Author:
Lemanski, Stuart Lucien

Title:
Static optimisation of prismatic structures as applied to helicopter rotor blades

STATIC OPTIMISATION OF PRISMATIC STRUCTURES AS APPLIED TO HELICOPTER ROTOR BLADES

by

Stuart Lucien Lemanski

A dissertation submitted to the University of Bristol in accordance with the requirements of the degree of Doctor of Philosophy in the Faculty of Engineering, Department of Aerospace Engineering

45688 words

ABSTRACT

The elastic coupling properties of anisotropic composite materials offer the potential for aeroelastic tailoring and other structural couplings that are not fully exploited in current helicopter rotor blade designs. The full 3-dimensional analysis of slender prismatic structures (such as helicopter rotor blades) is routinely reduced to analysis of a 1-dimensional beam with associated cross-sectional stiffness and mass properties. It is therefore desirable to design the cross-section of such prismatic structures to given values of these cross-sectional properties.

Although use of anisotropic composite materials offers additional degrees of freedom with which to obtain the desired values of cross-sectional properties, this introduces non-intuitive structural couplings and interactions between design variables, which increases the complexity of the design process. Rigorous optimisation techniques are therefore required to reliably and efficiently obtain an optimum design. This thesis addresses the main issues relating to the static optimisation of prismatic structures and their application to composite helicopter rotor blade design.

Existing literature in composite materials, optimisation, and helicopter blade design is surveyed. A 4-ply laminated cylindrical shell is examined from analytical and computational perspectives as a simplified case study, which is used to develop understanding of how the choice of design variables affects the nature of the design space, and hence the solution methods which can be used.

Flap-torsion coupling is an important variable in aeroelastic tailoring, and is therefore examined in some detail. A new analytical model is derived which is validated using finite element analysis, and compares favourably against existing models in the literature. Flap-torsion behaviour of laminated composite beams is studied experimentally, and compared with finite element results.

Finally, the validity of the method has been demonstrated through the application of this work to the design of a generic helicopter rotor blade section, which meets given target values of cross-sectional stiffness.

ACKNOWLEDGEMENTS

Thanks to Paul Weaver – for the priority treatment you gave me when proofreading this thesis, for the time you've invested in me throughout this project, and also for putting up with me on the (many) occasions I was upset, stressed, and frustrated over the last few years.

Thanks to Graham Hill – without your technical help I'd never have known how to get started on this project - let alone finished. It's been fun sharing an office with you.

Thanks to Luca Cecchini for being a good sounding board: for asking stupid, obvious questions, and for not laughing when I asked stupid, obvious questions of my own.

Thanks to Westland Helicopters for financially supporting this project, and also to Pete Wood, Wayland Chan and Dave Swabey whose assistance and advice have ensured this project remained industrially relevant and useful in the real world.

Thanks also to my friends and family – particularly to Kevin Knights for giving me his computer when mine died, and to my dad for providing me somewhere (free) to live while writing up (and for not hassling me to help with the DIY until this thesis was finished).

Finally, thank you Charlotte. Thank you for putting up with me while I was writing up, and thank you waiting for so long with me for my viva. Thank you for giving me the rest of our lives together in which I can begin to thank you properly.

AUTHOR'S DECLARATION

I hereby declare that the work in this dissertation was carried out in accordance with the regulations of the University of Bristol. The work is original except where indicated by special reference in the text and no part of the dissertation has been submitted for any other degree.

Any views expressed in the dissertation are those of the author and in no way represent those of the University of Bristol

The dissertation has not been presented to any other University for examination either in the United Kingdom or overseas

SIGNED:  DATE: 12th Jan '04

TABLE OF CONTENTS

LIST OF FIGURES

CHAPTER 2

CHAPTER 3

CHAPTER 4

CHAPTER 6

LIST OF TABLES

CHAPTER 2

CHAPTER 3

CHAPTER 4

CHAPTER 5

CHAPTER 6

NOMENCLATURE

The following nomenclature is used throughout this thesis, except where explicitly defined otherwise, or where quoting the work of others.

General

x	Value
$\underline{x}$	Vector
[X]	Matrix
f(x), g(x), h(x)	Functions of variable, x
f'(x)	First derivative of function f(x)
f''(x)	Second derivative of function f(x)
∇	Gradient operator

Structures and materials

E	Young's modulus
G	Shear modulus
v	Poisson ratio
A	Cross sectional area
I_{kk}	Second moment of area about kk-axis
J	Polar moment of area
EA	Axial stiffness
EI_{XX}	Flap bending stiffness
EI_{YY}	Lag bending stiffness
GJ	Torsional stiffness
$\underline{\sigma}$	Stress vector
σ_i	Direct stress in i-direction
σ_{ij}	Shear stress in ij-plane

$\underline{\varepsilon}$	Strain vector
ε_i	Strain in i-direction
γ_{ij}	Shear strain in ij-plane
κ_i	Curvature
κ_{ij}	Twist

Composite materials

E_i	Young's modulus in i-direction
G_{ij}	Shear modulus in ij-plane
v_{ij}	Major Poisson ratio
v_{ji}	Minor Poisson ratio
θ	Ply orientation angle
Q_{ij}	Lamina stiffness (lamina coordinates)
$[Q]$	Lamina stiffness matrix (lamina coordinates)
$\overline{Q}_{ij}$	Lamina stiffness (translated to laminate coordinates)
$[\overline{Q}_{ij}]$	Lamina stiffness matrix (translated to laminate coordinates)
A_{ij}	Laminate inplane stiffness term
B_{ij}	Laminate coupling stiffness term
D_{ij}	Laminate bending stiffness term
$[A]$	Laminate inplane stiffness matrix
$[B]$	Laminate coupling stiffness matrix
$[D]$	Laminate bending stiffness matrix
N_x, N_y, N_{xy}	Forces per unit width of laminate
M_x, M_y, M_{xy}	Bending and twisting moments per unit width of laminate
$\varepsilon_x, \varepsilon_y, \gamma_{xy}$	In-plane strains

κ_x, κ_y, κ_{xy},	Bending and twisting curvatures at the mid-surface
z_k, z_{k-1}	Distances from mid-plane to upper and lower surfaces of k^{th} lamina
U_i	Material invariant
ξ_i	Lamination parameter

Beam models

X	Axial direction
Y	Lag direction
Z	Flap direction
u,v,w or δ_x, δ_y, δ_z	Displacements in X-, Y- and Z-directions
ϕ_x, ϕ_y, ϕ_z	Rotations about X-, Y- and Z-axes
S_{ij}	Compliance term
$[S]$	Compliance matrix
K_{ij}	Stiffness term
$[K]$	Stiffness matrix
$\underline{F}$	Force vector
$\underline{F_x}$	Axial force
F_y	Lag-shear force
F_z	Flap-shear force
$\underline{M}$	Moment vector
M_x or M_{yz}	Torque
M_y	Flap-bending moment
M_z	Lag-bending moment
$[R]$	Transformation matrix

1 INTRODUCTION

1.1 BACKGROUND

The elastic coupling properties of anisotropic composite materials offer the potential of aeroelastic tailoring for vibration reduction. Such structural couplings are not fully exploited in current helicopter rotor blade designs. The full 3-dimensional analysis of slender prismatic structures (such as helicopter rotor blades) is routinely reduced to analysis of a 1-dimensional beam with associated cross-sectional stiffness and mass properties. It is therefore desirable to design the cross-section of such prismatic structures to meet given values of these cross-sectional properties.

Although use of anisotropic composite materials offers additional degrees of freedom with which to obtain the desired values of cross-sectional properties, this introduces non-intuitive structural couplings and interactions between design variables, which increases the complexity of the design process. Rigorous optimisation techniques are therefore required to reliably and efficiently obtain an optimal design.

The main objective of this research is therefore to produce a generic method for the analysis and optimisation of anisotropic 1-dimensional thin-walled beams. In so doing, this thesis particularly addresses the structural and optimisation issues relating to the static optimisation of composite helicopter rotor blades.

1.2 LITERATURE

Existing literature in composite materials, optimisation, and helicopter blade design is surveyed.

An introduction is given to the principles of composite laminate analysis and the main assumptions of this theory are considered. Lamination parameters are introduced, and their limitations discussed.

An overview of the main approaches to helicopter blade modelling and optimisation in the existing literature is given. Typically, research has focussed on either the

development of analytical models to give increased physical understanding of the behaviour of composite structures, or the optimisation of a specific blade property using a simplified finite element model and a limited choice of design variables.

An overview of optimisation theory is presented, including the visualisation of an optimisation problem, some basic concepts and techniques used in optimisation, and a discussion of a number of common optimisation algorithms.

1.3 CYLINDRICAL SHELL CASE STUDY

A 4-ply laminated cylindrical shell is examined from analytical and computational perspectives as a simplified case study, which is used to develop an understanding of how the choice of design variables affects the nature of the design space, and hence the solution methods which can be used.

The use of a multivariate global linear approximation method is detailed, wherein the problem is reduced to a number of simultaneous linear equations that can be solved using matrix methods. Three different classes of problem are considered and the types of solution that may result from these are discussed.

1.4 ANALYTICAL MODEL OF FLAP-TORSION COUPLING

Flap-torsion coupling is an important variable in aeroelastic tailoring, and is therefore examined in some detail. A new analytical model is derived which is based upon a stiffness of materials and shear flow approach. This model is validated by comparison with finite element analyses over a large range of design parameters. The analysis presented compares favourably against existing models for flap torsion coupling in the literature.

1.5 EXPERIMENTAL STUDY OF FLAP-TORSION COUPLING

An experiment is devised to measure the deflections of a eight laminated composite beams when subjected to shear load and torque at one end. From this behaviour, the bending, twisting and flap-torsion behaviour of these beams can be derived.

The results compare poorly with the predictions of classical laminate analysis. Since the assumptions of classical laminate analysis are not met for the beams studied, classical laminate analysis is inadequate for predicting the behaviour of the beams studied. The results are therefore compared with the results of finite element analyses, and good agreement is generally found.

1.6 OPTIMISATION OF A COMPOSITE ROTOR BLADE

The understanding gained through the work undertaken is applied to the design of a generic helicopter rotor blade section, which meets given target values of cross-sectional stiffness.

This is demonstrated in the first instance for the optimisation of cross-sectional properties that behave in an approximately linear fashion, using design variables that do not interact.

In the second instance, the optimisation of non-linear cross-sectional properties using potentially interactive design variables is demonstrated. Methods of minimising the interactions between design variables are discussed as this allows the continued use of deterministic optimisation methods that are based upon linear approximations. The effects of non-linearity of cross-sectional properties are discussed.

1.7 CONCLUSIONS

The final chapter concludes the thesis by summarising the work that has been presented and making suggestions for further study.

2 BACKGROUND AND LITERATURE

2.1 INTRODUCTION

Composite helicopter rotor blades "are normally of closed single- or multi-celled cross-sections and are thin walled, except near the root where they become thick walled" [1]. The properties of anisotropic composite materials (particularly elastic coupling) offer the potential for aeroelastic tailoring and other structural couplings that have not been fully exploited in current rotor designs.

2.1.1 Objectives

The main objective of this research is to produce a generic method for the analysis and optimisation of anisotropic 1-dimensional thin-walled beams, of which composite helicopter rotor blades are an example.

This research has developed a working optimisation code for use in industry that reliably designs the internal structure of a composite helicopter rotor blade to meet given cross-sectional properties. This process has been largely symbiotic with the overall academic goal described above.

2.1.2 Literature

In a survey of applications of design optimisation to rotorcraft, Celi [2] states that many helicopter engineering problems require a multidisciplinary approach, giving the example that flight dynamics and control system design are closely coupled with structural dynamics and aerodynamics. This approach has resulted in the development of comprehensive analysis codes, which attempt to integrate the mathematical models required by each helicopter engineering discipline. However, it is beneficial from an optimisation perspective to decompose a large, complex problem into smaller, simpler problems. Thus, optimising only the rotor blade structure is an important exercise, since it allows this aspect of the optimisation to be carried out in significantly more detail than otherwise possible.

Even a project with a highly directed focus such as this draws on a number of disciplines in its solution. To those involved in the research, this has been an attractive feature of this project. In particular, the following areas have been heavily called on during this research:

- composite laminate analysis
- analytical modelling
- finite element modelling
- optimisation

These broad areas encompass a vast amount of literature. Rapidly recognising and discarding the irrelevant material has been almost as important as understanding and critiquing the relevant in conducting the literature survey.

The remainder of this chapter approaches each for the above four subject areas in turn, outlining the basic concepts that are relevant to this work, with references to existing literature where appropriate.

2.2 COMPOSITE LAMINATE ANALYSIS

2.2.1 Classical laminate theory

There are good textbooks [3][4][5] that describe classical lamination theory, however, since its use is of such fundamental importance to the work presented elsewhere in this thesis, the basic theory is reproduced here.

Consider a flat orthotropic plate in a state of plane stress as shown in Figure 2.1 below.

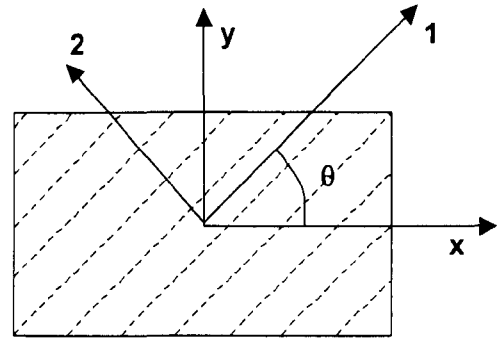

Figure 2.1 Plate axes (*x-y*) and Orthotropic axes (*1-2*)

The stress strain relations in the 1-2 axis system (aligned parallel with and perpendicular to the fibre direction) are given as

$$\begin{Bmatrix} \sigma_1 \\ \sigma_2 \\ \tau_{12} \end{Bmatrix} = \begin{bmatrix} Q_{11} & Q_{12} & 0 \\ Q_{12} & Q_{22} & 0 \\ 0 & 0 & Q_{66} \end{bmatrix} \begin{Bmatrix} \varepsilon_1 \\ \varepsilon_2 \\ \gamma_{12} \end{Bmatrix} \qquad (2.1)$$

where Q_{ij} terms are called the *reduced stiffnesses* (because the stiffness terms have been reduced from the engineering constants that populate the 6x6 stiffness matrix that is required to analyse the elastic behaviour of a fully 3-dimensional solid). These reduced stiffnesses are defined as

$$Q_{11} = \frac{E_1}{1 - \nu_{12}\nu_{21}} \qquad (2.1.a)$$

$$Q_{22} = \frac{E_2}{1 - \nu_{12}\nu_{21}} \qquad (2.1.b)$$

$$Q_{12} = \frac{\nu_{12}E_2}{1 - \nu_{12}\nu_{21}} = \frac{\nu_{21}E_1}{1 - \nu_{12}\nu_{21}} \qquad (2.1.c)$$

$$Q_{66} = G_{12} \qquad (2.1.d)$$

It is usually desirable to work in the plate *x-y* axis system (see Figure 2.1), so the above equations must be translated from the orthotropic *1-2* axis system to the *x-y* system. This gives

$$\begin{Bmatrix} \sigma_x \\ \sigma_y \\ \tau_{xy} \end{Bmatrix} = \begin{bmatrix} \overline{Q}_{11} & \overline{Q}_{12} & \overline{Q}_{16} \\ \overline{Q}_{12} & \overline{Q}_{22} & \overline{Q}_{26} \\ \overline{Q}_{16} & \overline{Q}_{26} & \overline{Q}_{66} \end{bmatrix} \begin{Bmatrix} \varepsilon_x \\ \varepsilon_y \\ \gamma_{xy} \end{Bmatrix} \qquad (2.2)$$

where the *translated reduced stiffnesses* ($\overline{Q}_{ij}$) are given as

$$\overline{Q}_{11} = Q_{11}\cos^4\theta + 2(Q_{12}+2Q_{66})\sin^2\theta\cos^2\theta + Q_{22}\sin^4\theta$$

$$\overline{Q}_{12} = (Q_{11}+Q_{22}-4Q_{66})\sin^2\theta\cos^2\theta + Q_{12}(\sin^4\theta + \cos^4\theta)$$

$$\overline{Q}_{22} = Q_{11}\sin^4\theta + 2(Q_{12} + 2Q_{66})\sin^2\theta\cos^2\theta + Q_{22}\cos^4\theta$$

$$\overline{Q}_{16} = (Q_{11}-Q_{12}-2Q_{66})\sin\theta\cos^3\theta + (Q_{12}-Q_{22}+2Q_{66})\sin^3\theta\cos\theta$$

$$\overline{Q}_{26} = (Q_{11}-Q_{12}-2Q_{66})\sin^3\theta\cos\theta + (Q_{12}-Q_{22}+2Q_{66})\sin\theta\cos^3\theta$$

$$\overline{Q}_{66} = (Q_{11}+Q_{22}-2Q_{12}-2Q_{66})\sin^2\theta\cos^2\theta + Q_{66}(\sin^4\theta + \cos^4\theta) \qquad (2.2.a\text{-}f)$$

Tsai and Pagano [6] define five material properties that are invariant with respect to ply orientation

$$U_1 = \frac{1}{8}(3Q_{11} + 3Q_{22} + 2Q_{12} + 4Q_{66})$$

$$U_2 = \frac{1}{2}(Q_{11} - Q_{22})$$

$$U_3 = \frac{1}{8}(Q_{11} + Q_{22} - 2Q_{12} - 4Q_{66})$$

$$U_4 = \frac{1}{8}(Q_{11} + Q_{22} + 6Q_{12} - 4Q_{66})$$

$$U_5 = \frac{1}{8}(Q_{11} + Q_{22} - 2Q_{12} + 4Q_{66}) \qquad (2.3.a\text{-}e)$$

Rearranging the above equations and using trigonometric identities gives the transformed reduced stiffnesses in terms of the material invariant properties.

$$\overline{Q}_{11} = U_1 + U_2 \cos 2\theta + U_3 \cos 4\theta$$

$$\overline{Q}_{12} = U_4 - U_3 \cos 4\theta$$

$$\overline{Q}_{22} = U_1 - U_2 \cos 2\theta + U_3 \cos 4\theta$$

$$\overline{Q}_{16} = -\frac{1}{2} U_2 \sin 2\theta - U_3 \sin 4\theta$$

$$\overline{Q}_{26} = -\frac{1}{2} U_2 \sin 2\theta + U_3 \sin 4\theta$$

$$\overline{Q}_{66} = U_5 - U_3 \cos 4\theta \qquad (2.4.a\text{-}f)$$

The behaviour of a composite material is defined in terms of the following constitutive relations for the laminate

$$\begin{Bmatrix} N_x \\ N_y \\ N_{xy} \\ M_x \\ M_y \\ M_{xy} \end{Bmatrix} = \begin{bmatrix} A_{11} & A_{12} & A_{16} & B_{11} & B_{12} & B_{16} \\ & A_{22} & A_{26} & B_{12} & B_{22} & B_{26} \\ & & A_{66} & B_{16} & B_{26} & B_{66} \\ & & & D_{11} & D_{12} & D_{16} \\ & Sym. & & & D_{22} & D_{26} \\ & & & & & D_{66} \end{bmatrix} \begin{Bmatrix} \varepsilon_x \\ \varepsilon_y \\ \gamma_{xy} \\ \kappa_x \\ \kappa_y \\ \kappa_{xy} \end{Bmatrix} \qquad (2.5)$$

where

$$A_{ij} = \sum_{k=1}^{N} (\overline{Q}_{ij})_k (z_k - z_{k-1})$$

$$B_{ij} = \frac{1}{2} \sum_{k=1}^{N} (\overline{Q}_{ij})_k (z_k^2 - z_{k-1}^2)$$

$$D_{ij} = \frac{1}{3} \sum_{k=1}^{N} (\overline{Q}_{ij})_k (z_k^3 - z_{k-1}^3) \qquad (2.5.a\text{-}c)$$

where z_k and z_{k-1} are the distances of the upper and lower surfaces of the k_{th} layer from the mid-plane of the laminate, as defined in the nomenclature.

The most important assumption inherent in the formulation of classical lamination theory is that the laminate is assumed to have (at most) linearly varying strains through its thickness. That is to say that there is no through thickness shear, and that lines normal to the surface of the laminate prior to deformation remain normal to the surface after deformation, as illustrated by Figure 2.2 below.

Figure 2.2 Normals to laminate before and after deformation

From the work of Tsai and Pagano [6], it is seen that the constitutive model can be expressed solely in terms of the sums of material invariant properties and ply angles through the thickness of the laminate. This leads naturally on to the idea of lamination parameters that have been explored by Fukunaga and Miki [7-10].

2.2.2 Lamination parameters

Lamination parameters have been developed by Fukunaga and Miki [7-10], and are now frequently used in the literature [11-16]. Although the direct use of Fukunaga and Miki's work on lamination parameters in this thesis is limited (due to the difficulty of obtaining explicit lay-ups and stacking sequences from particular lamination parameters), their approach gives valuable insight into the behaviour of composite laminates and has profound implications for design and optimisation. As a result, the inclusion of the basic theory is justified here.

Note that since lamination parameters are based upon the model derived from classical lamination theory, the same inherent assumptions apply here.

Fukunaga and Miki [7-10] have published a significant volume of work on the use of lamination parameters in structural design with composite materials. Comparison between the two authors shows that the lamination parameters used by each are equivalent. For continuity within this thesis, Fukunaga's notation will be adopted.

The properties of an anisotropic composite laminate are completely defined in terms of twelve lamination parameters $\xi_{1\text{-}12}$ and the five material invariant properties $U_{1\text{-}5}$ identified by Tsai and Pagano [6] as

$$\begin{Bmatrix} A_{11} \\ A_{12} \\ A_{22} \\ A_{66} \\ A_{16} \\ A_{26} \end{Bmatrix} = h \begin{bmatrix} 1 & \xi_1 & \xi_2 & 0 & 0 \\ 0 & 0 & -\xi_2 & 1 & 0 \\ 1 & -\xi_1 & \xi_2 & 0 & 0 \\ 0 & 0 & -\xi_2 & 0 & 1 \\ 0 & \frac{\xi_3}{2} & \xi_4 & 0 & 0 \\ 0 & \frac{\xi_3}{2} & -\xi_4 & 0 & 0 \end{bmatrix} \begin{Bmatrix} U_1 \\ U_2 \\ U_3 \\ U_4 \\ U_5 \end{Bmatrix} \qquad (2.6.a)$$

$$\begin{Bmatrix} B_{11} \\ B_{12} \\ B_{22} \\ B_{66} \\ B_{16} \\ B_{26} \end{Bmatrix} = \frac{h^2}{4} \begin{bmatrix} 0 & \xi_5 & \xi_6 & 0 & 0 \\ 0 & 0 & -\xi_6 & 0 & 0 \\ 0 & -\xi_5 & \xi_6 & 0 & 0 \\ 0 & 0 & -\xi_6 & 0 & 0 \\ 0 & \frac{\xi_7}{2} & \xi_8 & 0 & 0 \\ 0 & \frac{\xi_7}{2} & -\xi_8 & 0 & 0 \end{bmatrix} \begin{Bmatrix} U_1 \\ U_2 \\ U_3 \\ U_4 \\ U_5 \end{Bmatrix} \qquad (2.6.b)$$

$$\begin{Bmatrix} D_{11} \\ D_{12} \\ D_{22} \\ D_{66} \\ D_{16} \\ D_{26} \end{Bmatrix} = \frac{h^3}{12} \begin{bmatrix} 1 & \xi_9 & \xi_{10} & 0 & 0 \\ 0 & 0 & -\xi_{10} & 1 & 0 \\ 1 & -\xi_9 & \xi_{10} & 0 & 0 \\ 0 & 0 & -\xi_{10} & 0 & 1 \\ 0 & \frac{\xi_{11}}{2} & \xi_{12} & 0 & 0 \\ 0 & \frac{\xi_{11}}{2} & -\xi_{12} & 0 & 0 \end{bmatrix} \begin{Bmatrix} U_1 \\ U_2 \\ U_3 \\ U_4 \\ U_5 \end{Bmatrix} \qquad (2.6.c)$$

where h is the thickness of the laminate. The individual lamination parameters may be calculated from the following integrals

$$(\xi_1 \quad \xi_2 \quad \xi_3 \quad \xi_4) = \frac{1}{2}\int_{-1}^{1}(\cos 2\theta \quad \cos 4\theta \quad \sin 2\theta \quad \sin 4\theta)du$$

$$(\xi_5 \quad \xi_6 \quad \xi_7 \quad \xi_8) = \int_{-1}^{1}(\cos 2\theta \quad \cos 4\theta \quad \sin 2\theta \quad \sin 4\theta)udu$$

$$(\xi_9 \quad \xi_{10} \quad \xi_{11} \quad \xi_{12}) = \frac{3}{2}\int_{-1}^{1}(\cos 2\theta \quad \cos 4\theta \quad \sin 2\theta \quad \sin 4\theta)u^2du \qquad (2.7.a\text{-}l)$$

where

$$u = z/h \qquad (2.7.m)$$

As already stated, the reverse process of determining the ply orientations from a given set of lamination parameters is not straightforward, although much work in the literature has been directed towards this end.

Fukunaga [7] demonstrates a method applicable to *certain* cases for determining the laminate configurations from the lamination parameters. Diaconu *et al* [11][12] and Grediac [13] have developed work to determine lay-ups from lamination parameters.

These methods typically involve the optimisation of ply orientations and/or thicknesses. An initial guess is made for a lay-up, and the lamination parameters of the lay-up are determined. These lamination parameters are compared with the target values of lamination parameter, and an optimisation process is used to find the layer orientations and thicknesses that meet the desired values of lamination parameter. Both Diaconu *et al* [11] and Grediac [13] minimise an objective function of the form

$$\Delta\xi = \sum_{i=1}^{12}\left(\xi_{i(opt)} - \xi_i\right)^2 \qquad (2.8)$$

where $\xi_{i(opt)}$ is the optimum (i.e. target) value of lamination parameter i, and ξ_i is the calculated value of lamination parameter i at the current design point.

Depending on the number of layers in the laminate, there may be a number of possible (continuous) solutions. Since the design space is not discrete (ply layers have finite thickness, and manufacturing guidelines often limit the available ply orientations to 0°, ±45° or 90°) an exact, discrete solution is not normally possible. Typically, it is possible to match the lamination parameters with either the layer thicknesses or the ply orientations meeting the required discretisation, but not both.

It should be appreciated that because the lamination parameters are geometric functions of the ply angles, they are not independent of one another. Fukunaga [7] gives the relations between the A-matrix parameters, $\xi_{1\text{-}4}$, as

$$\xi_1^2 + \xi_3^2 \leq 1 \qquad (2.9.a)$$

$$\left(\xi_2 - \xi_1^2 + \xi_3^2\right)^2 + \left(\xi_4 - 2\xi_1\xi_3\right)^2 \leq \left(1 - \xi_1^2 - \xi_3^2\right)^2 \qquad (2.9.b)$$

Thus, any laminate will correspond to a given point within the boundaries shown by the following lamination parameter diagrams (Figure 2.3).

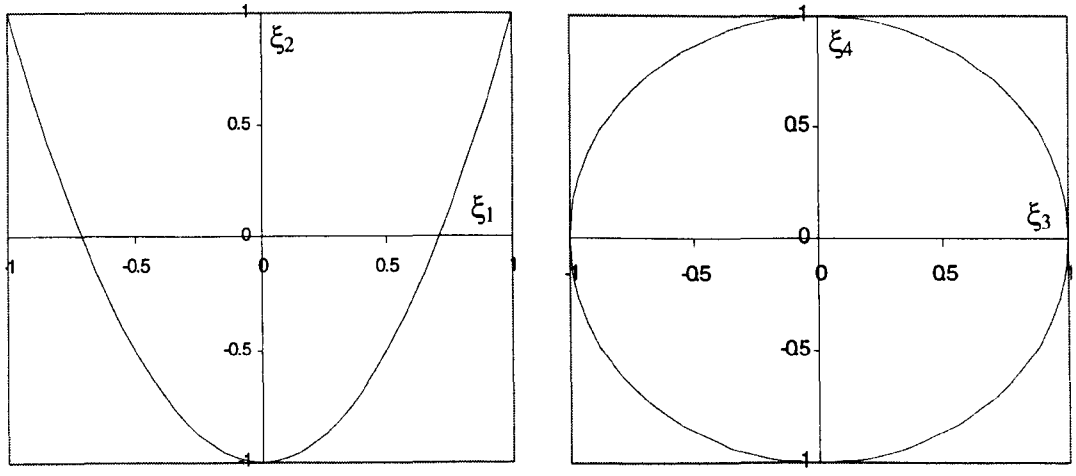

Figure 2.3 Lamination parameter diagrams for A-matrix parameters

The boundaries in ξ_1-ξ_2 and ξ_3-ξ_4 space are not independent, as demonstrated by equations *(2.8.a)* and *(2.8.b)*. Similar relations exist for the B and D matrix lamination parameters, although these are not detailed here.

The use of lamination parameters in optimisation results in the stiffness components being a linear function of the lamination parameters rather than a non-linear sinusoidal function of the ply angles. It is highly desirable for optimisation if the objective function and constraints are linear functions of the design variables.

Although Fukunaga's [7][8] notation has been adopted in this thesis Miki [9][10] has independently explored the idea of lamination parameter diagrams as a tool for designing laminates for in-plane and out-of-plane response. Since a symmetric, balanced laminate has no A_{16} or A_{26} coupling, the lamination parameters that correspond to these values (ξ_3 and ξ_4) are both zero. Therefore, only the ξ_1-ξ_2 lamination parameter diagram needs to be considered when designing such a laminate.

Any point inside this lamination parameter diagram corresponds to laminates with two or more fibre orientations. Assuming complete freedom in the choice of angle, only two different ply orientations are needed for designing laminates with prescribed in-plane stiffness requirements.

For a laminate with only one fibre orientation angle, θ, the lamination parameters are

$$\xi_1 = \cos 2\theta \qquad (2.7.a)$$

$$\xi_2 = \cos 4\theta \qquad (2.7.b)$$

Thus, double angle formulae give

$$\xi_2 = 2\xi_1^{\,2} - 1 \qquad (2.9.c)$$

Any single angle laminate will lie on the parabola defined by this expression and shown in Figure 2.3. It has been shown by Miki [9] that for two or more fibre orientations, the above equation becomes an inequality

$$\xi_2 \geq 2\xi_1^{\,2} - 1 \qquad (2.9.d)$$

and the laminate will lie within the bounded area shown on Figure 2.3. Each point in the allowable region is called a lamination point, and corresponds to a laminate with specific stiffness properties.

For symmetric balanced laminates, the values of the effective in-plane engineering constants are calculated from

$$E_x = \frac{1}{h}\left(\frac{A_{11}A_{22} - A_{12}^2}{A_{22}}\right) \qquad (2.20.a)$$

$$E_y = \frac{1}{h}\left(\frac{A_{11}A_{22} - A_{12}^2}{A_{11}}\right) \qquad (2.20.b)$$

$$G_{xy} = \frac{1}{h}A_{66} \qquad (2.20.c)$$

$$\nu_{xy} = \frac{A_{12}}{A_{22}} \qquad (2.20.d)$$

which may obviously be expressed in terms of lamination parameters if required. Contours of constant effective engineering constants can be obtained from the following equations and superimposed upon the allowable design space (Figure 2.4).

E_x contours

$$\xi_2 = \frac{U_2^2\xi_1^{\,2} - U_2E_x\xi_1 + E_xU_1 - U_1^2 + U_4^2}{U_3(2U_1 + 2U_4 - E_x)} \qquad (2.21.a)$$

E_y contours

$$\xi_2 = \frac{U_2^2 \xi_1^2 + U_2 E_y \xi_1 + E_y U_1 - U_1^2 + U_4^2}{U_3 (2U_1 + 2U_4 - E_y)} \qquad (2.21.b)$$

G_{xy} contours

$$\xi_2 = \frac{U_5 - G_{xy}}{U_3} \qquad (2.21.c)$$

ν_{xy} contours

$$\xi_2 = \frac{\nu_{xy} U_2 V_1^* - \nu_{xy} U_1 + U_4}{(1 + \nu_{xy}) U_3} \qquad (2.21.d)$$

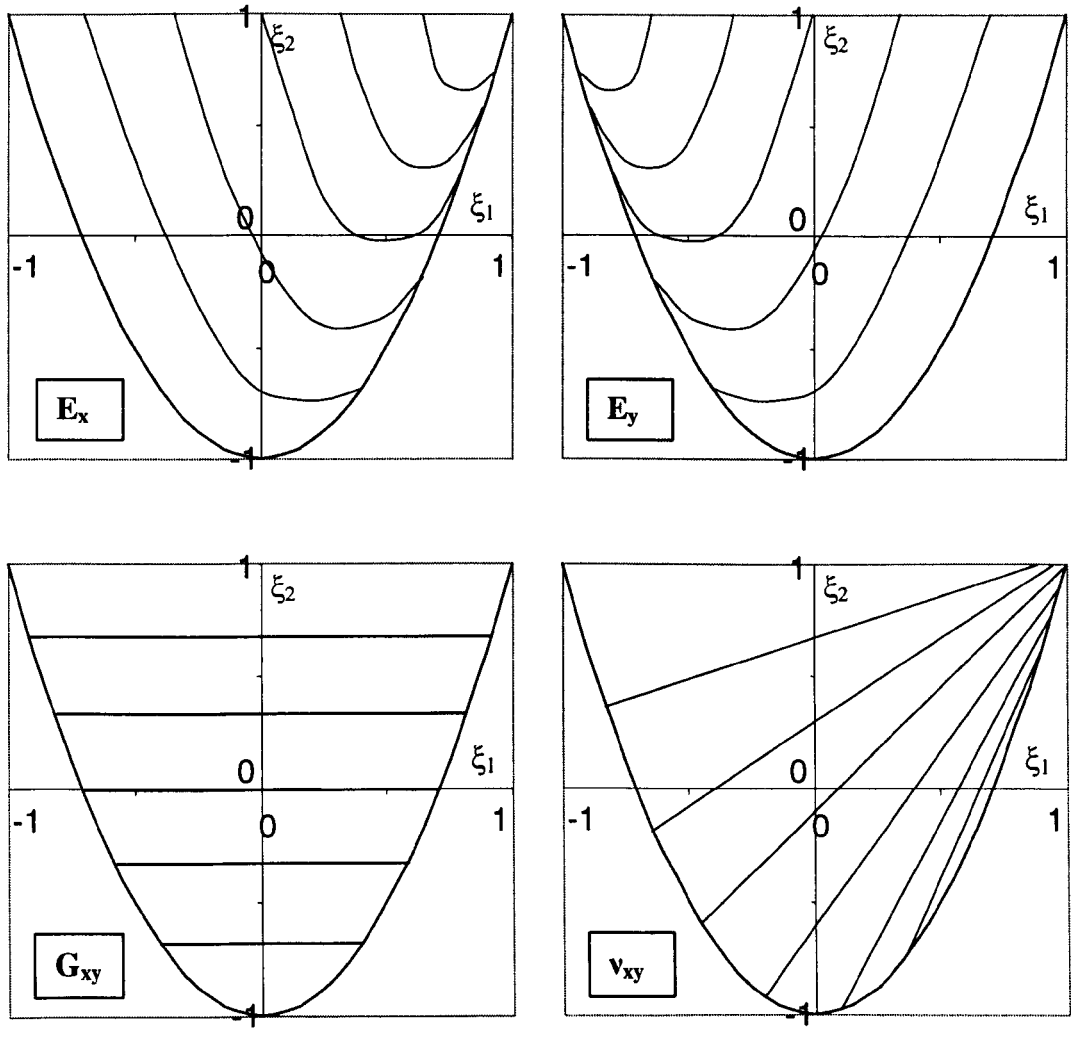

Figure 2.4 Contours of effective engineering constants in ξ_1-ξ_2 space

For design problems where one or more of the effective engineering constants are constrained, appropriate contours can be superimposed to identify the feasible design space and the lamination point that optimises the desired stiffness property.

In practice, a number of additional constraints are often added when designing a laminate (e.g. that the laminate be balanced, symmetric, and/or consists of only 0°/±45°/90° plies). Miki and Sugiyama [14] have shown that the feasible region for laminates with fixed ply angles is a polygon with vertices located on the envelope of the lamination parameter diagram. Points along the edges and interior points of the polygons correspond to laminates with combinations of the permissible orientations.

Thus, the in-plane properties of a balanced laminate consisting of only 0°/±45°/90° plies, will lie within the triangular shaded region of lamination parameter space shown in Figure 2.5. This indicates that constraining a design to only these ply angles does not significantly limit the properties of laminate that can be obtained.

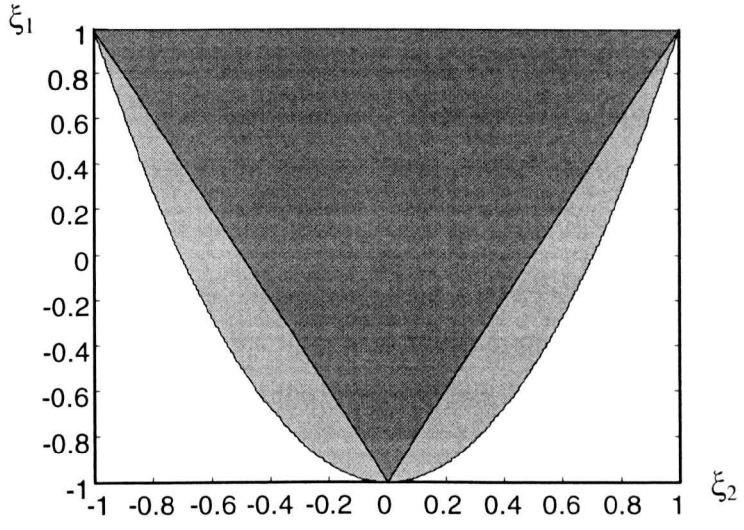

Figure 2.5 Lamination parameter space for balanced 0°/±45°/90° laminates

Assuming no discretisation of ply thickness, the lay-up can be chosen within these constraints that define any given point within the allowable triangular region, thus making lamination parameter diagrams particularly useful tool for designing laminates with predetermined ply orientation angles.

2.3 MODELLING ISSUES

2.3.1 Background

The usual industrial approach for design analysis is to use commercially available finite element analysis software. Since one of the objectives of this project is to satisfy industrial requirements, it is desired that finite element analysis software ultimately be coupled to an optimisation routine to obtain an optimal design. However, Haftka and Gurdal [17] state that "in optimisation, where hundreds or thousands of analyses may be required before convergence, the computational cost of using finite element analyses can become prohibitive". Analytical models are therefore often used as an alternative to finite element analysis based optimisation, or simply to give physical insight into a particular problem.

In his review of composite rotor blade modelling [18], Hodges classes "the work into two distinct areas: 1) the use of specialised, simple models for the blade cross-section in order to asses the stability of rotor blades for various values of ply orientation and other geometric parameters and 2) the development of modelling approaches so that the three-dimensional constitutive law from general, anisotropic elasticity can be reduced to a simple one-dimensional form of the beam problem." This thesis straddles both areas by examining analytical modelling approaches to determine the cross-sectional stiffness properties, and by then applying the insight to select appropriate design variables for the finite element based optimisation of the cross-section.

2.3.2 Analytical modelling approaches

Much work has already been published by Smith [19], Rehfield [20], Rehfield and Cheung [21], Rehfield *et al* [22], Jung *et al* [1] and others (reviewed by Hodges [18] and Jung *et al* [23]), that shows analytical modelling of the cross-sectional properties (and particularly the aeroelastic tailoring) of composite aerospace structures.

The obvious limitation of using analytical modelling as an alternative to finite element analysis is that the quality of the optimisation (and hence also the quality of the optimal design produced) is limited by the quality of the analytical model. When considering the behaviour of composite laminates in structures, the local coupling effects of a laminate must be transformed into the global co-ordinate system of the structure. Furthermore, the geometry of most real-life structures is too complex to model analytically; so geometric approximations are also required. As a result of these approximations, the results of many published analytical approaches are of little use from a practical design perspective.

One such example is Kameyama *et al.* [24] who examine aeroelastic tailoring of an aircraft wing. The choice to model the wing as a cantilevered laminated plate is overly simplified, and completely overlooks the geometric and structural complexity of any real-life aircraft wing. Although this work remains an interesting study into the use of lamination parameters to design composite plates with tailored composite coupling, it gives little practical help in producing a detailed optimal design of a real aeroelastically tailored wing.

From a practical design perspective, analytical modelling is used to give physical insight into the particular problem being studied. By identifying the underlying physics of the problem, the relationships between the different design variables and the properties being considered can be better understood. This can be used as justification for reducing the design space, by selecting only suitable design parameters as variables in the optimisation, and/or by limiting the range of values that such design variables may take. As shown later in this thesis, analytical considerations allow an otherwise intractable optimisation problem to be solved in a matter of minutes.

Although this project is posed as a real-world optimisation problem, analytical models are essential tools towards solving this problem because they give insight into the underlying physics of the problem, and in doing so they enable an appropriate optimisation tool to be selected.

2.3.3 The importance of cross-sectional properties

It is common practice (e.g. Smith [19], Rehfield [20], Rehfield and Cheung [21], Rehfield *et al* [22], Jung *et al* [1][23], Chattopadhyay *et al* [25][26][27], Ganguli and Chopra [28][29][30]) to idealise the helicopter blade as a 1-dimensional beam with calculated cross-sectional stiffnesses. Wörndle [31] goes some way towards summarising when he states that "the dynamic and static behaviour of rotor blades is mainly influenced by the co-ordinates of the shear centre and the centre of elasticity as well as the bending and shear stiffnesses. However the distribution of the shear stresses due to transverse and torsional shear, the location of the shear centre and the transverse deflection resulting from transverse shears are not easily found for beams with complicated cross-section configurations". He uses a finite element method to solve this problem for a restricted class of orthotropic rotor blades using a finite element model of the cross-section.

Jung *et al* [1][23] use a Cartesian *xyz*-coordinate system and define applied forces as shown in Figure 2.6 below.

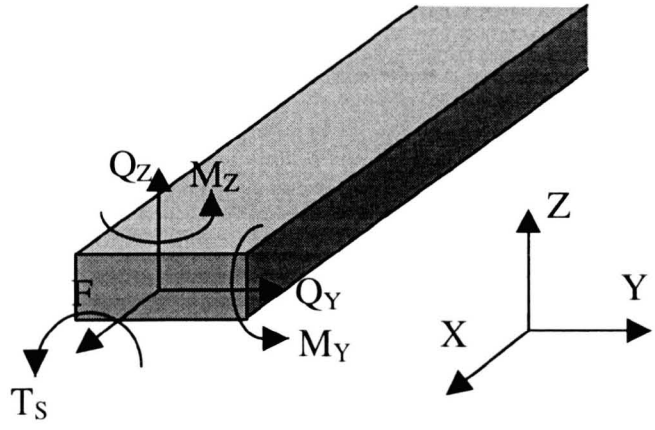

Figure 2.6 Coordinate system and forces defined by Jung *et al*

The cross-section stress resultants are related to the beam strain resultants with a 7 x 7 symmetric matrix *(2.22)*

$$\begin{Bmatrix} F \\ Q_y \\ Q_z \\ T_s \\ M_y \\ M_z \\ M_\omega \end{Bmatrix} = \begin{bmatrix} K_{11} & s_{12}K_{12} & s_{13}K_{13} & K_{14} & K_{15} & K_{16} & K_{17} \\ & s_{22}K_{22} & s_{23}K_{23} & K_{24} & K_{25} & K_{26} & K_{27} \\ & & s_{33}K_{33} & K_{34} & K_{35} & K_{36} & K_{37} \\ & & & K_{44} & K_{45} & K_{46} & K_{47} \\ & & & & K_{55} & K_{56} & K_{57} \\ & Sym. & & & & K_{66} & K_{67} \\ & & & & & & K_{77} \end{bmatrix} \begin{Bmatrix} u^0{}_{,x} \\ \gamma^0_{xy} \\ \gamma^0_{xz} \\ \phi_{,x} \\ \gamma^0_{xz,x} - w^0{}_{,xx} \\ \gamma^0_{xy,x} - v^0{}_{,xx} \\ \phi_{,xx} \end{Bmatrix} \qquad (2.22)$$

where

F	axial force
Q_y, Q_z	transverse shear forces along y- and z-axes respectively
T_s	torsion
M_y, M_z	bending moments about y- and z-axes respectively
M_ω	warping bimoment
$u^0{}_{,x}$	axial strain
γ^0_{xy}, γ^0_{xz}	transverse shear strains in xy- and xz-planes
$\phi_{,x}$	twist rate about x-axis
$w^0{}_{,xx}$, $v^0{}_{,xx}$	bending dispalcements about y- and z-axes respectively
$\phi_{,xx}$	warping displacement
K_{ij}	stiffness coefficients
s_{ij}	shear correction factors

Various researchers have applied different idealisations to both the beam and the cross-sectional shell aspects of the model, as summarised by Jung *et al* [23].

The work presented by Smith in his PhD thesis [19] is directed specifically towards aeroelastic response of composite helicopter rotor blades, and is particularly notable that by approximating the rotor blade to a thin walled rectangular box section, it derives expressions for each of the terms in a 6x6 cross-sectional stiffness matrix. Smith's thesis is considered detail in Chapter 3.

Rehfield *et al* [22] have also contributed significantly to the analytical modelling of cross-sectional stiffness properties. The rotor blade section is modelled as a thin walled box section, and various assumptions are made regarding the boundary conditions imposed upon the walls. Rehfield [20], and Rehfield and Cheung [21] use this method to examine the flap bending torsion coupling - an important variable in aeroelastic tailoring.

Jung *et al* [1] present a structural model that accounts for the effects of elastic couplings, shell wall thickness, section warping, warpnig restraint and transverse shear deformations. The approach is based on a mixed force and displacement method.

The analytical modelling of specific cross-sectional properties is considered in detail elsewhere in this thesis, since the highly specific and involved nature of such models makes it more appropriate to include such discussion in the relevant context rather than in the broad overview presented here.

2.3.4 Finite Element Modelling

In many respects, finite element modelling is generally regarded as a mature discipline, and great importance (and trust) is often placed on finite element results. The results from a well-constructed finite element model give confidence in the accuracy of experimental results and validate assumptions made in analytical work. By validating the analytical modelling in this way, and/or viewing the results in a suitable post-processor, finite element analysis can help to give insight into the underlying physics of the problem being studied.

The objective "to produce a working optimisation code for use in industry that reliably designs the internal structure of a composite helicopter rotor blade to meet given cross-sectional properties" requires that the analysis of a cross-section must be automated. The most appropriate approach for use in industry is the use of finite element analysis, with appropriate post-processing of results.

This project has been part supported by Westland Helicopters. For this reason NASTRAN [32] has been used as the finite element analysis code for this project, with a PATRAN [33] based interface and a PATRAN Command Language (PCL) routine based on the work of Hill and Weaver [34] which was written by Graham Hill as part of the wider research project at the University of Bristol.

2.3.5 Finite element optimisation models in existing literature

Sobieszczanski-Sobieski and Haftka [35] state "tradeoff of accuracy and cost through the judicious use of alternate models with different levels of complexity is another means for controlling computational cost. In single discipline optimisation, it is common to have an "**analysis model**" which is more accurate and more costly than an "**optimisation model**"."

Since their work was written, such vast improvements have been made in computational speed that "analysis models" are no longer strictly necessary in single discipline optimisation, although some trade off between model complexity and design flexibility is still required. Many examples of optimisation models are found in the literature that dates from this era.

He and Peters [36] use a 14-element box beam model to represent the structural component in the rotor blade. Each element has 12 degrees of freedom and the non-uniform *EI* and *GJ* are assumed linear over each element. The calculated results from their model are compared with measured data from a SA349/2 helicopter. It is claimed that the model predicts the basic characteristics of the structural loads, although it is also suggested that a better lag-damper model is needed for improvement.

McCarthy *et al.* [37] model the load carrying structural member of a tilt-rotor aircraft wing as a rectangular box beam with four independent wall thicknesses as design variables. To reduce the number of design variables while keeping the design space sufficiently large, spanwise variations of wall thickness are assumed similar to the rotor chord and twist distributions, although the wing root chord and taper ratio are also included as design variables. Subsequently, "each beam element was given ten degrees

of freedom, and the cross-sectional properties were calculated using thin walled theory. To obtain a realistic wing representation, the reference configuration used in the optimisation procedure is designed such that the first three frequencies, generalised masses and mode shapes are representative of NASTRAN data of the XV-15 tilting prop-rotor aircraft." [37] This provides some justification for the suitability of the model.

Ganguli and Chopra [28][29][30] have presented a significant volume of work that considers the optimisation of aerodynamic and/or dynamic behaviour of single and multi-celled helicopter rotor blades using simplified finite element models. Aeroelastic optimisation of helicopter blades with composite coupling was presented by Ganguli and Chopra in 1995 [28]. They modelled the cross-section as a single celled box-beam, with three of the ply angles as design variables. Although this is a severe limitation on the design space, they have successfully considered the global effects of composite coupling in a considerably more realistic model than that considered by Kameyama *et al* [24].

Subsequent to their 1995 paper [28], Ganguli and Chopra [29] state the importance of modelling the cross-section as a multicell beam, "since single cell representation of a multicell rotor blade can result in an overestimation of the torsional flexibility". They use an analysis based on Vlaslov theory for thin walled composite beams of arbitrary cross-section that includes the effect of out-of plane warping deformations, transverse shear related couplings, and constraining the warping deformation at the edges. The results of this analysis were validated by Chandra and Chopra [38].

Chattopadhyay has also published a significant volume of work with others [25][26][27] in the field of the multidisciplinary optimisation of aerodynamic and/or dynamic behaviour. Much of this work is directed towards the specific case of prop rotors on tilt-rotor aircraft, and so naturally has particular idiosyncrasies but is conceptually similar to that of Ganguli and Chopra and others inasmuch as it uses simplified finite element models.

Chattopadhyay *et al* [25] investigate the optimisation of a rotating wing structure for the prop-rotor of a tilt-rotor aircraft. Although the design resulting from their optimisation is compared with a reference solution, no discussion is given to indicate the accuracy of modelling the blade structure in this way.

When modelling a helicopter rotor blade, Chattopadhyay *et al.* [26] model the load carrying structural member "as a two-cell isotropic box beam with five independent wall thicknesses that are assumed to vary spanwise. Spanwise non-structural tuning masses are located at 2.5% chord location" and the beam is symmetrical about the x-axis. "Outer dimensions of the box at a blade section are based on constant percentages of the chord at a particular section". The accuracy of the model is not investigated, although their conclusions state "the procedure provides realistic design trends" in rotary blades, they acknowledge "the results obtained must be viewed within the context of the modelling assumptions used in the analysis".

The fundamental problem with the "optimisation model" approach is that the assumptions made in reducing the problem complexity (e.g. modelling rotor blade sections as thin walled rectangular boxes) potentially reduces the accuracy of the model, and in so doing it incurs the limitations that are inherent to analytical models. Much of the literature surveyed makes little or no attempt to validate the optimisation model with experimental or detailed finite element results.

The results of such optimisations are therefore often of less practical use to the industrial designer/manufacturer than desired, since if the optimisation model is not accurately representative of the real problem, the resulting solution may not be a true optimum. In such cases, a parametric study could potentially offer more insight into design trends at less overall effort.

2.3.6 Finite element analysis models

At the level of detail required by this project, the most pragmatic option for analysis of the cross-section is to use a detailed finite element model, since the final design will need to include details of exact internal geometry in terms of shapes, ply thicknesses,

lay-up, etc. However, the exact determination of the 1-dimensional cross-sectional properties from a finite element model is not straightforward.

Jung *et al* [23] have summarised the different idealisations applied by various researchers to both the beam and the cross-sectional shell aspects of the model.

Wörndle [31] uses a finite element model of the rotor blade cross-section (made from 2-D finite elements that assume no transverse pressure or in-plane shear exist in the cross-section) to determine the co-ordinates of the shear centre and the centre of elasticity as well as the bending and shear stiffnesses. Although his model is not strictly valid for non-homogeneous cross-sections, the effect is likely to be small. Since the work is concerned with accurately obtaining the beam section properties from a single analysis of the cross-section, the finite element model used is a detailed representation of an actual rotor blade cross-section.

Subsequent work was performed by Kosmatka and Dong [39] to "(1) formulate Saint-Venant's elasticity solutions for the extension, bending, torsion, and flexure of a prismatic beam whose cross-section is nonhomogeneous and completely anisotropic (i.e. like a composite rotor blade), and (2) determine the following important one-dimensional beam-theory properties; beam twist, flexural centre location, torsional constant, Saint-Venant torsion warping distribution, moment curvature relations, and shear correction factors." By assuming no variation of stress along the blade length, a large number of terms can be removed from the finite element stiffness matrix. Since the axial loading experienced by a beam rotating about one end is actually a parabolic function of the axial co-ordinate, this assumption is not strictly valid, although as with Wörndle's assumptions, the actual effect is likely to be small. Again, the finite element model of the cross-section is a detailed representation of an actual rotor blade cross-section

Work apparently overlooked by Jung *et al.* is that of Bartholomew and Mercer [40]. Their work takes a thin 3-D slice of a cross-section built from standard finite elements, with the ends constrained to remain planar. It is inherent in the approach taken that the assumptions made by Wörndle [31], and Kosmatka and Dong [39] are not required. This

approach has been subsequently adopted by Hatch and Lee [41], and Diamond [42]. Hill and Weaver [34] have extended Bartholomew and Mercer's work to automatically determine the coefficients of the fully populated 6 x 6 stiffness matrix from a finite element model of the cross-section. Having obtained this information the 1-D beam behaviour can be modelled. Automating this process allows it to be included in an optimisation routine.

Since the work of Hill and Weaver [34] forms the basis of the analysis code used in the optimisation routine for this thesis, the basic theory of their work (and the work that it was built upon) is presented below.

2.3.7 Basics of cross-sectional analysis method

Earlier work in this field was undertaken by Mansfield and Sobey [43], and Bartholomew and Mercer [40]. The following is paraphrased from Hill and Weaver [34]

2.3.7.1 Work of Bartholomew and Mercer

Bartholomew and Mercer [40] simplify the full 3-D problem by reducing it to a 2-D analysis of a cross-section of blade, using commercial finite element analysis packages. They establish shear and flexural centres, and in so doing, the bending-, extension- and torsion-stiffnesses are defined that may be used in subsequent 1-D beam analysis of the rotor blade (as described earlier in section 2.3).

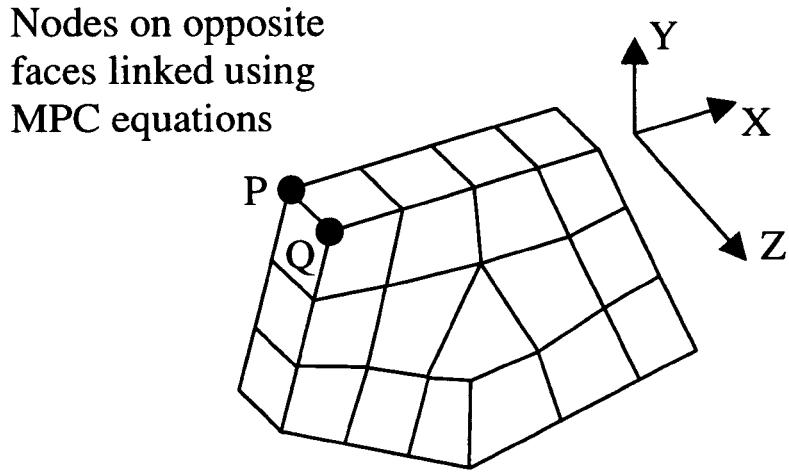

Figure 2.7 Generic Finite Element Cross-section

Note that the orientation of the global *XYZ*-coordinate system used for this work is different to that commonly used in beam analysis, which has been used elsewhere in this thesis.

The first step is to produce a 3-D slice of the section (depicted in Figure 2.7), with the nodes on opposite faces of the slice linked together by multi-point constraint (MPC) equations, defined in equations *(2.23.a-f)* below.

$$
\begin{aligned}
u(Q) &= u(P) + \mu_1 - \omega_3 y \\
v(Q) &= v(P) + \mu_2 + \omega_3 y \\
w(Q) &= w(P) + \mu_3 - \omega_2 x + \omega_1 y \\
r_x(Q) &= r_x(P) + \omega_1 \\
r_y(Q) &= r_y(P) + \omega_2 \\
r_z(Q) &= r_z(P) + \omega_3
\end{aligned}
\qquad \textit{(2.23.a-f)}
$$

These MPCs only control the *relative* displacements of the node pairs, which means that the two faces are not constrained to remain planar. The warping of the section is effectively unrestrained, and this work does not explicitly consider warping flexibilities.

By applying unit loads to the four active scalar freedoms (axial tension, flap-bending, lag-bending, and torsion), the loads are distributed to evenly to all the elements in the model.

For each load case, the four active scalar freedoms provide the overall displacements in the degree of freedom that they represent. The flexibility matrix of the section is found by dividing the relative displacements of the two faces by the length of the slice model to give

$$\begin{pmatrix} \delta_z \\ \phi_x \\ \phi_y \\ \phi_z \end{pmatrix} = \begin{pmatrix} S_{11} & S_{12} & S_{13} & S_{14} \\ S_{21} & S_{22} & S_{23} & S_{24} \\ S_{31} & S_{32} & S_{33} & S_{34} \\ S_{41} & S_{42} & S_{43} & S_{44} \end{pmatrix} \begin{pmatrix} F_z \\ M_x \\ M_y \\ M_z \end{pmatrix} \tag{2.24}$$

The stiffness matrix, K is found by inverting the flexibility matrix, S

$$[K] = [S]^{-1} \tag{2.25}$$

This flexibility matrix can be transformed to the elastic centroid of the beam by the transformation

$$[\bar{S}] = [R^T][S][R] \tag{2.26}$$

where

$$[R] = \begin{pmatrix} 1 & 0 & 0 & 0 \\ y_c & 1 & 0 & 0 \\ -x_c & 0 & 1 & 0 \\ 0 & 0 & 0 & 1 \end{pmatrix} \tag{2.26.a}$$

and

$$x_c = -\frac{K_{31}}{K_{11}} \qquad (2.26.b)$$

$$y_c = \frac{K_{21}}{K_{11}} \qquad (2.26.c)$$

The main assumption of this approach is that stresses are (at most) a linear function of the length.

2.3.7.2 Work of Hill and Weaver

The work of Bartholomew and Mercer [40] has been extended by Hill and Weaver [34] to produce a full 6x6 stiffness matrix. As with Bartholomew and Mercer, this work leaves the warping of the section unrestrained and does not explicitly consider warping stiffnesses (the 7th row and column in Jung's 7x7 matrix [1][23]). The 6 x 6 stiffness matrix is obtained in three stages.

Firstly, the X and Y scalar freedoms are *not* set to zero. This allows the shear flexibilities to be output as a part of the four load cases in the standard Bartholomew and Mercer method. Thus, the flexibility matrix will look like

$$\begin{pmatrix} \delta_x \\ \delta_y \\ \delta_z \\ \phi_x \\ \phi_y \\ \phi_z \end{pmatrix} = \begin{pmatrix} - & - & S_{13} & S_{14} & S_{15} & S_{16} \\ - & - & S_{23} & S_{24} & S_{25} & S_{26} \\ - & - & S_{33} & S_{34} & S_{35} & S_{36} \\ - & - & S_{43} & S_{44} & S_{45} & S_{46} \\ - & - & S_{53} & S_{54} & S_{55} & S_{56} \\ - & - & S_{63} & S_{64} & S_{65} & S_{66} \end{pmatrix} \begin{pmatrix} F_x \\ F_y \\ F_z \\ M_x \\ M_y \\ M_z \end{pmatrix} \qquad (2.27.a)$$

Eight of the remaining flexibilities are found by setting the shear freedoms to zero and applying the nodal forces from the bending cases. The displacements of the four active scalar freedoms will provide the flexibilities in those directions. The flexibility matrix now looks like

$$\begin{pmatrix} \delta_x \\ \delta_y \\ \delta_z \\ \phi_x \\ \phi_y \\ \phi_z \end{pmatrix} = \begin{pmatrix} - & - & S_{13} & S_{14} & S_{15} & S_{16} \\ - & - & S_{23} & S_{24} & S_{25} & S_{26} \\ S_{31} & S_{32} & S_{33} & S_{34} & S_{35} & S_{36} \\ S_{41} & S_{42} & S_{43} & S_{44} & S_{45} & S_{46} \\ S_{51} & S_{52} & S_{53} & S_{54} & S_{55} & S_{56} \\ S_{61} & S_{62} & S_{63} & S_{64} & S_{65} & S_{66} \end{pmatrix} \begin{pmatrix} F_x \\ F_y \\ F_z \\ M_x \\ M_y \\ M_z \end{pmatrix} \qquad (2.27.b)$$

The flexibilities in the shear directions are a little more complicated, but can be determined because the flexibility is a measure of the overall deflection of a section due to a load case. This means that the shear flexibility of the section can be calculated from the *mean slope* of either face of the section (calculated using a least square fit method using all the nodes). Note that since it is possible for the deformed shape to vary across the width of section, the results from *all* nodes must be considered. The flexibility matrix is now fully populated as

$$\begin{pmatrix} \delta_x \\ \delta_y \\ \delta_z \\ \phi_x \\ \phi_y \\ \phi_z \end{pmatrix} = \begin{pmatrix} S_{11} & S_{12} & S_{13} & S_{14} & S_{15} & S_{16} \\ S_{21} & S_{22} & S_{23} & S_{24} & S_{25} & S_{26} \\ S_{31} & S_{32} & S_{33} & S_{34} & S_{35} & S_{36} \\ S_{41} & S_{42} & S_{43} & S_{44} & S_{45} & S_{46} \\ S_{51} & S_{52} & S_{53} & S_{54} & S_{55} & S_{56} \\ S_{61} & S_{62} & S_{63} & S_{64} & S_{65} & S_{66} \end{pmatrix} \begin{pmatrix} F_x \\ F_y \\ F_z \\ M_x \\ M_y \\ M_z \end{pmatrix} \qquad (2.27.c)$$

The section stiffness matrix can be found by inverting the flexibility matrix, and this can be transformed to the elastic centroid (or any other section location) as described earlier.

2.4 EXPERIMENT

In the light of earlier statements about the maturity of finite element models as an analysis tool, an experimental program might be seen as unnecessary, since finite element analyses are sometimes considered to be "perfect experiments". It is not uncommon to see more trust to be placed in finite element results than in the results from a real experiment. However, any finite element model can only be as accurate as

the assumptions (such as boundary conditions and material behaviour) upon which it is based. Experimental results are therefore of critical importance to this research, since they give confidence that the finite element model is actually modelling the real life situation, and are thus used to validate the finite element approach adopted herein.

Where experimental results are already well published elsewhere, further experimental verification has been regarded as unnecessary, and indeed it has been our opinion that this would only distract from the analytical modelling and finite element optimisation work that is the main focus of this project. In such cases the models used have been verified against existing experimental results.

By contrast, when optimising the cross-sectional properties of a typical blade section (and also when investigating the phenomenon of K_{45} coupling) much less suitable experimental data is available in the literature, so tests were performed to verify the finite element models used, which were in turn used to verify the analytical work.

Monterro and Appleby [44] undertook a final year undergraduate project at the University of Bristol to determine the cross-sectional properties of several prismatic sections using a combination of deflection and strain gauge data. For the cross-sectional properties examined in the experimental section of this thesis, all the required data can be obtained from deflection results, considerably simplifying the experimental procedure. Their results generally compared well with their FE predictions, although their torsion results compared poorly with their FE model.

Rehfield *et al* [45] perform a four point bending test using a "sling supported method" to measure the camber produced in a tailored box beam under bending. Unfortunately, the use of such an experimental set up would make it difficult to apply or measure the torsion force (M_{xy}) required to prevent twisting of the section.

Diamond [46] predicted and measured the bending, torsion, and bending-torsion coupling of eight laminated composite beams manufactured by DERA. As part of the industrial collaboration for this project, these beams were made available for testing at the University of Bristol and Diamond's work is therefore referenced extensively in

Chapter 5 of this thesis. Diamond clamped each test specimen at one end and based his subsequent calculations on a linearly varying bending moment.

2.5 OPTIMISATION

2.5.1 Introduction and basics

As with classical laminate theory earlier, the processes and techniques of optimisation are so fundamental to this project that the inclusion of some general background is justified here.

The general formulation of an optimisation problem is:

Minimise $f(x)$

Such that $g_j(x) \geq 0\,, \quad j = 1\,, \ldots\,, n_g$

$h_k(x) = 0\,, \quad k = 1\,, \ldots\,, n_e$

The function $f(x)$ is called the objective function. Although the standard formulation requires $f(x)$ to be minimised, it is quite acceptable to minimise $-f(x)$ if the largest value of $f(x)$ is desired.

For some problems, it might be desirable to minimise more than one objective function. Optimisation for multiple objective functions is usually complex (or at least computationally expensive) and is generally avoided either by generating a single composite objective function that replaces the other objectives (Edgeworth-Pareto optimality criteria), or by selecting the most important objective function and placing constraints on the others.

2.5.2 Classification of optimisation problems and solution algorithms

Parks [47] characterises optimisation problems according to Table 2.1.

Characteristic	Property	Classification
Number of design variables	One	Univariate
	More than one	Multivariate
Type of design variables	Continuous real numbers	Continuous
	Discrete or integer values	Discrete
	Continuous and discrete values	Mixed integer
Problem functions	Linear functions of design variables	Linear
	Quadratic functions of design variables	Quadratic
	Non-linear functions of design variables	Non-linear
Problem formulation	Subject to constraints	Constrained
	Not subject to constraints	Unconstrained

Table 2.1 Classification of optimisation problems

Numerous attempts have been made to classify optimisation methods.

Parks [47] defines two basic classes of optimisation method

1. *Optimality criteria* are based on analytical methods and require that the objective function and constraints are known explicitly in terms of the design variables. Once the conditions for an optimum solution are established, either a candidate solution is tested to see if it meets the conditions, or the equations are solved analytically to determine the optimum solution.

2. *Search methods* are typically used when (1) the number of variables and constraints is large, (2) the problem functions are highly non-linear or (3) the problem functions are implicit in terms of the design variables.

Hajela [48] subdivides *search methods* into two categories

1. *Deterministic searches* are based on numerical methods and are used recursively to converge to an optimal solution.

2. *Stochastic searches* use sampling as a tool to guide the search in a manner that is considerably more efficient than random sampling.

Levin [49] splits optimisation algorithms into zeroth, first and second order categories, depending on the gradient information that is required of the objective function.

Haftka and Gurdal [17] illustrate many different optimisation methods without presenting a classification system.

The various attempts at classification referenced above are summarised by Table 2.2. Note that there is some tautology in the terms presented above, since many combinations of solution algorithm in the above table are not possible.

For example, stochastic methods are exclusively zeroth order, and deterministic methods are thus first order or higher. Most deterministic methods are linear methods - that is they treat the problem as linear about the current design point for the purpose of obtaining the next design point, and do not consider non-linear effects such as interaction between design variables. However, linear methods do implicitly recognise the non-linearity of the problem by recursively calling the method (in either a sequential or an iterative manner) to arrive at a solution.

Characteristic	Property	Classification
Type of approach	Equations that govern the behaviour of the system are known explicitly, and a direct solution to the problem is obtained	Analytical
	Governing equations are not know explicitly, and the solution must be obtained by "searching" the design space	Experimental
Method of searching	Probabilistic search is based on how the current design point compares to other design points	Stochastic
	Search direction is determined solely by the nature of the design space at the current design point	Deterministic
Problem function	Objective is assumed to be an approximately linear function of the design variables	Linear
	Objective may be a highly non-linear function of design variables	Non-linear
Order of method	The search requires no information other than the value of the objective function at the design point	Zeroth
	The search uses the derivative of the objective function (i.e. gradient) to determine the search direction	First
	The search uses higher order derivatives of the objective function to determine the search direction	Higher
Progress towards solution	The search moves step by step towards the solution until no further improvement is made	Sequential
	The search moves to an approximate solution and then repeats the process to improve the approximation.	Iterative

Table 2.2 Classification of solution algorithms

Based on the table above, it may be helpful to consider the classification of common experimental optimisation algorithms in terms of the hierarchical structure shown in Figure 2.8, below.

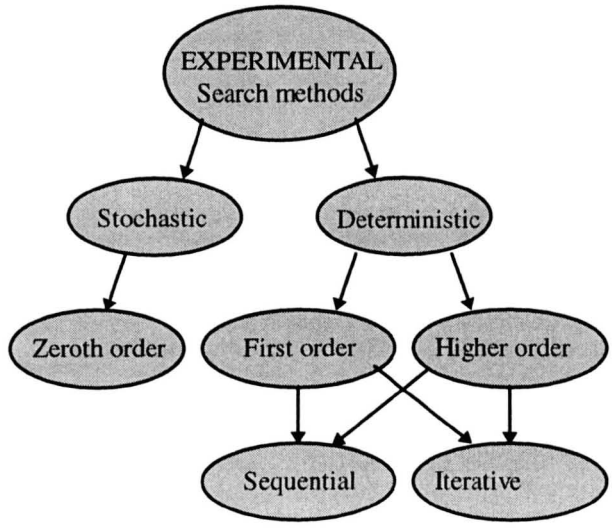

Figure 2.8 Hierarchical classifications of common optimisation methods

Given the variety of backgrounds that independently use optimisation techniques to varying degrees of rigour (e.g. academia, industry, or indeed anyone that creates or improves upon a design), it is perhaps not surprising that the classifications above have not been universally adopted. However, the terminology presented above will be used throughout this thesis. It is more surprising to note that no formal procedure exists for selecting the most efficient solution method for a given optimisation problem.

2.5.3 Visualisation of an optimisation problem

In visualising the process of trying to minimise the objective function, it is a helpful analogy to think of a two-dimensional optimisation problem - trying to find the lowest point (minimum value of objective function) on a section of landscape (representing the two dimensional N-S, E-W design space). This problem would be classified as a constrained, continuous, multivariate, non-linear problem. The maps below show contour lines that join points of equal elevation.

The landscape might look like Figure 2.9

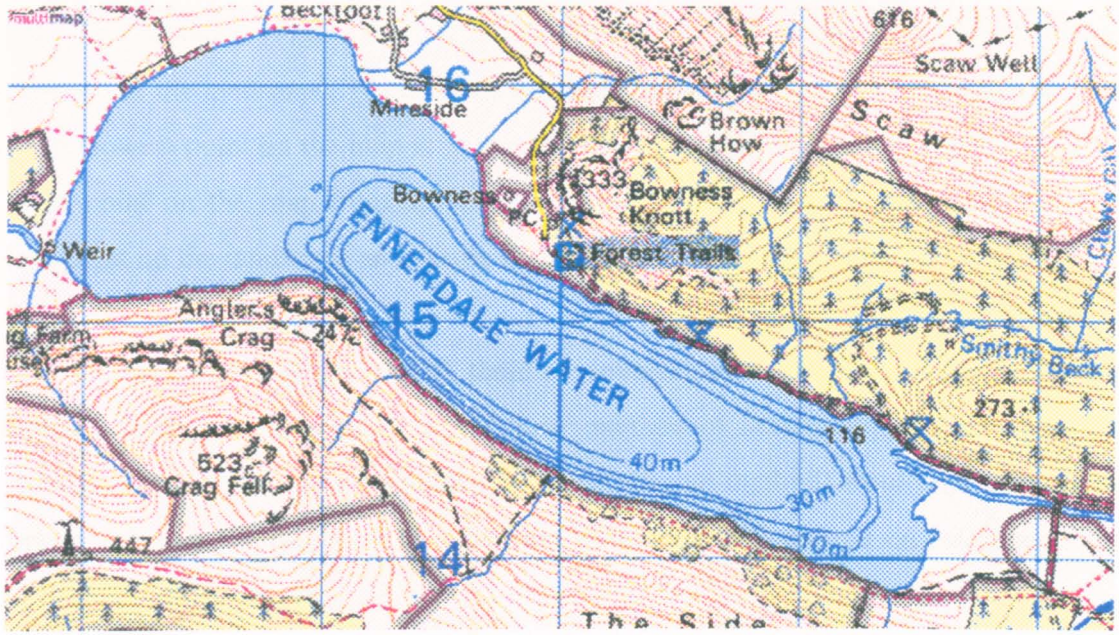

Figure 2.9 Elevation as an objective function of N-S, E-W grid position

or might look like Figure 2.10

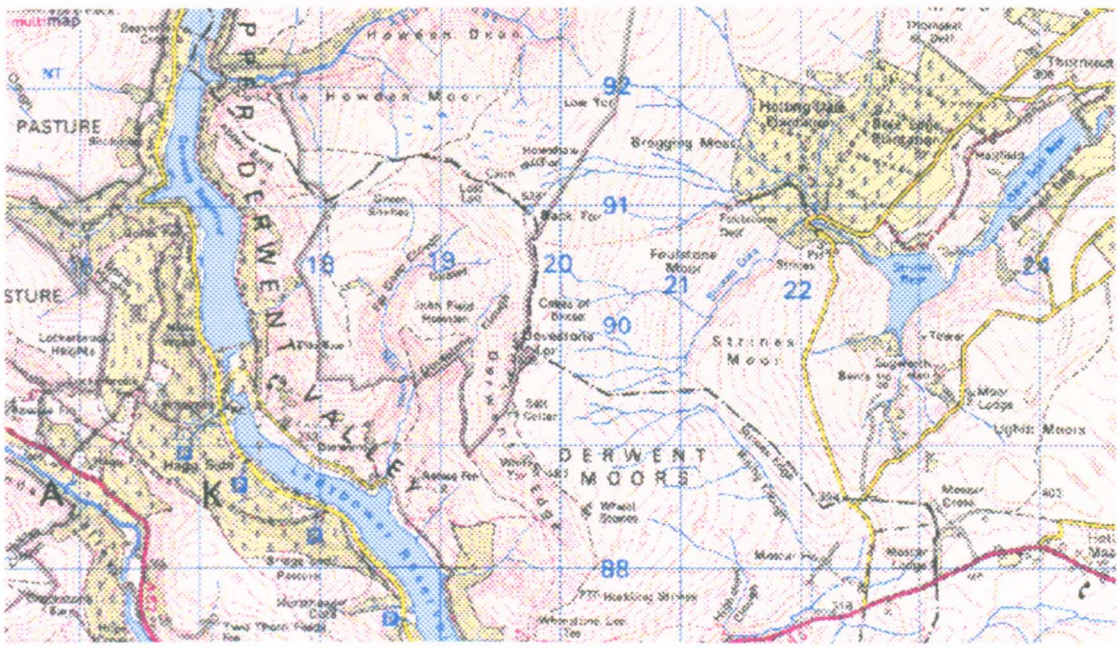

Figure 2.10 Elevation as an objective function of N-S, E-W grid position

Remember that in optimisation, no readymade map of the design space is available!

In the first instance (Figure 2.9), it is relatively easy to find the lowest point (*global optimum*) of the landscape. Water flows downhill into the lake, and it can easily be seen that the lowest point on the map is in the middle of the lake. It would be easy to find the lowest point on the map from an "experimental" point of view by dropping water at some point on the landscape and seeing that it collects at the lowest point.

In the second instance (Figure 2.10), there are several points where water collects (*local minima*), and the experimental "water flow" method of determining the lowest point used above (basically a type of sequential linear descent method) would not necessarily work in this case, as the point to which the water runs will depend on catchment area into which it initially falls.

Note that an objective function does not have to be a function of two variables - it may be a function of any number of variables, although obviously it is more difficult to clearly represent (and visualise) the variation of objective function over a design space of three (or more) dimensions.

2.5.4 Important concepts used in optimisation

Before moving on to consider some techniques applied to optimisation problems (section 2.5.5) and potentially suitable optimisation algorithms that may be used (section 2.5.6), it is necessary to understand some of the fundamental concepts upon which they are based, since such understanding is useful in selecting an appropriate solution algorithm and essential if modifying for a particular problem.

2.5.4.1 Convexity

Convexity has significant implications for the solution approaches that may be used. The term is also used in subtly different contexts, so it is therefore worth taking the time to understand this concept properly.

Convexity can be expressed mathematically as follows.

Define a function of x, $f(x)$. The **function is convex** over the range $x_1 < x < x_2$ provided that

$$\alpha x_2 + (1-\alpha)x_1 \leq \alpha f(x_2) + (1-\alpha) f(x_1) \qquad (2.28)$$

for $0 < \alpha < 1$

This is more easily understood pictorially. Figure 2.11 shows a univariate function, $f(x)$ where $f''(x) > 0$. It can be shown that an objective function is convex if its matrix of second derivatives (called the *Hessian* matrix) is positive semi-definite (i.e. that the determinants of the Hessian and all sub-matrices are positive) .

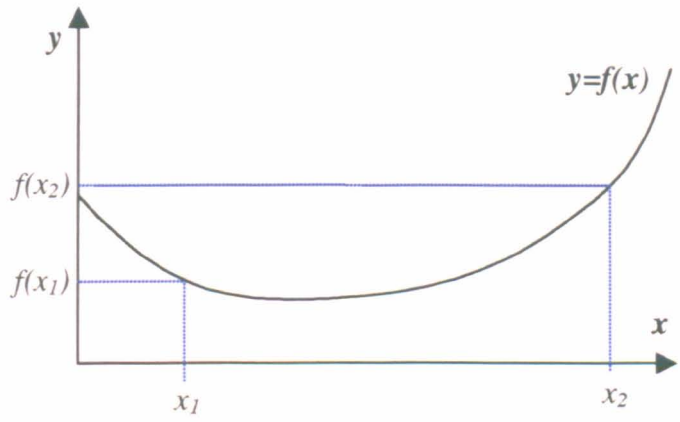

Figure 2.11 Illustration of a convex objective function, $f(x)$

A slightly different meaning applies when referring to a convex design space. The **design space is convex** if the line joining any (and every) two points that lie within the feasible area also lies entirely within the feasible area. This is illustrated by the two points s_1 and s_2 in Figure 2.12 below.

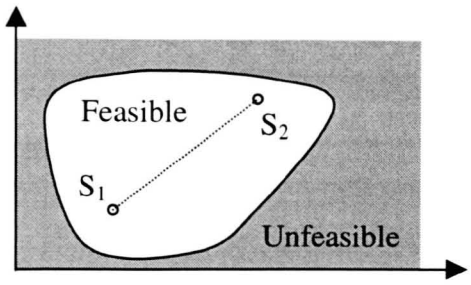

Figure 2.12 Illustration of convex design space

If a problem is convex, the Kuhn-Tucker conditions are not only necessary but also sufficient for a global minimum. A convex problem is defined as one having a convex objective function and a convex feasible domain. It has only one minimum and the Kuhn-Tucker conditions are therefore sufficient to establish it.

2.5.4.2 The Kuhn-Tucker conditions

The Lagrangian function is defined as

$$L(\mathbf{x},\boldsymbol{\lambda}) = f(\mathbf{x}) - \sum_{j=1}^{n_e} \lambda_j h_j(\mathbf{x}) \qquad (2.29)$$

The necessary conditions for a stationary point are

$$\frac{\partial L}{\partial x_i} = \frac{\partial f}{\partial x_i} - \sum_{j=1}^{n_e} \lambda_j \frac{\partial h_j}{\partial x_i} = 0 \quad , \quad i = 1,\ldots,n_e \qquad (2.30.a)$$

$$\frac{\partial L}{\partial \lambda_j} = h_j(\mathbf{x}) = 0 \quad , \quad j = 1,\ldots,n_e \qquad (2.30.b)$$

The above is only valid for a regular point – when inequality constraints are present, the inequality constraints are converted to equality constraints

$$g_j(\mathbf{x}) - t_j^2 = 0 \qquad (2.31.a)$$

$$L(\mathbf{x},\mathbf{t},\boldsymbol{\lambda}) = f - \sum_{j=1}^{n_g} \lambda_j (g_j - t_j^2) \tag{2.31.b}$$

Differentiating with respect to x, λ and t gives

$$\frac{\partial L}{\partial x_i} = \frac{\partial f}{\partial x_i} - \sum_{j=1}^{n_g} \lambda_j \frac{\partial g_j}{\partial x_i} = 0 \tag{2.32.a}$$

$$\frac{\partial L}{\partial \lambda_j} = -g_j + t_j^2 = 0 \tag{2.32.b}$$

$$\frac{\partial L}{\partial t_j} = 2\lambda_j t_j = 0 \tag{2.32.c}$$

The Kuhn-Tucker conditions are summarised by Haftka and Gurdal [17] that a point **x** is a local minimum of an inequality constrained problem only if a set of non-negative λ_j's can be found such that

1. $\partial L/\partial x_i = 0$
2. The corresponding λ_j is zero if a constraint is not active.

This can be interpreted geometrically, as illustrated by Figure 2.13 below.

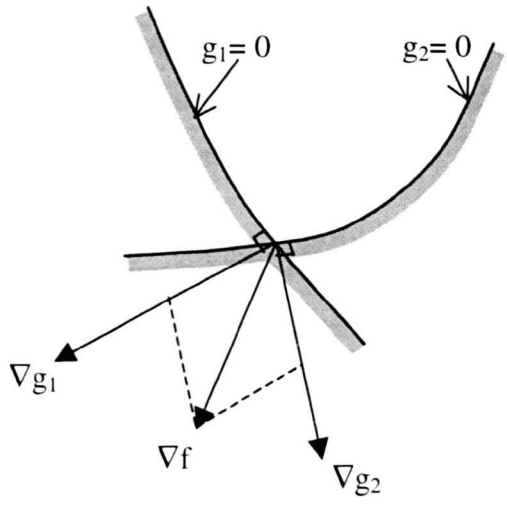

$$\frac{\partial f}{\partial x_i} = \sum_{j=1}^{n_g} \lambda_j \frac{\partial g_j}{\partial x_i}$$

Figure 2.13 Geometric interpretation of the Kuhn-Tucker conditions

If the Kuhn-Tucker conditions are satisfied, the point is a minimum. This only guarantees a local minimum - the Kuhn-Tucker conditions are only sufficient to define a global minimum if the problem can also be shown to be *convex*.

Although most optimisation problems encountered in practice cannot be shown to be convex, we can approximate most problems by a series of convex (e.g. linear) approximations. There is only one minimum to the approximate problem, and linear programming techniques can be used to rapidly converge on the optimum.

2.5.5 Techniques used in optimisation

2.5.5.1 Response surface approximation

Where a deterministic search method is being used, it is necessary to determine the direction in which to perturb the current design in order to obtain a better design. This requires some level of knowledge about how the objective function responds to the design variables. Since it is rare to have a closed form expression for the objective function in terms of the design variables, whatever method is being used must construct some sort of approximation to the objective function.

Conceptually, there are many possible methods of constructing such an approximation, but the most important distinction is to be made between a *global* approximation (used over the entire design space) and *local* approximations (each used over only a small region of the design space).

Schmit and Farshi [50] propose a method called *sequential approximate optimisation*, in which a number of points in the design space are analysed and a polynomial surface fitted through these points. Any appropriate optimisation algorithm can then be applied to solving the problem represented by this polynomial approximation. An in-depth prior knowledge of the problem may be required to determine the order of polynomial required to accurately model the global surface.

Obtaining global approximations becomes very costly as the number of design variables and/or the non-linearity of the problem increases. Roux *et al* [51] state that "finding an accurate global approximation is challenging, and sufficient accuracy could only be achieved ... by considering a smaller region of the design space." It is therefore common to use local approximations which are usually (but not necessarily) linear, based on derivatives of the objective function and constraints with respect to the design variables.

This approach is the basis for the method of sequential linear programming that is discussed later. Because such approximations are only useful in the neighbourhood of the initial design, it is necessary to impose *move limits* on the magnitudes of changes in the design that are permitted. Following an optimisation based on approximate analysis and move limits, an exact analysis is performed at the design point and new derivatives are calculated so that a new approximation for objective function and constraints can be constructed. This process is repeated until convergence is achieved.

The standard linear approximation is derived from the Taylor series.

$$f(x) = f(x_0) + (x - x_0) f'(x_0) \tag{2.33}$$

For highly non-linear functions, this approximation is often inaccurate even when x is relatively close to x_0. Accuracy could be improved by retaining higher order terms in the Taylor series as shown in the quadratic example below

$$f(x) = f(x_0) + (x - x_0) f'(x_0) + \frac{1}{2}(x - x_0)^2 f''(x_0) \tag{2.34}$$

however, this requires computationally expensive calculation of higher order derivatives, which rather defeats the object of reducing the computational cost.

Roux *et al* [51] concluded that the use of intervening variables can improve the accuracy of the linear approximation. That is, define $y_i = y_i(x)$ such that the linear approximation

$$f(y) = f(y_0) + (y - y_0) f'(y_0) \qquad (2.35)$$

gives better accuracy over the desired range. This has clearly been known since at least the mid-1970's, when Storaasli and Sobieszczanski [52], and Noor and Lowder [53] both found that the reciprocal approximation (i.e. $y_i = 1/x_i$) typically made constraints behave more linearly in structure resizing and reanalysis. Similarly, Vanderplaats and Salajegheh [54] found that forces approximate better than stresses i.e. a linear approximation of element forces followed by an exact calculation of stresses is more accurate than a linear approximation of the stresses.

Since the variation of the function, f will differ each of the design variables, sensitivity analysis (discussed next) is used to determine the size of the region over which the approximation is valid and hence the move limits imposed in each variable.

2.5.5.2 Sensitivity analysis

If a local approximating function (typically linear) is used to model a highly non-linear objective function (a common occurrence), the approximation is only valid over a small region. When using such approximations, move limits are imposed to prevent the design straying to a region where the approximations are no longer valid. If the move limits are too large, the approximation will be poor and the solution may be non-optimal. Conversely, if the move limits are small and the initial design point is some distance away from the optimum, an unnecessarily large number of iterations will be required for the solution to reach the optimum.

An appropriate size of move limit can be determined by *sensitivity analysis*. Although there are many approaches to sensitivity analysis, these usually require the partial first and second derivatives of the objective function and constraints (if appropriate).

If these functions are known explicitly in terms of the design variables, sensitivity derivatives may be calculated analytically. Since this is rare in problems where finite element models are employed, they are usually calculated by the finite difference

method (discussed next). Obtaining these derivatives is usually the greatest computational expense in an optimisation cycle.

2.5.5.3 The finite difference method

The most commonly used method of obtaining derivative information for an assumed-linear objective function is to use the finite difference method. It is very easy to program, but can be computationally expensive to use - especially if functions have large numbers of design variables and complex analyses.

Consider the curve $y = x^2$, shown in Figure 2.14.

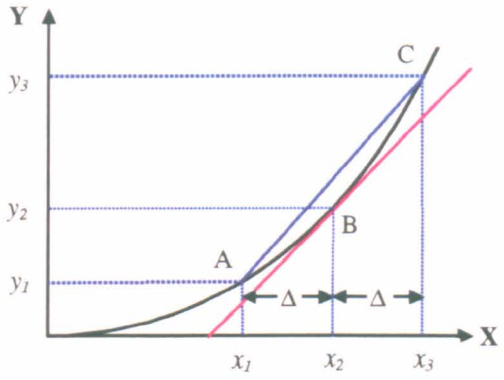

Figure 2.14 Gradient of a curve using finite differences

The gradient (m) of the blue line joining points A and C is easily calculated from the differences between the y-values and x-values of these two points, using

$$m = \frac{y_3 - y_1}{x_3 - x_1} = \frac{y_3 - y_1}{2\Delta} \qquad (2.36.a)$$

As Δ becomes increasingly small, and the gradient of the blue line becomes an increasingly good approximation of the tangent to the curve at x_2. This *centred finite difference method* thus approximates the gradient of the objective at the current design point (x_2) by dividing the difference of the values of objective function (y_1 and y_3) by the difference in value of nearby design points (x_1 and x_3) i.e.

$$\left(\frac{dy}{dx}\right)_B \approx \frac{y_3 - y_1}{x_3 - x_1} \qquad (2.36.b)$$

The calculation of all the (first order) derivatives of an objective function via the centred finite difference method requires $2N+1$ analyses, where N is the number of design variables.

Note that it is also possible to approximate the gradient at point B using

$$\left(\frac{dy}{dx}\right)_B \approx \frac{y_3 - y_2}{x_3 - x_2} \qquad (2.36.c)$$

Although the accuracy of the approximation will be less good than the centred finite difference method, the calculation of all the (first order) derivatives of an objective function via *(2.36.c)* requires only $N+1$ analyses. Provided the value of Δ is sufficiently small, it is usually preferable in optimisation to use equation *(2.36.c)* to determine approximate gradients, since it saves considerable computational expense.

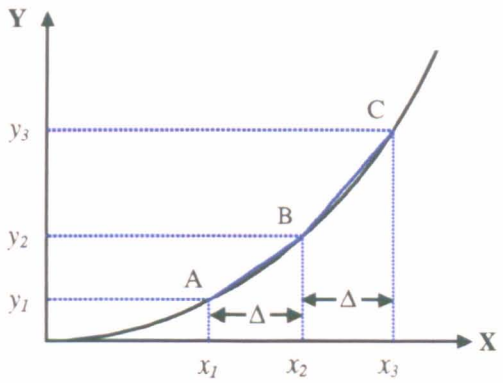

Figure 2.15 Second derivative of the curve using finite differences

For second order derivatives, finite difference principles are applied to give the second order derivative at point B as

$$\left(\frac{d^2y}{dx^2}\right)_B = \frac{y_3 - 2y_2 + y_1}{\Delta^2} \qquad (2.36.d)$$

which requires $2N+1$ analyses to obtain all the second order derivatives for an objective function of N design variables.

2.5.5.4 Penalty functions

Penalty functions are not optimisation methods in themselves, but rather a means of dealing with constraints in optimisation without actually having to use separate constraint equations. This is done by adding a penalty function to the original objective function, which penalises points outside the feasible region. The penalty associated with an infeasible solution will make such solutions unattractive. In this manner, the use of penalty functions turns a constrained problem into an unconstrained problem.

Exterior penalty functions

Since exterior penalty functions allow the search to move outside of the feasible region, the key to successful implementation of the exterior penalty function approach lies in setting the magnitude of the penalty function at an appropriate level. If the penalty function is too small, an infeasible solution may still be more attractive than the feasible optimum, whereas if the penalty function is too large, the search may produce ill-conditioned gradients and Hessians for deterministic search methods.

A common exterior penalty function defines the new objective, q as

$$q(\mathbf{x}, p) = f(\mathbf{x}) + p\sum_{i=1}^{m}(\max[0, g_i(\mathbf{x})])^2 \tag{2.37}$$

where m is the number of constraints. The value of the penalty parameter, p is usually determined by trial and error.

Interior Penalty Functions

Interior functions do not allow the search to proceed into the infeasible region. They achieve this by adding to the objective function a weighted sum of continuous functions

with a positive singularity at the boundary of the feasible region. This means that the new objective function is infinite along the edge of the feasible region, but also means that barrier functions cannot be used for equality constraints, or where the feasible region is disjoint.

Two common interior penalty functions are

- the *inverse barrier function*, where q is defined as

$$q(\mathbf{x}, r) = f(\mathbf{x}) - \frac{1}{r}\sum_{i=1}^{m}\frac{1}{g_i(\mathbf{x})} \qquad (2.38.a)$$

- the *logarithmic barrier function*, where q is defined as

$$q(\mathbf{x}, r) = f(\mathbf{x}) - \frac{1}{r}\sum_{i=1}^{m}\ln[-g_i(\mathbf{x})] \qquad (2.38.b)$$

As with exterior penalty functions, the value of the barrier parameter, r must be set to an appropriate value, which is usually determined by trial and error.

Comparison of interior and exterior penalty functions

Table 2.3 below compares the behaviour of interior and exterior penalty functions.

Interior Penalty Functions	Exterior Penalty Functions
Handles inequalities only	Handles equalities or inequalities
Starting point in feasible set	Arbitrary starting point
Only feasible iterates	Can iterate through infeasible region
Always yields feasible answer	Can get stuck in infeasible region

Table 2.3 Comparison of Interior and Exterior Penalty Functions

Notwithstanding the above, a suitable exterior penalty function can be useful to model a "guideline" (as opposed to a rigid constraint), which may be violated if the result is an improvement in overall objective function. Conversely, interior penalty functions do not allow the constraints to be violated in any way.

2.5.5.5 Discrete Variables

Many problems use design variables that can only take discrete values, for example the ply thickness in a CRFP laminate. Somewhat counter-intuitively, solving a discrete problem is usually harder than solving a continuous problem.

Thanedar and Vanderplaats [55] surveyed available methods for discrete variable structural optimisation, looking at three categories of methods – branch and bound, approximations using branch and bound and *ad-hoc* methods (such as simulated annealing and genetic algorithms).

Branch and Bound method

The branch and bound method begins with a continuous variable optimisation, which provides both an initial starting point for the discrete problem, and a lower bound on the solution. From this point, a single variable is selected and continuous optimisations are performed on the other variables. The value of the chosen (discretised) variable is changed until no further improvements can be found. The discretised variable is then allowed to vary subject to its currently imposed bound and the process is repeated for the next discrete variable. This process is repeated until all the discrete variables have been examined. The disadvantage of this method is that large number of non-linear optimisation tasks must be performed to locate the discrete optimum, and that the problem must be convex to guarantee optimality.

Sequential linear approximation

Olsen and Vanderplaats [56] have presented a numerical method based around an SLP approach that is suitable for the solution of non-linear discrete optimisation problems.

They demonstrated its suitability by solving several standard optimisation problems. The first stage is to linearise the problem about a design point $\mathbf{x}_0 = (x_1, x_2, \ldots, x_n)$ using a first order Taylor expansion. Each design variable, x_i can take on one of several discrete values $(d_{i1}, d_{i2}, \ldots, d_{iq})$, so we define x_i as

$$x_i = z_{i1}d_{i1} + z_{i2}d_{i2} + \ldots + z_{iq}d_{iq} \qquad (2.39)$$

where

$$\sum_{j=1}^{q} z_{ij} = 1$$

$$z_{ij} = 0 \text{ or } 1 \qquad (2.39.a\text{-}b)$$

The linearisation point $\mathbf{x}_0$ needs to be chosen. It is assumed that the discrete optimum lies near the continuous optimum, and thus this point is used for the initial value of $\mathbf{x}_0$. The design variables x_i are now rounded (in a direction away from constraint violation) to provide an initially feasible discrete solution. For all future linearisations, the result of the preceding approximate optimisation is used for $\mathbf{x}_0$.

In line with the assumption that the discrete optimum lies near the continuous one, the search is also narrowed to include only those values of discrete possibilities close to $\mathbf{x}_0$. This can significantly reduce the size of the approximate problem and hence improve overall efficiency.

Ad-hoc methods

Simulated annealing and genetic algorithms are both capable of dealing with discrete variables. When Thanedar and Vanderplaats' survey [55] was published in 1995, simulated annealing and genetic algorithms were "comparatively new insofar as their application to discrete structural design problems is concerned", although when Vanderplaats [57] later reviewed the status and direction of structural design optimisation, the use of these stochastic methods had become much more widespread. Since these approaches are complete solution methods in their own right, their application and the theory behind them is discussed in the next section.

2.5.6 Examples of experimental optimisation algorithms

Optimisation algorithms are the processes that are applied to solve optimisation problems. The choice of algorithm used will have significant implications for how efficiently an optimisation problem can be solved, or even if it can be solved at all.

Optimisation algorithms can be divided into two main categories: **stochastic** and **deterministic**.

2.5.6.1 Stochastic algorithms

Stochastic algorithms (of which simulated annealing and genetic algorithms are examples) are robust at finding an optimum solution (or family of solutions) from a large and non-convex design space. All purely stochastic algorithms are "zeroth order" methods. That is to say that they do not take any information about the gradient (or higher order derivatives) of the objective function - they simply analyse samples of the whole design space and direct the search towards the regions where the best results are returned. As a result, stochastic algorithms require many analyses to reliably find a good solution.

Despite the large number of analyses required for a reliable convergence, the rate of growth is less than linear. Thus, while a simple problem may be more efficiently solved by other methods, simulated annealing and genetic algorithms become progressively more attractive as the size of the problem increases. This is illustrated in the following table by Lombardi's results [58] for the problem of maximising buckling load of a composite laminate using simulated annealing.

Number of plies	Number of different possible designs	Approximate number of iterations for high reliability of convergence
32	6561	1000
64	43046721	3000

Table 2.4 Less than linear increase of iterations to convergence with design space size for simulated annealing

It should be pointed out that Lombardi's problem is relatively simple compared to many real-life problems, both in terms of the size of the design space and the relative simplicity with which the objective can be calculated. For optimisation problems where the objective function is expensive to evaluate (such as a large finite element model), the large number of evaluations required (for even a small problem) can be prohibitive for current computing technology.

Although stochastic methods do not guarantee that an optimum (either global or local) has been found, it is usual that many near-optimal solutions are obtained once the algorithm has converged. Obtaining a number of near-optimal solutions might be advantageous in some design problems.

Simulated annealing

The simulated annealing algorithm is based on the Metropolis algorithm as proposed by Metropolis *et al.* in 1953 [59] to model the annealing of metals in physical chemistry. The simulated annealing algorithm is so called precisely because of this physical analogy.

At a given temperature, T, the algorithm perturbs the design variables randomly and computes the new objective function to be minimised. If the objective function is lower than (i.e. an improvement upon) the initial objective function, then the new design point is accepted. If the objective is higher, the new state is accepted or rejected based upon a random probabilistic decision, the probability of acceptance being defined as

$$P(\Delta f) = e^{(\frac{-\Delta f}{k_b T})} \tag{2.40}$$

Where k_B is the Boltzmann constant and T is the system "temperature". If the temperature is high, the probability of acceptance is close to one; if low, the probability of acceptance is small. At each temperature, the design point is varied until a steady state energy level is reached, at which point the temperature is reduced and the process is begun again. The process continues until the minimum objective function is obtained.

The performance of the simulated annealing algorithm is highly dependent upon the initial temperature, T_0 and the rate of cooling. The value of T_0 must be high enough to permit virtually all moves in the design space to be acceptable, so that an almost random search is performed.

Once T_0 is set, the cooling rate must be set to an appropriate value that will allow the solution to escape from a local minimum. One popular method is a constant cooling update

$$T_{k+1} = \alpha T_k \quad , \quad k = 0,1,2,...,K \tag{2.41}$$

Another approach is that of Nahar [60], who suggests fixing the above number of decrement steps, K, and determines the values of T_k experimentally. Alternatively, it is possible simply to divide the interval $[0,T_0]$ into a fixed number, K, of equally spaced steps. Although a simulated annealing process only returns a single design, there are usually only small changes over the final temperature decrements. It is a straightforward process to archive these final few design points and thus obtain a number of near optimal solutions.

Genetic algorithms

As simulated annealing is analogous to a physical process in the metallurgical world, the genetic algorithm is analogous to evolutionary theory based on the biological laws of genetics and evolution of species according to Darwin's theory of natural selection. Genetic algorithms were developed by Holland [61] and are of particular use as robust multivariable search algorithms where there may be strong interactions between different design variables.

The design variable $\mathbf{x_0}$ must be represented as a binary string - analogous to a chromosome. The algorithm begins with a randomly chosen set of design points – analogous to a population each with one chromosome. The objective function of each of these points is evaluated and the design points are copied to form a new set. The copying process is biased so that the probability of being copied is higher for those points with good objective functions – analogous to survival of the fittest. In the new population, members are paired off randomly for crossover, where part of the design string is swapped – analogous to reproduction. Occasionally, a string location is selected at random and its binary value is changed – analogous to mutation.

Because every design variable must be represented as a binary string, genetic algorithms lend themselves particularly well to discrete valued problems. Genetic algorithms also inherently give a give a population of several near-optimal designs (rather than just a single optimum) so eliminating the need for an archiving process.

2.5.6.2 Deterministic algorithms

Deterministic algorithms consider the nature of the design space immediately surrounding the current design point and seek to improve upon the design by moving in the direction that gives the most rapid improvement. On a linear level, this approach simulates water running downhill, and finds a minimum with considerably fewer analyses than a stochastic method. A converged deterministic search guarantees that a minimum has been reached, but only guarantees that this is a global optimum if the

design space is convex. In non-convex problems, there *may* be local minima that are considerably sub-optimal (as illustrated earlier by Figure 2.10).

Simplex method

The Simplex method was first applied to the problem of function minimisation by Nelder and Mead [62] in 1965. For a linear optimisation problem, this is a computationally efficient matrix method of minimising an objective. However, this requires that the objective is both linear and known explicitly in terms of the design variables. Unfortunately, for real-world structural design problems, the objective is seldom known explicitly in terms of the design variables and can only be approximated as linear for small changes in design variables.

Steepest Descent Method

The steepest descent method was devised by Cauchy in 1847. Starting from an initial point, x_0, it involves evaluating the gradient vector, $\mathbf{g}(\mathbf{x}) = \nabla f(\mathbf{x})$, and then searching in the direction of steepest descent to minimise the objective function in that direction. If the objective function is not explicitly known in terms of the design variables, the gradient information is usually obtained from the finite difference method. The process of minimising in the direction of steepest descent is repeated until convergence is achieved.

Because the objective function is minimised along each particular search direction, each successive search direction is orthogonal to the previous one. Although the approach is intuitive, the rate of convergence is actually rather slow and additionally requires that the problem be convex in order to guarantee convergence to the global minimum.

Sequential Linear Programming (SLP)

The sequential linear program is based on a local linearisation of the optimisation problem. Much of the early work in this field is credited to Dantzig [63]. In this

approach, the standard optimisation problem is linearised by replacing the original problem with the Taylor series expansions about an initial design, x_k.

$$f(x_{k+1}) = f(x_k) + (x_{k+1} - x_k) f'(x_k) \qquad (2.42)$$

From an initial design point, the sequential linear program determines the maximum gradient of the objective function in the N-dimensional design space (which is physically interpreted as the direction of quickest improvement in the objective function). The current design is then perturbed as far as possible in that direction (i.e. until it reaches a move limit or constraint upon one of the design variables) to give a new design point.

Note that the sequential linear program recognises that a linear approximation may not be an accurate representation of the entire design space, and so limits the validity of this assumption to a small area of the design space that immediately surrounds the current design point. It does this by imposing "move limits" on each design variable, which set upper and lower bounds on the allowed change in x_k at each step. The move limits themselves are determined by any number of factors, such as the global upper and lower bounds of each design variable, the resolution of the design space, and any sensitivity information is available.

Provided the problem is sufficiently linear, and that the move limits are small enough to guarantee a good approximation within the allowable range, then the new design point will be closer to the optimum than the old one. At this new design point, the value of the objective function is re-evaluated, and the process is repeated until convergence is achieved, which indicates that an optimum has been found.

This sequential process of moving towards the optimum is illustrated graphically by the red arrows in Figure 2.16. Note that the length of the arrows remains constant – analogous to setting a fixed move limit.

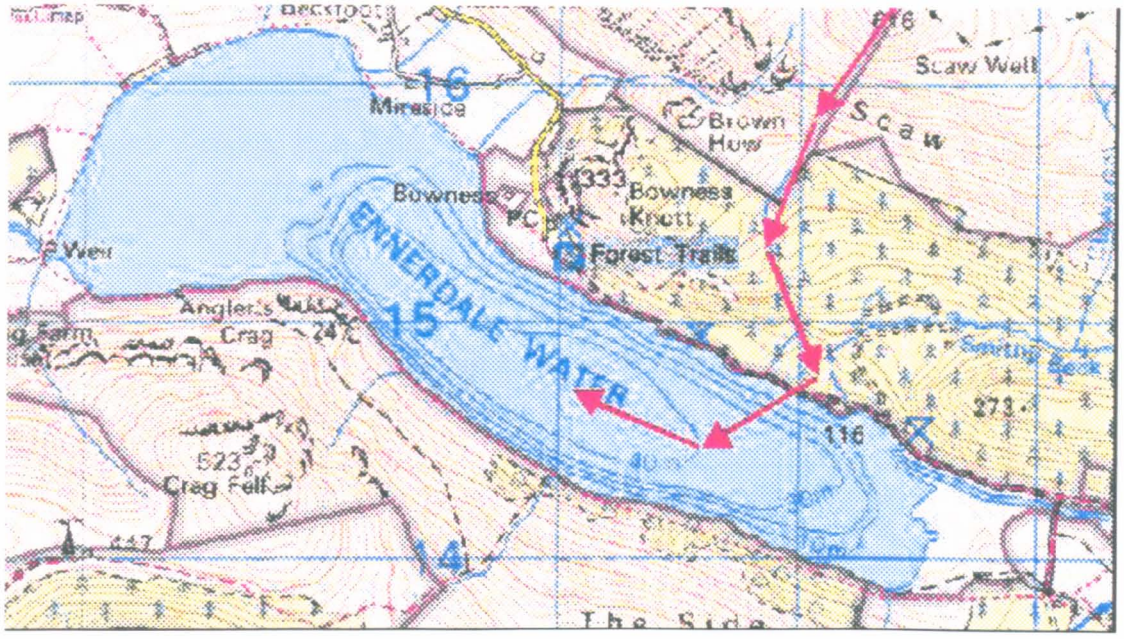

Figure 2.16 Movement of design towards optimum in a sequential linear program

Although sequential linear programs require the problem to be convex to guarantee convergence to a global minimum and converge less quickly than other methods, they remain popular optimisation tools due to the simplicity of implementation.

Newton's method

Newton's method is a second order iterative linear method. As with other deterministic methods, the derivative information is usually obtained from the finite difference method if the objective function is not known explicitly in terms of the design variables.

If terms of order greater than two are ignored, and the value of $f(x)$ is known at point x_k, then the value of $f(x_{k+1})$ is approximated by the Taylor expansion as

$$f(x_{k+1}) = f(x_k) + (x_{k+1}-x_k) f'(x_k) + \tfrac{1}{2} (x_{k+1}-x_k)^2 f''(x_k) \qquad (2.43)$$

Differentiate with respect to x to get

$$f'(x_{k+1}) = f'(x_k) + (x_{k+1} - x_k) f''(x_k) \qquad (2.44)$$

The minimum of $f(x)$ is located where $f'(x) = 0$. Thus if x_k is an estimate of the value that minimises $f(x)$, x_{k+1} will be a better estimate (i.e. assume $f'(x_{k+1}) = 0$) when

$$x_{k+1} = x_k - \frac{f'(x_k)}{f''(x_k)} \tag{2.45}$$

This is illustrated graphically by Figure 2.17, below.

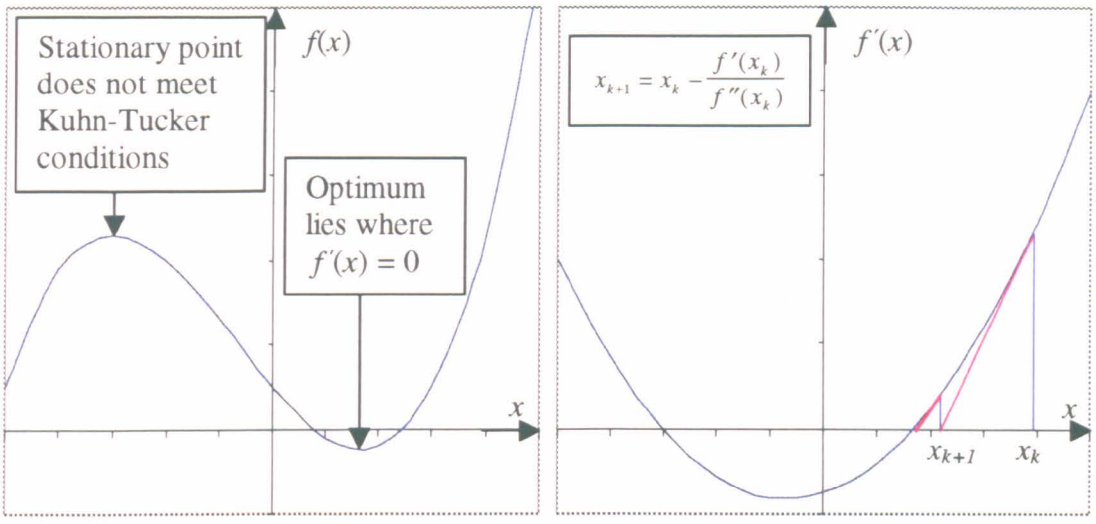

Figure 2.17 Illustration of Newton's method

The actual value of $f'(x_{k+1})$ is now evaluated. If this is acceptably close to zero, the minimum has been found. If not, the process may be iterated until suitably converged.

Although x has been treated above as a single variable, Newton's method can be equally well applied to multivariate problems and may be defined in terms of multiple design variables as

$$\underline{x_{k+1}} = \underline{x_k} + \underline{d_k} \tag{2.46}$$

where

$$\underline{d_k} = -\left[\nabla^2 f(\underline{x_k})\right]^{-1}\left[\nabla f(\underline{x_k})\right] \tag{2.47}$$

Since this is a second order method, the rate of convergence is much quicker than that for first order methods. However, the evaluation of the gradient and Hessian of $f(\underline{x})$ can be computationally expensive - especially if the design vector $\underline{x}$ is large in size and the finite difference method is used.

Global linear approximation

Surprisingly, this method has not been found in the literature, but was developed during the course of this research. It is a first order, iterative program that is based upon a global linear approximation of the design space. By recognising that it is often simpler to identify the solutions to an equation than it's stationary points, a considerable improvement in solution efficiency can be obtained for certain types of problem.

It is evident that many real-world problems do not specifically require the minimisation of an objective function - the objective function is simply an artificial construct used to objectively determine the overall fitness of a design by a single value.

One particularly relevant example of this is structural design to meet given stiffness properties. Rather than using the conventional approach, such problems can be set up in such a way that the goal is for the objective function to be zero, rather than a minimum value. This objective function is approximated as a linear function of the design variables over the whole design space. Once the N-dimensional gradient of the objective function has been determined (usually using the finite difference method) it is a simple process to calculate the exact solution to the linearised problem.

If terms of order greater than one are ignored, and the value of $f(x)$ is known at point x_k, then the value of $f(x_{k+1})$ is approximated by the Taylor expansion as

$$f(x_{k+1}) = f(x_k) + (x_{k+1} - x_k) f'(x_k) \qquad (2.48)$$

Obviously, the solution of $f(x)$ is located where $f(x) = 0$. Thus if x_k is an estimate of the value that solves $f(x)$, x_{k+1} will be a better estimate (i.e. assume $f(x_{k+1}) = 0$) when

$$x_{k+1} = x_k - \frac{f(x_k)}{f'(x_k)} \tag{2.49}$$

As with Newton's method and the sequential linear program, this method recognises that the linear approximation of the objective function may not be accurate over the entire design space. The objective function is therefore evaluated at the new design point. If the result is not sufficiently close to the optimum, then the gradient function is also re-evaluated and another iteration performed.

As before with Newton's method, this new method can be equally well applied to multivariate problems and may be defined in terms of multiple design variables.

2.5.7 Choice of solution method

It is surprising to note that, in spite of the classification of both problems and solution algorithms presented earlier, there is no formal procedure for selecting the most efficient solution algorithm for a particular problem.

Much work has been directed towards developing customised solution methods to highly specific problems. Haftka [64] presents a method of combining global approximations (typically based on a simplified theory or a coarse model) and local approximations (typically a linear model based on derivatives of the objective function at the design point). Furuya and Haftka [65] present a method that uses the genetic method to find the global region containing the optimum, and then quickly locating the local optimum in that region using deterministic methods.

Surprisingly little has been presented comparing the suitability of standard methods for different types of problem. It is argued that the vast diversity of optimisation problems makes such a task "all but impossible", although the fact that problems are routinely expressed in the standard format (described in 2.5.1) and that both problems and solutions can be classified (described in 2.5.2) appears to undermine this argument somewhat.

To produce a complete hierarchical classification of solution methods and selection tool is an undertaking which is beyond the scope of this thesis, although all choices of optimisation method used herein will be justified in terms of the characteristics of the problem being studied and the manner in which the optimisation problem is posed.

2.6 CONCLUSIONS

The overall aim of this research is the optimisation of composite helicopter rotor blades. This project is ambitious in that it seeks to solve a complex (and not necessarily convex) design optimisation problem using a computationally expensive finite element analysis routine. Given no prior knowledge of this design problem, a stochastic search algorithm would be required, which may need thousands of analyses to converge upon a near optimal solution even for a simple design problem. Given existing computing power, it is necessary to use a more efficient optimisation strategy. Considerably more efficient optimisation techniques can be employed if a problem is known to be convex, or is linear with respect to its design variables.

Analytical modelling, confirmed by appropriate finite element modelling and experimental results, gives an understanding of the underlying physics of the problem and enables the problem to be constrained to a convex design space and objective function and thus allow the use of efficient optimisation algorithms. From the broad overview provided in this chapter, the remaining chapters of this thesis go on to consider specific issues relevant to the problem of designing an anisotropic 1-dimensional beam structure:

Chapter 3 considers the simple example problem of a laminated cylindrical shell from both an analytical and a computational perspective, and addresses the optimisation and modelling issues that arise, such as how to obtain a convex design space and thus use an efficient optimisation tool. The solutions obtained for different types of problem are also discussed.

Chapter 4 considers the phenomenon of flap-torsion (K_{45}) coupling. Not only is this an important variable in the aeroelastic tailoring of aerodynamic structures, it is also highly interactive, non-linear function – the inclusion of which can make an optimisation problem difficult to solve using efficient deterministic methods that are based on linear approximations of the response. This analytical modelling (validated with computational and experimental results) shows that (by selecting appropriate design variables) this property can be included into an objective function whilst still allowing efficient optimisation methods to be employed.

Chapter 5 considers flap-torsion coupling from an experimental perspective. Eight laminated CFRP beams have been provided from the industrial sponsors. An experiment was devised and carried out to determine the cross-sectional bending and twisting properties, and the bend-twist coupling. These results were compared with analytical calculations (based on classical laminate analysis) and finite element results.

The work is then brought together in Chapter 6, which demonstrates the optimisation of a typical helicopter rotor blade to meet target values of various cross-section properties.

3 CYLINDRICAL SHELL

3.1 BACKGROUND

The aim of this thesis this is to produce a generic method for the analysis and optimisation of anisotropic 1-dimensional thin-walled beams, of which composite helicopter rotor blades are an example.

In this chapter, a laminated four layer cylindrical shell is used as the case study. A cylindrical shell is broadly similar to a helicopter rotor blade in terms of the underlying physics of the structure and the nature of the optimisation problem, but is much simpler to model analytically, allowing a better understanding of the more complex helicopter blade problem to be gained.

3.1.1 Case study problem

A laminated composite cylindrical shell was chosen as a case study for determining cross-sectional stiffness properties because an analytical derivation of the cross-sectional properties is relatively straightforward for a cylindrical shell, because a validated finite element model was available, and because cylindrical shells are commonly studied in the literature – providing a useful source of comparison.

As a case study, a problem is formulated to design a 4-layer composite cylindrical shell to meet predetermined target values of the four cross-sectional stiffnesses described below. The target values are arbitrarily chosen as

Axial stiffness (EA)	$= 6.0 \times 10^6$ N	
Flap bending stiffness (EI_{XX})	$= 1.2 \times 10^9$ Nmm^2	
Lag bending stiffness (EI_{YY})	$= 1.2 \times 10^9$ Nmm^2	
Torsional stiffness (GJ)	$= 1.8 \times 10^9$ Nmm^2	*(3.1.a-d)*

Note that since this investigation deals with a cylindrical shell, EI_{XX} must be equal to EI_{YY}.

These four cross-sectional stiffness properties are illustrated by Figure 3.1, below.

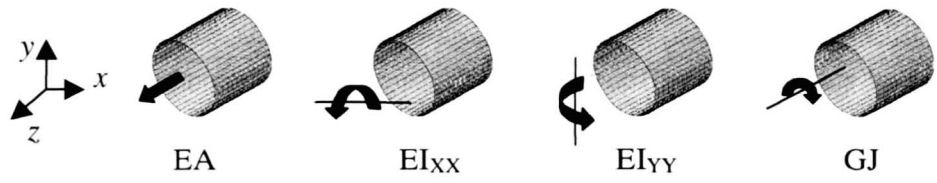

Figure 3.1 Four cross-sectional stiffness properties

Due to the high value of *GJ/EI*, this structure would be difficult to design from most real isotropic materials, thus making these values a good choice for this anisotropic design problem.

In addition to the target cross-sectional properties, typical "real world" constraints are included

- layer thicknesses are limited to multiples of typical ply thickness (0.125mm)
- internal shell radius is limited to "typical" mandrel sizes (0.2mm increments)

3.1.2 Choice of design variables

There are nine possible design variables for a 4-layer laminated cylindrical shell, x_1-x_9:

x_1 - Internal radius of shell
x_2-x_5 - Thickness of each layer
x_6-x_9 - Orientation of each layer

This would lead to a non-convex objective function, since the properties of each layer depend on trigonometric functions of the orientations. Additionally, if layer orientation is used as a design variable, this introduces several discrete design points with identical lay-ups (but different stacking sequences). Since the stacking sequence has only a small effect upon the cross-sectional stiffnesses of a thin walled structure, this would lead to

several discrete regions in the design space that have very similar properties and the objective function would have many local optima. The ply orientations and stacking sequence are therefore fixed at predetermined values: 0°, 45°, 90° and 135°. As discussed in Chapter 1 of this thesis, the work of Fukunaga [7][8] and Miki [9][10] shows that the vast majority of all possible in-plane stiffness properties for a laminate can still be obtained even if the ply orientations are constrained to these ply angles. It should be intuitive to the reader that the objective function is now convex.

The remaining five design variables for this problem are therefore

x_1 - Internal radius of the shell

x_2-x_5 - Thickness of each layer (+45°, 0°, 90°, -45°)

Note that the angle of each ply and the stacking sequence have now been fixed.

3.2 LITERATURE

3.2.1 Modified laminate stiffness matrix for curved shells

Fan *et al* [66] have published a modified ABD stiffness matrix for cylindrical shells that include terms neglected by Donnell's shallow shell theory. While this is only a small effect for the overall stiffness properties of a thin walled cylinder, the additional stiffness terms (due to the curvature of the shell) can have significant effects on the local stiffness of the shell, and thus on the potential stability of the cylinder under various loading conditions. For thick-walled cylinders

$$\begin{pmatrix} N_x \\ N_\theta \\ N_{x\theta} \\ N_{\theta x} \\ M_x \\ M_\theta \\ M_{x\theta} \\ M_{\theta x} \end{pmatrix} = \begin{bmatrix} A_{11}+\frac{B_{11}}{a} & A_{12}+\frac{B_{12}}{a} & A_{16}+\frac{B_{16}}{a}+\frac{D_{16}}{2a^2} & B_{11}+\frac{D_{11}}{a} & B_{12} & B_{16}+\frac{D_{16}}{2a} \\ A_{12} & A_{22} & A_{26}+\frac{D_{26}}{2a^2} & B_{12} & B_{22}-\frac{D_{22}}{a} & B_{26}-\frac{D_{26}}{2a} \\ A_{16}+\frac{B_{16}}{a} & A_{26}+\frac{B_{26}}{a} & A_{66}+\frac{B_{66}}{a}+\frac{D_{66}}{2a^2} & B_{16}+\frac{D_{16}}{a} & B_{26} & B_{66}+\frac{D_{66}}{2a} \\ A_{16} & A_{26} & A_{66}+\frac{D_{66}}{2a^2} & B_{16} & B_{26}-\frac{D_{26}}{a} & B_{66}-\frac{D_{66}}{2a} \\ B_{11}+\frac{D_{11}}{a} & B_{12}+\frac{D_{12}}{a} & B_{16}+\frac{D_{16}}{a} & D_{11} & D_{12} & D_{16} \\ B_{12} & B_{22} & B_{26} & D_{12} & D_{22} & D_{26} \\ B_{16}+\frac{D_{16}}{a} & B_{26}+\frac{D_{26}}{a} & B_{66}+\frac{D_{66}}{a} & D_{16} & D_{26} & D_{66} \\ B_{16} & B_{26} & B_{66} & D_{16} & D_{26} & D_{66} \end{bmatrix} \begin{pmatrix} e_x^{\,0} \\ e_\theta^{\,0} \\ e_{x\theta}^{\,0} \\ \chi_x \\ \chi_\theta \\ \chi_{x\theta} \end{pmatrix} \tag{3.2}$$

The results of this analysis have been compared with the laminate smear property analysis used later in this chapter. As expected for the cross-sectional stiffness of a thin walled structure, good agreement is generally found, indicating that the laminate smear property is an appropriate model to use in this optimisation problem.

3.2.2 Transformation of fibre orientation to global co-ordinate system

Since this work was begun, Lin and Chan [67] have published work on the stiffness evaluation of elliptical laminated composite tubes under bending. Their approach is considerably more involved than a laminate smear property approach, considering infinitesimally small shell sections of elliptical composite tubes as shown in Figure 3.2, below.

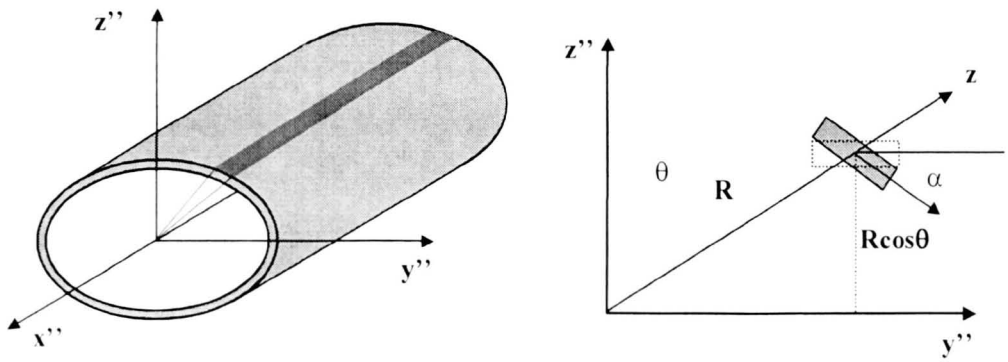

Figure 3.2 Infinitesimally small shell section of composite tube

The properties of each infinitesimal shell section are transformed into the global (x'', y'', z'') co-ordinate system and summed to give a global ABD matrix for the behaviour of the tube as a whole. This approach yields the following results

$$\overline{A}_{ij} = \sum_{k=1}^{n}\left(\int_0^{2\pi}\hat{Q}_{ij}^{k}\cdot\frac{ab}{\sqrt{b^2\sin^2\theta + a^2\cos^2\theta}}d\theta\right)\left(z_k' - z_{k-1}'\right) \tag{3.3.a}$$

$$\begin{aligned}\overline{B}_{ij} = &\sum_{k=1}^{n}\left(\int_0^{2\pi}\hat{Q}_{ij}^{k}\cdot\frac{ab}{\sqrt{b^2\sin^2\theta + a^2\cos^2\theta}}d\theta\right)\left(\frac{z_k'^{\,2} - z_{k-1}'^{\,2}}{2}\right)\\ &+\sum_{k=1}^{n}\left(\int_0^{2\pi}\hat{Q}_{ij}^{k}\cdot\left(\frac{ab}{\sqrt{b^2\sin^2\theta + a^2\cos^2\theta}}\right)^2\cos\theta\cdot d\theta\right)\left(z_k' - z_{k-1}'\right)\end{aligned} \tag{3.3.b}$$

$$\begin{aligned}\overline{D}_{ij} = &\sum_{k=1}^{n}\left(\int_0^{2\pi}\hat{Q}_{ij}^{k}\cdot\frac{ab}{\sqrt{b^2\sin^2\theta + a^2\cos^2\theta}}d\theta\right)\left(\frac{z_k'^{\,3} - z_{k-1}'^{\,3}}{3}\right)\\ &+2\sum_{k=1}^{n}\left(\int_0^{2\pi}\hat{Q}_{ij}^{k}\cdot\left(\frac{ab}{\sqrt{b^2\sin^2\theta + a^2\cos^2\theta}}\right)^2\cos\theta\cdot d\theta\right)\left(\frac{z_k'^{\,2} - z_{k-1}'^{\,2}}{2}\right)\\ &+\sum_{k=1}^{n}\left(\int_0^{2\pi}\hat{Q}_{ij}^{k}\cdot\left(\frac{ab}{\sqrt{b^2\sin^2\theta + a^2\cos^2\theta}}\right)^3\cos^2\theta\cdot d\theta\right)\left(z_k' - z_{k-1}'\right)\end{aligned} \tag{3.3.c}$$

where

$$\hat{Q}_{11} = c_z^4\overline{Q}_{11} + 2s_z^2c_z^2\left(c_x^2\overline{Q}_{12} + 2c_x^2\overline{Q}_{66}\right) + s_z^4c_x^4\overline{Q}_{22}$$

$$\hat{Q}_{12} = s_z^2c_z^2\left(\overline{Q}_{11} + c_x^4\overline{Q}_{22} - 4c_x^2\overline{Q}_{66}\right) + \left(s_z^4 + c_z^4\right)c_x^2\overline{Q}_{12}$$

$$\hat{Q}_{22} = s_z^4\overline{Q}_{11} + 2s_z^2c_z^2\left(c_x^2\overline{Q}_{12} + 2c_x^2\overline{Q}_{66}\right) + c_z^4c_x^4\overline{Q}_{22}$$

$$\hat{Q}_{16} = s_zc_z^3\left(\overline{Q}_{11} - c_x^2\overline{Q}_{12} - 2c_x^2\overline{Q}_{66}\right) + s_z^3c_z\left(c_x^2\overline{Q}_{12} - c_x^4\overline{Q}_{22} + 2c_x^2\overline{Q}_{66}\right)$$

$$\hat{Q}_{26} = s_z^3c_z\left(\overline{Q}_{11} - c_x^2\overline{Q}_{12} - 2c_x^2\overline{Q}_{66}\right) + s_zc_z^3\left(c_x^2\overline{Q}_{12} - c_x^4\overline{Q}_{22} + 2c_x^2\overline{Q}_{66}\right)$$

$$\hat{Q}_{66} = s_z^2c_z^2\left(\overline{Q}_{11} + c_x^4\overline{Q}_{22} - 2c_x^2\left(\overline{Q}_{12} + \overline{Q}_{66}\right)\right) + s_z^3c_z\left(c_x^2\overline{Q}_{12} - c_x^4\overline{Q}_{22} + 2c_x^2\overline{Q}_{66}\right)$$

(3.4.a-f)

where

$$s_x = \sin\alpha$$
$$c_x = \cos\alpha$$
$$s_z = \sin\beta$$
$$c_z = \cos\beta \qquad (3.5.a\text{-}d)$$

where

$$\alpha = \tan^{-1}\left(-\frac{b^2 \sin\theta}{a^2 \cos\theta}\right) \qquad (3.6)$$

and β is the fibre orientation angle.

Although these expressions reduce somewhat for circular sections (a=b, and α=θ), the expressions do not lend themselves to closed form solutions. Lin and Chan use a numerical method to evaluate the elliptical integrals for their cross-section.

Lin and Chan present a comparison of their method with finite element results (based on a 3D model in ANSYS 5.5) and the smear property approach. These are presented in the Table 3.1 below.

Their results (based on an elliptical tube with b/a=0.75) indicate that their method is closer to their finite element results than the laminate smear property approach used here. However, the results do also indicate that the discrepancy in bending stiffness between the finite element model and the laminate smear property approach used in the current research is fairly small (usually less than 5%), again providing justification for using the approximate closed form solution which is derived from the laminate smear property later in this chapter.

Major radius (in)	FEM result ($x10^4$ lb-in^4)	Smear property approach ($x10^4$ lb-in^4)	Lin and Chan approach ($x10^4$ lb-in^4)
2.6	1967.7	2096.4	1972.6
2.2	1201.1	1270.2	1195.1
1.8	662.85	695.92	654.65
1.4	314.19	327.61	308.08
1.0	115.22	119.55	112.33
0.8	59.139	61.300	57.548
0.6	25.000	25.944	24.309
0.5	14.486	15.063	14.086
0.4	7.3559	7.7578	7.2290
0.3	3.1249	3.3146	3.0652

Table 3.1 Comparison of results from Lin and Chan

It is difficult to justify the five significant figures given by Lin and Chan in the table above. Three significant figures would be perfectly adequate to allow accurate comparisons to be made between the different values.

3.3 ANALYTICAL MODEL

3.3.1 Analytical approach to geometric variables

The target values of axial stiffness and bending stiffness are prescribed. It will be appreciated that if assumptions of the laminate smear property approach are made, then these properties are both dependent on the same material parameter (E), and the ratio of these two target values is solely dependent upon the geometric parameters I and A. These parameters are determined by the internal radius of the shell (R_{inner}) and the overall wall thickness (t).

From the target values, the ratio *I/A* is determined as

$$EI/EA = 200\,\mathrm{mm}^2 \tag{3.7}$$

Since the geometry is a cylindrical shell,

$$I = \frac{\pi}{4}\left((R_{inner}+t)^4 - R_{inner}{}^4\right)$$
$$A = \pi\left((R_{inner}+t)^2 - R_{inner}{}^2\right) \tag{3.8.a-b}$$

Thus, taking all units to be in millimetres, we have

$$\frac{I}{A} = \frac{\frac{\pi}{4}\left((R_{inner}+t)^4 - R_{inner}{}^4\right)}{\pi\left((R_{inner}+t)^2 - R_{inner}{}^2\right)} = 200 \tag{3.9}$$

This can be simplified to

$$\left((R_{inner}+t)^2 + R_{inner}{}^2\right)\left((R_{inner}+t)^2 - R_{inner}{}^2\right) = 800\left((R_{inner}+t)^2 - R_{inner}{}^2\right)$$
$$\left((R_{inner}+t)^2 + R_{inner}{}^2\right) = 800$$
$$2R_{inner}{}^2 + 2R_{inner}t + t^2 = 800 \tag{3.10.a-c}$$

This gives a range of solutions for R_{inner} and t, which are plotted on Figure 3.3 below. It will be appreciated that as the radius increases and the wall thickness decreases (as described by the equation above) the cross-sectional area of the shell also decreases. In order to meet the axial stiffness target, the Young's modulus of the material will have to vary, according to

$$E = \frac{EA_{target}}{\pi\left(t + 2R_{inner}\right)} \tag{3.11}$$

Since the Young's modulus of CFRP can only take values between maximum and minimum values (typically around 9.2 GPa and 132.0 GPa) this constraint can be used to eliminate a large unfeasible region of the design space.

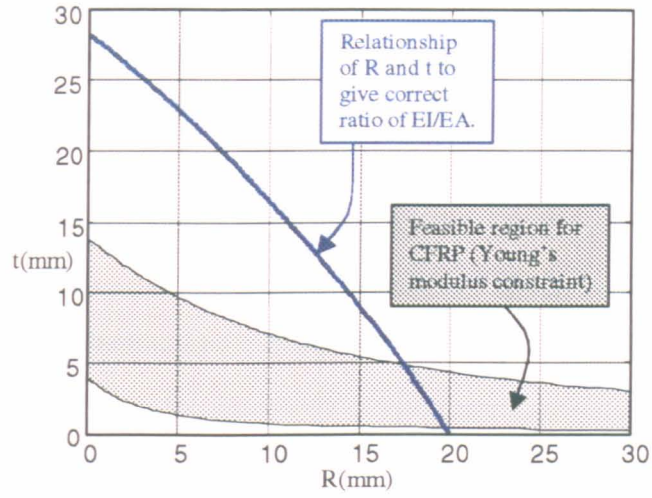

Figure 3.3 Material properties determine feasible design

The shaded region on the above diagram represents the region within which the Young's modulus requirement can be met by CFRP.

- The upper boundary to the shaded region represents the minimum modulus possible for CFRP (approximately 9.2 x 10^9 N/m^2 – corresponding to 90-degree plies).
- The lower boundary to the shaded region represents the maximum modulus possible for CFRP (approximately 1.32 x 10^{11} N/m^2 – corresponding to 0-degree plies).

Note that the torsional stiffness target will require that ±45-degree plies be used, and it can thus be predicted that any solution will not lie close to these boundaries, however the above analysis quickly gives upper and lower bounds of

18.0 mm < shell radius < 20.0 mm

0.0 mm < shell thickness < 5.0 mm

3.3.2 Analytical approach to lay-up

The target values of torsional stiffness (GJ) and bending stiffness (EI) are prescribed. Since the geometric properties (I and J) of a cylindrical cross-section are dependent the same geometric variables (shell radius and overall wall thickness), then using laminate smear property approach shows that the ratio of these cross-sectional properties is solely dependent upon the laminate stiffnesses, which in turn depend upon the lay-up of the material. It is therefore desirable to obtain a laminate that has the correct ratio of axial stiffness to shear stiffness. This task is particularly suited to a lamination parameter approach, since the values of lamination parameters ξ_1-ξ_4 (which determine the A-matrix properties of the laminate) are independent of stacking sequence.

For this problem, equations *(3.1.b-d)* are

$$\begin{aligned} EI_{XX} &= EI_{YY} = 1.2 \times 10^9 \text{ Nm}^2 \\ GJ &= 1.8 \times 10^9 \text{ Nm}^2 \end{aligned} \qquad (3.1.b\text{-}d)$$

so

$$\frac{EI}{GJ} = \frac{2}{3} \qquad (3.12)$$

Since the cross-section is circular,

$$I_{XX} = I_{YY} = J/2 \qquad (3.13)$$

so

$$\frac{E}{G} = \frac{4}{3} \qquad (3.14)$$

The required ratio of bending stiffness to torsional stiffness for the problem thus determines the required ratio of E to G for the laminate. The values E and G for the laminate are easily calculated from the stiffness matrix as

$$E = \frac{1}{h}\left(\frac{A_{11}A_{22} - A_{12}^{\,2}}{A_{22}}\right) \tag{3.15}$$

$$G = \frac{1}{h}A_{66} \tag{3.16}$$

so

$$\frac{E}{G} = \frac{A_{11}A_{22} - A_{12}^{\,2}}{A_{22}A_{66}} = \frac{4}{3} \tag{3.17}$$

The Young's modulus and shear modulus can be expressed in terms of the material invariants ($U_{1\text{-}5}$) and lamination parameters ($\xi_{1\text{-}4}$) as introduced in Chapter 1. Equation *(3.17)* may therefore be rewritten as

$$\frac{U_1^{\,2} + U_4^{\,2} - \xi_1^{\,2}U_2^{\,2} + 2\xi_2 U_3(U_1 + U_4)}{U_1U_5 - \xi_1U_2U_5 + \xi_2U_3(U_5 - U_1 - \xi_2U_3 - \xi_1U_2)} = \frac{4}{3} \tag{3.18}$$

Since $U_{1\text{-}5}$ are material invariants, the only two unknowns are ξ_1 and ξ_2, thus allowing one to be determined in terms of the other. The equation may be rearranged thus, to give the following (rather lengthy) equation

$$\begin{aligned} f(\xi_1,\xi_2) =& \xi_2^{\,2}\left(4U_3^{\,2}\right) + \xi_2\left(U_3\left(10U_1 + 6U_4 - 4U_5\right)\right) + \xi_1\xi_2\left(4U_2U_3\right) \\ &+ \xi_1\left(4U_2U_5\right) - \xi_1^{\,2}\left(3U_2^{\,2}\right) + \left(3\left(U_1^{\,2} + U_4^{\,2}\right) - 4U_1U_5\right) \\ &= 0 \end{aligned} \tag{3.19}$$

If either lamination parameter (ξ_1 or ξ_2) is known, this expression is a simple quadratic in the other lamination parameter. If neither is known (as is the case in this problem), the expression does not have a simple analytical solution, so a numerical solution is

applied. The MATLAB [68] output in Figure 3.4 shows the value of the above function over the range:

$$-1 < \xi_1, \xi_2 < 1 \qquad (3.20)$$

The curved black line on this surface is the contour where

$$f(\xi_1, \xi_2) = 0 \qquad (3.21)$$

This corresponds to the solution of equation *(3.19)* and hence shows the relationship between lamination parameters ξ_1 and ξ_2 required for the correct ratio of E to G.

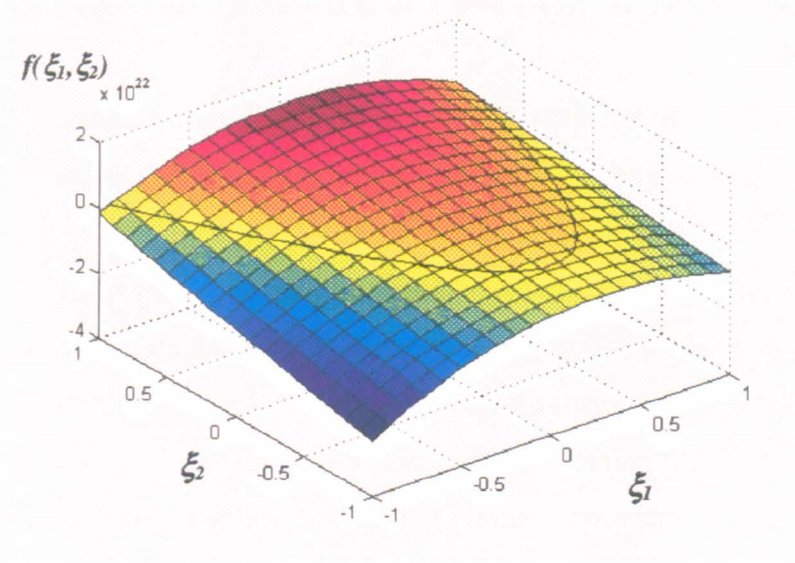

Figure 3.4 Allowable values of ξ_1 and ξ_2

By virtue of their geometric derivation, lamination parameters ξ_1 and ξ_2 can only take values within the region represented by the inequalities expressed in *(3.20)* and

$$2\xi_1^2 - \xi_2^2 - 1 \leq 0 \qquad (3.22)$$

This region is represented by the entire shaded area in Figure 3.5, below. Since this problem restricts the available ply angles to only 0°, ±45° and 90° plies, ξ_1 and ξ_2 are further restricted and can only take values within the darkly shaded triangular region in Figure 3.5.

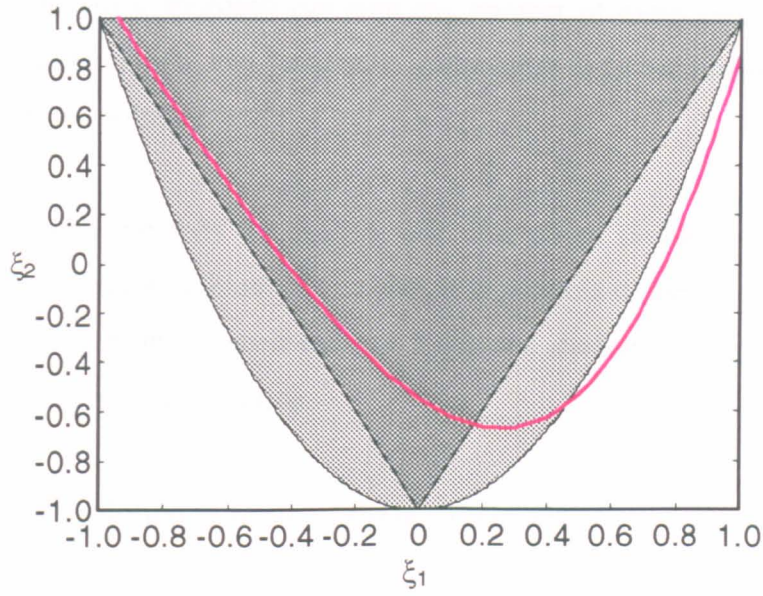

Figure 3.5 Lamination parameters that give required laminate properties

Any 0°/±45°/90° laminate with ξ_1 and ξ_2 lamination parameters that lie on the curved red line (within the dark shaded triangular region) will give the correct value of *E/G*.

Having determined the range of lamination parameters that give the correct value of *E/G*, there remain an infinite number of continuous solutions to the problem, which each refer to different shell radius and wall thickness. Any lay-up that corresponds to a solution of equation *(3.19)* is a potential solution to the problem. Having picked any one of these lay-ups, the required axial stiffness to bending stiffness ratio can be met by varying the shell radius and wall thickness as described earlier in section 3.3.1 and shown in Figure 3.3.

As in most real world problems, this problem has the additional complication of discretised design variables. It is not possible to choose the exact ply thicknesses and shell radii that give the required ξ_1 and ξ_2 values, but must round each of the ply thicknesses to the nearest 0.125mm, and the shell radius to the nearest 0.2mm. For very thin walled sections, the errors introduced through rounding the design variables in this way can be significant.

Although this analytical approach can give any number of exact solutions in terms of shell radius, wall thickness, and lamination parameters, it is not capable of finding an optimum discretised solution.

Formal optimisation methods for dealing with discretised problems are discussed in Chapter 1, although for a problem of this size, it is possible to use an exhaustive search of the solutions for different shell radii to locate the discrete design point that most closely matches the required solution.

3.3.3 Closed form solution in terms of design variables

Since one reason for the example problem used in this chapter is to gain a better understanding of the optimisation problem, it is important to have physical insight into how the design variables interact to affect the cross-sectional properties of the structure. It is therefore desirable to have a closed form solution for the objective function (i.e. the cross-sectional stiffnesses) in terms of the design variables. For this reason, the **laminate smear property** approach has been adopted.

The laminate smear property approach considers the inplane properties of a flat composite laminate and applies them to the structural properties of the (thin walled) cross-section being studied. Although this approach does not account for stacking sequence effects, and so is only strictly appropriate for thin walled sections, it may also be applied to thicker walled sections (albeit with an obvious reduction in accuracy). The approach is illustrated step by step below, in developing closed form solutions for the cross-sectional stiffnesses of the four layered composite cylindrical shell used as an example throughout this chapter.

It is first important to note that using the equations

$$\begin{aligned} E_0A_0 &= E_1A_1 + E_2A_2 + E_3A_3 + E_4A_4 \\ E_0I_0 &= E_1I_1 + E_2I_2 + E_3I_3 + E_4I_4 \\ G_0J_0 &= G_1J_1 + G_2J_2 + G_3J_3 + G_4J_4 \end{aligned} \qquad (3.23.a\text{-}c)$$

for the overall structural properties (indicated by the subscript "$_0$") in terms of the layer properties (indicated by the subscript "$_i$", where i=1-4) is *incorrect* for an anisotropic laminated structure because these equations do not take account of the interactions that occur between plies of different orientations. These interactions are fundamental to the overall behaviour of anisotropic laminates.

The laminate smear approach assumes that the cross-sectional stiffnesses are simply the effective material modulus of the (assumed flat) laminate, multiplied by the relevant function (e.g. area, second moment of area, or polar moment of area) of the overall cross-sectional shape.

3.3.3.1 Determination of effective moduli using laminate smear property approach

The behaviour of a flat composite laminate is described in terms of the usual ABD stiffness matrix

$$\begin{Bmatrix} N_x \\ N_y \\ N_{xy} \\ M_x \\ M_y \\ M_{xy} \end{Bmatrix} = \begin{bmatrix} A_{11} & A_{12} & A_{16} & B_{11} & B_{12} & B_{16} \\ & A_{22} & A_{26} & B_{12} & B_{22} & B_{26} \\ & & A_{66} & B_{16} & B_{26} & B_{66} \\ & & & D_{11} & D_{12} & D_{16} \\ & Sym. & & & D_{22} & D_{26} \\ & & & & & D_{66} \end{bmatrix} \begin{Bmatrix} \varepsilon_x \\ \varepsilon_y \\ \gamma_{xy} \\ \kappa_x \\ \kappa_y \\ \kappa_{xy} \end{Bmatrix} \qquad (3.24)$$

For a thin walled structure, the out of plane terms (i.e. B and D matrix terms) are less important for the overall stiffness properties of the cross-section than the inplane terms (i.e. A matrix terms), and these out of plane terms are therefore ignored as a small effect in the current analysis. The laminate behaviour is considered to be dominated by the in-plane stiffness, and is derived from the inverse of the A matrix where

$$A = \begin{bmatrix} A_{11} & A_{12} & A_{16} \\ A_{12} & A_{22} & A_{26} \\ A_{16} & A_{26} & A_{66} \end{bmatrix} \qquad (3.25)$$

$$A^{-1} = \frac{1}{|A|}\begin{bmatrix} \alpha_{11} & \alpha_{12} & \alpha_{16} \\ \alpha_{12} & \alpha_{22} & \alpha_{26} \\ \alpha_{16} & \alpha_{26} & \alpha_{66} \end{bmatrix} = \begin{bmatrix} a_{11} & a_{12} & a_{16} \\ a_{12} & a_{22} & a_{26} \\ a_{16} & a_{26} & a_{66} \end{bmatrix} \tag{3.26}$$

where

$$|A| = A_{11}(A_{22}A_{66} - A_{26}^{2}) - A_{12}(A_{12}A_{66} - A_{16}A_{26}) + A_{16}(A_{12}A_{26} - A_{16}A_{22})$$

$$\alpha_{11} = A_{22}A_{66} - A_{26}^{2}$$

$$\alpha_{12} = -A_{12}A_{66} + A_{16}A_{26}$$

$$\alpha_{16} = A_{12}A_{26} - A_{16}A_{22}$$

$$\alpha_{22} = A_{11}A_{66} - A_{16}^{2}$$

$$\alpha_{26} = -A_{11}A_{26} + A_{12}A_{16}$$

$$\alpha_{66} = A_{11}A_{22} - A_{12}^{2} \tag{3.26.a-g}$$

The effective engineering constants for the laminate are obtained directly from the inverse of the A-matrix (Jones [2]) as

$$E_x = \frac{1}{a_{11}t} \tag{3.27}$$

$$G = \frac{1}{a_{66}t} \tag{3.28}$$

Each stiffness matrix component may be expressed in terms of translated reduced stiffnesses and ply thicknesses as

$$A_{11} = \overline{Q_{11(1)}}t_1 + \overline{Q_{11(2)}}t_2 + \overline{Q_{11(3)}}t_3 + \overline{Q_{11(4)}}t_4$$

$$A_{12} = \overline{Q_{12(1)}}t_1 + \overline{Q_{12(2)}}t_2 + \overline{Q_{12(3)}}t_3 + \overline{Q_{12(4)}}t_4$$

$$A_{22} = \overline{Q_{22(1)}}t_1 + \overline{Q_{22(2)}}t_2 + \overline{Q_{22(3)}}t_3 + \overline{Q_{22(4)}}t_4$$

$$A_{66} = \overline{Q_{66(1)}}t_1 + \overline{Q_{66(2)}}t_2 + \overline{Q_{66(3)}}t_3 + \overline{Q_{66(4)}}t_4$$

$$A_{16} = \overline{Q_{16(1)}}t_1 + \overline{Q_{16(2)}}t_2 + \overline{Q_{16(3)}}t_3 + \overline{Q_{16(4)}}t_4$$

$$A_{26} = \overline{Q_{26(1)}}t_1 + \overline{Q_{26(2)}}t_2 + \overline{Q_{26(3)}}t_3 + \overline{Q_{26(4)}}t_4 \qquad (3.29.a.f)$$

so E_x and G for the laminate may be written in terms of transformed reduced stiffnesses and layer thicknesses as

$$E_x = \frac{|A|}{t(A_{22}A_{66} - A_{26}^{\ 2})} \qquad (3.30)$$

$$G = \frac{|A|}{t(A_{11}A_{22} - A_{12}^{\ 2})} \qquad (3.31)$$

Note that equations *(3.30)* and *(3.31)* above do not account for the curved shape of the laminate, and hence make no allowance for stacking sequence effects.

Once these are expanded into translated reduced stiffness terms for each layer, equations *(3.30)* and *(3.31)* become particularly large expressions that do not readily simplify. However, the expression can be simplified considerably by considering only balanced laminates. For this class of laminate, $A_{16} = A_{26} = 0$ and the expressions for E_x and G reduce to

$$E_x = \left(A_{11} - \frac{A_{12}^{\ 2}}{A_{22}} \right) \Big/ t \qquad (3.32)$$

$$G = A_{66}/t \qquad (3.33)$$

As before, E_x and G may be expressed in terms of material transformed reduced stiffnesses and ply thicknesses. Although not presented explicitly here, it is simple to substitute the A-matrix terms.

3.3.3.2 Closed form expressions for cross-sectional properties

Since the geometric stiffness properties of a cylindrical section are easily derived or looked up in the literature, it is straightforward to express the cross-sectional shell properties in terms of design variables.

The value of axial stiffness (*EA*) for the whole tube may now be written in terms of the material transformed reduced stiffnesses (which are constant for a given material at a given orientation) and design variables (R_{inner}, $t_{1\text{-}4}$) as

$$EA = \pi(2R_{inner} + t)\left(A_{11} - \frac{A_{12}^{\,2}}{A_{22}}\right)$$

$$= \pi(2R_{inner} + t)\left(\overline{Q_{11(1)}}t_1 + \overline{Q_{11(2)}}t_2 + \overline{Q_{11(3)}}t_3 + \overline{Q_{11(4)}}t_4 - \frac{\left(\overline{Q_{12(1)}}t_1 + \overline{Q_{12(2)}}t_2 + \overline{Q_{12(3)}}t_3 + \overline{Q_{12(4)}}t_2\right)^2}{\overline{Q_{22(1)}}t_1 + \overline{Q_{22(2)}}t_2 + \overline{Q_{22(3)}}t_3 + \overline{Q_{22(4)}}t_4}\right) \tag{3.34}$$

The partial derivatives of these target variables may now be determined with respect to the design variables as

$$\frac{\partial EA}{\partial R_{inner}} = 2\pi\left(A_{11} - \frac{A_{12}^{\,2}}{A_{22}}\right) \tag{3.35}$$

$$\frac{\partial EA}{\partial t_1} = \frac{\partial\left(\pi(K_{11} + t_1)\left(K_{12} + \overline{Q_{11(1)}}t_1 - \frac{\left(K_{13} + \overline{Q_{12(1)}}t_1\right)^2}{K_{14} + \overline{Q_{22(1)}}t_1}\right)\right)}{\partial t_1}$$

$$= \pi\left(\left(K_{12} + \overline{Q_{11(1)}}t_1 - \frac{\left(K_{13} + \overline{Q_{12(1)}}t_1\right)^2}{K_{14} + \overline{Q_{22(1)}}t_1}\right) + (K_{11} + t_1)\left(\overline{Q_{11(1)}} - \lambda_{11}\right)\right) \tag{3.36}$$

where

$$\lambda_{11} = \frac{\left(\begin{array}{l} 2\overline{Q_{12(1)}}\left(K_{14} + \overline{Q_{22(1)}}t_1\right)\left(K_{13} + \overline{Q_{12(1)}}t_1\right) \\ -\overline{Q_{22(1)}}\left(K_{13} + \overline{Q_{12(1)}}t_1\right)^2 \end{array}\right)}{\left(K_{14} + \overline{Q_{22(1)}}t_1\right)^2}$$

$$K_{11} = R_{inner} + t_2 + t_3 + t_4$$

$$K_{12} = \overline{Q_{11(2)}}t_2 + \overline{Q_{11(3)}}t_3 + \overline{Q_{11(4)}}t_4$$

$$K_{13} = \overline{Q_{12(2)}}t_2 + \overline{Q_{12(3)}}t_3 + \overline{Q_{12(4)}}t_4$$

$$K_{14} = \overline{Q_{22(2)}}t_2 + \overline{Q_{22(3)}}t_3 + \overline{Q_{22(4)}}t_4 \qquad \textit{(3.36.a-e)}$$

The remaining terms differentiate similarly. In general

$$\frac{\partial EA}{\partial t_i} = \frac{\partial\left(\pi\left(K_{i1} + t_i\right)\left(K_{i2} + \overline{Q_{11(i)}}t_i - \frac{\left(K_{i3} + \overline{Q_{12(i)}}t_i\right)^2}{K_{i4} + \overline{Q_{22(i)}}t_i}\right)\right)}{\partial t_i}$$

$$= \pi\left(\begin{array}{l} \left(K_{i2} + \overline{Q_{11(i)}}t_i - \frac{\left(K_{i3} + \overline{Q_{12(i)}}t_i\right)^2}{K_{i4} + \overline{Q_{22(i)}}t_i}\right) \\ +\left(K_{i1} + t_i\right)\left(\overline{Q_{11(i)}} - \lambda_{i1}\right) \end{array}\right) \qquad \textit{(3.37)}$$

where

$$\lambda_{i1} = \frac{\left(\begin{array}{l} 2\overline{Q_{12(i)}}\left(K_{i4} + \overline{Q_{22(i)}}t_i\right)\left(K_{i3} + \overline{Q_{12(i)}}t_i\right) \\ -\overline{Q_{22(i)}}\left(K_{i3} + \overline{Q_{12(i)}}t_i\right)^2 \end{array}\right)}{\left(K_{i4} + \overline{Q_{22(i)}}t_i\right)^2}$$

$$K_{i1} = R_{inner} + t - t_i$$

$$K_{i2} = -\overline{Q_{11(i)}}t_i + \sum_{j=0}^{n}\overline{Q_{11(j)}}t_j$$

$$K_{i3} = -\overline{Q_{12(i)}}t_i + \sum_{j=0}^{n}\overline{Q_{12(j)}}t_j$$

$$K_{i4} = -\overline{Q_{22(i)}} t_i + \sum_{j=0}^{n} \overline{Q_{22(j)}} t_j \qquad (3.37.a\text{-}e)$$

Similarly, the bending stiffness (EI) is given as

$$EI = \frac{\pi}{4t}\left((R_{inner} + t)^4 - R_{inner}^4\right)\left(A_{11} - \frac{A_{12}^2}{A_{22}}\right) \qquad (3.38)$$

and the partial derivatives with respect to EI are

$$\frac{\partial EI}{\partial R_{inner}} = \pi\left(3R_{inner}^2 + 3R_{inner}\,t + t^2\right)\left(A_{11} - \frac{A_{12}^2}{A_{22}}\right) \qquad (3.39)$$

$$\frac{\partial EI}{\partial t_i} = \frac{\partial\left(\frac{\pi}{4t}\left((R_{inner}+t)^4 - R_{inner}^4\right)\left(K_{i2} + \overline{Q_{11(i)}} t_i - \frac{\left(K_{i3} + \overline{Q_{12(i)}} t_i\right)^2}{K_{i4} + \overline{Q_{22(i)}} t_i}\right)\right)}{\partial t_i}$$

$$= \frac{\pi}{4}\left(\begin{array}{l}\left(6R_{inner}^2 + 8R_{inner}t + 3t^2\right)\left(K_{i2} + \overline{Q_{11(i)}} t_i - \dfrac{\left(K_{i3} + \overline{Q_{12(i)}} t_i\right)^2}{K_{i4} + \overline{Q_{22(i)}} t_i}\right) \\ + \left(4R_{inner}^3 + 6R_{inner}t + 4R_{inner}t^2 + t^3\right)\left(\overline{Q_{11(i)}} - \lambda_{i2}\right)\end{array}\right) \qquad (3.40)$$

where

$$\lambda_{i2} = \frac{2\overline{Q_{12(i)}}\left(K_{i4} + \overline{Q_{22(i)}} t_i\right)\left(K_{i3} + \overline{Q_{12(i)}} t_i\right) - \overline{Q_{22(i)}}\left(K_{i3} + \overline{Q_{12(i)}} t_i\right)^2}{\left(K_{i4} + \overline{Q_{22(i)}} t_i\right)^2} \qquad (3.40.a)$$

Finally the torsional stiffness (GJ) is given as

$$GJ = \frac{\pi}{2t} A_{66}\left((R_{inner} + t)^4 - R_{inner}^4\right) \qquad (3.41)$$

and the partial derivatives with respect to GJ are

$$\frac{\partial GJ}{\partial R_{inner}} = \pi(6R_{inner}{}^2 + 6R_{inner}t + 4R_{inner}t^2)A_{66} \tag{3.42}$$

$$\frac{\partial GJ}{\partial t_i} = \frac{\pi}{2}\left((6R_{inner}{}^2 + 8R_{inner}t + 3t^2)A_{66} + (4R_{inner}{}^3 + 6R_{inner}{}^2t + 4R_{inner}t^2 + t^3)\left(\overline{Q_{66(i)}}\right)\right) \tag{3.43}$$

The above closed form solutions for the target variables and partial derivatives in terms of the design variables can be used to check the gradients obtained from any finite difference calculations, and to check the solutions obtained from any optimisation performed on this problem.

3.4 FINITE ELEMENT MODELLING

3.4.1 Finite element model used

A finite element model of a cylindrical shell is analysed using ABAQUS [69]. A typical input file is given in Appendix 3.1. Code based on the method of Hill and Weaver [34] is used to analyse the cross-sectional properties of the model.

Although it may appear slightly crude, the mesh shown in Figure 3.6 below is suitable for use in this optimisation problem. Rather than using thin shell elements, 3-D solid brick elements were used to ensure that the effects of wall thickness are captured. Although only fifteen elements are used around the circumference of the shell, the general behaviour of cross-sectional properties is accurately represented by this mesh. A mesh refinement study showed that the increase in stiffness caused by using a low-resolution mesh is only a few percent, and significant computational expense is saved.

For the purposes of this study (i.e. to gain insight into the behaviour of cross-sectional properties and the issues associated with optimisation of these properties), the saving of computational expense is more important than the exact accuracy of the finite element model. Obviously, when actually applying any optimisation method to a real life

problem that requires accurate cross-sectional properties, it is important to use an appropriate finite element model.

Figure 3.6 Mesh used for finite element analysis of cylindrical shell properties

Using this mesh, the finite element analysis takes approximately 2.5 minutes (real time) to return the cross-sectional stiffness properties of the shell.

3.4.2 Variation of cross-sectional properties with design variables

The finite element model is used to demonstrate the variation of cross-sectional property with each design variable about the optimum design point, where

$$\underline{x} = (19.4 \quad 0.500 \quad 0.125 \quad 0.375 \quad 0.500)^T \qquad (3.44)$$

The results shown in Figure 3.7 (below) indicate that over the feasible region of design space, the cross-sectional properties are convex and are either approximately linear or increase monotonically, and may thus be approximated as linear for optimisation purposes.

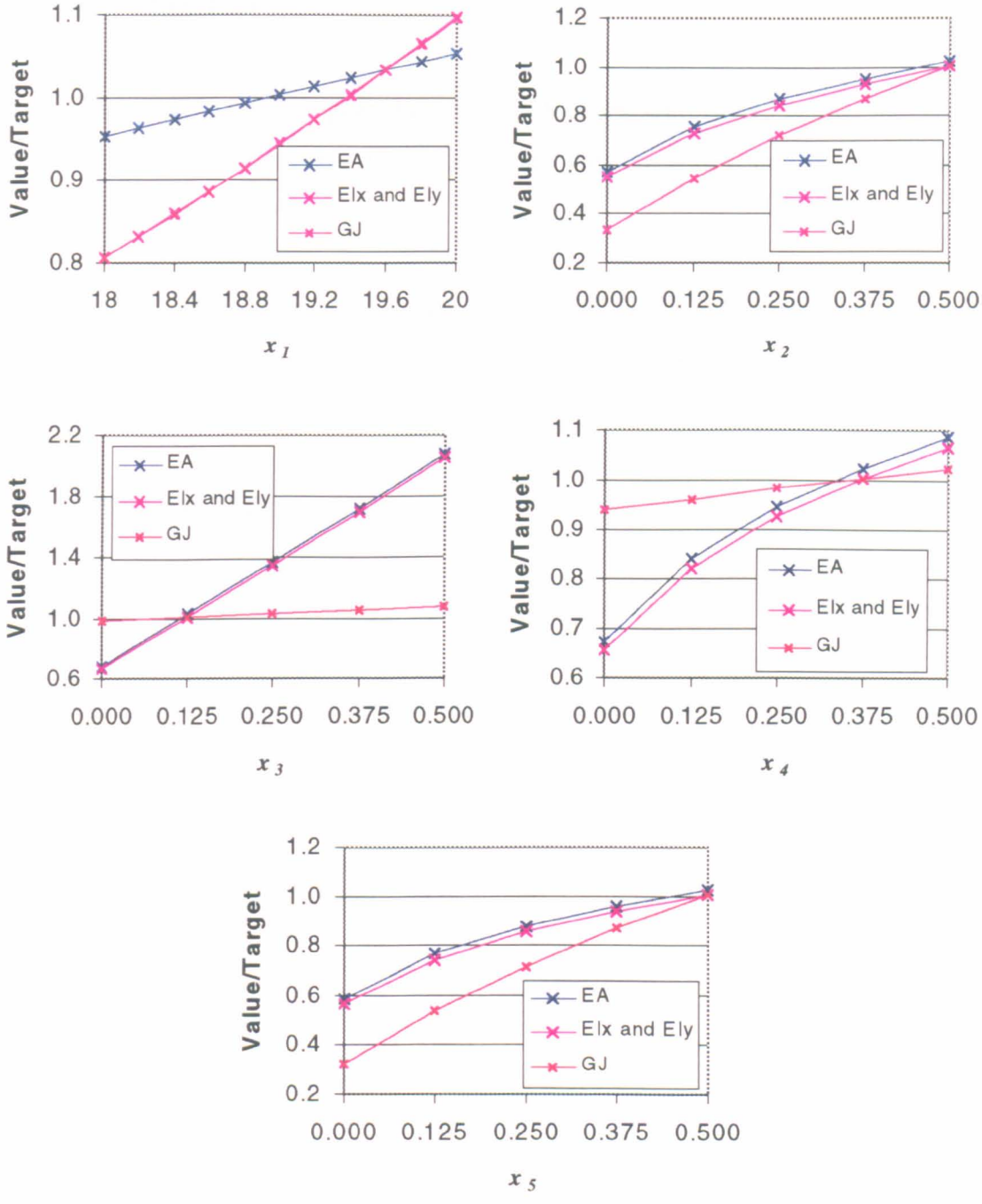

Figure 3.7 Variation of cross-sectional properties with design variables

Further investigation reveals that there is some interaction between the design variables – particularly between the thickness of +45° and –45° plies. This interaction limits the accuracy of the linearisation and hence increases the number of iterations until convergence. This interaction is therefore minimised by recoding the design variables, which will be discussed later in this chapter.

3.5 EXPERIMENT

No specific experimental program has been undertaken with regard to this part of the work, as results for the properties of cylindrical shells are widely quoted, based on the laminate smear property.

The results of Lin and Chan [67] presented earlier in Table 3.1 show good agreement between finite element and analytical models for elliptical shells, of which cylindrical shells are a sub-category.

3.6 OPTIMISATION

A suitable single objective function for this optimisation problem considers the square of the normalised N-dimensional Euclidean distance between each cross-sectional stiffness property and its target value. For this problem, such an objective would be written as

$$Objective = \left(\frac{EA_a - EA_t}{EA_t}\right)^2 + \left(\frac{EI_{xx_a} - EI_{xx_t}}{EI_{xx_t}}\right)^2 + \left(\frac{EI_{yy_a} - EI_{yy_t}}{EI_{yy_t}}\right)^2 + \left(\frac{GJ_a - GJ_t}{GJ_t}\right)^2 \tag{3.45}$$

Note that the objective is always positive, but reduces to zero when all of the target values have been met exactly. In this sense, this objective function may be thought of as consisting only of exterior penalty functions.

For more advanced problems, each term in the objective can be given a predetermined weighting factor (W_i) according to how important it is to match each individual term. Thus the objective function would be

$$Objective = W_1\left(\frac{EA_a - EA_t}{EA_t}\right)^2 + W_2\left(\frac{EI_{xx_a} - EI_{xx_t}}{EI_{xx_t}}\right)^2 + W_3\left(\frac{EI_{yy_a} - EI_{yy_t}}{EI_{yy_t}}\right)^2 + W_4\left(\frac{GJ_a - GJ_t}{GJ_t}\right)^2 \tag{3.46}$$

In this problem, all terms will considered of equal importance and consequently all weighing factors are all set to unity. Note that the weighting factors only affect the optimal solution if no exact solution exists.

3.6.1 Bounding the design space

As explained in the first chapter, the more information that is already known about the problem the easier to choose a suitable optimisation algorithm. As it is only possible to apply the most efficient algorithms to problems that are known to be convex and can be approximated as linear over at least a localised area about the current design point, it is appropriate to begin with simple analytical calculations to determine appropriate bounds for the design variables.

The analysis described in section 3.3 gives upper and lower bounds to the radius and wall thickness of the shell.

$$18.0 \text{ mm} < \text{shell radius} < 20.0 \text{ mm}$$
$$0.0 \text{ mm} < \text{shell thickness} < 5.0 \text{ mm}$$

3.6.2 Exhaustive search of the design space

The following technique is not really part of any practical optimisation procedure since it analyses every design point in the design space. However, since this is a relatively small optimisation problem, it is possible to search the entire design space by sampling discrete design points at regular, small intervals throughout the design space, much like surveying for a topographical map. Although this is not an efficient solution method for an optimisation problem (and would be too computationally expensive to use on anything but a small problem such as this one), it does provide a complete "map" of the objective function in the N-dimensional design space. This gives considerably more physical insight into the nature of the design space than a single optimal solution.

If continuous design variables are used in the problem, this approach requires that they either be discretised or sampled at discrete intervals, so that the design space to be searched effectively becomes a number of discrete design points in N-dimensional space. In this problem, the variables of shell radius and ply thicknesses are already discretised (to 0.2mm and 0.125mm increments respectively).

To use the bounds derived above at the desired resolution would lead to a design space with over 31 million design points. Assuming 2.5 minutes per analysis, an exhaustive search would take almost 150 years! The upper and lower bounds for searching the design variables were therefore chosen as

$$18.0 \text{ mm} < x_1 < 20.0 \text{ mm}$$
$$0.0 \text{ mm} < x_{2\text{-}5} < 0.5 \text{ mm}$$

This gives a design space of 6875 points, for which an exhaustive search would take just under 12 days. Although the above choice of design variables may not necessarily include every possible solution (particularly with the lower shell radii, the thickness of the shell wall may need to be larger than allowed for by the bounds chosen), it does include the majority of the feasible design space, and significantly reduces the number of discrete design points to be searched.

3.6.3 Presentation of search results

The results of this 5-dimensional search do not readily lend themselves to easy presentation. Printed in plain text, the complete search results would run to approximately 200 pages, and offer little physical insight to all but the most dedicated reader!

Presented below (Figure 3.8) is a graphical representation of the objective function plotted over a 3-dimensional cross-section of the 5-dimensional design space. In effect, what we have is a cross-section of a cross-section of the design space.

The position of each point in the 3-D grid depicted in the diagram is indicative of the value of the three design variables that correspond to each axis shown. The colour of each point is a measure of the value of the objective function as plotted in the key at the side of the graph.

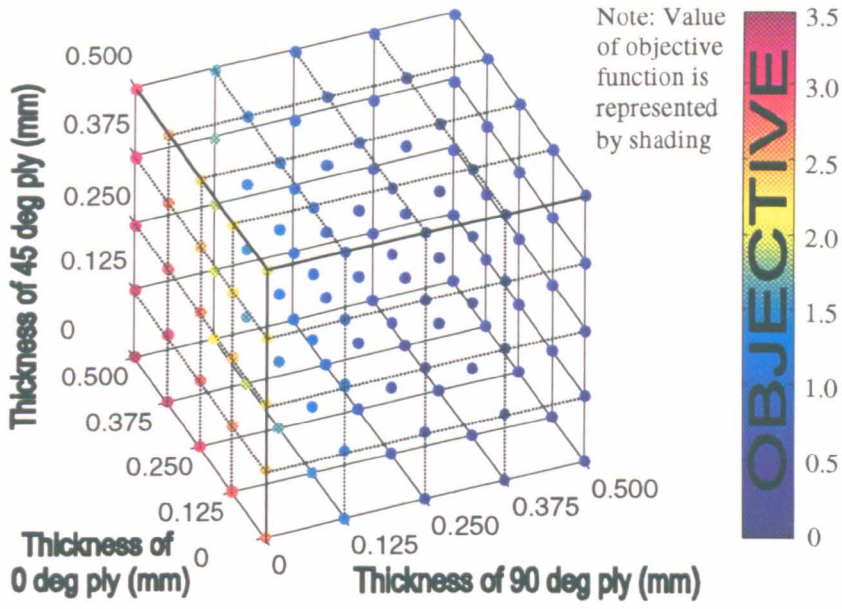

Figure 3.8 Variation of objective function across 3-dimensions of design space for 4-layer laminated cylindrical shell

Although the accuracy of the value of objective function at each point is limited by the colour perception of the human eye (or the quality of the printer or screen display used), this presentation does give physical insight into the nature of the design space in a compact, easy visual format.

From the earlier analytical work on this problem (section 3.3) and the exhaustive finite element results presented here (section 3.6), it is seen that this optimisation problem is convex provided that the design variables used are those described in section 3.1.

In this chapter, the exact location of the optimum discrete design point (given earlier in equation *(3.44)*) is only of incidental interest.

3.6.4 Sequential linear programming

With the knowledge that the design space is convex, it is possible to apply sequential linear programming (SLP) techniques to solve the problem.

The classical approach linearises the problem about the current design point (as described in Chapter 2) and evaluates the N-dimensional gradient of the objective function at this point using the finite difference method. The design is then perturbed in the direction of steepest descent (with appropriate move limits) and the process is repeated sequentially until convergence.

The objective function for this problem is highly non-linear in the chosen design space since there is a significant interaction between layers of +45° and -45° orientations in determining the torsional stiffness, GJ. This method nonetheless reliably succeeds in finding the optimum solution, since the problem is still convex, although the analysis requires several iterations. Since each iteration requires the gradients of the objective function to be evaluated via a computationally expensive finite-difference method, it is desirable to minimise the number of iterations required and hence the number of times that such gradients are calculated.

3.6.5 Global linear approximation based on multiple penalty functions.

A more efficient method considers each target variable (EA, EI_X, EI_Y and GJ) separately rather than combining them all into a single objective function. The problem then linearises the variation of the target variables about an initial design point.

3.6.5.1 Recoding design variables to minimise interactions

Some non-linearity of the target values with respect to design variables is acceptable as long as the problem is convex (since successive iterations of Newton's method will lead to convergence upon the optimum solution), however it is important to note that this approach approximates the whole design space in terms of simultaneous linear

equations. It is therefore important that there are minimal interactions between the design variables if this approach is to work robustly. If interactions between design variables are present, the design variables should be redefined such that interactions are minimised.

For example, the in-plane shear modulus of the laminate is mostly dependent on the interaction of +45° and -45° plies and not on the thickness of +45° or –45° on their own. Thus, in order to maximise the accuracy of the problem linearisation with respect to the design variables for this problem, it is necessary to choose the design variables to be

y_1 = internal radius of cylindrical shell
y_2 = thickness of balanced ±45° plies
y_3 = thickness of 0° plies
y_4 = thickness of 90° plies
y_5 = thickness of unbalanced 45° plies

The charts in Figure 3.9 plot the values of each cross-sectional property (normalised with respect to the target values) against the variation of each design variable, linearised about the point

$$\underline{y} = (18.0 \quad 0.001 \quad 0.001 \quad 0.001 \quad 0.001)^T \qquad (3.47.a)$$

(Since the FE code could not deal with zero-valued layer thicknesses, the analysis routine was written so that "zero" thicknesses were automatically set to 0.001 mm).

The charts in Figure 3.10 plot the same values, linearised about the optimum design point

$$\underline{y} = (19.4 \quad 1.000 \quad 0.125 \quad 0.375 \quad 0.001)^T \qquad (3.47.b)$$

These charts show that although each property varies almost linearly with each individual design variable over the entire design space, there is still some interaction

between the design variables. The coefficients for linearisation of the problem therefore vary from point to point within the design space.

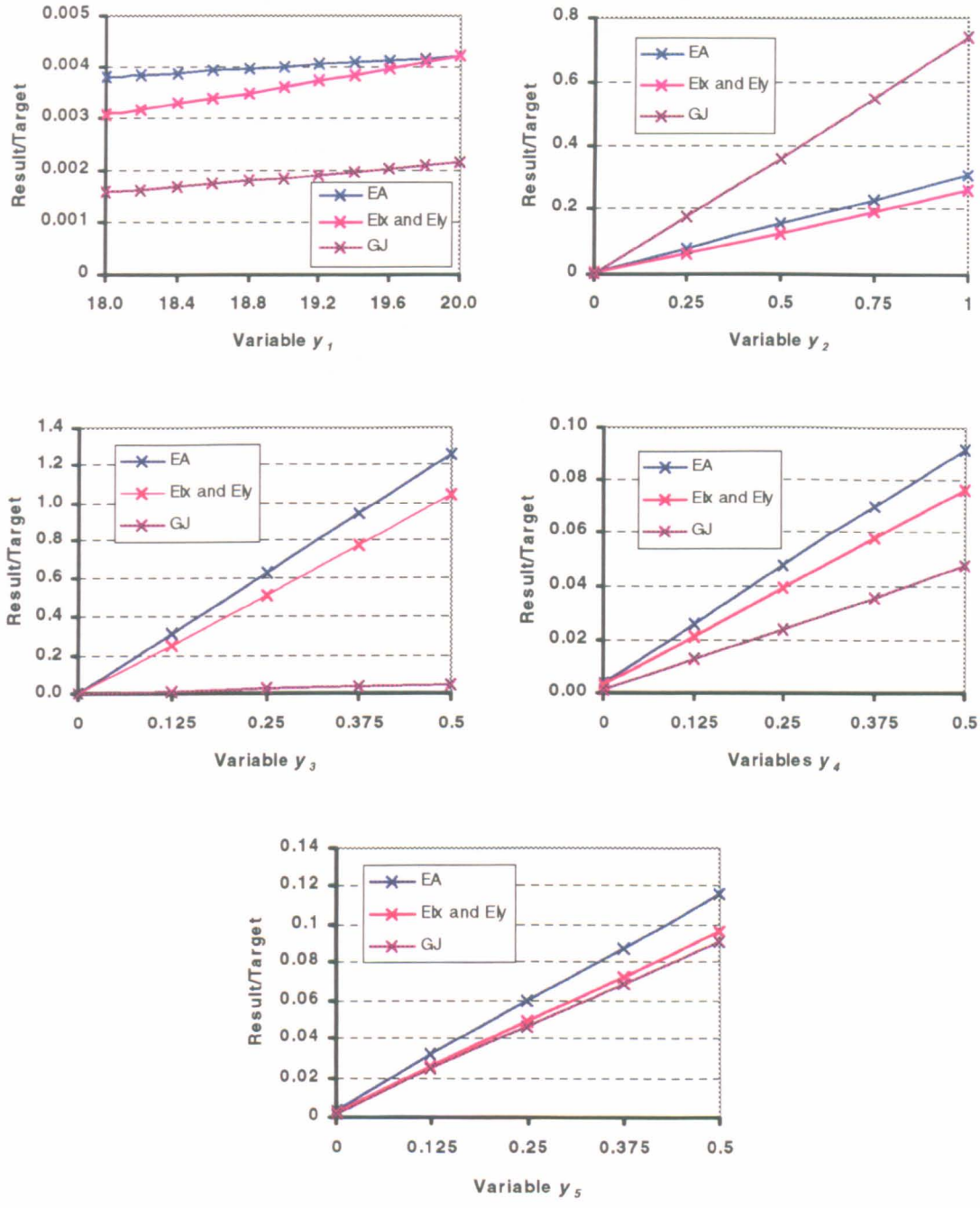

Figure 3.9 Variation of cross-sectional stiffness properties with respect to design variables, about an initial design point

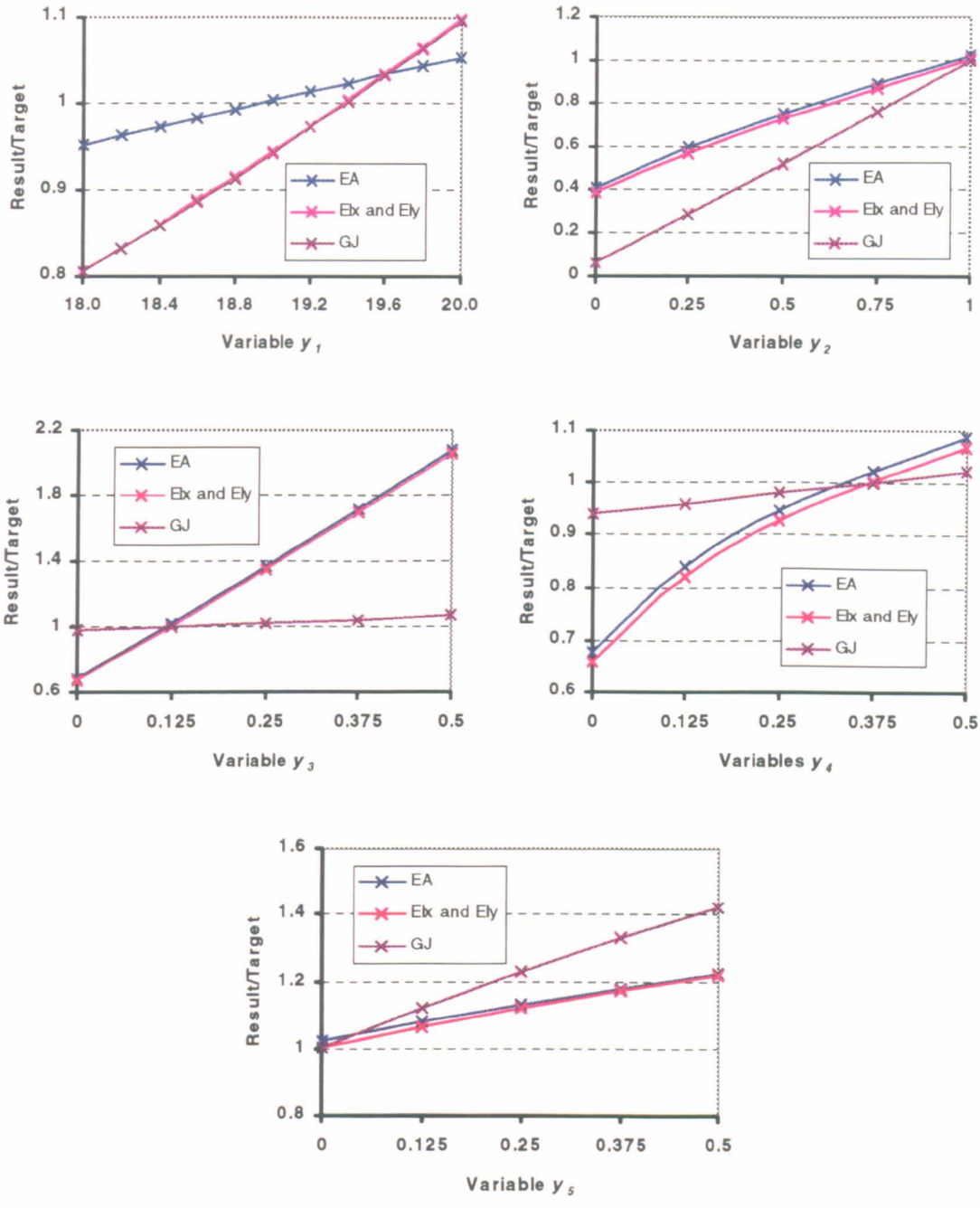

Figure 3.10 Variation of cross-sectional stiffness properties with respect to design variables, about optimum design point

Although there is still some non-linearity and interaction between the design variables, it is found that recoding the design variables from vector $\underline{x}$ to vector $\underline{y}$ has improved the linearity of the cross-sectional properties with respect to the design variables sufficiently to allow the optimum to be found by iterative application of a global linear approximation. This is discussed in the next section.

3.6.5.2 Solving the linearised problem

Assuming the targets may be approximated as being linearly related to the design variables, the problem can be expressed as N simultaneous linear equations where N is the number of target variables ($N = 4$ in this example). For this problem

$$
\begin{aligned}
EA_{new} &= EA_{old} + Z_{11}\Delta y_1 + Z_{12}\Delta y_2 + Z_{13}\Delta y_3 + Z_{14}\Delta y_4 + Z_{15}\Delta y_5 \\
EI_{Xnew} &= EI_{Xold} + Z_{21}\Delta y_1 + Z_{22}\Delta y_2 + Z_{23}\Delta y_3 + Z_{24}\Delta y_4 + Z_{25}\Delta y_5 \\
EI_{Ynew} &= EI_{Yold} + Z_{31}\Delta y_1 + Z_{32}\Delta y_2 + Z_{33}\Delta y_3 + Z_{34}\Delta y_4 + Z_{35}\Delta y_5 \\
GJ_{new} &= GJ_{old} + Z_{41}\Delta y_1 + Z_{42}\Delta y_2 + Z_{43}\Delta y_3 + Z_{44}\Delta y_4 + ZA_{45}\Delta y_5
\end{aligned}
\qquad (3.48.a\text{-}d)
$$

Since the linearisation about a given design point is (at least approximately) valid across the entire design space, the change in each design variable y_i (i.e. the perturbations, Δy_i) does not have to be small.

These simultaneous linear equations can be conveniently represented in matrix form as

$$
\begin{bmatrix}
Z_{11} & Z_{12} & Z_{13} & Z_{14} & Z_{15} \\
Z_{21} & Z_{22} & Z_{23} & Z_{24} & Z_{25} \\
Z_{31} & Z_{32} & Z_{33} & Z_{34} & Z_{35} \\
Z_{41} & Z_{42} & Z_{43} & Z_{44} & Z_{45}
\end{bmatrix}
\begin{pmatrix}
\Delta y_1 \\ \Delta y_2 \\ \Delta y_3 \\ \Delta y_4 \\ \Delta y_5
\end{pmatrix}
=
\begin{pmatrix}
EA_{new} - EA_{old} \\
EI_{Xnew} - EI_{Xold} \\
EI_{Ynew} - EI_{Yold} \\
GJ_{new} - GJ_{old}
\end{pmatrix}
\qquad (3.49)
$$

and generalised as

$$
\mathbf{Z}\,\Delta\underline{y} = \underline{b} \qquad (3.50)
$$

If weighting factors are to be included, this expression will take the form

$$
\mathbf{WZ}\,\Delta\underline{y} = \mathbf{W}\,\underline{b} \qquad (3.51)
$$

where

$$\mathbf{W} = \begin{pmatrix} W_1 & W_2 & W_3 & W_4 \end{pmatrix} \qquad (3.51.a)$$

As mentioned earlier, the inclusion of a weighting factor does not affect the position of the optimal solution if all of the target values can be matched exactly. However, if all target values cannot be matched simultaneously, the cross-sectional properties are "traded off" against each other. In such cases, the weightings do affect the solution, since a larger weighting implies that it is proportionally more important to match the cross-sectional property to which that weighting refers.

Both sides of the equation are premultiplied by $\mathbf{Z'}^{T}$, since this gives a least squared solution when the solution cannot be matched exactly - such as when the exact solution is infeasible, or when number of design variables is less than the number of target values. Thus, equation *(3.51)* becomes

$$\mathbf{Z'}^{T}\mathbf{Z'}\,\Delta\underline{y} = \mathbf{Z'}^{T}\mathbf{W}\,\underline{b} \qquad (3.52)$$

where

$$\mathbf{Z'} = \mathbf{WZ} \qquad (3.52.a)$$

from which $\Delta\underline{y}$ is found as

$$\Delta\underline{y} = (\mathbf{Z'}^{T}\mathbf{Z'})^{-1}\mathbf{Z'}^{T}\mathbf{W}\,\underline{b} \qquad (3.53)$$

to give a solution to the linearised problem. Since the real problem is not perfectly linear, Newton's method requires a few iterations of the linear solution to converge upon the solution to the real (non-linear) problem.

This global linear solution method has been coded into a C++ program and may be called as part of an optimisation routine. This program is listed in Appendix 6.3.

3.6.5.3 Types of linearised optimisation problem

Based upon the global linear approximation, three general types of optimisation problem are encountered. These three types of problems are discussed and illustrated with graphical examples to aid visualisation.

1. The number of design variables is less than the number of target values.

In some problems, the number of design variables is less than the number of target values. Consider the functions

$$f(x_1) = -4x_1 + 3$$
$$g(x_1) = 2x_1 - 1 \qquad (3.54.a\text{-}b)$$

which are shown on Figure 3.11. In this case the resulting matrix equation *(3.50)* is

$$\begin{bmatrix} -4 \\ 2 \end{bmatrix} x_1 = \begin{pmatrix} -3 \\ 1 \end{pmatrix} \qquad (3.55)$$

which is premultiplied by the transpose to give equation *(3.52)* as

$$\begin{bmatrix} -4 & 2 \end{bmatrix} \begin{bmatrix} -4 \\ 2 \end{bmatrix} x_1 = \begin{bmatrix} -4 & 2 \end{bmatrix} \begin{pmatrix} -3 \\ 1 \end{pmatrix} \qquad (3.56)$$

The solution of this equation ($x_1 = 0.7$) corresponds to a least squared error solution.

Figure 3.11 (below) illustrates that the solution to $f(x_1,0)$ lies at $x_1 = 0.75$, while the solution to $g(x_1,0)$ lies at $x_1 = 0.5$. The least squared error solution is $x_1 = 0.7$

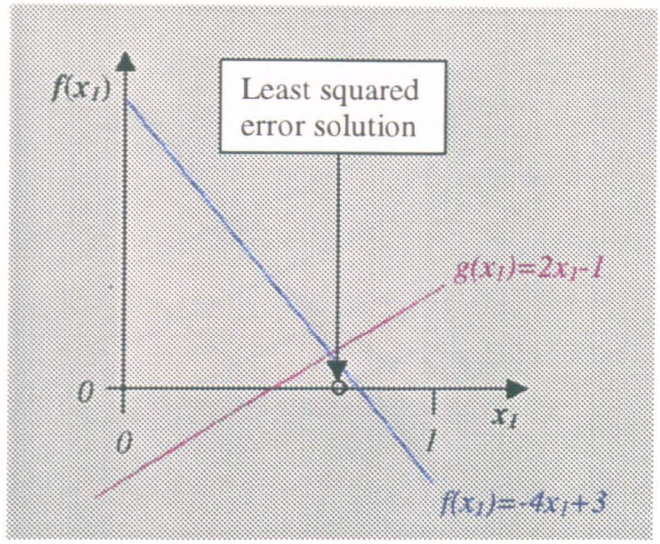

Figure 3.11 Two functions of one design variable

2. The number of design variables is exactly equal to the number of target values.

Figure 3.12 depicts contours of two independent functions (f, g) of two independent variables (x_1, x_2) where

$$f(x_1,x_2) = -4x_1 + 6x_2 + 3$$
$$g(x_1,x_2) = 2x_1 + 2x_2 - 2 \qquad (3.57.a\text{-}b)$$

and the design space is bounded by constraints that

$$0 \le x_1, x_2 \le 1 \qquad (3.57.c)$$

From Figure 3.12, it is obvious that there is only one solution (i.e. where $f(x_1,x_2) = g(x_1,x_2) = 0$), which lies at

$$x_1 = 0.9, x_2 = 0.1 \qquad (3.58)$$

which is marked on the figure.

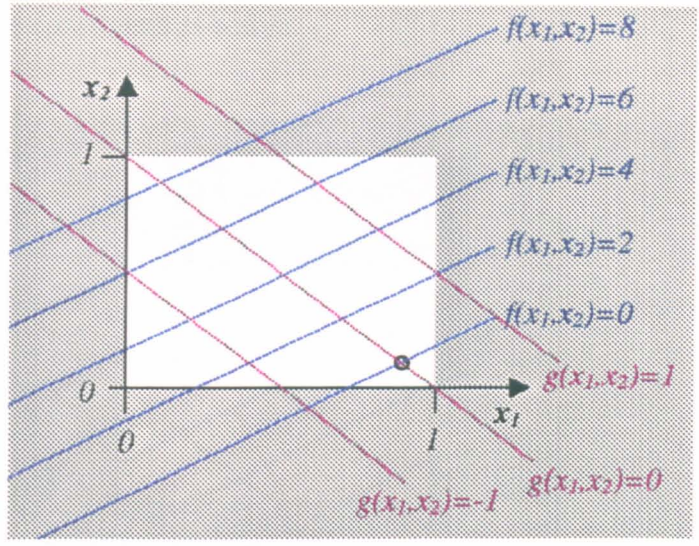

Figure 3.12 Two functions of two independent design variables

From an initial design, the solution of equation *(3.52)* moves the design directly to the solution as shown by the red arrow in Figure 3.13, below.

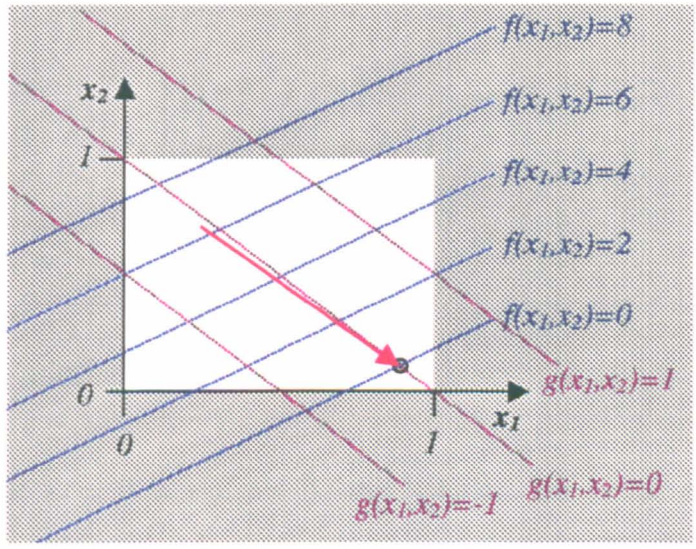

Figure 3.13 Solution lies within the feasible design space

Sometimes, the solution lies outside the feasible region. Figure 3.14 (below) shows contours of $f(x_1,x_2)$ and $g(x_1,x_2)$ where

$$f(x_1,x_2) = -4x_1 + 6x_2 + 3$$
$$g(x_1,x_2) = 2x_1 + 2x_2 - 1 \qquad (3.59.a\text{-}b)$$

subject to the same constraints as before.

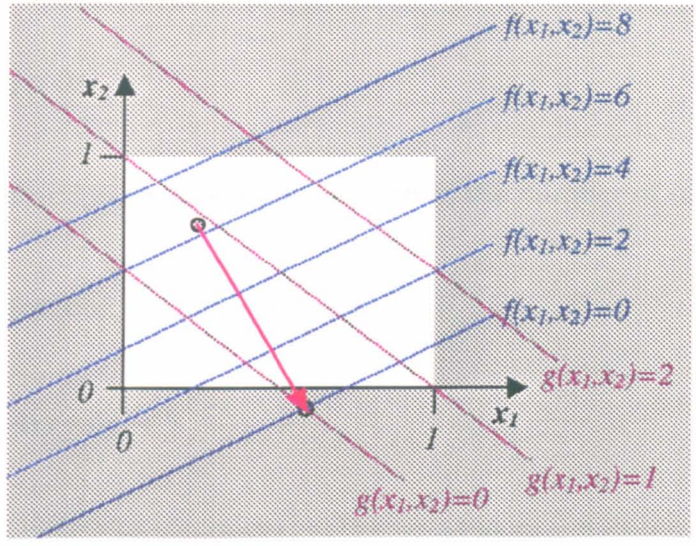

Figure 3.14 Solution lies outside the feasible design space

Equation *(3.52)* is written as

$$\begin{bmatrix} -4 & 2 \\ 6 & 2 \end{bmatrix}\begin{bmatrix} -4 & 6 \\ 2 & 2 \end{bmatrix}\begin{pmatrix} x_1 \\ x_2 \end{pmatrix}=\begin{bmatrix} -4 & 2 \\ 6 & 2 \end{bmatrix}\begin{pmatrix} -3 \\ 1 \end{pmatrix} \tag{3.60}$$

and the solution lies at

$$x_1 = 0.6,\ x_2 = -0.1 \tag{3.61}$$

The constraint that $x_2 = 0$ is violated by this solution. The value of x_2 is therefore returned to the feasible region ($x_2 = 0$) and made redundant. Equation *(3.52)* is then rewritten with only the remaining active variables as

$$\begin{bmatrix} -4 & 2 \end{bmatrix}\begin{bmatrix} -4 \\ 2 \end{bmatrix} x_1 = \begin{bmatrix} -4 & 2 \end{bmatrix}\begin{pmatrix} -3 \\ 1 \end{pmatrix} \tag{3.62}$$

and the solution process is repeated for variable x_1. Note that the optimum obtained is not an exact solution (since this lies outside the feasible design space), but it does

represent the best feasible solution. For this simple example, the optimum feasible solution is

$$x_1 = 0.7, x_2 = 0.0 \tag{3.63}$$

3. The number of design variables is greater than the number of target values

Consider a single function of two design variables

$$f(x_1,x_2) = -4x_1 + 6x_2 + 3 \tag{3.64}$$

which is subject to the same constraints as described earlier. As before, the dashed blue lines on the figure show contours of $f(x_1,x_2)$. However, in this case there are a number of feasible solutions, shown as the thick solid blue portion of the contour $f(x_1,x_2) = 0$ in Figure 3.15.

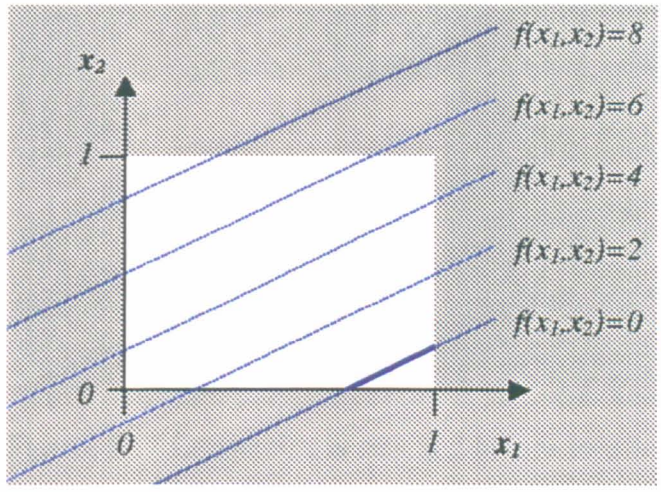

Figure 3.15 Range of solutions when number of design variables is greater than number of targets

When the design is perturbed from its initial point, one of two things will happen, depending upon the location of the initial design point. Either a solution is obtained as shown in Figure 3.16, below

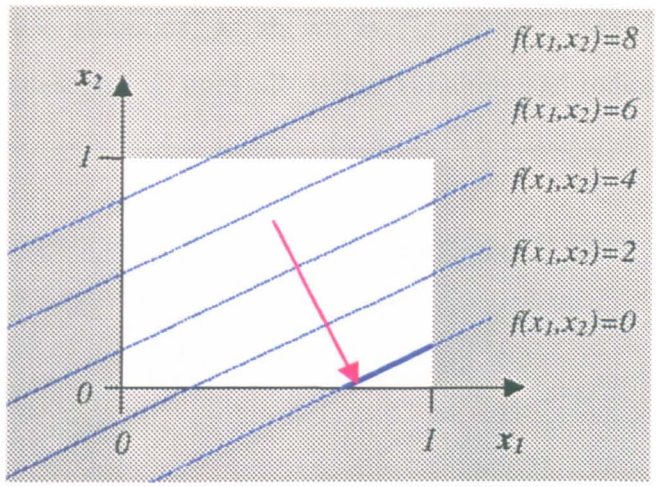

Figure 3.16 Solution is reached before constraint

or a constraint is reached (Figure 3.17, below). In the latter case, the design variable is returned to the edge of the feasible region, made redundant, and the optimisation is repeated with the active variables as described before.

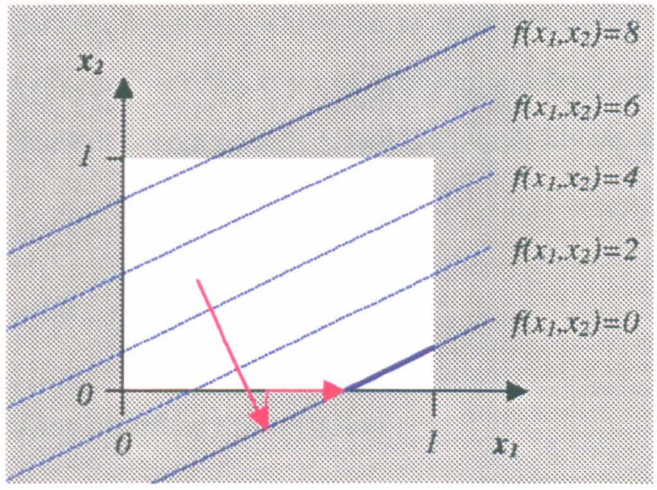

Figure 3.17 Constraint is reached before solution

In either case, the solution obtained is that which lies closest to the initial design point.

It is also possible that the solution lies outside of the feasible region. Consider the function

$$f(x_1,x_2) = -4x_1 + 6x_2 + 5 \qquad (3.65)$$

which has no feasible solutions, as shown in Figure 3.18, below. In this case, the optimisation keeps descending until all design variables are redundant due to active constraints.

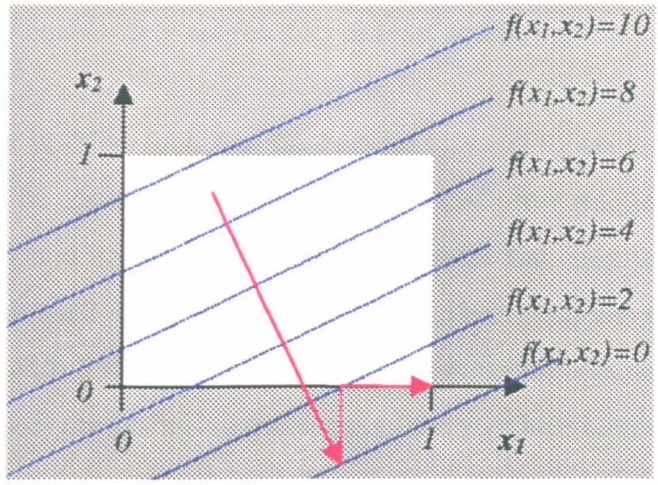

Figure 3.18 Solution lies outside feasible design space

As with the other classes of problem where the solution lies outside the feasible design space, the optimum obtained for this class of problem is a least squared error solution (i.e. the best design feasible design possible). In this example above, the optimum feasible solution is

$$x_1 = 1.0, x_2 = 0.0 \qquad (3.66)$$

3.6.6 Implications for practical optimisation

In the four-layer cylindrical shell case study presented in this chapter, it can be seen that there are four simultaneous equations *(3.48.a-d)* with five unknown design variables (y_1-y_5). Since two of the simultaneous equations are not independent ($EI_{XX} = EI_{YY}$ for a circular cylindrical shell), there are actually two degrees of redundancy and thus two of the design variables could be fixed (provided they are fixed at values so that the solution remains within the feasible design space).

Typically, a rotor blade optimisation might want to meet target values for a large number of cross-sectional properties. For complex problems, it is not straightforward to

determine the ranges of design variables that give feasible solutions, and many of the design variables will be subject to interdependent constraints (e.g. total thickness of a wall, rather than thickness of a particular layer). It is therefore usually preferable to allow redundant design variables to remain, since each redundancy gives an extra degree of freedom that may enable an exact solution to exist within the feasible design space.

If a design variable is fixed such that no feasible exact solution is possible, then the other variables will be optimised to give a least squared error solution. For example, if the cylindrical shell case study presented in this chapter had been to "design a 4-layer laminated cylindrical shell of 15mm internal radius", then the given target values could not have been met with a feasible solution. The optimisation routine returns a feasible solution that minimises the squares of the errors of the weighted target variables.

3.6.7 Effect of discretisation

The above discussion does not consider the effect of discretisation. This example problem is constrained because the ply thicknesses (variables y_2-y_5) are limited to 0.125mm increments.

Because the problem is convex, it is guaranteed that the best discretised solution is one that lies adjacent to the continuous solution. The simplest approach is to evaluate the discrete designs that immediately surround the continuous optimum and re-optimise the continuous variables for each point. Each solution can be obtained analytically by solving the matrix equation above, using the same values of Z_{ij} and searching through all the appropriate discretised combinations of Δy_i.

This will give 2^N discretised solutions, where N is the number of discretised variables. The best of these discrete solutions will be the discretised optimum. Depending on the accuracy of the linearisation and the degree of discretisation, the calculated discrete optimum may then be verified using finite element analysis.

As demonstrated by the work with lamination parameters, the case study used in this chapter did not have a single continuous optimum solution. The global linear

approximation method used to optimise the design highlights that this is because the problem has more design variables than target values. For this problem, the optimum discrete solution was found for this problem using the results of the exhaustive search.

In general, it is not straightforward to search every discrete point that lies adjacent to the continuous solution space in problems where there is not a unique continuous optimum. There remains no established procedure for determining the discrete optimum for such problems.

3.7 CONCLUSIONS

The iterative linear programming method presented here is considerably more efficient than either a stochastic method or a sequential linear program for the problem of meeting given cross-sectional properties.

This approach is possible because analytical calculations have enabled the design variables to be chosen such that the design space is convex and because simple approximations have been used to established suitable ranges for these design variables, and the problem may therefore be approximated by a number of linear relationships.

The iterative linear programming method cannot be reliably applied when the target variables are highly non-linear or non-convex functions of the design variables. One such target variable that is particularly important in the design of helicopter blades is flap-torsion coupling, as it is an important variable in aeroelastic tailoring. The next chapter looks at this property in detail, from analytical, computational and experimental perspectives.

4 MODELLING FLAP BENDING-TORSION COUPLING

4.1 BACKGROUND

4.1.1 Introduction

As a helicopter blade generates lift, it experiences a bending moment, which results in a bending deflection. If flap bending-torsion coupling is present, this bending moment will also generate a twist along the length of the blade, which will affect the angle of attack of the blade and hence the amount of lift and drag it produces. Coupling between flap bending and torsion is therefore of particular interest in helicopter blades, and is an important effect in the aeroelastic behaviour of any aerodynamic lifting surface.

This chapter details the development of an analytical model for the flap bending-torsion coupling term of a filled rectangular box section, which is similar to a rotor blade cross-section. The model is developed using a simple material stiffness based approach to determine the strains in an anisotropic cross section under an applied flap bending. The shear stresses throughout the cross-section are then calculated from these strains. The value of K_{45} is calculated from the moment of these shear stresses around the cross-section.

The analytical model is validated by comparison with finite element results. Comparison between finite element and experimental results is made in the next chapter.

Before treating this subject in any detail, it is necessary to define the co-ordinate system for the beam. The following global co-ordinate system (Figure 4.1) is commonly used in existing literature (e.g. Jung *et al* [1], Lin and Chan [67], Estivalez and Barrau [70], Rehfield *et al* [22]).

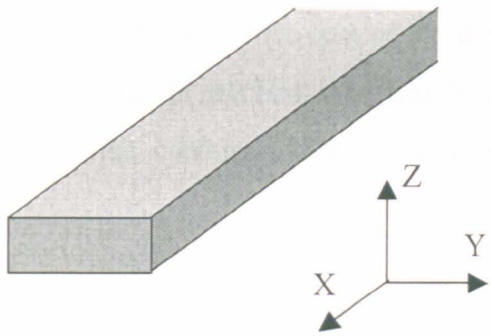

Figure 4.1 Global beam co-ordinate system

In addition to the co-ordinate system, it is also helpful to restate the nomenclature used in relation to the above co-ordinate system

Axial	– deflection in the *X*-direction
Lag	– deflection in the *Y*-direction
Flap	– deflection in the *Z*-direction

Thus, "flap bending" is bending about the *Y*-axis that results in *Z*-direction deflection of the beam. Twisting is the rate (per unit length) of twist about the *X*-axis. K_{45} is referred to as "flap bending-torsion coupling" because the value is given in the 4th row, 5th column of the stiffness matrix, which relates flap bending (κ_y) to the torsion force (M_{yz}) as highlighted on equation *(4.1)* below, which states

$$\begin{Bmatrix} N_x \\ N_{xy} \\ N_{xz} \\ M_{yz} \\ M_y \\ M_z \end{Bmatrix} = \begin{bmatrix} K_{11} & K_{12} & K_{13} & K_{14} & K_{15} & K_{16} \\ K_{12} & K_{22} & K_{23} & K_{24} & K_{25} & K_{26} \\ K_{13} & K_{23} & K_{33} & K_{34} & K_{35} & K_{36} \\ K_{14} & K_{24} & K_{34} & K_{44} & K_{45} & K_{46} \\ K_{15} & K_{25} & K_{35} & K_{45} & K_{55} & K_{56} \\ K_{16} & K_{26} & K_{36} & K_{46} & K_{56} & K_{66} \end{bmatrix} \begin{Bmatrix} \varepsilon_x \\ \gamma_{xy} \\ \gamma_{xz} \\ \kappa_{yz} \\ \kappa_y \\ \kappa_z \end{Bmatrix} \qquad (4.1)$$

Note that K_{45} also relates the flap bending moment (M_y) to the twist rate (κ_{yz}) in the 5th row, 4th column of the stiffness matrix.

Although K_{45} is commonly referred to simply as "flap-torsion coupling", this is not strictly correct since the total flap deflection is the sum of the shear deflection (due to γ_{xz}) and the bending deflection (due to κ_y). In practice, the shear deflection of a slender beam will be negligible compared to the bending deflection and the distinction is mostly semantic.

Since it is obtained directly from the stiffness matrix, K_{45} is not like other common stiffness terms (such as "axial stiffness", "bending stiffness" or "torsion stiffness" examined in Chapter 3), which are obtained by inverting the relevant term from the compliance matrix. The physical interpretation of K_{45} is therefore best not thought of in terms of conventional "stiffness", but "the torque (M_{yz}) required to prevent twisting when one unit of flapwise bending curvature (κ_y) is applied".

Implicit in this formulation of K_{45} directly from the stiffness matrix is the assumption that global axial (ε_x), flap-shear (γ_{xy}), lag-shear (γ_{xz}), and lag-bending (κ_z) strains for the cross-section are all constrained to be zero.

4.1.2 Sign conventions

The sign conventions for the beam coordinate system are based upon the conventional right-handed Cartesian axes shown in Figure 4.1 above. Figure 4.2 below shows the sign conventions that are used in classical laminate analysis.

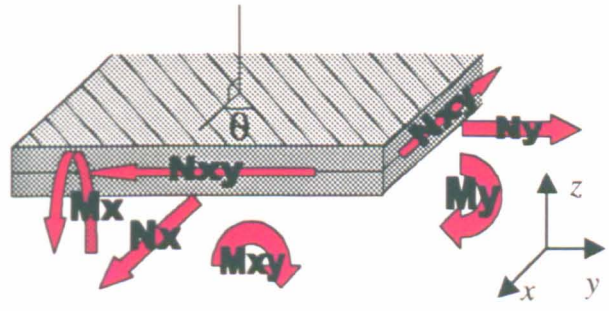

Figure 4.2 Laminate sign conventions

Note that although the *xyz* co-ordinate system is the same as that defined for the beam (described earlier) the associated stress and strain definitions for the laminate are not

necessarily consistent with those of the beam model. For example, the conventional definition of M_y in the beam coordinate system corresponds to $-M_x$ according to the conventions of classical laminate theory.

In order to maximise consistency with notation used in the relevant fields, the laminate strain calculations that follow later in this chapter are based on the laminate sign conventions, and the cross sectional shear stress calculations are based on the standard conventions for a Cartesian coordinate system.

4.1.3 Qualitative explanation of flap torsion coupling

Many subtle effects contribute to the overall flap torsion coupling behaviour of a section, which are considered in detail by the analytical model presented later. It is nonetheless useful to understand from a physical perspective how flap torsion coupling arises from a simplified, qualitative point of view. A suitable explanation is summarised below.

As the beam undergoes flap bending, the top and bottom surfaces will experience axial strain as shown in Figure 4.3 below.

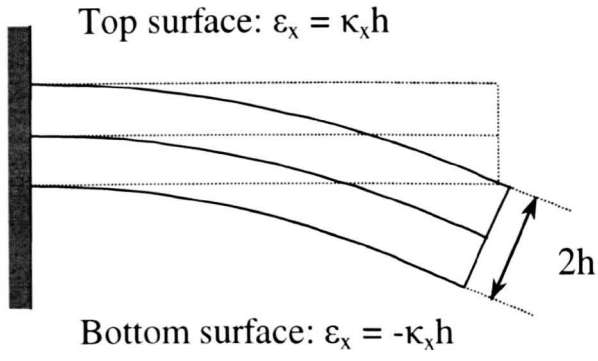

Figure 4.3 Axial strains on top and bottom surface due to flap bending

Consider the effect of these axial strains upon the anisotropic layers: the top and bottom laminates will want to shear in opposite directions as shown in Figure 4.4.

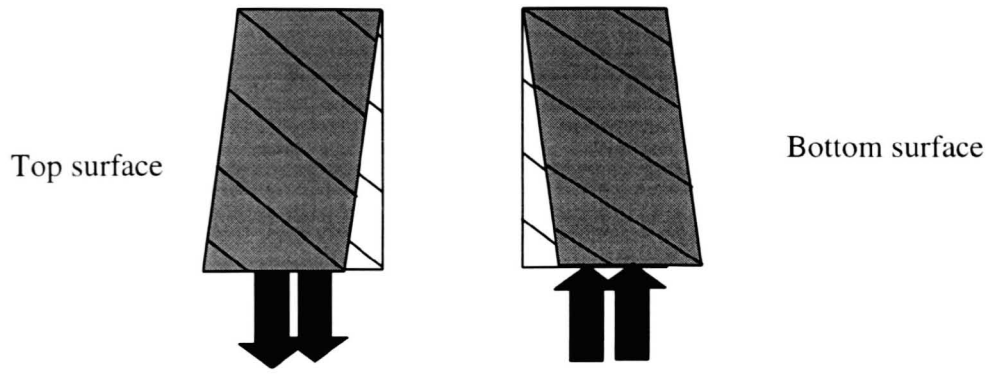

Figure 4.4 Top and bottom surfaces shear in opposite directions due to applied flap bending

If the cross-section is somehow constrained so that the top and bottom laminates cannot shear *relative to one another*, then the cross-section will have to twist (and/or warp) in order to accommodate the shearing of the top and bottom surfaces. This is shown on Figure 4.5 below.

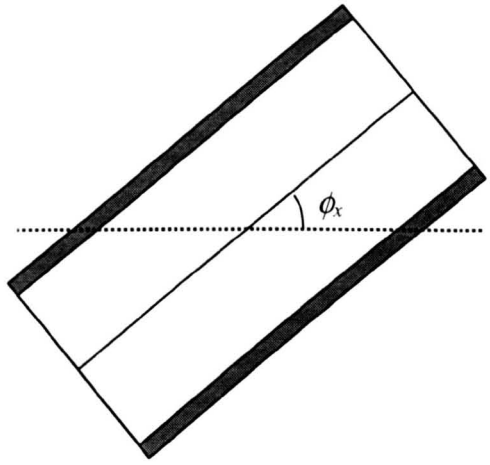

Figure 4.5 Cross-section tries to twist to accommodate differential shear of top and bottom surfaces

Since the definition of K_{45} prohibits twisting of the section, the value of K_{45} may be physically interpreted as the restraining moment required to prevent the section from twisting. Note that this is distinct from the "twist produced per unit bending deflection"

- K_{45} is not a direct measure of the twist rate along the length of a torsionally unrestrained beam.

4.2 LITERATURE

The two most comprehensive descriptions of stiffness matrix terms that are found in the literature are the thesis of Smith [19], and the work of Rehfield *et al* [22]. Their approaches and some of their inherent assumptions are summarised below.

4.2.1 Stiffness matrix analysis in Smith's thesis

The work of Smith [19] is not solely concerned with flap-torsion (K_{45}) coupling, but rather with the "Aeroelastic response and aeromechanical stability of Helicopters with elastically coupled composite rotor blades". However, the first section of the second chapter of that work is devoted to deriving the entire 6 x 6 stiffness matrix of the cross-section, of which K_{45} is only one term.

Smith models the rotor blade as a hollow, thin walled box section, shown in Figure 4.6 below.

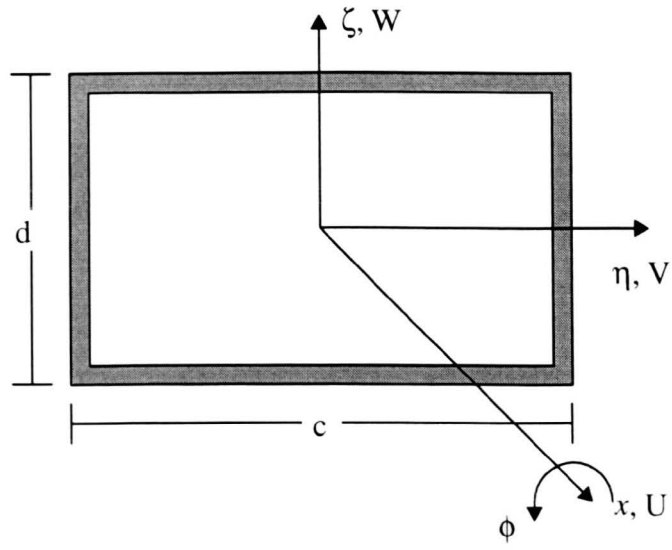

Figure 4.6 Smith's cross-sectional model

Smith assumes his total displacements in the x-, η- and ζ-directions to be

$$U = u(x) - \eta\left(v'(x) - \gamma^{o}_{x\eta}(x)\right) - \zeta\left(w'(x) - \gamma^{0}_{x\zeta}(x)\right) - \lambda\phi'(x) \qquad (4.2.a)$$

$$V = v(x) - \zeta\phi(x) \qquad (4.2.b)$$

$$W = w(x) + \eta\phi(x) \qquad (4.2.c)$$

respectively, where λ is the contour warping function and is transformed into the two dimensional cross sectional form, β, where

$$\lambda(\eta,\zeta) = \beta\eta\zeta \qquad (4.3.a)$$

$$\beta = -\frac{(1-\alpha)}{(1+\alpha)} \qquad (4.3.b)$$

$$\alpha = \left(\frac{c}{d}\right)\left(\frac{t_v}{t_h}\right)\left(\frac{G_v}{G_h}\right) \qquad (4.3.c)$$

Strains are determined by differentiating the displacement terms above. Smith assumes thin walls and neglects all strains except axial and inplane shear to give the following strain displacement relations.

For vertical walls

$$\varepsilon_{xx} = u' - \eta\left(v'' - \gamma'^{0}_{x\eta}\right) - \zeta\left(w'' - \gamma'^{0}_{x\zeta}\right) - \lambda\phi''$$

$$\varepsilon_{x\zeta} = \left(\eta - \frac{\partial\lambda}{\partial\zeta}\right)\phi' + \gamma^{0}_{x\zeta} \qquad (4.4.a\text{-}b)$$

For horizontal walls

$$\varepsilon_{xx} = u' - \eta\left(v'' - \gamma'^{0}_{x\eta}\right) - \zeta\left(w'' - \gamma'^{0}_{x\zeta}\right) - \lambda\phi''$$

$$\varepsilon_{x\eta} = -\left(\zeta + \frac{\partial\lambda}{\partial\eta}\right)\phi' + \gamma^{0}_{x\eta} \qquad (4.5.a\text{-}b)$$

Smith states "when the walls of the box beam are made of laminated composite-material plies, transverse inplane normal stresses and strains ... can become important". The inplane elastic constitutive relations for anisotropic laminate are therefore applied for vertical walls,

$$\begin{Bmatrix} \sigma_{xx} \\ \sigma_{\zeta\zeta} \\ \sigma_{x\zeta} \end{Bmatrix} = \begin{bmatrix} \overline{Q}_{11} & \overline{Q}_{12} & \overline{Q}_{16} \\ \overline{Q}_{12} & \overline{Q}_{22} & \overline{Q}_{26} \\ \overline{Q}_{16} & \overline{Q}_{26} & \overline{Q}_{66} \end{bmatrix} \begin{Bmatrix} \varepsilon_{xx} \\ \varepsilon_{\zeta\zeta} \\ \varepsilon_{x\zeta} \end{Bmatrix} \qquad (4.6)$$

and for horizontal walls

$$\begin{Bmatrix} \sigma_{xx} \\ \sigma_{\eta\eta} \\ \sigma_{x\eta} \end{Bmatrix} = \begin{bmatrix} \overline{Q}_{11} & \overline{Q}_{12} & \overline{Q}_{16} \\ \overline{Q}_{12} & \overline{Q}_{22} & \overline{Q}_{26} \\ \overline{Q}_{16} & \overline{Q}_{26} & \overline{Q}_{66} \end{bmatrix} \begin{Bmatrix} \varepsilon_{xx} \\ \varepsilon_{\eta\eta} \\ \varepsilon_{x\eta} \end{Bmatrix} \qquad (4.7)$$

and then imposes the following three conditions on the transverse inplane stresses:

$$\iint_h \sigma_{\eta\eta} dA + \iint_v \sigma_{\zeta\zeta} dA = 0$$

$$\iint_h \sigma_{\eta\eta} \eta dA + \iint_v \sigma_{\zeta\zeta} \eta dA = 0$$

$$\iint_h \sigma_{\eta\eta} \zeta dA + \iint_v \sigma_{\zeta\zeta} \zeta dA = 0 \qquad (4.8.a\text{-}c)$$

Smith's states that these conditions are "equivalent to setting the net inplane force and inplane bending moments to be zero".

The first assumption is clearly conservation of transverse force around the box section (equivalent to treating the box section as a membrane subject to an internal pressure), although physical interpretation of the second and third assumptions is unclear based on the co-ordinate system used by Smith (shown in Figure 4.6 above).

Moment equilibria for the inplane forces of horizontal and vertical walls might be expressed as

$$\iint_{h} \sigma_{\eta\eta} \zeta dA + \iint_{v} \sigma_{\zeta\zeta} \eta dA = 0 \qquad (4.8.d)$$

Despite the difficulties of interpretation, the use of the suggested inplane stress constraints ultimately leads to the correct derivation of Smith's cross sectional stiffness results.

The transverse inplane strains ($\varepsilon_{\eta\eta}$ and $\varepsilon_{\zeta\zeta}$) are determined to satisfy the conditions for transverse inplane stress. Based on Smith's conditions for transverse inplane stress, the transverse inplane strain is given as

$$\varepsilon_{\zeta\zeta} = au' + b\left(v'' - \gamma'^{0}_{x\eta}\right) + c\left(w'' - \gamma'^{0}_{x\zeta}\right) + d\phi' + e\phi'' + f\gamma^{0}_{x\eta} + g\gamma^{0}_{x\zeta} \qquad (4.9)$$

for a vertical wall. Smith assumes that the coefficients *a-g* are linear functions within the cross-section, i.e.

$$a = a_0 + a_1\eta + a_2\zeta$$
$$b = b_0 + b_1\eta + b_2\zeta \qquad (4.10.a\text{-}b)$$
$$etc.$$

where the constants a_i, b_i, *etc.* are determined by substituting the strain displacement equations *(4.4.a-b)* and *(4.9)* into the stress-strain relations of equation *(4.5)* to give stresses within the walls in terms of displacements of the beam cross-section, and then imposing the conditions on the inplane stresses *(4.7.a-c)*.

The stresses within the beam walls are now related to the net forces and moments acting over the cross-section by equilibrium as

$$F = \iint \sigma_{xx} dA$$

$$Q_y = \iint \sigma_{x\eta} dA$$

$$Q_z = \iint \sigma_{x\zeta} dA$$

$$T = \iint \left[\left(\eta - \frac{\partial \lambda}{\partial \zeta} \right) \sigma_{x\zeta} - \left(\zeta + \frac{\partial \lambda}{\partial \eta} \right) \sigma_{x\eta} \right] dA + \frac{\partial}{\partial x} \left[\iint \lambda \sigma_{xx} dA \right]$$

$$M_y = -\iint \sigma_{xx} \zeta dA$$

$$M_z = -\iint \sigma_{xx} \eta dA \qquad (4.11.a\text{-}f)$$

where

F	=	Axial force
Q_y	=	Lag shear force
Q_z	=	Flap shear force
T	=	Cross-section torque
M_y	=	Flap bending moment
M_z	=	Lag bending moment

Since the generalised internal forces are known explicitly in terms of displacements and membrane stiffness terms, and the relationship between internal forces, F, and generalised strains, u, may be expressed as

$$F = Ku \qquad (4.12)$$

where

$$F = \begin{bmatrix} F & Q_y & Q_z & T & M_y & M_z \end{bmatrix}^T \qquad (4.12.a)$$

$$u = \begin{bmatrix} u' & \gamma_{x\eta}^0 & \gamma_{x\zeta}^0 & \phi' & \left(w'' - \gamma_{x\zeta}'^0 \right) & \left(v'' - \gamma_{x\eta}'^0 \right) \end{bmatrix}^T \qquad (4.12.b)$$

The individual terms in the stiffness matrix are determined as the coefficients of the displacement terms from the force equilibrium integrals above. The full 21 terms of the stiffness matrix are not reproduced here, but the K_{45} term in the stiffness matrix (i.e. the expression for the flap torsion coupling) is determined by Smith to be

$$K_{45} = (1+\beta)\iint_{n} \overline{Q_{16}}\zeta^2 dA - (1+\beta)\iint_{n,v} \overline{Q_{12}}\zeta^2 dA \frac{\iint_{n,v} \overline{Q_{26}} dA}{\iint_{n,v} \overline{Q_{22}} dA} \qquad (4.13)$$

where the parameter β is the two dimensional cross-sectional form of the contour warping function, λ.

These calculations have been confirmed as correct if the analysis is based upon the assumptions stated earlier.

While the physical interpretation of equations *(4.7.b,c)* remains unclear, the expression Smith derives is of the same general form as derived in the present work, although the present work treats the cross-sections as laminates with full ABD matrix properties, as opposed to the purely in-plane properties of Smith's analysis.

4.2.2 Coupling parameters in Rehfield's work

A significant volume of work has been published on the coupling of aerospace structures. [18-23][28][31]. Rehfield *et al* [22] set out the calculation of the cross-sectional stiffness terms from first principles as described below. (Note that some variables have been renamed from the original paper for consistency with work elsewhere in this thesis). Their formulation has a pleasing mathematical elegance, and is not restricted to a particular cross-section, although it does make some assumptions about the behaviour of the cross-section.

A general thin walled prismatic beam is defined as shown in Figure 4.7 below, where

N_{xx} is the local axial stress in the shell.

N_{xs} is the local inplane shear stress in the shell

N_{ss} is the local transverse stress in the shell.

x, y, and z are the global co-ordinate axes

u, v, and w are the respective displacements in the x, y, and z directions

s is the circumferential coordinate around the shell

c is the circumference

Γ represents the cross-section shape

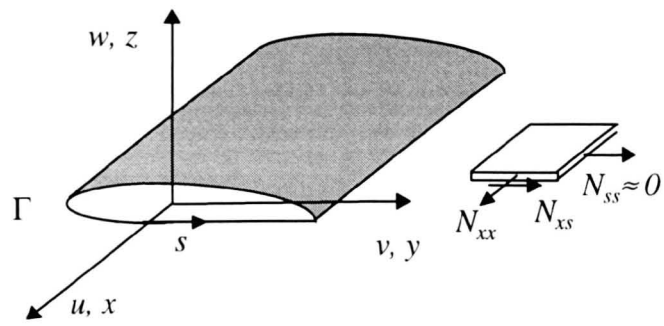

Figure 4.7 Coordinate system used by Rehfield *et al*

Firstly, the axial (ε_{xx}) and shear (γ_{xs}) strains are determined for any point in the cross-section (y, z), in terms of axial component of displacement ($U_{,x}$), twist and bending curvatures ($\phi_{,x}$, $\beta_{y,x}$, $\beta_{z,x}$), and a kinematic variable associated with torsional warping ($\phi_{,xx}$). The displacements are assumed to be (at most) linear functions of position.

$$\varepsilon_{xx} = U_{,x} - y\beta_{z,x} + z\beta_{y,x} + \psi\phi_{,xx}$$

$$\gamma_{xs} = \gamma_{xy}\frac{dy}{ds} + \gamma_{xz}\frac{dz}{ds} + \frac{2A}{c}\phi_{,x} \qquad (4.14.a\text{-}b)$$

The principle of virtual work states that the internal work (stresses and strains) is equal to the external work (applied forces and displacements) i.e.

$$\int_0^L \oint_\Gamma \left(N_{xx}\delta\varepsilon_{xx} + N_{xs}\delta\gamma_{xs}\right)dsdx - \delta W = 0 \qquad (4.15)$$

The equilibrium equations may thus be written as

$$\begin{aligned}
&N_{,x} + q_x = 0 \\
&Q_{y,x} + q_y = 0 \\
&Q_{z,x} + q_z = 0 \\
&M_{x,x} - Q_{w,xx} + m_x - q_{w,x} = 0 \\
&M_{y,x} - Q_z + m_y = 0 \\
&M_{z,x} + Q_y + m_z = 0
\end{aligned} \qquad (4.16.a\text{-}f)$$

where the seven generalised internal forces are defined as

$$\begin{aligned}
&\oint_\Gamma N_{xx}(1, z, -y, \psi)ds = \left(N, M_y, M_z, Q_w\right) \\
&\oint_\Gamma N_{xx}\left(\frac{dy}{ds}, \frac{dz}{ds}, \frac{2A}{c}\right)ds = \left(Q_y, Q_z, M_x\right)
\end{aligned} \qquad (4.17.a\text{-}g)$$

By assuming thin walled beams, local shell bending and twisting moments are ignored. By also assuming the internal pressure is zero; the hoop stress N_{ss} must also be zero. These are good assumptions when applied to hollow, thin walled cross-sections but may not be accurate when applied to filled, thick-walled cross-sections.

The constitutive relations for the membrane stiffness matrix are

$$\begin{aligned}
N_{xx} &= C_{11}\varepsilon_{xx} + C_{12}\gamma_{xs} \\
N_{xs} &= C_{12}\varepsilon_{xx} + C_{22}\gamma_{xs}
\end{aligned} \qquad (4.18.a\text{-}b)$$

where

$$C_{11} = A_{11} - \frac{A_{12}^2}{A_{22}}$$

$$C_{12} = A_{16} - \frac{A_{12}A_{26}}{A_{22}}$$

$$C_{22} = A_{66} - \frac{A_{26}^2}{A_{22}} \qquad (4.19.a\text{-}c)$$

with the A_{ij} terms determined from the translated reduced stiffnesses in the usual manner.

Thus, the generalised internal forces are known explicitly in terms of displacements and membrane stiffness terms, and the relationship between internal forces, F, and generalised strains, u, may be expressed as

$$F = Ku \qquad (4.20)$$

where

$$F = \begin{bmatrix} N & Q_y & Q_z & M_x & M_y & M_z & Q_w \end{bmatrix}^T$$

$$u = \begin{bmatrix} U_{,x} & \gamma_{xy} & \gamma_{xz} & \phi_{,x} & \beta_{y,x} & \beta_{z,x} & \phi_{,xx} \end{bmatrix} \qquad (4.20.a\text{-}b)$$

The stiffness matrix terms are determined by matching the relevant terms from the integrals for generalised internal forces, to obtain all 28 terms in the 7 x 7 beam stiffness matrix. The full 28 terms are not reproduced here, but the K_{45} term in the stiffness matrix (i.e. the expression for the flap torsion coupling) is determined to be

$$K_{45} = \frac{2A}{c} \oint C_{12} z ds \qquad (4.21)$$

where A is the area enclosed by the section and c is the distance around the cross section.

For the simplified cross-section studied in [21] (shown in Figure 4.8, below), this becomes

$$K_{45} = \frac{C_S^2 H^2}{(C_S + H)}\left(A_{16} - \frac{A_{26}A_{12}}{A_{22}}\right) \qquad (4.22)$$

where C_S and H are defined as illustrated.

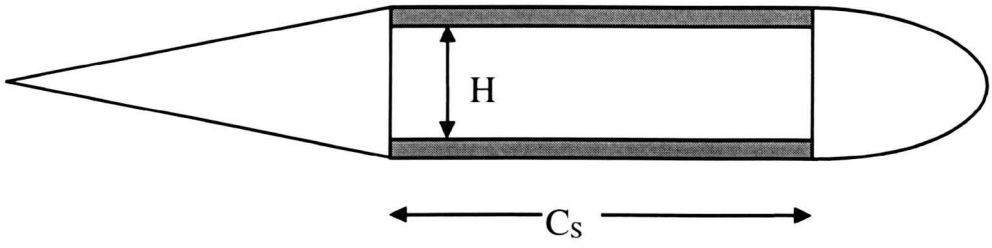

Figure 4.8 Rehfield and Cheung's cross-sectional model

Only the shaded parts are assumed to be load bearing - the other elements are non-structural. Although Rehfield and Cheung [21] do not detail the calculations, the process is clearly based on the results of earlier work [22]. For the case of identical upper and lower covers, the result for K_{45} is

$$\begin{aligned} K_{45} &= \frac{2A}{c}\oint C_{12} z ds \\ &= \frac{C_S^2 H^2}{(C_S + H)} C_{12} \end{aligned} \qquad (4.23)$$

where C_{12} is defined in equation *(4.19.b)* above.

The assumptions of Rehfield's work are that there is no transverse force upon the load bearing structure. i.e.

$$N_y = 0 \qquad (4.24)$$

While this assumption may be appropriate for sandwich sections with a low modulus core (or for box sections with very flexible vertical walls), it is unlikely to accurately model a real helicopter rotor blade cross-section. The effect of this upon the cross-sectional coupling terms is investigated later by comparing this model with the results of finite element analyses of various box sections.

It is interesting to note Rehfield and Cheung [21] define a "bend-twist parameter", β as

$$\beta = \frac{C_{45}^{\ 2}}{C_{44}C_{55}} = \frac{(A_{16} - A_{12}A_{26})^2}{(A_{11} - A_{12}^{\ 2})(A_{66} - A_{26}^{\ 2})} \tag{4.25}$$

The bend-twist parameter, β is possibly a more intuitive measure of bend twist coupling than K_{45}, since its value is effectively a measure of the amount of rotation for a given bending deflection.

Note that Rehfield and Cheung's bend twist parameter, β is not in any way related to Smith's cross-sectional warping function, β.

4.3 ANALYTICAL MODEL

In contrast to the work of Smith [19] and Rehfield *et al* [22], this thesis is seeking to produce a model only for flap torsion coupling of a section that has features that are more representative of a typical helicopter rotor blade. This will help to determine which design parameters are important in determining the value of K_{45}, and give increased physical understanding of the interactions that cause K_{45} coupling in helicopter rotor blade sections – thereby enabling suitable design variables to be chosen for the optimisation of this property.

A stiffness of materials based approach is adopted, which allows significantly more freedom in modelling specific features of the cross-section while producing a mathematical model with a manageable level of complexity. The values for K_{45} derived using this method are compared later with those obtained using the methods of Smith [19] and Rehfield *et al* [22].

4.3.1 Features of the analytical model

The analysis of K_{45} in this thesis looks at a general filled box section, as depicted in Figure 4.9 below. Although some ply angles and lay-up examined have been pre-specified in this work, the analysis method is valid for any laminate configuration. A number of variables are defined in relation to the geometry of the section, as shown on the figure.

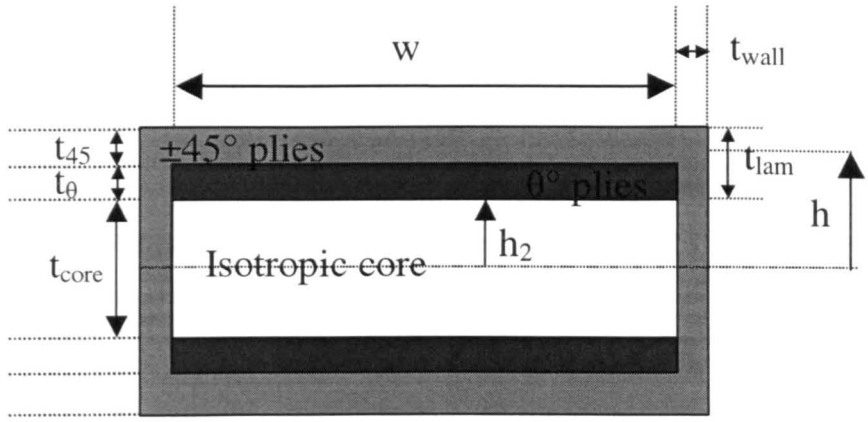

Figure 4.9 Cross-sectional features of analytical model

A local *xyz* co-ordinate system is defined for the cross-section such that when the beam is undeformed, the *xyz*-local (cross-sectional) and *XYZ*-global (beam) co-ordinate systems are coincident. i.e.

x = spanwise direction

y = lag direction

z = flap direction

The cross-sectional model has several features, some of which (e.g. lay-up and stacking of laminates) have been constrained here for simplicity of analysis, although the analyses described in this chapter are valid for any general filled box section.

1. **Horizontal laminates** made from balanced ±45° plies (which are assumed to be homogeneous in this model) and unbalanced plies laid up at a variable angle $\theta°$. The thickness of the ±45° plies (t_{45}) and the θ° plies (t_θ) are independently variable, and the mid-plane of these top and bottom laminates are placed a variable distance (h) from the neutral axis of the cross-section.

2. **Vertical laminated walls** to the box section are assumed to be made from balanced ±45° plies (which are again assumed to be homogeneous in this model). The thickness of the vertical walls (t_v) is independently variable, and the inside edge of the vertical walls is set at a width (w) apart.

3. The box section is filled with an isotropic **core material**. The Poisson ratio (ν) can be varied, but is set to 0.3 in this work. The Young's modulus (E) and (by implication) the shear modulus (G) are variable.

Note that this model explicitly considers both the thicknesses and out of plane behaviour of the laminates and the effect of the core material - features that are not considered in the analyses of Smith [19] and Rehfield *et al* [22].

4.3.2 Analysis procedure

The analysis procedure may be broken down into a number of steps, outlined below

1. Apply a unit bending deflection to the cross-section, and write down expressions for strains in the horizontal laminates
2. Determine the forces acting on laminate due to vertical walls and core material
3. Determine the resulting strains on the horizontal laminates from the ABD stiffness matrix, and hence strains throughout the entire cross-section.
4. Calculate shear stresses over the entire cross-section.
5. Integrate the moment of shear flow (about the beam centroid) around the entire cross-section

These stages are now detailed below.

4.3.3 Strains on the top and bottom laminates

Based on the simplified, qualitative physical interpretation of how K_{45} arises (section 4.1.3), it will be appreciated that applying flap-bending to the beam will generate shear stresses in the top and bottom laminates. This understanding is supported by Smith's statement that "elastic coupling between flap bending and torsion, K_{45} arises from the top and bottom walls of the beam" [19], and also by Ganguli and Chopra [30].

Obviously, the independent, unconstrained deformations of the laminates, walls and core would usually be incompatible with each other under an applied loading. Since the cross-section does not come apart under loading, the actual strains of each of these component parts must be compatible. Enforcing compatibility between these component parts gives rise to internal stresses and resultant forces between them.

Consider the deflection of a simple piece of isotropic core material as it is placed under unit flap bending curvature. The strains (ε_x, ε_y, γ_{xy}) and curvatures (κ_x, κ_y, κ_{xy}) of the top surface of the core (to which the upper horizontal laminate would be attached) would be

$$\varepsilon_x = h\kappa_x$$
$$\varepsilon_y = -\nu h\kappa_x$$
$$\gamma_{xy} = 0$$
$$\kappa_x = 1$$
$$\kappa_y = -\nu\kappa_x$$
$$\kappa_{xy} = 0 \qquad \textit{(4.26.a-f)}$$

Consider that for a complete box section, the vertical walls and the top and bottom horizontal laminates will cause the strains of the top and bottoms surface of the core material to differ from those of the unconstrained isotropic core material by some finite amount (Δ_1, Δ_2, and Δ_3) where

Δ_1 is the change in transverse strain, ε_y

Δ_2 is the change in shear strain, γ_{xy}

Δ_3 is the change in transverse bending curvature, κ_y

The strains of the top surface of the core are therefore

$$\varepsilon_x = h\kappa_x$$
$$\varepsilon_y = -\nu h\kappa_x + \Delta_1$$
$$\gamma_{xy} = \Delta_2$$
$$\kappa_x = 1$$
$$\kappa_y = -\nu\kappa_x + \Delta_3$$
$$\kappa_{xy} = 0 \qquad (4.27.a\text{-}f)$$

and each of the component parts of the cross-section (laminates, walls and core) will be in a state of internal stress and will exert forces on the components around them. Note that since the deformations of the upper horizontal laminate are constrained to be compatible with the structures to which they are joined, equations *(4.27.a-f)* also represent the strains on the upper horizontal laminate.

Note that equation *(4.27.f)* above assumes that the twist (κ_{xy}) of the upper horizontal laminate is zero. In fact, the definition of K_{45} only requires that the twist of the cross section *as a whole* is zero. This raises interesting questions about the nature of the idealisation of a slender 3-dimensional structure as a 1-dimensional beam and the deformations that are acceptable, such as "What *specifically* constitutes twist of a 1-D beam?" and "Can a beam be considered not to have twisted if parts of its substructure have twisted?"

More importantly, the principle of considering 1-D beam with an associated *cross sectional stiffness matrix* implies that the cross sectional stiffness matrix is based solely on the cross section, i.e. that it is independent of length. Any proposed cross sectional

deformation must therefore be compatible over an infinitely long beam. Figure 4.10 illustrates two possible deformations of the beam at intervals along its length if the top and bottom laminates are allowed to twist.

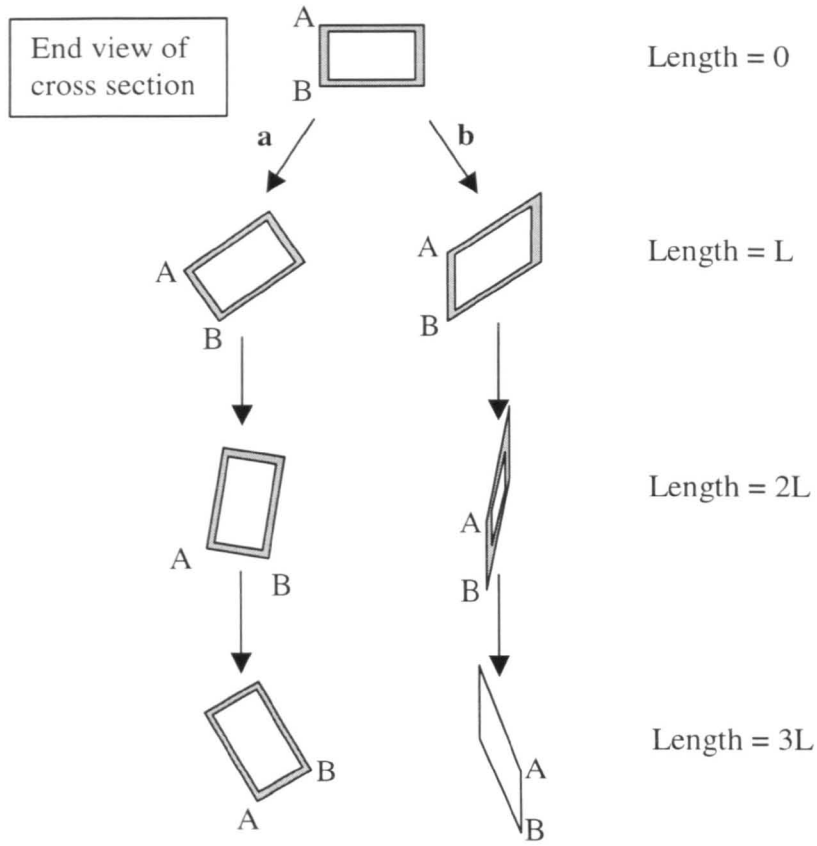

Figure 4.10 Deformation of cross section along the length of a beam if horizontal laminates are allowed to twist ($\kappa_{xy} \neq 0$)

In case (a), twist is accommodated by twist of the whole beam. Although this deformation is compatible with an infinitely long beam, it clearly violates the definition of K_{45} as "the torque (M_{yz}) required *to prevent twisting* when one unit of flapwise bending curvature (κ_y) is applied".

Considering case (b), it is clear that if the "top" and "bottom" laminates have a twist rate of say, 40/L °/m, then (based on the 1-D idealisation) these laminates will have twisted 80° in length 2L, and by 120° in length 3L. Looking at the positions of nodes A and B on the corners of the cross section, it becomes clear that case (b) cannot be a valid

deformation for a 1-D idealisation of a 3-D structure, since the cross sectional deformations become unfeasible for an infinitely long beam.

The twist of the top laminate (κ_{xy}) is therefore assumed to be zero in the beam cross section.

When flap-bending is applied, the cross-section of the beam may deform to look something like that shown in Figure 4.11.

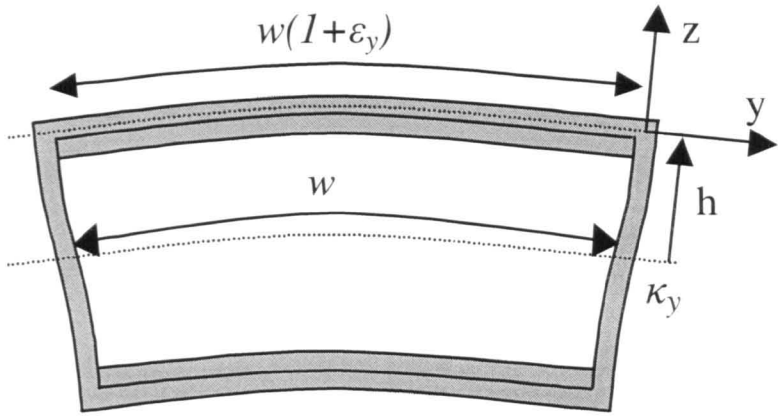

Figure 4.11 Deformation of cross-section due to applied bending

4.3.4 Forces on the top and bottom laminates

This section determines the forces acting upon the top laminate that are caused by enforcing compatibility of strains between the component parts of the cross-section as described above.

4.3.4.1 Transverse force, N_y.

Contribution from walls

If the vertical walls are not completely stiff, it can be seen that the walls will deflect by some amount, δ. The overall deformation is shown on the diagram below, and the deflection of the walls is highlighted on Figure 4.12, below.

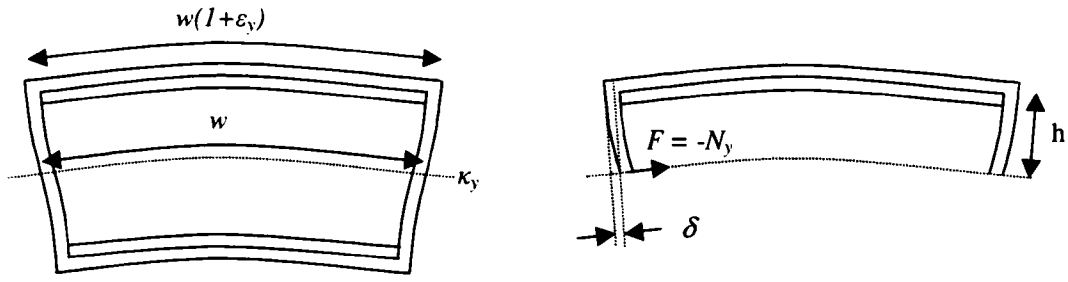

Figure 4.12 Deflection of vertical walls and resultant force on laminates

From geometry, it can be seen that

$$(w+2\delta)(1+h\kappa_y) = w(1+\varepsilon_y) \tag{4.28}$$

This formulation leads to non-linear equations. However, provided that

$$2\delta << w$$
$$h\kappa_y << 1 \tag{4.29.a-b}$$

then

$$\varepsilon_y = h\kappa_y + \frac{2\delta}{w} \tag{4.30}$$

Note that the theory of reducing a 3-dimensional structure to a 1-dimensional beam with a cross-sectional stiffness matrix implicitly assumes small deformations (i.e. linear geometry) so the above assumption is automatically justified.

From static equilibrium, the transverse forces upon the top laminate are

$$N_y = -F \tag{4.31}$$

The deflection of each vertical wall is given by a standard bending deflection term, plus a Timoshenko shear term

$$\delta = -N_y \left(\frac{h^3}{3E_{wall} I_{wall}} + \frac{h}{t_{wall} G_{yz(wall)}} \right) \tag{4.32}$$

where $E_{wall}I_{wall}$ is the bending stiffness of a vertical wall in the y-direction and $G_{yz(wall)}$ is the shear modulus of the vertical wall in the yz plane. Substituting into equation *(4.30)* gives

$$h\kappa_y = \varepsilon_y + N_y \frac{2h}{w} \left(\frac{h^2}{3E_{wall} I_{wall}} + \frac{1}{t_{wall} G_{yz(wall)}} \right) \tag{4.33}$$

Thus, the transverse force due to the vertical walls is

$$\begin{aligned} N_y &= \frac{h\kappa_y - \varepsilon_y}{\frac{2h}{w} \left(\frac{h^2}{3E_{wall} I_{wall}} + \frac{1}{t_{wall} G_{yz(wall)}} \right)} \\ &= \frac{h\Delta_3 - \Delta_1}{\frac{2h}{w} \left(\frac{h^2}{3E_{wall} I_{wall}} + \frac{1}{t_{wall} G_{yz(wall)}} \right)} \end{aligned} \tag{4.34}$$

Contribution from core material

If the horizontal laminates and vertical walls had no effect, the core material would simply deform according to its Poisson behaviour, and the strain on the top surface would be

$$\varepsilon_y = -\nu h \kappa_x \tag{4.35}$$

The effect of the laminates and walls will cause the actual transverse strain of the top surface to differ by some amount, Δ_1, so that

$$\varepsilon_y = -\nu h \kappa_x + \Delta_1 \tag{4.36}$$

and as a result, there will be a resultant force on the laminate from the core material. The transverse strain in the section is assumed to vary linearly through the depth, and is analogous to bending. However, for clarity, a change in transverse strain of the top surface (Δ_1) is illustrated in Figure 4.13 without any bending deformation shown.

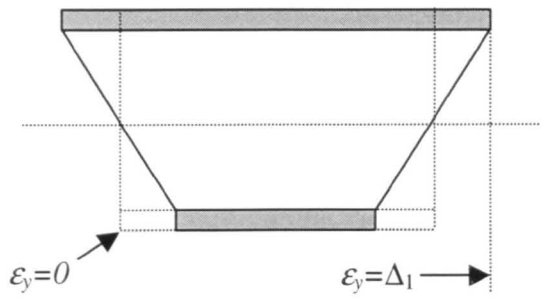

Figure 4.13 Strain on laminates due to deflection of core

The overall deviation of the core from its unrestrained deflection is δ_K, where

$$\delta_K = \frac{-\Delta_1}{h} \tag{4.37}$$

The moment required to produce this deviation is

$$\begin{aligned} M_y &= -\frac{1}{2} E_{core} I_{core} \delta_K \\ &= \frac{E_{core} I_{core} \Delta_1}{2h} \end{aligned} \tag{4.38}$$

where $E_{core}I_{core}$ is the bending stiffness of the core material. The transverse inplane force on the laminates, N_y that produces such a bending moment on the section is

$$\begin{aligned} N_y &= -\frac{M_y}{h} \\ &= -\frac{E_{core} I_{core} \Delta_1}{2h^2} \end{aligned} \tag{4.39}$$

Total transverse force, N_y

The total transverse force on one laminate is therefore given by

$$N_y = \frac{h\Delta_3 - \Delta_1}{\frac{2h}{w}\left(\frac{h^2}{3E_{wall}I_{wall}} + \frac{1}{t_{wall}G_{yz(wall)}}\right)} - \frac{E_{core}I_{core}\Delta_1}{2h^2} \qquad (4.40)$$

4.3.4.2 Shear force, N_{xy}

The physical visualisation and calculation of shear force is particularly interesting. Since the beam is infinitely long, the top and bottom surfaces cannot displace relative to one another in the conventional sense, since this would lead to infinite displacements of the vertical walls and core material, as illustrated in Figure 4.14 below.

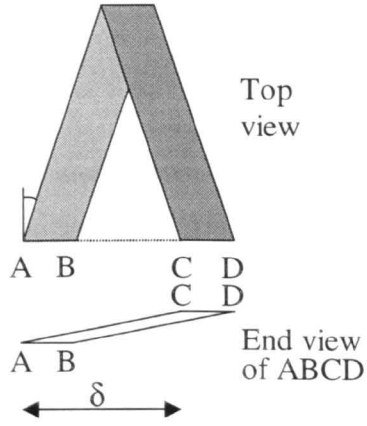

Figure 4.14 Relative shear of top and bottom surfaces

A possible deformation of the beam that incorporates shear of the top and bottom laminates would be for the section to twist along its length at a twist rate of

$$\frac{\phi}{l} = \frac{\gamma}{h} \qquad (4.41)$$

as shown in Figure 4.5. Since twisting of the section is explicitly restrained by the working definition of K_{45} given earlier, this type of deformation cannot occur. The only other deformation of the beam that allows the top and bottom laminates to shear is longitudinal warping.

The actual restraints imposed on a helicopter blade cross-section might not allow longitudinal warping near the blade root. In this case,

$$\gamma_{xy} = \Delta_2 = 0 \tag{4.42}$$

however, since restrained warping is only of importance at a constraint such as a fixed end, warping freedom is retained in this analysis. The work of Hill and Weaver [34] (based on the work of Bartholomew and Mercer [40]) implicitly assumes that the beam is free to undergo longitudinal warping, so the results this modelling should be consistent with finite element analysis based on their work.

Contribution from walls

Consider a box section where the top and bottom laminates have sheared by γ_{xy}, and that the structure has warped to accommodate this deflection, as shown by Figure 4.15.

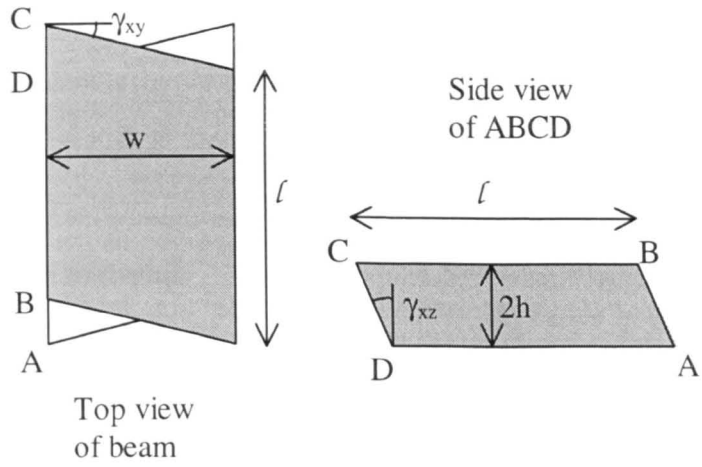

Figure 4.15 Shear deflection of top and bottom laminates accommodated by warping of the section

Consider the shear force (S) on the edge BC. Considering equilibrium of the horizontal laminate gives

$$S = N_{xy} l \tag{4.43.a}$$

and considering equilibrium of the vertical wall gives

$$S = G_{xz(wall)} t_{wall} l \gamma_{xz(wall)} \tag{4.43.b}$$

Now consider the out of plane warping deflection, δ. Equating longitudinal displacements when looking from above gives

$$\delta(\frac{w}{2}, h) = \frac{w}{2} \gamma_{xy(lam)} \tag{4.44.a}$$

When looking from the side view it is clear that

$$\delta(\frac{w}{2}, h) = h \gamma_{xz(wall)} \tag{4.44.b}$$

Thus, eliminating δ, $\gamma_{xz(wall)}$, and S gives

$$N_{xy} = \frac{G_{xz(wall)} t_{wall} w}{2h} \gamma_{xy(lam)} \tag{4.45}$$

Contribution from core material

The same approach is used to calculate the contribution of the core material, except that in this case, the shear of the core material is assumed to vary linearly across the width of the section, from a value of $\gamma_{xz}(w/2,z)$ at $y=w/2$ (as shown on Figure 4.15) to $\gamma_{xz}(-w/2,z)$ at $y=-w/2$. The shear, $\gamma_{xz}(y,z)$ at a point a distance, y from the vertical mid-plane of the section is therefore given by

$$\gamma_{xz}(y,z) = \gamma_{xz}(w/2,z)\frac{2y}{w} \qquad (4.46.a)$$

Consider the shear force from laminate balanced by varying shear force from core. Moments of S about a vertical axis through the laminate give

$$S = N_{xy}l \qquad (4.46.b)$$

and moments of shear force from a strip of core material of width δy give

$$dS = G_{core}l\gamma_{xz}(y,z)dy \qquad (4.46.c)$$

Thus

$$\int dS = \frac{2G_{core}l\gamma_{xz}(w/2,z)}{w}\int_0^{w/2} ydy \qquad (4.47.a)$$

$$S = \frac{1}{4}G_{core}lw\gamma_{xz}(w/2,z) \qquad (4.47.b)$$

Now consider the out of plane warping deflection, δ. Equating displacements when looking from above gives

$$\delta = w\gamma_{xy(lam)} \qquad (4.48.a)$$

When looking from the side view it is clear that

$$\delta = 2h\gamma_{xz}(w/2,z) \qquad (4.48.b)$$

Thus, eliminating δ, $\gamma_{xz}(w/2,z)$, and S gives

$$N_{xy} = \frac{1}{4}\frac{G_{core}w^2}{2h}\gamma_{xy(lam)} \tag{4.49}$$

However, this is only part of the resistance provided by the core material. So far, only the shearing of the core material evident from the side view has been considered. When viewed from the top, it is seen that the core material also shears in this direction. The amount of shearing resistance in the through-depth direction is calculated in the same way as the shearing resistance in the across-width direction. The total shearing resistance from the core material is

$$N_{xy} = \frac{1}{4}\frac{G_{core}\left(w^2+4h^2\right)}{2h}\gamma_{xy} \tag{4.50}$$

Total inplane shear force, N_{xy}

The total inplane shear force on one laminate is given by

$$\begin{aligned} N_{xy} &= \left(\frac{G_{xz(wall)}t_{wall}w}{2h} + \frac{1}{4}\frac{G_{core}\left(w^2+4h^2\right)}{2h}\right)\gamma_{xy} \\ &= \left(\frac{G_{xz(wall)}t_{wall}w}{2h} + \frac{1}{4}\frac{G_{core}\left(w^2+4h^2\right)}{2h}\right)\Delta_2 \end{aligned} \tag{4.51}$$

4.3.4.3 Anticlastic bending force, M_y

Contribution from walls

Consider the forces acting in the cross-section, as shown by the free body diagram in Figure 4.16.

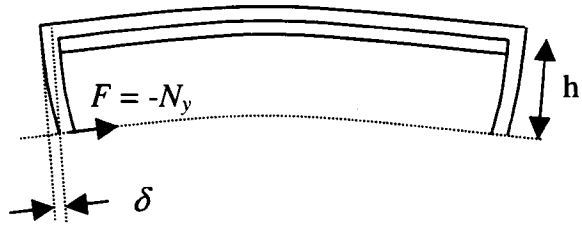

Figure 4.16 Free body diagram showing forces on laminate due to vertical walls

The resultant transverse inplane moment upon the top surface is given by

$$\begin{aligned} M_y &= -hN_y \\ &= \frac{-h}{\frac{2h}{w}\left(\frac{h^2}{3E_{wall}I_{wall}} + \frac{1}{t_{wall}G_{yz(wall)}}\right)}\left(h\kappa_y - \varepsilon_y\right) \\ &= \frac{-h}{\frac{2h}{w}\left(\frac{h^2}{3E_{wall}I_{wall}} + \frac{1}{t_{wall}G_{yz(wall)}}\right)}\left(h\Delta_3 - \Delta_1\right) \end{aligned} \qquad (4.52)$$

Contribution from core material

If the horizontal and vertical walls had no effect, the core material would simply deform according to its Poisson behaviour,

$$\kappa_y = -\nu\kappa_x \qquad (4.26.e)$$

The effect of the horizontal laminates will cause the actual behaviour to differ by some amount,

$$\kappa_y = -\nu\kappa_x + \Delta_3 \qquad (4.27.e)$$

A change in curvature Δ_3 is illustrated by Figure 4.17 below, which (for clarity) is shown without any associated transverse strain on the top and bottom surfaces.

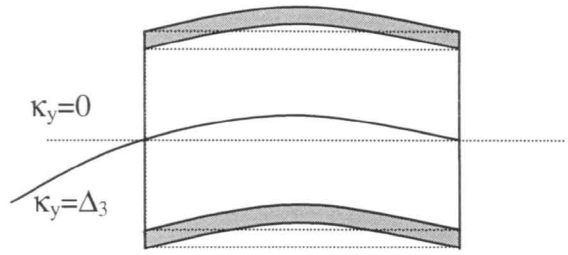

Figure 4.17 Increase in curvature from $\kappa_y=0$ to $\kappa_y=\Delta_3$

The overall deviation of the core from its unrestrained behaviour is Δ_3, which requires a total resultant bending moment of

$$M = E_{core} I_{core} \Delta_3 \tag{4.53}$$

Since this bending force is distributed between the top and bottom horizontal laminates, the resultant bending force that reacts upon each laminate is

$$M_y = -\frac{1}{2} E_{core} I_{core} \Delta_3 \tag{4.54}$$

Total transverse bending moment, M_y

The total transverse bending force on the one laminate is given by

$$M_y = \frac{-h}{\frac{2h}{w}\left(\frac{h^2}{3E_{wall} I_{wall}} + \frac{1}{t_{wall} G_{yz(wall)}}\right)} (h\Delta_3 - \Delta_1) - \frac{1}{2} E_{core} I_{core} \Delta_3 \tag{4.55}$$

4.3.5 Calculation of laminate strains

All the above expressions can be substituted into the second, third and fifth lines of the laminate stiffness equation

$$\begin{Bmatrix} N_x \\ N_y \\ N_{xy} \\ M_x \\ M_y \\ M_{xy} \end{Bmatrix} = \begin{bmatrix} A_{11} & A_{12} & A_{16} & B_{11} & B_{12} & B_{16} \\ A_{12} & A_{22} & A_{26} & B_{12} & B_{22} & B_{26} \\ A_{16} & A_{26} & A_{66} & B_{16} & B_{26} & B_{66} \\ B_{11} & B_{12} & B_{16} & D_{11} & D_{12} & D_{16} \\ B_{12} & B_{22} & B_{26} & D_{12} & D_{22} & D_{26} \\ B_{16} & B_{26} & B_{66} & D_{16} & D_{26} & D_{66} \end{bmatrix} \begin{Bmatrix} \varepsilon_x \\ \varepsilon_y \\ \gamma_{xy} \\ \kappa_x \\ \kappa_y \\ \kappa_{xy} \end{Bmatrix} \tag{4.56}$$

Thus, the deviations from isotropic core material deflections are expressed in terms of the applied curvature and the geometric and material properties of the cross-section.

Note that the majority of other analyses in the literature do not consider the out-of-plane behaviour of the laminates (thus effectively ignoring the B and D matrix terms). While it may be argued that these terms are small for thin walled sections, helicopter rotor blades are often quite thick walled near the root.

The **second line** of equation *(4.56)* gives

$$\frac{h\Delta_3 - \Delta_1}{\frac{2h}{w}\left(\frac{h^2}{3E_{wall}I_{wall}} + \frac{1}{t_{wall}G_{yz(wall)}}\right)} - \frac{E_{core}I_{core}\Delta_1}{2h^2} =$$

$$A_{12}h\kappa_x + A_{22}\left(-\nu h\kappa_x + \Delta_1\right) + A_{26}\Delta_2 + B_{12}\kappa_x + B_{22}\left(-\nu\kappa_x + \Delta_3\right) \tag{4.57}$$

The **third line** of equation *(4.56)* gives

$$\left(\frac{G_{xz(wall)}t_{wall}w}{2h} + \frac{1}{2}\frac{G_{core}\left(w^2 + 4h^2\right)}{2h}\right)\Delta_2 =$$

$$A_{16}h\kappa_x + A_{26}\left(-\nu h\kappa_x + \Delta_1\right) + A_{66}\Delta_2 + B_{16}\kappa_x + B_{26}\left(-\nu\kappa_x + \Delta_3\right) \tag{4.58}$$

The **fifth line** of equation (4.56) gives

$$\frac{-h}{\frac{2h}{w}\left(\frac{h^2}{3E_{wall}I_{wall}}+\frac{1}{t_{wall}G_{yz(wall)}}\right)}\left(h\Delta_3-\Delta_1\right)-\frac{1}{2}E_{core}I_{core}\Delta_3 =$$

$$B_{12}h\kappa_x + B_{22}\left(-\nu h\kappa_x+\Delta_1\right)+B_{26}\Delta_2 + D_{12}\kappa_x + D_{22}\left(-\nu\kappa_x+\Delta_3\right) \qquad (4.59)$$

It is a straightforward procedure to solve as a linear problem to obtain the values of Δ_1, Δ_2, and Δ_3 by rearranging equations *(4.57)*, *(4.58)* and *(4.59)* into matrix form, as

$$\begin{bmatrix} A_{22}+C_1+\frac{C_3}{h^2} & A_{26} & B_{22}+C_1h \\ +A_{26} & C_2+A_{66} & B_{26} \\ B_{22}-C_1h & B_{26} & D_{22}+C_1h^2+C_3 \end{bmatrix}\begin{pmatrix}\Delta_1\\ \Delta_2\\ \Delta_3\end{pmatrix} = -\begin{pmatrix} A_{12}h-A_{22}\nu h+B_{12}-B_{22}\nu \\ A_{16}h-A_{26}\nu h+B_{16}-B_{26}\nu \\ B_{12}h-B_{22}\nu h+D_{12}-D_{22}\nu \end{pmatrix}\kappa_x \qquad (4.60)$$

where $$C_1=\frac{w}{2h\left(\frac{h^2}{3E_{wall}I_{wall}}+\frac{1}{t_{wall}G_{yz(wall)}}\right)} \qquad (4.61.a)$$

$$C_2=\frac{G_{xz(wall)}t_{wall}w}{2h}+\frac{1}{4}\frac{G_{core}\left(w^2+4h^2\right)}{2h} \qquad (4.61.b)$$

$$C_3=\frac{E_{core}I_{core}}{2h^2} \qquad (4.61.c)$$

Once the values of Δ_1, Δ_2, and Δ_3 are determined, all the laminate strains are known, from which the strains throughout the cross-section may be determined.

The laminate forces (per unit width) may be calculated directly from equation *(4.56)*.

4.3.6 Expression for K_{45} from shear stresses in the section

The total moment acting on the section is equal to the sum of the horizontal and vertical components of shear stresses generated within every part of the cross-section, i.e. the horizontal and vertical components of the shear stresses in the horizontal laminates, vertical walls and core material.

The value of K_{45} is thus calculated as the moment of the horizontal and vertical components of shear flow (about the centroid of the section) summed around the entire section. This may be expressed mathematically as

$$\begin{aligned} K_{45} &= M_h + M_v \\ &= \iint_{2hw} \sigma_{xy}(y,z) z dy dz + \iint_{2hw} \sigma_{xz}(y,z) y dy dz \end{aligned} \tag{4.62}$$

where the vertical and horizontal components of shear stress (σ_{xy} and σ_{xz}) are generally assumed to be functions of cross-sectional location (y and z).

Note that considering only the shear stresses developed in the horizontal laminates will give only a loose correlation with the actual K_{45} behaviour of the section, and will generally be smaller than actually seen. This is illustrated by considering the example of shear flow around a box section as shown in Figure 4.18 below.

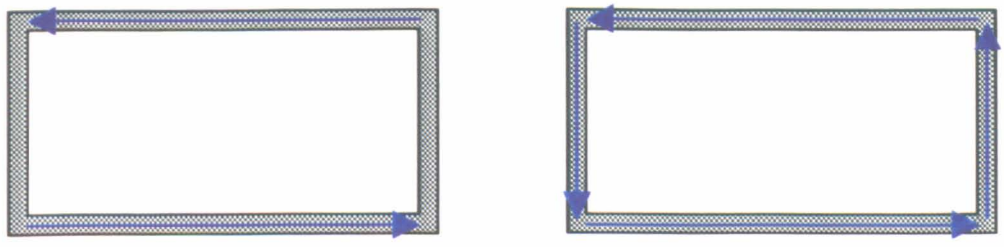

Figure 4.18 Moment of shear flow around section is greater than moment of shear in horizontal laminates alone

The moment of the shear stresses that flow about the section is double the moment of the shear stresses in the horizontal laminates alone. Since shear flow around the section is clearly of importance in this analysis, it is unsurprising that considering only the contribution from the horizontal laminates does not give accurate values.

This model therefore proceeds by considering the moments of shear forces in each of the components – laminates, walls, and core.

4.3.7 Notation

To avoid confusion in the shear flow analysis presented later in this chapter, shear force and stress components that refer to a specific substructure of the section will be followed by a subscript in parentheses that indicates which component of the blade section to which they refer.

Thus, for forces

$N_{xy(lam)}$ refers to the laminate shear force in the xy plane.
$N_{xz(wall)}$ refers to the vertical wall shear force in the xz plane.

for stresses

$\sigma_{xy(lam)}$ refers to the laminate shear stress in the xy plane.
$\sigma_{xz(wall)}$ refers to the vertical wall shear stress in the xz plane.
$\sigma_{xy(core)}$ refers to the core shear stress in the xy plane.
$\sigma_{xz(core)}$ refers to the core shear stress in the xz plane.

and for shear strains.

$\gamma_{xy(lam)}$ refers to the laminate shear strain in the xy plane.
$\gamma_{xz(wall)}$ refers to the vertical wall shear strain in the xz plane.
$\gamma_{xy(core)}$ refers to the core shear strain in the xy plane.
$\gamma_{xz(core)}$ refers to the core shear strain in the xz plane.

Where a stress or strain component is a function of cross-sectional yz-coordinate (i.e. in the core), the generalised or specific value of cross-sectional location is included in non-subscript parentheses. Thus

$\sigma_{xy(core)}(y,z)$ refers to xy-shear stress in the core at any y- or z-coordinate.
$\sigma_{xz(core)}(y,h)$ refers to xz-shear stress in the core at any y-coordinate and $z=h$.
$\sigma_{xz(core)}(w/2,z)$ refers to xz-shear stress in the core at $y=w/2$ and any z-coordinate.
$\sigma_{xz(core)}(w/2,h)$ refers to xz-shear stress in the core at $y=w/2$ and $z=h$.

and similarly for shear strains.

4.3.8 Calculation of laminate forces

Since all laminate strains are known, the relevant laminate forces can be calculated directly from equation *(4.56)*. For K_{45}, the shear and twisting forces arising in the horizontal laminates are calculated from the third and sixth lines of the laminate stiffness matrix *(4.56)* as

$$N_{xy(lam)} = A_{16}\varepsilon_{x(lam)} + A_{26}\varepsilon_{y(lam)} + A_{66}\gamma_{xy(lam)} + B_{16}\kappa_{x(lam)} + B_{26}\kappa_{y(lam)} + B_{66}\kappa_{xy(lam)}$$

$$M_{xy(lam)} = B_{16}\varepsilon_{x(lam)} + B_{26}\varepsilon_{y(lam)} + B_{66}\gamma_{xy(lam)} + D_{16}\kappa_{x(lam)} + D_{26}\kappa_{y(lam)} + D_{66}\kappa_{xy(lam)} \qquad (4.56.a,b)$$

Note that the laminate forces given are the *force per unit width* of laminate. The assumptions of classical laminate theory indicate that the laminate forces are constant across the width of the laminate.

4.3.9 Contribution to K_{45} from shear stresses in the horizontal laminates

Classical lamination theory gives two laminate forces that contribute towards the overall moment on the section: $N_{xy(lam)}$ and $M_{xy(lam)}$. The contributions of the overall moment on the section from the laminate forces due to $N_{xy(lam)}$ and $M_{xy(lam)}$ must therefore be

calculated. The overall moment contribution from the laminate might appear to be given by

$$M_{(lam)} = -wM_{xy(top)} + whN_{xy(top)} - wM_{xy(bottom)} - whN_{xy(bottom)} \qquad (4.63)$$

as shown on Figure 4.19, below.

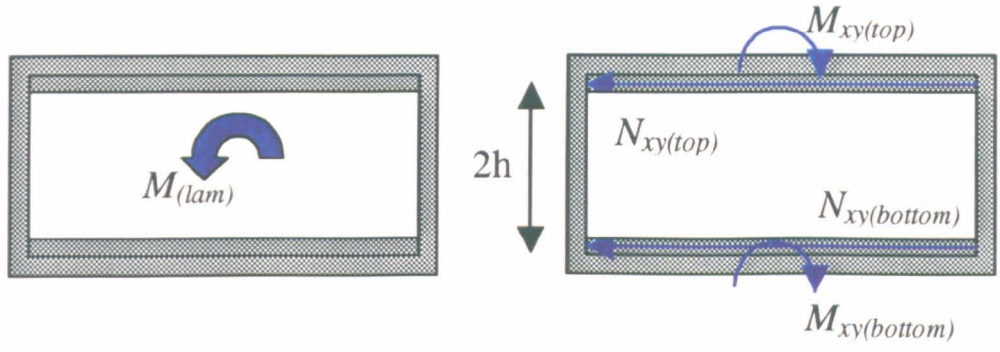

Figure 4.19 Section moment contribution from laminate forces

Note that due to the construction of the horizontal laminates,

$$N_{xy(top)} = -N_{xy(bottom)}$$
$$M_{xy(top)} = M_{xy(bottom)} \qquad (4.63.a,b)$$

$N_{xy(lam)}$ and $M_{xy(lam)}$ refer to the forces on the top laminates.

4.3.9.1 Contribution to section moment from $N_{xy(lam)}$

The calculation of $N_{xy(lam)}$ is based on the assumptions of classical laminate theory i.e. that edge effects can be ignored. This approximation does not have a significant impact on the overall contribution to section moment arising from $N_{xy(lam)}$. The moment contribution from $N_{xy(lam)}$ is therefore given by $M_{(Nxy(lam))}$ where

$$M_{(Nxy(lam))} = 2N_{xy(lam)}wh \qquad (4.64)$$

4.3.9.2 Contribution to section moment from $M_{xy(lam)}$

The calculation of $M_{xy(lam)}$ is based on the assumptions of classical laminate theory i.e. that edge effects can be ignored. The results of FE analyses show that edge effects do significantly affect the overall contribution to section moment arising from $M_{xy(lam)}$ contribution to K_{45}. $M_{xy(lams)}$ arises for the reasons described below, and the actual moment contribution from $M_{xy(lams)}$ will be demonstrated.

$M_{xy(lam)}$ arises from shear flow *within* the horizontal laminates. Shear stress generated in the unbalanced plies can flow within the horizontal laminates through the balanced ±45° plies. This is shown on Figure 4.20 below.

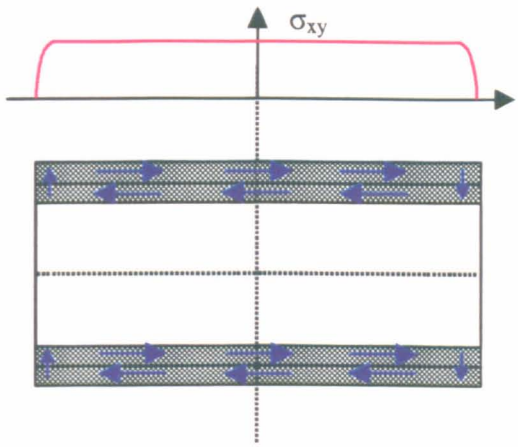

Figure 4.20 Shear flow within horizontal laminates

This effect can also be seen on Figure 4.21 below, which shows the *xy* component of shear stress for a section comprising two CFRP laminates separated by a very low modulus core, when subjected to flap bending. This figure is obtained from a finite element analysis of the section.

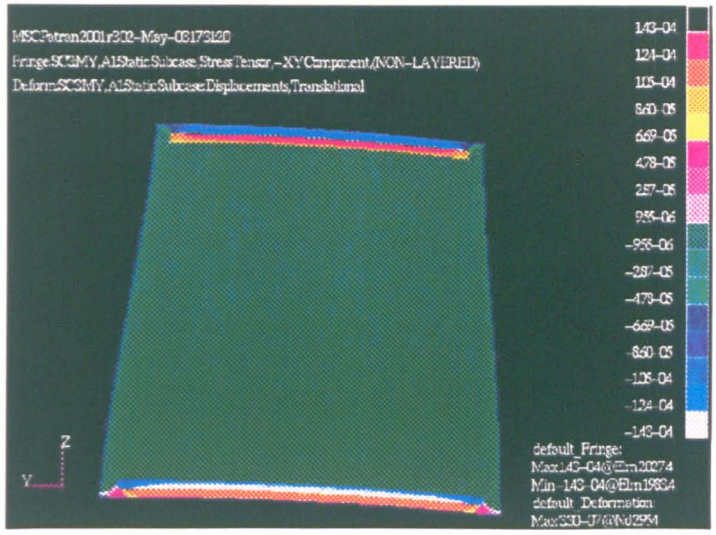

Figure 4.21 Finite element output showing value of horizontal component of shear flow in a cross-section under flap-bending

This shear flow within the laminates is most significant when the section undergoes out of plane warping. This is because when warping occurs, shear stress is generated in the ±45° plies in the opposite direction to the shear stress that is generated in the θ° plies. In the most extreme case (where two laminates are separated by a core of negligible stiffness) the shear stress generated in the ±45° plies is equal and opposite to the shear stress in the θ° plies. Shear flow remains entirely within the horizontal laminates and no shear stress is carried by the core.

Generally, it will be appreciated that any shear flow within the horizontal laminates contributes towards the overall moment acting on the section, which is represented by the M_{xy} term that is obtained from the sixth line of the laminate stiffness matrix. It will be appreciated that for the cross-sectional model considered in this work, the shear flow within the laminates occurs in the opposite direction to shear flow around the cross-section as a whole, and so the contribution to overall moment will be negative.

Classical laminate analysis assumes laminar sections (i.e. infinitely wide and thin laminates), and does not explicitly account for the effects of shear flow in its calculation of M_{xy}. It merely sums the moments caused by the horizontal components of shear stress in the layers, as illustrated by Figure 4.22 below

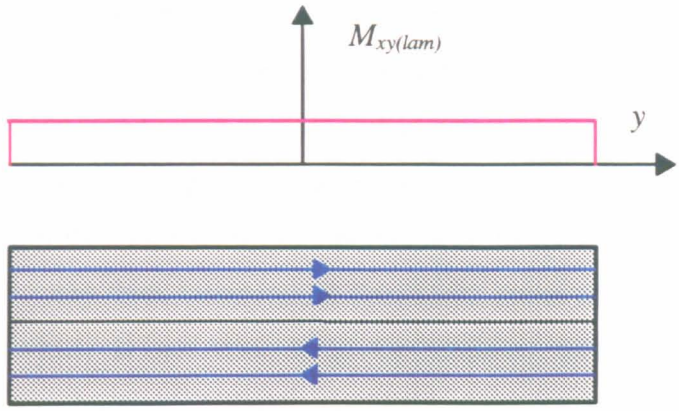

Figure 4.22 Shear stresses in laminate according to classical laminate theory

In reality, the section is not laminar. The laminate is of finite width, and has non-negligible thickness. The shear flow within the horizontal laminates therefore will look more like that shown in Figure 4.23 below.

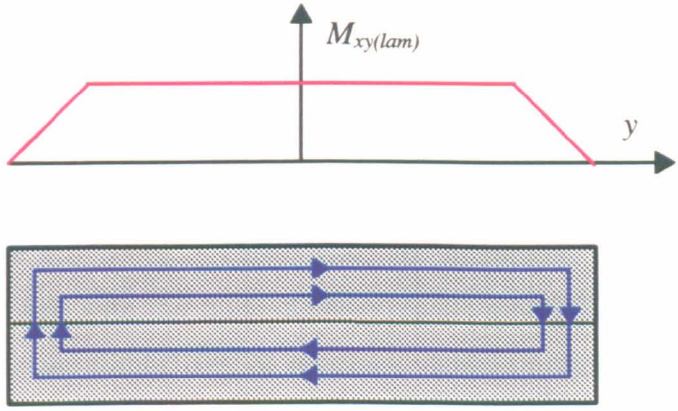

Figure 4.23 Idealised shear flow within a laminate of finite size

Because the flow around the section has vertical as well as horizontal components, the overall moment caused by a shear flow within a finitely sized laminate is larger than the simple sum of moments from each layer as calculated by classical laminate analysis. It is relatively straightforward to calculate the approximate contribution to the overall moment on the section from the shear flow *within* the horizontal laminates by modifying the M_{xy} term as described below.

It will be appreciated that shear stress must reduce to zero at a free surface i.e. the boundary condition $\sigma_{xy(lam)} = 0$ is imposed at the edges of the horizontal laminates. This effect can be seen on the finite element output of Figure 4.21 earlier - the shear flow is not generated all the way to the edge of the laminate. It is therefore appropriate to reduce the "effective" width of the laminate by an amount equal to its thickness. Although this may be inaccurate for very thick laminates, it does make some allowance for the effect of the free edge (which is not considered by laminate theory), and is a good approximation for the majority of laminates used in practical structures.

It will also be appreciated that (when compared to considering the horizontal component of shear flow alone) the total contribution to the moment is doubled by considering both the horizontal and vertical components of shear stress that flow around the section. Note that this is independent of the aspect ratio of the laminate.

The contribution to section moment from $M_{xy(lam)}$ is therefore given by

$$M_{(Mxy(lam))} = -2M_{xy(lam)}(w - t_{lam}) \qquad (4.65)$$

Using this analysis, the results for sandwich sections with a low modulus core material (where almost all the K_{45} coupling comes from the moment of shear flow within the laminates) correlate well with the finite element results presented later in this chapter. The analytical results are within 10% of the finite element results - even for relatively thick walled sections. Although a slightly better fit can be obtained empirically, the method presented here has a sound theoretical basis and should therefore be applicable for all geometries and material properties (within the limitations of the modelling assumptions).

4.3.10 Contribution to K_{45} of shear stresses in the walls and core

Since K_{45} is the total moment on the section, this is equal to the sum of the moment of the horizontal component of shear stresses (M_h) and the moment of the vertical component of shear stress (M_v) around the entire section i.e.

$$\begin{aligned} K_{45} &= M_h + M_v \\ &= \int_{2hw}\int \sigma_{xy}(y,z)zdydz + \int_{2hw}\int \sigma_{xz}(y,z)ydydz \end{aligned} \tag{4.66}$$

where the general vertical and horizontal components of shear stress (σ_{xy} and σ_{xz}) are assumed to be functions of cross-sectional location (y and z).

Note that this generalised expression already includes the contribution from the horizontal laminates, which was discussed in the section above. Only the contribution to K_{45} caused by the moments of shear stresses in the vertical walls and core are considered in this section.

For clarity of example, the calculation of the moment of shear stress due to walls and core are calculated separately by looking at the two extreme cases (i.e. a box section, and a sandwich section).

4.3.10.1 Moment of shear stresses in vertical walls – illustrated by box section

The analytical model presented can represent a box section, by setting the modulus of the core material to zero.

The section undergoes out of plane warping, and a shear strain is calculated for the horizontal laminates. For compatibility of the structure, there must also be a shear strain (that gives an equal and opposite out of plane warping deformation) in the vertical walls as shown in Figure 4.24 below.

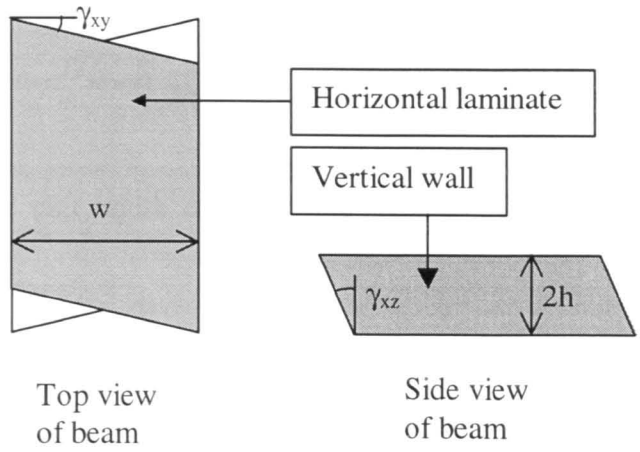

Figure 4.24 Out of plane warping displacements give rise to shear strains in horizontal laminates and vertical walls

The constant *xz* shear strain in the horizontal walls is thus calculated from the warping deformation as

$$\gamma_{xz(wall)} = \gamma_{xy(lam)} \frac{w}{2h} \tag{4.67}$$

Note that the warping deformation of the horizontal laminates $\gamma_{xy(lam)}$ has already been determined from the laminate stiffness matrix (equation *(4.57)*).

The *xz* shear stress in the horizontal walls will therefore be given by

$$\sigma_{xz(wall)} = \gamma_{xz(wall)} G_{xz(wall)} \tag{4.68}$$

Since the vertical inplane shear modulus of the vertical walls, $G_{xz(walls)}$ is known, the shear stress in the vertical walls can be written as

$$\sigma_{xz(wall)} = \gamma_{xy(lam)} G_{xz(wall)} \frac{w}{2h} \tag{4.69}$$

The vertical shear force per unit depth of the vertical walls is equal to the integral of this shear stress over the wall thickness.

$$N_{xz(wall)} = \gamma_{xy(lam)} G_{xz(wall)} \frac{w}{2h} t_{wall} \tag{4.70}$$

The shear force per unit width of horizontal laminate, N_{xy} is known from equation *(4.45)*, where

$$N_{xy(lam)} = \frac{G_{xz(wall)} t_{wall} w}{2h} \gamma_{xy(lam)} \tag{4.45}$$

Thus it can be seen that the horizontal shear force per unit width in the horizontal laminates is equal to the vertical shear force per unit depth in the vertical walls. i.e.

$$N_{xy(lam)} = N_{xz(wall)} \tag{4.71}$$

There is no horizontal component to the shear stress in the vertical walls. The moment of the shear forces in the vertical walls is therefore

$$\begin{aligned} M_{(wall)} &= \int \sigma_{xz(wall)} y dA \\ &= 2N_{xz(wall)} 2h \frac{w}{2} \\ &= G_{xz(wall)} t_{wall} w^2 \gamma_{xy(lam)} \end{aligned} \tag{4.72}$$

It is instructive to note that the moment contribution from the $N_{xy(lam)}$ shear force in the horizontal laminates is given by

$$\begin{aligned} M_{(Nxy(lam))} &= \int \sigma_{xy(lam)} z dA \\ &= 2N_{xy(lam)} wh \\ &= G_{xz(wall)} t_{wall} w^2 \gamma_{xy(lam)} \end{aligned} \tag{4.73}$$

which shows that for a hollow box section, the moment of $N_{xy(lam)}$ shear forces in the horizontal laminates is equal to the moment of shear stresses in the vertical walls. i.e.

$$M_{(Nxy(lam))} = M_{(wall)} = 2N_{xy(lam)}wh \tag{4.74}$$

For a hollow box section, the total moment of the horizontal and vertical components of shear stress around the entire section is therefore

$$\begin{aligned} K_{45(box)} &= M_{(wall)} + M_{(lam)} \\ &= \left[M_{(wall)}\right] + \left[M_{(Nxy(lam))} + M_{(Mxy(lam))}\right] \\ &= \left[2N_{xy(lam)}wh\right] + \left[2N_{xy(lam)}wh - 2(w - t_{lam})M_{xy(lam)}\right] \\ &= 4N_{xy(lam)}wh - 2(w - t_{lam})M_{xy(lam)} \end{aligned} \tag{4.75}$$

For most box sections,

$$N_{xy(lam)} >> M_{xy(lam)} \tag{4.76}$$

and the value of K_{45} will be approximately double that of the contribution from the horizontal laminates alone.

The analysis of a box section may alternatively be thought of in terms of shear flow around the section as follows.

Since shear flow around the cross-section is constant, the net shear generated in the horizontal laminates (i.e. $N_{xy(lam)}$) must flow from these laminates and into the vertical walls, as shown in Figure 4.25 below. The contribution to overall moment on the section from the shear flow in the vertical walls is exactly equal (and in the same direction as) to that generated by the net shear flow from the top and bottom laminates. This is shown on the figure below.

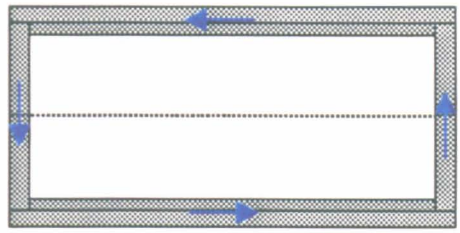

Figure 4.25 Shear flow around a box section

Since the shear modulus of the core is zero, the shear flow takes place entirely within the walls of the section. Since shear flow around the sections must be conserved, the (constant) shear flow in the vertical walls, $N_{xz(wall)}$ is equal to the (constant) shear flow in the horizontal laminates, $N_{xy(lam)}$. i.e.

$$N_{xz(wall)} = N_{xy(lam)} \tag{4.77}$$

Thus, taking either approach leads to the same result for the total moment from the shear stresses in the horizontal laminates and vertical walls i.e.

$$\begin{aligned} K_{45(box)} &= M_{(wall)} + M_{(Nxy(lam))} + M_{(Mxy(lam))} \\ &= 4N_{xy(lam)}wh - 2(w - t_{lam})M_{xy(lam)} \end{aligned} \tag{4.75}$$

which is approximately double the value obtained if considering only the contribution to overall moment on the section from the horizontal laminates.

4.3.10.2 Moment of shear stresses in core – illustrated by sandwich section

This analytical model can also be used to model a sandwich section, by setting the thickness of the vertical walls to zero. If there are no vertical walls, the shear flow must be carried by the core material. Obviously, the net shear force in the horizontal laminate remains constant across its width, and is determined from laminate stiffness calculations.

For the case of shear flow through the core, it is easiest to use the shear strains approach (based on the out-of-plane warping displacements of the core), as the pattern of shear flow around the section is not intuitive. Consider the out of plane warping of a sandwich panel, Figure 4.26.

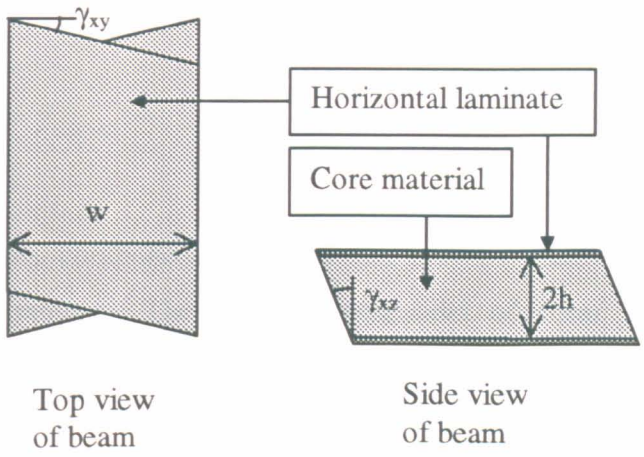

Figure 4.26 Out of plane warping displacements give rise to shear strains in horizontal laminates and core material

The idealised shear strain distribution in the core of this cross-section is shown in Figure 4.27 below.

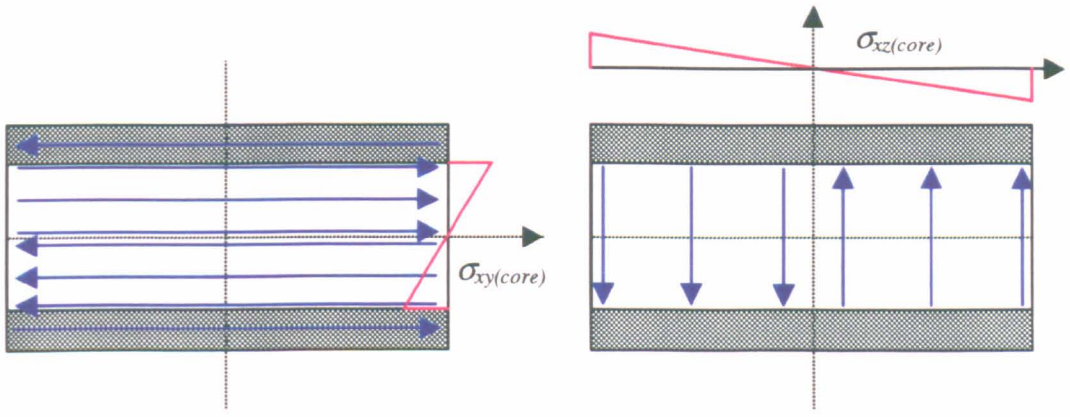

Figure 4.27 Horizontal and vertical shear stresses in a sandwich section

Assuming the core material has constant material properties, then the distribution of horizontal shear stress in the core ($\sigma_{xy(core)}$) varies linearly with z-coordinate, and that of vertical shear stress in the core ($\sigma_{xz(core)}$) varies linearly with y-coordinate.

The horizontal shear strain in the core is independent of y-coordinate and is given by

$$\gamma_{xy(core)}(y,z) = \gamma_{xy(lam)}\frac{z}{h} \tag{4.78}$$

and the vertical shear strain in the core is independent of z-coordinate and is given by

$$\gamma_{xz(core)}(y,z) = \gamma_{xz(core)}(\frac{w}{2},z)\frac{2y}{w} \tag{4.79}$$

Note that the horizontal component of shear strain at $z=h$ is that which was determined for the horizontal laminate. The vertical component of shear strain at $y=w/2$ is calculated by compatibility of the out-of-plane warping displacements

$$\gamma_{xz(core)}(\frac{w}{2},z) = \gamma_{xy(lam)}\frac{w}{2h} \tag{4.80}$$

Now that the horizontal and vertical components of shear strain are known at any position in the cross-section, the components of shear stress may be easily calculated from

$$\sigma_{xy(core)}(y,z) = G_{xy(core)}\gamma_{xy(core)}(y,z)$$
$$\sigma_{xz(core)}(y,z) = G_{xz(core)}\gamma_{xz(core)}(y,z) \tag{4.81.a-b}$$

Assuming the core material is isotropic, $G_{xy(core)}=G_{xz(core)}=G_{(core)}$, which gives

$$\sigma_{xz(core)}(\frac{w}{2},z) = \sigma_{xy(core)}(y,h)\frac{w}{2h} \tag{4.82}$$

Finally, the moments of these shear stresses must be summed to determine the overall moment acting on the section due to the core.

The moment of horizontal component of shear flow in the core is given by $M_{h(core)}$ where

$$\begin{aligned} M_{h(core)} &= -2\int_0^h \sigma_{xy(core)}(y,z)zdA \\ &= -2\int_0^h \sigma_{xy(core)}(y,h)\frac{z}{h}zwdz \\ &= -2\sigma_{xy(core)}(y,h)\frac{w}{h}\left[\frac{z^3}{3}\right]_0^h \\ &= -\frac{2}{3}\sigma_{xy(core)}(y,h)wh^2 \end{aligned} \qquad (4.83)$$

The moment of vertical component of shear flow *in the core* is given by $M_{v(core)}$ where

$$\begin{aligned} M_{v(core)} &= 2\int_0^{w/2} \sigma_{xz(core)}(y,z)ydA \\ &= 2\int_0^{w/2} \sigma_{xz(core)}(\frac{w}{2},z)\frac{2y}{w}y2hdy \\ &= 2\sigma_{xz(core)}(\frac{w}{2},z)\frac{4h}{w}\left[\frac{y^3}{3}\right]_0^{w/2} \\ &= \frac{1}{3}\sigma_{xz(core)}(\frac{w}{2},z)w^2h \end{aligned} \qquad (4.84)$$

The total moment on the blade section due to shear flow in the core is given by $M_{(core)}$ where

$$\begin{aligned} M_{(core)} &= M_{v(core)} + M_{h(core)} \\ &= \frac{1}{3}\sigma_{xz(core)}(\frac{w}{2},z)w^2h - \frac{2}{3}\sigma_{xy(core)}(y,h)wh^2 \\ &= \frac{1}{6}\sigma_{xy(core)}(y,h)w\left(w^2-4h^2\right) \\ &= \frac{1}{6}G_{(core)}\gamma_{xy(lam)}w\left(w^2-4h^2\right) \end{aligned} \qquad (4.85)$$

This is an interesting result, as it shows that if *2h* is greater than *w*, then the shear flow around the core will actually contribute a negative moment to the overall section and will cause a decrease in predicted K_{45}.

The total moment on the section is obviously equal to the moment of shear stresses in the laminates plus the moment of shear stresses in the core. i.e.

$$K_{45(sandwich)} = M_{(lams)} + M_{(core)}$$
$$= \left[2N_{xy(lams)}wh - 2(w - t_{lam})M_{xy(lam)}\right] + \left[\frac{1}{6}G_{(core)}\gamma_{xy(lam)}w(w_2 - 4h_2)\right] \quad (4.86)$$

4.3.11 Combining moments from all components in filled box section analysis

Using the out of plane warping deformations and associated shear stiffnesses of the vertical walls and core material to calculate the shear stresses throughout the cross-section allows a filled box section to be analysed easily, as it is simply the sum of moment contributions from all the components of the cross-section (i.e. horizontal laminates, vertical walls, and core material) all of which are calculated as presented above.

The value of K_{45} for a filled box section is therefore given by

$$K_{45(filledbox)} = M_{(lam)} + M_{(wall)} + M_{(core)}$$
$$= \left[2N_{xy(lams)}wh + 2(w - t_{lam})M_{xy(lam)}\right] + \left[2G_{xz(wall)}t_{wall}w^2\gamma_{xy(lam)}\right] + \left[\frac{1}{6}G_{(core)}\gamma_{xy(lam)}w(w_2 - 4h_2)\right] \quad (4.87)$$

The analytical results using this "sum of moments of shear stresses" approach gives good agreement with the finite element results.

4.4 FINITE ELEMENT MODELLING

4.4.1 Parametric study

The analytical model is tested by comparison with finite element results using code developed by Hill, based on the work of Bartholomew and Mercer [40]. The theoretical basis for this analysis is presented fully by Hill and Weaver [34] but is summarised in Chapter 2 of this thesis. Such a generalised model allows the validity of various assumptions to be tested individually, by parameterising the different variables and investigating the effect of each parameter upon the behaviour of the section. A suitable postprocessor allows increased physical insight from the finite element results.

A representation of the finite element model used is shown on Figure 4.28 below. The model was constructed from 3D reduced-integration brick elements. In order to facilitate the automation of model generation (necessary because several hundred analyses were run during the course of the parametric study), the cross section of each element was fixed at 1 mm square, irrespective of the geometry of the model. Although this gives less than ideal through-thickness resolution for thin laminates, the effect upon the overall behaviour of the cross section is likely to be small. Figure 4.28 also shows the parameters that were varied as part of the finite element study.

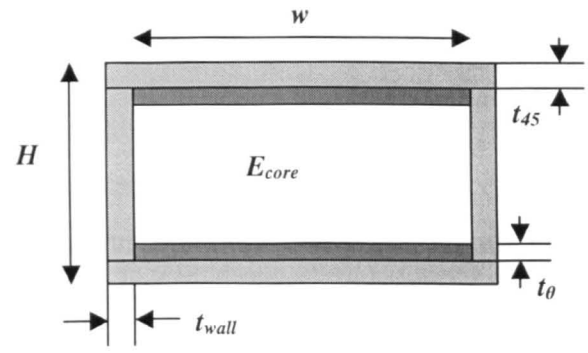

Figure 4.28 Finite element model of cross-section

The parameters being varied in the following investigations are the height of the cross-section (H), the width of the unbalanced coupling plies (w), the Young's modulus of core material (E_{core}), and thickness of vertical walls (t_{wall}).

The material properties for the CFRP used in the finite element modelling are given in the table below.

Properties	E_1 (GPa)	E_2 (GPa)	E_3 (GPa)	G_{12} (GPa)	G_{13} (GPa)	G_{23} (GPa)	ν_{12}	ν_{13}	ν_{23}
"Generic" Carbon	132.0	9.2	9.2	4.34	4.34	4.34	0.3	0.3	0.3

Table 4.1 Generic CFRP material properties used in Finite Element Analyses

Height and Width of cross-section

Each value is independently varied in 10 mm increments over the ranges of 10-40 mm (height) and 10-50 mm (width). This gives a range of sizes and aspect ratios whilst ensuring that the finite element model does not become too large to be analysed.

Young's modulus of isotropic core material

Core modulus was varied in a logarithmic manner from 7 MPa (a very floppy core, offering very little warping restraint) to 7000 GPa (a very stiff core, offering negligible warping freedom).

Thickness of vertical walls

Vertical wall thickness was varied in 1 mm increments from 0 mm (which is unable to offer any warping restraint) to 5 mm (which offers significant warping restraint, but beginning to exhibit thick-walled effects)

Although the analytical model allows the thickness of both the ±45° plies in the horizontal walls and the thickness of the coupling plies to be varied, these were left constant during the following investigations.

The assumptions of classical laminate theory upon which the analytical calculations have been based become less accurate as the thickness of the horizontal and vertical laminates increase. In classical laminate analysis, through thickness effects are neglected, and (since the laminate is assumed to be of infinite size) no consideration is made of edge effects. Analysing thin-walled sections will therefore give the most accurate comparison between the analytical model (based on classical laminate theory) and the finite element results.

4.4.2 Thin-walled sections

Thin walled sections are inherently simpler to consider than thick walled sections, since B and D matrix terms have a relatively small effect, and non-uniform variation of strains through the thickness can generally be ignored. The analytical work presented earlier is based on classical laminate theory, and thus inherently assumes that thick walled effects can be ignored.

The analytical work presented in section 4.3 above examines both sandwich panels and box sections, and presents a single, unified approach for the analysis of both cross-sections. It is seen that several factors have varying significance on the behaviour of the cross-section, including cross-sectional geometry (i.e. size and aspect ratio), the vertical walls (which affect both transverse strains and out-of plane warping), and the core material (which also affects transverse strains and out-of plane warping).

These factors (and their effect upon the accuracy of the analysis) are investigated here by comparing the analytical predictions with the finite element results for a range of sandwich, box and filled-box sections.

4.4.2.1 Discussion of Finite Element results for sandwich panels

Figure 4.29, below, shows how the finite element analysis results for K_{45} vary with ply angle for a 50 x 40 mm sandwich section. Each curve represents results obtained for a different Young's modulus of isotropic core material. Similar graphs are included in Appendix 4.1, which show the same results for a range of width and height values.

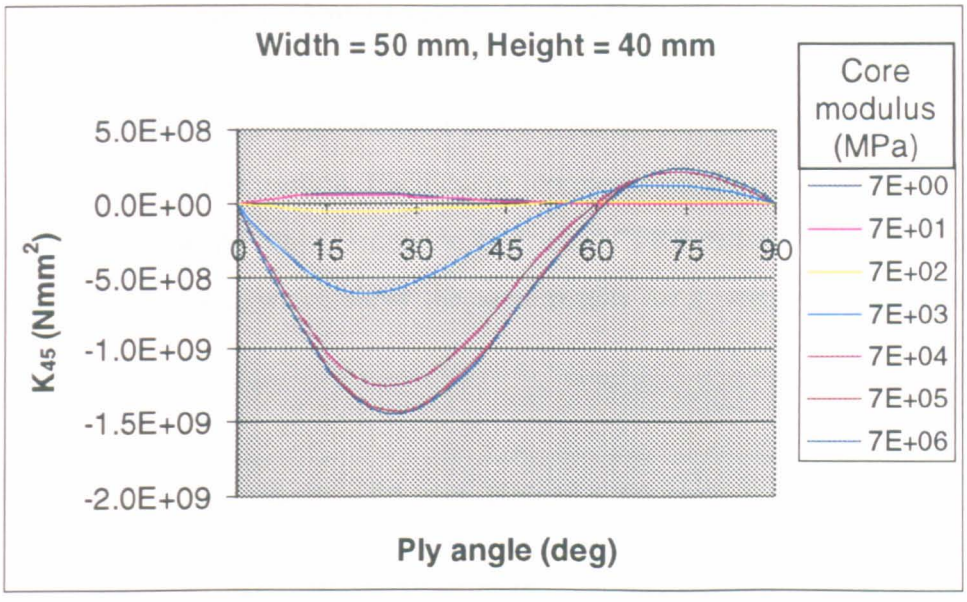

Figure 4.29 Finite element prediction of variation of K_{45} with ply angle for sandwich panels of varying core modulus

It can be seen that as the Young's modulus of the core material increases from a low value of 7 MPa (which allows warping to occur with hardly any restraint) through to a "mathematically large" value of 7E+06 MPa (which effectively restrains the warping completely), the value of K_{45} changes sign and magnitude. This observation is explained below.

Very low modulus core material does not restrain the out of plane warping of the section. The shear flow therefore remains within the laminates, and overall value of K_{45} is almost entirely due to the moment of this shear flow within the laminates i.e. the modified M_{xy} component from the laminate stiffness matrix. This gives a small value of K_{45}.

Very high modulus core material almost totally restrains the out of plane warping of the section. Any shear stresses generated in the unbalanced plies of the top and bottom laminates flow through the core and the overall value of K_{45} is almost entirely due to the moment of this shear flow around the section i.e. the modified N_{xy} component from the laminate stiffness matrix.

4.4.2.2 Discussion of Finite Element results for box sections

Figure 4.30, shows how the finite element analysis results for K_{45} vary with ply angle for a 50 x 40 mm hollow box section. Each curve represents results obtained for a different thickness of vertical walls, which are made from ±45° CFRP material. Similar graphs are included in Appendix 4.2, which show the same results for a range of width and height values.

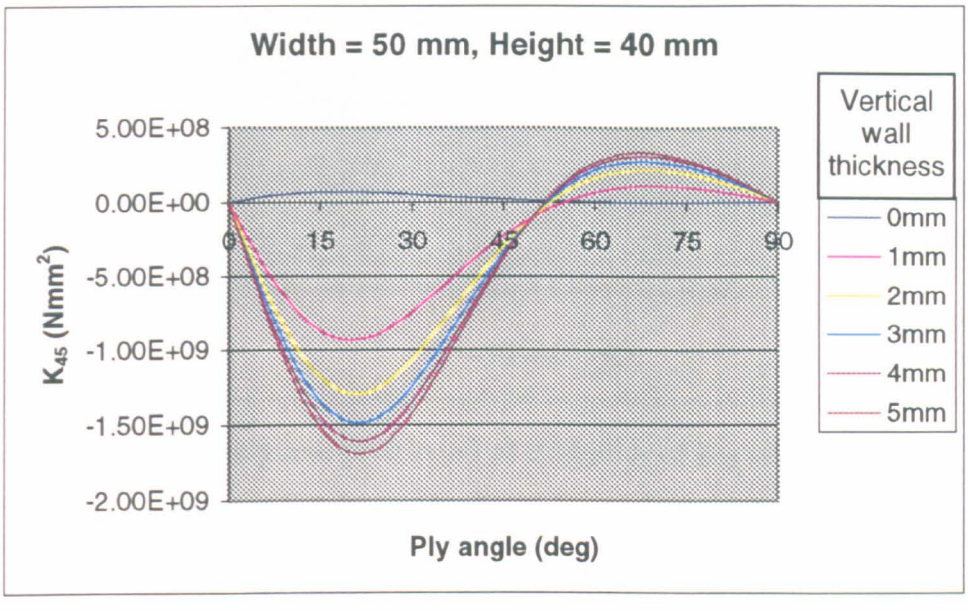

Figure 4.30 Finite element prediction of variation of K_{45} with ply angle for hollow box sections with varying vertical wall thickness

It can be seen from the graphs that even 1 mm thin vertical walls provide enough warping restraint for shear flow around the section (rather than within the horizontal laminates) to dominate the response. As these vertical walls become stiffer (i.e. by increasing in thickness), the out of plane warping is restrained even more effectively, and behaviour of the cross-section tends towards the fully warping restrained value.

4.4.2.3 Comparison of FE and Analytical results for sandwich sections

The analysis method presented in this chapter can be used to derive results for the K_{45} term for the entire range of cross-sections studied by the finite element method discussed above. Appendix 4.3 shows the graphs obtained for sandwich sections.

Figure 4.31 below shows the curves obtained for 50 mm x 40 mm sandwich sections of varying core modulus.

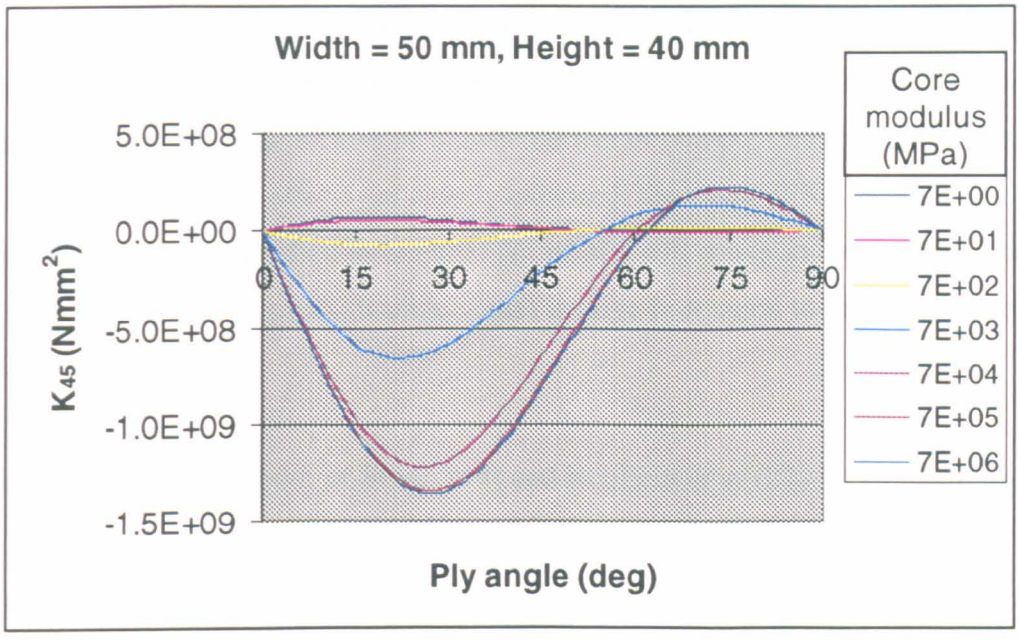

Figure 4.31 Analytical prediction of variation of K_{45} with ply angle for sandwich panels of varying core modulus

As can be seen from comparison with Figure 4.29, the analytical results closely match the finite element results at this cross-sectional geometry.

Appendix 4.4 shows graphs comparing the finite element results with the analytical results from both the "basic laminate forces" and "full shear flow effects" analytical models for sandwich section beams over a wide range of cross-sectional geometries.

These results show the importance of considering shear flow effects around the section. Although the basic laminate forces method does capture the general trend of behaviour seen in the finite element results, it is inaccurate in magnitude (because the vertical component of shear flow is neglected) and does not model the change in K_{45} seen over a range of different geometries (because the distribution of shear flow around the section is neglected).

As can be seen from the graphs in Appendix 4.4, the full shear flow analytical model accurately predicts the value of K_{45} for a range of cross-sectional geometries and core moduli.

The poorest correlations occur when the behaviour of the core is somewhere between low modulus behaviour to high modulus behaviour. This is not surprising - numerically, K_{45} is determined from the difference between effect of two possible paths of shear flow N_{xy} and M_{xy}. When these effects are closely balanced, the value of K_{45} is small, and thus any small errors in the prediction of either N_{xy} or M_{xy} will cause an error in the value of K_{45} that (although still a small absolute value) is large in relation to the small, predicted value of K_{45}.

A comparison with the work of Smith [19] and Rehfield *et al* [22] is not made because their work cannot be directly applied to sandwich sections.

4.4.2.4 Comparison of FE and Analytical results for box sections

The analysis method presented in this chapter can be used to derive results for the K_{45} term for the entire range of cross-sections studied by the finite element method discussed above. Appendix 4.5 shows the graphs obtained for box sections. Figure 4.32 below shows the curves obtained for 50 mm x 40 mm sandwich sections of varying core modulus.

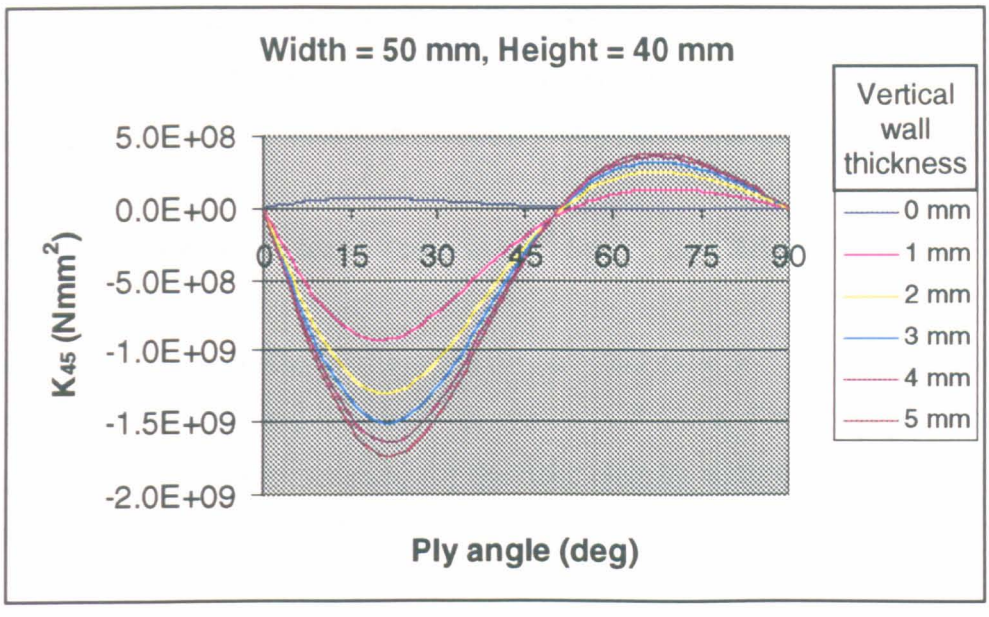

Figure 4.32 Analytical prediction of variation of K_{45} with ply angle for box sections of varying vertical wall thickness

As can be seen from comparison with Figure 4.30, the analytical results closely match the finite element results at this cross-sectional geometry – the two value for K_{45} generally agreeing to within 10%.

Appendix 4.6 shows graphs comparing the finite element results with the analytical results from both the "basic laminate forces" and "full shear flow effects" analytical models for box section beams over a wide range of cross-sectional geometries.

These results again show the importance of considering shear flow effects around the section. The basic laminate forces method captures the general trend of behaviour seen in the finite element results, but is only half the magnitude of the finite element results because the vertical component of shear flow is neglected. Since the shear stresses are limited to flowing within the walls of the box section, the effects of shear flow distribution are not significant, and the magnitude of this error does not change significantly with cross-sectional geometry.

As can be seen from the graphs in Appendix 4.6, the full shear flow analytical model predicts the value of K_{45} over a range of cross-sectional geometries and vertical wall thicknesses. The poorest correlation occurs as the thickness of the vertical wall increases.

This is because the calculations assume uniform shear flow in the vertical walls. As the walls become thicker, the shear flow in them can take on a non-uniform distribution (as was seen for the core in the sandwich section), giving rise to the discrepancy.

4.4.2.5 Comparison of box section results with Smith, and Rehfield *et al*

A comparison with the methods of Smith [19] and Rehfield *et al* [22] is possible for box sections. Appendices 4.7 and 4.8 show the results of Smith and Rehfield over the same range geometries that were presented for the finite element method in Appendix 4.2 and for the present analytical method in Appendix 4.5.

Figure 4.33 below shows the cross-sectional results for a 40 mm x 30 mm box section with varying vertical wall thickness, as obtained using Smith's method. Smith's variable, β gives a good approximation to the warping restraint offered by vertical walls of different thickness, although it is noted that when the section is completely free to undergo out of plane warping (i.e. zero vertical wall thickness), Smith's analysis does not capture the effect of shear flow within the laminates.

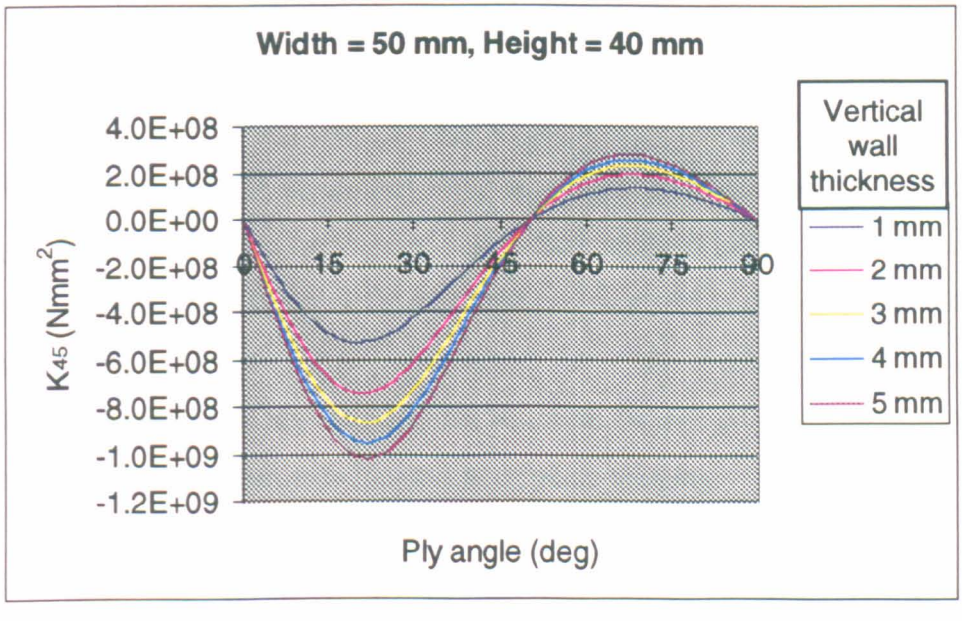

Figure 4.33 Smith's results for K_{45} of various box sections

Since Rehfield *et al* [22] derive a 7 x 7 stiffness matrix (where the out of plane warping is explicitly considered as a separate variable) the K_{45} term obtained using this method is

derived by implicitly assuming restrained warping. Since it is the amount of warping restraint offered by the vertical walls that dominates the behaviour of the different wall thicknesses studied, the analysis of Rehfield *et al* produces only one type of solution, which is shown on Figure 4.34, below. The small differences between analyses of different wall thicknesses are due to the slight change in the effective values of area enclosed and circumference of cross-section as vertical wall thickness varies but width of unbalanced plies remains constant.

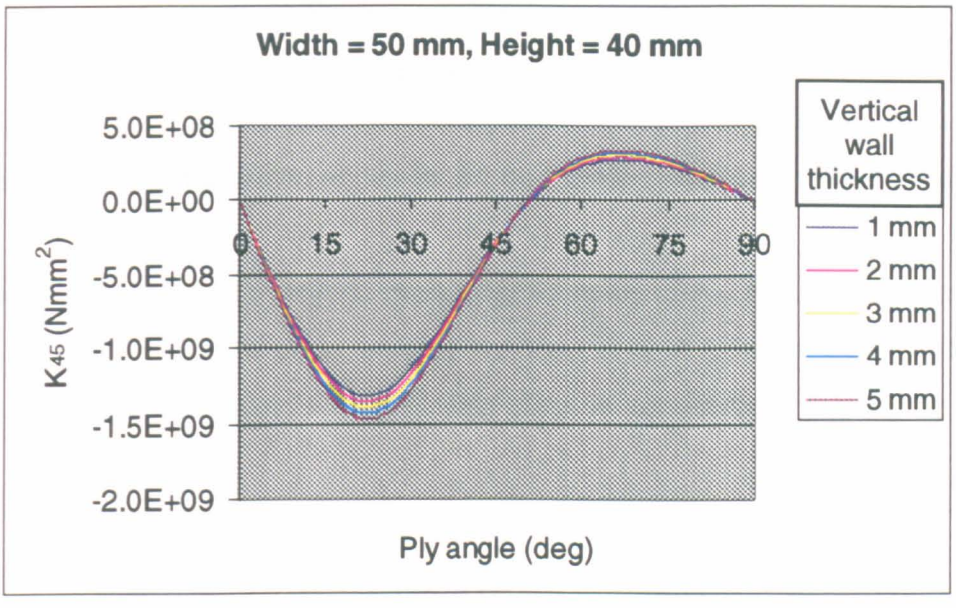

Figure 4.34 Rehfield's results for K_{45} of various box sections

It is not suggested that the method of Rehfield *et al* doesn't account for the effects of warping – is simply that the meaning of K_{45} in their analysis (which explicitly considers out of plane warping) is slightly different to the meaning of K_{45} that is used in this thesis (and that of Smith). When analysing the overall behaviour of a box section, the method of Rehfield *et al* will explicitly consider the K_{47} term (warping torsion coupling), which will give a response that accounts for the out of plane warping.

As a result, considering only the K_{45} values given by each method does not give a strictly fair comparison. The values of K_{45} for a 50mm x 40mm box section with 1mm vertical walls that are given by each method are nonetheless plotted on Figure 4.35 below.

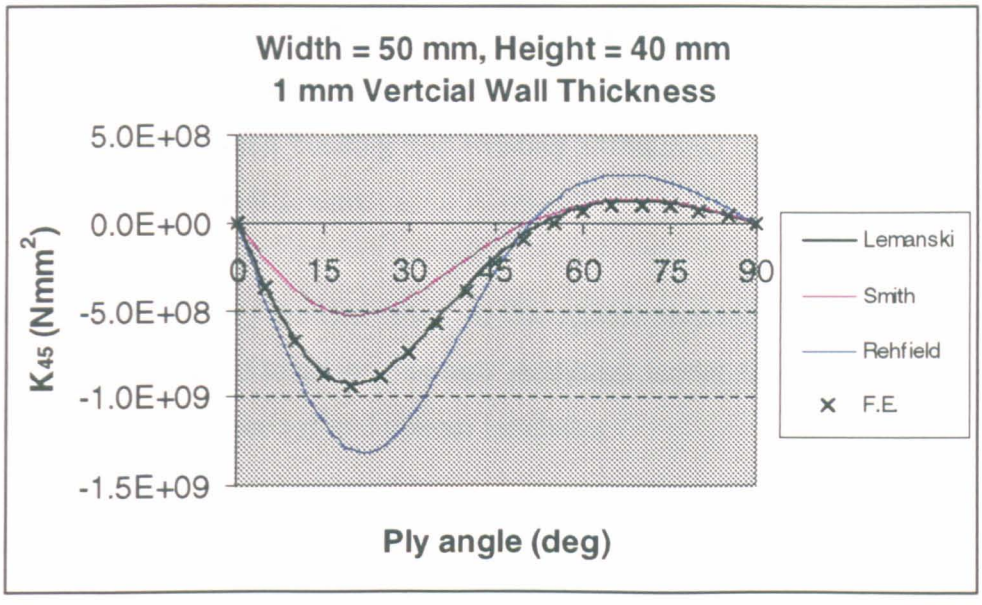

Figure 4.35 Comparison of results for box section with 1mm vertical walls

As can be seen, Rehfield's analysis gives a higher value of K_{45} than the other methods. This is because the out of plane warping has the effect of reducing the effective flap-torsion coupling. In Rehfield's analysis, this effect is considered separately by the K_{47} term.

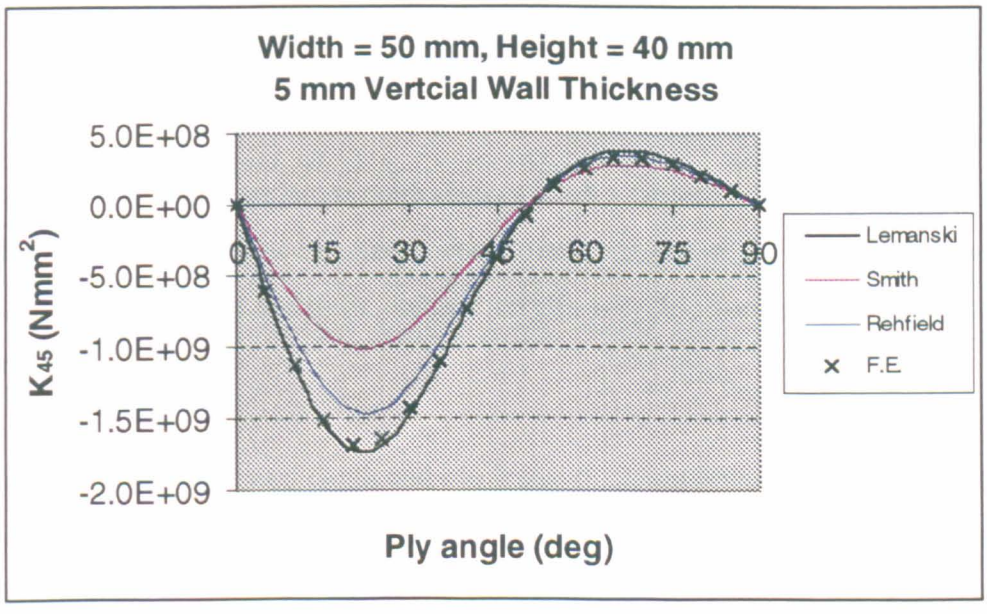

Figure 4.36 Comparison of results for box section with 5mm vertical walls

Figure 4.36 shows the values of K_{45} for a box section with 5mm vertical walls. The inplane shear stiffness of 5mm vertical walls is sufficient to effectively restrain out of plane warping, and the predictions should be comparable. It is interesting to note that the

method of Rehfield *et al* gives results which are approximately 20% *lower* than the FE analysis. This is most likely due to the use of only membrane stiffnesses in their analysis (i.e. ignoring shell bending and twisting stiffnesses), and the assumption that that hoop stress in the shell is zero.

As was discussed during the derivation of the model presented in this chapter, it is relatively straightforward to adapt this new analytical model for a restrained warping case by setting $\gamma_{xy}=0$ on the top and bottom laminates.

4.4.2.6 Conclusion

A new analytical model has been developed that accurately models the flap torsion coupling of a cross section that has similar features to a real composite helicopter rotor blade. A parametric study is undertaken, and the values of K_{45} are plotted for a range of cross-sectional geometries and material parameters as shown in the appendices. The results obtained from this new analytical model are shown to correlate well with finite element results, and also compared favourably with existing methods in the literature.

4.4.3 Thick-walled effects

Helicopter rotor blades are often quite thick walled – particularly near the root. Due to the inherent assumptions of laminate theory (discussed earlier), the agreement between the analytical model and the finite element results will deteriorate as the walls become thicker.

A section that is 10 mm total depth and has 2 mm thick laminates on the top and bottom surfaces may be considered relatively thick walled. The graphs in the appendices show that although the accuracy of the analytical method deteriorates as the wall thickness increases relative to the dimensions of the cross-section, the general trends remain the same.

For the majority of cases, the prediction is still accurate to within 10% even for wall thicknesses equal to 10% of the total section depth. Even in these cases, the analytical

results continue to describe the qualitative behaviour of the K_{45} value for the cross-section.

For thick walled sections, the largest source of error is due to the non-uniform deformation of the top and bottom laminates. The deformations of the cross-section in Figure 4.37 below clearly show the laminates exhibiting significant through thickness variation of in-plane strains, which leads to non-uniform distribution of shear stresses in the laminates (plotted in colour).

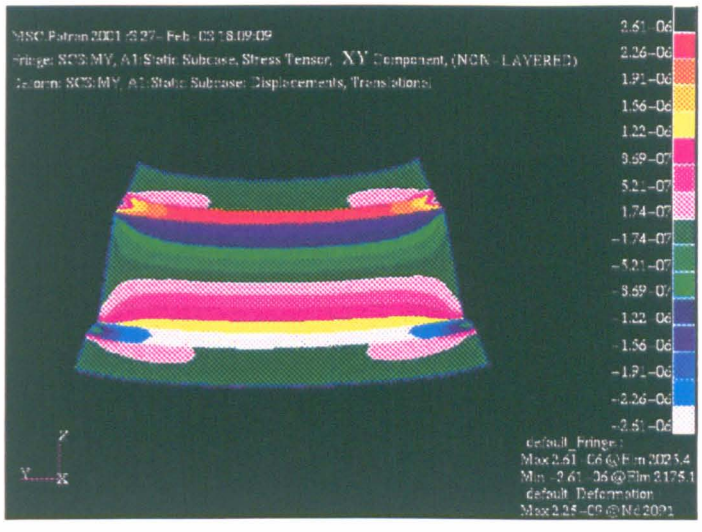

Figure 4.37 Finite element output showing non-uniform deformation and non-uniform shear stress of thick laminates

The main cause of these non-uniform deformations is the forces that are imposed upon the laminate by the core material, and hence this source of error is most significant for sections with high core modulus.

4.5 OPTIMISATION ISSUES

K_{45} coupling is obviously not a linear function of any of the design variables. K_{45} is not even a convex function of many of the possible variables *cf.* variation of K_{45} with ply angle.

This poses potential problems if using an optimisation algorithm based on a linearised problem – the method which was found to be the most efficient for other cross-sectional properties.

It is seen from the studies so far that, as K_{45} varies with unbalanced ply angle, the value of ply angle that maximises K_{45} for a given thickness of unbalanced laminate is in the range 15°-30°. From a design perspective, it is desirable to use as little material as possible to produce the required amount of K_{45}. It is therefore justifiable to pre-select a ply angle of, say, 22.5° to remove one source of non-convexity.

Since ply angle is no longer a variable, the only remaining factors that determine K_{45} are the geometry of the section, and the A, B and D matrix terms of the horizontal laminates.

Recalling Smith's results

$$K_{45} = (1+\beta)\iint \overline{Q_{16}}\zeta^2 dA - (1+\beta)\iint_{n,v} \overline{Q_{12}}\zeta^2 dA \frac{\iint_{n,v} \overline{Q_{26}} dA}{\iint_{n,v} \overline{Q_{22}} dA} \tag{4.95}$$

and Rehfield's results

$$K_{45} = \frac{C_S^2 H^2}{(C_S + H)}\left(A_{16} - \frac{A_{26}A_{12}}{A_{22}}\right) \tag{4.96}$$

it is appreciated that K_{45} may be generally approximated as a function of four translated reduced stiffness terms

$$K_{45} = f_1(\overline{Q}_{16}) - f_2(\overline{Q}_{26})\frac{f_3(\overline{Q}_{12})}{f_4(\overline{Q}_{22})} \qquad (4.97)$$

Thus, at a pre-selected coupling angle, the value of K_{45} is mostly dependent upon the Q_{16} term. Since the rest of the laminate is balanced, the Q_{16} term will be directly proportional to the thickness of unbalanced laminate (as will the Q_{26} term).

While this is not a good approximation for large changes in unbalanced ply thickness or in the overall lay-up or (since these would have a significant effect upon the Q_{12} and Q_{22} terms), it is acceptable to simplify the optimisation problem in this way, by assuming linearity with respect to thickness of unbalanced coupling material.

This allows the use of efficient optimisation methods such as sequential linear programs, or iterative global linear approximations as presented in the previous chapter.

4.6 CONCLUSIONS

A new analytical model for flap bending-torsion (K_{45}) coupling has been presented which models the cross-sectional features of a typical rotor blade in considerably more detail than existing models. The simplified cross sectional model on which this analysis is based consists of a box section with CFRP walls, additional unbalanced CFRP coupling plies in the top and bottom surfaces of the box section, and an isotropic core material. The analysis procedure is applicable to a wide range of geometry and material properties.

A parametric investigation is undertaken using finite element analysis, and the predictions from this new analytical model are found to correlate well with the finite element results over a wide range of cross-sectional parameters - including aspect ratio of cross-section, ply orientation, vertical wall thickness, and core material modulus.

Although a closed form solution for K_{45} is not presented explicitly, it is seen that this stiffness term is based upon the translated reduced stiffness terms of the laminates on the top and bottom surfaces and may generally be approximated to be of form

$$K_{45} = f_1(\overline{Q}_{16}) - f_2(\overline{Q}_{26})\frac{f_3(\overline{Q}_{12})}{f_4(\overline{Q}_{22})} \qquad (4.97)$$

By fixing the angle of unbalanced plies in the upper and lower surfaces of the cross-section, the thickness of this unbalanced layer can be used as a suitable design variable in a global linear approximation optimisation algorithm.

The following chapter details the experimental measurement of K_{45} for a number of DERA-manufactured solid rectangular section CFRP beams, and compares these results with finite element analysis. In so doing, the finite element analysis method of Hill and Weaver [34] is independently validated, and further insight is gained into the physical interpretation of K_{45} (and other) stiffness matrix terms.

5 EXPERIMENTAL VALIDATION OF K_{45} FOR SOLID SECTIONS

5.1 INTRODUCTION

The anisotropic coupling behaviour of composite beams is not a new discovery. In an early experimental study, Diamond [46] of the former Defence Engineering Research Agency (DERA) manufactured and tested eight CFRP spars with a solid rectangular cross-section to investigate these anisotropic couplings. As part of the collaboration between Westland Helicopters and University of Bristol, these spars were made available to this project and used as test specimens.

Since the test specimens used in this study are solid CFRP laminates and the K_{45} model presented in the previous chapter applies to filled box- and sandwich-sections, the experimental results presented here clearly do not directly validate the analytical model presented in the previous chapter. Rather, the experimental results are used to validate the finite element method of Hill and Weaver [34] that is used elsewhere in this project. The previous chapter has already shown that the analytical model developed therein concurs with the finite element method of Hill and Weaver.

Since the finite element method of Hill and Weaver is applicable to any prismatic beam section, it is perfectly acceptable to use a solid section spar as an experimental validation of the method. Indeed, the existence of Diamond's [46] results (which were obtained completely independently of this project) makes these spars ideal specimens for experimental testing and validation of the finite element method.

5.2 LITERATURE

Since familiar isotropic structures do not exhibit the same couplings as anisotropic structures, the physical interpretation of individual terms in the stiffness matrix requires careful thought. Intuition cannot always be relied upon to give the correct interpretation of a stiffness term.

Monterro & Appleby [44] measured the coupling of various anisotropic prismatic beams as part of an undergraduate project at the University of Bristol. They measured a

variety of strains and deflections to determine various terms from the 1-dimensional beam stiffness matrix. For the cross-sectional properties examined in the experimental section of this thesis, all the required data can be obtained from deflection results, considerably simplifying the experimental procedure.

Clearly the most significant piece of literature for this chapter is that of Diamond [46] at DERA, and his work is referred to extensively throughout this chapter.

5.3 BACKGROUND

5.3.1 Physical interpretation of Stiffness Matrix terms

Using the same global *xyz* beam co-ordinate system described in Chapter 4 gives the 1-dimensional 6 x 6 beam stiffness matrix as

$$\begin{Bmatrix} N_x \\ N_{xy} \\ N_{xz} \\ M_{yz} \\ M_y \\ M_z \end{Bmatrix} = \begin{bmatrix} K_{11} & K_{12} & K_{13} & K_{14} & K_{15} & K_{16} \\ K_{12} & K_{22} & K_{23} & K_{24} & K_{25} & K_{26} \\ K_{13} & K_{23} & K_{33} & K_{34} & K_{35} & K_{36} \\ K_{14} & K_{24} & K_{34} & K_{44} & \textcircled{K_{45}} & K_{46} \\ K_{15} & K_{25} & K_{35} & \textcircled{K_{45}} & K_{55} & K_{56} \\ K_{16} & K_{26} & K_{36} & K_{46} & K_{56} & K_{66} \end{bmatrix} \begin{Bmatrix} \varepsilon_x \\ \gamma_{xy} \\ \gamma_{xz} \\ \kappa_{yz} \\ \kappa_y \\ \kappa_z \end{Bmatrix} \qquad (5.1)$$

where the K_{45} terms are highlighted. Equation *(5.1)* may also be written as

$$\begin{Bmatrix} \varepsilon_x \\ \gamma_{xy} \\ \gamma_{xz} \\ \kappa_{yz} \\ \kappa_y \\ \kappa_z \end{Bmatrix} = \begin{bmatrix} S_{11} & S_{12} & S_{13} & S_{14} & S_{15} & S_{16} \\ S_{12} & S_{22} & S_{23} & S_{24} & S_{25} & S_{26} \\ S_{13} & S_{23} & S_{33} & S_{34} & S_{35} & S_{36} \\ S_{14} & S_{24} & S_{34} & S_{44} & S_{45} & S_{46} \\ S_{15} & S_{25} & S_{35} & S_{45} & S_{55} & S_{56} \\ S_{16} & S_{26} & S_{36} & S_{46} & S_{56} & S_{66} \end{bmatrix} \begin{Bmatrix} N_x \\ N_{xy} \\ N_{xz} \\ M_{yz} \\ M_y \\ M_z \end{Bmatrix} \qquad (5.2)$$

where the compliance matrix is the inverse of the stiffness matrix. It will be appreciated that each term in the stiffness matrix is not simply the inverse of the corresponding term in the compliance matrix.

Because it is obtained directly from the stiffness matrix, K_{45} is not like other common stiffness terms (which are defined as the inverse of the relevant term from the compliance matrix), as explained in Chapter 4.

Experimentally, it is much easier to derive compliance terms than it is to derive stiffness terms, and hence the value of K_{45} must be calculated from the inverse of the compliance matrix. For many classes of beam (including the specimens tested in this project) this does not require the entire compliance matrix to be derived, since the K_{45} term can be (partially) decoupled from the full 6 x 6.

The working definition of K_{45} used so far is "the torque (M_{yz}) when one unit of flapwise bending curvature (κ_y) is applied and all other strains are constrained to be zero", i.e.

$$M_{yz} = K_{14}\varepsilon_x + K_{24}\gamma_{xy} + K_{34}\gamma_{xz} + K_{44}\kappa_{yz} + K_{45}\kappa_y + K_{46}\kappa_z \qquad (5.1.a)$$

although from the above matrix *(5.1)*, it can be seen that K_{45} may equally well be expressed as "the moment (M_y) when one unit of twist (κ_{yz}) is applied and all other strains are constrained to be zero".

$$M_y = K_{15}\varepsilon_x + K_{25}\gamma_{xy} + K_{35}\gamma_{xz} + K_{45}\kappa_{yz} + K_{55}\kappa_y + K_{56}\kappa_z \qquad (5.1.b)$$

If required, this can be used to provide an alternative experimental procedure for determining K_{45}, since the value should be independent of which experimental method of calculating K_{45} has been used.

5.3.2 Test specimens

Eight DERA-manufactured solid CFRP spars were provided by Westland Helicopters for experimental testing. These spars were originally the subject of testing undertaken by Diamond [46].

All the spars are 1 metre long and share a common cross-sectional geometry of 40.2 mm x 8 mm (to within manufacturing tolerances). Each spar is constructed from 60 plies of unidirectional carbon, laid up in the global *xy*-plane as shown on Figure 5.1 below.

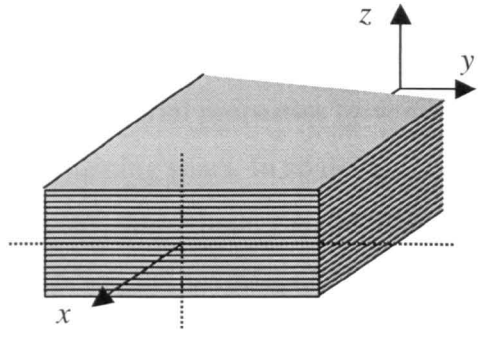

Figure 5.1 Coordinate system and orientation of layers in DERA spars

Each spar was manufactured with a unique lay-up. Obviously, it was not possible for DERA to manufacture each spar to precisely the dimension given above. The lay-up and exact cross sectional geometry of each spar is summarised by Table 5.1, below.

Spar	Lay-up	Mean width (mm)	Mean depth (mm)
1	$[0]_{60}$	40.18	7.932
2	$[+45]_{60}$	40.41	7.968
3	$[+45]_{30}[-45]_{30}$	40.29	7.922
4	$[+/-45]_{30}[-/+45]_{30}$	40.28	7.956
5	$[+15]_{60}$	40.19	7.962
6	$[+15]_{30}[-15]_{30}$	40.71	8.004
7	$[+30]_{60}$	40.15	7.994
8	$[+30]_{30}[-30]_{30}$	40.13	7.986

Table 5.1 Geometry and lay-ups of available test specimens

One important feature of the DERA beams is that they are made up from 60 plies of 0.125mm thick UD carbon. This would normally give a total thickness of 7.5mm; however the beams are all approximately 8mm thick.

The additional thickness is made up from excess resin. This will have a significant impact on the resulting material properties, since the values quoted by the supplier are only valid for a specific fibre-resin ratio.

Diamond [46] addressed this problem by measuring the overall bending and twisting flexibilities of Spar 1 (manufactured from 0° plies) and back calculating the material properties. These values of material properties (given in Table 5.2) were then applied to the calculations for the remaining spars. In so doing, Diamond assumed this excess resin to be uniformly distributed throughout the thickness of the laminate, although the validity of this assumption was not investigated.

Properties	E_1 (GPa)	E_2 (GPa)	E_3 (GPa)	G_{12} (GPa)	G_{13} (GPa)	G_{23} (GPa)	ν_{12}	ν_{13}	ν_{23}
Carbon XAS 913c	124.0	9.4	9.4	4.6	4.6	2.4	0.26	0.26	0.30

Table 5.2 CFRP material properties calculated by Diamond [46]

The material property values determined by Diamond have *not* been adopted for use within this thesis. One reason for this is that the beams are at least 7 years old, with an unknown history. It is not necessarily safe to assume that the material properties have not changed during this time due to delaminations, prolonged exposure to moisture or UV light, or to other factors.

Values for generic CFRP (given in Table 5.3) are used in the FE and laminate analyses of these sections. Although it is appreciated that this will be a source of error, the source is known and some attempt can be made to quantify the magnitude of this error based on the results obtained.

Properties	E_1 (GPa)	E_2 (GPa)	E_3 (GPa)	G_{12} (GPa)	G_{13} (GPa)	G_{23} (GPa)	ν_{12}	ν_{13}	ν_{23}
Generic CFRP	132.0	9.2	9.2	4.34	4.34	4.34	0.3	0.3	0.3

Table 5.3 Generic CFRP material properties used in Finite Element Analyses

5.3.3 Classical laminate theory

Due to the construction of the spars (each spar is effectively a thick laminate of finite width), there is a direct parallel between some of the terms in the laminate stiffness matrix and those in the 1-dimensional beam stiffness matrix. Equivalent terms in Figure 5.2 (below) are shown by identically coloured boxes around those terms.

Laminate stiffness matrix

$$\begin{bmatrix} A_{11} & A_{12} & A_{16} & B_{11} & B_{12} & B_{16} \\ A_{12} & A_{22} & A_{26} & B_{12} & B_{22} & B_{26} \\ A_{16} & A_{26} & A_{66} & B_{16} & B_{26} & B_{66} \\ B_{11} & B_{12} & B_{16} & D_{11} & D_{12} & D_{16} \\ B_{12} & B_{22} & B_{26} & D_{12} & D_{22} & D_{26} \\ B_{16} & B_{26} & B_{66} & D_{16} & D_{26} & D_{66} \end{bmatrix}$$

1-D beam stiffness matrix

$$\begin{bmatrix} K_{11} & K_{12} & K_{13} & K_{14} & K_{15} & K_{16} \\ K_{12} & K_{22} & K_{23} & K_{24} & K_{25} & K_{26} \\ K_{13} & K_{23} & K_{33} & K_{34} & K_{35} & K_{36} \\ K_{14} & K_{24} & K_{34} & K_{44} & K_{45} & K_{46} \\ K_{15} & K_{25} & K_{35} & K_{45} & K_{55} & K_{56} \\ K_{16} & K_{26} & K_{36} & K_{46} & K_{56} & K_{66} \end{bmatrix}$$

Figure 5.2 Equivalence of terms in laminate stiffness matrix and 1-D beam stiffness matrix

The inherent assumptions of classical laminate theory severely limit the accuracy of the analysis where the laminate used cannot be approximated to a mathematical lamina (i.e. infinitely wide and thin). For the samples studied here, where the laminate thickness is approximately 20% of the laminate width, classical laminate theory is clearly not expected to give a good correlation with the experimental and finite element results. However, it is seen that each of the spar lay-ups fall into one of the following three general categories, which gives some insight into their general behaviour.

5.3.3.1 Symmetric, balanced (Spars 1, 4)

The 6 x 6 flexibility matrix for these balanced symmetric spars is expected to be populated as

$$\begin{bmatrix} S_{11} & 0 & 0 & 0 & 0 & 0 \\ 0 & S_{22} & 0 & 0 & 0 & 0 \\ 0 & 0 & S_{33} & 0 & 0 & 0 \\ 0 & 0 & 0 & S_{44} & S_{45} & 0 \\ 0 & 0 & 0 & S_{45} & S_{55} & 0 \\ 0 & 0 & 0 & 0 & 0 & S_{66} \end{bmatrix} \qquad (5.2.a)$$

5.3.3.2 Symmetric, unbalanced (Spars 2, 5, 7)

The 6 x 6 flexibility matrix for these unbalanced symmetric spars is expected to be populated as

$$\begin{bmatrix} S_{11} & S_{12} & 0 & 0 & 0 & 0 \\ S_{12} & S_{22} & 0 & 0 & 0 & 0 \\ 0 & 0 & S_{33} & 0 & 0 & 0 \\ 0 & 0 & 0 & S_{44} & S_{45} & 0 \\ 0 & 0 & 0 & S_{45} & S_{55} & 0 \\ 0 & 0 & 0 & 0 & 0 & S_{66} \end{bmatrix} \qquad (5.2.b)$$

5.3.3.3 Anti-symmetric (Spars 3, 6, 8)

The 6 x 6 flexibility matrix for these anti-symmetric spars is expected to be populated as

$$\begin{bmatrix} S_{11} & 0 & 0 & S_{14} & 0 & 0 \\ 0 & S_{22} & 0 & 0 & S_{25} & 0 \\ 0 & 0 & S_{33} & 0 & 0 & S_{36} \\ S_{14} & 0 & 0 & S_{44} & 0 & 0 \\ 0 & S_{25} & 0 & 0 & S_{55} & 0 \\ 0 & 0 & S_{36} & 0 & 0 & S_{66} \end{bmatrix} \qquad (5.2.c)$$

Note that since all plies lie parallel to the *x-y* plane, in all cases the third and sixth rows and columns can be decoupled from the rest of the matrix.

For symmetric beams, the 2 x 2 sub-matrix containing the S_{44}, S_{45} and S_{55} terms can be decoupled from the full 6 x 6 compliance matrix. The sub matrix may be inverted to obtain the K_{44}, K_{45} and K_{55} terms in the stiffness matrix.

It is important to note that, although K_{44} is a term that relates the twisting of the section (κ_{yz}) to the applied torque (M_{yz}), it is not equal to the "torsional stiffness" of the beam (which is given by the inverse of the S_{44} term).

Similarly, K_{55} is a term that relates the bending of the section to the applied bending moment, but is not equal to the "bending stiffness" of the beam (which is given by the inverse of the S_{55} term).

5.4 EXPERIMENTAL DESIGN AND METHOD

5.4.1 Conceptual design

For this work, the first of the conceptual approaches discussed in section 5.3 above was used. If a constant (known) bending curvature is applied to the beam section, and the value of K_{45} can be calculated directly from the torque required to give no end rotation.

In practice, it is not straightforward to apply a constant bending curvature without adding unwanted constraints upon the system. The standard method of applying a *constant* bending moment (and hence obtaining a constant curvature) to a section of a beam is to use a four point bending test as depicted schematically in Figure 5.3 below.

Rehfield *et al* [45] perform a four point bending test using a "sling supported method" to measure the camber produced in a tailored box beam under bending. Unfortunately, the use of such an experimental set up would make it difficult to measure the torsion force (M_{xy}) required to prevent twisting of the section.

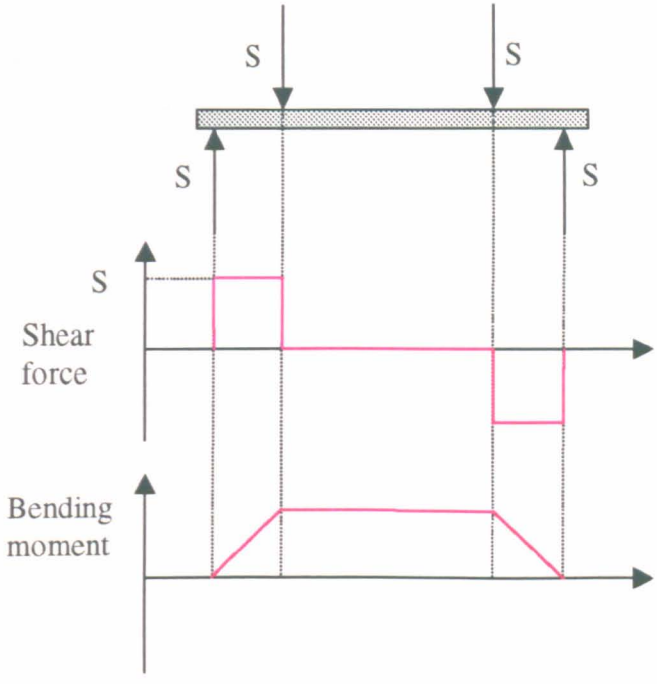

Figure 5.3 Bending moment and shear force diagram for four-point bending test

Since the reduction of the 3-dimensional blade behaviour to a 1-dimensional beam inherently assumes a linear system, it is straightforward to calculate the stiffness matrix terms from the results of a cantilever bend test. The torsion force required to prevent twisting is relatively easy to determine in this type of test. A schematic diagram of the experimental set-up (complete with charts of bending moment, shear force and torque along the length of the beam) is shown below in Figure 5.4.

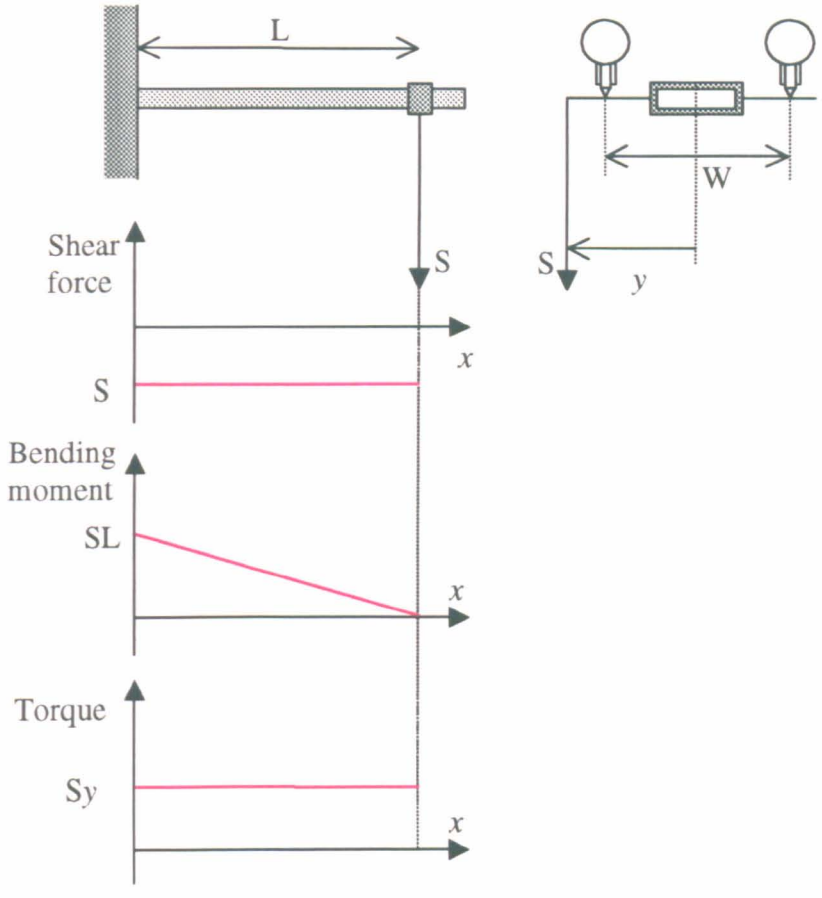

Figure 5.4 Schematic diagram of experimental set up

For a given shear force, S, at a given (measured) length, L, the applied flap-bending moment will vary linearly along the length of the beam as shown in the figure above, but will be independent of the offset, y. The applied torque is constant along the length of the beam, but varies linearly with the offset, y.

5.4.2 Shear deflection of beam

Timoshenko beam theory tells us that the flap deflection of the beam (δ_z) comes from bending and shear deformations, and is given by

$$\delta_z = \frac{SL^3}{3EI} + \frac{SL}{Gtw} \qquad (5.3)$$

Thus for a three point bend test, there will be some flap shear deformation (γ_{xz}) in addition to the flap bending deformation (κ_y).

Although this should be negligibly small for a slender beam, any source of error is undesirable. It is possible to determine exactly how much shear deformation is present by conducting tests for two different lengths and measuring the flap deflections of each. It is then straightforward to calculate the amount of shear deformation and bending deformation by solving the simultaneous equation. By so doing, it is possible to eliminate this source of error from the results.

No flap shear-torsion coupling was predicted for any of the test specimens, and initial results indicated that the shear deformation accounted for less than 1% of the total flap deflection. Further tests were therefore conducted at one length only, and corrections for flap shear deflection are not performed.

5.4.3 Constraint of unwanted strains

Implicit in the calculation of K_{45} directly from the stiffness matrix is the assumption that the axial (ε_x), flap-shear (γ_{xy}), lag-shear (γ_{xz}), and lag-bending (κ_z) strains are all zero. In practice, this is difficult to achieve without interfering with the necessary bending displacements and imposing unknown torsion restraint forces on the section.

For symmetric lay-ups (i.e. Spars 1, 2, 4, 5 and 7) the axial, lag-shear, and lag-bending strains were all predicted to be zero under an applied flap-bending. These strains are therefore not constrained (although strain gauges could be used to confirm the validity of these predictions).

For anti-symmetric lay-ups (i.e. Spars 3, 6 and 8), a lag-shear deformation was predicted under an applied flap-bending. It was assumed that any lag-shear bending does not interfere with the accuracy of any measurements taken. This makes explicit calculation of K_{45} impossible from the limited measurements that could be taken, since the K_{45} term does not decouple easily from the 6 x 6 stiffness matrix. However, since K_{45} is predicted to be zero for anti-symmetric lay-ups, it is relatively straightforward to

confirm (or refute) this prediction by simply determining the location of the shear centre of the spar.

5.4.4 Experimental set up and procedure

The apparatus was set up as shown in Figure 5.5 below. The spar was clamped securely at one end between two large steel blocks. Although this clamping arrangement restrains out of plane warping, the sections tested here are solid, and hence the stress effects of end restraints will die away rapidly along the length of the beam. It is assumed that this warping restraint does not significantly affect the end deflections.

The lengths L and W (as marked on the schematic diagram – Figure 5.4) were measured. Typically, L ≈ 0.6-0.7 m and W ≈ 0.6 m.

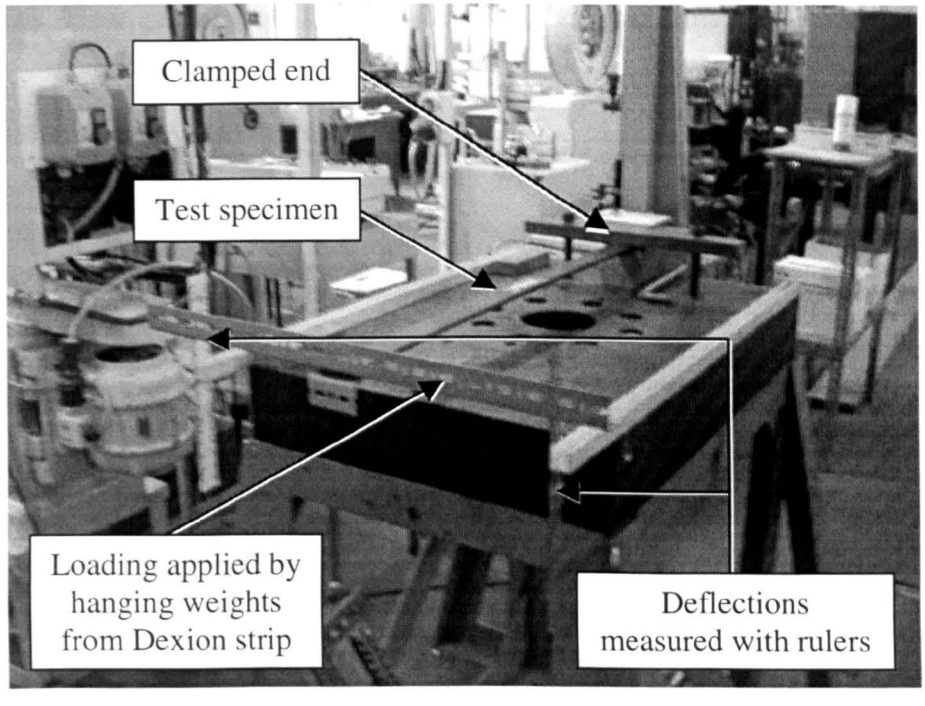

Figure 5.5 Experimental set up

An offset shear force was applied at the end of the spar, by hanging a mass from the Dexion strip attached to the end of the beam. The offset, y, was measured and the end deflection and end rotation of the spar (relative to the unloaded case) were noted. The value of y was changed and the new relative deflections were noted.

Since it was only possible to measure the end deflections to a resolution of 0.5 mm, the magnitude of the applied shear force, S was chosen such that the measured deflections were approximately 10 cm. With an end deflection of this size, the inability to measure deflections more accurately than 0.5 mm will introduce errors of less than 0.5%. Typically, a loading with a mass of 1-3 kg gave a suitable end deflection.

Preliminary results (which measured the end deflection and end rotation of Spar 1 for a range of shear offsets) indicated that the response of the beam was linear because the deflections involved are small. Deflection and rotation readings at two different offsets therefore provide sufficient information to enable the location of the shear centre to be deduced. For symmetric lay-ups, the values of K_{44}, K_{45} and K_{55} could be calculated using the method described in section 5.4.5 below.

This procedure was repeated three times, to test the spar in the apparatus in all possible orientations. Mean values were calculated for the stiffness terms.

5.4.5 Calculations for symmetric lay-ups

The following analysis uses the standard terms for moments, stiffnesses and strains from the 1-dimensional beam equation *(5.1)* based on the standard global *xyz* co-ordinate system used here and elsewhere in the literature. Measured values are marked on the Figure 5.4.

For an end-loaded cantilever beam of length, L, first principles Euler bending theory gives the bending moment as a function of applied shear load, S and coordinate, x, as

$$M_y = S(L-x) \qquad (5.4)$$

and the flap deflection, $\delta_z(x)$ at coordinate x is determined from

$$\delta_z(x) = \iint \kappa_y(x)dx \qquad (5.5)$$

The torque acting on the beam is constant along the length of the beam

$$M_{yz} = Sy \tag{5.6}$$

and the twist, $\phi_x(x)$ is determined from

$$\phi_x(x) = \int \kappa_{yz}(x)dx \tag{5.7}$$

For a beam with no coupling, these calculations would be trivially simple. For beams with anisotropic couplings, the strains κ_{yz} and κ_y are expressed in terms of the full 6 x 6 matrix. For symmetric lay-ups, the K_{44}, K_{45} and K_{55} stiffness terms may be decoupled from the rest of the matrix, to give

$$\begin{pmatrix} M_{yz} \\ M_y \end{pmatrix} = \begin{bmatrix} K_{44} & K_{45} \\ K_{45} & K_{55} \end{bmatrix} \begin{pmatrix} \kappa_{yz} \\ \kappa_y \end{pmatrix} \tag{5.8}$$

and hence

$$\begin{pmatrix} \kappa_{yz} \\ \kappa_y \end{pmatrix} = \begin{bmatrix} S_{44} & S_{45} \\ S_{45} & S_{55} \end{bmatrix} \begin{pmatrix} M_{yz} \\ M_y \end{pmatrix} \tag{5.9}$$

Thus

$$\begin{aligned} \delta_z(x) &= S\iint (S_{45}(y) + S_{55}(L-x))dx \\ &= S\left(S_{45}\frac{yx^2}{2} + S_{55}\left(\frac{Lx^2}{2} - \frac{x^3}{6}\right)\right) \end{aligned} \tag{5.10}$$

and the end deflection is given by

$$\delta_z(L) = S\left(S_{45}\frac{yL^2}{2} + S_{55}\frac{L^3}{3}\right) \tag{5.11}$$

Similarly,

$$\begin{aligned}\phi_x(x) &= \int \kappa_{yz} dx \\ &= \int (S_{44} M_{yz} + S_{45} M_y) dx \\ &= S \int (S_{44}(y) + S_{45}(L-x)) dx \\ &= S\left(S_{44} yx + S_{45}\left(Lx - \frac{x^2}{2} \right) \right)\end{aligned} \tag{5.12}$$

and the end rotation is thus given by

$$\phi_x(L) = S\left(S_{44} yL + \frac{S_{45} L^2}{2} \right) \tag{5.13}$$

It is straightforward to experimentally determine the rate of change of $\phi(L)$ with respect to y. The value of S_{44} may be calculated from

$$\frac{d\phi_x(L)}{dy} = S_{44} LS \tag{5.14}$$

It is also straightforward to experimentally determine the value of y for which $\phi(L) = 0$. This gives the value of S_{45} as

$$S_{45} = -2S_{44} \frac{y}{L} \tag{5.15}$$

The end deflection for no end rotation is also easily determined, to give S_{55} from

$$\delta_x(L) = S\left(S_{45} \frac{yL^2}{2} + S_{55} \frac{L^3}{3} \right) \tag{5.11}$$

The flexibility terms S_{44}, S_{45} and S_{55} are now all known and the stiffness terms K_{44}, K_{45} and K_{55} may thus be calculated by inverting the 2 x 2 flexibility matrix.

5.5 RESULTS

The analytical K_{45} model presented in the previous chapter cannot be applied to the cross-sections tested here. Since the eight spars tested here are simply thick laminates of finite width, classical laminate theory can be applied – Figure 5.2 shows that the K_{44}, K_{45} and K_{55} terms in the 1-dimensional beam stiffness matrix are respectively equivalent to the D_{66}, D_{16} and D_{11} terms of the laminate stiffness matrix (ABD matrix) of classical lamination theory.

As stated earlier, due to the assumptions of classical laminate analysis, the ABD matrix terms are not expected to accurately quantify the behaviour of the spars studied here.

Spar	Lay-up	Stiffness terms from laminate theory (x10^5 Nmm^2)		
		$K_{44} = D_{66}$	$K_{45} = D_{16}$	$K_{55} = D_{11}$
1	$[0]_{60}$	74.0	0	2270
2	$[+45]_{60}$	584	528	704
3	$[+45]_{30}[-45]_{30}$	584	0	704
4	$[+/-45]_{30}[-/+45]_{30}$	584	26.4	704
5	$[+15]_{60}$	201	484	2000
6	$[+15]_{30}[-15]_{30}$	201	0	2000
7	$[+30]_{60}$	456	676	1360
8	$[+30]_{30}[-30]_{30}$	456	0	1360

Table 5.4 Predictions of classical laminate analysis

The finite element results for each of the 8 beams are summarised by Tables 5.5 and 5.6, below. Finite element results were determined from a model that used a nominal 40 mm x 8 mm section and typical CFRP material properties as given in Table 5.3.

Spar	Lay-up	Finite Element Predictions ($x10^{-10}$ $N^{-1}mm^{-2}$)		
		S_{44}	S_{45}	S_{55}
1	$[0]_{60}$	343	0	44.6
2	$[+45]_{60}$	212	148	464
3	$[+45]_{30}[-45]_{30}$	138	0	403
4	$[+/-45]_{30}[-/+45]_{30}$	67.5	2.22	340
5	$[+15]_{60}$	301	127	115
6	$[+15]_{30}[-15]_{30}$	237	0	91.3
7	$[+30]_{60}$	237	182	285
8	$[+30]_{30}[-30]_{30}$	154	0	206

Table 5.5 Finite Element flexibility results for DERA manufactured beams

Since the full 6 x 6 flexibility matrix is returned from the finite element output, the entire 6 x 6 stiffness matrix can be derived for any beam section by inverting the flexibility matrix. The values of K_{44}, K_{45} and K_{55} are presented in Table 5.6, below.

Spar	Lay-up	Finite Element Predictions ($x10^{5}$ Nmm^{2})		
		K_{44}	K_{45}	K_{55}
1	$[0]_{60}$	291	0	2240
2	$[+45]_{60}$	605	193	277
3	$[+45]_{30}[-45]_{30}$	813	0	318
4	$[+/-45]_{30}[-/+45]_{30}$	1480	9.65	294
5	$[+15]_{60}$	627	695	1640
6	$[+15]_{30}[-15]_{30}$	635	0	1770
7	$[+30]_{60}$	824	525	685
8	$[+30]_{30}[-30]_{30}$	928	0	937

Table 5.6 Finite Element stiffness results for DERA manufactured beams

The values obtained from finite element analysis (Table 5.6) confirm that classical laminate analysis (Table 5.4) does not give an accurate prediction of the stiffness terms.

The values of deflections are determined experimentally as described in section 5.4.4. The values of flexibilities S_{44}, S_{45} and S_{55} are determined from these deflections and are presented in Table 5.7 below.

Spar	Lay-up	Experimental Results ($x10^{-10}$ $N^{-1}mm^{-2}$)		
		S_{44}	S_{45}	S_{55}
1	$[0]_{60}$	346	<1	52.2
2	$[+45]_{60}$	229	156	497
3	$[+45]_{30}[-45]_{30}$	152	<1	441
4	$[+/-45]_{30}[-/+45]_{30}$	80.4	3.72	346
5	$[+15]_{60}$	313	128	125
6	$[+15]_{30}[-15]_{30}$	259	<1	121
7	$[+30]_{60}$	249	180	293
8	$[+30]_{30}[-30]_{30}$	261	<1	103

Table 5.7 Experimental flexibility results

Although it is most comprehensive to compare flexibility terms (S_{44}, S_{45} and S_{55}) from the experimental results and finite element model, it is often more intuitive to think about stiffness terms (K_{44}, K_{45} and K_{55}). Based on the assumptions discussed in section 5.3, the values of K_{44}, K_{45} and K_{55} may be derived from these flexibility results for symmetric lay-ups. These derived stiffness terms are presented in Table 5.8 below.

Spar	Lay-up	Experimental Results ($x10^{5}$ Nmm^{2})		
		K_{44}	K_{45}	K_{55}
1	$[0]_{60}$	289	<1	1920
2	$[+45]_{60}$	557	175	256
4	$[+/-45]_{30}[-/+45]_{30}$	1240	13.3	289
5	$[+15]_{60}$	548	559	1370
7	$[+30]_{60}$	726	448	617

Table 5.8 Experimental stiffness results for symmetric lay-ups

In the general case, the 2 x 2 S_{44}, S_{45}, S_{55} sub-matrix cannot be decoupled from the full 6 x 6 flexibility matrix. This is the case for non-symmetric lay-ups, and hence for spars 3, 6 and 8 the values of K_{44}, K_{45} and K_{55} cannot be determined explicitly from the measurements available. However, the flexibility terms obtained experimentally (Table 5.7) can be compared directly with those that are obtained from the finite element model (Table 5.5), and it can be seen that the results generally agree to an acceptable level of accuracy. A detailed discussion of results for flexibility and stiffness terms is presented later in this chapter.

Since K_{45} was predicted to be zero for each of the non-symmetric specimens tested, it is possible to validate this prediction directly from the location of the shear centre, where the shear centre is defined as the axis through which an applied shear force will produce no twisting. The location of the shear centre relative to the centroid of the beam is shown by the variable y_0 on Figure 5.6, below.

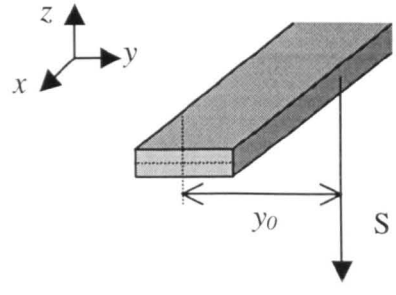

Figure 5.6 Location of shear centre, y_0 is taken relative to centroid of spar cross-section

It is obvious that if the shear centre passes through the centroid of the cross-section, then K_{45}=0. The distance of the shear centre from the centroid of the section was determined from the results as shown in Table 5.9 below.

Spar	Lay-up	Location of Shear Centre, y_0 (mm)				
		Test 1	Test 2	Test 3	Test 4	**Mean**
3	$[+45]_{30}[-45]_{30}$	-40.3	22.7	33.0	-15.6	**-0.05**
6	$[+15]_{30}[-15]_{30}$	0.5	0.5	-3.9	-0.9	**-0.94**
8	$[+30]_{30}[-30]_{30}$	-1.1	0.3	2.5	2.2	**0.96**

Table 5.9 Location of shear centre for anti-symmetric lay-up DERA manufactured beams

Note that four tests have been carried out for each spar. These tests correspond to the four possible orientations of the beam in the loading arrangement. i.e. After the initial test, the beam was turned over (so the bottom surface became the top) and the test repeated. The beam was then turned around (so that it was then clamped at the previously free end) and the test repeated again. Finally, the beam was turned over again and the test repeated one final time to compete the set of four results.

5.5.1 Discussion of experimental accuracy

Geometric, material, and experimental factors will affect the accuracy of these experimental results. These are discussed below.

5.5.1.1 Geometric issues

The geometric results are of some interest in determining the manufacturing variability of each beam, since both the cross-section and width varied slightly along the length of each beam.

The magnitude of the variation in width was typically 0.1-0.2 mm, although since this corresponds to less than 0.5% of the total width, this does not have a particularly significant effect upon K_{45}.

The magnitude of the through thickness variation was typically slightly under 0.1 mm, which corresponds to a variation of the order of 1% of the total depth. Since flap-torsion coupling is dependent upon depth to the third power, this may contribute to an overall error of up to 3% in the analysis.

5.5.1.2 Material properties

A number of issues are unknown which will affect the properties of the CFRP material. The effect of a non-standard fibre-to-resin ratio was noted by Diamond [46] in his investigation of the beams. Subsequent to the Diamond's study, additional factors may have an effect upon the material properties. The effect of age upon the material properties of CFRP is difficult to quantify with any certainty, especially as the history of each individual specimen is not known and a number of factors could affect the overall behaviour (e.g. presence of delaminations, exposure to moisture, and exposure to UV light).

The angle of the plies that compose the test specimens could not be confirmed with any degree of certainty. The best approximation was to visually determine the angle of plies on the top and bottom surfaces and assume that the remaining plies had all been laid up identically. As seen from the finite element predictions, altering the coupling angle can have a significant effect upon K_{45} over some ranges.

Nominal values from the material properties (based on data from Westland Helicopters Ltd) were used in the finite element model. A discrepancy of 10% between nominal and actual values for material stiffness properties may be expected.

5.5.1.3 Experimental procedure

The experimental procedure allowed the shear centre of a spar to be repeatably determined to an accuracy of better than 5 millimetres. In most cases, this corresponds to an uncertainty in K_{45} of about 5E+5 Nmm^2. It is obviously more meaningful to talk of accuracy in these terms than in terms of percentage error, since the percentage error depends on both the predicted location of the shear centre and the choice of datum from which it is measured. By determining the shear centre of the spar four times (loading

both sides for both ends) and taking a mean, confidence in the accuracy of the results could (in most cases) be improved further.

It was noted that the shear centre varied for each of the four cases – often by a significant amount. The repeatability of the results indicates that this is not a fault of the experimental procedure, but rather an inherent feature of the test specimens. This confirms that the manufacturing issues mentioned above can significantly affect the stiffness terms.

5.5.1.4 Expected overall accuracy

Considering the sources of error discussed above (i.e. geometric variability, material properties, and experimental resolution and repeatability), it is expected that the experimentally derived stiffness terms and the finite element predictions may vary by up to 20%.

5.6 DISCUSSION OF RESULTS

The experimental results generally supported the finite element predictions, although a few anomalies are noted in the discussion below. Because the sections tested are solid (rather than thin-walled) sections, St Venant's principle applies, and the warping restraint created by clamping the root of the cantilever does not greatly affect the results.

The results for each individual spar are now considered and discussed below. Note that the following discussions refer to the experimental and finite element results presented earlier in Tables 5.5 to 5.9.

5.6.1 Spar 1: $0_{[60]}$ lay-up

The experimentally determined value of S_{44} agreed with the finite element model to within 1%, while S_{55} was found to be 117% of that predicted by FE (i.e. more flexible

than predicted). These correlations were reflected in the derived values of K_{44} (within 1% of FE) and K_{55} (85% of FE value).

For a spar with 0° lay-up, the bending stiffness is determined by the axial stiffness of the plies. Since the fibre-to-resin ratio is less than that specified by the manufacturer, the axial stiffness will be lower than predicted by finite element analysis (which is based on the quoted material values of CFRP).

For a spar with 0° lay-up, the torsion stiffness is largely determined by the shear modulus of the material. Even for 0° plies, this is dependent upon the volume fraction, but not as sensitively as axial stiffness. The fact that the fibre-to-resin ratio is less than specified by the manufacturer would suggest that torsional stiffness of the section would be slightly less than predicted. The close agreement (1%) between the experimental results and the finite element analysis is therefore slightly surprising, but within the expected accuracy of the experimental procedure.

The experimentally determined value of K_{45} (1.59E+04 Nmm^2) compares exceptionally well with the predicted value. Obviously, a percentage error is not meaningful since the predicted value is zero, however the experimental result corresponds to a 0.06 mm discrepancy in the location of the shear centre of the beam.

This lack of any significant K_{45} coupling indicates that the orientation of plies was probably accurate to within a few degrees, since parametric studies of K_{45} with ply angle indicates that K_{45} increases rapidly as ply angle varies.

5.6.2 Spar 2: $+45_{[60]}$ lay-up

The experimentally determined stiffness values (K_{44}, K_{45} and K_{55}) were all lower (i.e. more flexible) than predicted by the finite element model. This was expected considering the excess resin in the lay-up. The discrepancy was within 10% in all cases - well within an acceptable range considering the accuracy issues described earlier in section 5.5.1.

5.6.3 Spar 3: $+45_{[30]},-45_{[30]}$ lay-up

Due to the expected presence of flap-bending to lag-shear coupling, the values of K_{44}, K_{45} and K_{55} cannot be decoupled from the rest of the 6 x 6 1-dimensional stiffness matrix, and hence these values cannot be evaluated directly from the experimental results. As expected, the values of the flexibility terms S_{44} and S_{55} were larger (i.e. more flexible) than predicted due to the reduced fibre-to-resin ratio. The discrepancy between experimental and finite element results was less than 10%, which is within the expected accuracy.

The experimental results confirmed the expected result that no significant flap torsion coupling (S_{45} or K_{45}) was present. Since the predicted value of K_{45} was zero, a percentage error is not meaningful; however the mean location of the shear centre was less than 0.1 mm from the centroid of the beam.

Although the mean experimentally derived location for the shear centre is (close to) zero, the location of the shear centre varies in sign depending on the direction of the applied bending moment. The magnitude of the discrepancy in shear centre location (up to 60 mm) cannot be attributed to experimental inaccuracies. This behaviour is not predicted, and the reason for it is unclear.

It is interesting to note that Spar 3 exhibits a large amount of initial twist (approx 0.2 rad m^{-1}), which Diamond considered was caused by thermal stresses during cure [46]. This pre-twist is shown on Figure 5.7 below.

Figure 5.7 Pre-twist of Spar 3 due to thermal stresses

Although this pre-twist should not have any effect on the value of K_{45} obtained from the experimental procedure (since measurements were made relative to the initial deflection), this would have a significant effect on the performance of an aerodynamic structure such as a rotor blade.

5.6.4 Spar 4: $+/-45_{[30]},-/+45_{[30]}$ lay-up

The experimentally determined value of S_{44} was 19% larger (i.e. more flexible) than that predicted by the finite element model while S_{55} agreed with the FE predicted value to within 2%.

Since the torsional stiffness of a ±45° laminate is highly dependent upon the interactions between +45° plies in one layer and -45° plies in the next, it is unsurprising that the presence of excess resin between the layers reduces these interactions and hence reduces the overall torsional stiffness.

The DERA report suggested that no K_{45} was predicted for this spar, the experimentally determined value of K_{45} was too large to be attributed to experimental error. The test was repeated and the results were confirmed as repeatable to within 5%.

If it is assumed that the ±45° plies are effectively homogeneous through the thickness of the spar, then DERA's prediction of no K_{45} coupling is correct. However, considering classical laminate theory, it is clear that a symmetric laminate manufactured from alternate +45° and -45° plies *will* exhibit some K_{45} coupling, due to the different distances of each successive layer from the mid-plane of the laminate. Admittedly this effect will be small, but it is quantifiable (even for a 60-layer laminate) and measurable.

Although the value of K_{45} calculated from the experimental results was 38% larger than predicted by finite element analysis, it must be emphasised that the predicted value of K_{45} is a small value, and hence difficult to measure accurately. This error in K_{45} corresponds to an error of 3 mm in the experimentally-determined location of the shear centre, which is within the accuracy of the experimental procedure claimed earlier.

5.6.5 Spar 5: $+15_{[60]}$ lay-up

As expected, the reduced fibre-to-resin ratio caused the spar to be more flexible than predicted. The experimentally determined values of stiffness terms (K_{44}, K_{45} and K_{55}) were 10-20% less (i.e. more flexible) than those predicted by the FE model. These results are within the expected range considering the accuracy issues described in section 5.5.1.

5.6.6 Spar 6: $+15_{[30]}$,$-15_{[30]}$ lay-up

Due to the expected presence of flap-bending to lag-shear coupling, the values of K_{44}, K_{45} and K_{55} cannot be decoupled from the rest of the 6 x 6 1-dimensional stiffness matrix, and hence these values cannot be evaluated directly from the experimental results.

The experimental value of the S_{44} term is 9% larger (i.e. more flexible) than predicted by the finite element model and the value of the S_{55} term is 31% larger (i.e. more flexible) than predicted. Given the reduction in interactions between layers and the effective reduction in axial stiffness of the section, (both effects being caused by excess resin in the lay-up) these results are within the expected range.

The experimental results confirmed that no significant flap torsion coupling was present, since the mean location of the shear centre (y_0) was only half a millimetre from the centroid of the beam (the predicted location of the shear centre). As with Spars 1 and 3, a percentage error is not meaningful.

As with Spar 3, some pre-twist was evident due to thermal stresses during cure. The fact that the location of the shear centre was consistent with the FE predictions (to within the expected accuracy of the experiment) indicates that pre-twist is unlikely to be the cause of the discrepancy noted for Spar 3.

5.6.7 Spar 7: $+30_{[60]}$ lay-up

As expected, the reduced fibre-to-resin ratio caused the spar to be more flexible than predicted. The experimentally determined values of the stiffness terms (K_{44}, K_{45} and K_{55}) were 10-15% smaller (i.e. more flexible) than those predicted by the FE model. These results are within an acceptable range considering the issues described above.

5.6.8 Spar 8: $+30_{[30]}$,$-30_{[30]}$ lay-up

Due to the expected presence of flap-bending to lag-shear coupling, the values of K_{44}, K_{45} and K_{55} cannot be decoupled from the rest of the 6 x 6 1-dimensional stiffness matrix, and hence these values cannot be evaluated directly from the experimental results.

However, the experimental results confirm that no significant flap torsion coupling was present since the location of the shear centre was less than a millimetre from the centroid of the beam, which is the location of predicted shear centre. As with Spars 1, 3 and 6, a percentage error is not meaningful.

As with Spar 3, some pre-twist was evident due to thermal stresses during cure. The fact that the location of the shear centre was consistent with the FE predictions (to within the expected accuracy of the experiment) indicates that pre-twist is unlikely to be the cause of the discrepancy noted for Spar 3.

It can be seen from the flexibility terms, the results for Spar 8 were very similar to those obtained from Spar 6, and quite significantly different to those predicted by finite element analysis of the section. The orientation of plies on the top and bottom surfaces was measured using a protractor. The angle of these plies was found to be approximately 18° on average. Assuming the orientation of the plies is consistent through the depth of the section, this explains the discrepancy in between experimental and predicted results for Spar 8, and also the similarity between the results for Spars 6 and 8.

5.7 CONCLUSIONS

The problem brief has indicated the desirability of designing helicopter rotor blade cross sections to meet given values of K_{45} since it is widely acknowledged to be an important variable in aeroelastic tailoring. Considering the two physical interpretations of K_{45} presented in section 5.2, it is clear that the interpretation obtained from the fifth line of the 1-dimensional beam stiffness matrix equation highlights the coupling behaviour that is most important in the aeroelastic tailoring of a helicopter rotor blade section. i.e.

$$M_y = K_{15}\varepsilon_x + K_{25}\gamma_{xy} + K_{35}\gamma_{xz} + K_{45}\kappa_{yz} + K_{55}\kappa_y + K_{56}\kappa_z \qquad (5.1.b)$$

In order to lift the helicopter, a rotor blade must produce a vertical lifting force. This (distributed) lifting force, will create a varying flap-bending moment (M_y) along the length of the rotor blade. K_{45} relates the value of this flap-bending moment to the resulting twist of the rotor blade along its length (κ_{yz}). The blade twist directly affects the angle of attack of the blade, which in turn has significant implications for lift and drag produced as well as dynamic behaviour. It is therefore important to be able to predict (or control) how the section will twist as it produces lift by designing a blade with an appropriate value of K_{45}.

The experimental results generally supported the finite element predictions. Because the sections tested are solid (rather than thin-walled) sections, the warping restraint created

by clamping the root of the cantilever does not greatly affect the results. The experimental work presented here therefore gives increased confidence in the finite element method of Hill and Weaver that is used throughout this thesis and elsewhere.

The following chapter incorporates the insight from the work presented so far into an optimisation strategy that is used to determine a detailed design for a generic composite helicopter rotor blade that meets given target values of various cross-sectional properties. This has been coded into a C++ program, and results from a number of optimisation runs are presented.

6 FULL BLADE ANALYSIS AND OPTIMISATION

6.1 BACKGROUND

A large amount of literature has been published on the optimisation of various aspects of helicopter blade designs. As discussed in Chapter 2, most of this literature approaches the subject from one of two perspectives. The first of these is the development of simplified analytical models (e.g. Smith [19] and Rehfield *et al* [22], which were discussed at length in Chapter 4), and which give understanding to the underlying physics of the design problem. The second approach is directed towards the optimisation of a specific rotor blade property using simplified finite element models with few design variables (e.g. Chattopdahyay *et al* [25-27], Ganguli and Chopra [28-30], McCarthy [37] and Chandra and Chopra [38]). While these two approaches have produced a large volume of literature and have brought many valuable contributions to the field in terms of both physical insight and optimisation techniques, further methods that produce results in greater detail are required by the industrial designer who wishes to produce a finished design.

6.2 MODELLING ISSUES

One of the goals of this research has been the development of a method that can be used in an industrial context to reliably design composite helicopter rotor blade sections to meet given physical properties.

Since an accurate analytical model is obviously not possible due to the geometric and material complexity of the section, the design must be analysed using a suitable finite element model. The earlier analytical modelling of cylinders and box sections is nonetheless important because it gives an understanding of the underlying physics involved in these problems. It is assumed that these principles can be applied equally well to the complete blade section, and hence the lessons learned from these examples can be applied to the problem of optimising a helicopter rotor blade section.

6.3 FINITE ELEMENT MODEL

6.3.1 Finite element modelling and analysis procedure

The finite element model of a blade section can be built up automatically from data about the external profile and interior construction using BLADEBUILDER - code developed in-house at Westland Helicopters Ltd and made available to the University of Bristol for this project. BLADEBUILDER is a subroutine that runs within the PATRAN [33] modelling environment and uses NASTRAN [32] as the solver. This is consequently written in PATRAN Command Language (PCL). Although BLADEBUILDER can also be run interactively (useful for debugging, and also for investigating particular designs or design features in more detail), its implementation in an optimisation routine requires that it be called as a non-interactive background process.

BLADEBUILDER not only creates the geometry and structure of the cross-section from the input data, but also automatically generates a mesh suitable for finite element analysis of the section. The step-by step procedure for producing a finite element model of the cross-section using BLADEBUILDER is outlined by the flowchart in Figure 6.1 below.

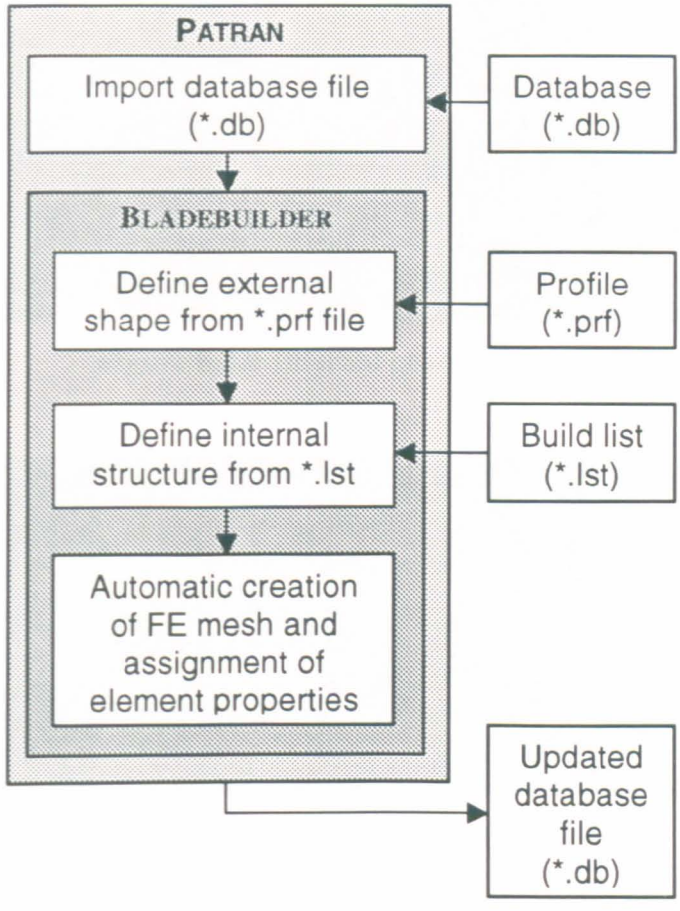

Figure 6.1 Finite element model creation using BLADEBUILDER within the PATRAN environment

The PATRAN output at each step of finite element model creation using BLADEBUILDER is shown on Figures 6.2.a-e below.

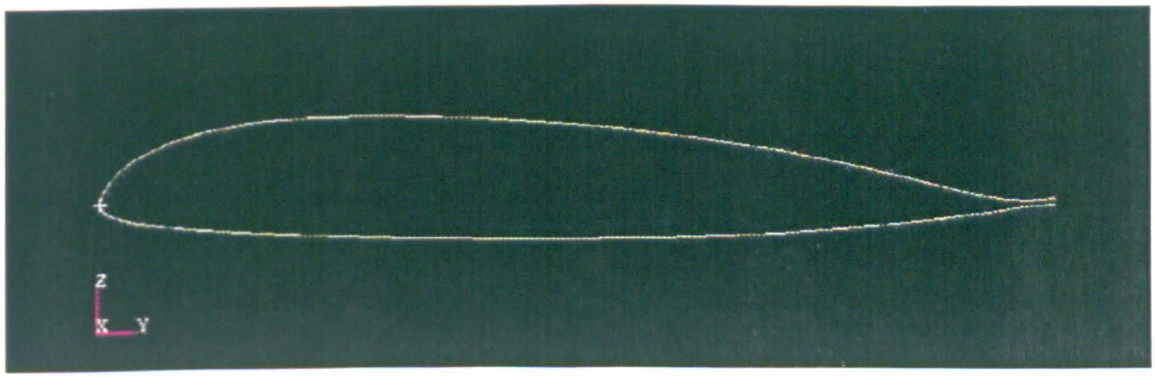

Figure 6.2.a Profile definition

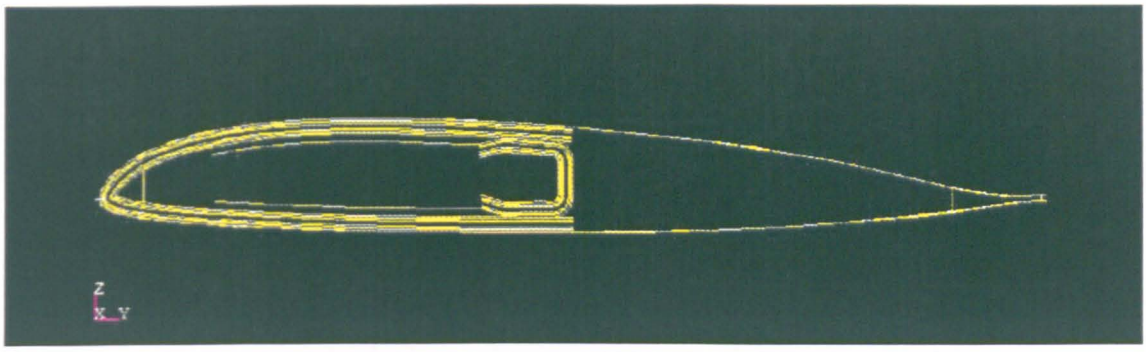

Figure 6.2.b Internal geometry of blade

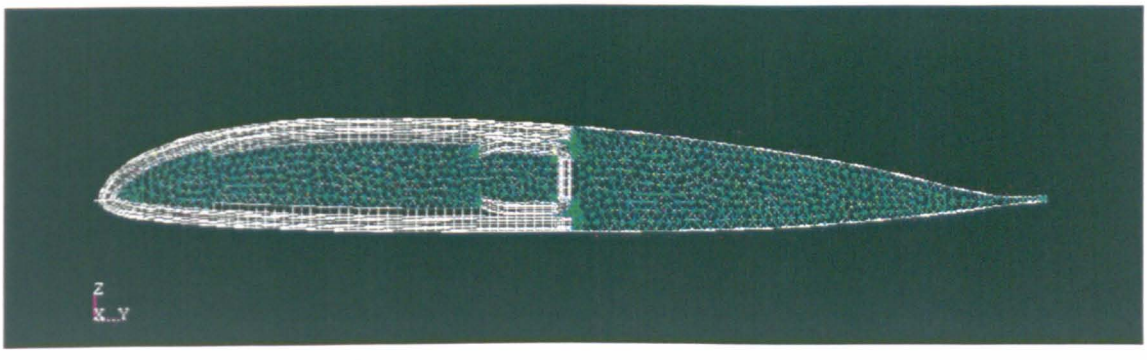

Figure 6.2.c Mesh generated automatically

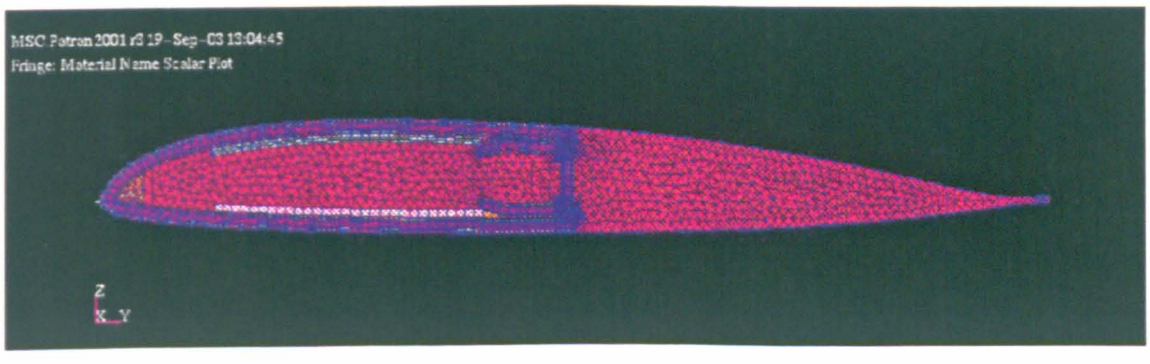

Figure 6.2.d Materials and Element properties defined

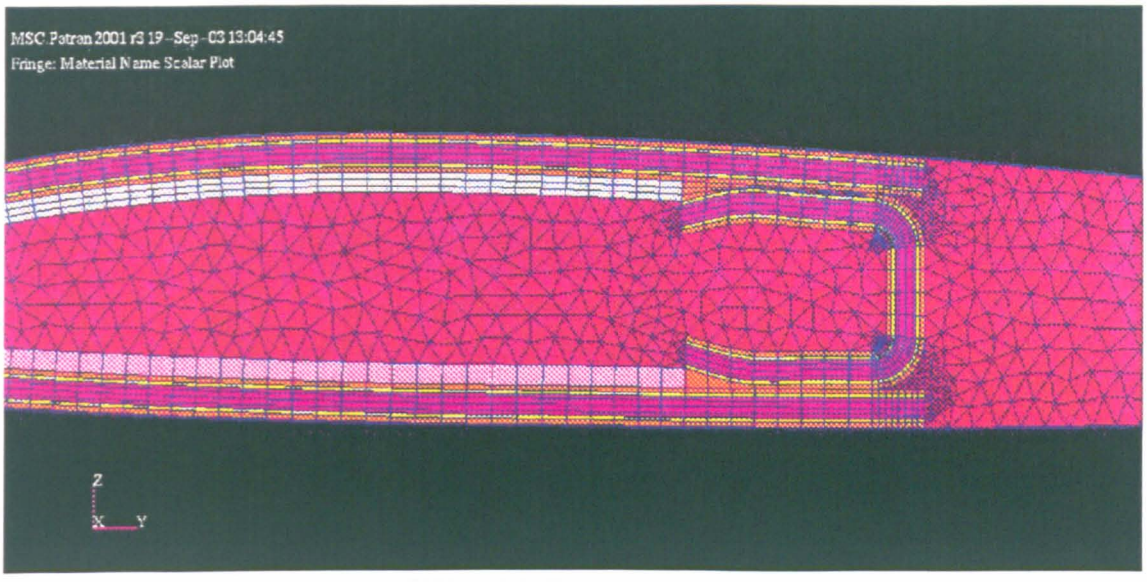

Figure 6.2.e Close-up of materials definition

The code written by Hill at the University of Bristol (based on the work of Hill and Weaver [34]) is then used to extrude this 2-dimensional cross-sectional model to a 3-D slice. This model is analysed under four different loading conditions and the cross-sectional properties calculated. The underlying theory for these calculations is described earlier in Chapter 1 of this thesis.

As part of the industrial collaboration on this project, this code has been adopted by Westland Helicopters for the analysis of helicopter blade cross-sections. This code has been called NASSAN (NAStran Section ANalysis). The step-by step procedure for determining the cross-sectional properties from a finite element model using NASSAN is outlined by the flowchart in Figure 6.3 below.

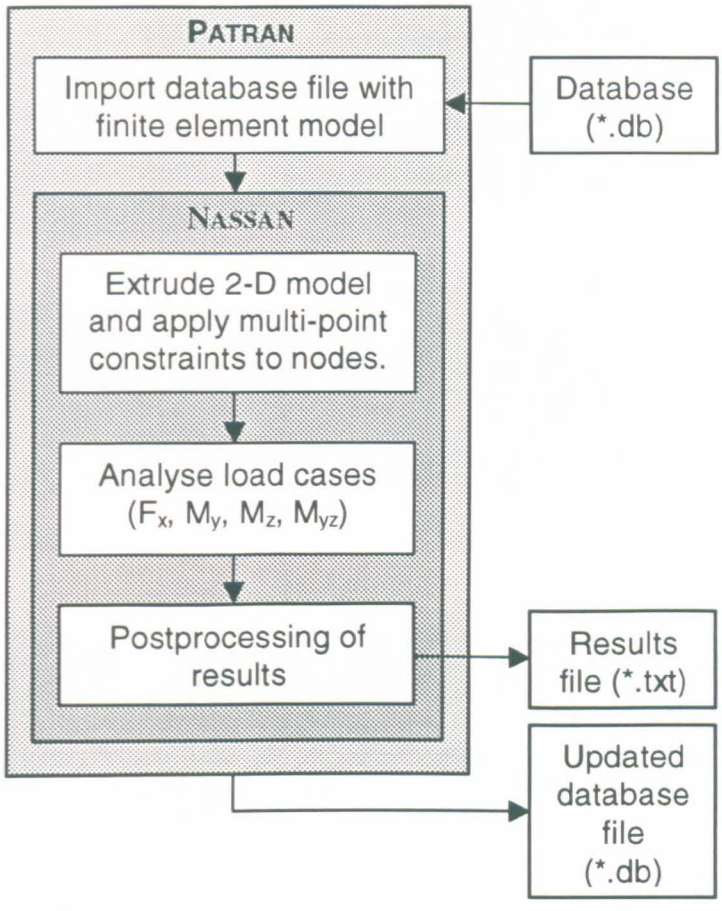

Figure 6.3 Finite element model analysis using NASSAN within the PATRAN environment

The figures below show typical PATRAN outputs/results during the NASSAN analysis.

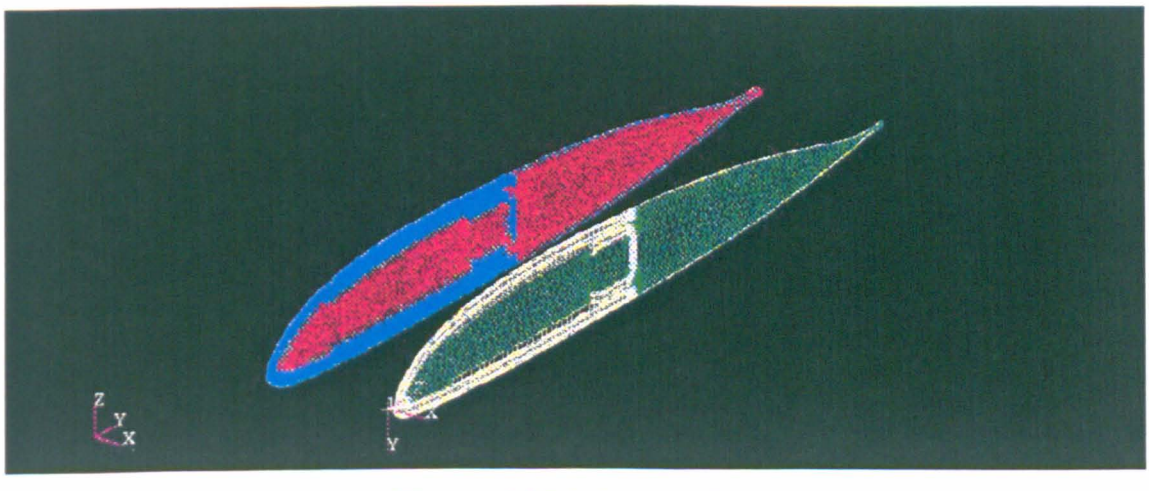

Figure 6.4 Blade extrusion

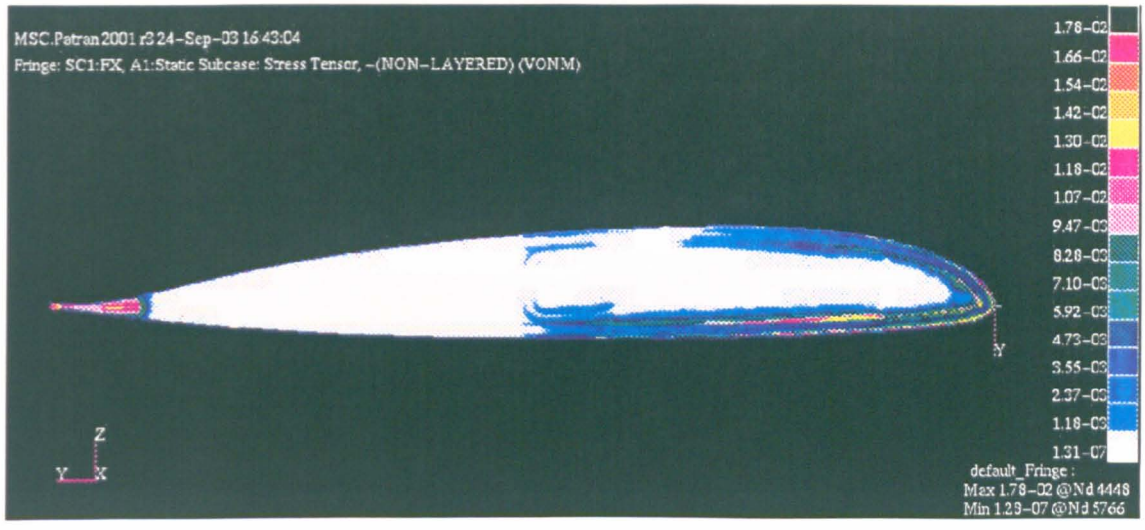

Figure 6.5.a Stress tensor under axial force load case

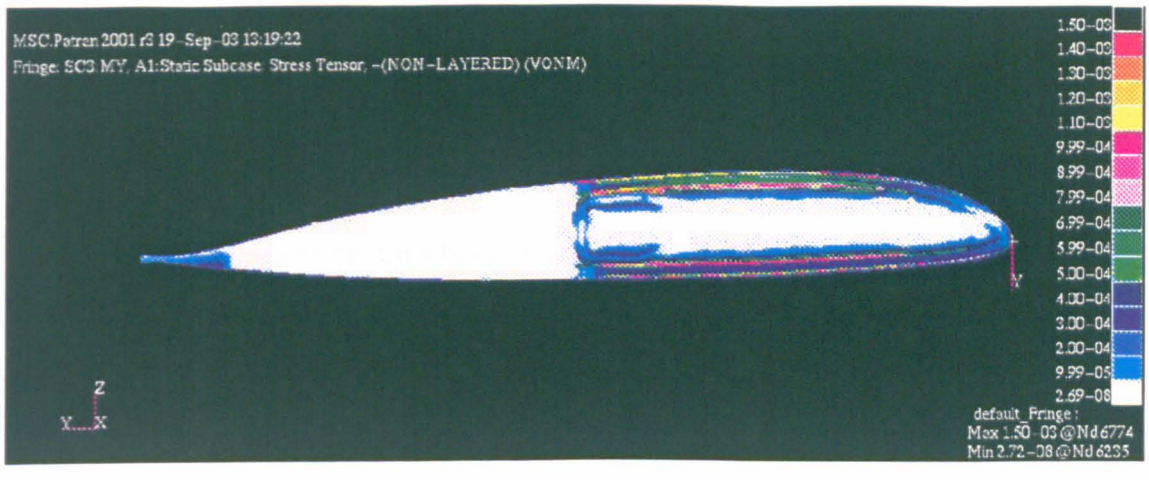

Figure 6.5.b Stress tensor under flap bending load case

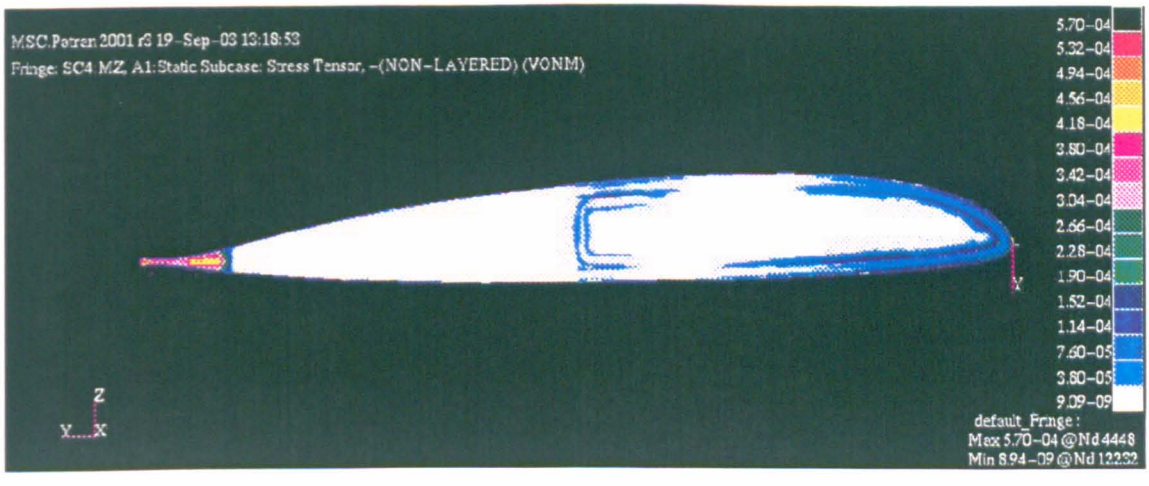

Figure 6.5.c Stress tensor under lag bending load case

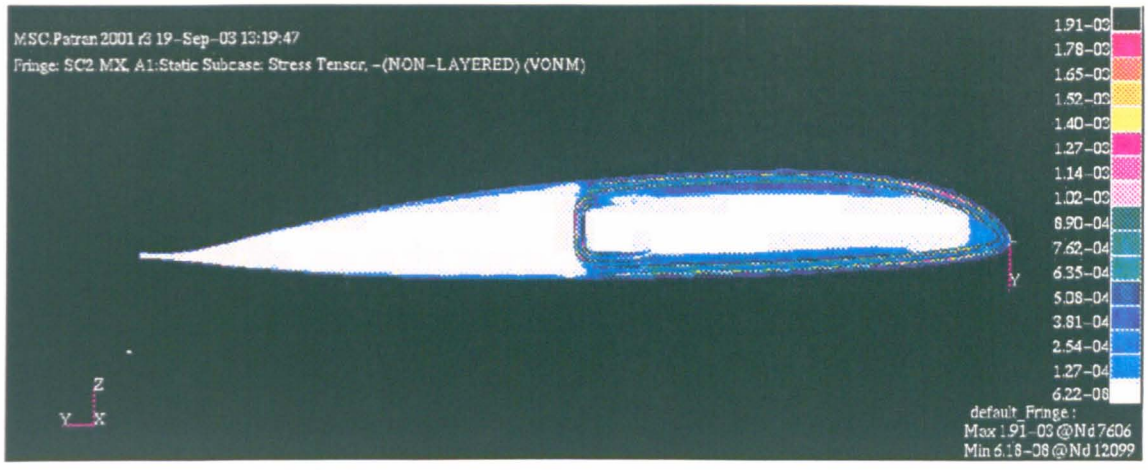

Figure 6.5.d Stress tensor under torsion load case

It is very important to ensure that the design to be analysed is feasible. For example, it would not be possible to analyses a blade section that has a total depth of 10 mm if the upper and lower surfaces are each 6 mm thick. In particular, meshing problems may be experienced with BLADEBUILDER where thick laminates are laid up around tight radii (typically at the nose). These problems are overcome by ensuring that laminates are less than a specified maximum thickness. This is achieved in the optimisation routine by setting suitable upper and lower bounds on the design variables.

6.3.2 Physical insight from finite element analysis results

It should be noted that during the optimisation procedure, all steps are automated and run as background processes. As a result, the outputs presented above are not usually seen, although running a single analysis and examining the outputs can offer valuable physical insight. Figures 6.5.a-d above show the stress distributions in the blade cross-sections under the different loadings to be as expected.

Under an applied flap bending moment, the stress is carried predominantly in the top and bottom surfaces. This is why unbalanced plies are placed in the top and bottom surfaces of the section to tailor flap-torsion coupling. Due to their high axial stiffness (compared to $\pm 45°$ and $90°$ plies) most of the stress from the applied bending moment is carried in the $0°$ plies of the top and bottom surfaces. The thickness of these $0°$ plies is one of the

most significant design variables in determining flap bending stiffness, and also significantly affects the axial stiffness and (to a slightly lesser extent) lag stiffness.

Under an applied lag bending moment, the stress is carried by axial plies in the front part of the torsion box, and by the axial plies in the carbon wedge at the trailing edge of the section. The size of this rear wedge is the most significant design variable in determining the lag bending stiffness, and also significantly affects the axial stiffness and location of the centre of gravity (CG). The size of the nose-mass can be used as a variable to return the CG to its target location, as it contributes relatively little towards the overall stiffness properties of the section.

Under an applied torsion force, the stress is carried by the torsion box. In particular, the ±45° plies carry the most stress (due to their high shear stiffness compared to 0° and 90° plies), and the thickness of ±45° plies is therefore one of the most significant design variables in determining torsion stiffness of the section.

The size of the torsion box (controlled by the chordwise location of the centre wall) will affect torsion, flap, lag and axial stiffness, as well as mass and centre of gravity location.

It can therefore be seen that (before even considering interactions between the design variables) the optimisation of a rotor blade section is not a straightforward procedure, justifying the requirement for rigorous optimisation techniques to be applied to this problem.

6.4 EXPERIMENT

6.4.1 Experimental set up and procedure

As part of ongoing collaborative work, a section of BTP-7 blade was donated by Westland Helicopters. This section is the same as those actually used on the Lynx tail rotor. The cross-sectional properties of this blade were tested at the University of Bristol by Dr Ian Farrow, to verify the chordwise location of the shear centre. The following is a summary of Farrow's work.

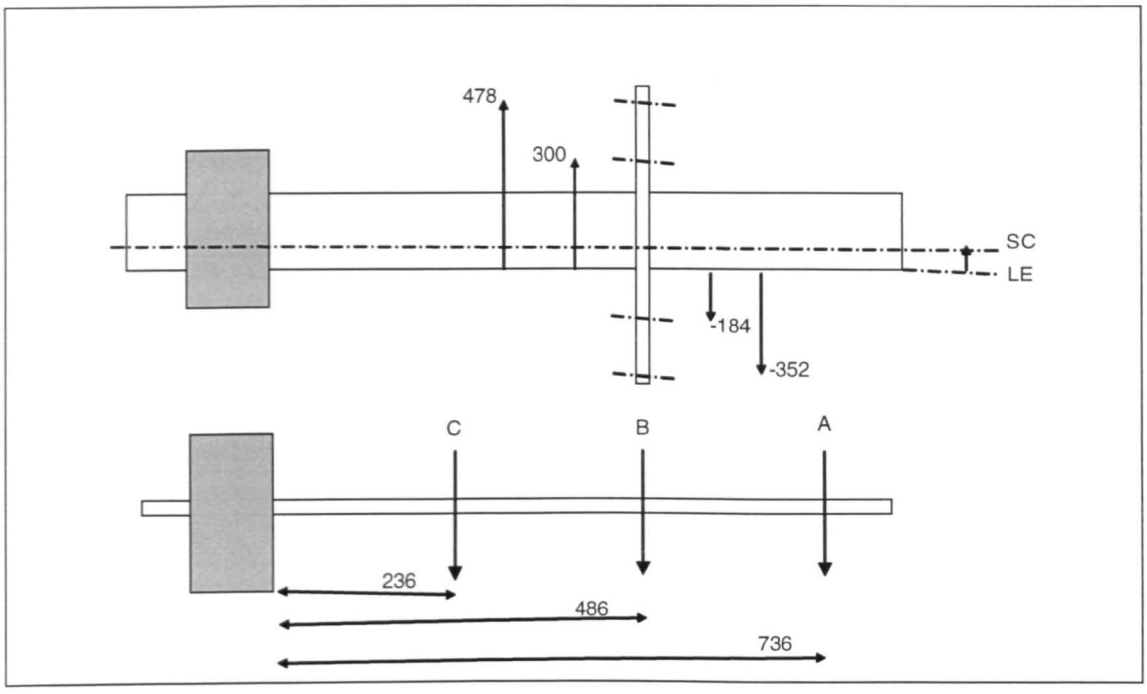

Figure 6.6 Schematic diagram of BTP-7 blade, showing loading stations

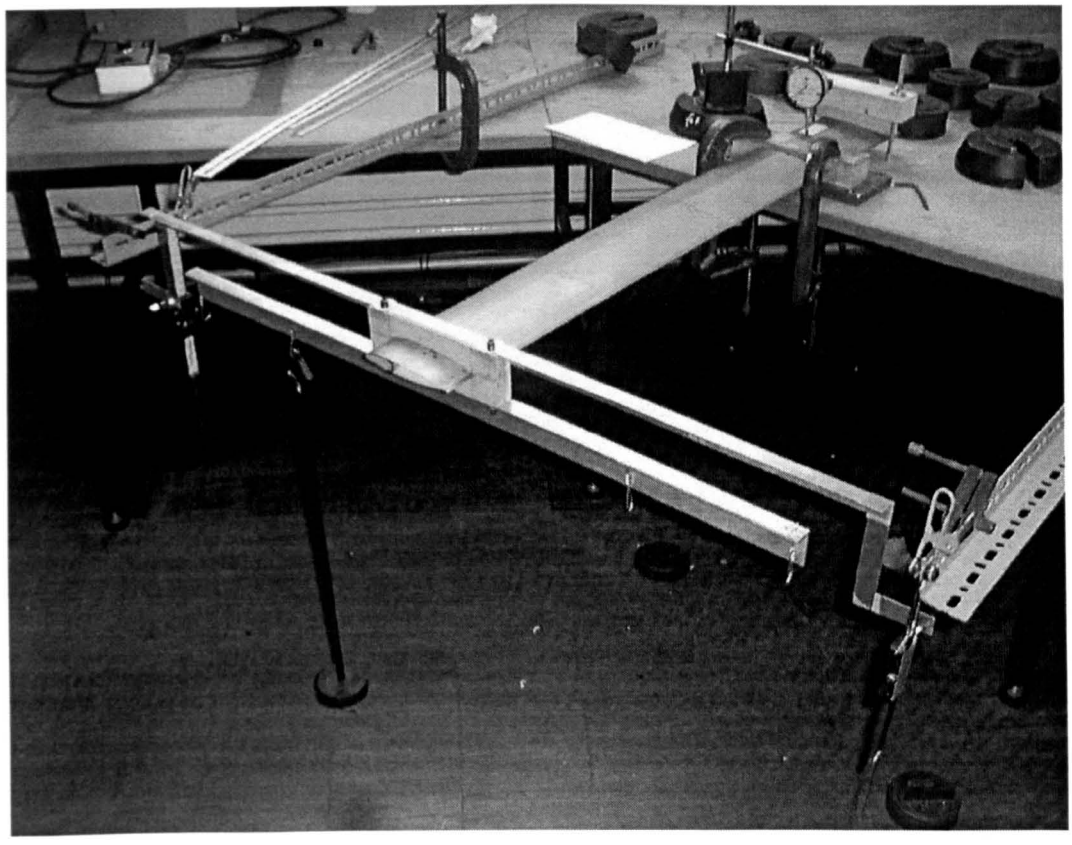

Figure 6.7.a Experimental set-up

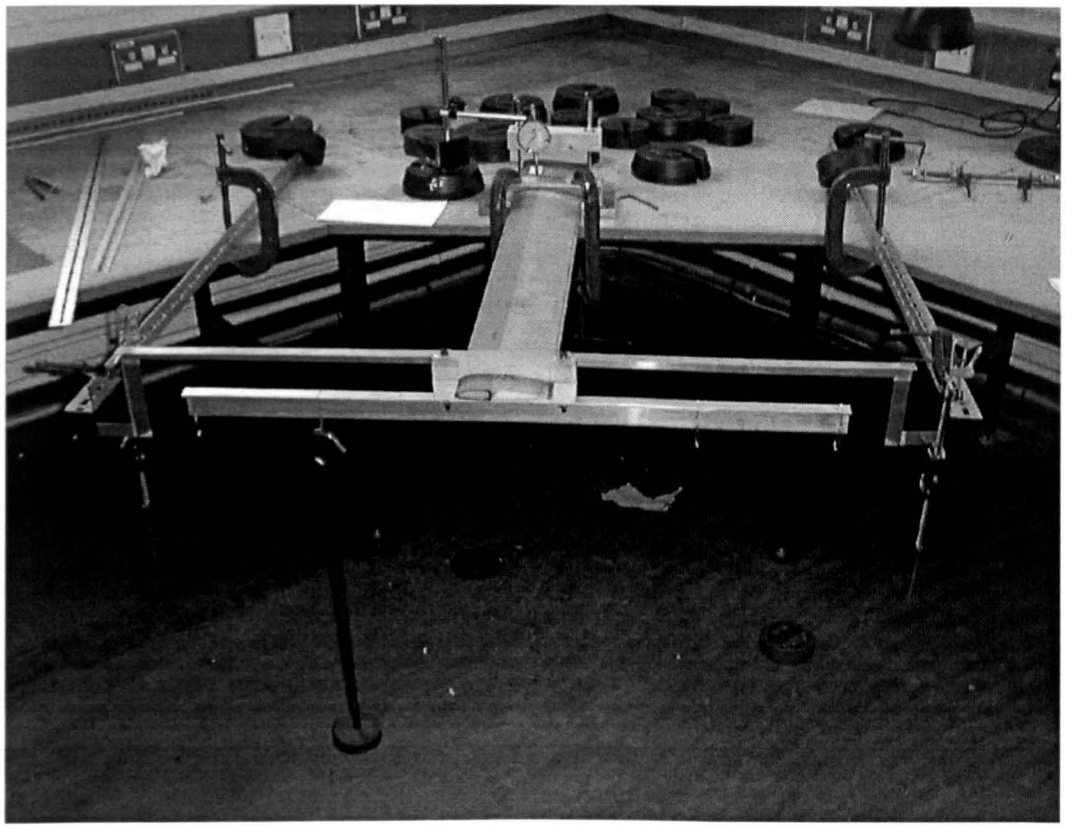

Figure 6.7.b Experimental set-up

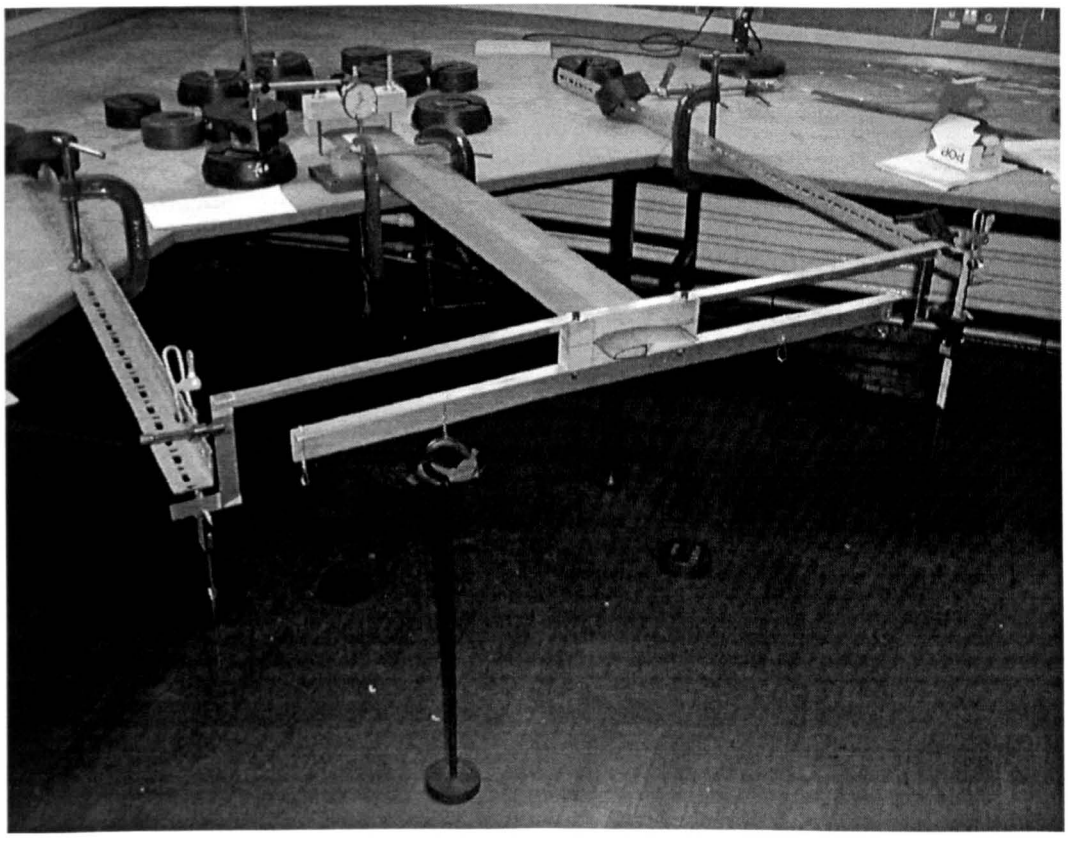

Figure 6.7.c Experimental set up

This work is conceptually very similar to that used in the previous chapter to determine the cross-sectional properties of the eight laminated CFRP beams manufactured by DERA.

Farrow loads the blade section at three points along the blade span - referred to as Stations A, B and C. These are shown on Figure 6.6. At each station, the load is applied at four offsets – referred to as Moments 1, 2, 3 and 4. These are also shown on Figure 6.6.

The relative displacements of the ends of the loading apparatus are measured. These measurements can be used to determine the bending and twisting displacements under each loading case. The bending, torsion and bend-torsion flexibilities of the blade section may be calculated from these displacements according to the calculations described in the previous chapter.

Note that since the cross-section of the blade is not a uniform shape, the location of the axis about which the cross-sectional stiffness matrix should be calculated is not immediately obvious.

Although the elastic centre is used by Westland Helicopters (and is also the default output for NASSAN), the exact location of the elastic centre of this section cannot be determined from the measurements taken. However, Farrow's measurements do give the location of the shear centre (the axis through which an applied shear force will give no twisting). Calculations may be made based around this origin, although obviously no flap-torsion coupling will be present (from the very definition of the shear centre).

6.4.2 Experimental results

Farrow's results are included in Appendix 6.1. From these results, it is possible to calculate the bending and shear stiffnesses for the blade section. These are summarised (along with Farrow's results for shear centre location) in the following table.

Length (mm)	Shear load (kg)	Location of shear centre (mm)	Torsion flexibility S_{44} ($x10^{-9}$ $N^{-1}mm^{-2}$)	Bending flexibility S_{55} ($x10^{-9}$ $N^{-1}mm^{-2}$)
736	0.5	31.38	14.3	9.07
736	1.0	32.95	6.90	4.77
736	1.5	29.97	6.94	4.79
486	1.5	29.61	7.54	5.82
486	2.0	32.11	7.60	5.48
486	2.5	28.25	7.68	6.07
236	2.5	28.73	9.53	9.54
236	3.0	27.20	8.12	8.13
236	3.5	34.84	8.21	8.22

Table 6.1 Bending and twisting flexibilities of blade section based on Farrow's results and assuming Euler beam behaviour

Farrow's results show that the chordwise location of the shear centre is approximately 30.5 mm behind the leading edge of the blade section, although the first row of results in Table 6.1 appears anomalous and has been ignored. This has presumably been caused by friction in the system taking up some of the (small) applied load. The result for shear centre location is nonetheless repeatable (to within ±3.5 mm) over the entire range of blade stations and applied shear loads.

Euler bending calculations based on Farrow's results suggest that the cross-sectional bending and torsion flexibilities both show a general decrease with the length of the section. While it is obvious that the bending and twisting *displacements* will increase with length, the terms from cross-sectional flexibility matrix should be independent of length.

This observation is difficult to explain for twisting flexibilities, however for bending flexibilities, this could be explained if Timoshenko shear displacements are not negligibly small i.e. the overall flap displacement is a function of the form

$$\delta_z = S(AL^3 + BL) \qquad (6.1)$$

where

S is the applied end loading

L is the length at which the loading is applied

A is a constant that incorporates the flap-bending flexibility

B is a constant that incorporates the flap-shear flexibility

Surprisingly, analysis of the displacements at each length suggest that the overall flap displacement is a function of the form

$$\delta = S(AL^3 + BL^2) \qquad (6.2)$$

The squared term in the relationship between flap displacement and length suggests that the results data cannot be used to accurately determine the flap-shear and flap-bending displacements. Even if it could be found that Timoshenko shear deflection was significant, this would not explain the general decrease in twisting flexibility with increasing length that is seen in the results of Table 6.1.

Considering also the relatively large variation of results data at any given length, it is safest to conclude that the flexibility terms cannot be calculated with any degree of confidence. The values for bending and torsion flexibilities presented above cannot therefore be taken as anything more than approximate figures.

Further work could examine this blade section using non-destructive testing techniques to determine whether the internal structure has damage (such as local delaminations) that could cause these apparently anomalous results. If localised damage were present, it would be possible to re-test an undamaged section of the blade to determine the cross-sectional bending and torsion flexibilities more accurately.

6.5 OPTIMISATION ISSUES

6.5.1 Optimising near-linear cross-sectional properties

If the cross-sectional properties to be optimised are linear functions of the design variables (or can be approximated to be linear functions of the design variables), a blade section may be most efficiently designed in the same manner as the cylindrical shell of Chapter 2 – by using an iterative global approximation method, which is summarised by the flowchart below (Figure 6.8).

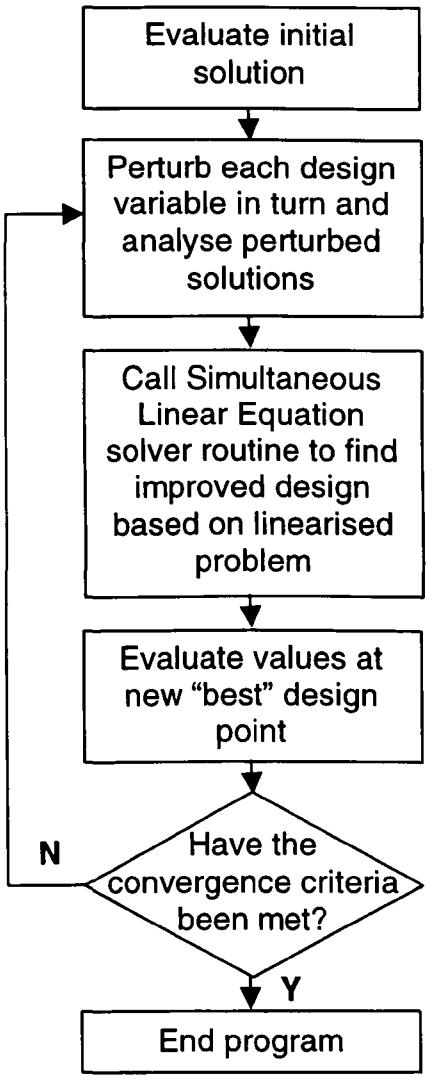

Figure 6.8 Flowchart of Iterative Global Approximation method

This iterative global approximation method assumes that a linearisation of the problem is valid over the whole design space. The problem is therefore reduced to solving a number of simultaneous equations, which can be solved quickly and easily using matrix methods as described in detail in Chapter 3. Due to the obvious fact that the problem is only approximately linear, the calculated solution will differ from the target values by some small amount. The linear solution process is thus called in an iterative fashion until convergence is achieved. This process is implemented by the Simultaneous Linear Equation solver routine and is shown by Figure 6.9 below.

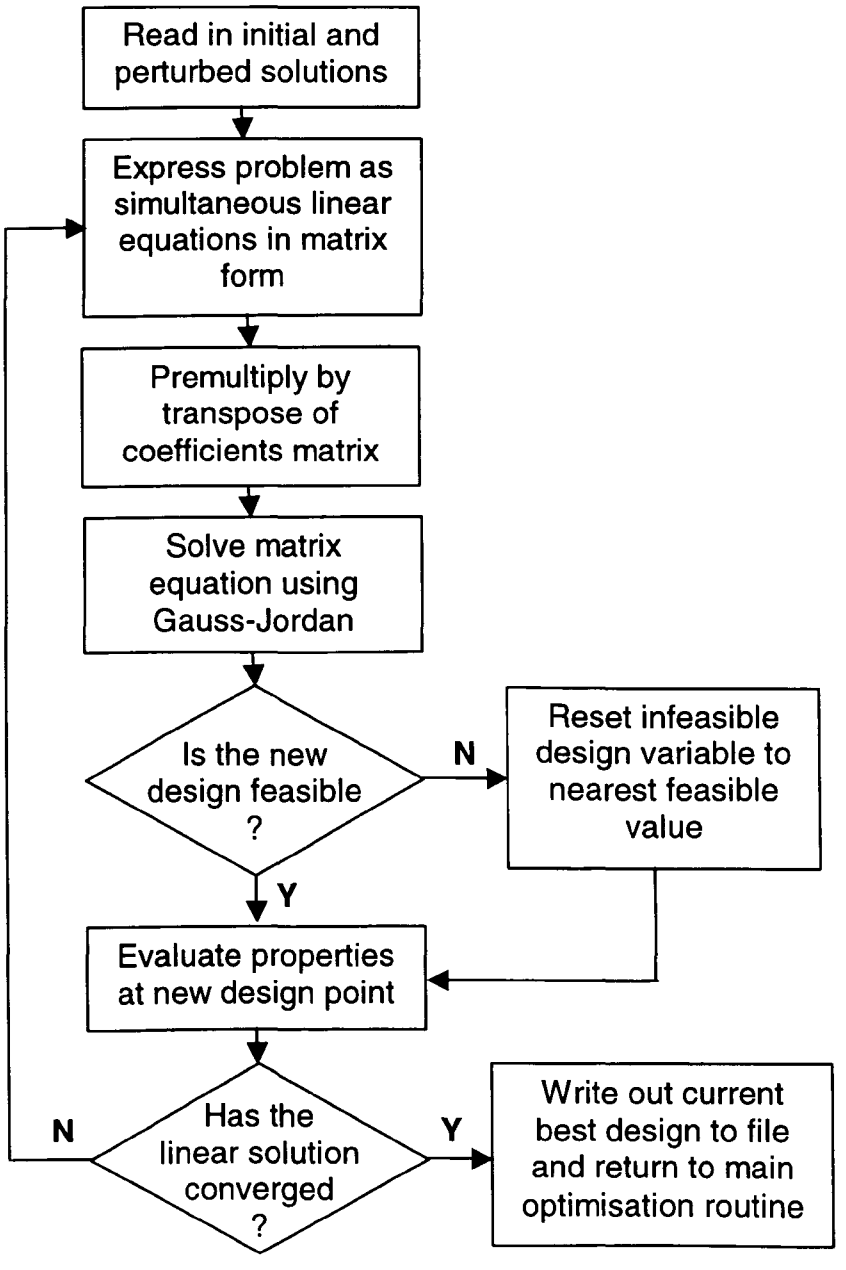

Figure 6.9 Flowchart for Simultaneous Linear Equation Solver routine

6.5.1.1 Problem definition

The design of a composite helicopter rotor blade to meet (linear) cross-sectional stiffness properties was presented at the European Rotorcaft Forum in Bristol 2002 [72].

The problem formulated is to design a composite helicopter rotor blade to meet predetermined target values of the four cross-sectional stiffnesses. Figure 6.10 below, shows the generic blade section used for this analysis, with the main features labelled.

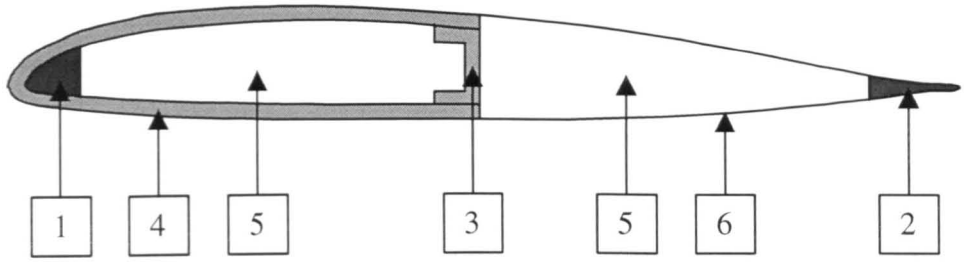

Figure 6.10 Generic helicopter blade design

The main features of this generic blade design are

1. Nose weight
2. 0° unidirectional CFRP rear wedge
3. CFRP composite spar wall
4. CFRP composite blade wall
5. Rohacell foam filler
6. GFRP surface layer

The independent design variables for this problem are

$x[0]$ location of end of nose weight (% chord)

$x[1]$ location of start of rear wedge (% chord)

$x[2]$ thickness of each CFRP composite wall

Target values were chosen for four cross-sectional properties

Flap bending stiffness (EI_{XX})	=	2.72×10^8	Nmm^2
Lag bending stiffness (EI_{YY})	=	4.79×10^9	Nmm^2
Mass	=	0.397	g/mm
Location of CG	=	23.0	% chord

Since the number of target values exceeds the number of design variables, an exact continuous solution is not necessarily possible, and the optimum design will be that with the minimum value of the sum of squared errors for each design variable (i.e. a least squared error solution).

Note that it is very important to set appropriate constraints on the design to ensure that it is feasible. This has been achieved by setting suitable upper and lower bounds on each of the design variables.

Although it is not explicitly used as part of the optimisation routine, it is useful to define a single objective function that measures how closely a give design meets the objective of matching all of the cross-sectional properties. In general, this objective is defined as

$$Objective = \sum_{i=1}^{N} W_i \left(\frac{Z_i - T_i}{T_i} \right)^2 \qquad (6.3)$$

where

N is the number of cross-sectional properties to be matched

W_i is the weighting factor of target value i

Z_i is the value of cross-sectional property i at the current design point

T_i is the target value of cross-sectional property i

In the case of the problem considered here, this becomes

$$Objective = W_1\left(\frac{EI_{xx_a} - EI_{xx_t}}{EI_{xx_t}}\right)^2 + W_2\left(\frac{EI_{yy_a} - EI_{yy_t}}{EI_{yy_t}}\right)^2 + W_3\left(\frac{Mass_a - Mass_t}{Mass_t}\right)^2 + W_4\left(\frac{CG_a - CG_t}{CJ_t}\right)^2 \quad (6.4)$$

Note that this objective is not explicitly used as part of the optimisation procedure, but is a useful tool for simply and concisely presenting how well a given design meets the target values.

6.5.1.2 Searching the design space

As with the cylindrical shell problem of Chapter 3, the design space for this problem is relatively small and can be exhaustively searched in order to provide a full "map" of the design space and help gain a better understanding of the exact behaviour of the objective function with respect to the design variables. Due to the simple (3-variable) nature of this problem, a sufficiently high-resolution search was obtained by discretising the entire design space into 512 design points. This design space required 2 days to exhaustively search.

6.5.1.3 Presentation of results

Despite the limitations imposed by discretisation, it is possible to meet the target values to a mean error of less than 1% at the optimum point. The optimum design values are summarised in Table 6.2, below.

Design variable	x[0]	x[1]	x[2]
Value	4.0	98	1.375

Table 6.2 Optimum discrete design

The results of this search indicated that if stacking sequence effects are ignored, the design space becomes convex. Figure 6.11, below, illustrates the variation of the objective function (plotted in colour) within the 3-dimensional design space.

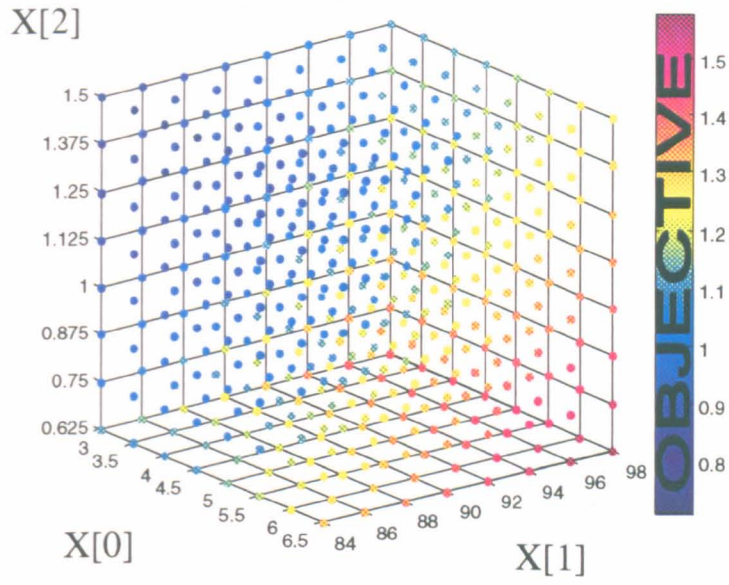

Figure 6.11 Variation of objective function over 3-D design space

Work with the composite cylindrical shells in Chapter 3 suggests that this design space is convex because the design variables in this problem are wall locations and ply thicknesses. The inclusion of ply orientations or stacking sequences would lead to a non-convex objective function. If this were the case, the problem would have to be either solved using stochastic methods, or simplified by the use of lamination parameters.

The visualisation of an objective function within a design space that has more than three dimensions is not intuitive for most people, and is certainly not easy to represent in a concise pictorial format. However, despite the obvious difficulties of representation, these results presented above have significant consequences for the optimisation of helicopter blades.

6.5.2 Optimising highly coupled and non-linear properties

6.5.2.1 The problem of non-linear properties and interactive design variables

If K_{45} coupling and/or other highly non-linear functions are included among the target properties to be optimised, then the optimisation problem is not so straightforward.

For properties that are highly non-linear functions of the design variables, a linearisation of the problem about the current design point will only be valid for small changes in design variables. In general, this will not cause a deterministic linearised algorithm to fail completely, but will reduce the rate of convergence. However, if the objective is highly non-linear, it may be necessary to limit the magnitude of changes in design variables at each step. This technique is known as sequential linear programming (*SLP*), and was discussed in Chapter 2. Although this approach is less efficient than the global linear approximation method, it does robustly find a minimum for highly non-linear convex problems.

In certain non-convex problems, it is possible that even SLP methods will not converge upon an optimum. This occurs because the SLP method implicitly assumes that the objective is a linear function of the design variables, and hence does not consider any interaction between design variables when determining the gradient information.

Figure 6.12 shows two examples of functions that have strong interactions between design variables for which an SLP optimisation method would not be guaranteed to find the global optimum.

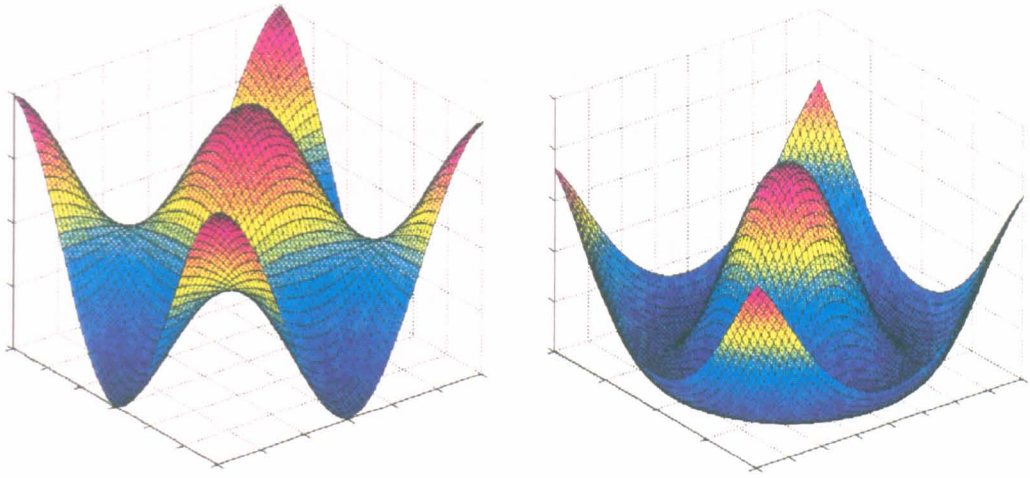

Figure 6.12 Examples of interactive design variables

If there is a high degree of interaction between design variables, it is possible that an optimisation algorithm based on an approximate linearisation of the problem will not converge upon a solution at all. Because many of the possible design variables for a helicopter blade cross-section potentially interact with one another, it is not necessarily possible to produce a converged solution by the global linear approximation method used for the cylindrical shell problem of Chapter 3.

Although Jung's statement that composite helicopter rotor blades "are thin walled, except near the root where they become thick walled" [1] may be a valid approximation for analysis purposes, thickness effects can still have an implication for optimisation. Deterministic methods rely on derivative information to predict the next design iteration, and hence are sensitive to interactions between design variables.

6.5.2.2 Importance of minimising variable interactions

As discussed above, it is highly desirable to minimise interactions between variables, since they reduce the robustness of deterministic optimisation routines – increasing the number of iterations required for convergence and preventing convergence entirely in some cases. Fortunately, it is quite possible to minimise such interactions by redefining the design variables so that the interactions between them are minimised. This approach has already been demonstrated for the cylindrical shell in Chapter 3.

Although this approach requires considerable knowledge about the underlying physics of the particular problem being studied, it does potentially allow the continued use of methods based upon linear approximations. The approximations may be either local or global, depending upon the behaviour of the objective with respect to the new design variables, although it has been shown [72] that the iterative global approximation method converges considerably quicker than the sequential local approximations of a SLP.

The following strategies for minimising variable interactions (or conditions for allowing interactions to remain) have been justified on the basis of the work presented earlier in this thesis and the insight offered by the finite element output in section 6.3.

6.5.2.3 Thickness of CFRP plies in the torsion box

It will be appreciated that due to their low axial modulus and low shear modulus, 90° plies contribute relatively little to the cross-sectional stiffness properties of the blade. Thus, rather than having three independent design variables for the thicknesses of 0°, 90° and ±45° plies, set

$$t_0 + t_{45} + t_{90} = T \qquad (6.4)$$

where T is a preselected, overall thickness of laminate wall, t_0 and t_{45} are independent design variables, and t_{90} takes a value that is dependent upon the other variables. Note that in general, it is usually appropriate to select the least sensitive variable (or define a variable that is insensitive) as the dependent variable.

By defining this constant-thickness laminate (comprising the 0°, 90° and 45° plies) to be laid up symmetrically, the interactions between design variables is minimised and the linearity of the cross-sectional stiffness properties with respect to the design variables is improved.

6.5.2.4 Unbalanced CFRP plies material to tailor flap torsion coupling

From the work on flap torsion coupling of a box section, it can be seen that the value of K_{45} does not vary linearly with ply orientation. Indeed, if ply orientation were used as a variable, the problem would not even be convex, since K_{45} is a function of the form

$$K_{45} = f_1(\overline{Q}_{16}) - f_2(\overline{Q}_{26}) f_3(\overline{Q}_{12}) / f_4(\overline{Q}_{22}) \qquad (6.5)$$

As concluded in Chapter 3, the most suitable approach to ensure problem convexity is to preselect the angle of coupling ply, and use its thickness as a design variable. If either the thickness of the coupling ply is small in relation to the thickness of the torsion box, or the change in thickness of coupling ply is small, then the linear approximation of K_{45} with respect to ply thickness will be good. In any case, use of thickness as a design variable will give a convex design space.

6.5.2.5 Size of nose-mass

The size of the nose-mass is determined by the chordwise location of its rear wall. Since the thickness of the cross-section does not remain constant (the external profile is aerofoil shaped), the cross-sectional properties do not vary linearly with this location. Note that because an increase in chordwise location will always lead to an increase in size of nose-mass, the behaviour is convex. The nose-mass does not interact with any other design features, so this non-linearity is overcome by a few iterations of the optimisation procedure.

6.5.2.6 Size of torsion box

The size of the torsion box is determined by the chordwise location of the spar wall. This variable interacts with many of the other design variables and this has direct implications for almost all of cross-sectional properties. Despite these interactions, the behaviour with respect to this design variable is convex because for the generic cross-section and design variables used in this study the interactions themselves behave in a convex manner. The range of allowable values for the torsion box has been found to be

significant in determining the efficiency with which a global approximation will converge upon the optimum solution.

6.5.2.7 Size of rear wedge

In a similar manner to the nose-mass, the size of the rear wedge is determined by the chordwise location of its free wall. Since the thickness of the cross-section is not constant as the blade tapers towards the trailing edge, the cross-sectional properties do not vary linearly with this location, although (as with the nose-mass) the behaviour is convex. As with the nose-mass, the trailing edge wedge does not interact strongly with the other design variables and the non-linearity is therefore overcome by a few iterations of the optimisation procedure.

6.6 OPTIMISATION OF A COMPOSITE HELICOPTER ROTOR BLADE

Based on the principles addressed so far in this thesis, it is now possible to produce a detailed design of a helicopter blade cross-section that meets given cross-sectional properties. This is demonstrated by the following example, wherein the design of a helicopter blade cross-section is optimised to meet given values of cross-sectional properties.

6.6.1 Problem definition

Design a helicopter blade section within a BTP-7 profile that meets the following cross-sectional properties:

Axial stiffness	=	1.492×10^7	N
Flap bending stiffness	=	3.866×10^8	Nmm^2
Lag bending stiffness	=	8.797×10^9	Nmm^2
Torsional stiffness	=	4.496×10^8	Nmm^2
Centre of mass location	=	19.90	% chord
Flap torsion coupling	=	6.454×10^6	Nmm^2
Mass	=	0.6391	g/mm

These values were chosen because they corresponded to the results of a known design, and the solution was therefore known to lie within the feasible design space. The weighting factors were all set to unity (i.e. it is equally important to match each cross-sectional property), although since the targets correspond to a unique known feasible solution, the value of the weighting factor will not affect the location optimum solution.

The generic design is shown in Figure 6.13 below, and the main features are illustrated.

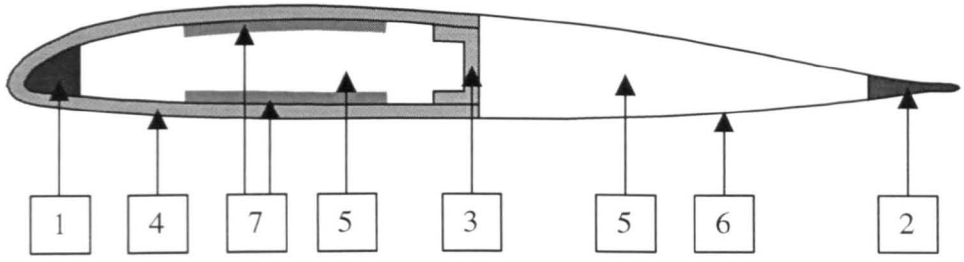

Figure 6.13 Generic design features for helicopter rotor blade section

1. Nose weight
2. 0° unidirectional CFRP rear wedge
3. Composite spar wall, comprising 0°, 90° and balanced ±45° plies
4. Composite blade wall, comprising 0°, 90° and balanced ±45° plies
5. Rohacell foam filler
6. GFRP surface layer
7. Coupling layers, comprising unbalanced 23° plies

Note that ply orientation of the coupling layers is fixed at 23°. The results presented for box sections in Chapter 4 show that this angle is usually close to that which maximises K_{45} for a given thickness of coupling material.

6.6.2 Appropriate design variables

The following six parameters are used as design variables

$x[0]$ Chordwise location of rear of nose weight

$x[1]$ Chordwise location of front of rear wedge

$x[2]$ Chordwise location of spar wall

$x[3]$ Thickness of 0° plies in spar/blade wall

$x[4]$ Thickness of balanced ±45° plies in spar/blade wall

$x[5]$ Thickness of coupling layer

Since the number of target properties exceeds the number of design variables, this problem does not necessarily have an exact solution. However for the case study presented here, the values of cross-sectional target properties correspond to a real design, for which the optimum solution is given in Table 6.3.

Design variable	x[0]	x[1]	x[2]	x[3]	x[4]	x[5]
Value	7	95	48	0.5	0.5	0.5

Table 6.3 Design values at optimum design

Although a discretisation has not been imposed upon this example problem, discretised variables may be dealt with as described earlier in this thesis.

6.6.3 Refinements to the optimisation algorithm

An optimisation routine was written in C++ to apply a modified global linear approximation method to design a rotor blade cross-section to meet given cross-sectional properties. The finished source code is fully commented, and is attached as Appendices 6.2 and 6.3.

Although this optimisation routine is based on the global linear approximation method described earlier in this thesis and follows the procedure outlined in the flowcharts of

Figures 6.8 and 6.9, some modifications were required to ensure that a solution was obtained efficiently and reliably. The most significant of these modifications was the introduction of a varying scale factor and associated move limit.

Due to the significant non-linearity of some variables and the potential interactions between design variables, a varying scale factor (and associated move limit) was introduced into the optimisation routine. This *varying* scale factor ensured that the linearisation was based over a large region of the design space for early iterations (i.e. when the design vector might change by quite a lot and it is important that the linearisation is valid for potentially large changes in the design vector), but was based over a smaller region for later iterations (i.e. when the design vector is close to converging upon the solution, and requires a linearisation that is accurate in the immediate vicinity of the design point).

A convergence criterion was set that ended the optimisation once all the cross-sectional properties were met to within 1%, or no further improvement in objective function was found after five iterations of the linearised solution had been completed.

6.6.4 Discussion of results

The optimisation code writes out a history file, which allows the step-by-step progress of the optimisation run to be examined - either during the optimisation process or after it is complete. The results of several optimisation runs are attached as Appendix 6.4. These show that the optimisation reliably converges upon the optimum solution, irrespective of the initial design point.

Each complete optimisation run took a few hours to converge upon an optimum solution. Figure 6.14 shows how the square root of the value of the objective function varied with the number of finite element analyses performed for each of the four optimisation runs detailed in Appendix 6.4. Note that since each finite element analysis is a computationally expensive step in the optimisation procedure, the number of FE analyses performed (rather than the number of optimisation iterations) gives the best indication of overall computational expense. The plateaux occur where the optimisation

algorithm performs many finite element analyses to determine the gradient function via a finite difference method. Although the objective does not actually improve because of these analyses, it is necessary to determine the gradient function so that new designs are based on an accurate linearisation of the optimisation problem.

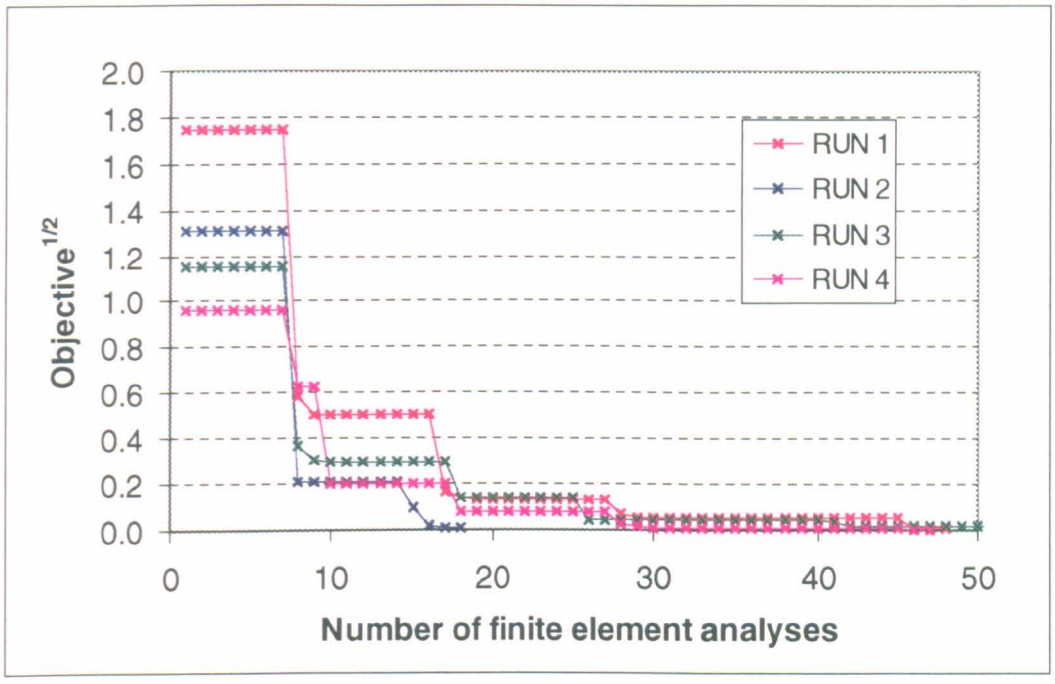

Figure 6.14 Improvement of design with number of FE analyses performed

The square root of the objective function (as defined in equation *(6.3)*) can be physically interpreted as the *N*-dimensional distance between the current cross-sectional properties and the target values. The figure above clearly shows that the optimisation algorithm very quickly finds solutions that are reasonably close to the required solution. The rate of convergence then typically slows down as the scale factor gradually reduces (with iteration number). As a result, the time required for an optimisation run only varies slightly with the choice of initial solution.

Further development of this scale factor (possibly by making it dependent upon the current value of objective function) could possibly enable the optimisation routine to converge upon a solution even more quickly.

6.7 CONCLUSIONS

An experiment was performed by Dr Ian Farrow at the University of Bristol to determine the shear centre location of a composite helicopter tail rotor blade. The cross sectional bending and torsion flexibilities of this blade section have been calculated from the experimental results. Surprisingly, the flexibility appears to vary with the length of blade section tested, which indicates that there is either some error in the experimental set-up and/or procedure, or that the blade structure has been damaged in some way that is not evident from a visual inspection.

The general design of a helicopter rotor blade is well known. Industry requires an automated method, which produces a detailed design of a helicopter rotor blade that will meet desired values of many cross-sectional properties. The method must produce an optimal design that has sufficient design information to enable the blade to be built. Industry is also generally reluctant to adopt radical changes to a tried and tested concept – it would generally be preferable to optimise an existing generic design than to produce an entirely new internal helicopter blade structure, not least because of the stringent requirements of aerospace airworthiness legislation.

This chapter has demonstrated the optimal detailed design of a rotor blade cross-section to meet target values for multiple cross-sectional properties from an initial generic section. In order to produce a robust and efficient solution algorithm, an optimisation algorithm has been developed that is based on a linear approximation of the design problem and pseudo-inverse method to determine the solution to the approximate linear problem. This approximation is called iteratively until the solution converges upon an optimal design. In order to maximise the robustness and efficiency of the optimisation, it is necessary to place appropriate constraints upon the design variables, and to minimise the interactions between design variables as discussed.

The novel method presented here fulfils the requirements of a typical helicopter rotor blade designer described above, and is therefore of practical use in an industrial context. Indeed Westland Helicopters have adopted the methodology presented herein to speed up the design process for their helicopter rotor blades.

7. CONCLUSIONS

The main objective of this research is to produce a generic method for the analysis and optimisation of anisotropic 1-dimensional thin-walled beams, of which composite helicopter rotor blades are an example.

This research has developed a working optimisation code for use in industry that reliably designs the internal structure of a composite helicopter rotor blade to meet given cross-sectional properties. This process has been largely symbiotic with the overall academic goal described above.

Since the methodology applied to the helicopter rotor blade problem can equally well be applied to the design of any prismatic structure, this work has wider applications – including the design of sports equipment (e.g. bicycle tubing, golf club shafts, skis), or indeed any prismatic structure which is designed to meet given cross-sectional properties.

7.1 SUMMARY OF WORK PRESENTED

7.1.1 Literature survey

Existing literature in the relevant fields is surveyed. In composite materials, an introduction is given to the principles and underlying assumptions of composite laminate analysis. Lamination parameters are introduced and their limitations as design variables in optimisation problems are discussed. It is shown that the majority of inplane laminate properties can be obtained by using laminates with only 0°, 90° and ±45° plies.

In helicopter blade design, an overview is given of the main approaches to helicopter blade modelling and optimisation in the existing literature. These generally fall into one of two categories

- the use of specialised, simple finite element models for the blade cross-section in order to optimise various values of ply orientation and other geometric parameters to improve the suitability of rotor blades for a particular application.
- the development of analytical modelling approaches so that the three-dimensional constitutive law from general, anisotropic elasticity can be reduced to a simple one-dimensional form of the beam problem.

In optimisation, an overview of optimisation theory is presented, including the visualisation of an optimisation problem, some basic concepts, and common techniques used in optimisation. A number of common optimisation methods are discussed.

7.1.2 Laminated shell case study

A 4-ply laminated cylindrical shell is examined from analytical and computational perspectives as a simplified case study, which is used to develop understanding of how the choice of design variables affects the nature of the design space, and hence the solution methods which may be used.

It is found that using layer thicknesses as design variables gives a convex problem, whereas the use of ply orientation angles gives a non-convex problem. The former approach allows the use of efficient, deterministic solution algorithms. The problem of linearity of (and interactions between) design variables is introduced and it is found that redefining the design variables can help to minimise interactions and improve the problem linearity, which leads to a more robust and efficient solution.

The use of a multivariate global linear approximation method is introduced, wherein the problem is reduced to a number of simultaneous linear equations that can be solved using pseudo-inverse matrix method that gives a least squares solution.

7.1.3 Flap-Torsion coupling

A new analytical model is derived which is based upon a stiffness of materials approach. The features of this model are intended to reflect the main features of a composite helicopter rotor blade section, and include a CFRP box section of variable

size and wall thickness, with variable thickness of unbalanced CFRP plies in the top and bottom surfaces of the box to produce K_{45} coupling. The box is filled with an isotropic core material of variable modulus. This model is novel in that it includes the effects of a core material (for which existing literature has not been found), and thus has the capability to model both hollow box sections (common in the literature), sandwich sections with no vertical walls, and box sections that have been filled with foam (or other core materials).

This model is validated by comparison with finite element analyses over a large range of design parameters, specifically including section height and width, vertical wall thickness, core material modulus, and fibre orientation in the coupling plies. The analysis presented compares favourably against existing models for flap-torsion coupling of box sections in the literature.

The flap-torsion behaviour of laminated composite beams is studied experimentally. The results are compared with finite element results, and good agreement is generally found. Classical laminate analysis is shown to be inadequate for predicting the flap-torsion coupling of the beams studied.

7.1.4 Optimisation of a composite helicopter rotor blade

The understanding gained through the work undertaken is applied to the design of a generic helicopter rotor blade section, which meets given target values of cross-sectional stiffness.

This is presented in the first instance for the optimisation of cross-sectional properties that behave in an approximately linear fashion, using design variables that do not interact. This optimisation can be achieved using the multivariate global linear approximation method presented in Chapter 3.

In the second instance, the optimisation of non-linear cross-sectional properties using potentially interactive design variables is demonstrated. Since the use of highly non-linear or interactive design variables can cause a deterministic method to fail, methods of minimising the interactions between design variables are discussed. Although this

approach requires some physical understanding of the behaviour of section properties with respect to the different design variables, this does allow the continued use of efficient deterministic optimisation methods that are based upon linear approximations.

The multivariate linear approximation method is again used to solve this problem, although additional refinements are made to the optimisation procedure to improve the robustness and efficiency of the solution process for this (more demanding) optimisation problem. One novel improvement has been to use *varying* finite differences (and associated move limits) in the evaluation of gradient information. This *varying* scale factor ensured that the linearisation is based over a large region of the design space for early iterations when the design vector may change a lot, but is based over a smaller region for later iterations when the design is already close to the optimum.

7.2 SUGGESTIONS FOR FURTHER RESEARCH

7.2.1 Non-destructive investigation of blade section

The apparently anomalous flexibility results of Farrow's experiment could have been caused by some internal structural damage (such as localised delaminations) to the blade. Non-destructive (e.g. ultrasound) testing could determine whether such damage was present, and the blade section could then be loaded again avoiding any localised areas of damage to obtain a better estimate of the cross sectional bending and torsion flexibilities.

7.2.2 Parametric study of K_{45} in a rotor blade section

As stated in the literature survey, the analysis of a box beam (or any other simplified section) as an idealised helicopter blade model will not necessarily give accurate values for the properties studied, although it is generally accepted that such simplified models do reflect the main trends.

It may prove interesting to carry out further detailed parametric studies of the cross-sectional properties of helicopter rotor blade sections. In particular, flap-torsion (K_{45})

coupling in helicopter blade sections is worth further attention. Although the flap-torsion behaviour of rotor blade sections is not presented explicitly in this thesis, the underlying physics and main trends were observed from the detailed analytical and parametric study of K_{45} presented in Chapter 4.

7.2.2 Further development of optimisation algorithms

There is scope to further improve the efficiency of the solution algorithm. By altering the size of finite difference upon which the linear approximation is based, the range over which this linear approximation is valid was altered. Appropriate move limits must then be set for the design variables based on the range of validity of the linear approximation.

The existing optimisation algorithm uses a reciprocal of iteration number to modify the size of finite difference perturbation. While this does give a robust algorithm, the finite differences are unnecessarily large for problems where the initial design is relatively close to the optimum. An algorithm where the size of finite difference perturbation used is dependent upon the value of the objective function may prove to be even more efficient.

REFERENCES

[1] Jung, S.N., Nagaraj, V.T., Chopra, I,. "Refined Structural Model for Thin- and Thick-Walled Composite Rotor Blades", AIAA Journal, Vol. 40, No. 1, pp. 105-116, 2002.

[2] Celi, R., "Recent Applications of Design Optimization to Rotorcraft – A Survey," Journal of Aircraft, Vol. 36, No. 1, pp. 176-189, 1999.

[3] Jones, R. M., "Mechanics of Composite Materials," Taylor & Francis, 2nd Ed, 1999.

[4] Tsai, S.W., Hahn, H.T., "Introduction to Composite Materials," Technomic Publishing Co., Inc., Lancaster, Pa., pp. 300-345, 1984.

[5] Datoo, M.H., "Mechanics of Fibrous Composites," Kluwer Academic Publishers, 1991.

[6] Tsai, S.W., Pagano, N.J., "Invariant Properties of Composite Materials," in Composite Materials Workshop, Technomic Publishing Co., Westport, pp. 233-253, 1968.

[7] Fukunaga, H., "A solution procedure for determining laminate configurations from lamination parameters," Advanced Composite Materials, Vol. 1, No. 3, pp. 209-224, 1991.

[8] Fukunaga, H., Sekine, H., "Stiffness design method of symmetric laminates using lamination parameters," AIAA Journal, Vol. 30, pp. 2791-2793, 1992.

[9] Miki, M., "Material Design of Composite Laminates with Required In-Plane Elastic Properties," Progress in Science and Engineering of Composites, Eds., T. Hayashi, K. Kawata, and S. Umekawa, ICCM-IV, Tokyo, Vol.2, pp. 1725-1731, 1982.

[10] Miki, M., "A Graphical Method for Designing Fibrous Laminated Composites with Required In-Plane Stiffness," Trans. JSCM, Vol. 9, No. 2, pp. 51-55, 1983.

[11] Diaconu, C.G., Sato, M., Sekine, H., "Buckling characteristics and layup optimisation of long laminated composite cylindrical shells subjected to combined loads using lamination parameters", Composite Structures, Vol. 58, pp. 423-433, 2002.

[12] Diaconu, C.G., Sato, M., Sekine, H., "Layup optimisation of symmetrically laminated thick plates for fundamental frequencies using lamination parameters", Structural Multidisciplinary Optimisation, Vol. 24, pp. 302-311, 2002.

[13] Grediac, M., "On the stiffness design of thin woven composites", Composite Structures, Vol. 51, pp. 245-255, 2001.

[14] Miki, M., Sugiyama, Y., "Optimum Design of Laminated Composite Plates Using Lamination Parameters," Proceedings of the AIAA/ASME/ASCE/AHS/ASC 32nd Structures, Structural Dynamics, and Materials Conference, Baltimore, MA., Part I, pp. 275-283, April 1991.

[15] Miki, M., "Optimum Design of Laminated Composite Plates Subject to Axial Compression," Composites '86: Recent Advances in Japan and the United States, Eds., K. Kawata, S. Umekawa, and A. Kobayashi, Proceedings of Japan-U.S. CCM-III, Tokyo, pp. 673-680, 1986.

[16] Pedersen, P., "On Sensitivity Analysis and Optimal Design of Specially Orthotropic Laminates," Engineering Optimization, Vol. 9, pp. 233-248, 1986.

[17] Haftka, R.T., Gurdal, Z., "Elements of Structural Optimisation," Kluwer Academic Publishers, 3rd Ed, 1993.

[18] Hodges, D.H., "Review of Composite Rotor Blade Modelling". AIAA Journal, Vol. 28, No. 3, pp. 561-565.

[19] Smith, E.C., "Aeroelastic Response and Aeromechanical Stability of Helicopters with Elastically Coupled Composite Rotor Blades", PhD Thesis, University of Maryland, 1992.

[20] Rehfield, L.W., "A Refined Simple Model for Tailoring Box Beams with Composites", Proc. 42nd AIAA/ASME/ASCE/AHS/ASC Structures, Structural Dynamics, and Materials Conference, Seattle, WA, 2001

[21] Rehfield, L.W., Cheung, R.H., "Some Basic Strategies for Aeroelastic Tailoring of Wings with Bend-Twist Coupling: Part One", Proc. 44th AIAA/ASME/ASCE/AHS/ASC Structures, Structural Dynamics, and Materials Conference, Norfolk, VA, 2003 .

[22] Rehfield, L.W., Atilgan, A.R., Hodges, D.H., "Nonclassical behaviour of Thin-Walled Composite Beams with Closed Cross Sections", Journal of the American Helicopter Society, Vol. 35, No. 2, pp. 42-50, 1990.

[23] Jung, S.N., Nagaraj, V.T., Chopra I., "Assessment of Composite Helicopter Blade Modelling Techniques," Journal of the American Helicopter Society, Vol. 44, No. 3, pp. 188-205, 1999.

[24] Kameyama, M., Fukunaga, H., Sekine, H., "Optimum Design of Composite Wing Model for Aeroelastic Properties," Proc. 5th Japan Intl. SAMPE Symposium, 1997.

[25] Chattopadhyay, A., McCarthy, T.R., Seeley, C.E., "Decomposition-Based Optimisation Procedure for High-Speed Prop-Rotors Using Composite Tailoring," Journal of Aircraft, Vol. 32, No. 5, pp. 1026-1033, 1995.

[26] Chattopadhyay, A., Narayan, J., "Optimum Design of High Speed Prop-Rotors Using a Multidisciplinary Approach," Engineering Optimization, Vol. 22, pp. 1-17, 1993.

[27] Chattopadhyay, A., McCarthy, T.R., Pagaldipti, N., "Multilevel Decomposition Procedure for Efficient Design Optimization of Helicopter Rotor Blades," AIAA Journal, Vol. 33, No. 2, pp. 223-230, 1995.

[28] Ganguli, R., Chopra, I., "Aeroelastic Optimization of a Helicopter Rotor with Composite Coupling," Journal of Aircraft, Vol. 32, No. 6, pp. 1326-1334, 1995.

[29] Ganguli, R., Chopra, I., "Aeroelastic Optimization of a Helicopter Rotor with Two-Cell Composite Blades," AIAA Journal, Vol. 34, No. 4, pp. 835-854, 1996.

[30] Ganguli, R., Chopra, I., "Aeroelastic Optimization of a Helicopter Rotor to Reduce Vibration and Dynamic Stresses," Journal of Aircraft, Vol. 33, No. 4, pp. 808-815, 1996.

[31] Wörndle, R., "Calculation of the Cross-section Properties and the Shear Stresses of Composite Rotor Blades," Vertica, Vol. 6, pp. 111-129, 1982.

[32] MSC NASTRAN, MacNeal-Schwendler Corporation, 2975 Redhill Avenue, Costa Mesa, California 92626, USA.

[33] MSC PATRAN, MacNeal-Schwendler Corporation, 2975 Redhill Avenue, Costa Mesa, California 92626, USA.

[34] Hill G.F.J., Weaver, P.M., "Analysis of Arbitrary Beam Sections with Non-Homogeneous Anisotropic Material Properties", Proc. ICCM13, Beijing, China, 2001.

[35] Sobieszczanski-Sobieski, J.; Haftka, R. T., "Multidisciplinary Aerospace Design Optimization: Survey of Recent Developments," Structural Optimization, Vol. 14, No. 1, pp. 1-23, 1997.

[36] He, C., Peters, D.A., "Finite State Aeroelastic Model for Use in Rotor Design Optimisation," Journal of Aircraft, Vol. 30, No. 5, pp. 777-784, 1993.

[37] McCarthy, T.R., Chattopadhyay, A., Zhang, S., "A Coupled Rotor/Wing Optimization Procedure for High Speed Tilt-Rotor Aircraft," Proceedings of American Helicopter Society 51st Annual Forum, Vol. 2, 1995.

[38] Chandra, R., Chopra, I., "Structural Behaviour of Two-Cell Composite Rotor Blades with Elastic Couplings," AIAA Journal, Vol. 30, No. 12, pp. 2914-2924, 1992.

[39] Kosmatka, J.B., Dong, S.B, "Saint-Venant Solutions for Prismatic Anisotropic Beams," Int. Journal of Solids and Structures, Vol. 28, No. 7, pp. 917-938, 1991.

[40] Bartholomew, P., Mercer, A.D., "Analysis of an Anisotropic Beam with Arbitrary Cross-Section," Technical Report 84058, Royal Aircraft Establishment, 1984.

[41] Hatch, C., Lee, A.R., "Determination of the Structural Properties of Helicopter Rotor Blades by Theoretical and Experimental Methods," Paper No. 67 presented at the 12th European Rotorcraft Forum, 1986.

[42] Diamond, S.W., "Theoretical Prediction of Composite Model Rotor Blade Structural Properties Using Various F.E. Modelling Idealisations," Defence Research Agency, Farnborough, 1996.

[43] Mansfield, E.H., Sobey A.J., "The Fibre Composite Helicopter Blade", Aeronautical Quarterly, pp.413-417, May 1979.

[44] Monterro, P., Appleby, R., "Determination of cross sectional stiffnesses of anisotropic prismatic structures," Undergraduate research project, University of Bristol, UK, 2003.

[45] Rehfield, L.W., Zischka, P.J., Chang, S., Fentress, M.L., Ambur, D.R., "Experimental Evaluation of a Box Beam Specifically Tailored for Chordwise Deformation", AIAA Journal, Vol. 33, No. 1, pp. 116-119, 1995.

[46] Diamond, S.W., "The Theoretical Prediction and Experimental Measurement of Sectional Properties of Coupled Composite Beams," Defence Research Agency, Farnborough, 1996.

[47] Parks, G.T., "F13 Lecture Notes – Optimisation Techniques," Cambridge University Engineering Dept., Cambridge, UK, 1998.

[48] Hajela, P., "Nongradient Methods in Multidisciplinary Design Optimization – Status and Potential," Journal of Aircraft, Vol. 36, No. 1, pp. 255-265, 1999.

[49] Levin, R.I., "Dynamic Finite Element Model Updating Using Neural Networks," PhD Thesis, University of Bristol, 1998.

[50] Schmit, L.A. Jr., Farshi, B., "Some approximation concepts for structural synthesis," AIAA Journal, Vol. 12, No. 5, 692-699, 1974.

[51] Roux, W.J., Stander, N., Haftka, R.T., "Response Surface Approximations for Structural Optimisation," Int. J. Numer. Meth. Engng., Vol. 42, pp. 517-534, 1998.

[52] Storaasli, O.O., Sobieszczanski, J., "On the Accuracy of the Taylor Approximation for Structure Resizing," AIAA Journal, Vol. 12, No. 2, 231-233, 1974.

[53] Noor, A.K., Lowder, H.E., "Structural Reanalysis via a Mixed Method," Computers and Structures, Vol. 5, Nos. 9-12, 1975.

[54] Vanderplaats, G.N., Salajeghah, E., "A New Approximation Method for Stress Constraints in Structural Synthesis," AIAA Journal, Vol. 27, No. 3, pp. 352-358, 1989.

[55] Thanedar, P.B., Vanderplaats, G.N., "Survey of Discrete Variable Optimization for Structural Design," Journal of Structural Engineering, Vol. 121, No. 2, pp. 301-305, 1995.

[56] Olsen, G.R., Vanderplaats, G.N., "Method for Non-linear Optimization with Discrete Design Variables," AIAA Journal, Vol. 27, pp. 1584-1589, 1987.

[57] Vanderplaats, G.N., "Structural Design Optimization Status and Direction," Journal of Aircraft, Vol. 36, No. 1, pp. 11-20, 1999.

[58] Lombardi, M., "Ottomizzazione di Lastre in Materiale Composito con l'uso di un Metodo di Annealing Simulato," Tesi di Laurea, Dept. of Structural Mechanics, University of Pavia, 1990.

[59] Metropolis, N., Rosenbluth, A.W., Rosenbluth, M.N., Teller, A.H., Teller, E., "Equation of State Calculations by Fast Computing Machines," J. Chem. Physics, Vol. 21, No. 6, pp. 1087-1092, 1953.

[60] Nahar, S., Sahni, S., Shragowithz, E. V., Proceedings of 22nd Design Automation Conf., Las Vegas, pp. 748-752, June 1985.

[61] Holland, J.H., Adaptation of Natural and Artificial Systems, The University of Michigan Press, Ann Arbor, MI, 1975.

[62] Nelder, J.A., Mead, R., "A Simplex Method for Function Minimization," Computer Journal, Vol. 7, pp. 308-313, 1965.

[63] Dantzig, G., "Linear Programming and Extensions," Princeton University Press, Princeton, NJ, 1963.

[64] Haftka, R.T., "Combining Global and Local Approximations," AIAA Journal, Vol. 29, No. 9, pp. 1523-1525, 1991.

[65] Furuya, H., Haftka, R.T., "Combining Genetic and Deterministic Algorithms for Locating Actuators on Space Structures," Journal of Spacecraft and Rockets, Vol. 33, No. 3, pp. 422-427, 1996.

[66] Fan, S.R., Geier, B., Rohwer, K., Liu, D.C., "Stability of Layered Anisotropic Cylindrical Shells under Combined Loading", Z. Flugweiss. Weltraumforsch. Vol. 7, No. 5, 1983.

[67] Lin, C.Y., Chan, W.S., "Stiffness Evaluation of Elliptical Laminated Composite Tube under Bending", Proc. 42nd AIAA/ASME/ASCE/AHS/ASC Structures, Structural Dynamics, and Materials Conference, Seattle, WA, 2001

[68] MATLAB, Version 6.1, The MathWorks, Inc., 3 Apple Hill Drive, Natick, MA 01760-2098, USA.

[69] ABAQUS Version 6.2, ABAQUS, INC., 1080 Main Street, Pawtucket, Rhode Island, 02860-4847, USA.

[70] Estivalez, E., Barrau, J-J., "Analytical theory for an approach calculation of composite box beams subjected to tension and bending", Composites Part B, Vol. 29B, pp. 371-376, 1998.

[71] Chandra, R., Stemple, A.D., and Chopra, I., "Thin-Walled Composite Beams under Bending, Torsional and Extensional Loads", Journal of Aircraft, Vol. 27, No. 7, pp. 619-626, 1990.

[72] Lemanski, S.L., Weaver, P.M.W., Hill, G.F.J., "Optimisation of laminated cylindrical shells to meet given cross sectional stiffness properties", Proc. 43rd AIAA/ASME/ASCE/AHS/ASC Structures, Structural Dynamics, and Materials Conference, Denver, CO, 2002.

APPENDIX 3.1

ABAQUS INPUT FILE FOR CYLINDRICAL SHELL ANALYSIS

```
*HEADING
Cylinder model
*NODE,NSET=NF1
1,21.625,0,0
30,21.625,348,0
*NGEN,NSET=NF1
1,30,1
*NODE,NSET=NF1
31,21.875,0,0
59,21.875,336,0
*NGEN,NSET=NF1
31,59,2
*NODE,NSET=NF1
61,22.125,0,0
90,22.125,348,0
*NGEN,NSET=NF1
61,90,1
*NODE,NSET=NF1
91,22.375,0,0
119,22.375,336,0
*NGEN,NSET=NF1
91,119,2
*NODE,NSET=NF1
121,22.625,0,0
150,22.625,348,0
*NGEN,NSET=NF1
121,150,1
*NODE,NSET=NF1
151,22.875,0,0
179,22.875,336,0
*NGEN,NSET=NF1
151,179,2
*NODE,NSET=NF1
181,23.125,0,0
210,23.125,348,0
*NGEN,NSET=NF1
181,210,1
*NODE,NSET=NF1
211,23.375,0,0
239,23.375,336,0
*NGEN,NSET=NF1
211,239,2
*NODE,NSET=NF1
241,23.625,0,0
270,23.625,348,0
*NGEN,NSET=NF1
241,270,1
*NODE,NSET=MIDS
271,21.625,0,0.5
299,21.625,336,0.5
*NGEN,NSET=MIDS
271,299,2
*NODE,NSET=MIDS
301,22.125,0,0.5
```

```
329,22.125,336,0.5
*NGEN,NSET=MIDS
301,329,2
*NODE,NSET=MIDS
331,22.625,0,0.5
359,22.625,336,0.5
*NGEN,NSET=MIDS
331,359,2
*NODE,NSET=MIDS
361,23.125,0,0.5
389,23.125,336,0.5
*NGEN,NSET=MIDS
361,389,2
*NODE,NSET=MIDS
391,23.625,0,0.5
419,23.625,336,0.5
*NGEN,NSET=MIDS
391,419,2
*NODE,NSET=NF2
421,21.625,0,1
450,21.625,348,1
*NGEN,NSET=NF2
421,450,1
*NODE,NSET=NF2
451,21.875,0,1
479,21.875,336,1
*NGEN,NSET=NF2
451,479,2
*NODE,NSET=NF2
481,22.125,0,1
510,22.125,348,1
*NGEN,NSET=NF2
481,510,1
*NODE,NSET=NF2
511,22.375,0,1
539,22.375,336,1
*NGEN,NSET=NF2
511,539,2
*NODE,NSET=NF2
541,22.625,0,1
570,22.625,348,1
*NGEN,NSET=NF2
541,570,1
*NODE,NSET=NF2
571,22.875,0,1
599,22.875,336,1
*NGEN,NSET=NF2
571,599,2
*NODE,NSET=NF2
601,23.125,0,1
630,23.125,348,1
*NGEN,NSET=NF2
601,630,1
*NODE,NSET=NF2
631,23.375,0,1
659,23.375,336,1
*NGEN,NSET=NF2
631,659,2
*NODE,NSET=NF2
661,23.625,0,1
690,23.625,348,1
```

```
*NGEN,NSET=NF2
661,690,1
*NSET,NSET=ALLND
NF1,MIDS,NF2
*NMAP,NSET=ALLND,TYPE=CYLINDRICAL
0.,0.,0.,0.,0.,1.
0.,1.,0.
1.,1.,1.
*ELEMENT,TYPE=C3D20,ELSET=LYR1
1,1,3,423,421,61,63,483,481,2,273,422,271,62,303,482,
301,31,33,453,451
*ELGEN,ELSET=LYR1
1,14,2,1
*ELEMENT,TYPE=C3D20,ELSET=LYR1
15,29,1,421,449,89,61,481,509,30,271,450,299,90,301,510,
329,59,31,451,479
*ELEMENT,TYPE=C3D20,ELSET=LYR2
16,61,63,483,481,121,123,543,541,62,303,482,301,122,333,542,
331,91,93,513,511
*ELGEN,ELSET=LYR2
16,14,2,1
*ELEMENT,TYPE=C3D20,ELSET=LYR2
30,89,61,481,509,149,121,541,569,90,301,510,329,150,331,570,
359,119,91,511,539
*ELEMENT,TYPE=C3D20,ELSET=LYR3
31,121,123,543,541,181,183,603,601,122,333,542,331,182,363,602,
361,151,153,573,571
*ELGEN,ELSET=LYR3
31,14,2,1
*ELEMENT,TYPE=C3D20,ELSET=LYR3
45,149,121,541,569,209,181,601,629,150,331,570,359,210,361,630,
389,179,151,571,599
*ELEMENT,TYPE=C3D20,ELSET=LYR4
46,181,183,603,601,241,243,663,661,182,363,602,361,242,393,662,
391,211,213,633,631
*ELGEN,ELSET=LYR4
46,14,2,1
*ELEMENT,TYPE=C3D20,ELSET=LYR4
60,209,181,601,629,269,241,661,689,210,361,630,389,270,391,690,
419,239,211,631,659
*ORIENTATION,NAME=TUBE,DEFINITION=COORDINATES,SYSTEM=CYLINDRICAL
0.,0.,0.,0.,0.,1.
2,-90.
*SOLID SECTION,ELSET=LYR1,MATERIAL=LYR1,ORIENTATION=TUBE
*MATERIAL,NAME=LYR1
*USER MATERIAL,CONSTANTS=8
131500.,9200.,0.3,0.45,4340.,3103.,45,1.
*DEPVAR
5
*SOLID SECTION,ELSET=LYR2,MATERIAL=LYR2,ORIENTATION=TUBE
*MATERIAL,NAME=LYR2
*USER MATERIAL,CONSTANTS=8
131500.,9200.,0.3,0.45,4340.,3103.,0,1.
*DEPVAR
5
*SOLID SECTION,ELSET=LYR3,MATERIAL=LYR3,ORIENTATION=TUBE
*MATERIAL,NAME=LYR3
*USER MATERIAL,CONSTANTS=8
131500.,9200.,0.3,0.45,4340.,3103.,90,1.
*DEPVAR
5
```

```
*SOLID SECTION,ELSET=LYR4,MATERIAL=LYR4,ORIENTATION=TUBE
*MATERIAL,NAME=LYR4
*USER MATERIAL,CONSTANTS=8
131500.,9200.,0.3,0.45,4340.,3103.,135,1.
*DEPVAR
5
**
** Beam
**
*NODE,NSET=BEAM
99999,0.,0.,0.
100000,0.,0.,0.1
*element,type=b31,elset=beam
10000,99999,100000
*beam general section,elset=beam
.01,.000001,.0000001,.000001,.000001
1.,0.,0.
1.,.2,0.
**
** The following equations are the MPC's for every node
**
*EQUATION
4
1,1,-1.,421,1,1.,99999,1,1.,99999,6,-21.625
4
1,2,-1.,421,2,1.,99999,2,1.,99999,6,-0
5
1,3,-1.,421,3,1.,99999,3,1.,99999,5,0,
99999,4,21.625
4
2,1,-1.,422,1,1.,99999,1,1.,99999,6,-21.1524
4
2,2,-1.,422,2,1.,99999,2,1.,99999,6,-4.49609
5
2,3,-1.,422,3,1.,99999,3,1.,99999,5,4.49609,
99999,4,21.1524
4
3,1,-1.,423,1,1.,99999,1,1.,99999,6,-19.7554
4
3,2,-1.,423,2,1.,99999,2,1.,99999,6,-8.79568
5
3,3,-1.,423,3,1.,99999,3,1.,99999,5,8.79568,
99999,4,19.7554
4
4,1,-1.,424,1,1.,99999,1,1.,99999,6,-17.495
4
4,2,-1.,424,2,1.,99999,2,1.,99999,6,-12.7109
5
4,3,-1.,424,3,1.,99999,3,1.,99999,5,12.7109,
99999,4,17.495
4
5,1,-1.,425,1,1.,99999,1,1.,99999,6,-14.4699
4
5,2,-1.,425,2,1.,99999,2,1.,99999,6,-16.0705
5
5,3,-1.,425,3,1.,99999,3,1.,99999,5,16.0705,
99999,4,14.4699
4
6,1,-1.,426,1,1.,99999,1,1.,99999,6,-10.8125
4
6,2,-1.,426,2,1.,99999,2,1.,99999,6,-18.7278
```

```
5
6,3,-1.,426,3,1.,99999,3,1.,99999,5,18.7278,
99999,4,10.8125
4
7,1,-1.,427,1,1.,99999,1,1.,99999,6,-6.68249
4
7,2,-1.,427,2,1.,99999,2,1.,99999,6,-20.5666
5
7,3,-1.,427,3,1.,99999,3,1.,99999,5,20.5666,
99999,4,6.68249
4
8,1,-1.,428,1,1.,99999,1,1.,99999,6,-2.26043
4
8,2,-1.,428,2,1.,99999,2,1.,99999,6,-21.5065
5
8,3,-1.,428,3,1.,99999,3,1.,99999,5,21.5065,
99999,4,2.26043
4
9,1,-1.,429,1,1.,99999,1,1.,99999,6,2.26043
4
9,2,-1.,429,2,1.,99999,2,1.,99999,6,-21.5065
5
9,3,-1.,429,3,1.,99999,3,1.,99999,5,21.5065,
99999,4,-2.26043
4
10,1,-1.,430,1,1.,99999,1,1.,99999,6,6.68249
4
10,2,-1.,430,2,1.,99999,2,1.,99999,6,-20.5666
5
10,3,-1.,430,3,1.,99999,3,1.,99999,5,20.5666,
99999,4,-6.68249
4
11,1,-1.,431,1,1.,99999,1,1.,99999,6,10.8125
4
11,2,-1.,431,2,1.,99999,2,1.,99999,6,-18.7278
5
11,3,-1.,431,3,1.,99999,3,1.,99999,5,18.7278,
99999,4,-10.8125
4
12,1,-1.,432,1,1.,99999,1,1.,99999,6,14.4699
4
12,2,-1.,432,2,1.,99999,2,1.,99999,6,-16.0705
5
12,3,-1.,432,3,1.,99999,3,1.,99999,5,16.0705,
99999,4,-14.4699
4
13,1,-1.,433,1,1.,99999,1,1.,99999,6,17.495
4
13,2,-1.,433,2,1.,99999,2,1.,99999,6,-12.7109
5
13,3,-1.,433,3,1.,99999,3,1.,99999,5,12.7109,
99999,4,-17.495
4
14,1,-1.,434,1,1.,99999,1,1.,99999,6,19.7554
4
14,2,-1.,434,2,1.,99999,2,1.,99999,6,-8.79568
5
14,3,-1.,434,3,1.,99999,3,1.,99999,5,8.79568,
99999,4,-19.7554
4
15,1,-1.,435,1,1.,99999,1,1.,99999,6,21.1524
```

```
4
15,2,-1.,435,2,1.,99999,2,1.,99999,6,-4.49609
5
15,3,-1.,435,3,1.,99999,3,1.,99999,5,4.49609,
99999,4,-21.1524
4
16,1,-1.,436,1,1.,99999,1,1.,99999,6,21.625
4
16,2,-1.,436,2,1.,99999,2,1.,99999,6,-0
5
16,3,-1.,436,3,1.,99999,3,1.,99999,5,0,
99999,4,-21.625
4
17,1,-1.,437,1,1.,99999,1,1.,99999,6,21.1524
4
17,2,-1.,437,2,1.,99999,2,1.,99999,6,4.49609
5
17,3,-1.,437,3,1.,99999,3,1.,99999,5,-4.49609,
99999,4,-21.1524
4
18,1,-1.,438,1,1.,99999,1,1.,99999,6,19.7554
4
18,2,-1.,438,2,1.,99999,2,1.,99999,6,8.79568
5
18,3,-1.,438,3,1.,99999,3,1.,99999,5,-8.79568,
99999,4,-19.7554
4
19,1,-1.,439,1,1.,99999,1,1.,99999,6,17.495
4
19,2,-1.,439,2,1.,99999,2,1.,99999,6,12.7109
5
19,3,-1.,439,3,1.,99999,3,1.,99999,5,-12.7109,
99999,4,-17.495
4
20,1,-1.,440,1,1.,99999,1,1.,99999,6,14.4699
4
20,2,-1.,440,2,1.,99999,2,1.,99999,6,16.0705
5
20,3,-1.,440,3,1.,99999,3,1.,99999,5,-16.0705,
99999,4,-14.4699
4
21,1,-1.,441,1,1.,99999,1,1.,99999,6,10.8125
4
21,2,-1.,441,2,1.,99999,2,1.,99999,6,18.7278
5
21,3,-1.,441,3,1.,99999,3,1.,99999,5,-18.7278,
99999,4,-10.8125
4
22,1,-1.,442,1,1.,99999,1,1.,99999,6,6.68249
4
22,2,-1.,442,2,1.,99999,2,1.,99999,6,20.5666
5
22,3,-1.,442,3,1.,99999,3,1.,99999,5,-20.5666,
99999,4,-6.68249
4
23,1,-1.,443,1,1.,99999,1,1.,99999,6,2.26043
4
23,2,-1.,443,2,1.,99999,2,1.,99999,6,21.5065
5
23,3,-1.,443,3,1.,99999,3,1.,99999,5,-21.5065,
99999,4,-2.26043
```

```
4
24,1,-1.,444,1,1.,99999,1,1.,99999,6,-2.26043
4
24,2,-1.,444,2,1.,99999,2,1.,99999,6,21.5065
5
24,3,-1.,444,3,1.,99999,3,1.,99999,5,-21.5065,
99999,4,2.26043
4
25,1,-1.,445,1,1.,99999,1,1.,99999,6,-6.68249
4
25,2,-1.,445,2,1.,99999,2,1.,99999,6,20.5666
5
25,3,-1.,445,3,1.,99999,3,1.,99999,5,-20.5666,
99999,4,6.68249
4
26,1,-1.,446,1,1.,99999,1,1.,99999,6,-10.8125
4
26,2,-1.,446,2,1.,99999,2,1.,99999,6,18.7278
5
26,3,-1.,446,3,1.,99999,3,1.,99999,5,-18.7278,
99999,4,10.8125
4
27,1,-1.,447,1,1.,99999,1,1.,99999,6,-14.4699
4
27,2,-1.,447,2,1.,99999,2,1.,99999,6,16.0705
5
27,3,-1.,447,3,1.,99999,3,1.,99999,5,-16.0705,
99999,4,14.4699
4
28,1,-1.,448,1,1.,99999,1,1.,99999,6,-17.495
4
28,2,-1.,448,2,1.,99999,2,1.,99999,6,12.7109
5
28,3,-1.,448,3,1.,99999,3,1.,99999,5,-12.7109,
99999,4,17.495
4
29,1,-1.,449,1,1.,99999,1,1.,99999,6,-19.7554
4
29,2,-1.,449,2,1.,99999,2,1.,99999,6,8.79568
5
29,3,-1.,449,3,1.,99999,3,1.,99999,5,-8.79568,
99999,4,19.7554
4
30,1,-1.,450,1,1.,99999,1,1.,99999,6,-21.1524
4
30,2,-1.,450,2,1.,99999,2,1.,99999,6,4.49609
5
30,3,-1.,450,3,1.,99999,3,1.,99999,5,-4.49609,
99999,4,21.1524
4
31,1,-1.,451,1,1.,99999,1,1.,99999,6,-21.875
4
31,2,-1.,451,2,1.,99999,2,1.,99999,6,-0
5
31,3,-1.,451,3,1.,99999,3,1.,99999,5,0,
99999,4,21.875
4
33,1,-1.,453,1,1.,99999,1,1.,99999,6,-19.9838
4
33,2,-1.,453,2,1.,99999,2,1.,99999,6,-8.89736
5
```

```
33,3,-1.,453,3,1.,99999,3,1.,99999,5,8.89736,
99999,4,19.9838
4
35,1,-1.,455,1,1.,99999,1,1.,99999,6,-14.6372
4
35,2,-1.,455,2,1.,99999,2,1.,99999,6,-16.2563
5
35,3,-1.,455,3,1.,99999,3,1.,99999,5,16.2563,
99999,4,14.6372
4
37,1,-1.,457,1,1.,99999,1,1.,99999,6,-6.75975
4
37,2,-1.,457,2,1.,99999,2,1.,99999,6,-20.8044
5
37,3,-1.,457,3,1.,99999,3,1.,99999,5,20.8044,
99999,4,6.75975
4
39,1,-1.,459,1,1.,99999,1,1.,99999,6,2.28656
4
39,2,-1.,459,2,1.,99999,2,1.,99999,6,-21.7552
5
39,3,-1.,459,3,1.,99999,3,1.,99999,5,21.7552,
99999,4,-2.28656
4
41,1,-1.,461,1,1.,99999,1,1.,99999,6,10.9375
4
41,2,-1.,461,2,1.,99999,2,1.,99999,6,-18.9443
5
41,3,-1.,461,3,1.,99999,3,1.,99999,5,18.9443,
99999,4,-10.9375
4
43,1,-1.,463,1,1.,99999,1,1.,99999,6,17.6972
4
43,2,-1.,463,2,1.,99999,2,1.,99999,6,-12.8578
5
43,3,-1.,463,3,1.,99999,3,1.,99999,5,12.8578,
99999,4,-17.6972
4
45,1,-1.,465,1,1.,99999,1,1.,99999,6,21.397
4
45,2,-1.,465,2,1.,99999,2,1.,99999,6,-4.54807
5
45,3,-1.,465,3,1.,99999,3,1.,99999,5,4.54807,
99999,4,-21.397
4
47,1,-1.,467,1,1.,99999,1,1.,99999,6,21.397
4
47,2,-1.,467,2,1.,99999,2,1.,99999,6,4.54807
5
47,3,-1.,467,3,1.,99999,3,1.,99999,5,-4.54807,
99999,4,-21.397
4
49,1,-1.,469,1,1.,99999,1,1.,99999,6,17.6972
4
49,2,-1.,469,2,1.,99999,2,1.,99999,6,12.8578
5
49,3,-1.,469,3,1.,99999,3,1.,99999,5,-12.8578,
99999,4,-17.6972
4
51,1,-1.,471,1,1.,99999,1,1.,99999,6,10.9375
4
```

```
51,2,-1.,471,2,1.,99999,2,1.,99999,6,18.9443
5
51,3,-1.,471,3,1.,99999,3,1.,99999,5,-18.9443,
99999,4,-10.9375
4
53,1,-1.,473,1,1.,99999,1,1.,99999,6,2.28656
4
53,2,-1.,473,2,1.,99999,2,1.,99999,6,21.7552
5
53,3,-1.,473,3,1.,99999,3,1.,99999,5,-21.7552,
99999,4,-2.28656
4
55,1,-1.,475,1,1.,99999,1,1.,99999,6,-6.75975
4
55,2,-1.,475,2,1.,99999,2,1.,99999,6,20.8044
5
55,3,-1.,475,3,1.,99999,3,1.,99999,5,-20.8044,
99999,4,6.75975
4
57,1,-1.,477,1,1.,99999,1,1.,99999,6,-14.6372
4
57,2,-1.,477,2,1.,99999,2,1.,99999,6,16.2563
5
57,3,-1.,477,3,1.,99999,3,1.,99999,5,-16.2563,
99999,4,14.6372
4
59,1,-1.,479,1,1.,99999,1,1.,99999,6,-19.9838
4
59,2,-1.,479,2,1.,99999,2,1.,99999,6,8.89736
5
59,3,-1.,479,3,1.,99999,3,1.,99999,5,-8.89736,
99999,4,19.9838
4
61,1,-1.,481,1,1.,99999,1,1.,99999,6,-21.875
4
61,2,-1.,481,2,1.,99999,2,1.,99999,6,-0
5
61,3,-1.,481,3,1.,99999,3,1.,99999,5,0,
99999,4,21.875
4
62,1,-1.,482,1,1.,99999,1,1.,99999,6,-21.397
4
62,2,-1.,482,2,1.,99999,2,1.,99999,6,-4.54807
5
62,3,-1.,482,3,1.,99999,3,1.,99999,5,4.54807,
99999,4,21.397
4
63,1,-1.,483,1,1.,99999,1,1.,99999,6,-19.9838
4
63,2,-1.,483,2,1.,99999,2,1.,99999,6,-8.89736
5
63,3,-1.,483,3,1.,99999,3,1.,99999,5,8.89736,
99999,4,19.9838
4
64,1,-1.,484,1,1.,99999,1,1.,99999,6,-17.6972
4
64,2,-1.,484,2,1.,99999,2,1.,99999,6,-12.8578
5
64,3,-1.,484,3,1.,99999,3,1.,99999,5,12.8578,
99999,4,17.6972
4
```

```
65,1,-1.,485,1,1.,99999,1,1.,99999,6,-14.6372
4
65,2,-1.,485,2,1.,99999,2,1.,99999,6,-16.2563
5
65,3,-1.,485,3,1.,99999,3,1.,99999,5,16.2563,
99999,4,14.6372
4
66,1,-1.,486,1,1.,99999,1,1.,99999,6,-10.9375
4
66,2,-1.,486,2,1.,99999,2,1.,99999,6,-18.9443
5
66,3,-1.,486,3,1.,99999,3,1.,99999,5,18.9443,
99999,4,10.9375
4
67,1,-1.,487,1,1.,99999,1,1.,99999,6,-6.75975
4
67,2,-1.,487,2,1.,99999,2,1.,99999,6,-20.8044
5
67,3,-1.,487,3,1.,99999,3,1.,99999,5,20.8044,
99999,4,6.75975
4
68,1,-1.,488,1,1.,99999,1,1.,99999,6,-2.28656
4
68,2,-1.,488,2,1.,99999,2,1.,99999,6,-21.7552
5
68,3,-1.,488,3,1.,99999,3,1.,99999,5,21.7552,
99999,4,2.28656
4
69,1,-1.,489,1,1.,99999,1,1.,99999,6,2.28656
4
69,2,-1.,489,2,1.,99999,2,1.,99999,6,-21.7552
5
69,3,-1.,489,3,1.,99999,3,1.,99999,5,21.7552,
99999,4,-2.28656
4
70,1,-1.,490,1,1.,99999,1,1.,99999,6,6.75975
4
70,2,-1.,490,2,1.,99999,2,1.,99999,6,-20.8044
5
70,3,-1.,490,3,1.,99999,3,1.,99999,5,20.8044,
99999,4,-6.75975
4
71,1,-1.,491,1,1.,99999,1,1.,99999,6,10.9375
4
71,2,-1.,491,2,1.,99999,2,1.,99999,6,-18.9443
5
71,3,-1.,491,3,1.,99999,3,1.,99999,5,18.9443,
99999,4,-10.9375
4
72,1,-1.,492,1,1.,99999,1,1.,99999,6,14.6372
4
72,2,-1.,492,2,1.,99999,2,1.,99999,6,-16.2563
5
72,3,-1.,492,3,1.,99999,3,1.,99999,5,16.2563,
99999,4,-14.6372
4
73,1,-1.,493,1,1.,99999,1,1.,99999,6,17.6972
4
73,2,-1.,493,2,1.,99999,2,1.,99999,6,-12.8578
5
73,3,-1.,493,3,1.,99999,3,1.,99999,5,12.8578,
```

```
99999,4,-17.6972
4
74,1,-1.,494,1,1.,99999,1,1.,99999,6,19.9838
4
74,2,-1.,494,2,1.,99999,2,1.,99999,6,-8.89736
5
74,3,-1.,494,3,1.,99999,3,1.,99999,5,8.89736,
99999,4,-19.9838
4
75,1,-1.,495,1,1.,99999,1,1.,99999,6,21.397
4
75,2,-1.,495,2,1.,99999,2,1.,99999,6,-4.54807
5
75,3,-1.,495,3,1.,99999,3,1.,99999,5,4.54807,
99999,4,-21.397
4
76,1,-1.,496,1,1.,99999,1,1.,99999,6,21.875
4
76,2,-1.,496,2,1.,99999,2,1.,99999,6,-0
5
76,3,-1.,496,3,1.,99999,3,1.,99999,5,0,
99999,4,-21.875
4
77,1,-1.,497,1,1.,99999,1,1.,99999,6,21.397
4
77,2,-1.,497,2,1.,99999,2,1.,99999,6,4.54807
5
77,3,-1.,497,3,1.,99999,3,1.,99999,5,-4.54807,
99999,4,-21.397
4
78,1,-1.,498,1,1.,99999,1,1.,99999,6,19.9838
4
78,2,-1.,498,2,1.,99999,2,1.,99999,6,8.89736
5
78,3,-1.,498,3,1.,99999,3,1.,99999,5,-8.89736,
99999,4,-19.9838
4
79,1,-1.,499,1,1.,99999,1,1.,99999,6,17.6972
4
79,2,-1.,499,2,1.,99999,2,1.,99999,6,12.8578
5
79,3,-1.,499,3,1.,99999,3,1.,99999,5,-12.8578,
99999,4,-17.6972
4
80,1,-1.,500,1,1.,99999,1,1.,99999,6,14.6372
4
80,2,-1.,500,2,1.,99999,2,1.,99999,6,16.2563
5
80,3,-1.,500,3,1.,99999,3,1.,99999,5,-16.2563,
99999,4,-14.6372
4
81,1,-1.,501,1,1.,99999,1,1.,99999,6,10.9375
4
81,2,-1.,501,2,1.,99999,2,1.,99999,6,18.9443
5
81,3,-1.,501,3,1.,99999,3,1.,99999,5,-18.9443,
99999,4,-10.9375
4
82,1,-1.,502,1,1.,99999,1,1.,99999,6,6.75975
4
82,2,-1.,502,2,1.,99999,2,1.,99999,6,20.8044
```

```
5
82,3,-1.,502,3,1.,99999,3,1.,99999,5,-20.8044,
99999,4,-6.75975
4
83,1,-1.,503,1,1.,99999,1,1.,99999,6,2.28656
4
83,2,-1.,503,2,1.,99999,2,1.,99999,6,21.7552
5
83,3,-1.,503,3,1.,99999,3,1.,99999,5,-21.7552,
99999,4,-2.28656
4
84,1,-1.,504,1,1.,99999,1,1.,99999,6,-2.28656
4
84,2,-1.,504,2,1.,99999,2,1.,99999,6,21.7552
5
84,3,-1.,504,3,1.,99999,3,1.,99999,5,-21.7552,
99999,4,2.28656
4
85,1,-1.,505,1,1.,99999,1,1.,99999,6,-6.75975
4
85,2,-1.,505,2,1.,99999,2,1.,99999,6,20.8044
5
85,3,-1.,505,3,1.,99999,3,1.,99999,5,-20.8044,
99999,4,6.75975
4
86,1,-1.,506,1,1.,99999,1,1.,99999,6,-10.9375
4
86,2,-1.,506,2,1.,99999,2,1.,99999,6,18.9443
5
86,3,-1.,506,3,1.,99999,3,1.,99999,5,-18.9443,
99999,4,10.9375
4
87,1,-1.,507,1,1.,99999,1,1.,99999,6,-14.6372
4
87,2,-1.,507,2,1.,99999,2,1.,99999,6,16.2563
5
87,3,-1.,507,3,1.,99999,3,1.,99999,5,-16.2563,
99999,4,14.6372
4
88,1,-1.,508,1,1.,99999,1,1.,99999,6,-17.6972
4
88,2,-1.,508,2,1.,99999,2,1.,99999,6,12.8578
5
88,3,-1.,508,3,1.,99999,3,1.,99999,5,-12.8578,
99999,4,17.6972
4
89,1,-1.,509,1,1.,99999,1,1.,99999,6,-19.9838
4
89,2,-1.,509,2,1.,99999,2,1.,99999,6,8.89736
5
89,3,-1.,509,3,1.,99999,3,1.,99999,5,-8.89736,
99999,4,19.9838
4
90,1,-1.,510,1,1.,99999,1,1.,99999,6,-21.397
4
90,2,-1.,510,2,1.,99999,2,1.,99999,6,4.54807
5
90,3,-1.,510,3,1.,99999,3,1.,99999,5,-4.54807,
99999,4,21.397
4
91,1,-1.,511,1,1.,99999,1,1.,99999,6,-22.125
```

```
4
91,2,-1.,511,2,1.,99999,2,1.,99999,6,-0
5
91,3,-1.,511,3,1.,99999,3,1.,99999,5,0,
99999,4,22.125
4
93,1,-1.,513,1,1.,99999,1,1.,99999,6,-20.2122
4
93,2,-1.,513,2,1.,99999,2,1.,99999,6,-8.99905
5
93,3,-1.,513,3,1.,99999,3,1.,99999,5,8.99905,
99999,4,20.2122
4
95,1,-1.,515,1,1.,99999,1,1.,99999,6,-14.8045
4
95,2,-1.,515,2,1.,99999,2,1.,99999,6,-16.4421
5
95,3,-1.,515,3,1.,99999,3,1.,99999,5,16.4421,
99999,4,14.8045
4
97,1,-1.,517,1,1.,99999,1,1.,99999,6,-6.837
4
97,2,-1.,517,2,1.,99999,2,1.,99999,6,-21.0421
5
97,3,-1.,517,3,1.,99999,3,1.,99999,5,21.0421,
99999,4,6.837
4
99,1,-1.,519,1,1.,99999,1,1.,99999,6,2.31269
4
99,2,-1.,519,2,1.,99999,2,1.,99999,6,-22.0038
5
99,3,-1.,519,3,1.,99999,3,1.,99999,5,22.0038,
99999,4,-2.31269
4
101,1,-1.,521,1,1.,99999,1,1.,99999,6,11.0625
4
101,2,-1.,521,2,1.,99999,2,1.,99999,6,-19.1608
5
101,3,-1.,521,3,1.,99999,3,1.,99999,5,19.1608,
99999,4,-11.0625
4
103,1,-1.,523,1,1.,99999,1,1.,99999,6,17.8995
4
103,2,-1.,523,2,1.,99999,2,1.,99999,6,-13.0047
5
103,3,-1.,523,3,1.,99999,3,1.,99999,5,13.0047,
99999,4,-17.8995
4
105,1,-1.,525,1,1.,99999,1,1.,99999,6,21.6415
4
105,2,-1.,525,2,1.,99999,2,1.,99999,6,-4.60005
5
105,3,-1.,525,3,1.,99999,3,1.,99999,5,4.60005,
99999,4,-21.6415
4
107,1,-1.,527,1,1.,99999,1,1.,99999,6,21.6415
4
107,2,-1.,527,2,1.,99999,2,1.,99999,6,4.60005
5
107,3,-1.,527,3,1.,99999,3,1.,99999,5,-4.60005,
99999,4,-21.6415
```

```
4
109,1,-1.,529,1,1.,99999,1,1.,99999,6,17.8995
4
109,2,-1.,529,2,1.,99999,2,1.,99999,6,13.0047
5
109,3,-1.,529,3,1.,99999,3,1.,99999,5,-13.0047,
99999,4,-17.8995
4
111,1,-1.,531,1,1.,99999,1,1.,99999,6,11.0625
4
111,2,-1.,531,2,1.,99999,2,1.,99999,6,19.1608
5
111,3,-1.,531,3,1.,99999,3,1.,99999,5,-19.1608,
99999,4,-11.0625
4
113,1,-1.,533,1,1.,99999,1,1.,99999,6,2.31269
4
113,2,-1.,533,2,1.,99999,2,1.,99999,6,22.0038
5
113,3,-1.,533,3,1.,99999,3,1.,99999,5,-22.0038,
99999,4,-2.31269
4
115,1,-1.,535,1,1.,99999,1,1.,99999,6,-6.837
4
115,2,-1.,535,2,1.,99999,2,1.,99999,6,21.0421
5
115,3,-1.,535,3,1.,99999,3,1.,99999,5,-21.0421,
99999,4,6.837
4
117,1,-1.,537,1,1.,99999,1,1.,99999,6,-14.8045
4
117,2,-1.,537,2,1.,99999,2,1.,99999,6,16.4421
5
117,3,-1.,537,3,1.,99999,3,1.,99999,5,-16.4421,
99999,4,14.8045
4
119,1,-1.,539,1,1.,99999,1,1.,99999,6,-20.2122
4
119,2,-1.,539,2,1.,99999,2,1.,99999,6,8.99905
5
119,3,-1.,539,3,1.,99999,3,1.,99999,5,-8.99905,
99999,4,20.2122
4
121,1,-1.,541,1,1.,99999,1,1.,99999,6,-22.125
4
121,2,-1.,541,2,1.,99999,2,1.,99999,6,-0
5
121,3,-1.,541,3,1.,99999,3,1.,99999,5,0,
99999,4,22.125
4
122,1,-1.,542,1,1.,99999,1,1.,99999,6,-21.6415
4
122,2,-1.,542,2,1.,99999,2,1.,99999,6,-4.60005
5
122,3,-1.,542,3,1.,99999,3,1.,99999,5,4.60005,
99999,4,21.6415
4
123,1,-1.,543,1,1.,99999,1,1.,99999,6,-20.2122
4
123,2,-1.,543,2,1.,99999,2,1.,99999,6,-8.99905
5
```

```
123,3,-1.,543,3,1.,99999,3,1.,99999,5,8.99905,
99999,4,20.2122
4
124,1,-1.,544,1,1.,99999,1,1.,99999,6,-17.8995
4
124,2,-1.,544,2,1.,99999,2,1.,99999,6,-13.0047
5
124,3,-1.,544,3,1.,99999,3,1.,99999,5,13.0047,
99999,4,17.8995
4
125,1,-1.,545,1,1.,99999,1,1.,99999,6,-14.8045
4
125,2,-1.,545,2,1.,99999,2,1.,99999,6,-16.4421
5
125,3,-1.,545,3,1.,99999,3,1.,99999,5,16.4421,
99999,4,14.8045
4
126,1,-1.,546,1,1.,99999,1,1.,99999,6,-11.0625
4
126,2,-1.,546,2,1.,99999,2,1.,99999,6,-19.1608
5
126,3,-1.,546,3,1.,99999,3,1.,99999,5,19.1608,
99999,4,11.0625
4
127,1,-1.,547,1,1.,99999,1,1.,99999,6,-6.837
4
127,2,-1.,547,2,1.,99999,2,1.,99999,6,-21.0421
5
127,3,-1.,547,3,1.,99999,3,1.,99999,5,21.0421,
99999,4,6.837
4
128,1,-1.,548,1,1.,99999,1,1.,99999,6,-2.31269
4
128,2,-1.,548,2,1.,99999,2,1.,99999,6,-22.0038
5
128,3,-1.,548,3,1.,99999,3,1.,99999,5,22.0038,
99999,4,2.31269
4
129,1,-1.,549,1,1.,99999,1,1.,99999,6,2.31269
4
129,2,-1.,549,2,1.,99999,2,1.,99999,6,-22.0038
5
129,3,-1.,549,3,1.,99999,3,1.,99999,5,22.0038,
99999,4,-2.31269
4
130,1,-1.,550,1,1.,99999,1,1.,99999,6,6.837
4
130,2,-1.,550,2,1.,99999,2,1.,99999,6,-21.0421
5
130,3,-1.,550,3,1.,99999,3,1.,99999,5,21.0421,
99999,4,-6.837
4
131,1,-1.,551,1,1.,99999,1,1.,99999,6,11.0625
4
131,2,-1.,551,2,1.,99999,2,1.,99999,6,-19.1608
5
131,3,-1.,551,3,1.,99999,3,1.,99999,5,19.1608,
99999,4,-11.0625
4
132,1,-1.,552,1,1.,99999,1,1.,99999,6,14.8045
4
```

```
132,2,-1.,552,2,1.,99999,2,1.,99999,6,-16.4421
5
132,3,-1.,552,3,1.,99999,3,1.,99999,5,16.4421,
99999,4,-14.8045
4
133,1,-1.,553,1,1.,99999,1,1.,99999,6,17.8995
4
133,2,-1.,553,2,1.,99999,2,1.,99999,6,-13.0047
5
133,3,-1.,553,3,1.,99999,3,1.,99999,5,13.0047,
99999,4,-17.8995
4
134,1,-1.,554,1,1.,99999,1,1.,99999,6,20.2122
4
134,2,-1.,554,2,1.,99999,2,1.,99999,6,-8.99905
5
134,3,-1.,554,3,1.,99999,3,1.,99999,5,8.99905,
99999,4,-20.2122
4
135,1,-1.,555,1,1.,99999,1,1.,99999,6,21.6415
4
135,2,-1.,555,2,1.,99999,2,1.,99999,6,-4.60005
5
135,3,-1.,555,3,1.,99999,3,1.,99999,5,4.60005,
99999,4,-21.6415
4
136,1,-1.,556,1,1.,99999,1,1.,99999,6,22.125
4
136,2,-1.,556,2,1.,99999,2,1.,99999,6,-0
5
136,3,-1.,556,3,1.,99999,3,1.,99999,5,0,
99999,4,-22.125
4
137,1,-1.,557,1,1.,99999,1,1.,99999,6,21.6415
4
137,2,-1.,557,2,1.,99999,2,1.,99999,6,4.60005
5
137,3,-1.,557,3,1.,99999,3,1.,99999,5,-4.60005,
99999,4,-21.6415
4
138,1,-1.,558,1,1.,99999,1,1.,99999,6,20.2122
4
138,2,-1.,558,2,1.,99999,2,1.,99999,6,8.99905
5
138,3,-1.,558,3,1.,99999,3,1.,99999,5,-8.99905,
99999,4,-20.2122
4
139,1,-1.,559,1,1.,99999,1,1.,99999,6,17.8995
4
139,2,-1.,559,2,1.,99999,2,1.,99999,6,13.0047
5
139,3,-1.,559,3,1.,99999,3,1.,99999,5,-13.0047,
99999,4,-17.8995
4
140,1,-1.,560,1,1.,99999,1,1.,99999,6,14.8045
4
140,2,-1.,560,2,1.,99999,2,1.,99999,6,16.4421
5
140,3,-1.,560,3,1.,99999,3,1.,99999,5,-16.4421,
99999,4,-14.8045
4
```

```
141,1,-1.,561,1,1.,99999,1,1.,99999,6,11.0625
4
141,2,-1.,561,2,1.,99999,2,1.,99999,6,19.1608
5
141,3,-1.,561,3,1.,99999,3,1.,99999,5,-19.1608,
99999,4,-11.0625
4
142,1,-1.,562,1,1.,99999,1,1.,99999,6,6.837
4
142,2,-1.,562,2,1.,99999,2,1.,99999,6,21.0421
5
142,3,-1.,562,3,1.,99999,3,1.,99999,5,-21.0421,
99999,4,-6.837
4
143,1,-1.,563,1,1.,99999,1,1.,99999,6,2.31269
4
143,2,-1.,563,2,1.,99999,2,1.,99999,6,22.0038
5
143,3,-1.,563,3,1.,99999,3,1.,99999,5,-22.0038,
99999,4,-2.31269
4
144,1,-1.,564,1,1.,99999,1,1.,99999,6,-2.31269
4
144,2,-1.,564,2,1.,99999,2,1.,99999,6,22.0038
5
144,3,-1.,564,3,1.,99999,3,1.,99999,5,-22.0038,
99999,4,2.31269
4
145,1,-1.,565,1,1.,99999,1,1.,99999,6,-6.837
4
145,2,-1.,565,2,1.,99999,2,1.,99999,6,21.0421
5
145,3,-1.,565,3,1.,99999,3,1.,99999,5,-21.0421,
99999,4,6.837
4
146,1,-1.,566,1,1.,99999,1,1.,99999,6,-11.0625
4
146,2,-1.,566,2,1.,99999,2,1.,99999,6,19.1608
5
146,3,-1.,566,3,1.,99999,3,1.,99999,5,-19.1608,
99999,4,11.0625
4
147,1,-1.,567,1,1.,99999,1,1.,99999,6,-14.8045
4
147,2,-1.,567,2,1.,99999,2,1.,99999,6,16.4421
5
147,3,-1.,567,3,1.,99999,3,1.,99999,5,-16.4421,
99999,4,14.8045
4
148,1,-1.,568,1,1.,99999,1,1.,99999,6,-17.8995
4
148,2,-1.,568,2,1.,99999,2,1.,99999,6,13.0047
5
148,3,-1.,568,3,1.,99999,3,1.,99999,5,-13.0047,
99999,4,17.8995
4
149,1,-1.,569,1,1.,99999,1,1.,99999,6,-20.2122
4
149,2,-1.,569,2,1.,99999,2,1.,99999,6,8.99905
5
149,3,-1.,569,3,1.,99999,3,1.,99999,5,-8.99905,
```

```
99999,4,20.2122
4
150,1,-1.,570,1,1.,99999,1,1.,99999,6,-21.6415
4
150,2,-1.,570,2,1.,99999,2,1.,99999,6,4.60005
5
150,3,-1.,570,3,1.,99999,3,1.,99999,5,-4.60005,
99999,4,21.6415
4
151,1,-1.,571,1,1.,99999,1,1.,99999,6,-22.375
4
151,2,-1.,571,2,1.,99999,2,1.,99999,6,-0
5
151,3,-1.,571,3,1.,99999,3,1.,99999,5,0,
99999,4,22.375
4
153,1,-1.,573,1,1.,99999,1,1.,99999,6,-20.4406
4
153,2,-1.,573,2,1.,99999,2,1.,99999,6,-9.10073
5
153,3,-1.,573,3,1.,99999,3,1.,99999,5,9.10073,
99999,4,20.4406
4
155,1,-1.,575,1,1.,99999,1,1.,99999,6,-14.9718
4
155,2,-1.,575,2,1.,99999,2,1.,99999,6,-16.6279
5
155,3,-1.,575,3,1.,99999,3,1.,99999,5,16.6279,
99999,4,14.9718
4
157,1,-1.,577,1,1.,99999,1,1.,99999,6,-6.91426
4
157,2,-1.,577,2,1.,99999,2,1.,99999,6,-21.2799
5
157,3,-1.,577,3,1.,99999,3,1.,99999,5,21.2799,
99999,4,6.91426
4
159,1,-1.,579,1,1.,99999,1,1.,99999,6,2.33882
4
159,2,-1.,579,2,1.,99999,2,1.,99999,6,-22.2524
5
159,3,-1.,579,3,1.,99999,3,1.,99999,5,22.2524,
99999,4,-2.33882
4
161,1,-1.,581,1,1.,99999,1,1.,99999,6,11.1875
4
161,2,-1.,581,2,1.,99999,2,1.,99999,6,-19.3773
5
161,3,-1.,581,3,1.,99999,3,1.,99999,5,19.3773,
99999,4,-11.1875
4
163,1,-1.,583,1,1.,99999,1,1.,99999,6,18.1018
4
163,2,-1.,583,2,1.,99999,2,1.,99999,6,-13.1517
5
163,3,-1.,583,3,1.,99999,3,1.,99999,5,13.1517,
99999,4,-18.1018
4
165,1,-1.,585,1,1.,99999,1,1.,99999,6,21.8861
4
165,2,-1.,585,2,1.,99999,2,1.,99999,6,-4.65202
```

```
5
165,3,-1.,585,3,1.,99999,3,1.,99999,5,4.65202,
99999,4,-21.8861
4
167,1,-1.,587,1,1.,99999,1,1.,99999,6,21.8861
4
167,2,-1.,587,2,1.,99999,2,1.,99999,6,4.65202
5
167,3,-1.,587,3,1.,99999,3,1.,99999,5,-4.65202,
99999,4,-21.8861
4
169,1,-1.,589,1,1.,99999,1,1.,99999,6,18.1018
4
169,2,-1.,589,2,1.,99999,2,1.,99999,6,13.1517
5
169,3,-1.,589,3,1.,99999,3,1.,99999,5,-13.1517,
99999,4,-18.1018
4
171,1,-1.,591,1,1.,99999,1,1.,99999,6,11.1875
4
171,2,-1.,591,2,1.,99999,2,1.,99999,6,19.3773
5
171,3,-1.,591,3,1.,99999,3,1.,99999,5,-19.3773,
99999,4,-11.1875
4
173,1,-1.,593,1,1.,99999,1,1.,99999,6,2.33882
4
173,2,-1.,593,2,1.,99999,2,1.,99999,6,22.2524
5
173,3,-1.,593,3,1.,99999,3,1.,99999,5,-22.2524,
99999,4,-2.33882
4
175,1,-1.,595,1,1.,99999,1,1.,99999,6,-6.91426
4
175,2,-1.,595,2,1.,99999,2,1.,99999,6,21.2799
5
175,3,-1.,595,3,1.,99999,3,1.,99999,5,-21.2799,
99999,4,6.91426
4
177,1,-1.,597,1,1.,99999,1,1.,99999,6,-14.9718
4
177,2,-1.,597,2,1.,99999,2,1.,99999,6,16.6279
5
177,3,-1.,597,3,1.,99999,3,1.,99999,5,-16.6279,
99999,4,14.9718
4
179,1,-1.,599,1,1.,99999,1,1.,99999,6,-20.4406
4
179,2,-1.,599,2,1.,99999,2,1.,99999,6,9.10073
5
179,3,-1.,599,3,1.,99999,3,1.,99999,5,-9.10073,
99999,4,20.4406
4
181,1,-1.,601,1,1.,99999,1,1.,99999,6,-22.375
4
181,2,-1.,601,2,1.,99999,2,1.,99999,6,-0
5
181,3,-1.,601,3,1.,99999,3,1.,99999,5,0,
99999,4,22.375
4
182,1,-1.,602,1,1.,99999,1,1.,99999,6,-21.8861
```

```
4
182,2,-1.,602,2,1.,99999,2,1.,99999,6,-4.65202
5
182,3,-1.,602,3,1.,99999,3,1.,99999,5,4.65202,
99999,4,21.8861
4
183,1,-1.,603,1,1.,99999,1,1.,99999,6,-20.4406
4
183,2,-1.,603,2,1.,99999,2,1.,99999,6,-9.10073
5
183,3,-1.,603,3,1.,99999,3,1.,99999,5,9.10073,
99999,4,20.4406
4
184,1,-1.,604,1,1.,99999,1,1.,99999,6,-18.1018
4
184,2,-1.,604,2,1.,99999,2,1.,99999,6,-13.1517
5
184,3,-1.,604,3,1.,99999,3,1.,99999,5,13.1517,
99999,4,18.1018
4
185,1,-1.,605,1,1.,99999,1,1.,99999,6,-14.9718
4
185,2,-1.,605,2,1.,99999,2,1.,99999,6,-16.6279
5
185,3,-1.,605,3,1.,99999,3,1.,99999,5,16.6279,
99999,4,14.9718
4
186,1,-1.,606,1,1.,99999,1,1.,99999,6,-11.1875
4
186,2,-1.,606,2,1.,99999,2,1.,99999,6,-19.3773
5
186,3,-1.,606,3,1.,99999,3,1.,99999,5,19.3773,
99999,4,11.1875
4
187,1,-1.,607,1,1.,99999,1,1.,99999,6,-6.91426
4
187,2,-1.,607,2,1.,99999,2,1.,99999,6,-21.2799
5
187,3,-1.,607,3,1.,99999,3,1.,99999,5,21.2799,
99999,4,6.91426
4
188,1,-1.,608,1,1.,99999,1,1.,99999,6,-2.33882
4
188,2,-1.,608,2,1.,99999,2,1.,99999,6,-22.2524
5
188,3,-1.,608,3,1.,99999,3,1.,99999,5,22.2524,
99999,4,2.33882
4
189,1,-1.,609,1,1.,99999,1,1.,99999,6,2.33882
4
189,2,-1.,609,2,1.,99999,2,1.,99999,6,-22.2524
5
189,3,-1.,609,3,1.,99999,3,1.,99999,5,22.2524,
99999,4,-2.33882
4
190,1,-1.,610,1,1.,99999,1,1.,99999,6,6.91426
4
190,2,-1.,610,2,1.,99999,2,1.,99999,6,-21.2799
5
190,3,-1.,610,3,1.,99999,3,1.,99999,5,21.2799,
99999,4,-6.91426
```

```
4
191,1,-1.,611,1,1.,99999,1,1.,99999,6,11.1875
4
191,2,-1.,611,2,1.,99999,2,1.,99999,6,-19.3773
5
191,3,-1.,611,3,1.,99999,3,1.,99999,5,19.3773,
99999,4,-11.1875
4
192,1,-1.,612,1,1.,99999,1,1.,99999,6,14.9718
4
192,2,-1.,612,2,1.,99999,2,1.,99999,6,-16.6279
5
192,3,-1.,612,3,1.,99999,3,1.,99999,5,16.6279,
99999,4,-14.9718
4
193,1,-1.,613,1,1.,99999,1,1.,99999,6,18.1018
4
193,2,-1.,613,2,1.,99999,2,1.,99999,6,-13.1517
5
193,3,-1.,613,3,1.,99999,3,1.,99999,5,13.1517,
99999,4,-18.1018
4
194,1,-1.,614,1,1.,99999,1,1.,99999,6,20.4406
4
194,2,-1.,614,2,1.,99999,2,1.,99999,6,-9.10073
5
194,3,-1.,614,3,1.,99999,3,1.,99999,5,9.10073,
99999,4,-20.4406
4
195,1,-1.,615,1,1.,99999,1,1.,99999,6,21.8861
4
195,2,-1.,615,2,1.,99999,2,1.,99999,6,-4.65202
5
195,3,-1.,615,3,1.,99999,3,1.,99999,5,4.65202,
99999,4,-21.8861
4
196,1,-1.,616,1,1.,99999,1,1.,99999,6,22.375
4
196,2,-1.,616,2,1.,99999,2,1.,99999,6,-0
5
196,3,-1.,616,3,1.,99999,3,1.,99999,5,0,
99999,4,-22.375
4
197,1,-1.,617,1,1.,99999,1,1.,99999,6,21.8861
4
197,2,-1.,617,2,1.,99999,2,1.,99999,6,4.65202
5
197,3,-1.,617,3,1.,99999,3,1.,99999,5,-4.65202,
99999,4,-21.8861
4
198,1,-1.,618,1,1.,99999,1,1.,99999,6,20.4406
4
198,2,-1.,618,2,1.,99999,2,1.,99999,6,9.10073
5
198,3,-1.,618,3,1.,99999,3,1.,99999,5,-9.10073,
99999,4,-20.4406
4
199,1,-1.,619,1,1.,99999,1,1.,99999,6,18.1018
4
199,2,-1.,619,2,1.,99999,2,1.,99999,6,13.1517
5
```

```
199,3,-1.,619,3,1.,99999,3,1.,99999,5,-13.1517,
99999,4,-18.1018
4
200,1,-1.,620,1,1.,99999,1,1.,99999,6,14.9718
4
200,2,-1.,620,2,1.,99999,2,1.,99999,6,16.6279
5
200,3,-1.,620,3,1.,99999,3,1.,99999,5,-16.6279,
99999,4,-14.9718
4
201,1,-1.,621,1,1.,99999,1,1.,99999,6,11.1875
4
201,2,-1.,621,2,1.,99999,2,1.,99999,6,19.3773
5
201,3,-1.,621,3,1.,99999,3,1.,99999,5,-19.3773,
99999,4,-11.1875
4
202,1,-1.,622,1,1.,99999,1,1.,99999,6,6.91426
4
202,2,-1.,622,2,1.,99999,2,1.,99999,6,21.2799
5
202,3,-1.,622,3,1.,99999,3,1.,99999,5,-21.2799,
99999,4,-6.91426
4
203,1,-1.,623,1,1.,99999,1,1.,99999,6,2.33882
4
203,2,-1.,623,2,1.,99999,2,1.,99999,6,22.2524
5
203,3,-1.,623,3,1.,99999,3,1.,99999,5,-22.2524,
99999,4,-2.33882
4
204,1,-1.,624,1,1.,99999,1,1.,99999,6,-2.33882
4
204,2,-1.,624,2,1.,99999,2,1.,99999,6,22.2524
5
204,3,-1.,624,3,1.,99999,3,1.,99999,5,-22.2524,
99999,4,2.33882
4
205,1,-1.,625,1,1.,99999,1,1.,99999,6,-6.91426
4
205,2,-1.,625,2,1.,99999,2,1.,99999,6,21.2799
5
205,3,-1.,625,3,1.,99999,3,1.,99999,5,-21.2799,
99999,4,6.91426
4
206,1,-1.,626,1,1.,99999,1,1.,99999,6,-11.1875
4
206,2,-1.,626,2,1.,99999,2,1.,99999,6,19.3773
5
206,3,-1.,626,3,1.,99999,3,1.,99999,5,-19.3773,
99999,4,11.1875
4
207,1,-1.,627,1,1.,99999,1,1.,99999,6,-14.9718
4
207,2,-1.,627,2,1.,99999,2,1.,99999,6,16.6279
5
207,3,-1.,627,3,1.,99999,3,1.,99999,5,-16.6279,
99999,4,14.9718
4
208,1,-1.,628,1,1.,99999,1,1.,99999,6,-18.1018
4
```

```
208,2,-1.,628,2,1.,99999,2,1.,99999,6,13.1517
5
208,3,-1.,628,3,1.,99999,3,1.,99999,5,-13.1517,
99999,4,18.1018
4
209,1,-1.,629,1,1.,99999,1,1.,99999,6,-20.4406
4
209,2,-1.,629,2,1.,99999,2,1.,99999,6,9.10073
5
209,3,-1.,629,3,1.,99999,3,1.,99999,5,-9.10073,
99999,4,20.4406
4
210,1,-1.,630,1,1.,99999,1,1.,99999,6,-21.8861
4
210,2,-1.,630,2,1.,99999,2,1.,99999,6,4.65202
5
210,3,-1.,630,3,1.,99999,3,1.,99999,5,-4.65202,
99999,4,21.8861
4
211,1,-1.,631,1,1.,99999,1,1.,99999,6,-22.625
4
211,2,-1.,631,2,1.,99999,2,1.,99999,6,-0
5
211,3,-1.,631,3,1.,99999,3,1.,99999,5,0,
99999,4,22.625
4
213,1,-1.,633,1,1.,99999,1,1.,99999,6,-20.669
4
213,2,-1.,633,2,1.,99999,2,1.,99999,6,-9.20242
5
213,3,-1.,633,3,1.,99999,3,1.,99999,5,9.20242,
99999,4,20.669
4
215,1,-1.,635,1,1.,99999,1,1.,99999,6,-15.1391
4
215,2,-1.,635,2,1.,99999,2,1.,99999,6,-16.8137
5
215,3,-1.,635,3,1.,99999,3,1.,99999,5,16.8137,
99999,4,15.1391
4
217,1,-1.,637,1,1.,99999,1,1.,99999,6,-6.99151
4
217,2,-1.,637,2,1.,99999,2,1.,99999,6,-21.5177
5
217,3,-1.,637,3,1.,99999,3,1.,99999,5,21.5177,
99999,4,6.99151
4
219,1,-1.,639,1,1.,99999,1,1.,99999,6,2.36496
4
219,2,-1.,639,2,1.,99999,2,1.,99999,6,-22.5011
5
219,3,-1.,639,3,1.,99999,3,1.,99999,5,22.5011,
99999,4,-2.36496
4
221,1,-1.,641,1,1.,99999,1,1.,99999,6,11.3125
4
221,2,-1.,641,2,1.,99999,2,1.,99999,6,-19.5938
5
221,3,-1.,641,3,1.,99999,3,1.,99999,5,19.5938,
99999,4,-11.3125
4
```

```
223,1,-1.,643,1,1.,99999,1,1.,99999,6,18.304
4
223,2,-1.,643,2,1.,99999,2,1.,99999,6,-13.2986
5
223,3,-1.,643,3,1.,99999,3,1.,99999,5,13.2986,
99999,4,-18.304
4
225,1,-1.,645,1,1.,99999,1,1.,99999,6,22.1306
4
225,2,-1.,645,2,1.,99999,2,1.,99999,6,-4.704
5
225,3,-1.,645,3,1.,99999,3,1.,99999,5,4.704,
99999,4,-22.1306
4
227,1,-1.,647,1,1.,99999,1,1.,99999,6,22.1306
4
227,2,-1.,647,2,1.,99999,2,1.,99999,6,4.704
5
227,3,-1.,647,3,1.,99999,3,1.,99999,5,-4.704,
99999,4,-22.1306
4
229,1,-1.,649,1,1.,99999,1,1.,99999,6,18.304
4
229,2,-1.,649,2,1.,99999,2,1.,99999,6,13.2986
5
229,3,-1.,649,3,1.,99999,3,1.,99999,5,-13.2986,
99999,4,-18.304
4
231,1,-1.,651,1,1.,99999,1,1.,99999,6,11.3125
4
231,2,-1.,651,2,1.,99999,2,1.,99999,6,19.5938
5
231,3,-1.,651,3,1.,99999,3,1.,99999,5,-19.5938,
99999,4,-11.3125
4
233,1,-1.,653,1,1.,99999,1,1.,99999,6,2.36496
4
233,2,-1.,653,2,1.,99999,2,1.,99999,6,22.5011
5
233,3,-1.,653,3,1.,99999,3,1.,99999,5,-22.5011,
99999,4,-2.36496
4
235,1,-1.,655,1,1.,99999,1,1.,99999,6,-6.99151
4
235,2,-1.,655,2,1.,99999,2,1.,99999,6,21.5177
5
235,3,-1.,655,3,1.,99999,3,1.,99999,5,-21.5177,
99999,4,6.99151
4
237,1,-1.,657,1,1.,99999,1,1.,99999,6,-15.1391
4
237,2,-1.,657,2,1.,99999,2,1.,99999,6,16.8137
5
237,3,-1.,657,3,1.,99999,3,1.,99999,5,-16.8137,
99999,4,15.1391
4
239,1,-1.,659,1,1.,99999,1,1.,99999,6,-20.669
4
239,2,-1.,659,2,1.,99999,2,1.,99999,6,9.20242
5
239,3,-1.,659,3,1.,99999,3,1.,99999,5,-9.20242,
```

```
99999,4,20.669
4
241,1,-1.,661,1,1.,99999,1,1.,99999,6,-22.625
4
241,2,-1.,661,2,1.,99999,2,1.,99999,6,-0
5
241,3,-1.,661,3,1.,99999,3,1.,99999,5,0,
99999,4,22.625
4
242,1,-1.,662,1,1.,99999,1,1.,99999,6,-22.1306
4
242,2,-1.,662,2,1.,99999,2,1.,99999,6,-4.704
5
242,3,-1.,662,3,1.,99999,3,1.,99999,5,4.704,
99999,4,22.1306
4
243,1,-1.,663,1,1.,99999,1,1.,99999,6,-20.669
4
243,2,-1.,663,2,1.,99999,2,1.,99999,6,-9.20242
5
243,3,-1.,663,3,1.,99999,3,1.,99999,5,9.20242,
99999,4,20.669
4
244,1,-1.,664,1,1.,99999,1,1.,99999,6,-18.304
4
244,2,-1.,664,2,1.,99999,2,1.,99999,6,-13.2986
5
244,3,-1.,664,3,1.,99999,3,1.,99999,5,13.2986,
99999,4,18.304
4
245,1,-1.,665,1,1.,99999,1,1.,99999,6,-15.1391
4
245,2,-1.,665,2,1.,99999,2,1.,99999,6,-16.8137
5
245,3,-1.,665,3,1.,99999,3,1.,99999,5,16.8137,
99999,4,15.1391
4
246,1,-1.,666,1,1.,99999,1,1.,99999,6,-11.3125
4
246,2,-1.,666,2,1.,99999,2,1.,99999,6,-19.5938
5
246,3,-1.,666,3,1.,99999,3,1.,99999,5,19.5938,
99999,4,11.3125
4
247,1,-1.,667,1,1.,99999,1,1.,99999,6,-6.99151
4
247,2,-1.,667,2,1.,99999,2,1.,99999,6,-21.5177
5
247,3,-1.,667,3,1.,99999,3,1.,99999,5,21.5177,
99999,4,6.99151
4
248,1,-1.,668,1,1.,99999,1,1.,99999,6,-2.36496
4
248,2,-1.,668,2,1.,99999,2,1.,99999,6,-22.5011
5
248,3,-1.,668,3,1.,99999,3,1.,99999,5,22.5011,
99999,4,2.36496
4
249,1,-1.,669,1,1.,99999,1,1.,99999,6,2.36496
4
249,2,-1.,669,2,1.,99999,2,1.,99999,6,-22.5011
```

```
5
249,3,-1.,669,3,1.,99999,3,1.,99999,5,22.5011,
99999,4,-2.36496
4
250,1,-1.,670,1,1.,99999,1,1.,99999,6,6.99151
4
250,2,-1.,670,2,1.,99999,2,1.,99999,6,-21.5177
5
250,3,-1.,670,3,1.,99999,3,1.,99999,5,21.5177,
99999,4,-6.99151
4
251,1,-1.,671,1,1.,99999,1,1.,99999,6,11.3125
4
251,2,-1.,671,2,1.,99999,2,1.,99999,6,-19.5938
5
251,3,-1.,671,3,1.,99999,3,1.,99999,5,19.5938,
99999,4,-11.3125
4
252,1,-1.,672,1,1.,99999,1,1.,99999,6,15.1391
4
252,2,-1.,672,2,1.,99999,2,1.,99999,6,-16.8137
5
252,3,-1.,672,3,1.,99999,3,1.,99999,5,16.8137,
99999,4,-15.1391
4
253,1,-1.,673,1,1.,99999,1,1.,99999,6,18.304
4
253,2,-1.,673,2,1.,99999,2,1.,99999,6,-13.2986
5
253,3,-1.,673,3,1.,99999,3,1.,99999,5,13.2986,
99999,4,-18.304
4
254,1,-1.,674,1,1.,99999,1,1.,99999,6,20.669
4
254,2,-1.,674,2,1.,99999,2,1.,99999,6,-9.20242
5
254,3,-1.,674,3,1.,99999,3,1.,99999,5,9.20242,
99999,4,-20.669
4
255,1,-1.,675,1,1.,99999,1,1.,99999,6,22.1306
4
255,2,-1.,675,2,1.,99999,2,1.,99999,6,-4.704
5
255,3,-1.,675,3,1.,99999,3,1.,99999,5,4.704,
99999,4,-22.1306
4
256,1,-1.,676,1,1.,99999,1,1.,99999,6,22.625
4
256,2,-1.,676,2,1.,99999,2,1.,99999,6,-0
5
256,3,-1.,676,3,1.,99999,3,1.,99999,5,0,
99999,4,-22.625
4
257,1,-1.,677,1,1.,99999,1,1.,99999,6,22.1306
4
257,2,-1.,677,2,1.,99999,2,1.,99999,6,4.704
5
257,3,-1.,677,3,1.,99999,3,1.,99999,5,-4.704,
99999,4,-22.1306
4
258,1,-1.,678,1,1.,99999,1,1.,99999,6,20.669
```

```
4
258,2,-1.,678,2,1.,99999,2,1.,99999,6,9.20242
5
258,3,-1.,678,3,1.,99999,3,1.,99999,5,-9.20242,
99999,4,-20.669
4
259,1,-1.,679,1,1.,99999,1,1.,99999,6,18.304
4
259,2,-1.,679,2,1.,99999,2,1.,99999,6,13.2986
5
259,3,-1.,679,3,1.,99999,3,1.,99999,5,-13.2986,
99999,4,-18.304
4
260,1,-1.,680,1,1.,99999,1,1.,99999,6,15.1391
4
260,2,-1.,680,2,1.,99999,2,1.,99999,6,16.8137
5
260,3,-1.,680,3,1.,99999,3,1.,99999,5,-16.8137,
99999,4,-15.1391
4
261,1,-1.,681,1,1.,99999,1,1.,99999,6,11.3125
4
261,2,-1.,681,2,1.,99999,2,1.,99999,6,19.5938
5
261,3,-1.,681,3,1.,99999,3,1.,99999,5,-19.5938,
99999,4,-11.3125
4
262,1,-1.,682,1,1.,99999,1,1.,99999,6,6.99151
4
262,2,-1.,682,2,1.,99999,2,1.,99999,6,21.5177
5
262,3,-1.,682,3,1.,99999,3,1.,99999,5,-21.5177,
99999,4,-6.99151
4
263,1,-1.,683,1,1.,99999,1,1.,99999,6,2.36496
4
263,2,-1.,683,2,1.,99999,2,1.,99999,6,22.5011
5
263,3,-1.,683,3,1.,99999,3,1.,99999,5,-22.5011,
99999,4,-2.36496
4
264,1,-1.,684,1,1.,99999,1,1.,99999,6,-2.36496
4
264,2,-1.,684,2,1.,99999,2,1.,99999,6,22.5011
5
264,3,-1.,684,3,1.,99999,3,1.,99999,5,-22.5011,
99999,4,2.36496
4
265,1,-1.,685,1,1.,99999,1,1.,99999,6,-6.99151
4
265,2,-1.,685,2,1.,99999,2,1.,99999,6,21.5177
5
265,3,-1.,685,3,1.,99999,3,1.,99999,5,-21.5177,
99999,4,6.99151
4
266,1,-1.,686,1,1.,99999,1,1.,99999,6,-11.3125
4
266,2,-1.,686,2,1.,99999,2,1.,99999,6,19.5938
5
266,3,-1.,686,3,1.,99999,3,1.,99999,5,-19.5938,
99999,4,11.3125
```

```
4
267,1,-1.,687,1,1.,99999,1,1.,99999,6,-15.1391
4
267,2,-1.,687,2,1.,99999,2,1.,99999,6,16.8137
5
267,3,-1.,687,3,1.,99999,3,1.,99999,5,-16.8137,
99999,4,15.1391
4
268,1,-1.,688,1,1.,99999,1,1.,99999,6,-18.304
4
268,2,-1.,688,2,1.,99999,2,1.,99999,6,13.2986
5
268,3,-1.,688,3,1.,99999,3,1.,99999,5,-13.2986,
99999,4,18.304
4
269,1,-1.,689,1,1.,99999,1,1.,99999,6,-20.669
4
269,2,-1.,689,2,1.,99999,2,1.,99999,6,9.20242
5
269,3,-1.,689,3,1.,99999,3,1.,99999,5,-9.20242,
99999,4,20.669
4
270,1,-1.,690,1,1.,99999,1,1.,99999,6,-22.1306
4
270,2,-1.,690,2,1.,99999,2,1.,99999,6,4.704
5
270,3,-1.,690,3,1.,99999,3,1.,99999,5,-4.704,
99999,4,22.1306
*BOUNDARY
100000,1,6
99999,1,2
*STEP
*STATIC
*CLOAD
99999,3,1.
*NODE PRINT,NSET=BEAM
U
*EL PRINT,ELSET=beam
S
*END STEP
*STEP
*STATIC
*CLOAD
99999,3,0.
99999,4,1.
*NODE PRINT,NSET=BEAM
U
*EL PRINT,ELSET=beam
S
*END STEP
*STEP
*STATIC
*CLOAD
99999,4,0.
99999,5,1.
*NODE PRINT,NSET=BEAM
U
*EL PRINT,ELSET=beam
S
*END STEP
*STEP
```

```
*STATIC
*CLOAD
99999,5,0.
99999,6,1.
*NODE PRINT,NSET=BEAM
U
*EL PRINT,ELSET=beam
S
*END STEP
```

APPENDIX 4.1

Finite Element results for K_{45} of sandwich section

Variation of K_{45} with orientation of coupling plies is shown for:

Width in 10 mm increments from 10mm to 50mm

Height in 10 mm increments from 10mm to 40mm

Core modulus in exponential increments from 7 MPa to $7x10^6$ MPa

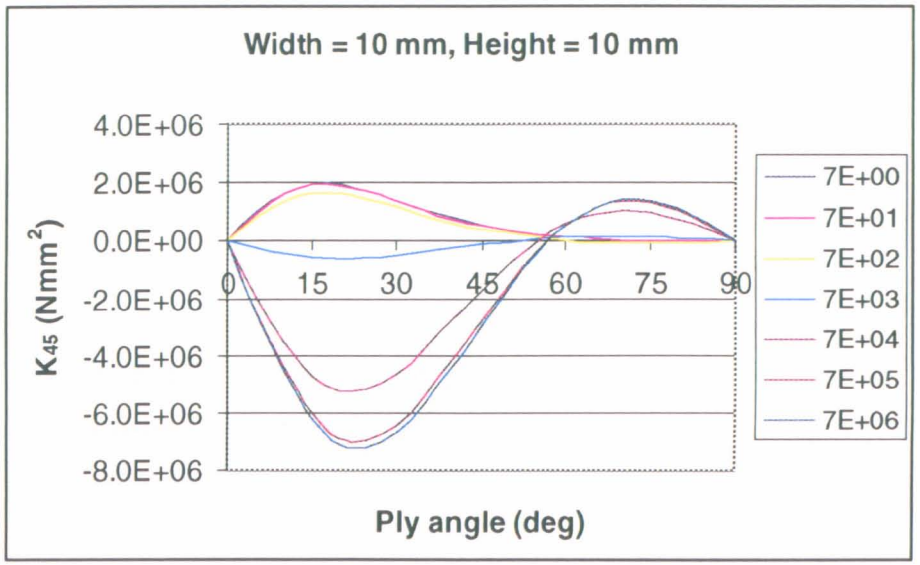
Width = 10 mm, Height = 10 mm
4.0E+06
2.0E+06
0.0E+00
-2.0E+06
-4.0E+06
-6.0E+06
-8.0E+06
K45 (Nmm2)
0
15
30
45
60
75
90
Ply angle (deg)
7E+00
7E+01
7E+02
7E+03
7E+04
7E+05
7E+06

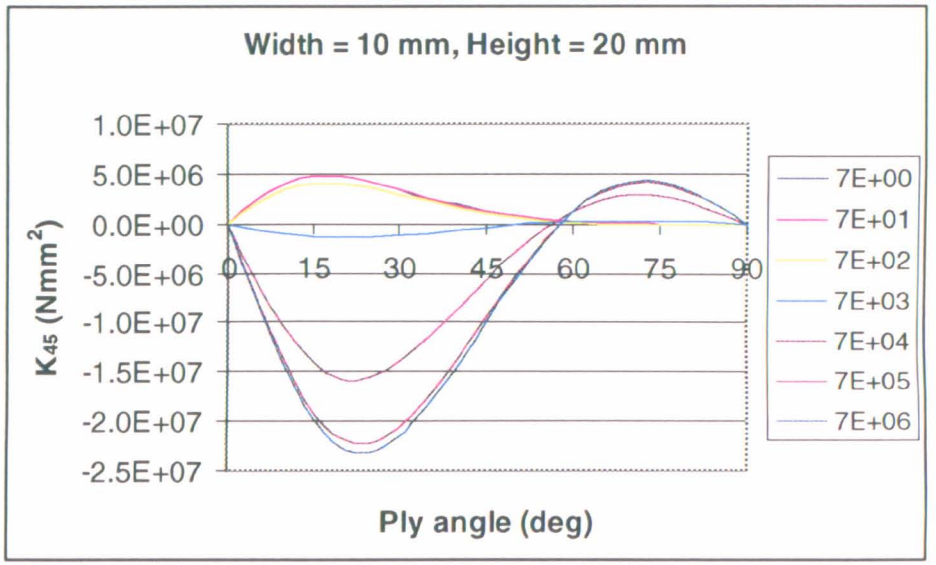
Width = 10 mm, Height = 20 mm
1.0E+07
5.0E+06
0.0E+00
-5.0E+06
-1.0E+07
-1.5E+07
-2.0E+07
-2.5E+07
K45 (Nmm2)
0
15
30
45
60
75
90
Ply angle (deg)
7E+00
7E+01
7E+02
7E+03
7E+04
7E+05
7E+06

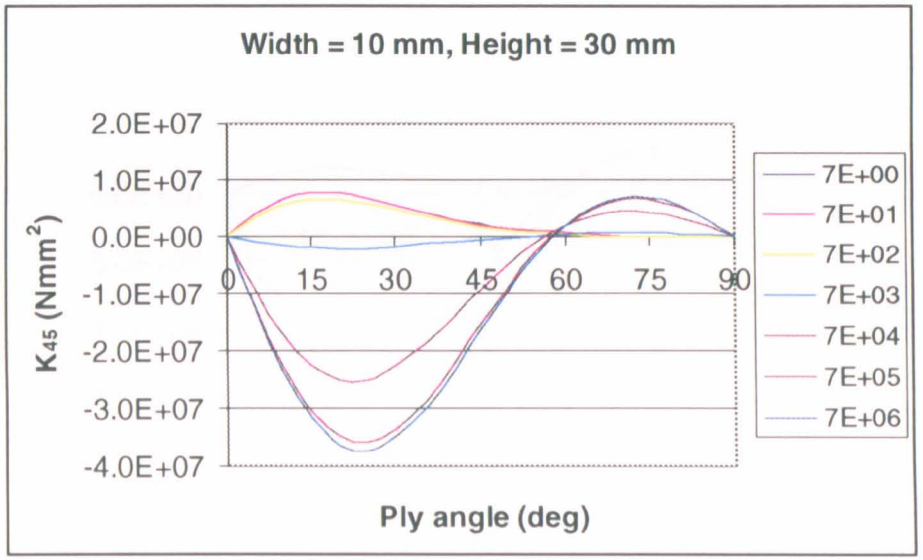
Width = 10 mm, Height = 30 mm
2.0E+07
1.0E+07
0.0E+00
-1.0E+07
-2.0E+07
-3.0E+07
-4.0E+07
K45 (Nmm2)
0
15
30
45
60
75
90
Ply angle (deg)
7E+00
7E+01
7E+02
7E+03
7E+04
7E+05
7E+06

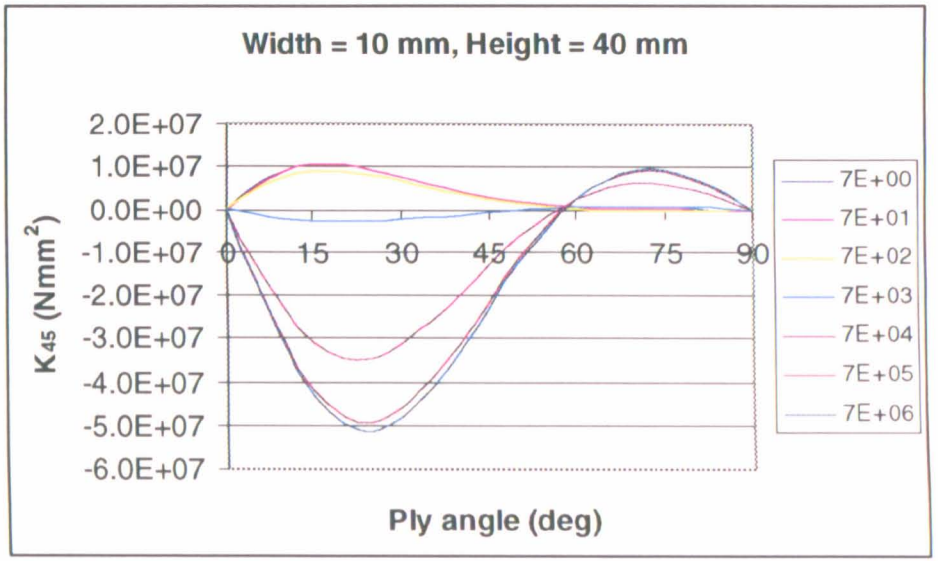
Width = 10 mm, Height = 40 mm
2.0E+07
1.0E+07
0.0E+00
-1.0E+07
-2.0E+07
-3.0E+07
-4.0E+07
-5.0E+07
-6.0E+07
K45 (Nmm2)
0
15
30
45
60
75
90
Ply angle (deg)
7E+00
7E+01
7E+02
7E+03
7E+04
7E+05
7E+06

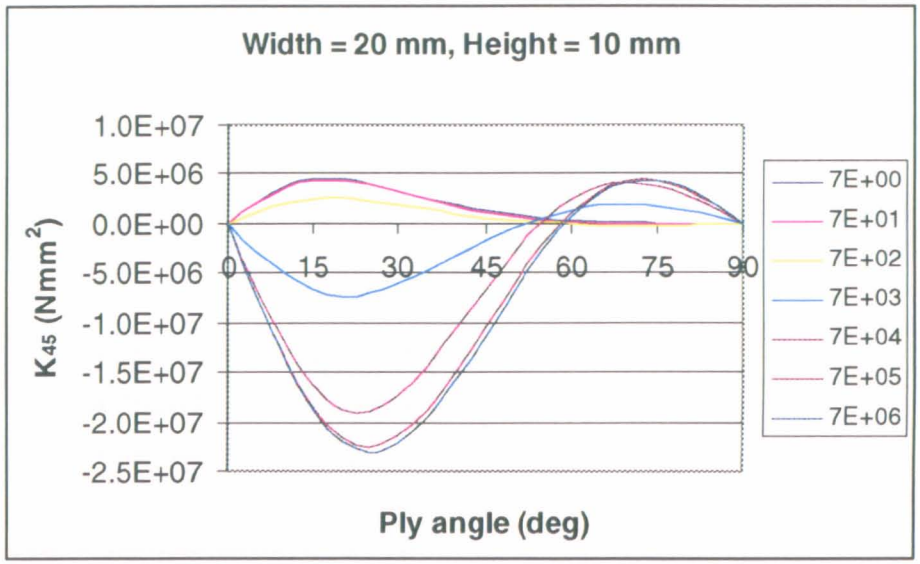
Width = 20 mm, Height = 10 mm
1.0E+07
5.0E+06
0.0E+00
-5.0E+06
-1.0E+07
-1.5E+07
-2.0E+07
-2.5E+07
K45 (Nmm2)
0
15
30
45
60
75
90
Ply angle (deg)
7E+00
7E+01
7E+02
7E+03
7E+04
7E+05
7E+06

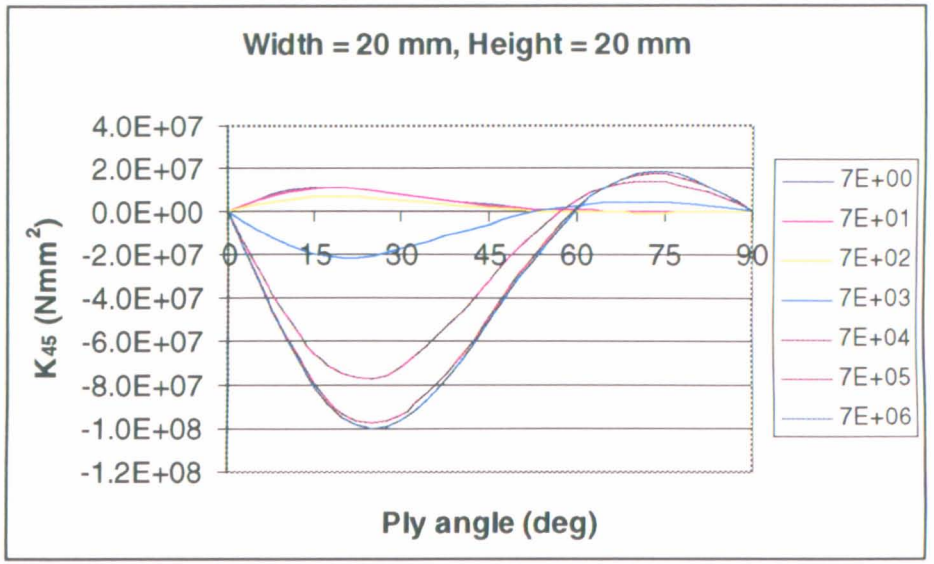
Width = 20 mm, Height = 20 mm
4.0E+07
2.0E+07
0.0E+00
-2.0E+07
-4.0E+07
-6.0E+07
-8.0E+07
-1.0E+08
-1.2E+08
K45 (Nmm2)
0
15
30
45
60
75
90
Ply angle (deg)
7E+00
7E+01
7E+02
7E+03
7E+04
7E+05
7E+06

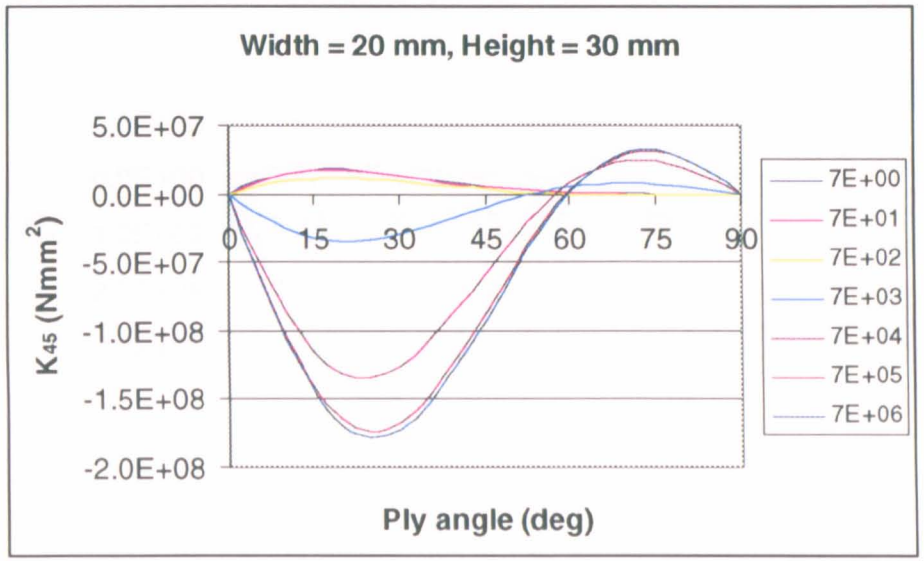
Width = 20 mm, Height = 30 mm
5.0E+07
0.0E+00
-5.0E+07
-1.0E+08
-1.5E+08
-2.0E+08
K45 (Nmm2)
0
15
30
45
60
75
90
Ply angle (deg)
7E+00
7E+01
7E+02
7E+03
7E+04
7E+05
7E+06

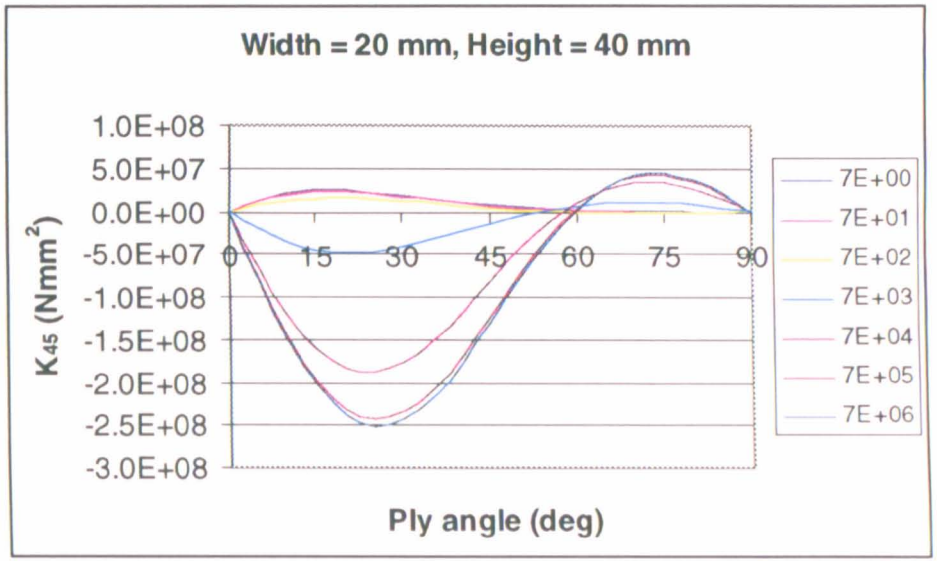
Width = 20 mm, Height = 40 mm
1.0E+08
5.0E+07
0.0E+00
-5.0E+07
-1.0E+08
-1.5E+08
-2.0E+08
-2.5E+08
-3.0E+08
K45 (Nmm2)
0
15
30
45
60
75
90
Ply angle (deg)
7E+00
7E+01
7E+02
7E+03
7E+04
7E+05
7E+06

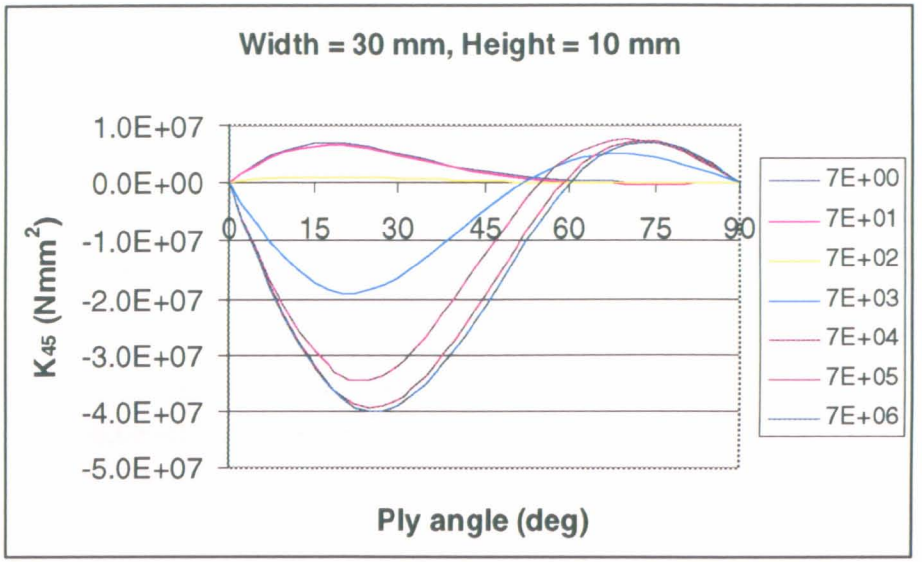
Width = 30 mm, Height = 10 mm
1.0E+07
0.0E+00
-1.0E+07
-2.0E+07
-3.0E+07
-4.0E+07
-5.0E+07
K45 (Nmm2)
0
15
30
45
60
75
90
Ply angle (deg)
7E+00
7E+01
7E+02
7E+03
7E+04
7E+05
7E+06

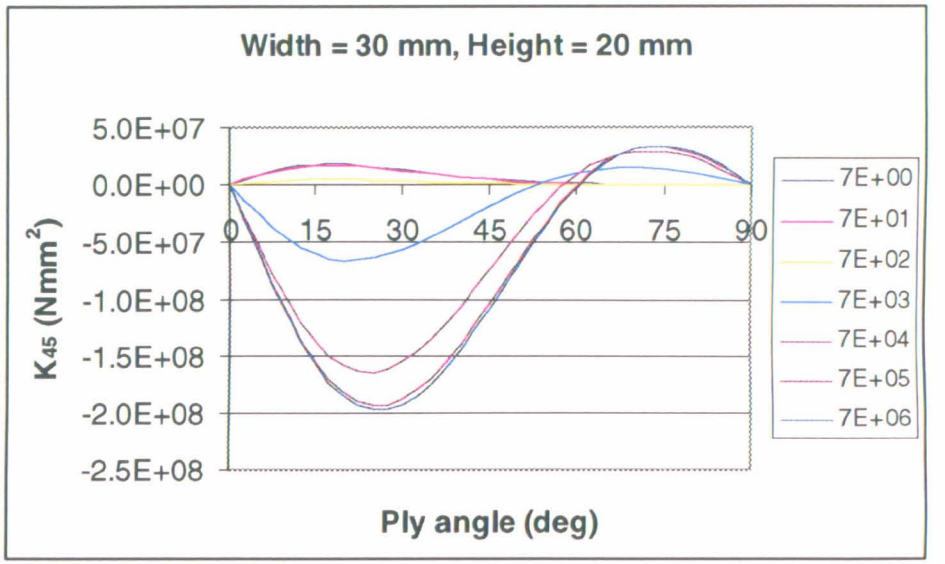
Width = 30 mm, Height = 20 mm
5.0E+07
0.0E+00
-5.0E+07
-1.0E+08
-1.5E+08
-2.0E+08
-2.5E+08
K45 (Nmm2)
0
15
30
45
60
75
90
Ply angle (deg)
7E+00
7E+01
7E+02
7E+03
7E+04
7E+05
7E+06

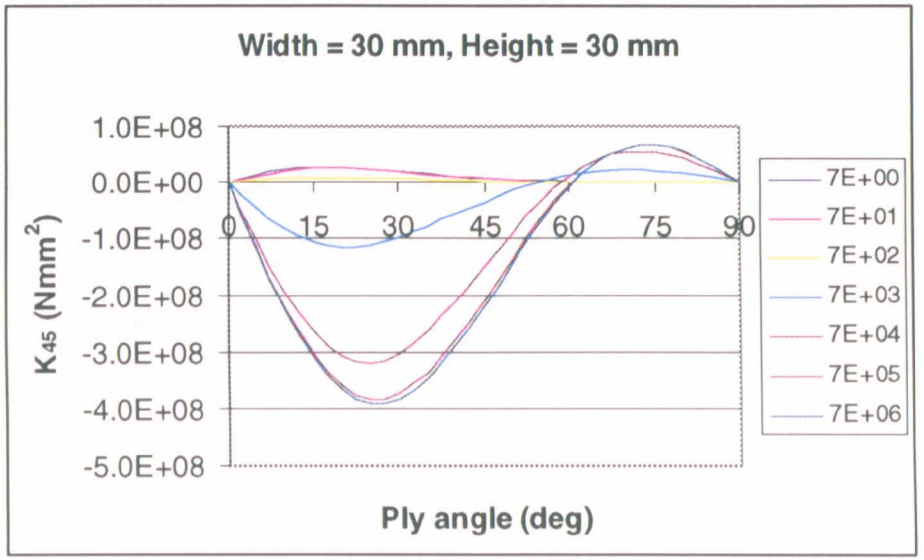
Width = 30 mm, Height = 30 mm
1.0E+08
0.0E+00
-1.0E+08
-2.0E+08
-3.0E+08
-4.0E+08
-5.0E+08
K45 (Nmm2)
0
15
30
45
60
75
90
Ply angle (deg)
7E+00
7E+01
7E+02
7E+03
7E+04
7E+05
7E+06

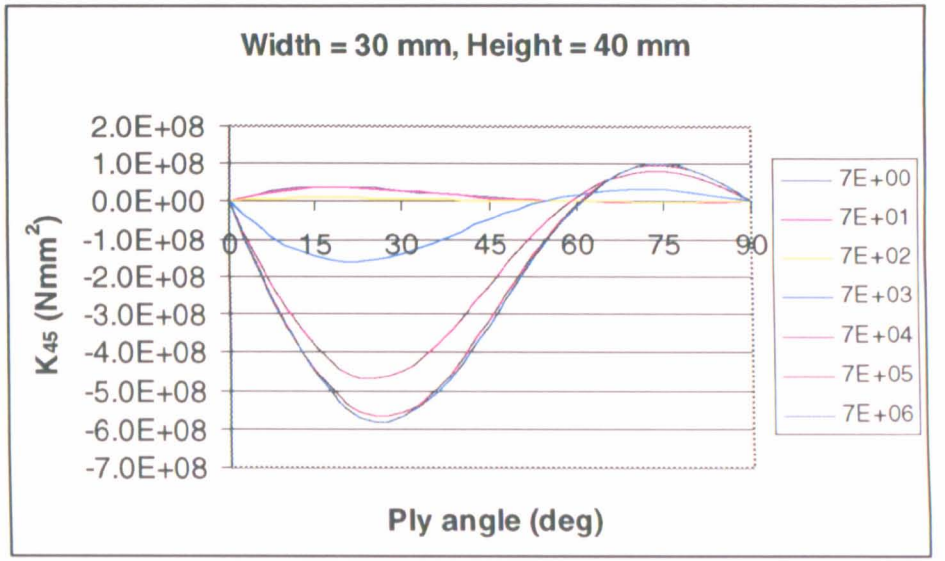
Width = 30 mm, Height = 40 mm
2.0E+08
1.0E+08
0.0E+00
-1.0E+08
-2.0E+08
-3.0E+08
-4.0E+08
-5.0E+08
-6.0E+08
-7.0E+08
K45 (Nmm2)
0
15
30
45
60
75
90
Ply angle (deg)
7E+00
7E+01
7E+02
7E+03
7E+04
7E+05
7E+06

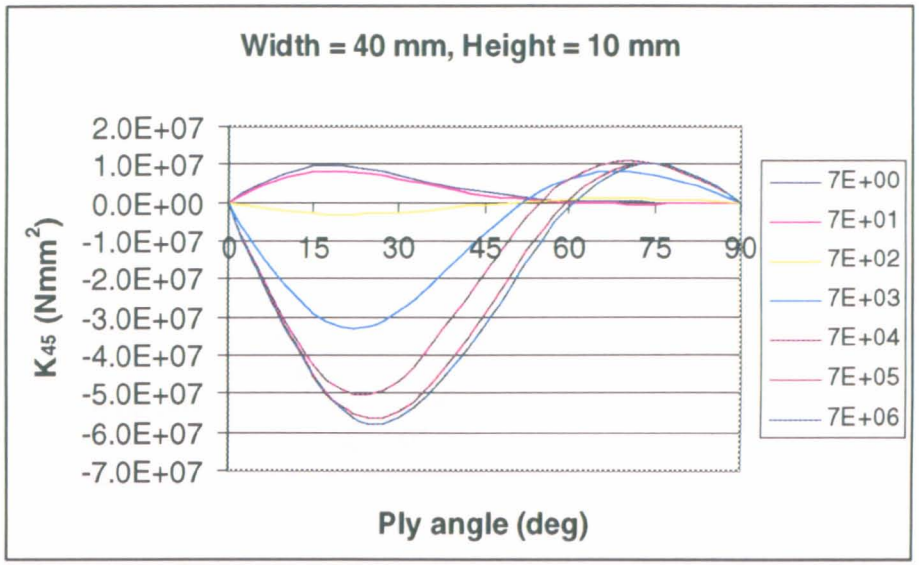
Width = 40 mm, Height = 10 mm
2.0E+07
1.0E+07
0.0E+00
-1.0E+07
-2.0E+07
-3.0E+07
-4.0E+07
-5.0E+07
-6.0E+07
-7.0E+07
0
15
30
45
60
75
90
K45 (Nmm2)
Ply angle (deg)
7E+00
7E+01
7E+02
7E+03
7E+04
7E+05
7E+06

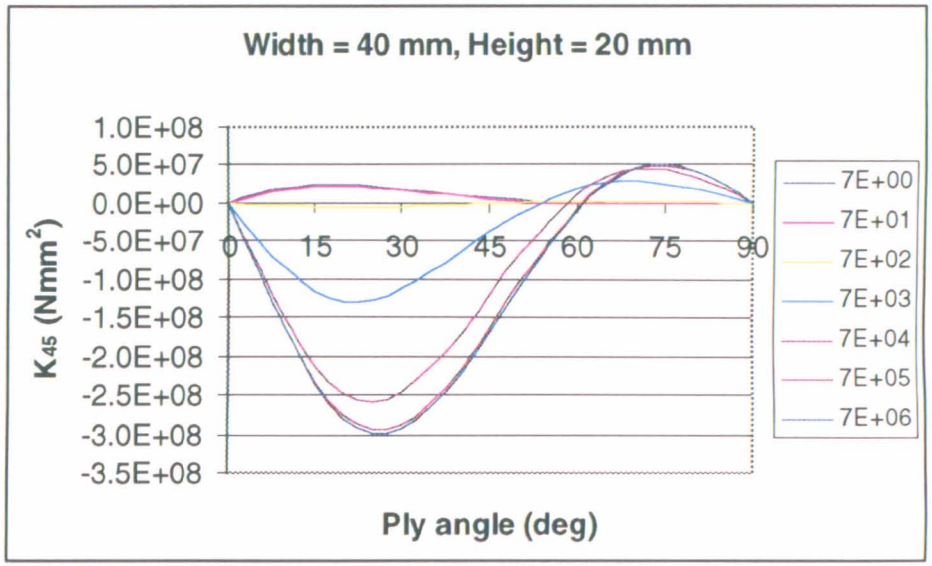
Width = 40 mm, Height = 20 mm
1.0E+08
5.0E+07
0.0E+00
-5.0E+07
-1.0E+08
-1.5E+08
-2.0E+08
-2.5E+08
-3.0E+08
-3.5E+08
0
15
30
45
60
75
90
K45 (Nmm2)
Ply angle (deg)
7E+00
7E+01
7E+02
7E+03
7E+04
7E+05
7E+06

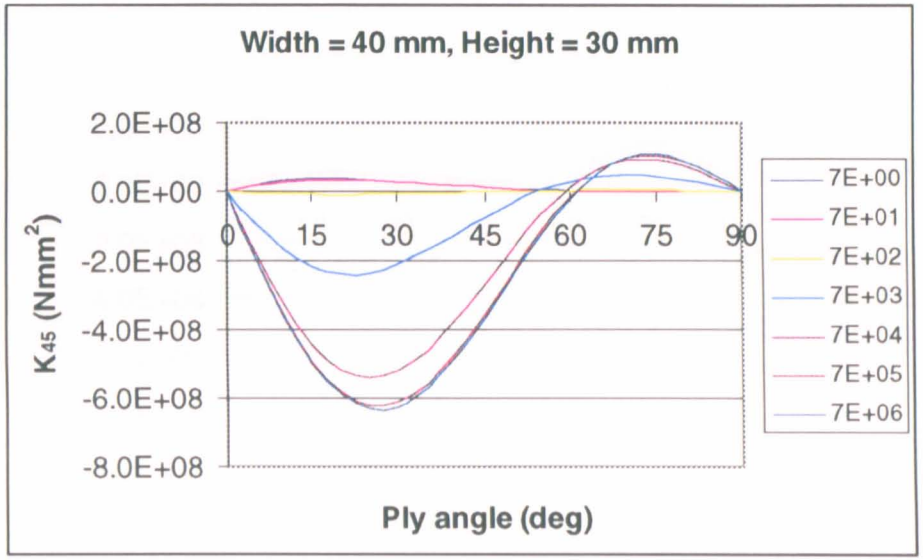
Width = 40 mm, Height = 30 mm
2.0E+08
0.0E+00
-2.0E+08
-4.0E+08
-6.0E+08
-8.0E+08
0
15
30
45
60
75
90
K45 (Nmm2)
Ply angle (deg)
7E+00
7E+01
7E+02
7E+03
7E+04
7E+05
7E+06

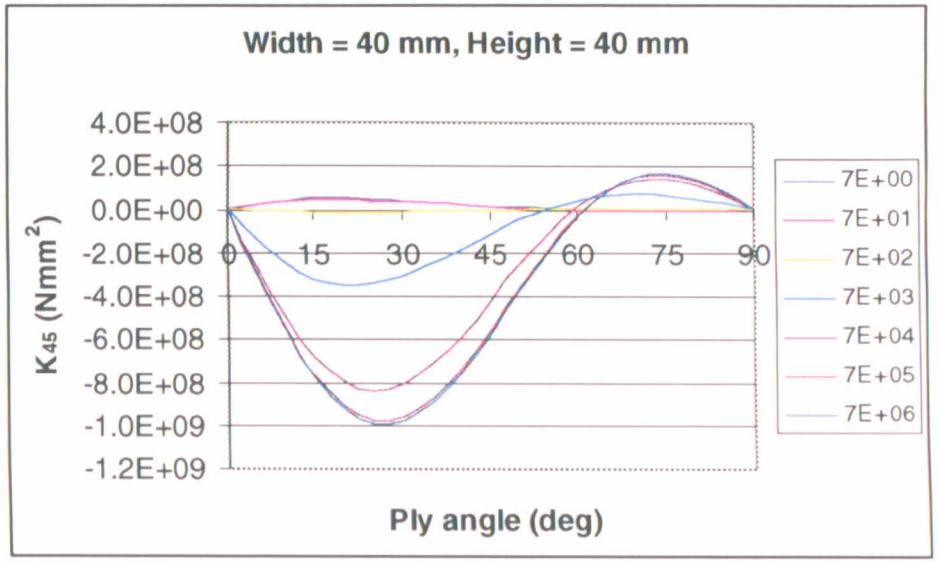
Width = 40 mm, Height = 40 mm
4.0E+08
2.0E+08
0.0E+00
-2.0E+08
-4.0E+08
-6.0E+08
-8.0E+08
-1.0E+09
-1.2E+09
0
15
30
45
60
75
90
K45 (Nmm2)
Ply angle (deg)
7E+00
7E+01
7E+02
7E+03
7E+04
7E+05
7E+06

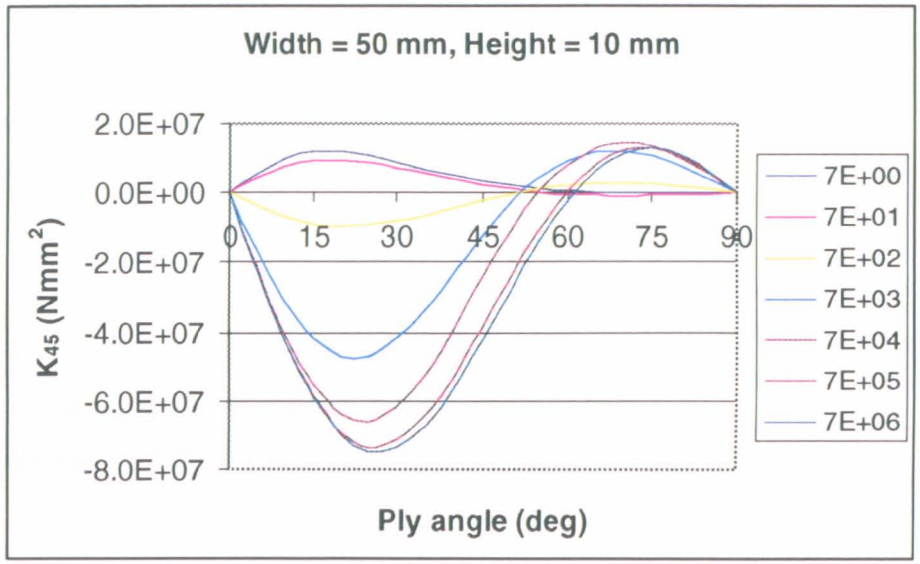
Width = 50 mm, Height = 10 mm
2.0E+07
0.0E+00
-2.0E+07
-4.0E+07
-6.0E+07
-8.0E+07
K45 (Nmm2)
0
15
30
45
60
75
90
Ply angle (deg)
7E+00
7E+01
7E+02
7E+03
7E+04
7E+05
7E+06

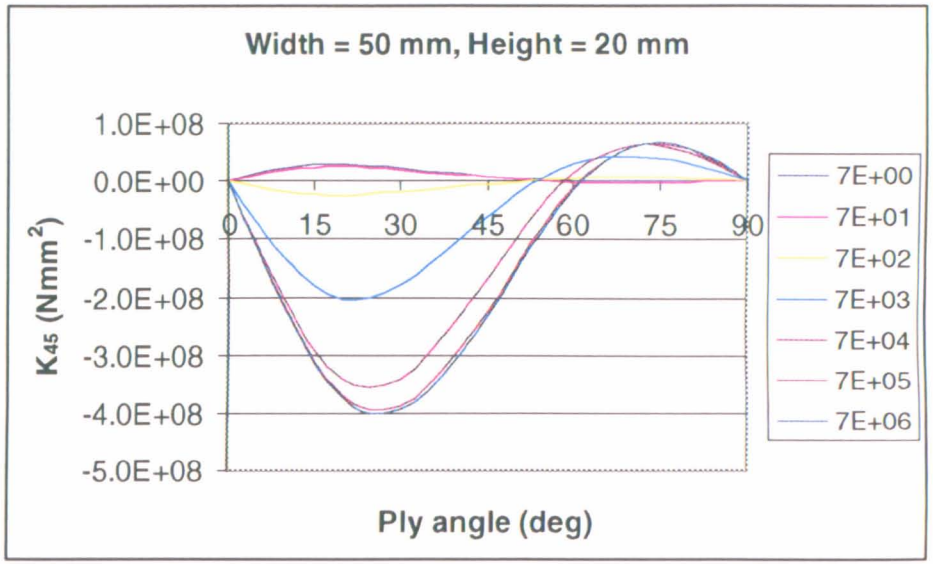
Width = 50 mm, Height = 20 mm
1.0E+08
0.0E+00
-1.0E+08
-2.0E+08
-3.0E+08
-4.0E+08
-5.0E+08
K45 (Nmm2)
0
15
30
45
60
75
90
Ply angle (deg)
7E+00
7E+01
7E+02
7E+03
7E+04
7E+05
7E+06

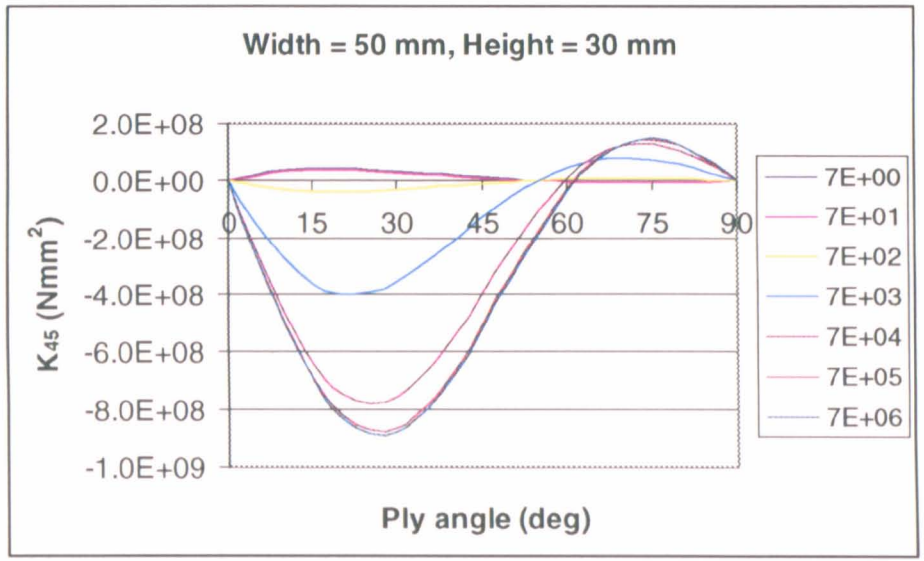
Width = 50 mm, Height = 30 mm
2.0E+08
0.0E+00
-2.0E+08
-4.0E+08
-6.0E+08
-8.0E+08
-1.0E+09
K45 (Nmm2)
0
15
30
45
60
75
90
Ply angle (deg)
7E+00
7E+01
7E+02
7E+03
7E+04
7E+05
7E+06

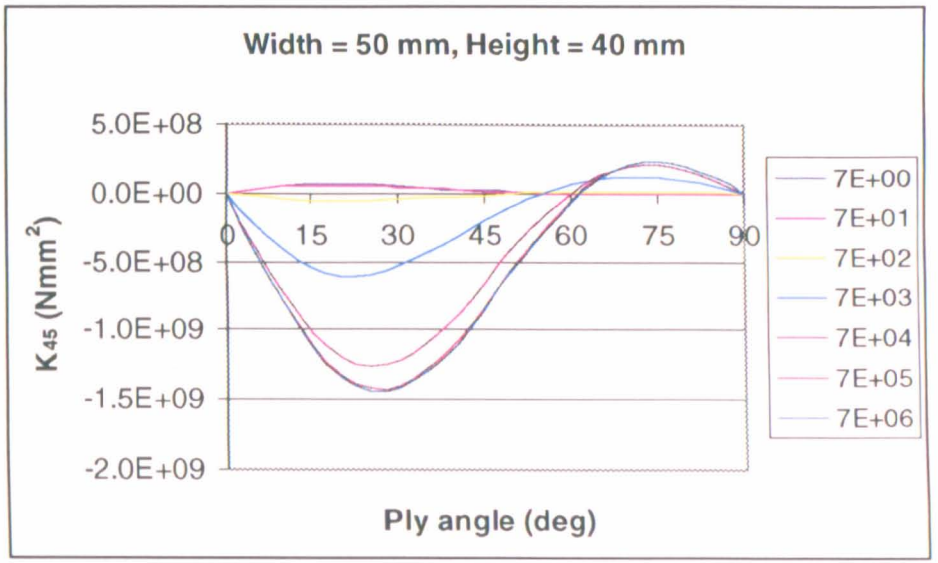
Width = 50 mm, Height = 40 mm
5.0E+08
0.0E+00
-5.0E+08
-1.0E+09
-1.5E+09
-2.0E+09
K45 (Nmm2)
0
15
30
45
60
75
90
Ply angle (deg)
7E+00
7E+01
7E+02
7E+03
7E+04
7E+05
7E+06

APPENDIX 4.2

Finite element results of box sections

Variation of K_{45} with orientation of coupling plies is shown for:

Width in 10 mm increments from 10mm to 50mm

Height in 10 mm increments from 10mm to 40mm

Vertical wall thickness in 1mm increments from 0mm to 5mm

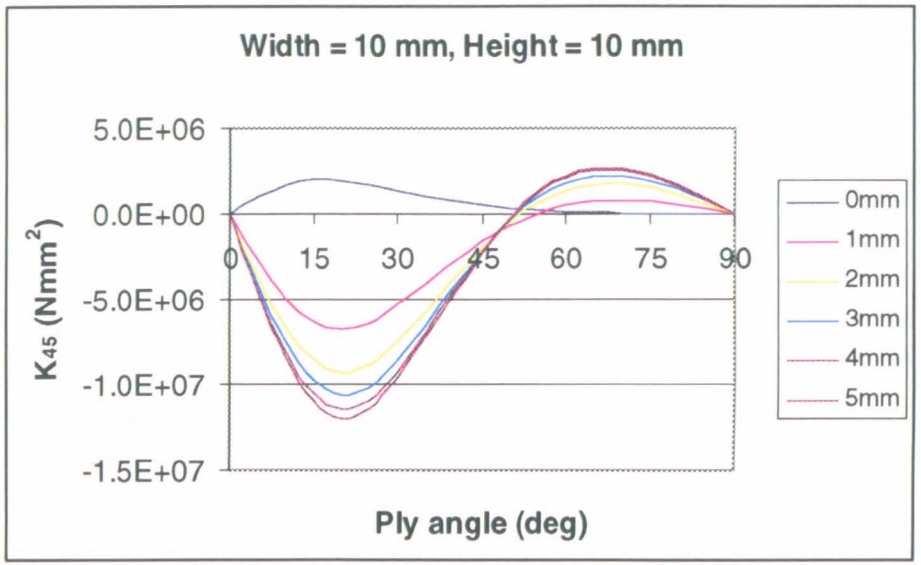
Width = 10 mm, Height = 10 mm
5.0E+06
0.0E+00
-5.0E+06
-1.0E+07
-1.5E+07
K45 (Nmm2)
0
15
30
45
60
75
90
Ply angle (deg)
0mm
1mm
2mm
3mm
4mm
5mm

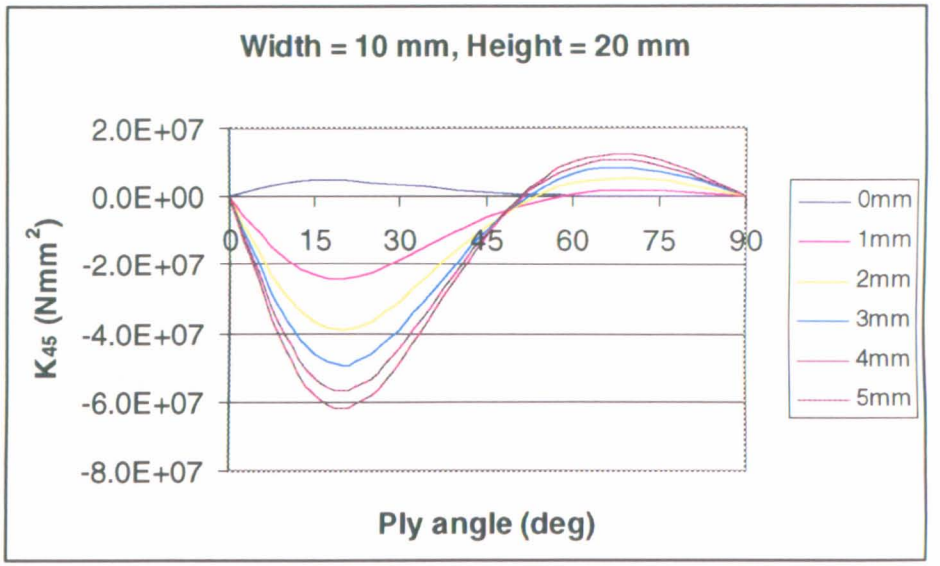
Width = 10 mm, Height = 20 mm
2.0E+07
0.0E+00
-2.0E+07
-4.0E+07
-6.0E+07
-8.0E+07
K45 (Nmm2)
0
15
30
45
60
75
90
Ply angle (deg)
0mm
1mm
2mm
3mm
4mm
5mm

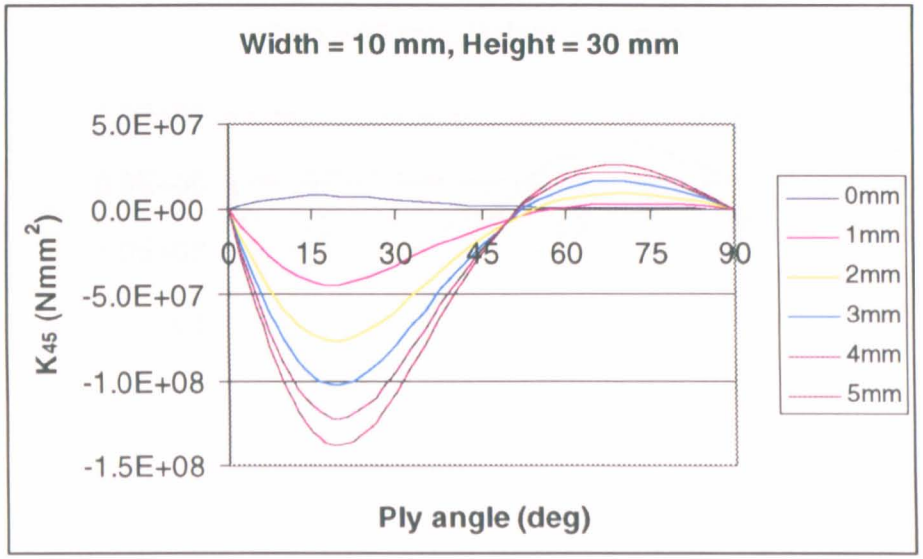
Width = 10 mm, Height = 30 mm
5.0E+07
0.0E+00
-5.0E+07
-1.0E+08
-1.5E+08
K45 (Nmm2)
0
15
30
45
60
75
90
Ply angle (deg)
0mm
1mm
2mm
3mm
4mm
5mm

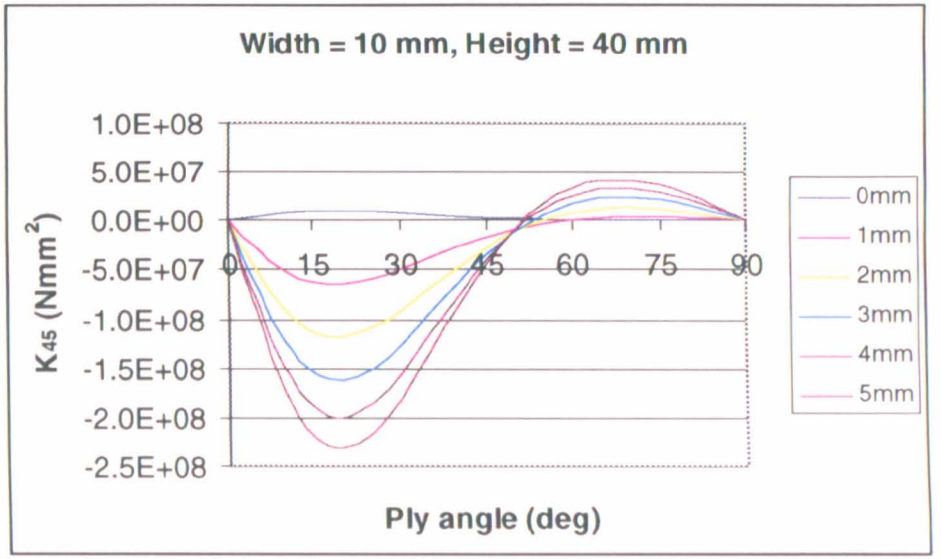
Width = 10 mm, Height = 40 mm
1.0E+08
5.0E+07
0.0E+00
-5.0E+07
-1.0E+08
-1.5E+08
-2.0E+08
-2.5E+08
K45 (Nmm2)
0
15
30
45
60
75
90
Ply angle (deg)
0mm
1mm
2mm
3mm
4mm
5mm

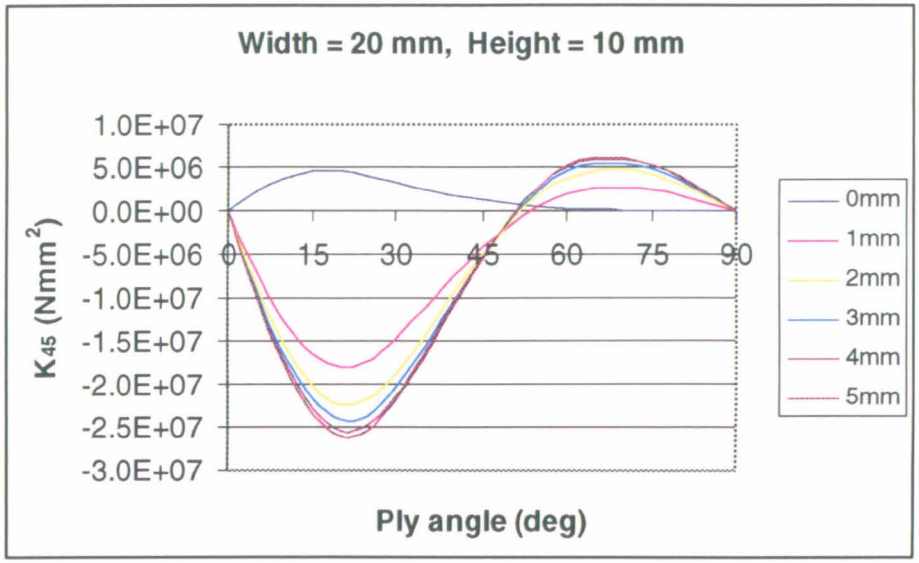
Width = 20 mm, Height = 10 mm
1.0E+07
5.0E+06
0.0E+00
-5.0E+06
-1.0E+07
-1.5E+07
-2.0E+07
-2.5E+07
-3.0E+07
0
15
30
45
60
75
90
K45 (Nmm2)
Ply angle (deg)
0mm
1mm
2mm
3mm
4mm
5mm

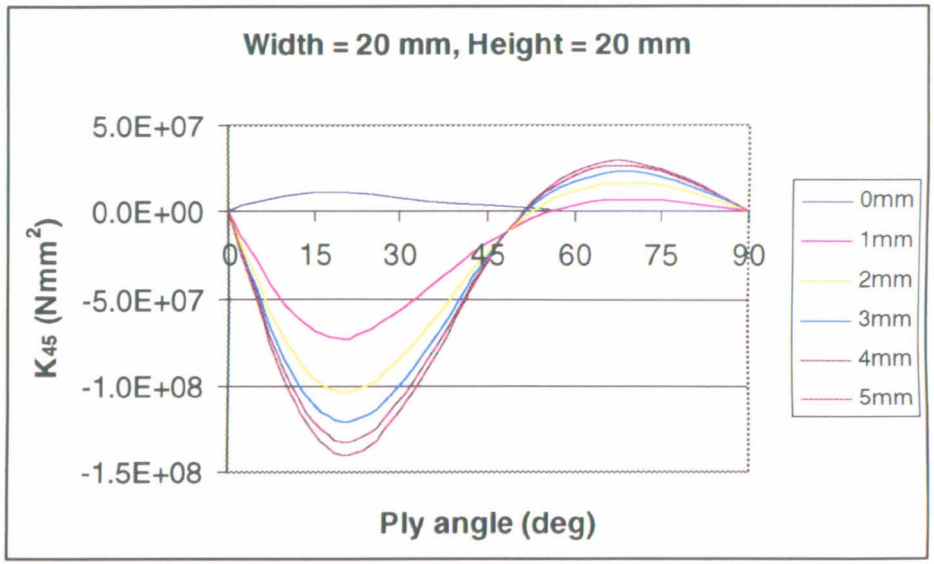
Width = 20 mm, Height = 20 mm
5.0E+07
0.0E+00
-5.0E+07
-1.0E+08
-1.5E+08
0
15
30
45
60
75
90
K45 (Nmm2)
Ply angle (deg)
0mm
1mm
2mm
3mm
4mm
5mm

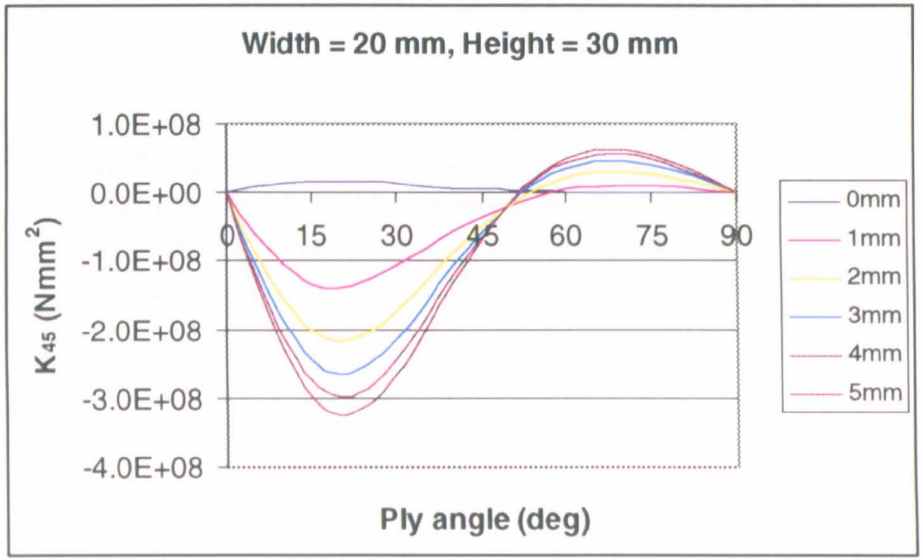
Width = 20 mm, Height = 30 mm
1.0E+08
0.0E+00
-1.0E+08
-2.0E+08
-3.0E+08
-4.0E+08
0
15
30
45
60
75
90
K45 (Nmm2)
Ply angle (deg)
0mm
1mm
2mm
3mm
4mm
5mm

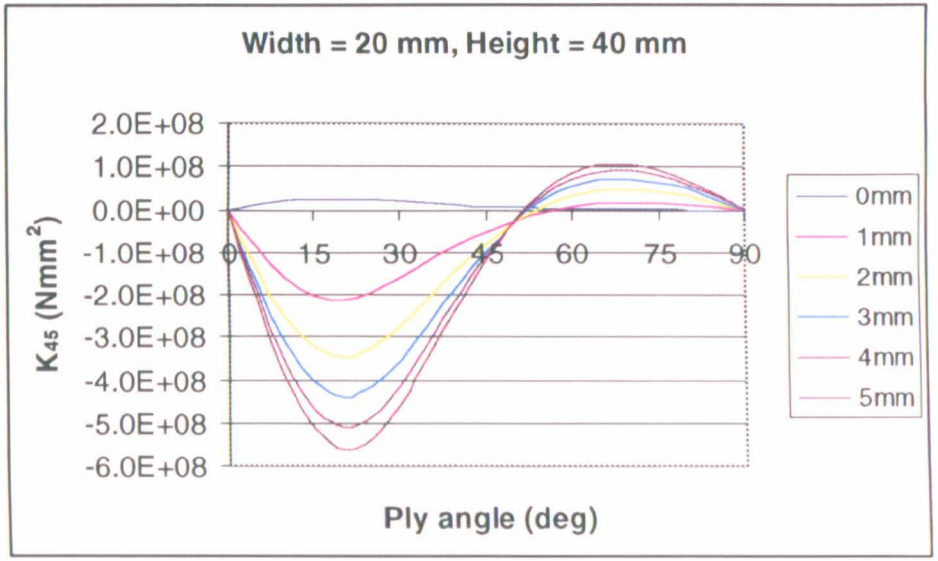
Width = 20 mm, Height = 40 mm
2.0E+08
1.0E+08
0.0E+00
-1.0E+08
-2.0E+08
-3.0E+08
-4.0E+08
-5.0E+08
-6.0E+08
0
15
30
45
60
75
90
K45 (Nmm2)
Ply angle (deg)
0mm
1mm
2mm
3mm
4mm
5mm

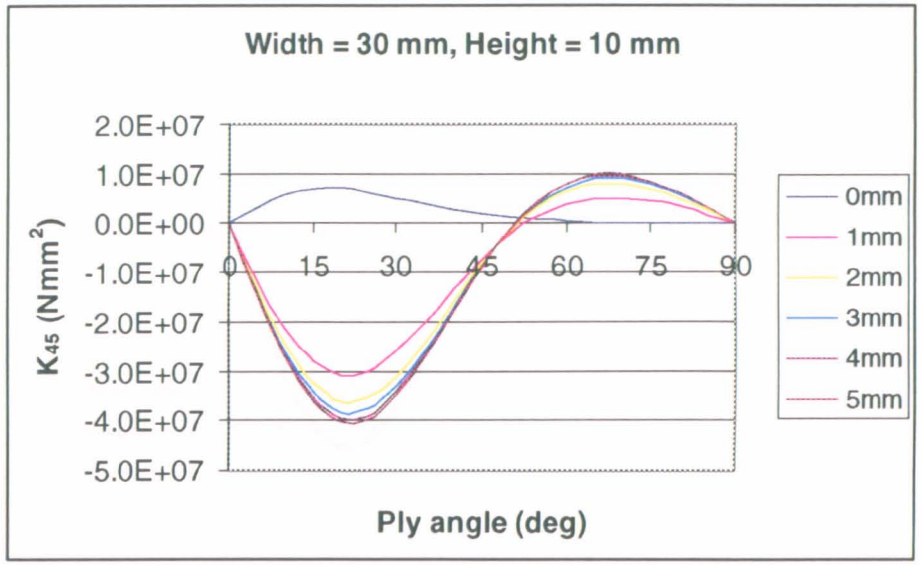
Width = 30 mm, Height = 10 mm
2.0E+07
1.0E+07
0.0E+00
-1.0E+07
-2.0E+07
-3.0E+07
-4.0E+07
-5.0E+07
0
15
30
45
60
75
90
K45 (Nmm2)
Ply angle (deg)
0mm
1mm
2mm
3mm
4mm
5mm

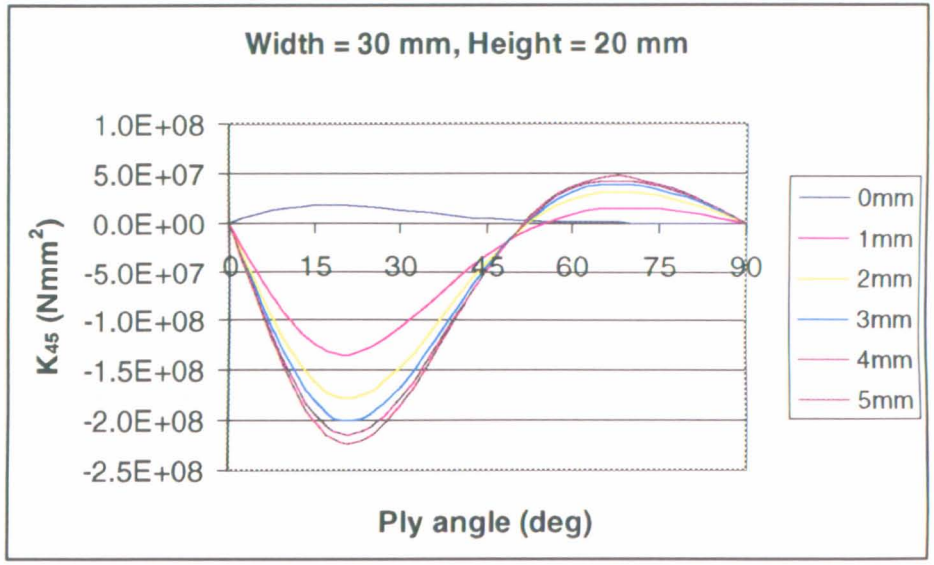
Width = 30 mm, Height = 20 mm
1.0E+08
5.0E+07
0.0E+00
-5.0E+07
-1.0E+08
-1.5E+08
-2.0E+08
-2.5E+08
0
15
30
45
60
75
90
K45 (Nmm2)
Ply angle (deg)
0mm
1mm
2mm
3mm
4mm
5mm

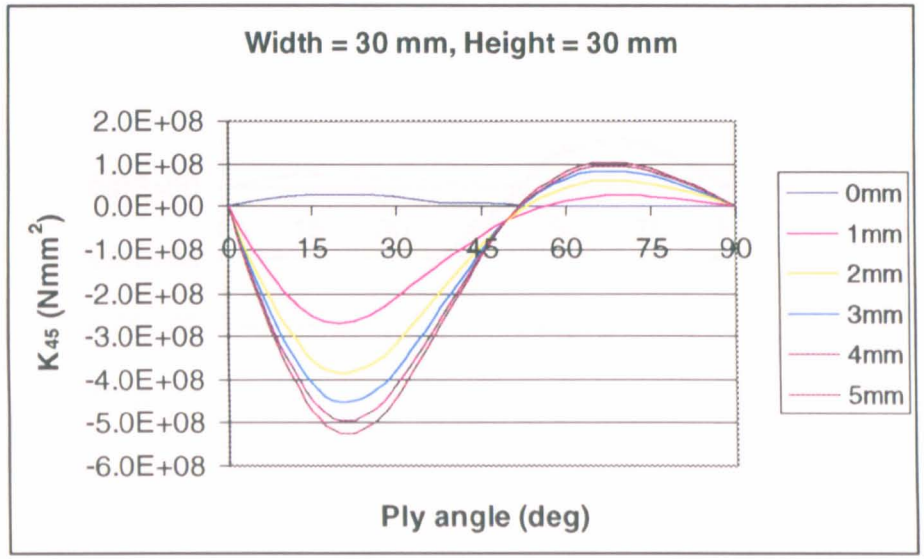
Width = 30 mm, Height = 30 mm
2.0E+08
1.0E+08
0.0E+00
-1.0E+08
-2.0E+08
-3.0E+08
-4.0E+08
-5.0E+08
-6.0E+08
0
15
30
45
60
75
90
K45 (Nmm2)
Ply angle (deg)
0mm
1mm
2mm
3mm
4mm
5mm

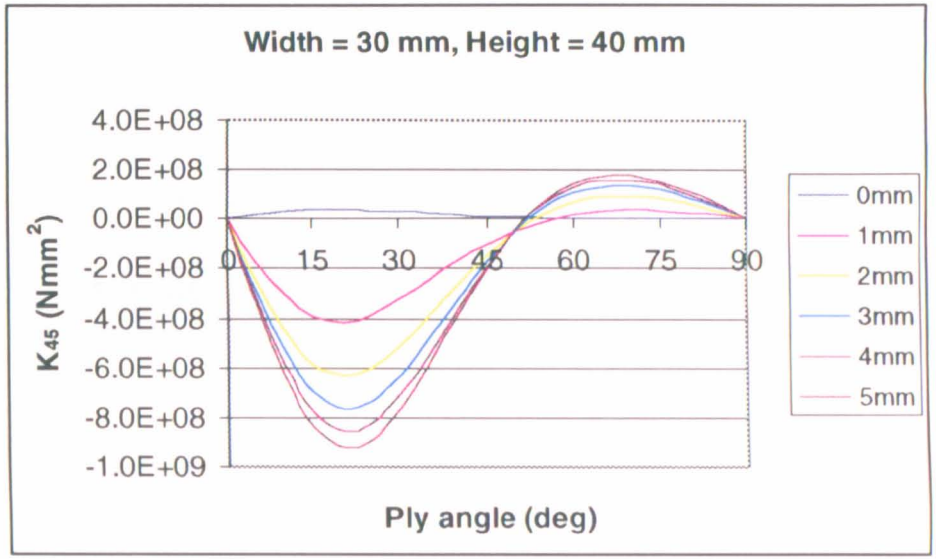
Width = 30 mm, Height = 40 mm
4.0E+08
2.0E+08
0.0E+00
-2.0E+08
-4.0E+08
-6.0E+08
-8.0E+08
-1.0E+09
0
15
30
45
60
75
90
K45 (Nmm2)
Ply angle (deg)
0mm
1mm
2mm
3mm
4mm
5mm

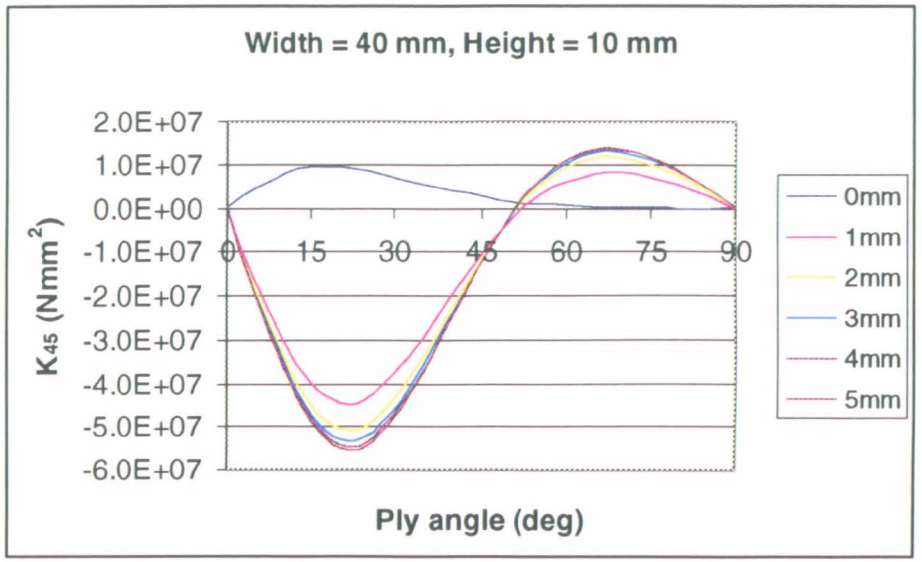
Width = 40 mm, Height = 10 mm
2.0E+07
1.0E+07
0.0E+00
-1.0E+07
-2.0E+07
-3.0E+07
-4.0E+07
-5.0E+07
-6.0E+07
0
15
30
45
60
75
90
K45 (Nmm2)
Ply angle (deg)
0mm
1mm
2mm
3mm
4mm
5mm

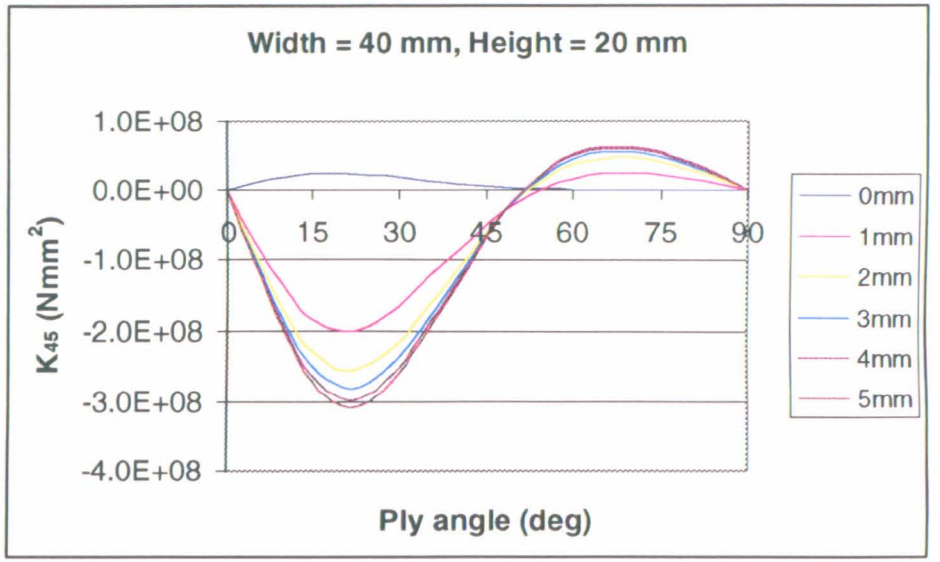
Width = 40 mm, Height = 20 mm
1.0E+08
0.0E+00
-1.0E+08
-2.0E+08
-3.0E+08
-4.0E+08
0
15
30
45
60
75
90
K45 (Nmm2)
Ply angle (deg)
0mm
1mm
2mm
3mm
4mm
5mm

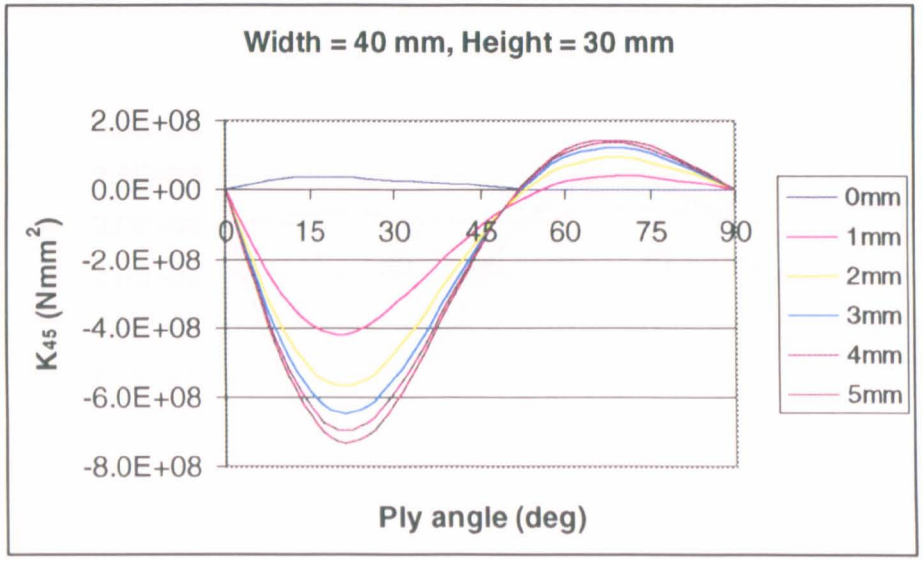
Width = 40 mm, Height = 30 mm
2.0E+08
0.0E+00
-2.0E+08
-4.0E+08
-6.0E+08
-8.0E+08
0
15
30
45
60
75
90
K45 (Nmm2)
Ply angle (deg)
0mm
1mm
2mm
3mm
4mm
5mm

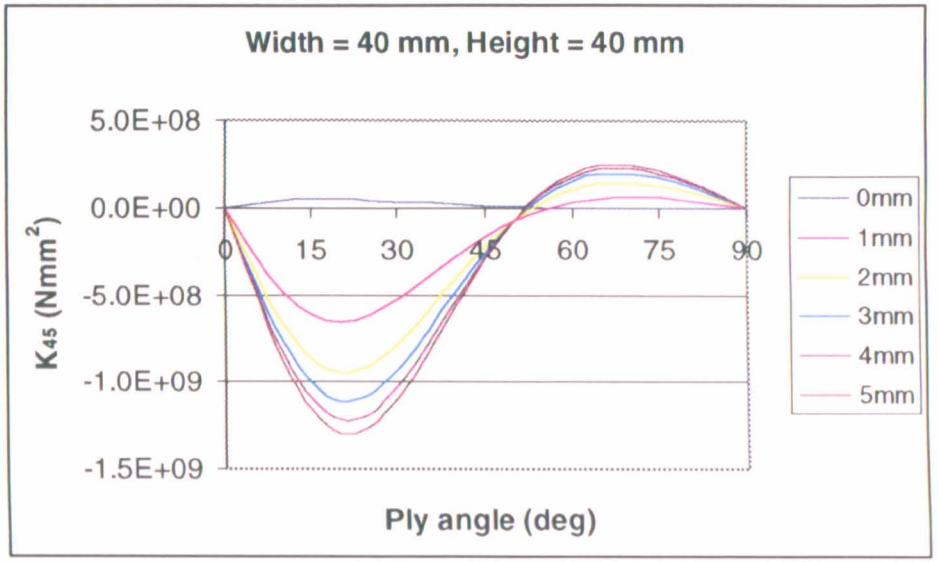
Width = 40 mm, Height = 40 mm
5.0E+08
0.0E+00
-5.0E+08
-1.0E+09
-1.5E+09
0
15
30
45
60
75
90
K45 (Nmm2)
Ply angle (deg)
0mm
1mm
2mm
3mm
4mm
5mm

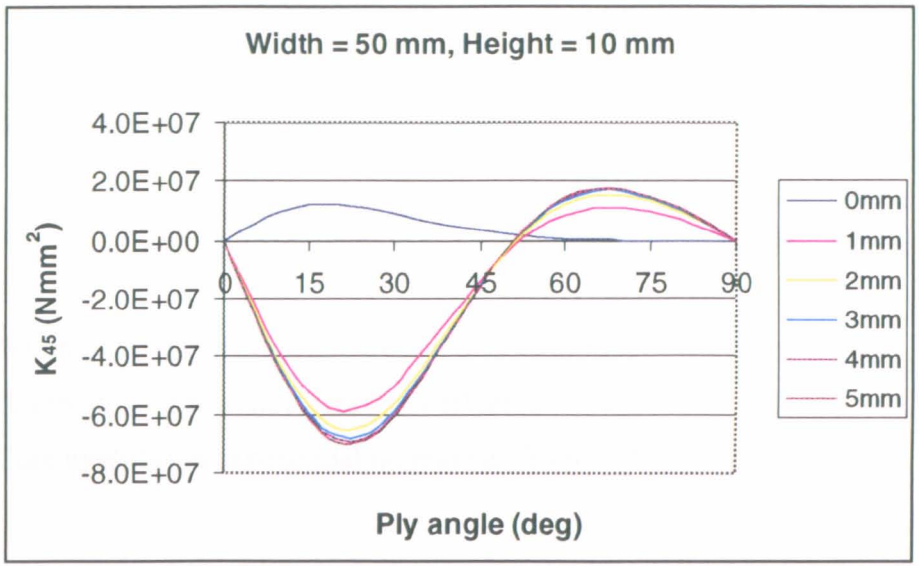
Width = 50 mm, Height = 10 mm
4.0E+07
2.0E+07
0.0E+00
-2.0E+07
-4.0E+07
-6.0E+07
-8.0E+07
K45 (Nmm2)
0
15
30
45
60
75
90
Ply angle (deg)
0mm
1mm
2mm
3mm
4mm
5mm

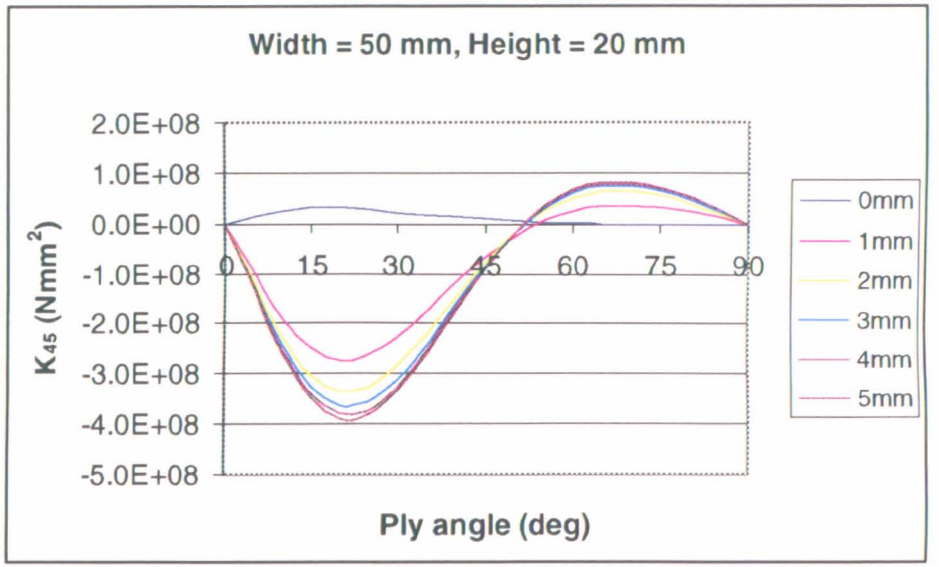
Width = 50 mm, Height = 20 mm
2.0E+08
1.0E+08
0.0E+00
-1.0E+08
-2.0E+08
-3.0E+08
-4.0E+08
-5.0E+08
K45 (Nmm2)
0
15
30
45
60
75
90
Ply angle (deg)
0mm
1mm
2mm
3mm
4mm
5mm

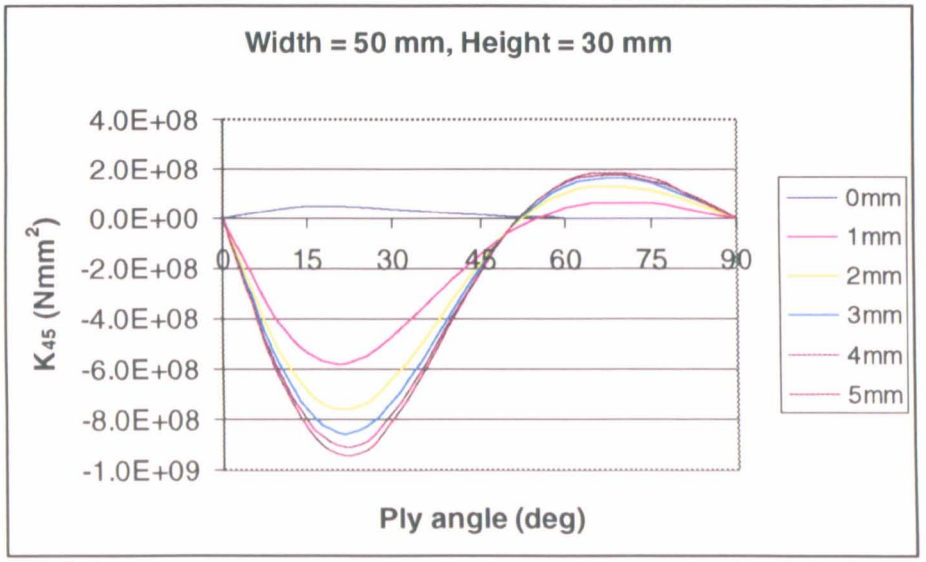
Width = 50 mm, Height = 30 mm
4.0E+08
2.0E+08
0.0E+00
-2.0E+08
-4.0E+08
-6.0E+08
-8.0E+08
-1.0E+09
K45 (Nmm2)
0
15
30
45
60
75
90
Ply angle (deg)
0mm
1mm
2mm
3mm
4mm
5mm

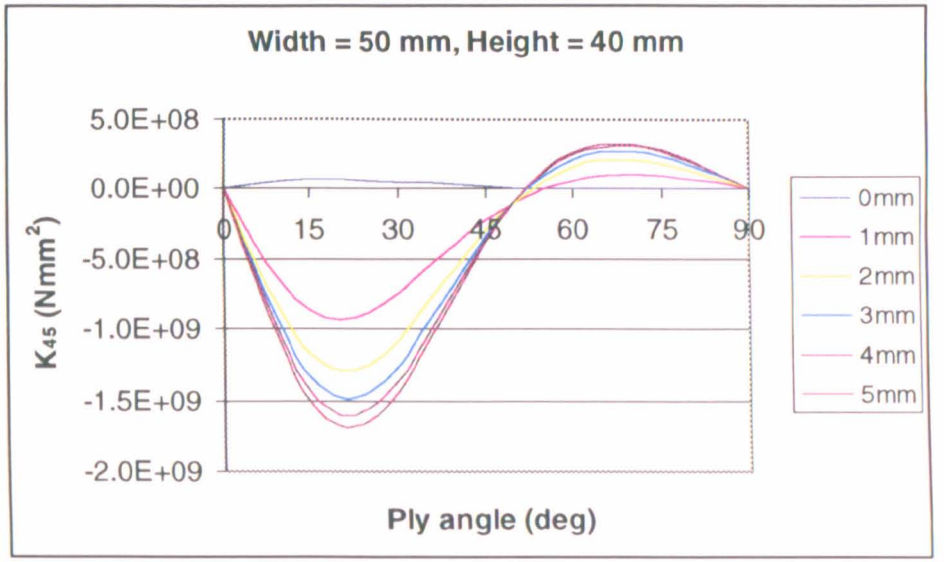
Width = 50 mm, Height = 40 mm
5.0E+08
0.0E+00
-5.0E+08
-1.0E+09
-1.5E+09
-2.0E+09
K45 (Nmm2)
0
15
30
45
60
75
90
Ply angle (deg)
0mm
1mm
2mm
3mm
4mm
5mm

APPENDIX 4.3

Analytical results for sandwich sections

Variation of K_{45} with orientation of coupling plies is shown for:

Width in 10 mm increments from 10mm to 50mm

Height in 10 mm increments from 10mm to 40mm

Core modulus in exponential increments from 7 MPa to $7x10^6$ MPa

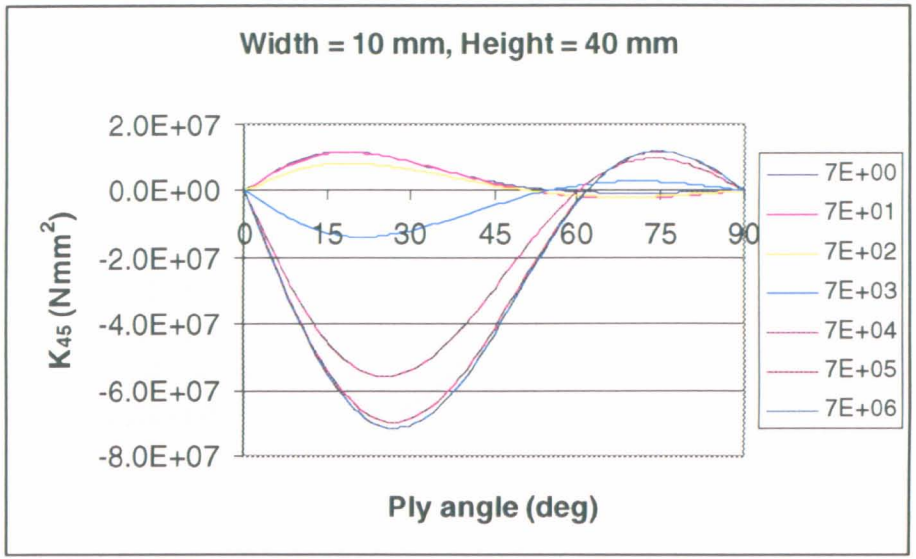
Width = 10 mm, Height = 40 mm
2.0E+07
0.0E+00
-2.0E+07
-4.0E+07
-6.0E+07
-8.0E+07
K45 (Nmm2)
0
15
30
45
60
75
90
Ply angle (deg)
7E+00
7E+01
7E+02
7E+03
7E+04
7E+05
7E+06

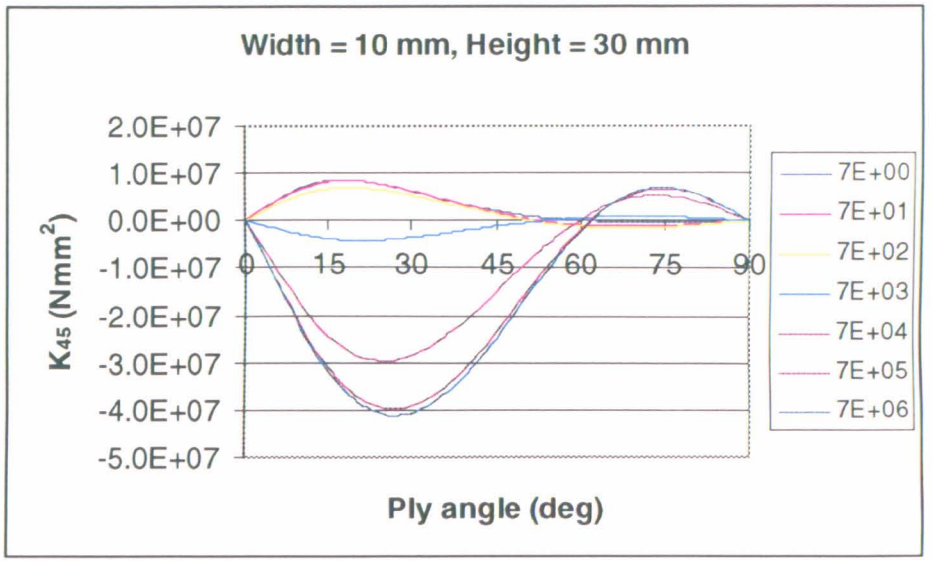
Width = 10 mm, Height = 30 mm
2.0E+07
1.0E+07
0.0E+00
-1.0E+07
-2.0E+07
-3.0E+07
-4.0E+07
-5.0E+07
K45 (Nmm2)
0
15
30
45
60
75
90
Ply angle (deg)
7E+00
7E+01
7E+02
7E+03
7E+04
7E+05
7E+06

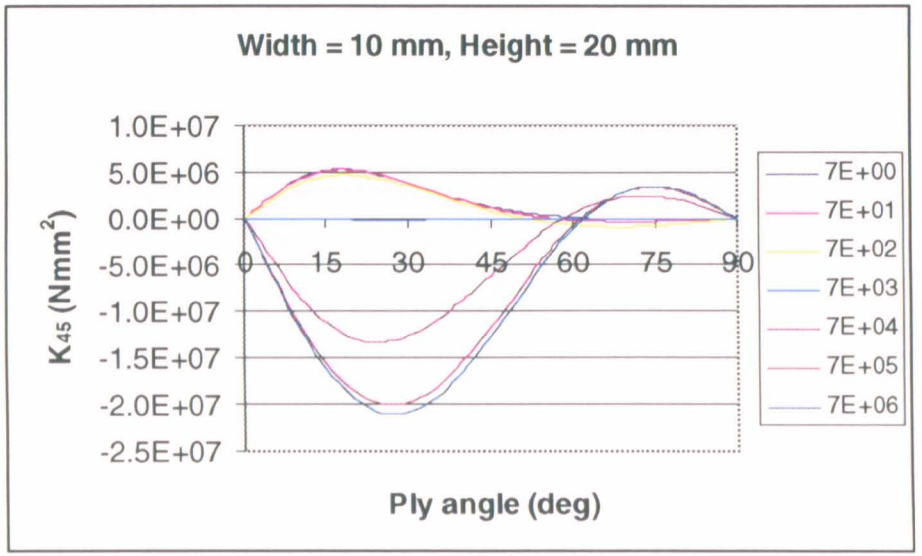
Width = 10 mm, Height = 20 mm
1.0E+07
5.0E+06
0.0E+00
-5.0E+06
-1.0E+07
-1.5E+07
-2.0E+07
-2.5E+07
K45 (Nmm2)
0
15
30
45
60
75
90
Ply angle (deg)
7E+00
7E+01
7E+02
7E+03
7E+04
7E+05
7E+06

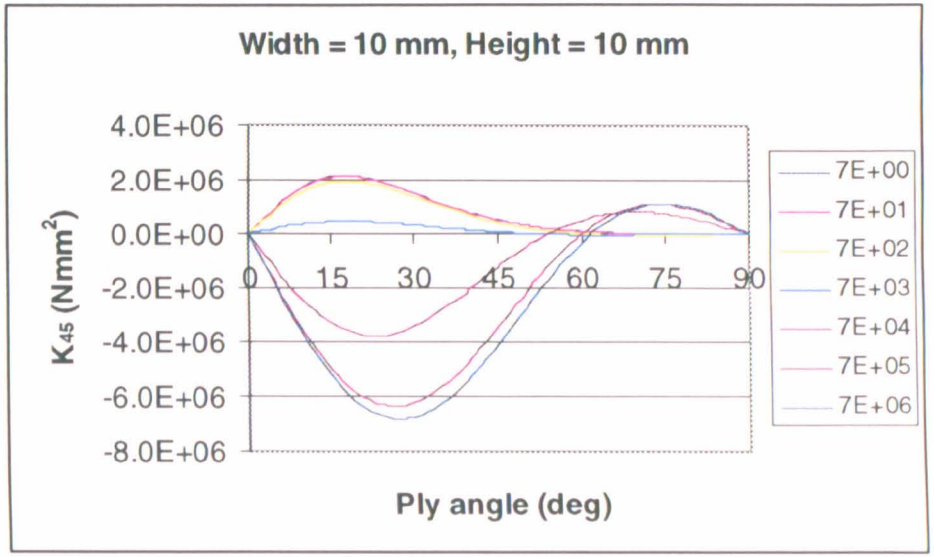
Width = 10 mm, Height = 10 mm
4.0E+06
2.0E+06
0.0E+00
-2.0E+06
-4.0E+06
-6.0E+06
-8.0E+06
K45 (Nmm2)
0
15
30
45
60
75
90
Ply angle (deg)
7E+00
7E+01
7E+02
7E+03
7E+04
7E+05
7E+06

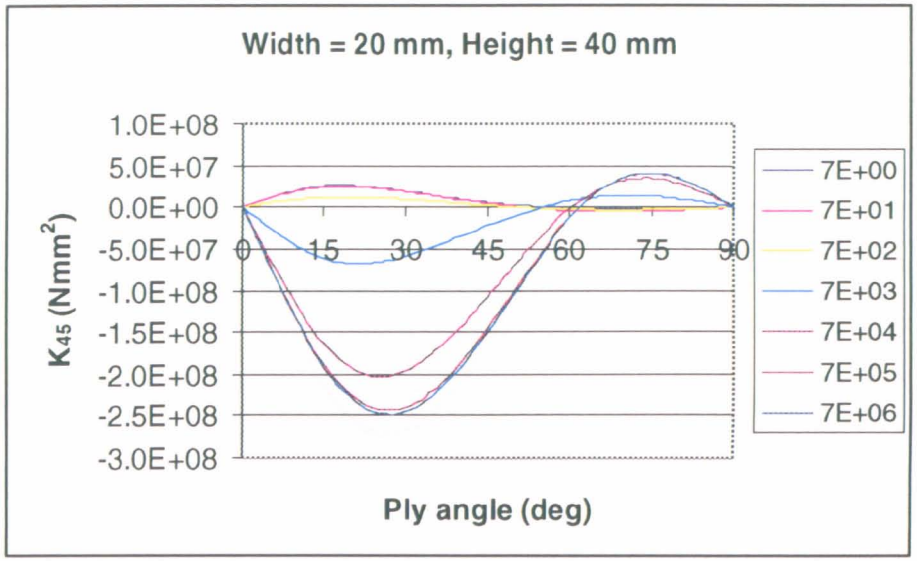
Width = 20 mm, Height = 40 mm
1.0E+08
5.0E+07
0.0E+00
-5.0E+07
-1.0E+08
-1.5E+08
-2.0E+08
-2.5E+08
-3.0E+08
0
15
30
45
60
75
90
K45 (Nmm2)
Ply angle (deg)
7E+00
7E+01
7E+02
7E+03
7E+04
7E+05
7E+06

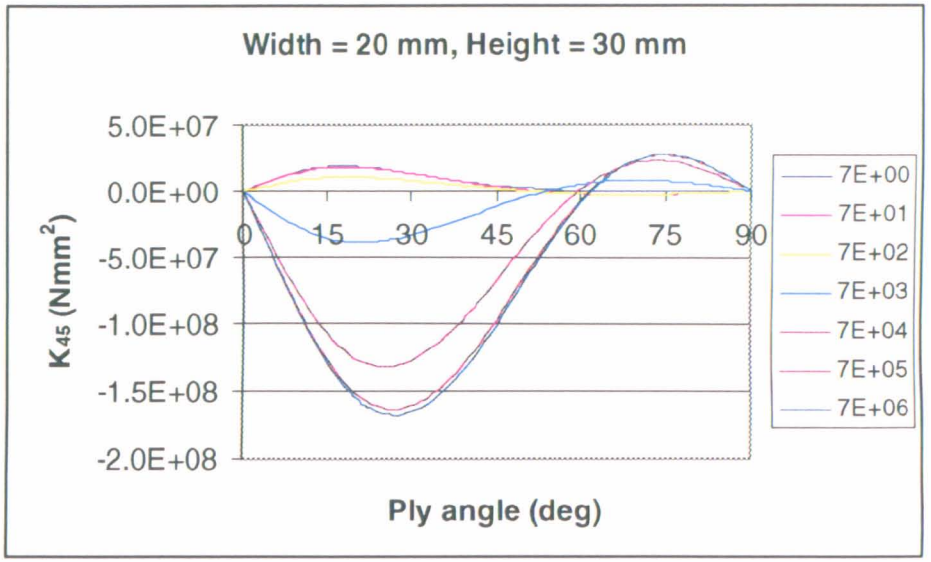
Width = 20 mm, Height = 30 mm
5.0E+07
0.0E+00
-5.0E+07
-1.0E+08
-1.5E+08
-2.0E+08
0
15
30
45
60
75
90
K45 (Nmm2)
Ply angle (deg)
7E+00
7E+01
7E+02
7E+03
7E+04
7E+05
7E+06

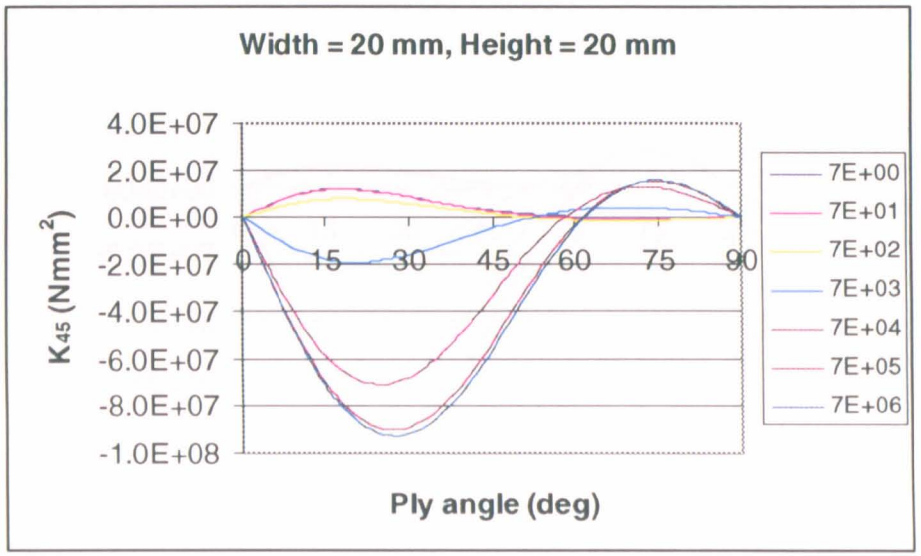
Width = 20 mm, Height = 20 mm
4.0E+07
2.0E+07
0.0E+00
-2.0E+07
-4.0E+07
-6.0E+07
-8.0E+07
-1.0E+08
0
15
30
45
60
75
90
K45 (Nmm2)
Ply angle (deg)
7E+00
7E+01
7E+02
7E+03
7E+04
7E+05
7E+06

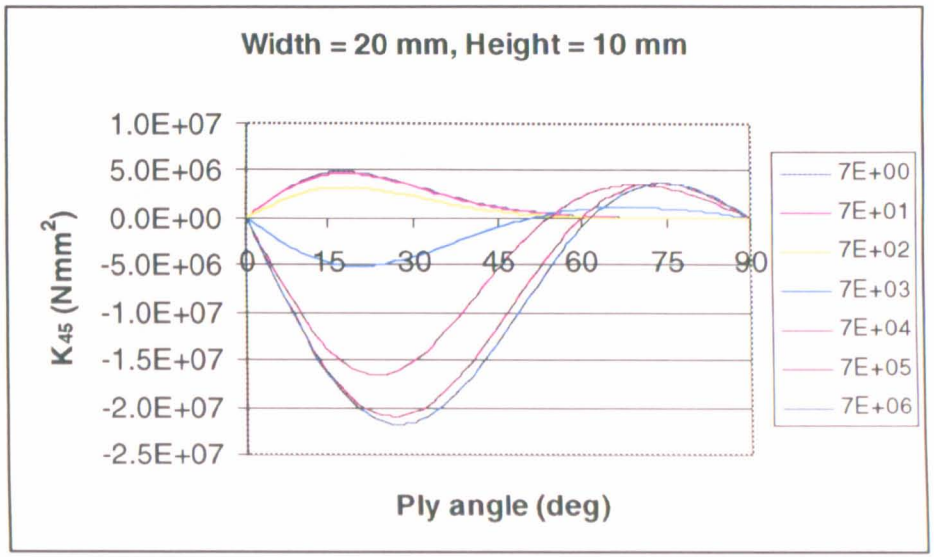
Width = 20 mm, Height = 10 mm
1.0E+07
5.0E+06
0.0E+00
-5.0E+06
-1.0E+07
-1.5E+07
-2.0E+07
-2.5E+07
0
15
30
45
60
75
90
K45 (Nmm2)
Ply angle (deg)
7E+00
7E+01
7E+02
7E+03
7E+04
7E+05
7E+06

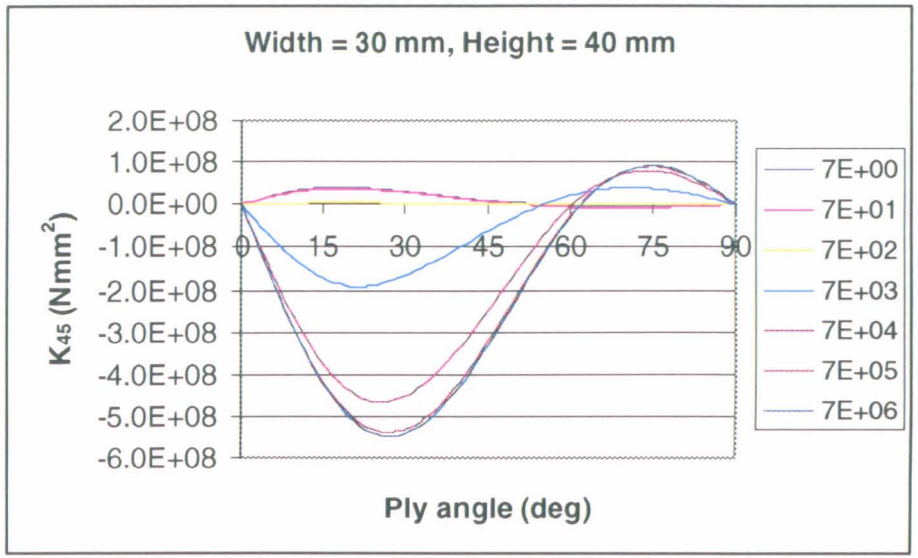
Width = 30 mm, Height = 40 mm
2.0E+08
1.0E+08
0.0E+00
-1.0E+08
-2.0E+08
-3.0E+08
-4.0E+08
-5.0E+08
-6.0E+08
0
15
30
45
60
75
90
K45 (Nmm2)
Ply angle (deg)
7E+00
7E+01
7E+02
7E+03
7E+04
7E+05
7E+06

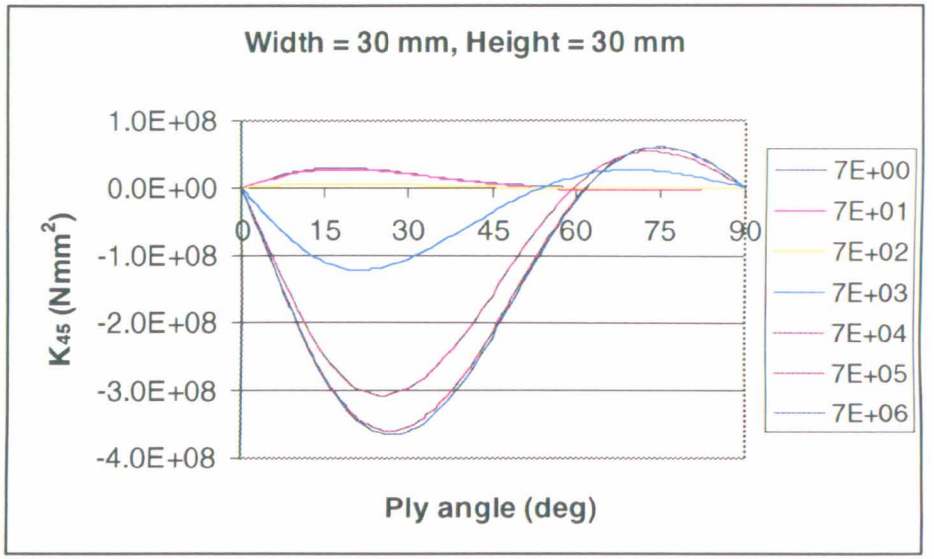
Width = 30 mm, Height = 30 mm
1.0E+08
0.0E+00
-1.0E+08
-2.0E+08
-3.0E+08
-4.0E+08
0
15
30
45
60
75
90
K45 (Nmm2)
Ply angle (deg)
7E+00
7E+01
7E+02
7E+03
7E+04
7E+05
7E+06

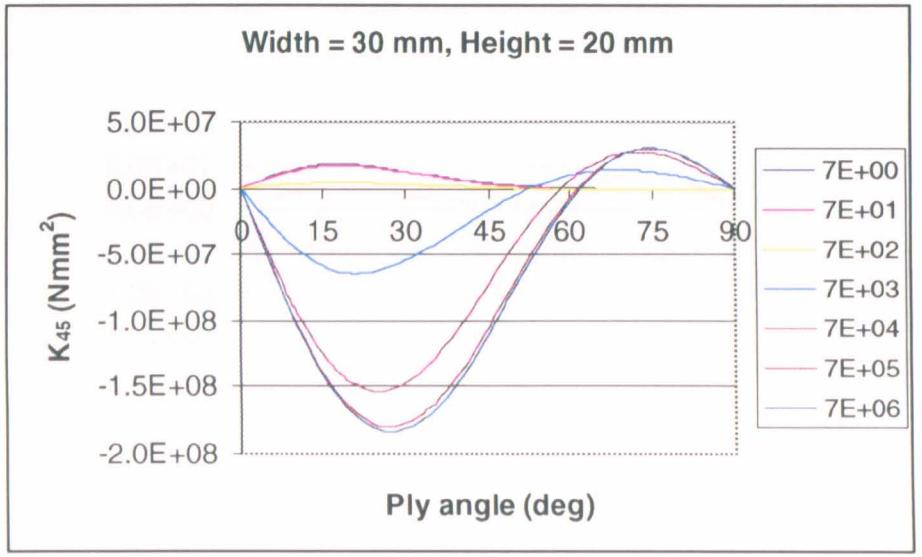
Width = 30 mm, Height = 20 mm
5.0E+07
0.0E+00
-5.0E+07
-1.0E+08
-1.5E+08
-2.0E+08
0
15
30
45
60
75
90
K45 (Nmm2)
Ply angle (deg)
7E+00
7E+01
7E+02
7E+03
7E+04
7E+05
7E+06

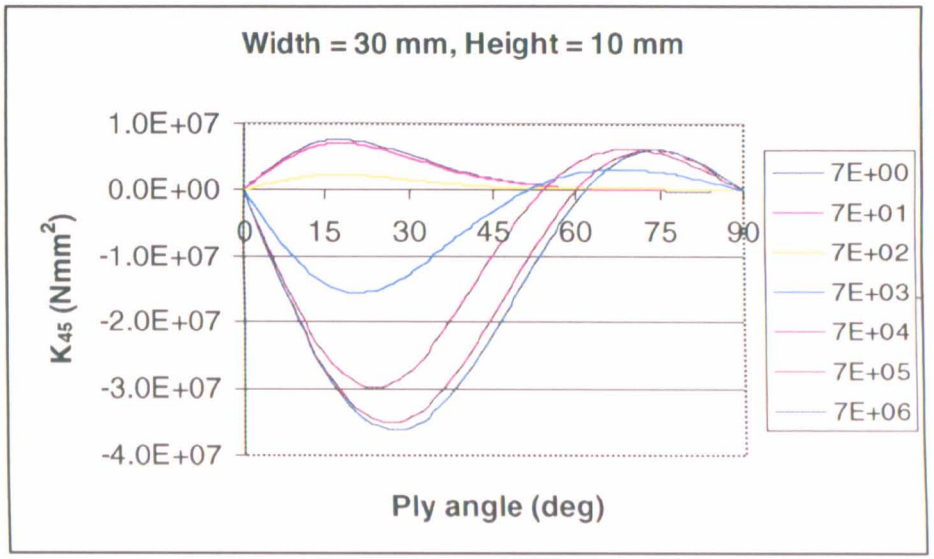
Width = 30 mm, Height = 10 mm
1.0E+07
0.0E+00
-1.0E+07
-2.0E+07
-3.0E+07
-4.0E+07
0
15
30
45
60
75
90
K45 (Nmm2)
Ply angle (deg)
7E+00
7E+01
7E+02
7E+03
7E+04
7E+05
7E+06

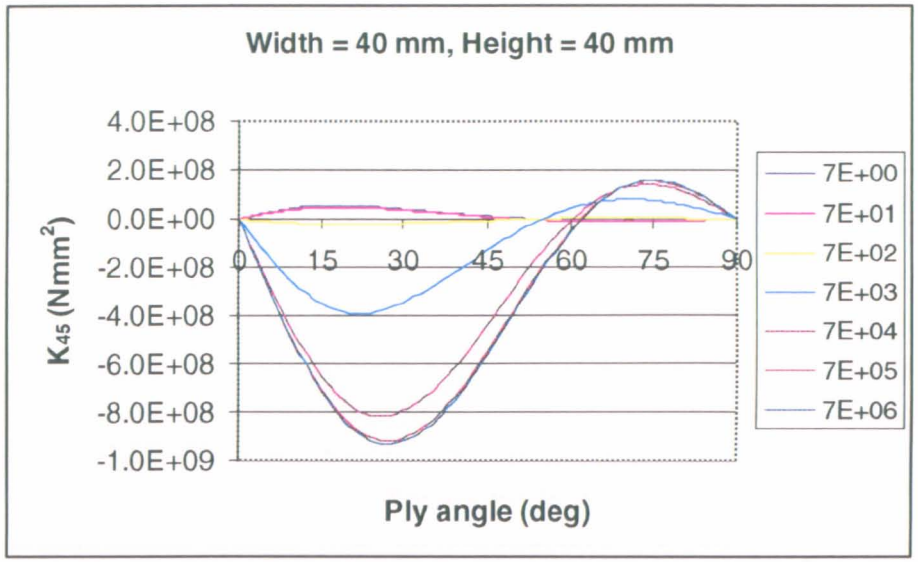
Width = 40 mm, Height = 40 mm
4.0E+08
2.0E+08
0.0E+00
-2.0E+08
-4.0E+08
-6.0E+08
-8.0E+08
-1.0E+09
0
15
30
45
60
75
90
K45 (Nmm2)
Ply angle (deg)
7E+00
7E+01
7E+02
7E+03
7E+04
7E+05
7E+06

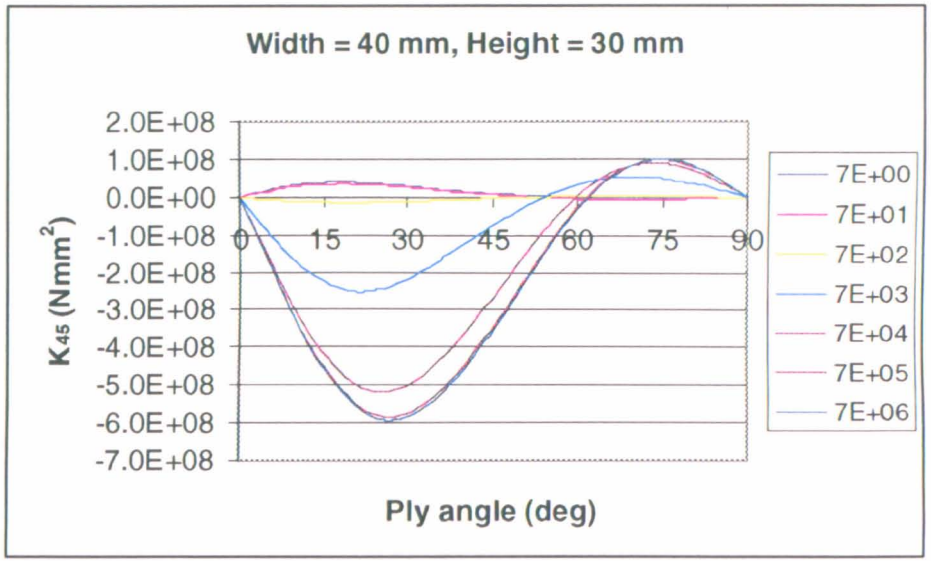
Width = 40 mm, Height = 30 mm
2.0E+08
1.0E+08
0.0E+00
-1.0E+08
-2.0E+08
-3.0E+08
-4.0E+08
-5.0E+08
-6.0E+08
-7.0E+08
0
15
30
45
60
75
90
K45 (Nmm2)
Ply angle (deg)
7E+00
7E+01
7E+02
7E+03
7E+04
7E+05
7E+06

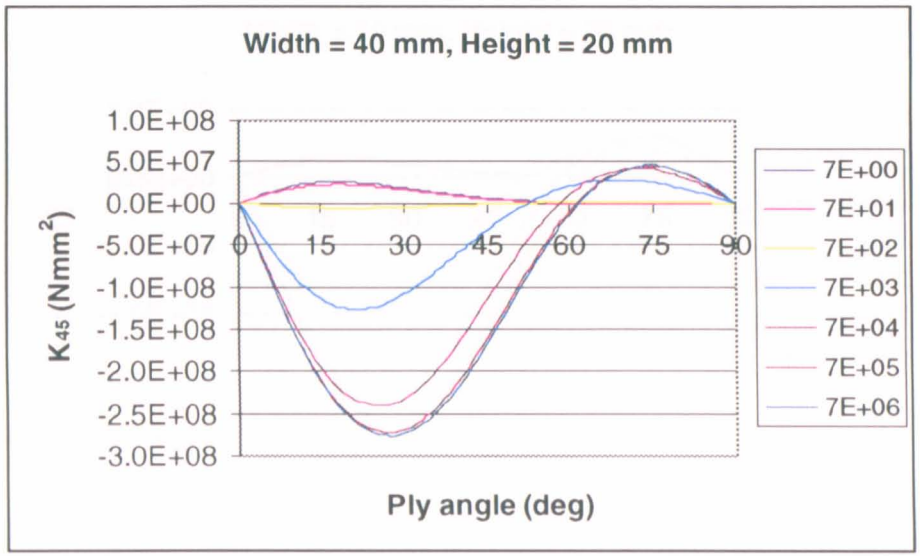
Width = 40 mm, Height = 20 mm
1.0E+08
5.0E+07
0.0E+00
-5.0E+07
-1.0E+08
-1.5E+08
-2.0E+08
-2.5E+08
-3.0E+08
0
15
30
45
60
75
90
K45 (Nmm2)
Ply angle (deg)
7E+00
7E+01
7E+02
7E+03
7E+04
7E+05
7E+06

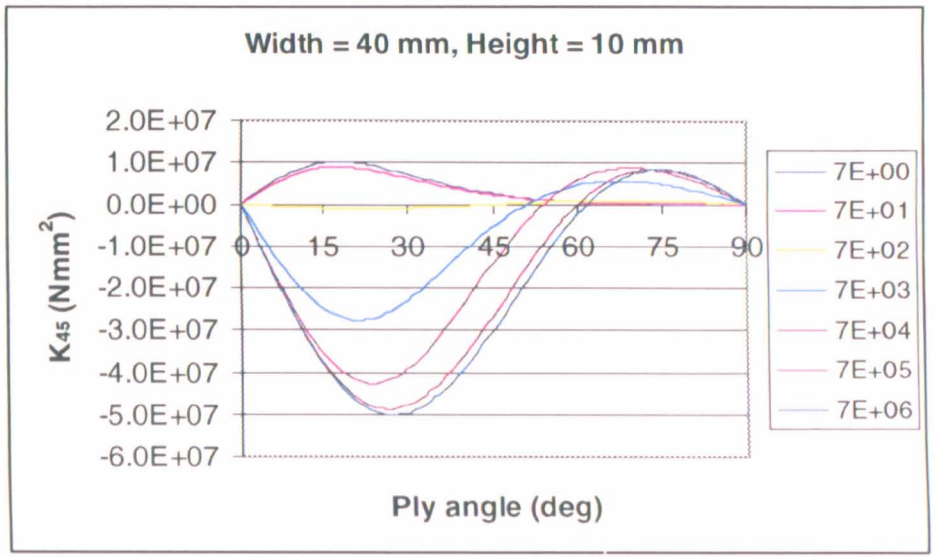
Width = 40 mm, Height = 10 mm
2.0E+07
1.0E+07
0.0E+00
-1.0E+07
-2.0E+07
-3.0E+07
-4.0E+07
-5.0E+07
-6.0E+07
0
15
30
45
60
75
90
K45 (Nmm2)
Ply angle (deg)
7E+00
7E+01
7E+02
7E+03
7E+04
7E+05
7E+06

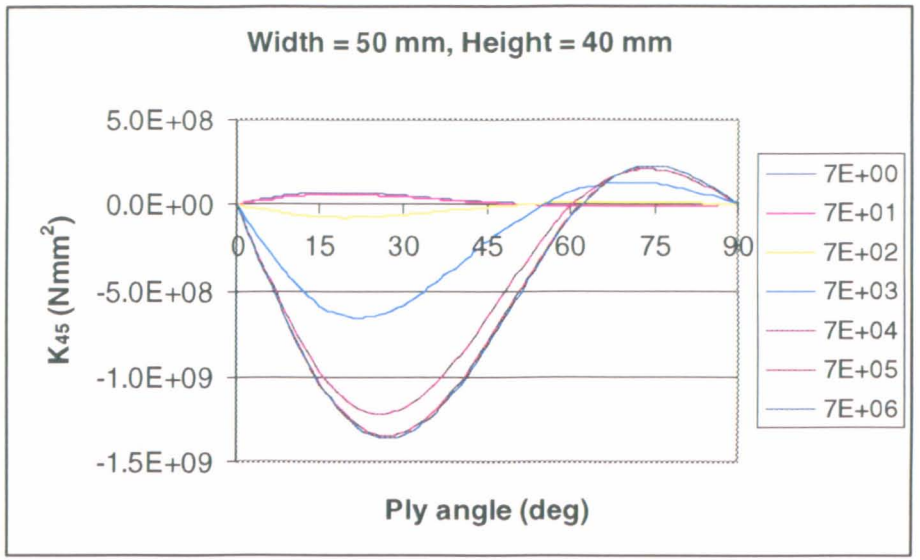
Width = 50 mm, Height = 40 mm
5.0E+08
0.0E+00
-5.0E+08
-1.0E+09
-1.5E+09
K45 (Nmm2)
0
15
30
45
60
75
90
Ply angle (deg)
7E+00
7E+01
7E+02
7E+03
7E+04
7E+05
7E+06

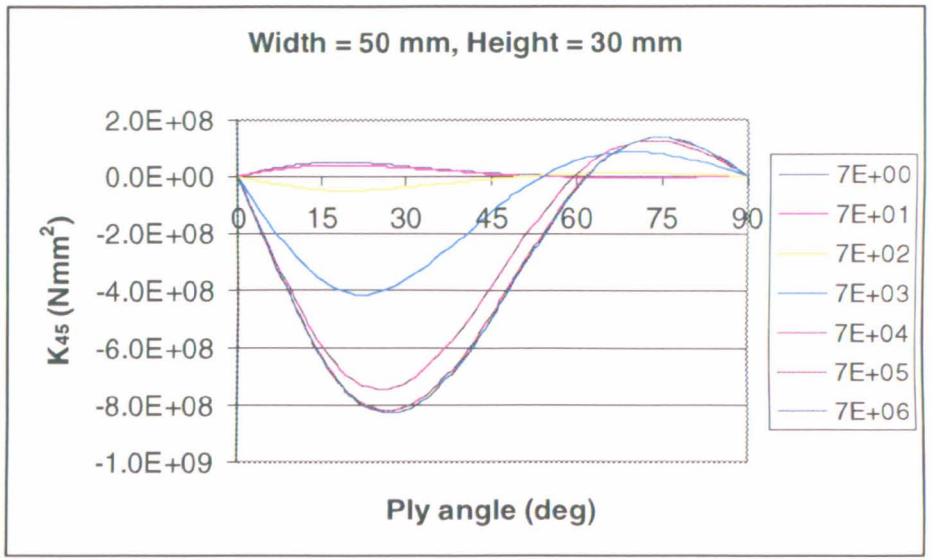
Width = 50 mm, Height = 30 mm
2.0E+08
0.0E+00
-2.0E+08
-4.0E+08
-6.0E+08
-8.0E+08
-1.0E+09
K45 (Nmm2)
0
15
30
45
60
75
90
Ply angle (deg)
7E+00
7E+01
7E+02
7E+03
7E+04
7E+05
7E+06

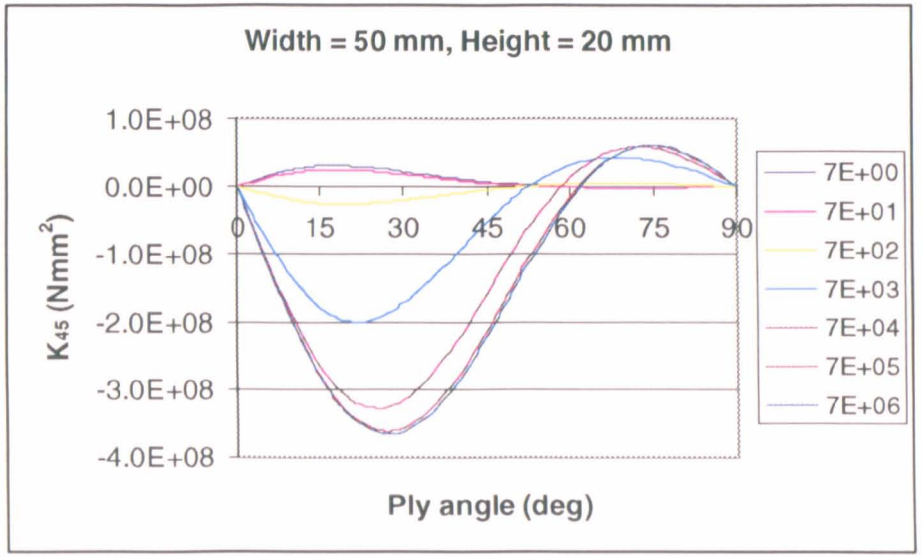
Width = 50 mm, Height = 20 mm
1.0E+08
0.0E+00
-1.0E+08
-2.0E+08
-3.0E+08
-4.0E+08
K45 (Nmm2)
0
15
30
45
60
75
90
Ply angle (deg)
7E+00
7E+01
7E+02
7E+03
7E+04
7E+05
7E+06

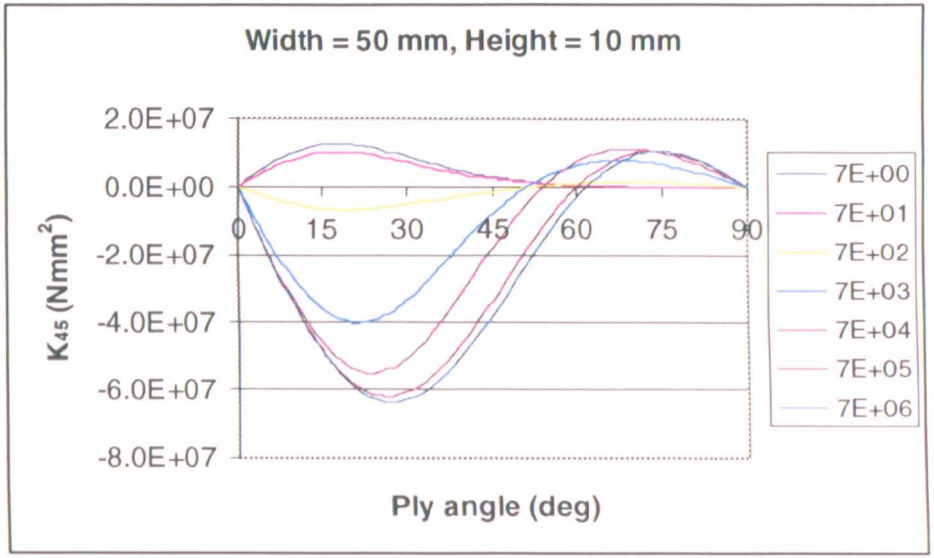
Width = 50 mm, Height = 10 mm
2.0E+07
0.0E+00
-2.0E+07
-4.0E+07
-6.0E+07
-8.0E+07
K45 (Nmm2)
0
15
30
45
60
75
90
Ply angle (deg)
7E+00
7E+01
7E+02
7E+03
7E+04
7E+05
7E+06

APPENDIX 4.4

Comparison of Analytical and Finite Element results for Sandwich Sections

Peak value of K_{45} is shown for:

Width in 10 mm increments from 10mm to 50mm

Height in 10 mm increments from 10mm to 40mm

Core modulus in exponential increments from 7 MPa to $7x10^6$ MPa

7e+00 MPa core modulus

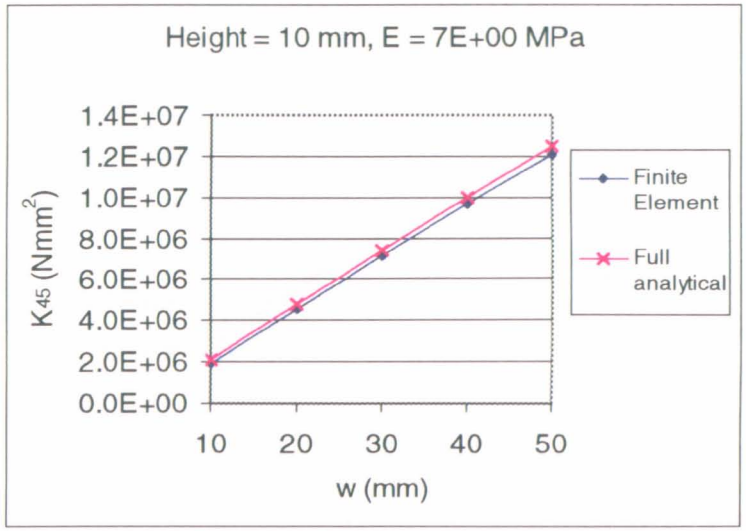

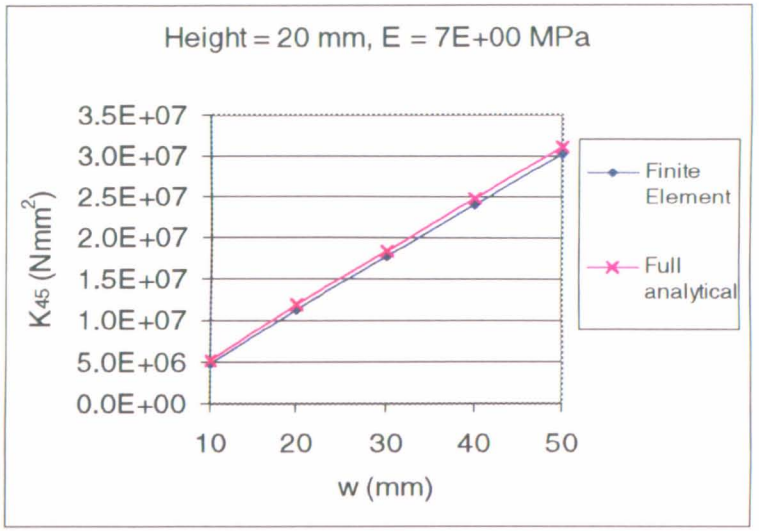

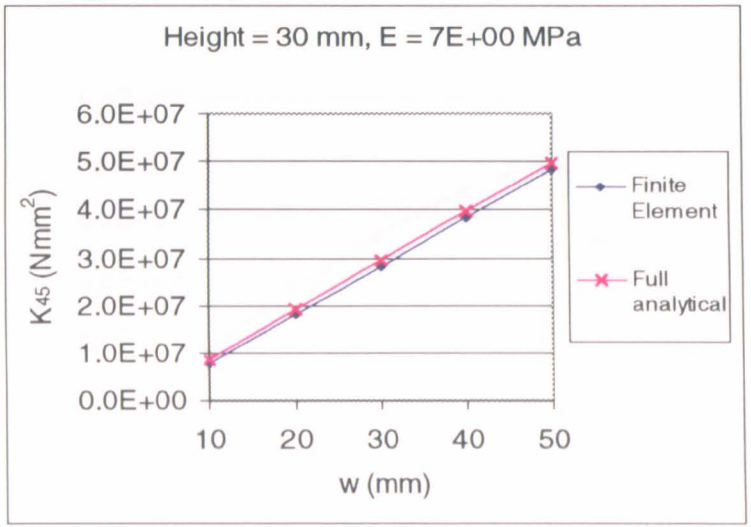

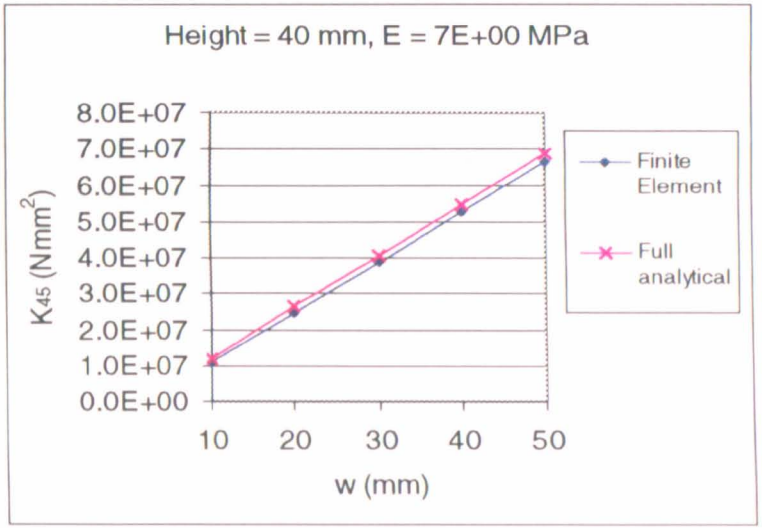

7e+01 MPa core modulus

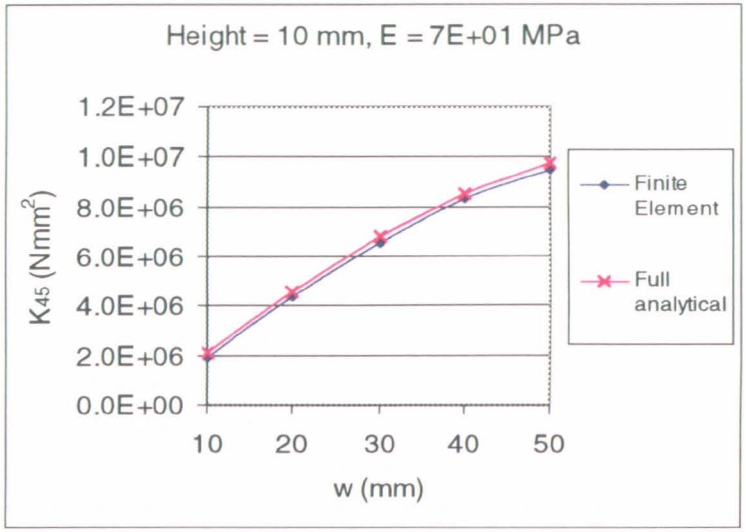

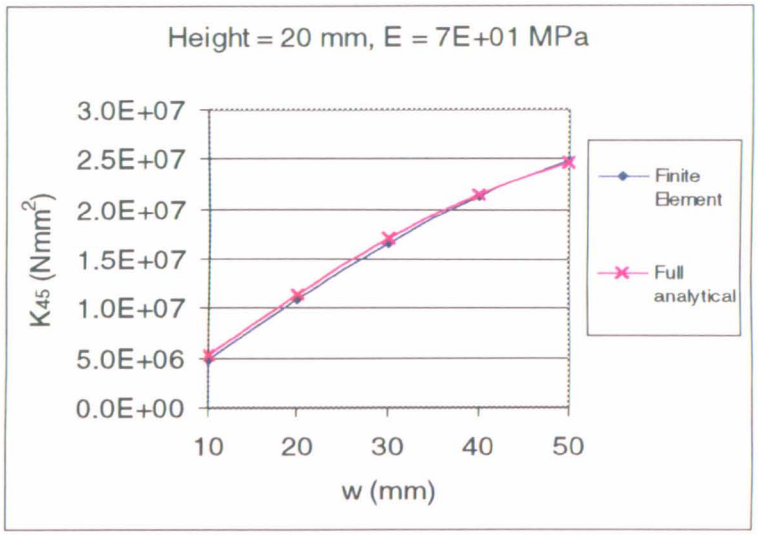

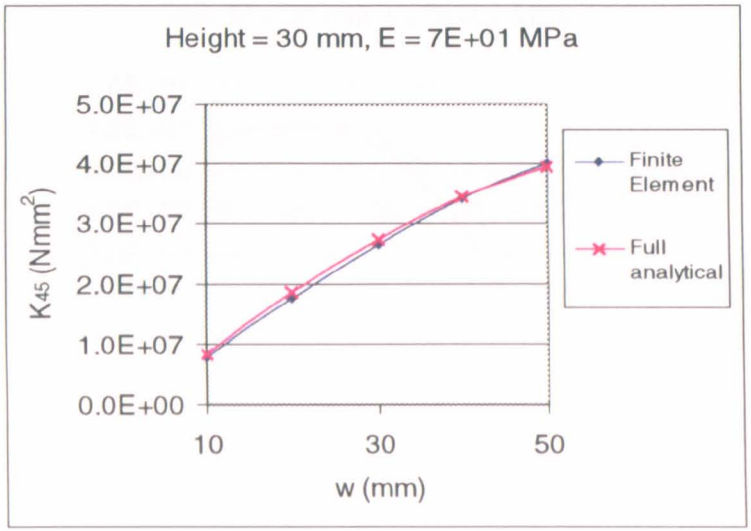

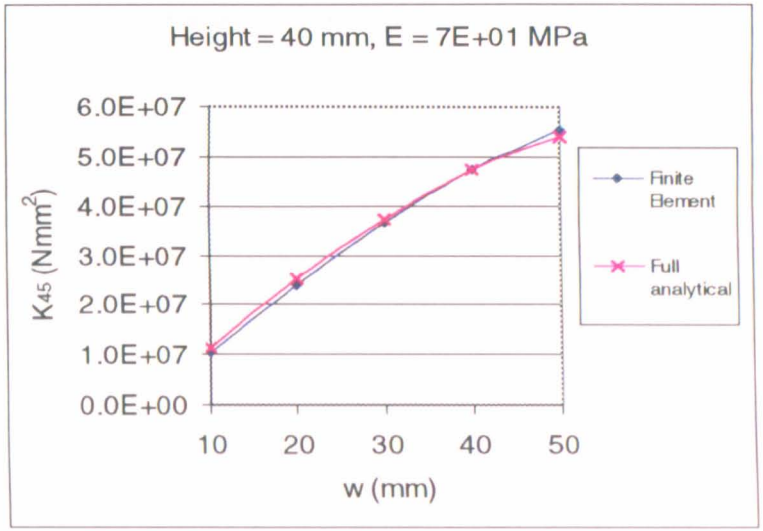

7e+02 MPa core modulus

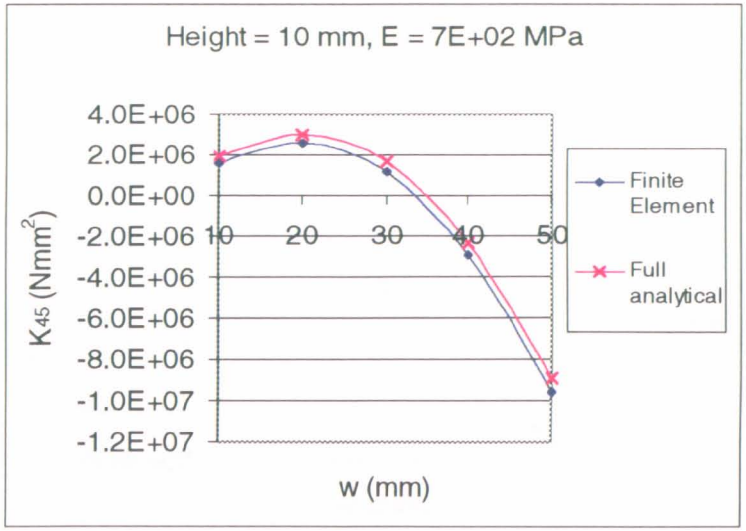

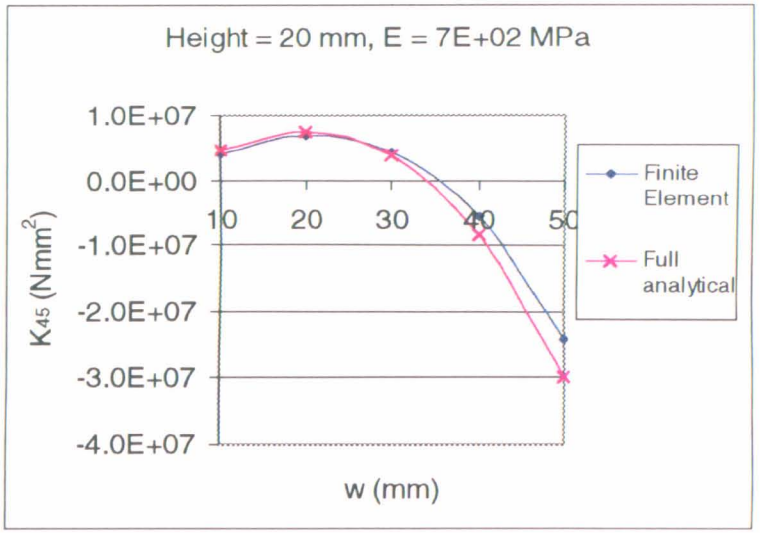

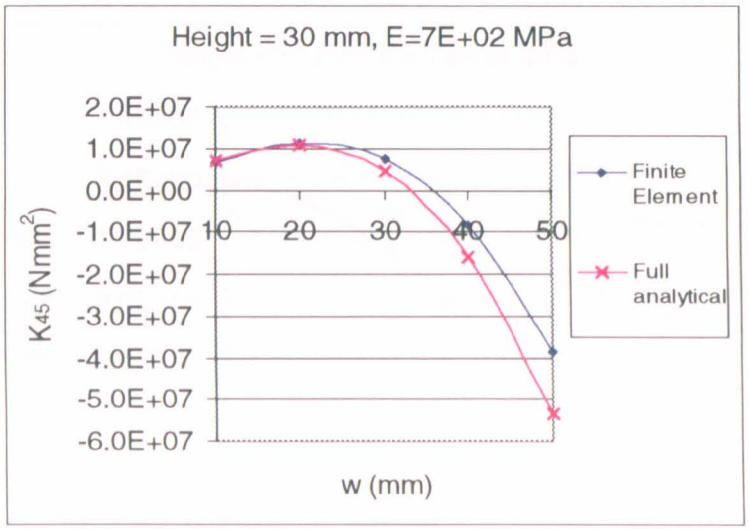

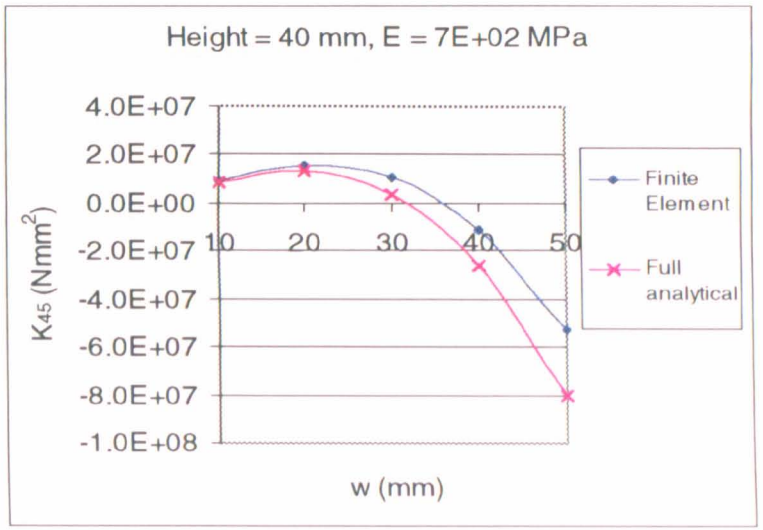

7e+03 MPa core modulus

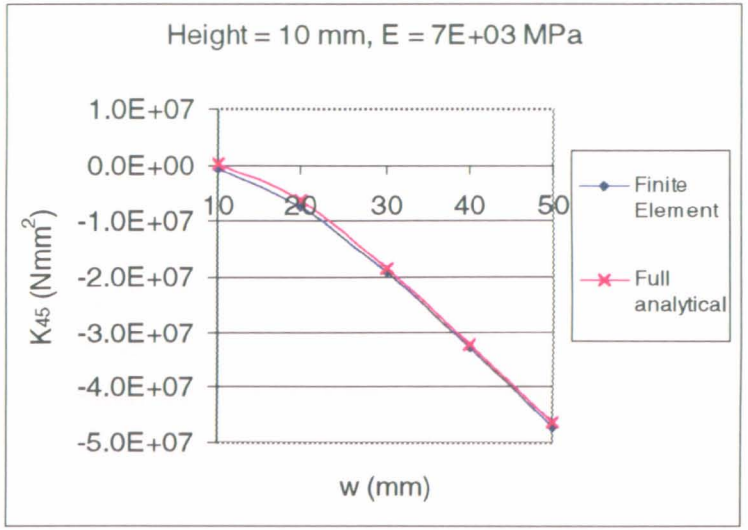

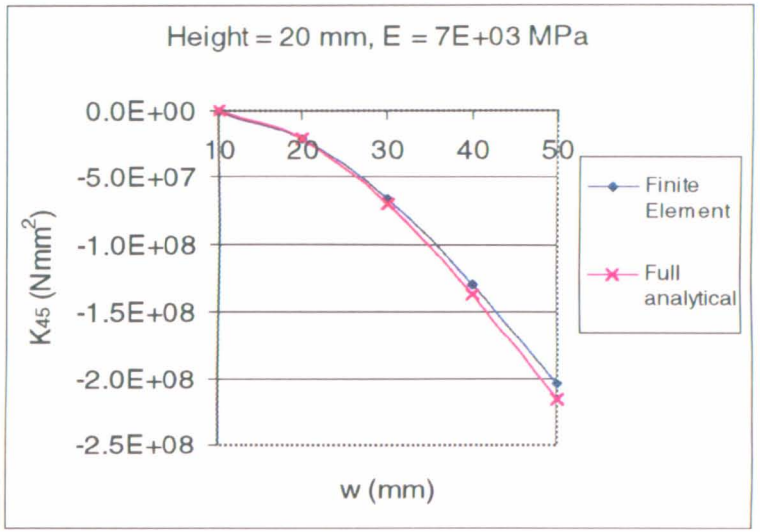

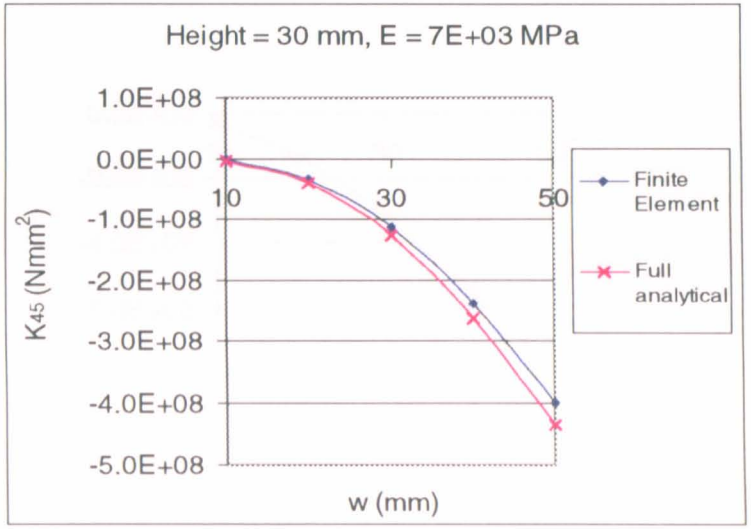

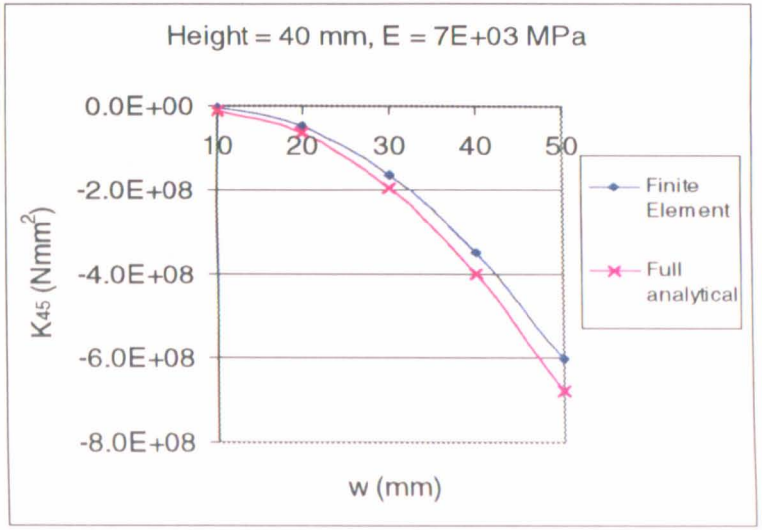

7e+04 MPa core modulus

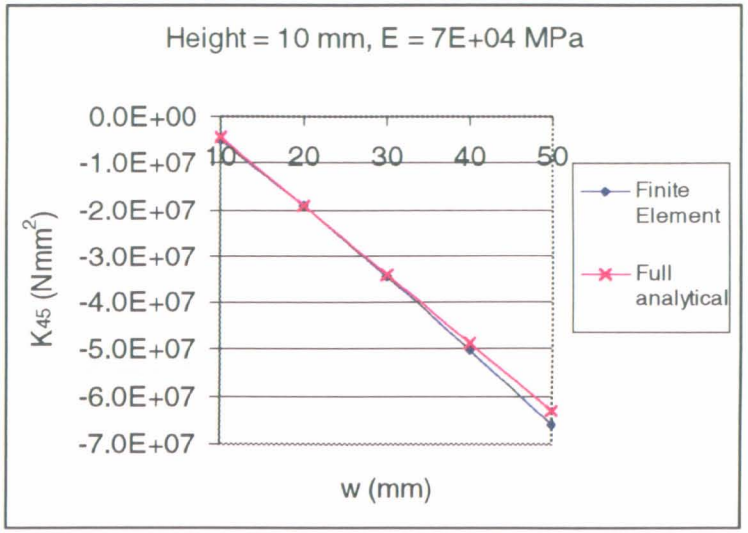

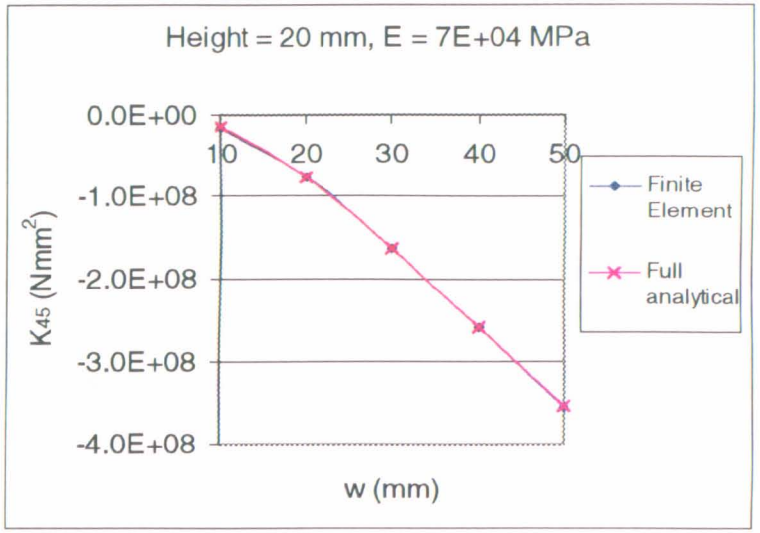

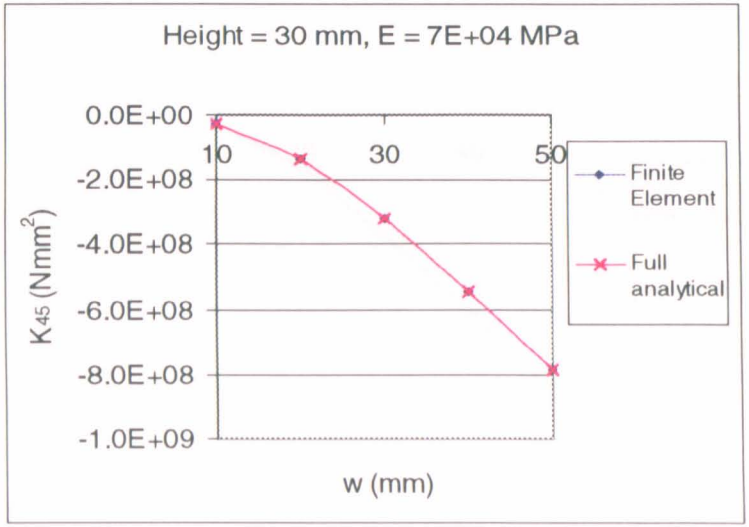

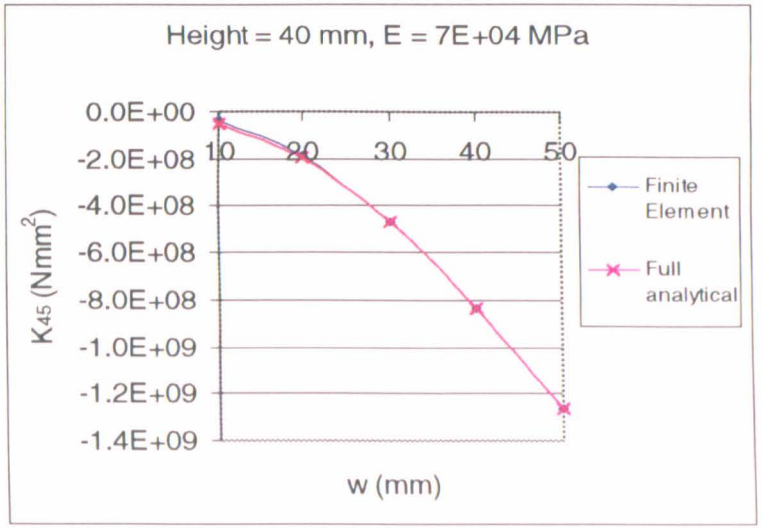

7e+05 MPa core modulus

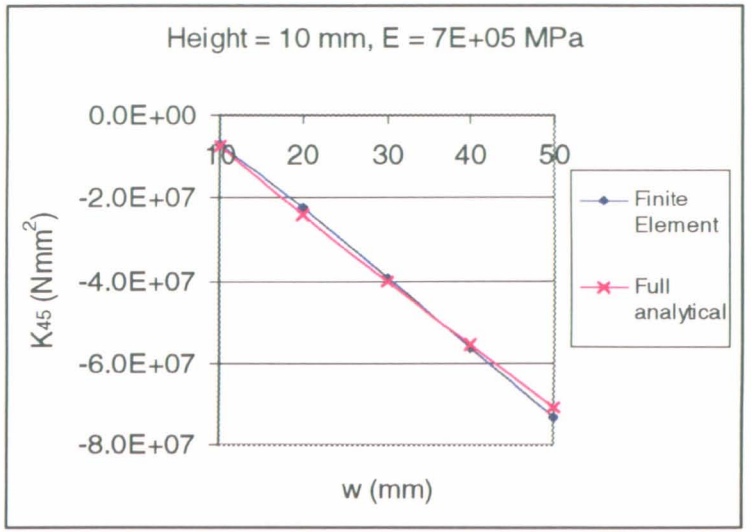

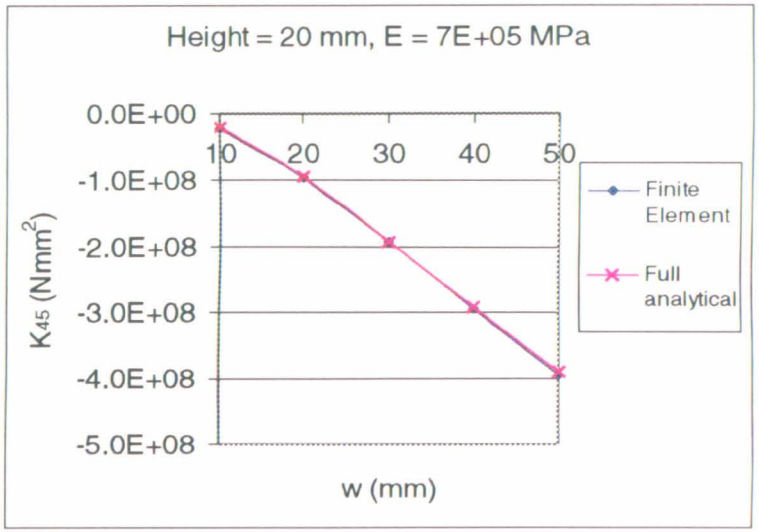

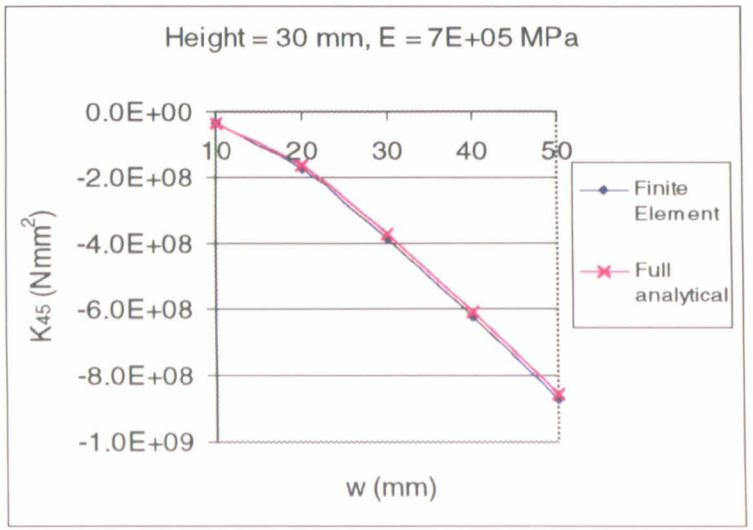

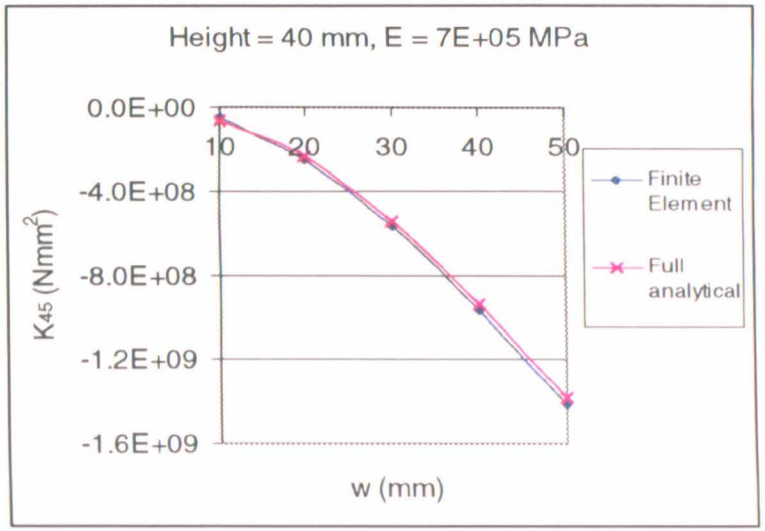

7e+06 MPa core modulus

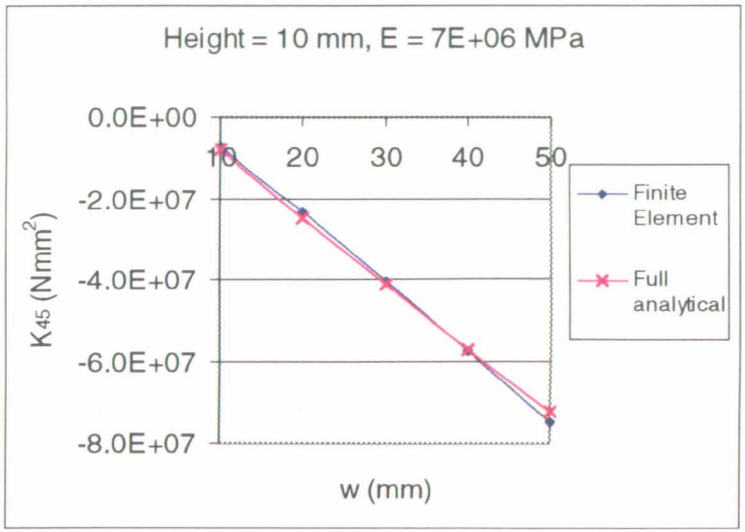

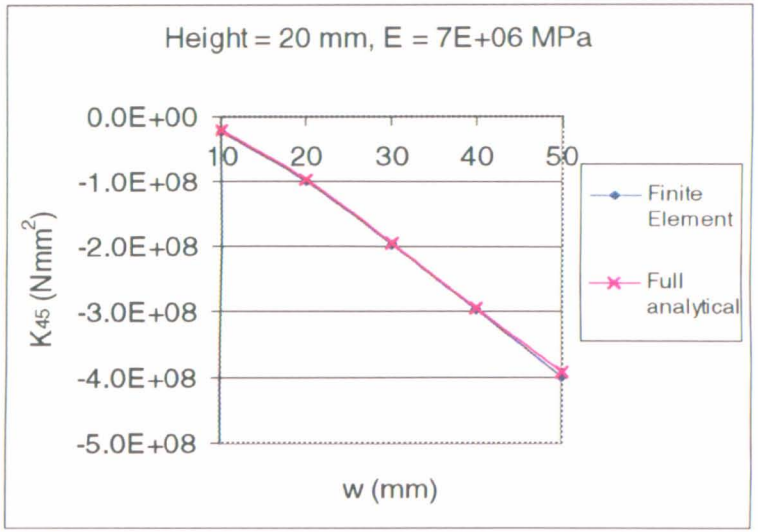

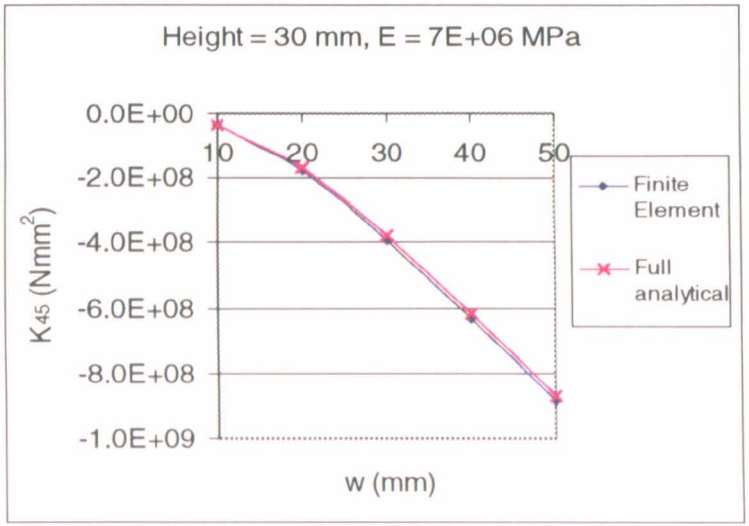

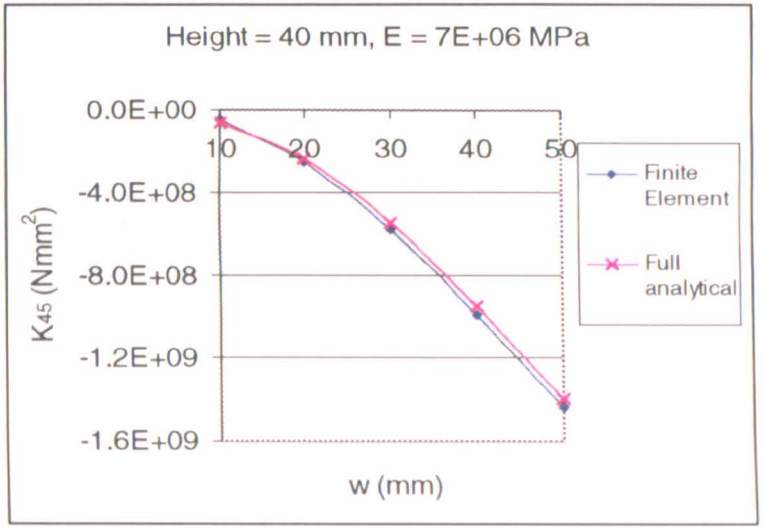

APPENDIX 4.5

Analytical results for K_{45} of box sections

Variation of K_{45} with orientation of coupling plies is shown for:

Width in 10 mm increments from 10mm to 50mm

Height in 10 mm increments from 10mm to 40mm

Vertical wall thickness in 1mm increments from 0mm to 5mm

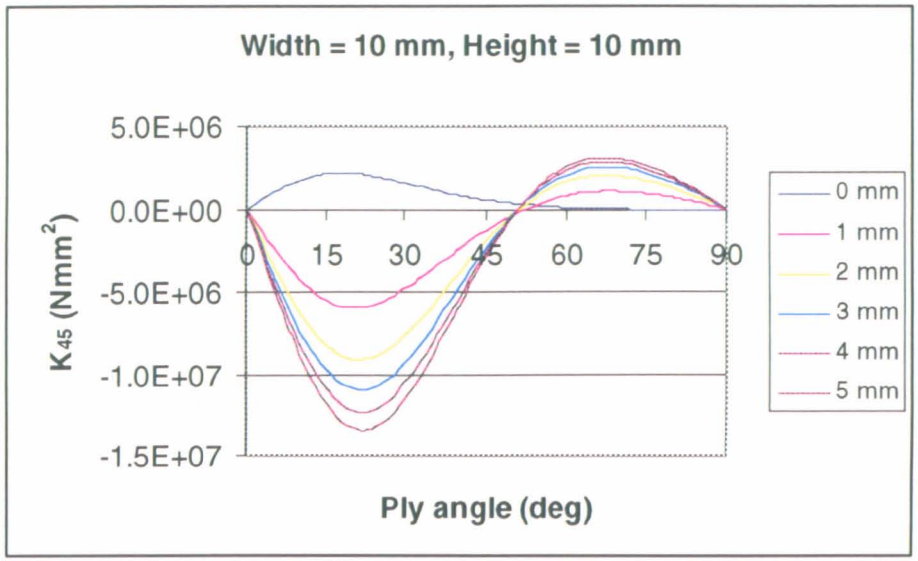
Width = 10 mm, Height = 10 mm
5.0E+06
0.0E+00
-5.0E+06
-1.0E+07
-1.5E+07
K45 (Nmm2)
0
15
30
45
60
75
90
Ply angle (deg)
0 mm
1 mm
2 mm
3 mm
4 mm
5 mm

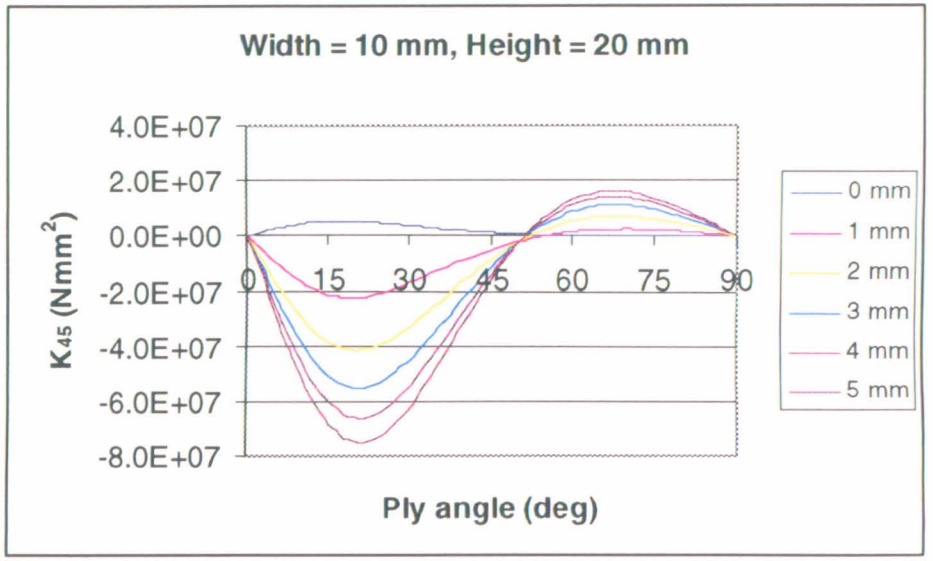
Width = 10 mm, Height = 20 mm
4.0E+07
2.0E+07
0.0E+00
-2.0E+07
-4.0E+07
-6.0E+07
-8.0E+07
K45 (Nmm2)
0
15
30
45
60
75
90
Ply angle (deg)
0 mm
1 mm
2 mm
3 mm
4 mm
5 mm

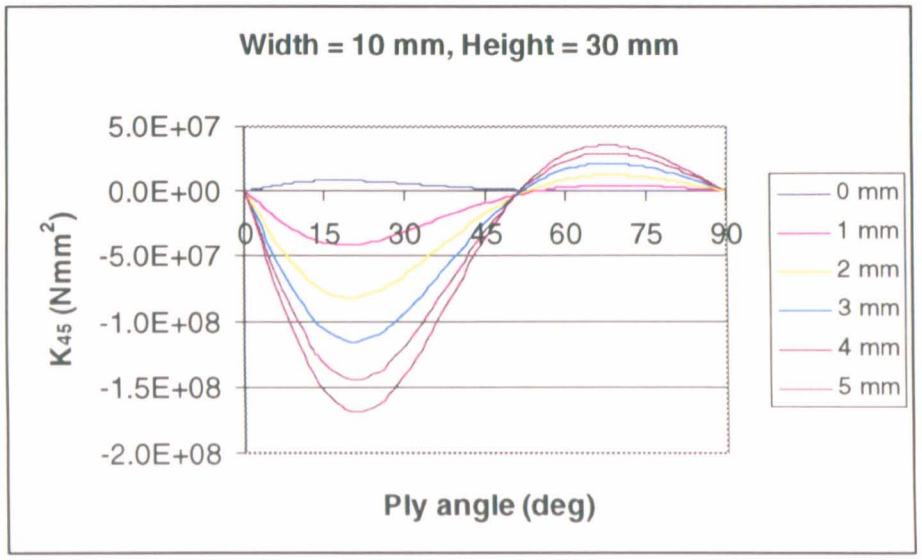
Width = 10 mm, Height = 30 mm
5.0E+07
0.0E+00
-5.0E+07
-1.0E+08
-1.5E+08
-2.0E+08
K45 (Nmm2)
0
15
30
45
60
75
90
Ply angle (deg)
0 mm
1 mm
2 mm
3 mm
4 mm
5 mm

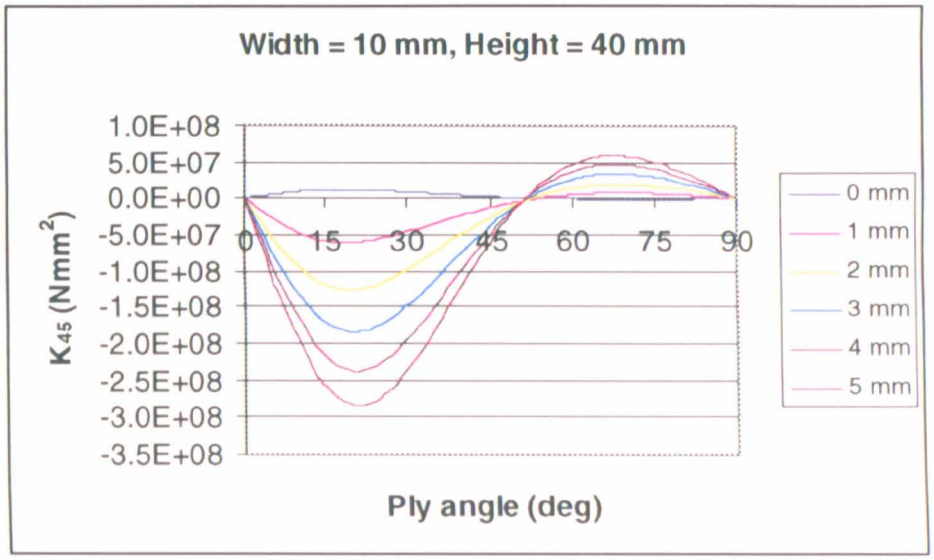
Width = 10 mm, Height = 40 mm
1.0E+08
5.0E+07
0.0E+00
-5.0E+07
-1.0E+08
-1.5E+08
-2.0E+08
-2.5E+08
-3.0E+08
-3.5E+08
K45 (Nmm2)
0
15
30
45
60
75
90
Ply angle (deg)
0 mm
1 mm
2 mm
3 mm
4 mm
5 mm

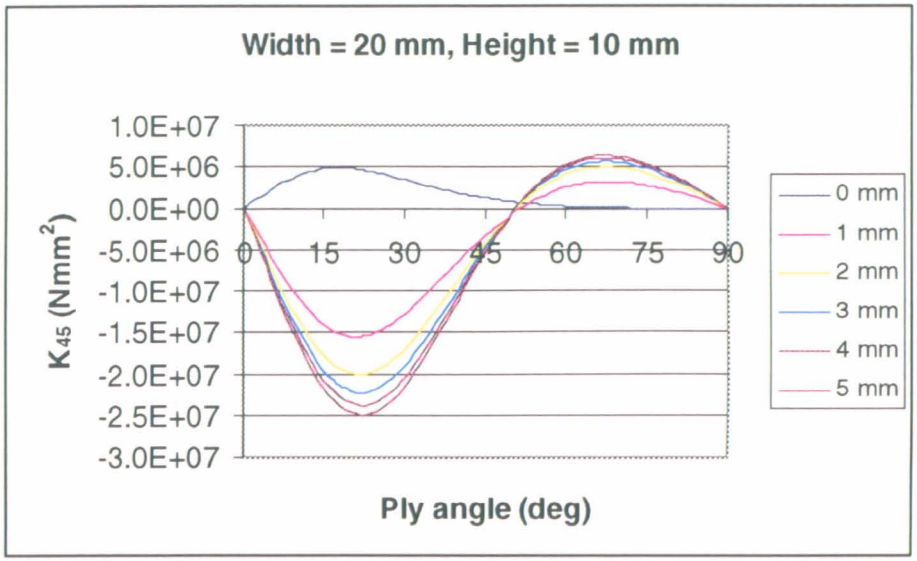
Width = 20 mm, Height = 10 mm
1.0E+07
5.0E+06
0.0E+00
-5.0E+06
-1.0E+07
-1.5E+07
-2.0E+07
-2.5E+07
-3.0E+07
0
15
30
45
60
75
90
K45 (Nmm2)
Ply angle (deg)
0 mm
1 mm
2 mm
3 mm
4 mm
5 mm

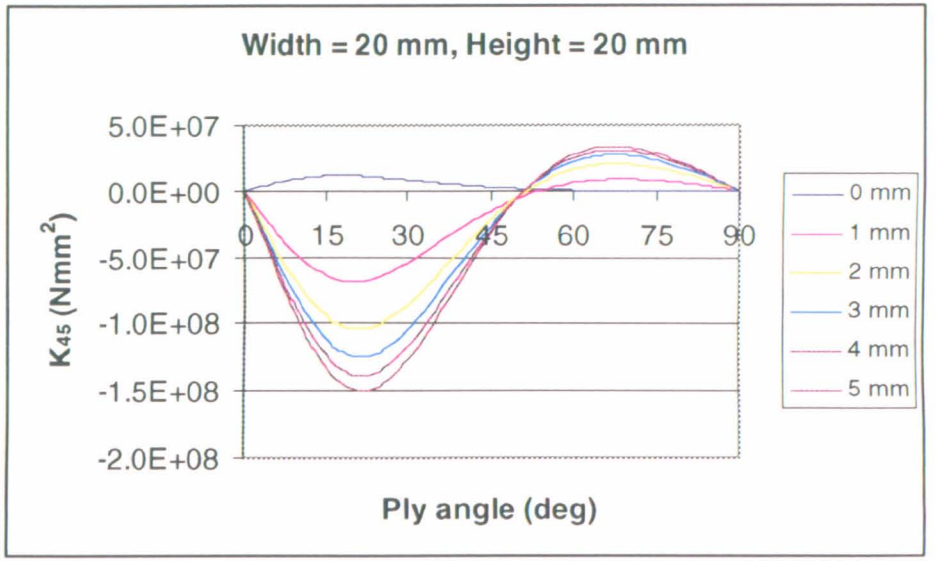
Width = 20 mm, Height = 20 mm
5.0E+07
0.0E+00
-5.0E+07
-1.0E+08
-1.5E+08
-2.0E+08
0
15
30
45
60
75
90
K45 (Nmm2)
Ply angle (deg)
0 mm
1 mm
2 mm
3 mm
4 mm
5 mm

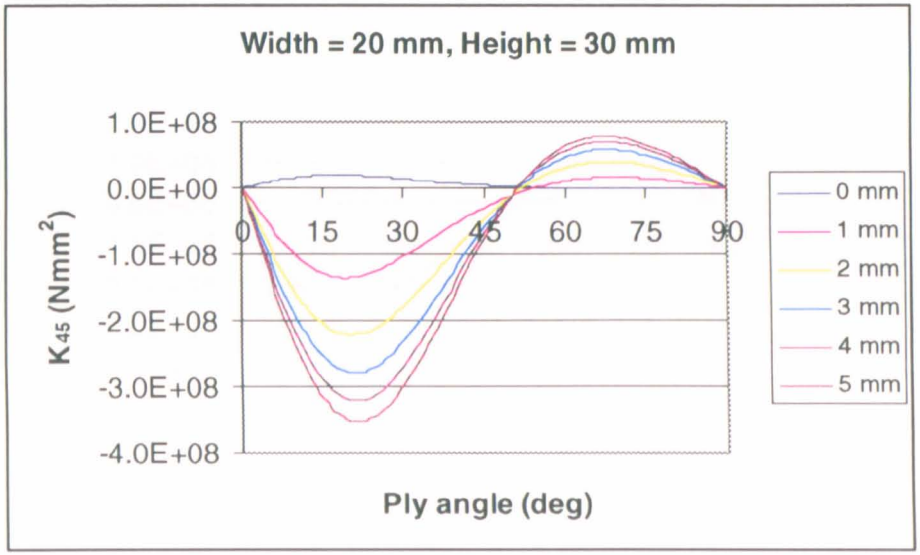
Width = 20 mm, Height = 30 mm
1.0E+08
0.0E+00
-1.0E+08
-2.0E+08
-3.0E+08
-4.0E+08
0
15
30
45
60
75
90
K45 (Nmm2)
Ply angle (deg)
0 mm
1 mm
2 mm
3 mm
4 mm
5 mm

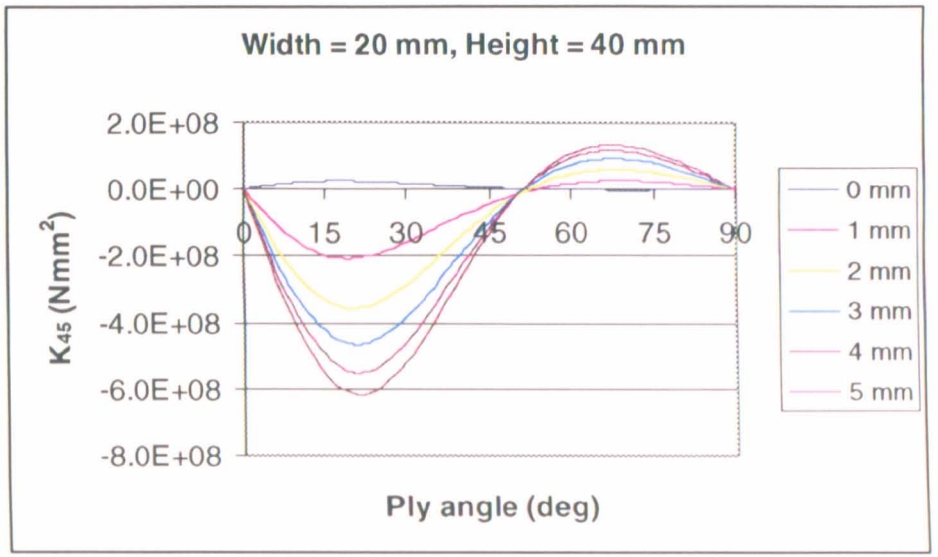
Width = 20 mm, Height = 40 mm
2.0E+08
0.0E+00
-2.0E+08
-4.0E+08
-6.0E+08
-8.0E+08
0
15
30
45
60
75
90
K45 (Nmm2)
Ply angle (deg)
0 mm
1 mm
2 mm
3 mm
4 mm
5 mm

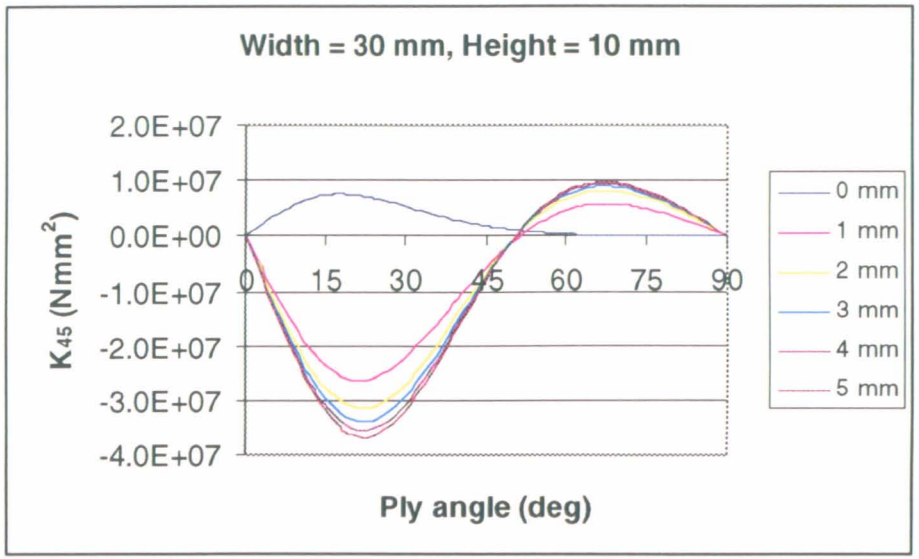
Width = 30 mm, Height = 10 mm
2.0E+07
1.0E+07
0.0E+00
-1.0E+07
-2.0E+07
-3.0E+07
-4.0E+07
0
15
30
45
60
75
90
K45 (Nmm2)
Ply angle (deg)
0 mm
1 mm
2 mm
3 mm
4 mm
5 mm

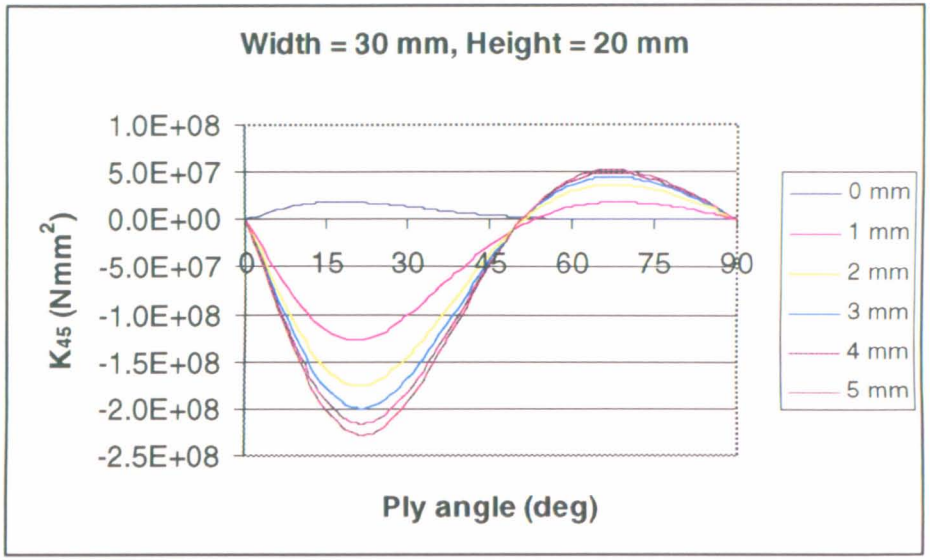
Width = 30 mm, Height = 20 mm
1.0E+08
5.0E+07
0.0E+00
-5.0E+07
-1.0E+08
-1.5E+08
-2.0E+08
-2.5E+08
0
15
30
45
60
75
90
K45 (Nmm2)
Ply angle (deg)
0 mm
1 mm
2 mm
3 mm
4 mm
5 mm

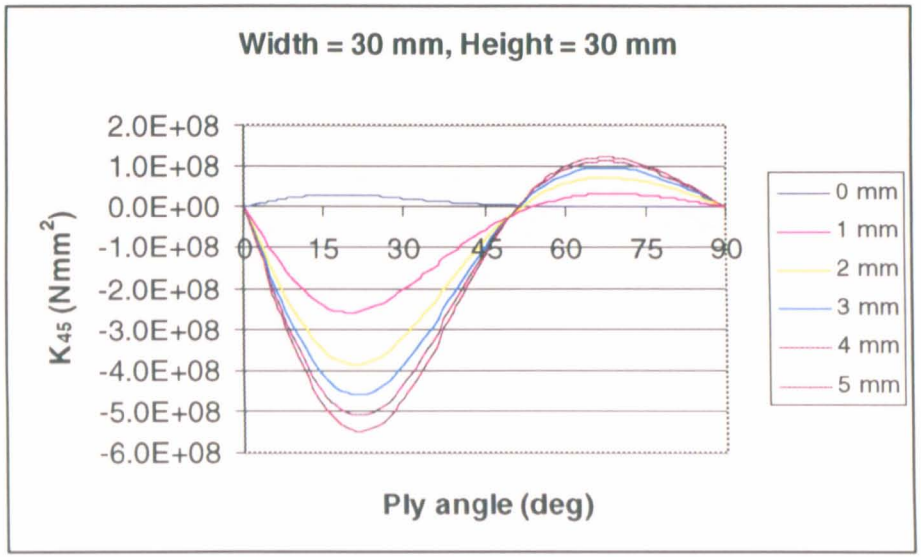
Width = 30 mm, Height = 30 mm
2.0E+08
1.0E+08
0.0E+00
-1.0E+08
-2.0E+08
-3.0E+08
-4.0E+08
-5.0E+08
-6.0E+08
0
15
30
45
60
75
90
K45 (Nmm2)
Ply angle (deg)
0 mm
1 mm
2 mm
3 mm
4 mm
5 mm

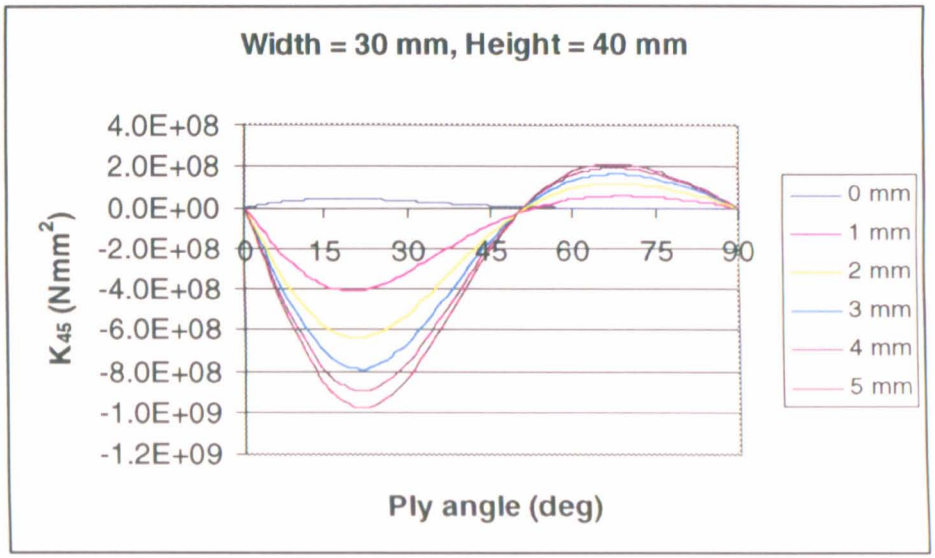
Width = 30 mm, Height = 40 mm
4.0E+08
2.0E+08
0.0E+00
-2.0E+08
-4.0E+08
-6.0E+08
-8.0E+08
-1.0E+09
-1.2E+09
0
15
30
45
60
75
90
K45 (Nmm2)
Ply angle (deg)
0 mm
1 mm
2 mm
3 mm
4 mm
5 mm

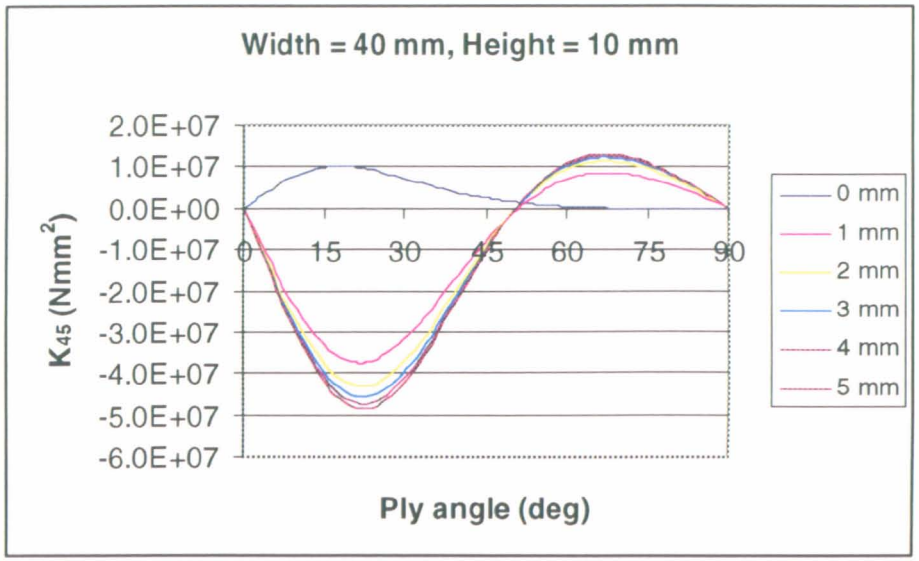
Width = 40 mm, Height = 10 mm
2.0E+07
1.0E+07
0.0E+00
-1.0E+07
-2.0E+07
-3.0E+07
-4.0E+07
-5.0E+07
-6.0E+07
0
15
30
45
60
75
90
K45 (Nmm2)
Ply angle (deg)
0 mm
1 mm
2 mm
3 mm
4 mm
5 mm

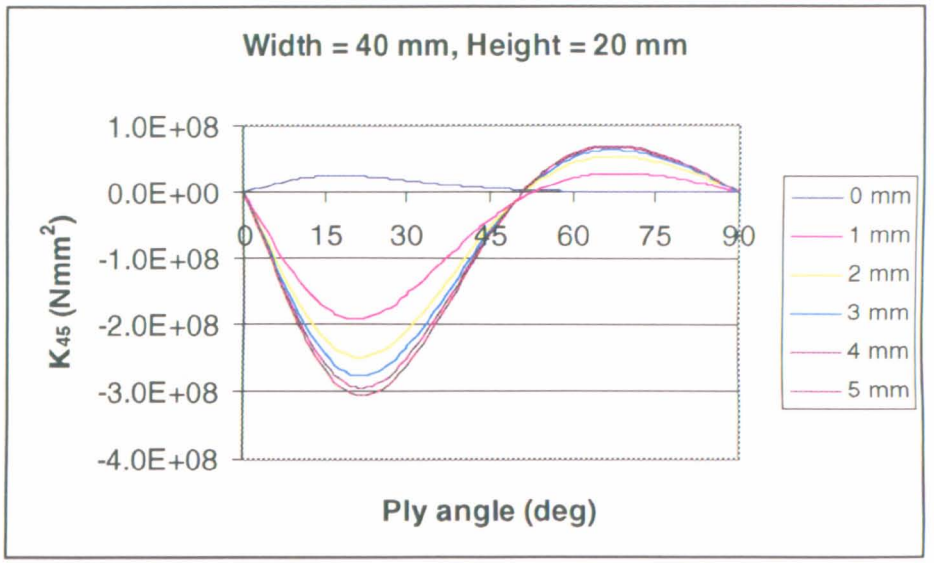
Width = 40 mm, Height = 20 mm
1.0E+08
0.0E+00
-1.0E+08
-2.0E+08
-3.0E+08
-4.0E+08
0
15
30
45
60
75
90
K45 (Nmm2)
Ply angle (deg)
0 mm
1 mm
2 mm
3 mm
4 mm
5 mm

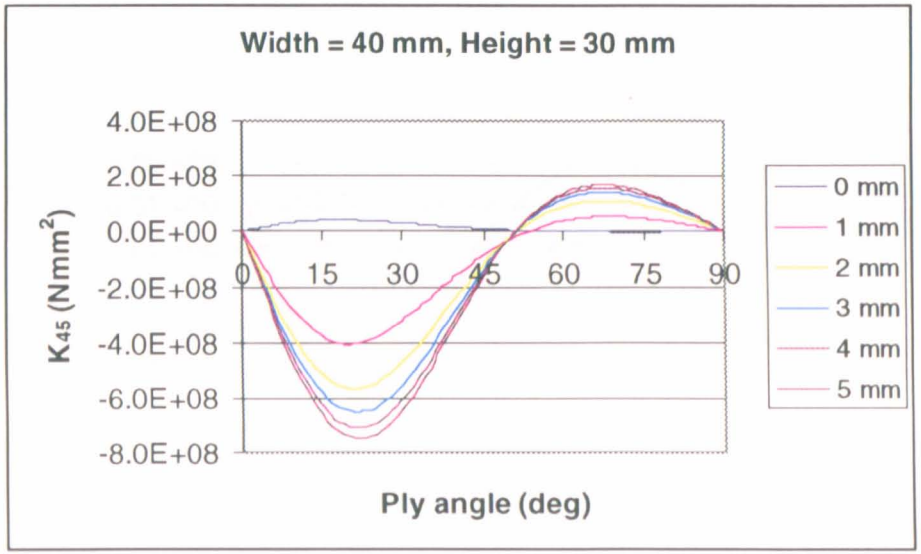
Width = 40 mm, Height = 30 mm
4.0E+08
2.0E+08
0.0E+00
-2.0E+08
-4.0E+08
-6.0E+08
-8.0E+08
0
15
30
45
60
75
90
K45 (Nmm2)
Ply angle (deg)
0 mm
1 mm
2 mm
3 mm
4 mm
5 mm

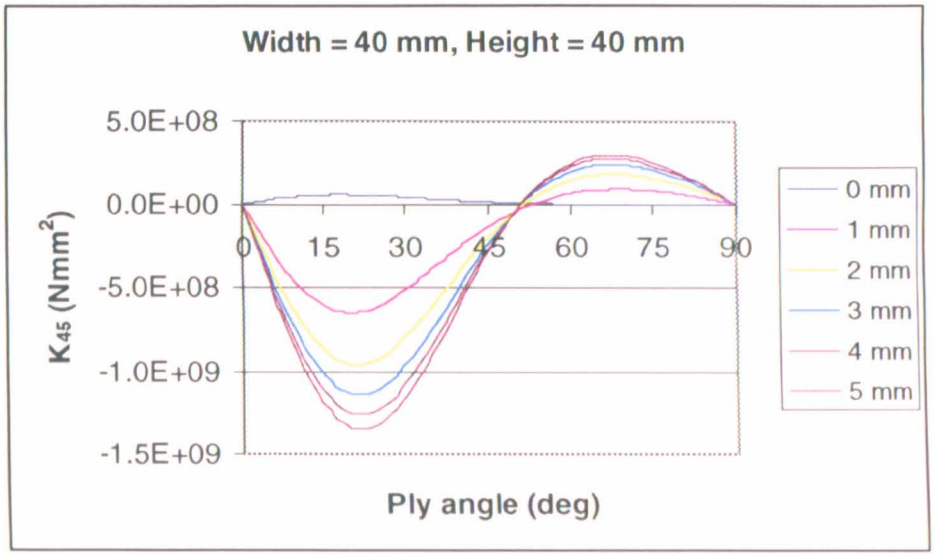
Width = 40 mm, Height = 40 mm
5.0E+08
0.0E+00
-5.0E+08
-1.0E+09
-1.5E+09
0
15
30
45
60
75
90
K45 (Nmm2)
Ply angle (deg)
0 mm
1 mm
2 mm
3 mm
4 mm
5 mm

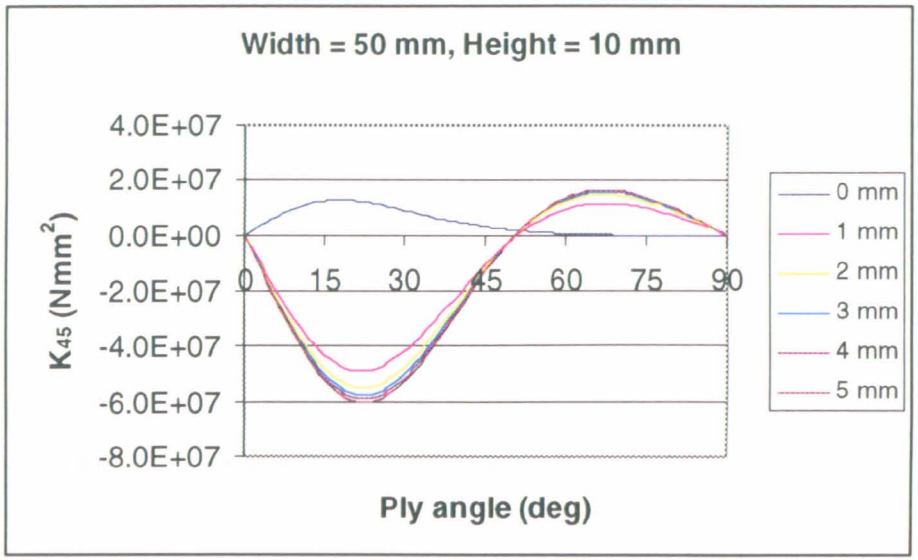
Width = 50 mm, Height = 10 mm
4.0E+07
2.0E+07
0.0E+00
-2.0E+07
-4.0E+07
-6.0E+07
-8.0E+07
K45 (Nmm2)
0
15
30
45
60
75
90
Ply angle (deg)
0 mm
1 mm
2 mm
3 mm
4 mm
5 mm

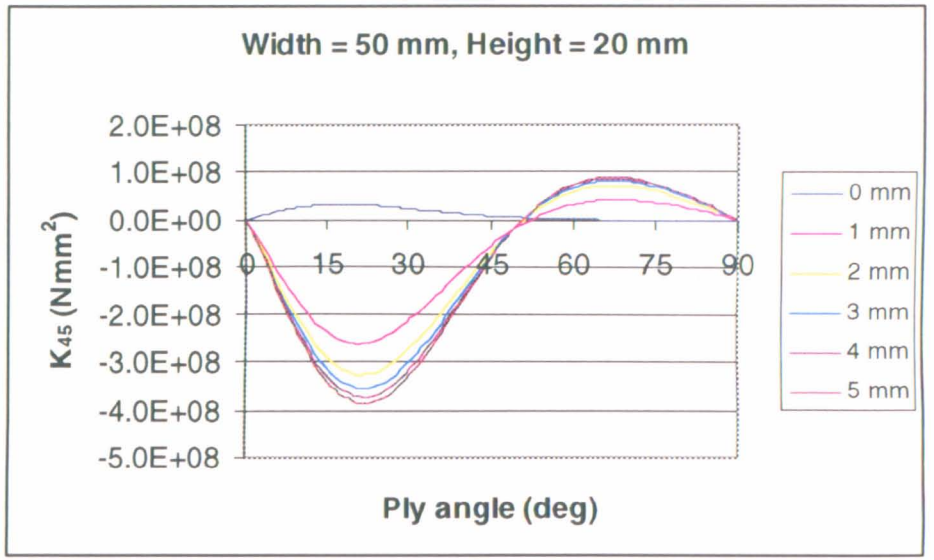
Width = 50 mm, Height = 20 mm
2.0E+08
1.0E+08
0.0E+00
-1.0E+08
-2.0E+08
-3.0E+08
-4.0E+08
-5.0E+08
K45 (Nmm2)
0
15
30
45
60
75
90
Ply angle (deg)
0 mm
1 mm
2 mm
3 mm
4 mm
5 mm

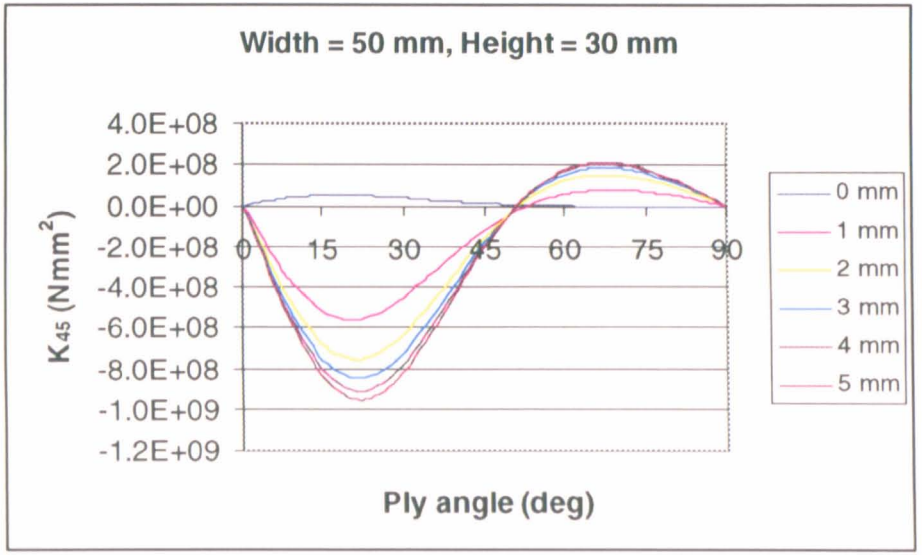
Width = 50 mm, Height = 30 mm
4.0E+08
2.0E+08
0.0E+00
-2.0E+08
-4.0E+08
-6.0E+08
-8.0E+08
-1.0E+09
-1.2E+09
K45 (Nmm2)
0
15
30
45
60
75
90
Ply angle (deg)
0 mm
1 mm
2 mm
3 mm
4 mm
5 mm

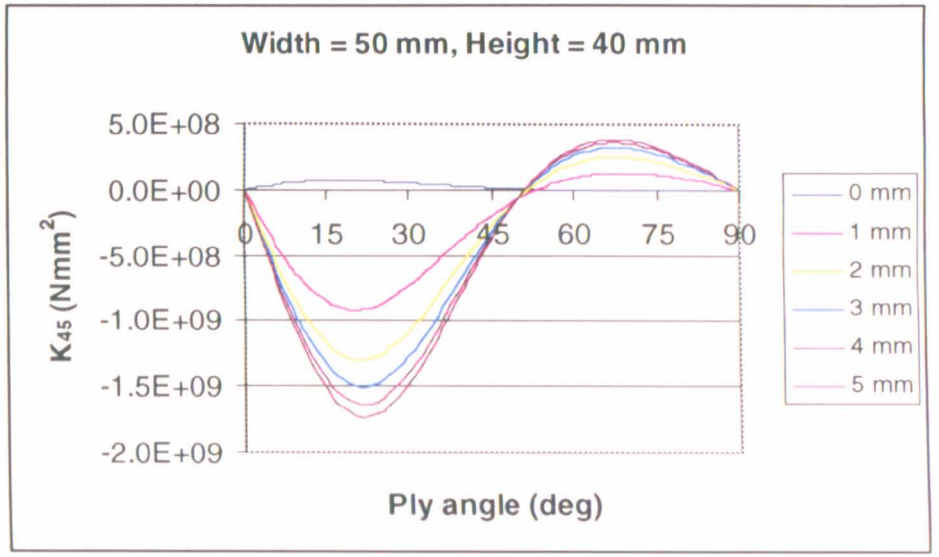
Width = 50 mm, Height = 40 mm
5.0E+08
0.0E+00
-5.0E+08
-1.0E+09
-1.5E+09
-2.0E+09
K45 (Nmm2)
0
15
30
45
60
75
90
Ply angle (deg)
0 mm
1 mm
2 mm
3 mm
4 mm
5 mm

APPENDIX 4.6

Comparison of Analytical and Finite Element results for Box Sections

Peak value of K_{45} is shown for:

Width in 10 mm increments from 10mm to 50mm

Height in 10 mm increments from 10mm to 40mm

Vertical wall thickness in 1mm increments from 1mm to 5mm

1 mm vertical wall thickness

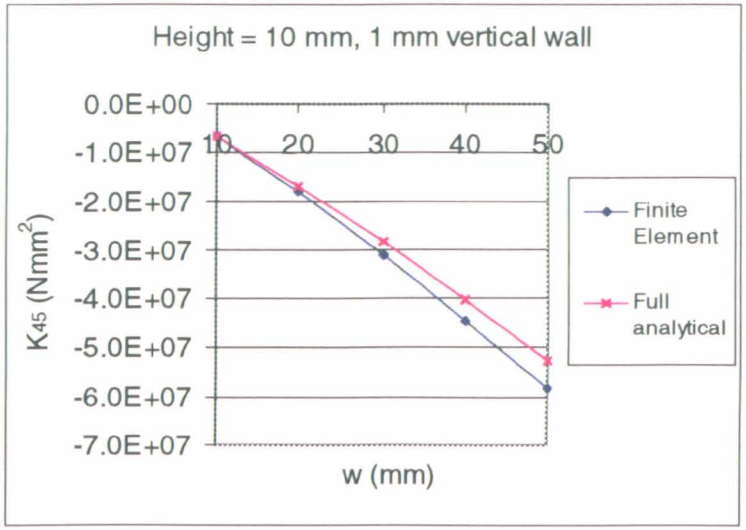

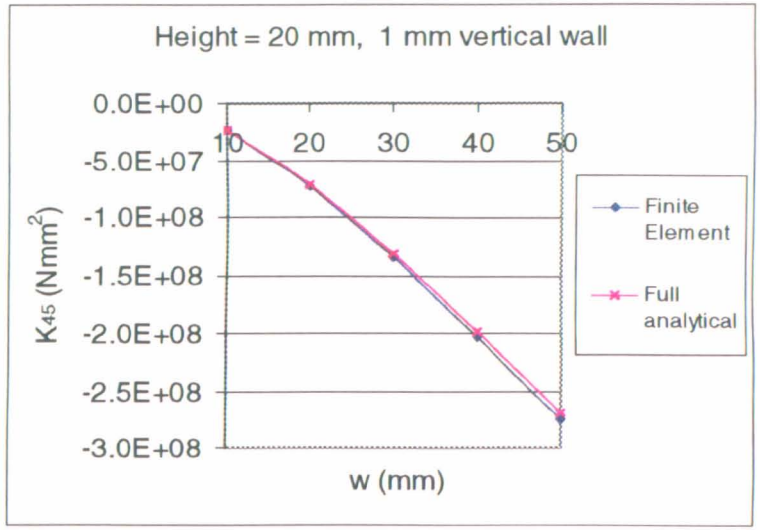

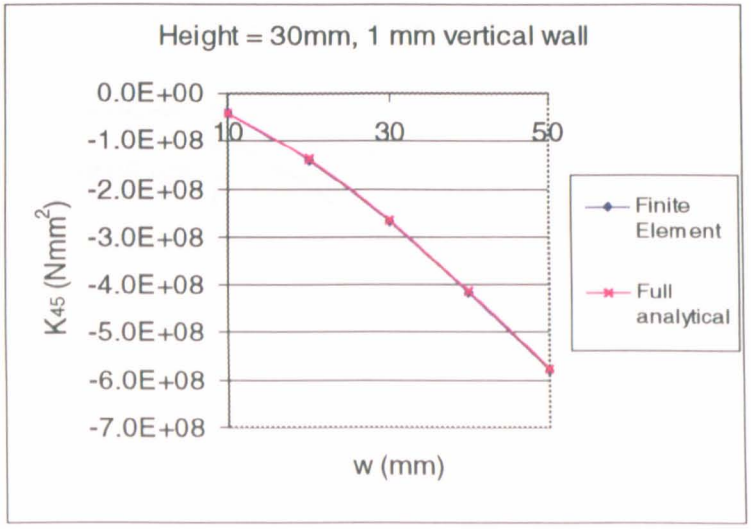

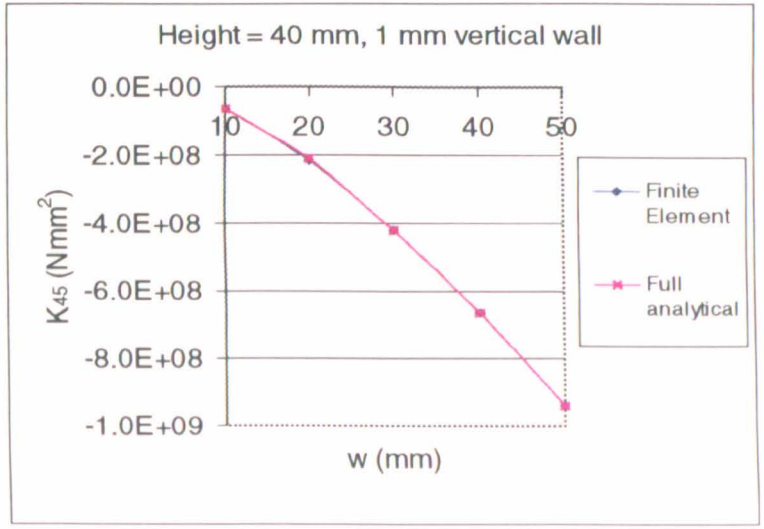

2 mm vertical wall thickness

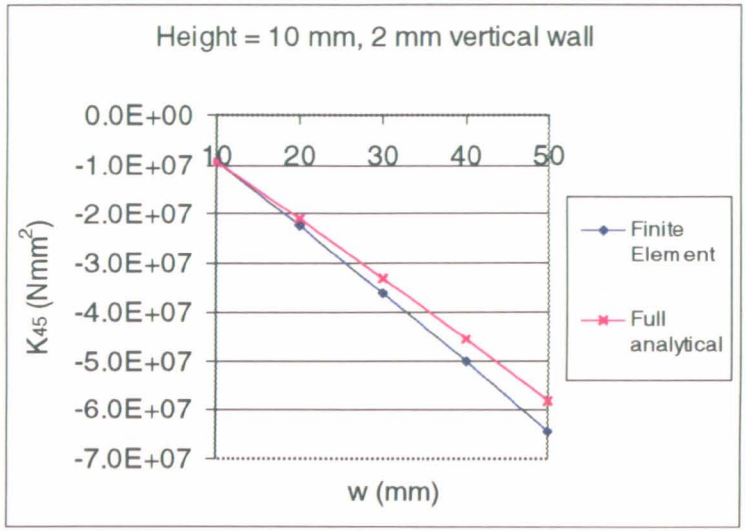

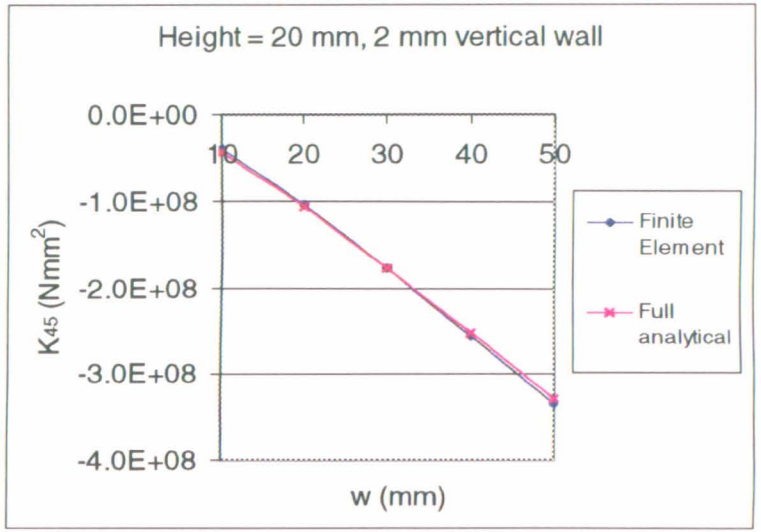

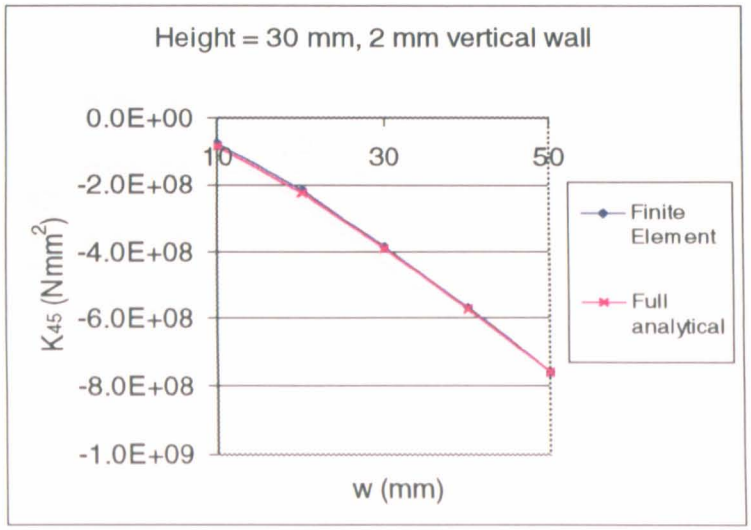

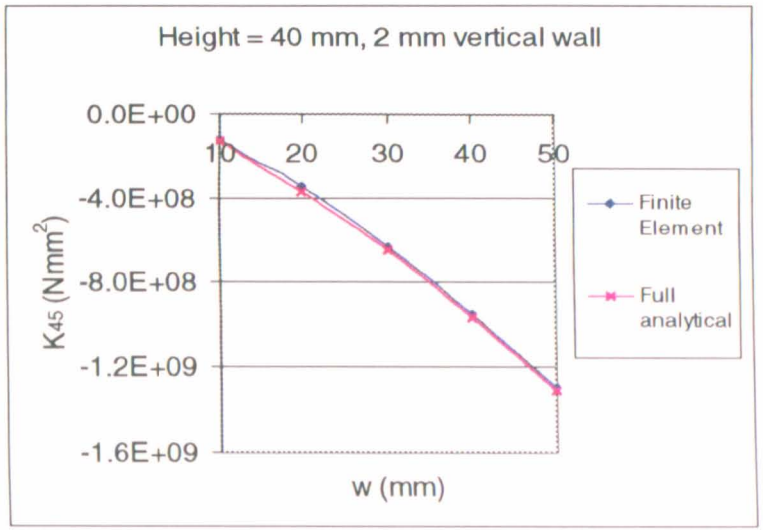

3 mm vertical wall thickness

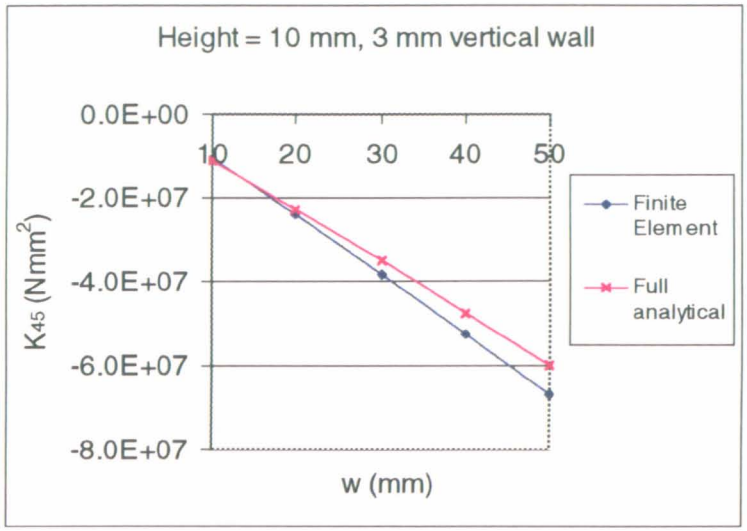

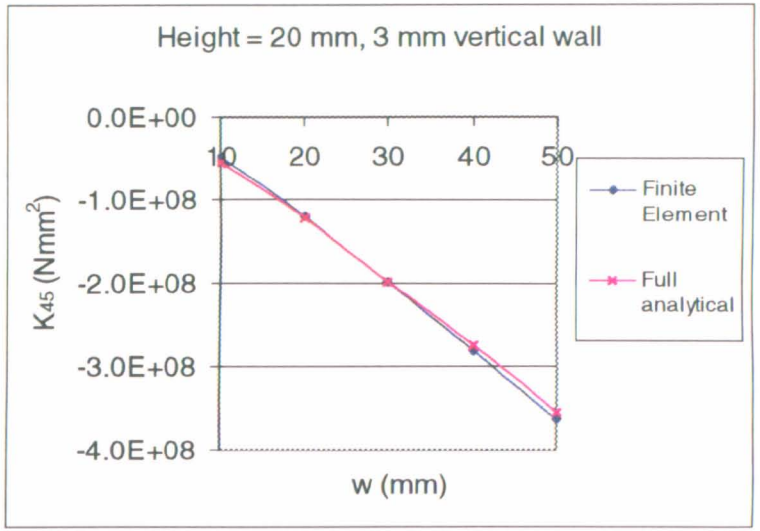

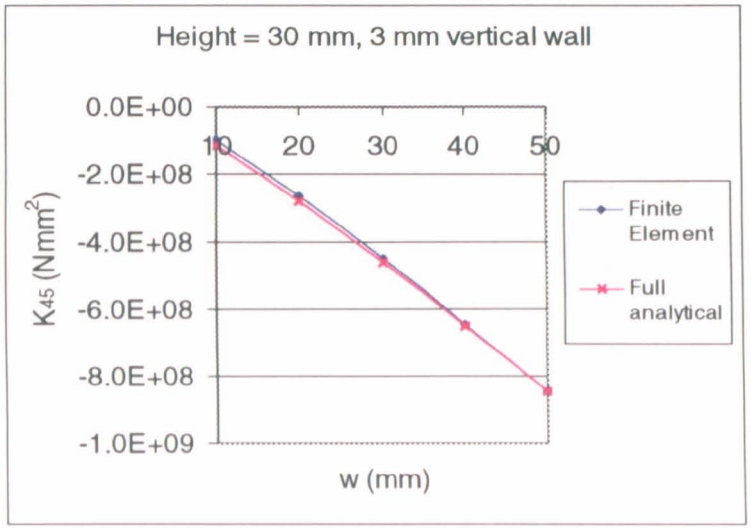

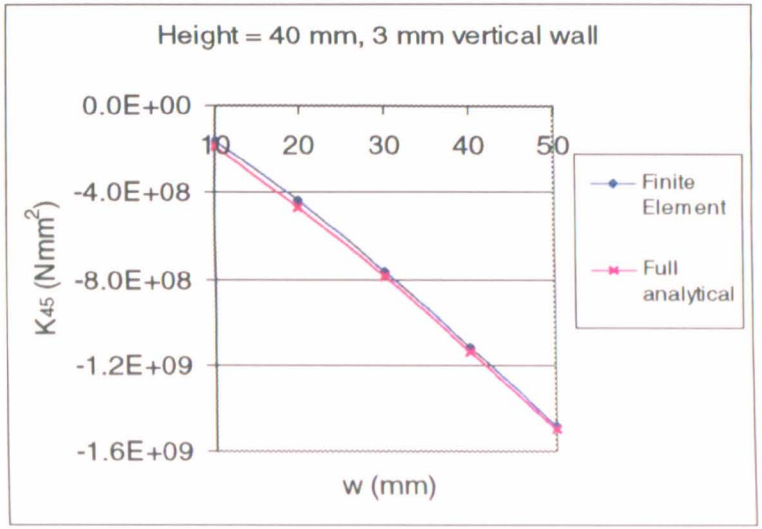

4 mm vertical wall thickness

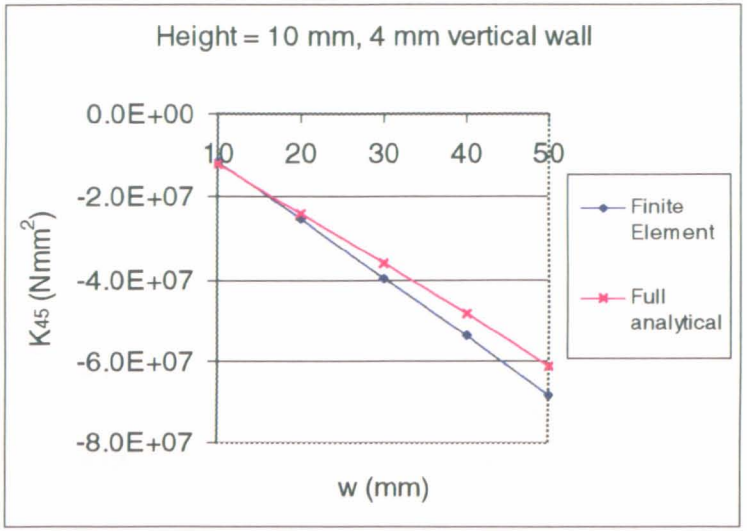

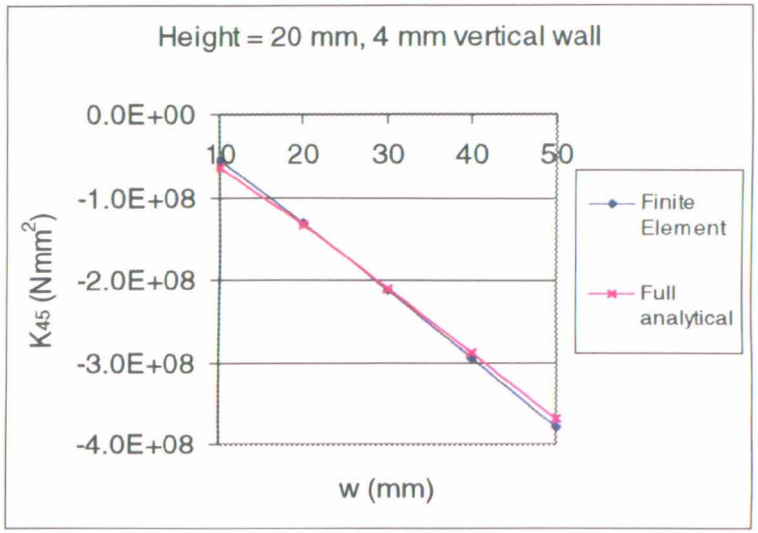

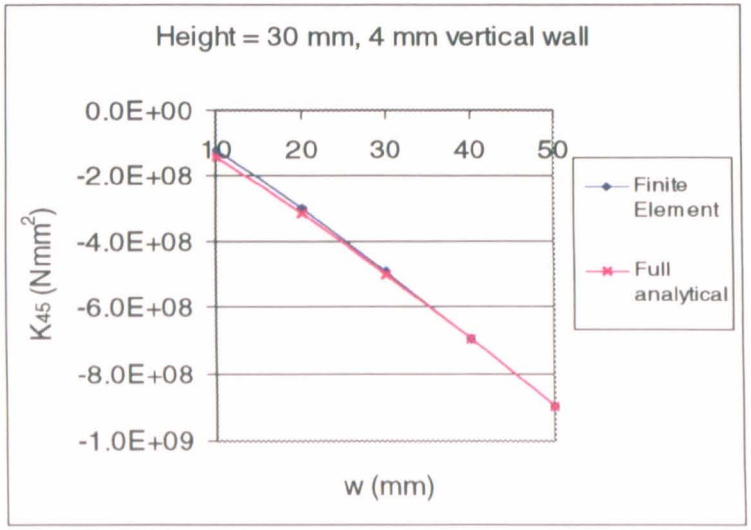

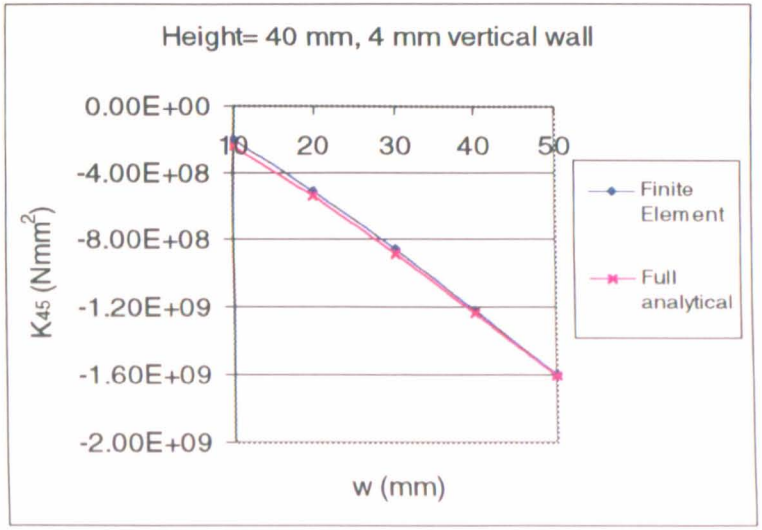

5 mm vertical wall thickness

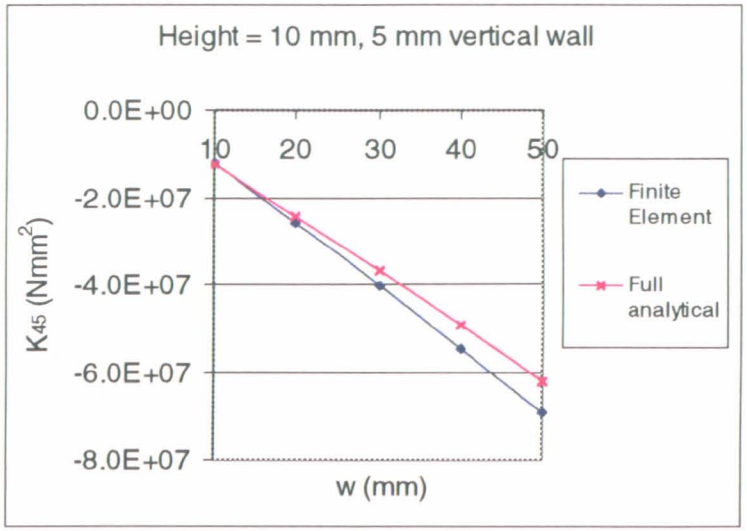

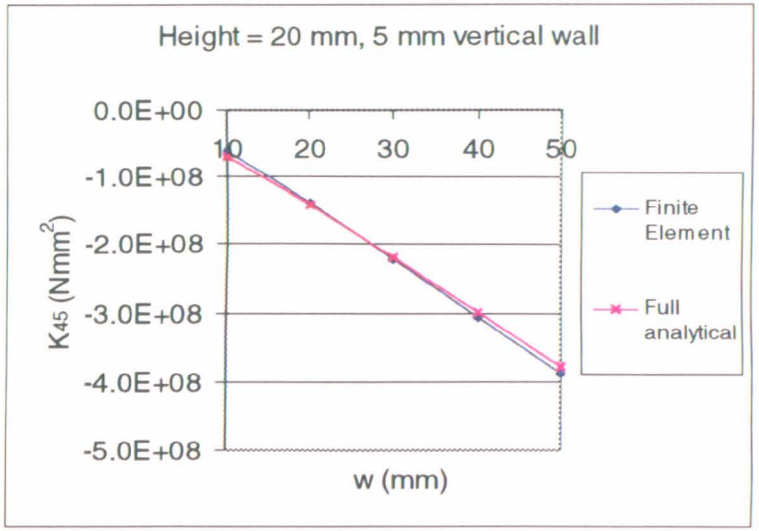

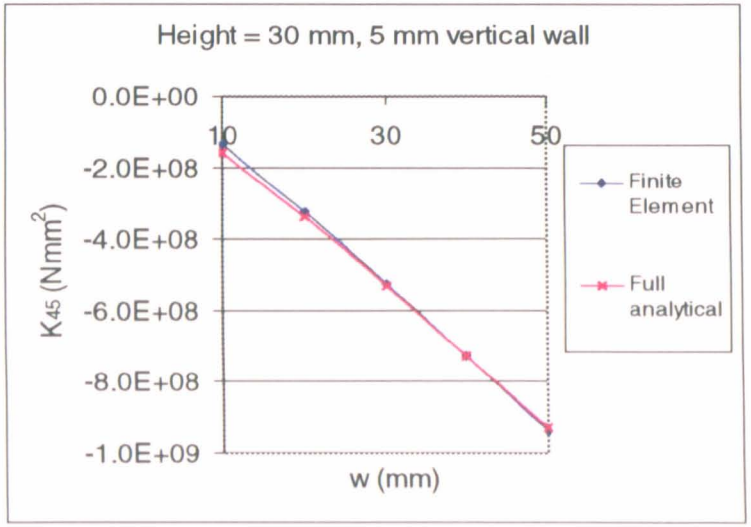

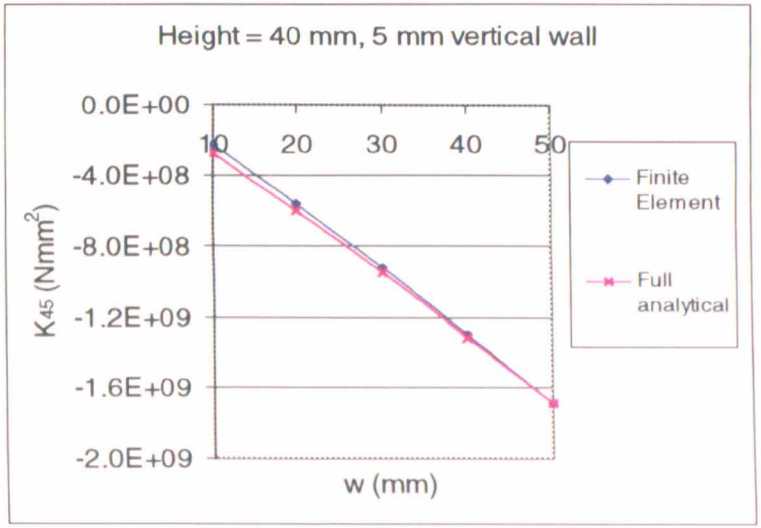

APPENDIX 4.7

Smith's analytical results for box sections

Variation of K_{45} with orientation of coupling plies is shown for:

Width in 10 mm increments from 10mm to 50mm

Height in 10 mm increments from 10mm to 40mm

Vertical wall thickness in 1mm increments from 0mm to 5mm

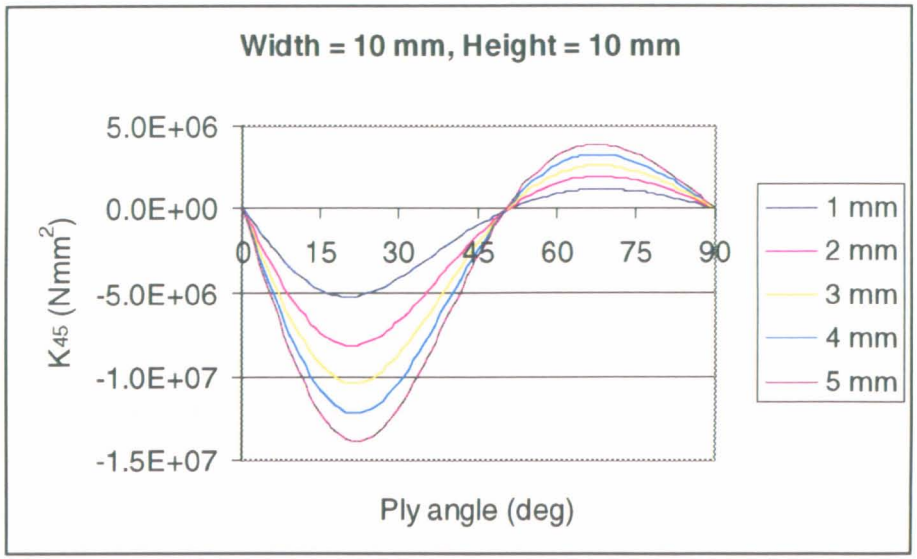
Width = 10 mm, Height = 10 mm
5.0E+06
0.0E+00
-5.0E+06
-1.0E+07
-1.5E+07
K45 (Nmm2)
0
15
30
45
60
75
90
Ply angle (deg)
1 mm
2 mm
3 mm
4 mm
5 mm

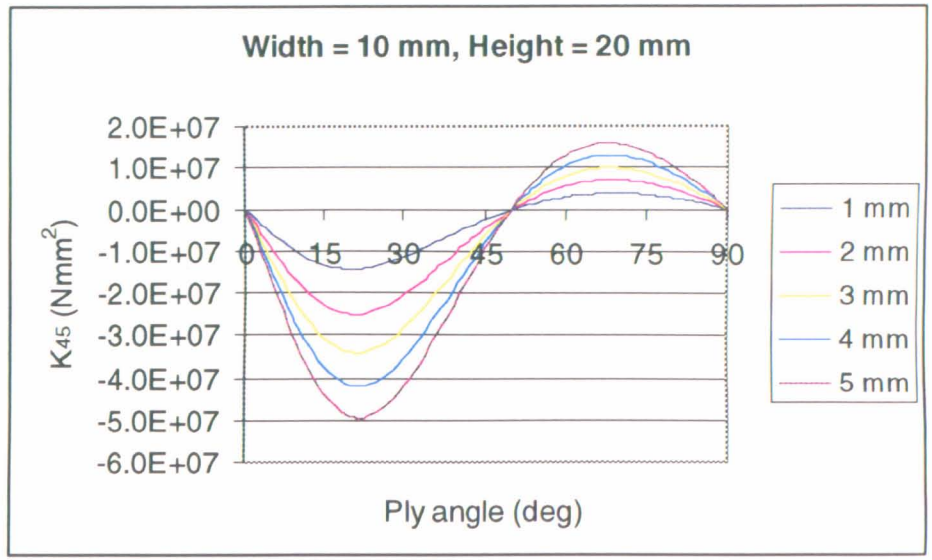
Width = 10 mm, Height = 20 mm
2.0E+07
1.0E+07
0.0E+00
-1.0E+07
-2.0E+07
-3.0E+07
-4.0E+07
-5.0E+07
-6.0E+07
K45 (Nmm2)
0
15
30
45
60
75
90
Ply angle (deg)
1 mm
2 mm
3 mm
4 mm
5 mm

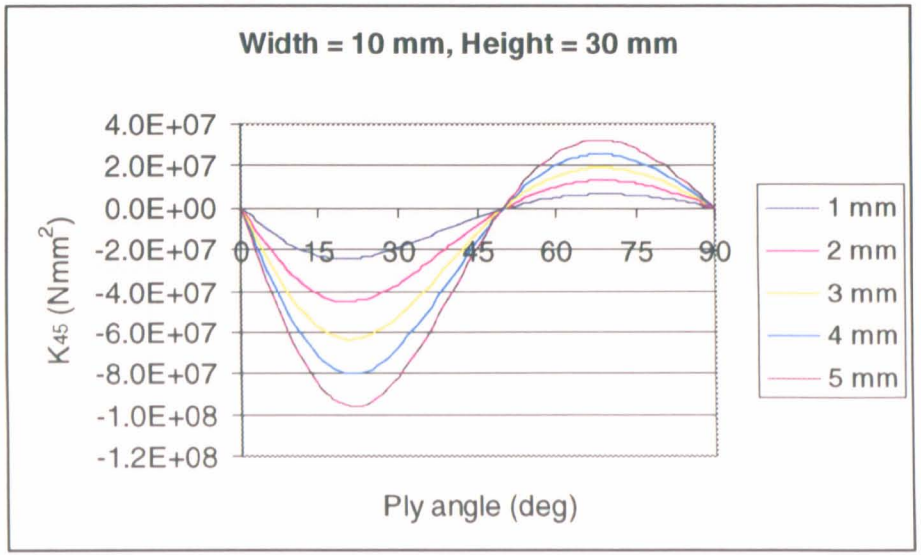
Width = 10 mm, Height = 30 mm
4.0E+07
2.0E+07
0.0E+00
-2.0E+07
-4.0E+07
-6.0E+07
-8.0E+07
-1.0E+08
-1.2E+08
K45 (Nmm2)
0
15
30
45
60
75
90
Ply angle (deg)
1 mm
2 mm
3 mm
4 mm
5 mm

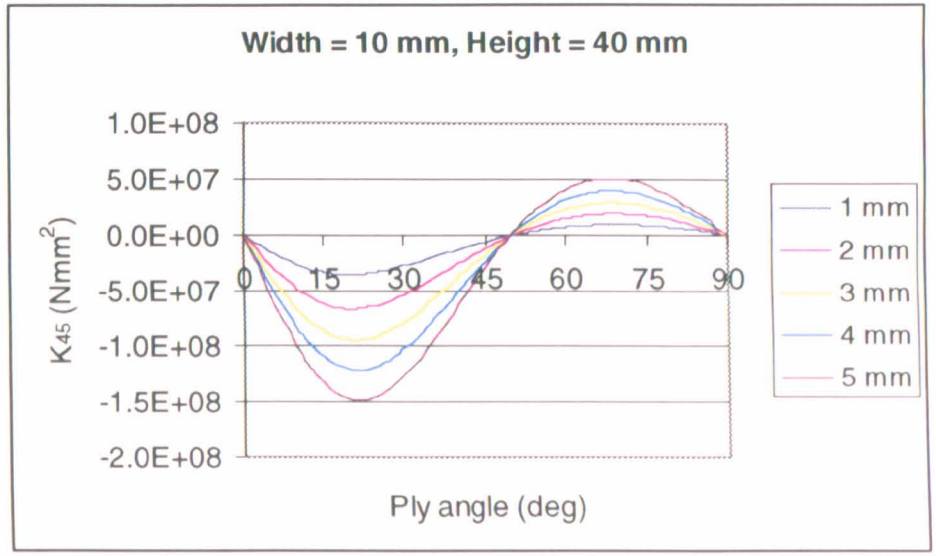
Width = 10 mm, Height = 40 mm
1.0E+08
5.0E+07
0.0E+00
-5.0E+07
-1.0E+08
-1.5E+08
-2.0E+08
K45 (Nmm2)
0
15
30
45
60
75
90
Ply angle (deg)
1 mm
2 mm
3 mm
4 mm
5 mm

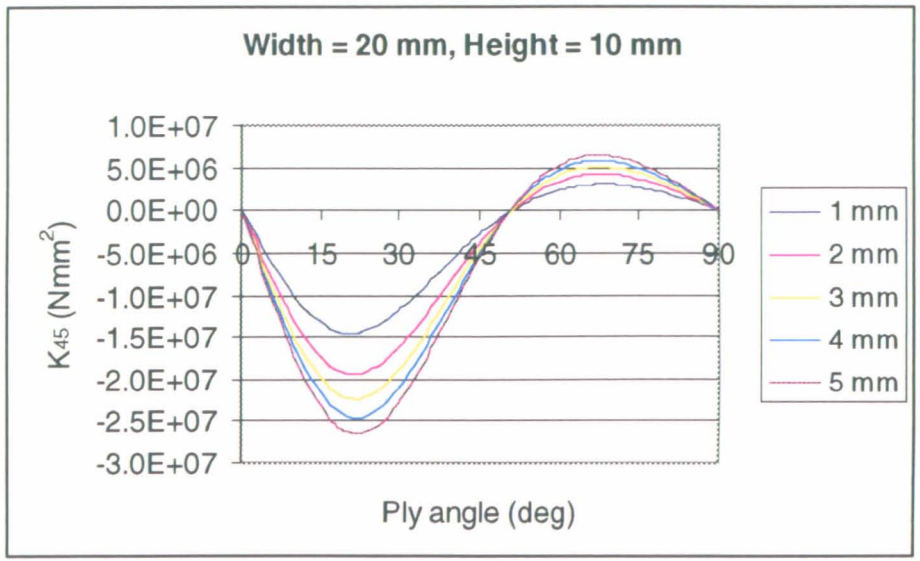
Width = 20 mm, Height = 10 mm
1.0E+07
5.0E+06
0.0E+00
-5.0E+06
-1.0E+07
-1.5E+07
-2.0E+07
-2.5E+07
-3.0E+07
K45 (Nmm2)
0
15
30
45
60
75
90
Ply angle (deg)
1 mm
2 mm
3 mm
4 mm
5 mm

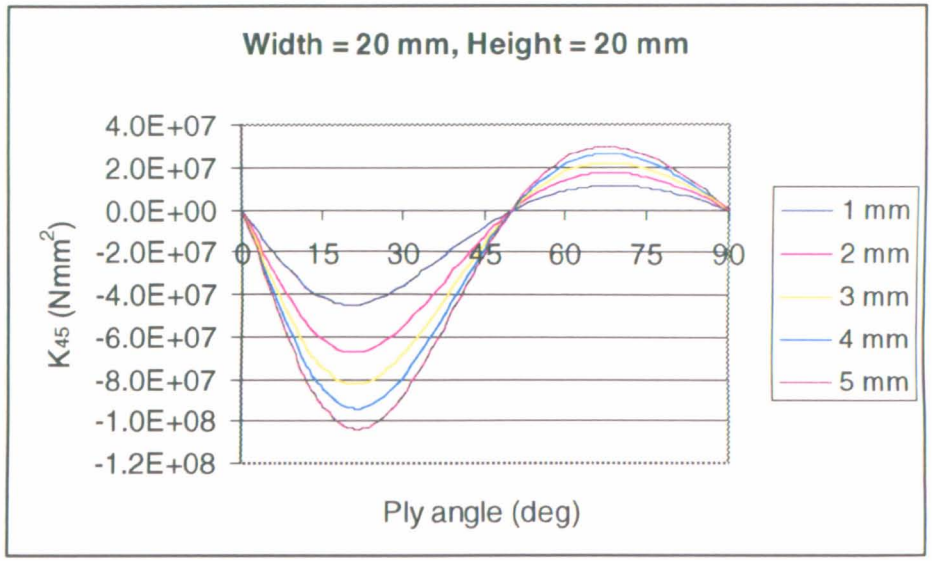
Width = 20 mm, Height = 20 mm
4.0E+07
2.0E+07
0.0E+00
-2.0E+07
-4.0E+07
-6.0E+07
-8.0E+07
-1.0E+08
-1.2E+08
K45 (Nmm2)
0
15
30
45
60
75
90
Ply angle (deg)
1 mm
2 mm
3 mm
4 mm
5 mm

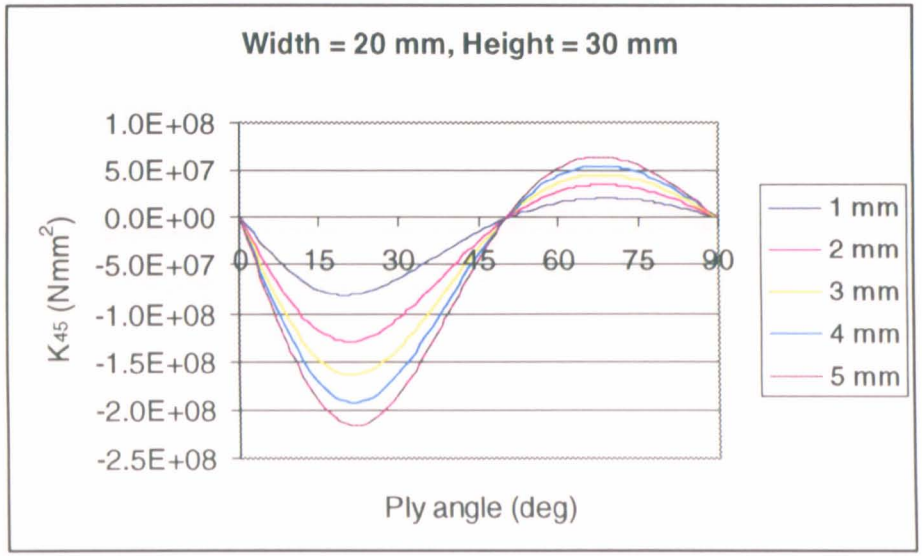
Width = 20 mm, Height = 30 mm
1.0E+08
5.0E+07
0.0E+00
-5.0E+07
-1.0E+08
-1.5E+08
-2.0E+08
-2.5E+08
K45 (Nmm2)
0
15
30
45
60
75
90
Ply angle (deg)
1 mm
2 mm
3 mm
4 mm
5 mm

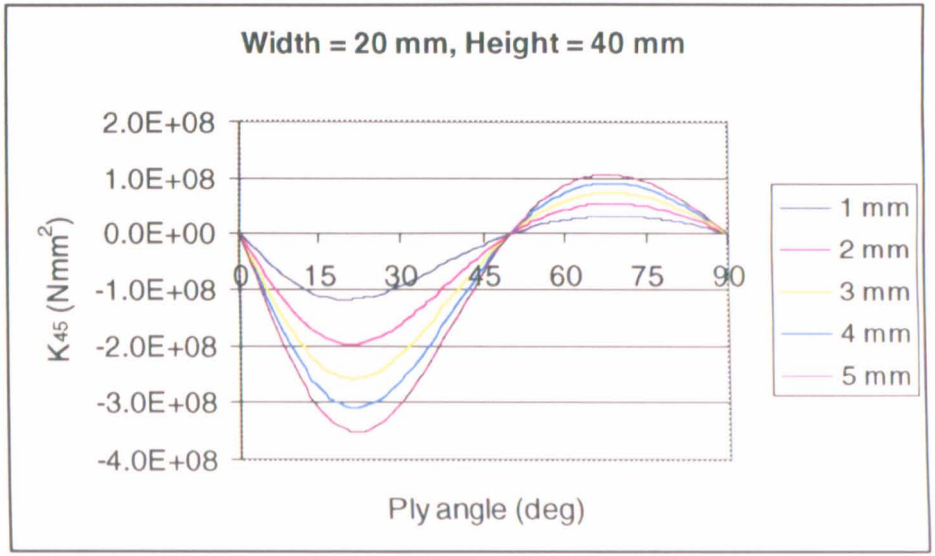
Width = 20 mm, Height = 40 mm
2.0E+08
1.0E+08
0.0E+00
-1.0E+08
-2.0E+08
-3.0E+08
-4.0E+08
K45 (Nmm2)
0
15
30
45
60
75
90
Ply angle (deg)
1 mm
2 mm
3 mm
4 mm
5 mm

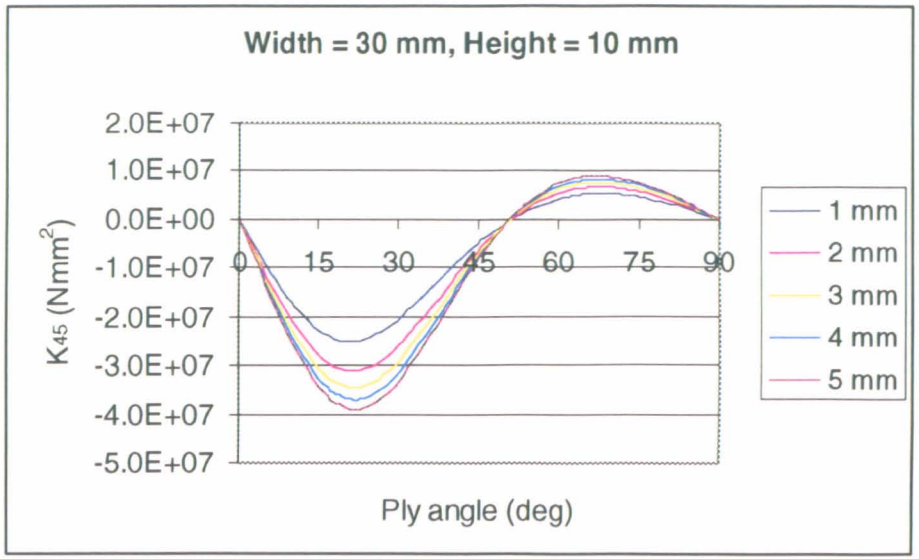
Width = 30 mm, Height = 10 mm
2.0E+07
1.0E+07
0.0E+00
-1.0E+07
-2.0E+07
-3.0E+07
-4.0E+07
-5.0E+07
K45 (Nmm2)
0
15
30
45
60
75
90
Ply angle (deg)
1 mm
2 mm
3 mm
4 mm
5 mm

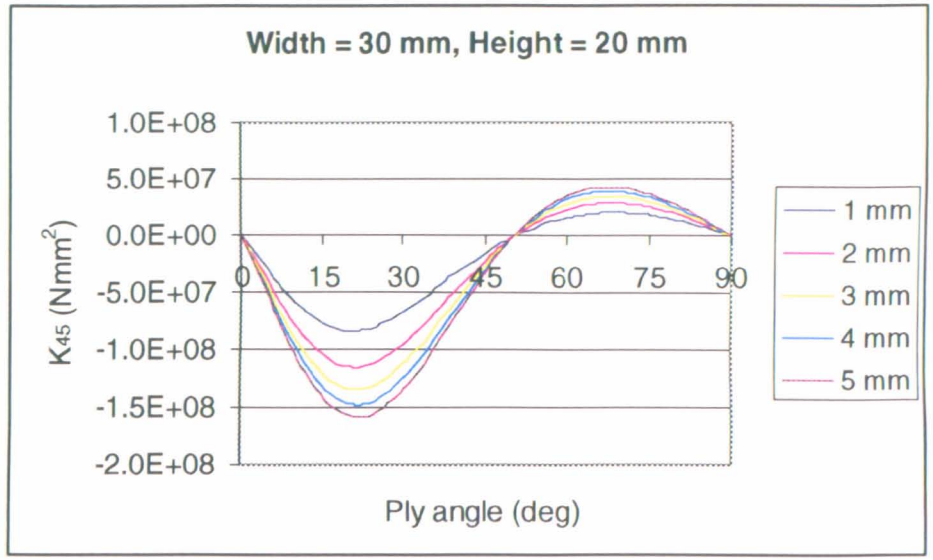
Width = 30 mm, Height = 20 mm
1.0E+08
5.0E+07
0.0E+00
-5.0E+07
-1.0E+08
-1.5E+08
-2.0E+08
K45 (Nmm2)
0
15
30
45
60
75
90
Ply angle (deg)
1 mm
2 mm
3 mm
4 mm
5 mm

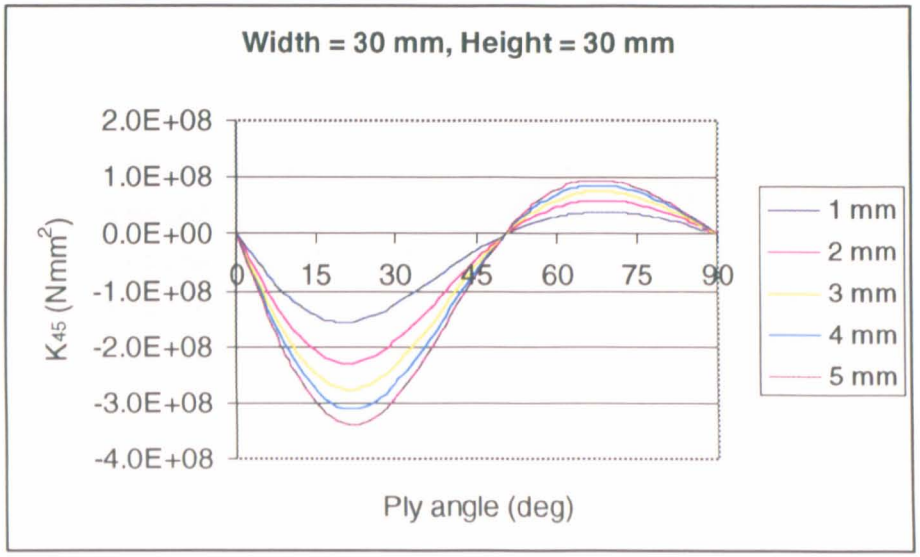
Width = 30 mm, Height = 30 mm
2.0E+08
1.0E+08
0.0E+00
-1.0E+08
-2.0E+08
-3.0E+08
-4.0E+08
K45 (Nmm2)
0
15
30
45
60
75
90
Ply angle (deg)
1 mm
2 mm
3 mm
4 mm
5 mm

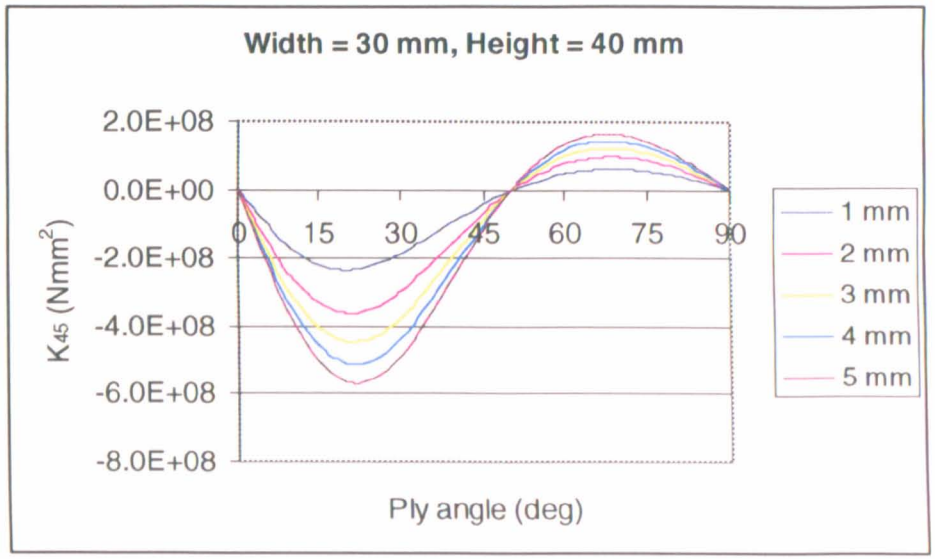
Width = 30 mm, Height = 40 mm
2.0E+08
0.0E+00
-2.0E+08
-4.0E+08
-6.0E+08
-8.0E+08
K45 (Nmm2)
0
15
30
45
60
75
90
Ply angle (deg)
1 mm
2 mm
3 mm
4 mm
5 mm

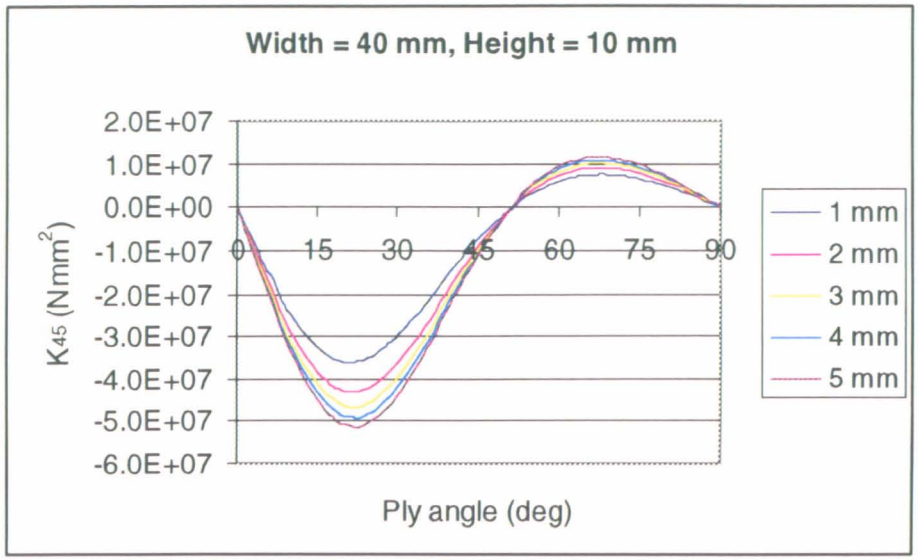
Width = 40 mm, Height = 10 mm
2.0E+07
1.0E+07
0.0E+00
-1.0E+07
-2.0E+07
-3.0E+07
-4.0E+07
-5.0E+07
-6.0E+07
0
15
30
45
60
75
90
K45 (Nmm2)
Ply angle (deg)
1 mm
2 mm
3 mm
4 mm
5 mm

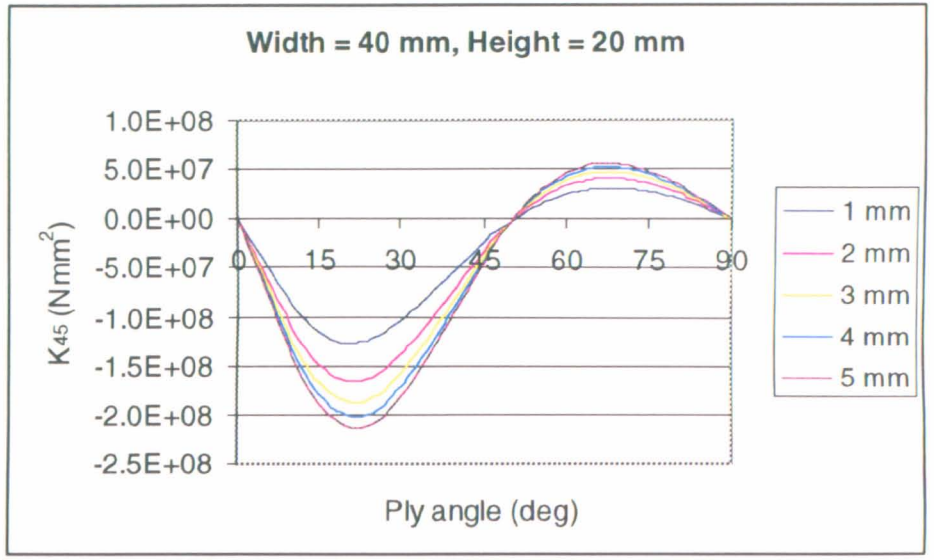
Width = 40 mm, Height = 20 mm
1.0E+08
5.0E+07
0.0E+00
-5.0E+07
-1.0E+08
-1.5E+08
-2.0E+08
-2.5E+08
0
15
30
45
60
75
90
K45 (Nmm2)
Ply angle (deg)
1 mm
2 mm
3 mm
4 mm
5 mm

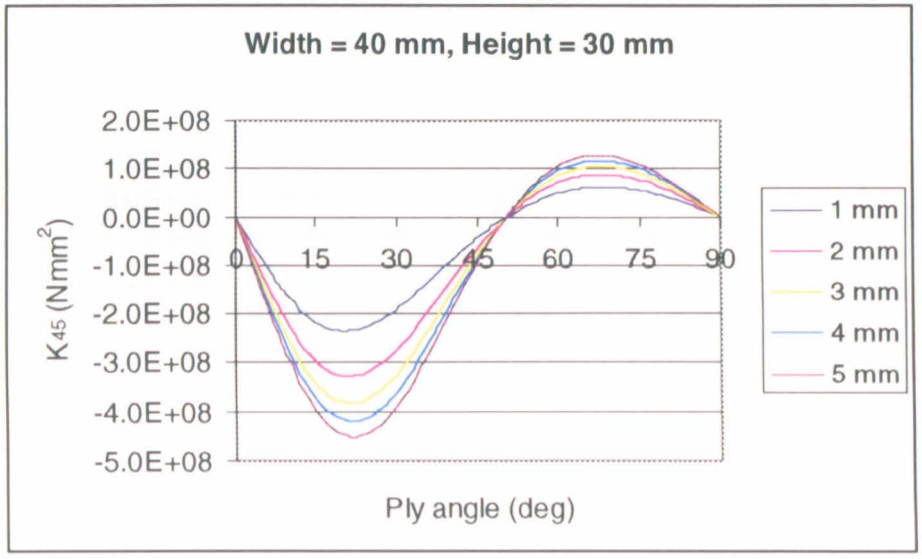
Width = 40 mm, Height = 30 mm
2.0E+08
1.0E+08
0.0E+00
-1.0E+08
-2.0E+08
-3.0E+08
-4.0E+08
-5.0E+08
0
15
30
45
60
75
90
K45 (Nmm2)
Ply angle (deg)
1 mm
2 mm
3 mm
4 mm
5 mm

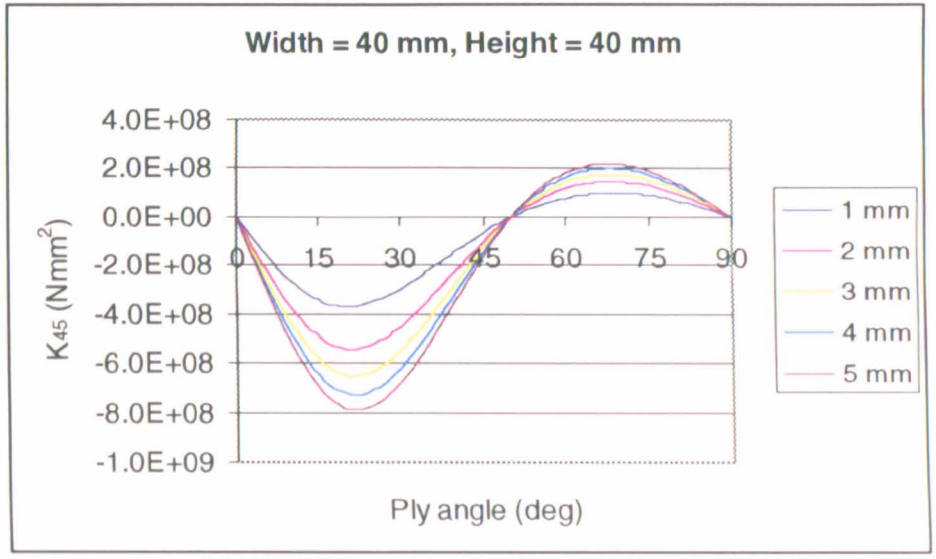
Width = 40 mm, Height = 40 mm
4.0E+08
2.0E+08
0.0E+00
-2.0E+08
-4.0E+08
-6.0E+08
-8.0E+08
-1.0E+09
0
15
30
45
60
75
90
K45 (Nmm2)
Ply angle (deg)
1 mm
2 mm
3 mm
4 mm
5 mm

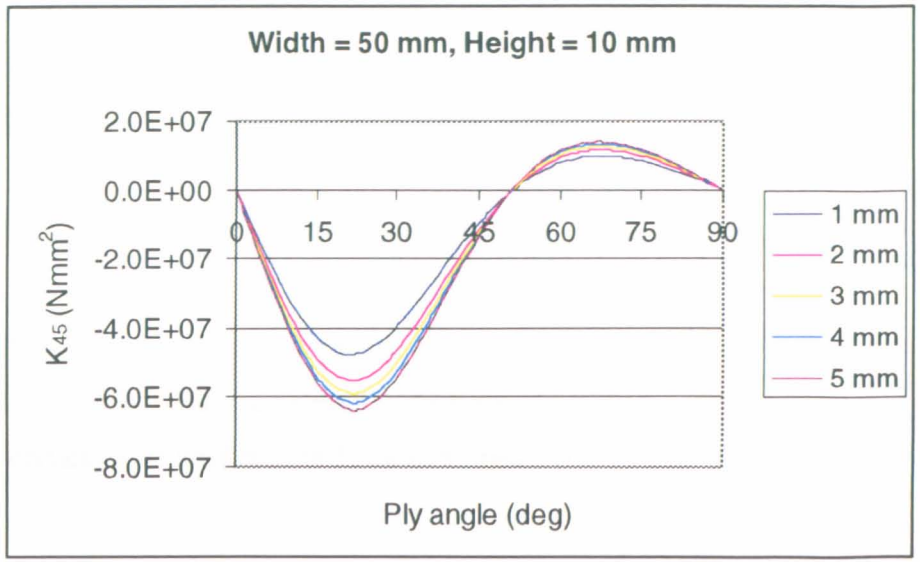
Width = 50 mm, Height = 10 mm
2.0E+07
0.0E+00
-2.0E+07
-4.0E+07
-6.0E+07
-8.0E+07
K45 (Nmm2)
0
15
30
45
60
75
90
Ply angle (deg)
1 mm
2 mm
3 mm
4 mm
5 mm

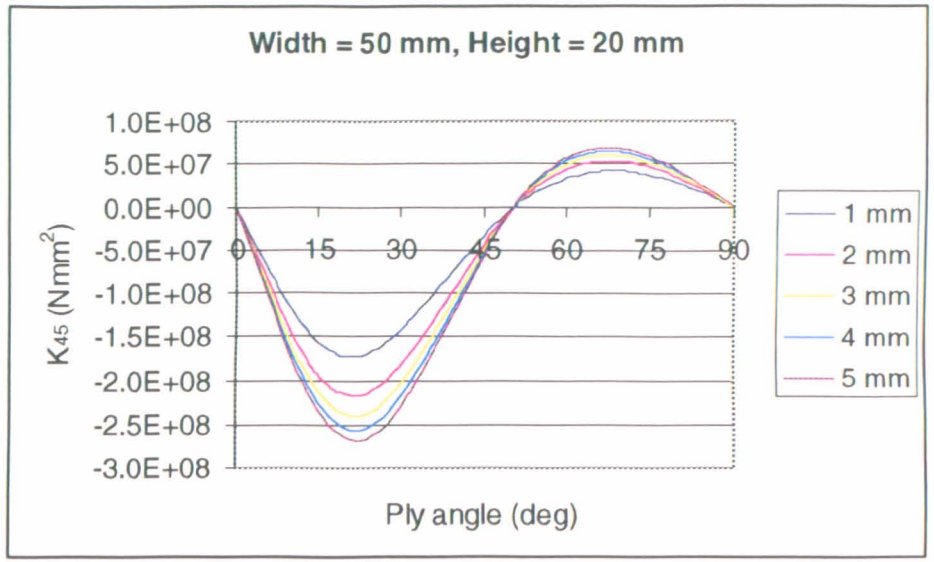
Width = 50 mm, Height = 20 mm
1.0E+08
5.0E+07
0.0E+00
-5.0E+07
-1.0E+08
-1.5E+08
-2.0E+08
-2.5E+08
-3.0E+08
K45 (Nmm2)
0
15
30
45
60
75
90
Ply angle (deg)
1 mm
2 mm
3 mm
4 mm
5 mm

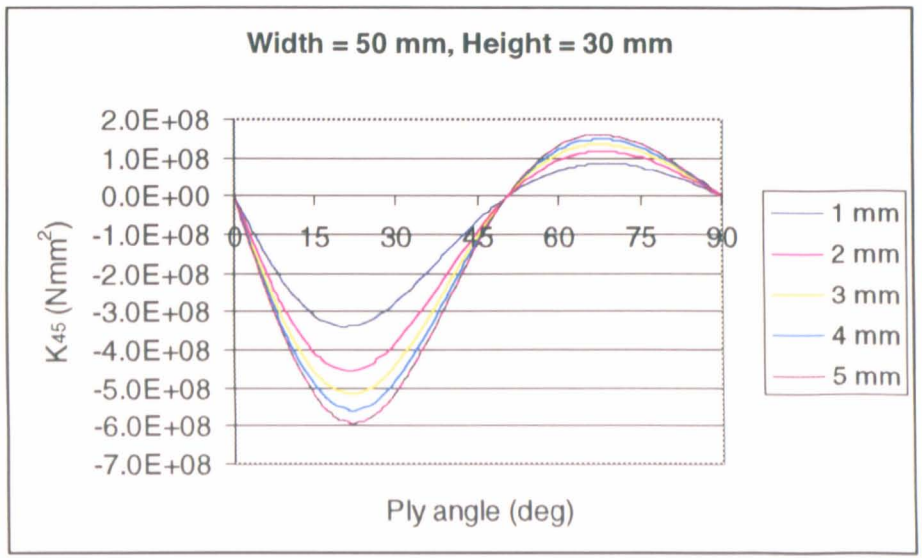
Width = 50 mm, Height = 30 mm
2.0E+08
1.0E+08
0.0E+00
-1.0E+08
-2.0E+08
-3.0E+08
-4.0E+08
-5.0E+08
-6.0E+08
-7.0E+08
K45 (Nmm2)
0
15
30
45
60
75
90
Ply angle (deg)
1 mm
2 mm
3 mm
4 mm
5 mm

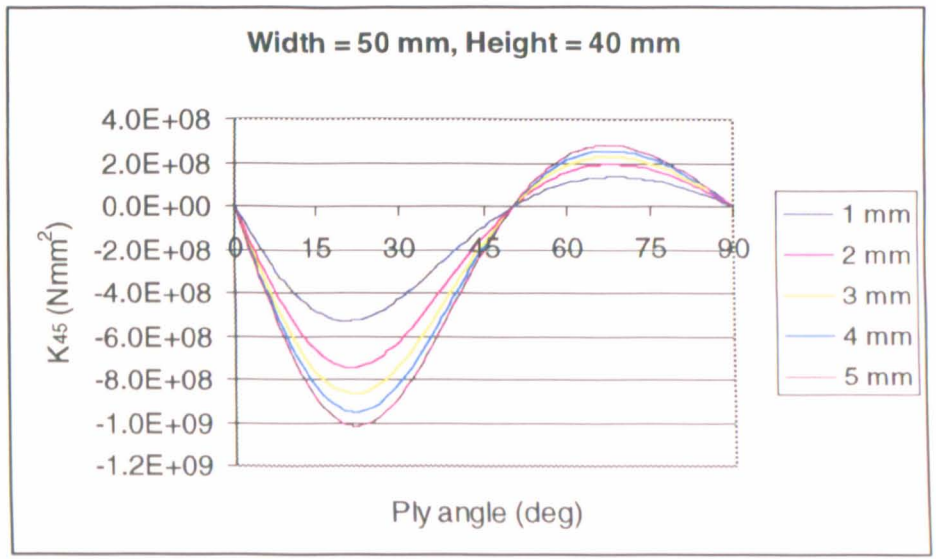
Width = 50 mm, Height = 40 mm
4.0E+08
2.0E+08
0.0E+00
-2.0E+08
-4.0E+08
-6.0E+08
-8.0E+08
-1.0E+09
-1.2E+09
K45 (Nmm2)
0
15
30
45
60
75
90
Ply angle (deg)
1 mm
2 mm
3 mm
4 mm
5 mm

APPENDIX 4.8

Rehfield's analytical results for box sections

Variation of K_{45} with orientation of coupling plies is shown for:

Width in 10 mm increments from 10mm to 50mm

Height in 10 mm increments from 10mm to 40mm

Vertical wall thickness in 1mm increments from 0mm to 5mm

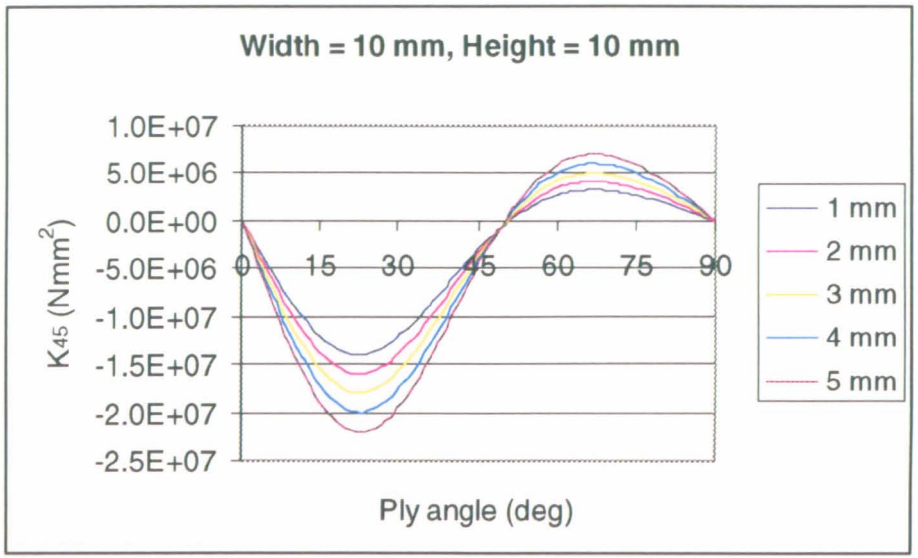
Width = 10 mm, Height = 10 mm
1.0E+07
5.0E+06
0.0E+00
-5.0E+06
-1.0E+07
-1.5E+07
-2.0E+07
-2.5E+07
K45 (Nmm2)
0
15
30
45
60
75
90
Ply angle (deg)
1 mm
2 mm
3 mm
4 mm
5 mm

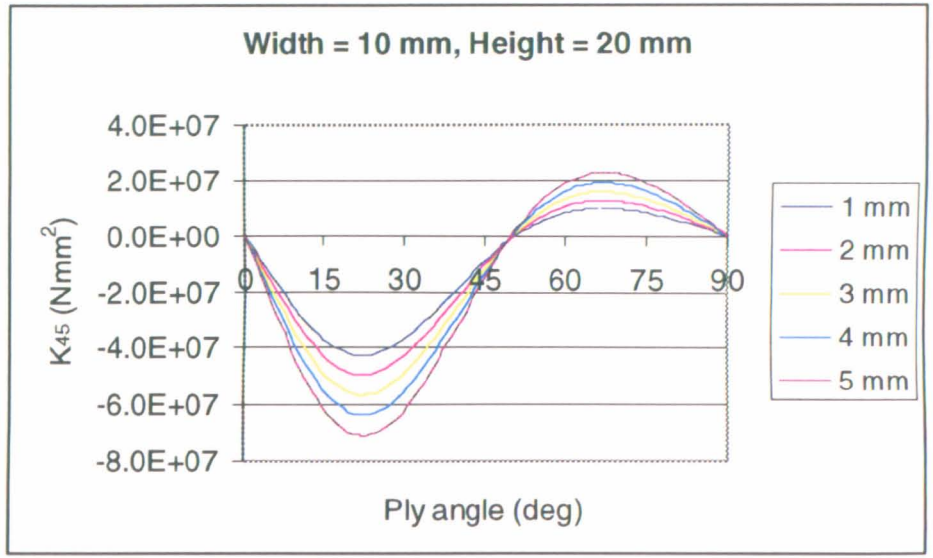
Width = 10 mm, Height = 20 mm
4.0E+07
2.0E+07
0.0E+00
-2.0E+07
-4.0E+07
-6.0E+07
-8.0E+07
K45 (Nmm2)
0
15
30
45
60
75
90
Ply angle (deg)
1 mm
2 mm
3 mm
4 mm
5 mm

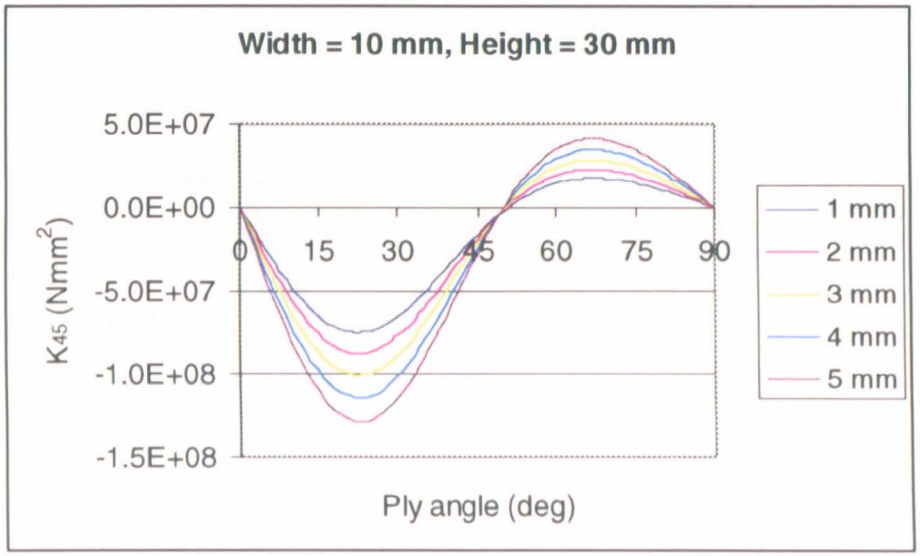
Width = 10 mm, Height = 30 mm
5.0E+07
0.0E+00
-5.0E+07
-1.0E+08
-1.5E+08
K45 (Nmm2)
0
15
30
45
60
75
90
Ply angle (deg)
1 mm
2 mm
3 mm
4 mm
5 mm

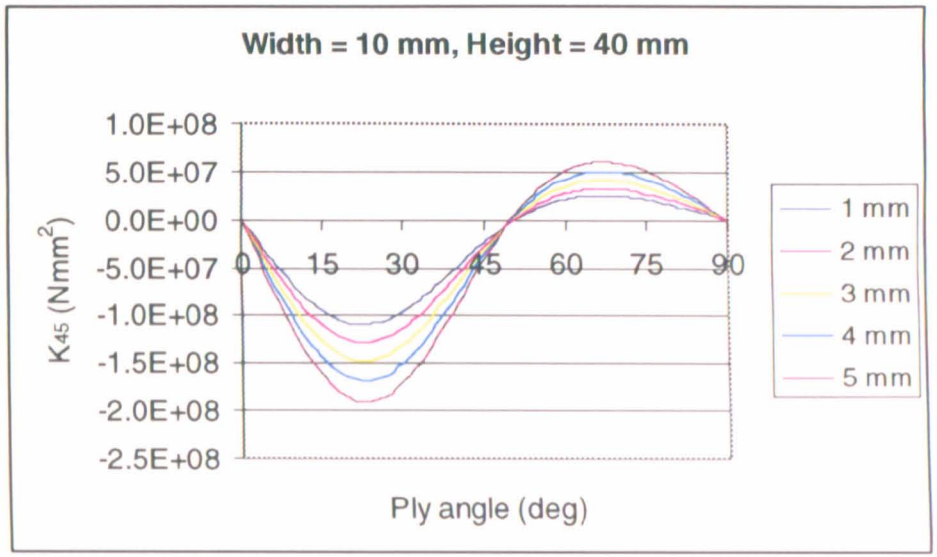
Width = 10 mm, Height = 40 mm
1.0E+08
5.0E+07
0.0E+00
-5.0E+07
-1.0E+08
-1.5E+08
-2.0E+08
-2.5E+08
K45 (Nmm2)
0
15
30
45
60
75
90
Ply angle (deg)
1 mm
2 mm
3 mm
4 mm
5 mm

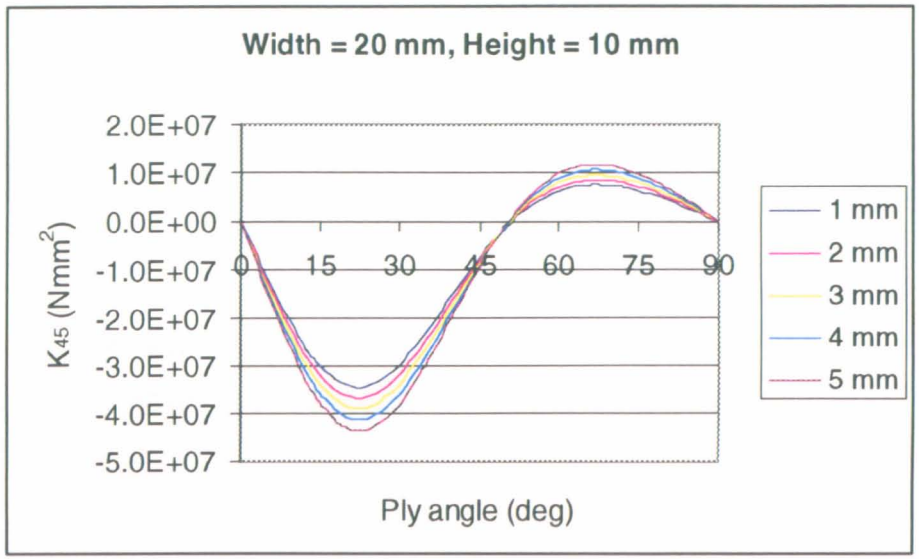
Width = 20 mm, Height = 10 mm
2.0E+07
1.0E+07
0.0E+00
-1.0E+07
-2.0E+07
-3.0E+07
-4.0E+07
-5.0E+07
K45 (Nmm2)
0
15
30
45
60
75
90
Ply angle (deg)
1 mm
2 mm
3 mm
4 mm
5 mm

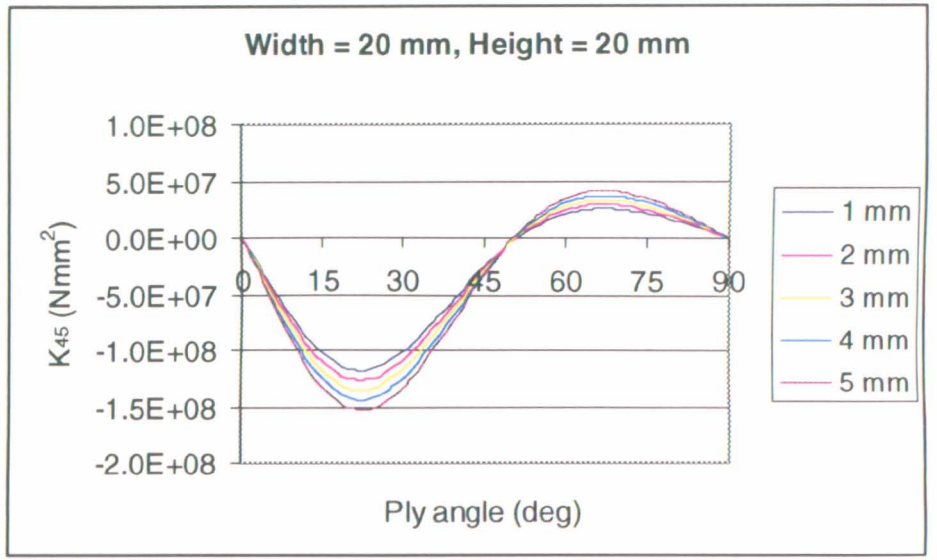
Width = 20 mm, Height = 20 mm
1.0E+08
5.0E+07
0.0E+00
-5.0E+07
-1.0E+08
-1.5E+08
-2.0E+08
K45 (Nmm2)
0
15
30
45
60
75
90
Ply angle (deg)
1 mm
2 mm
3 mm
4 mm
5 mm

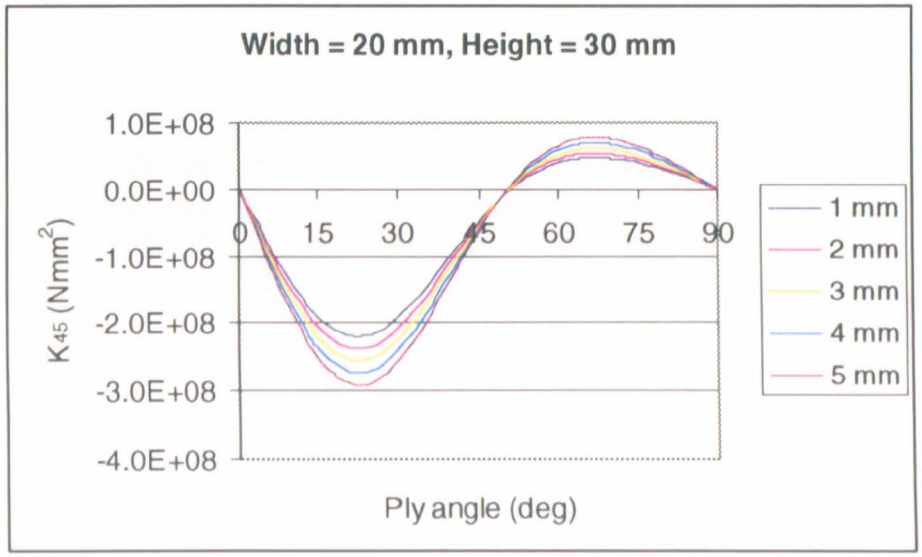
Width = 20 mm, Height = 30 mm
1.0E+08
0.0E+00
-1.0E+08
-2.0E+08
-3.0E+08
-4.0E+08
K45 (Nmm2)
0
15
30
45
60
75
90
Ply angle (deg)
1 mm
2 mm
3 mm
4 mm
5 mm

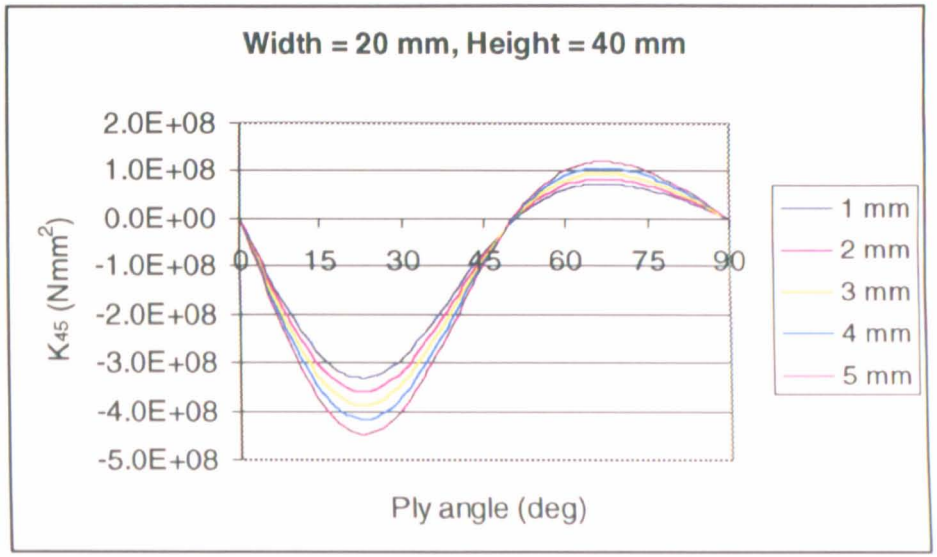
Width = 20 mm, Height = 40 mm
2.0E+08
1.0E+08
0.0E+00
-1.0E+08
-2.0E+08
-3.0E+08
-4.0E+08
-5.0E+08
K45 (Nmm2)
0
15
30
45
60
75
90
Ply angle (deg)
1 mm
2 mm
3 mm
4 mm
5 mm

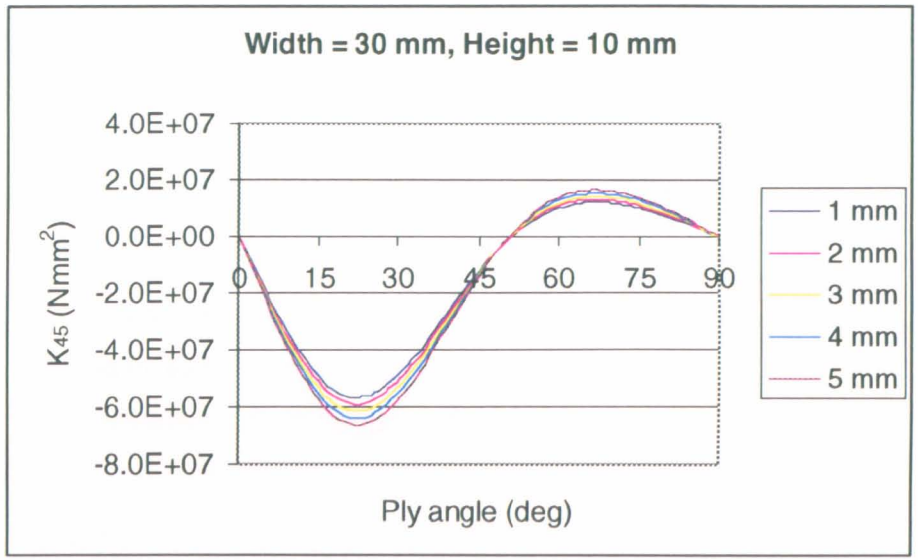
Width = 30 mm, Height = 10 mm
4.0E+07
2.0E+07
0.0E+00
-2.0E+07
-4.0E+07
-6.0E+07
-8.0E+07
K45 (Nmm2)
0
15
30
45
60
75
90
Ply angle (deg)
1 mm
2 mm
3 mm
4 mm
5 mm

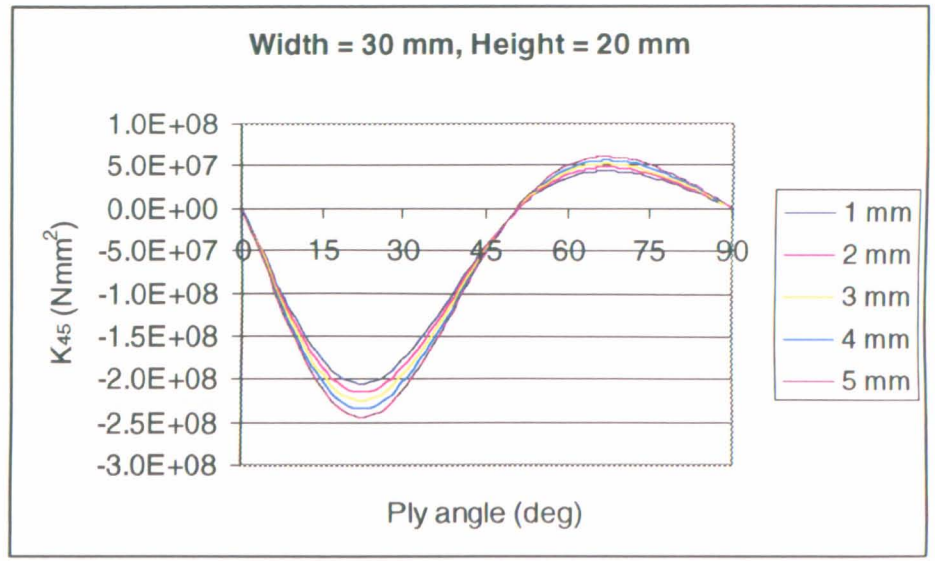
Width = 30 mm, Height = 20 mm
1.0E+08
5.0E+07
0.0E+00
-5.0E+07
-1.0E+08
-1.5E+08
-2.0E+08
-2.5E+08
-3.0E+08
K45 (Nmm2)
0
15
30
45
60
75
90
Ply angle (deg)
1 mm
2 mm
3 mm
4 mm
5 mm

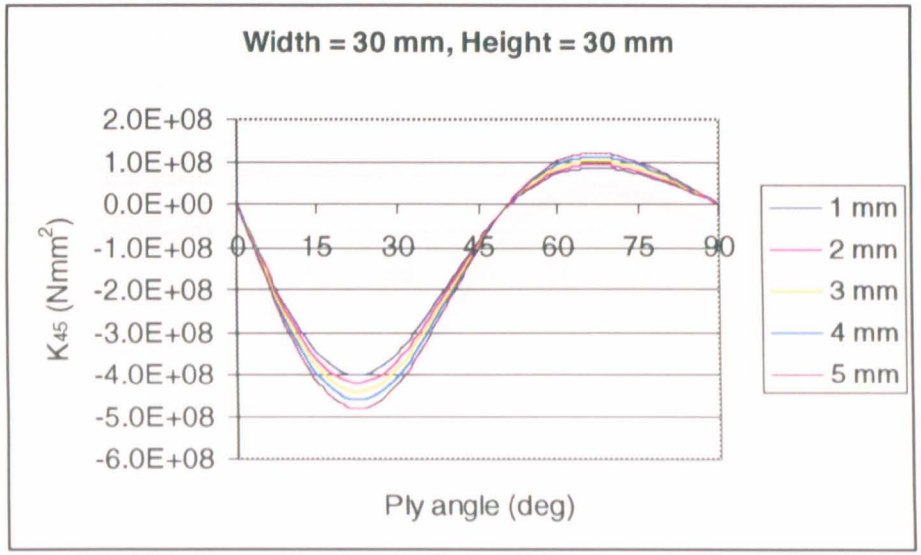
Width = 30 mm, Height = 30 mm
2.0E+08
1.0E+08
0.0E+00
-1.0E+08
-2.0E+08
-3.0E+08
-4.0E+08
-5.0E+08
-6.0E+08
K45 (Nmm2)
0
15
30
45
60
75
90
Ply angle (deg)
1 mm
2 mm
3 mm
4 mm
5 mm

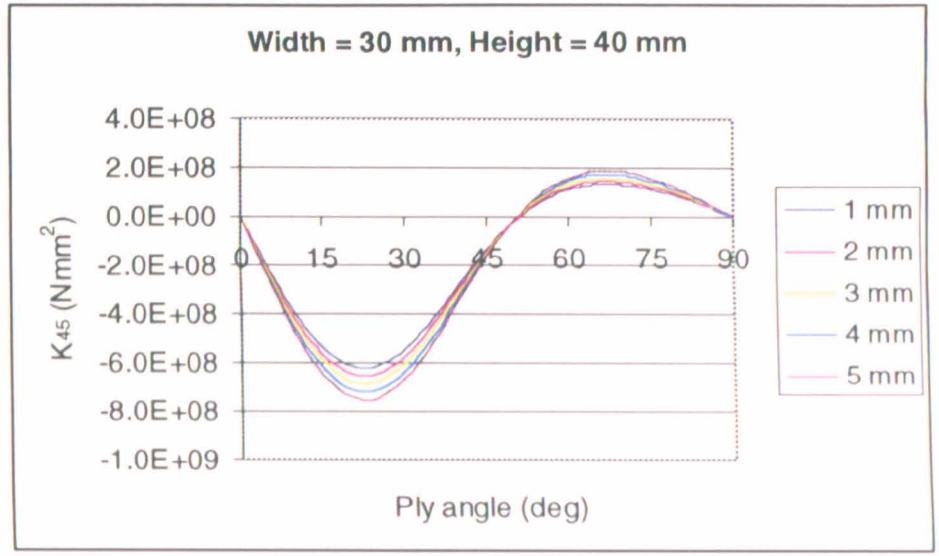
Width = 30 mm, Height = 40 mm
4.0E+08
2.0E+08
0.0E+00
-2.0E+08
-4.0E+08
-6.0E+08
-8.0E+08
-1.0E+09
K45 (Nmm2)
0
15
30
45
60
75
90
Ply angle (deg)
1 mm
2 mm
3 mm
4 mm
5 mm

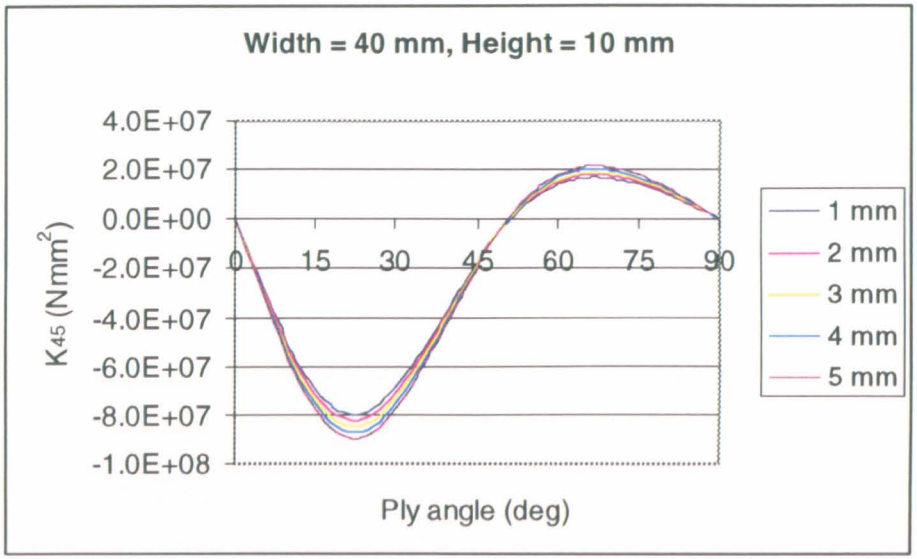
Width = 40 mm, Height = 10 mm
4.0E+07
2.0E+07
0.0E+00
-2.0E+07
-4.0E+07
-6.0E+07
-8.0E+07
-1.0E+08
K45 (Nmm2)
0
15
30
45
60
75
90
Ply angle (deg)
1 mm
2 mm
3 mm
4 mm
5 mm

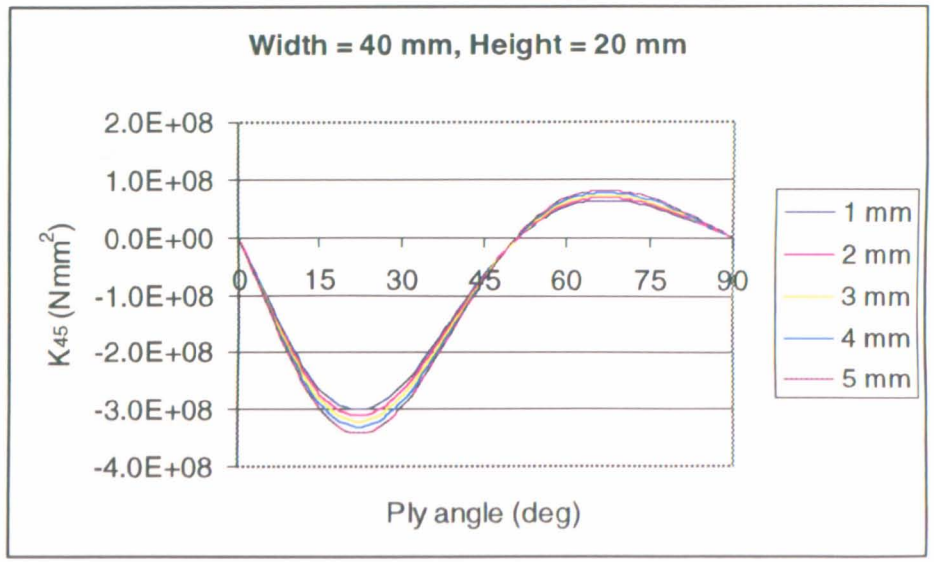
Width = 40 mm, Height = 20 mm
2.0E+08
1.0E+08
0.0E+00
-1.0E+08
-2.0E+08
-3.0E+08
-4.0E+08
K45 (Nmm2)
0
15
30
45
60
75
90
Ply angle (deg)
1 mm
2 mm
3 mm
4 mm
5 mm

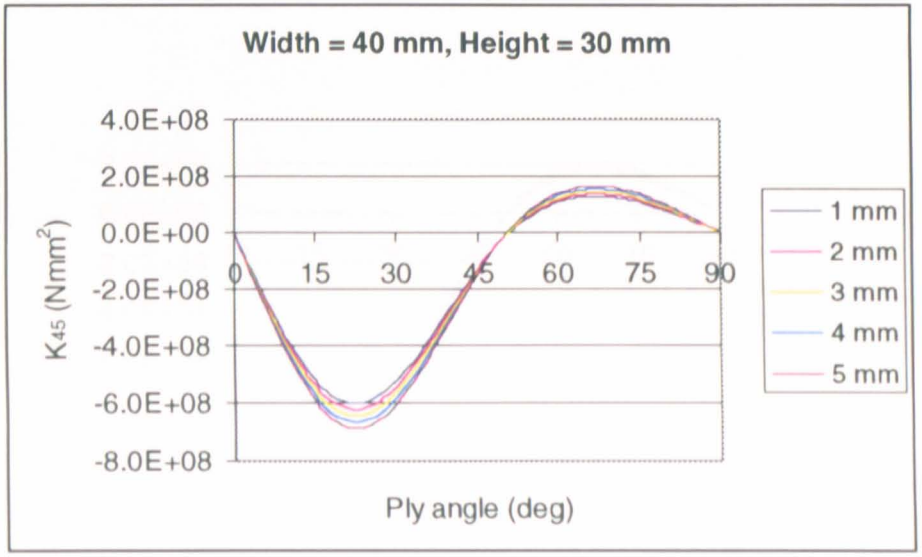
Width = 40 mm, Height = 30 mm
4.0E+08
2.0E+08
0.0E+00
-2.0E+08
-4.0E+08
-6.0E+08
-8.0E+08
K45 (Nmm2)
0
15
30
45
60
75
90
Ply angle (deg)
1 mm
2 mm
3 mm
4 mm
5 mm

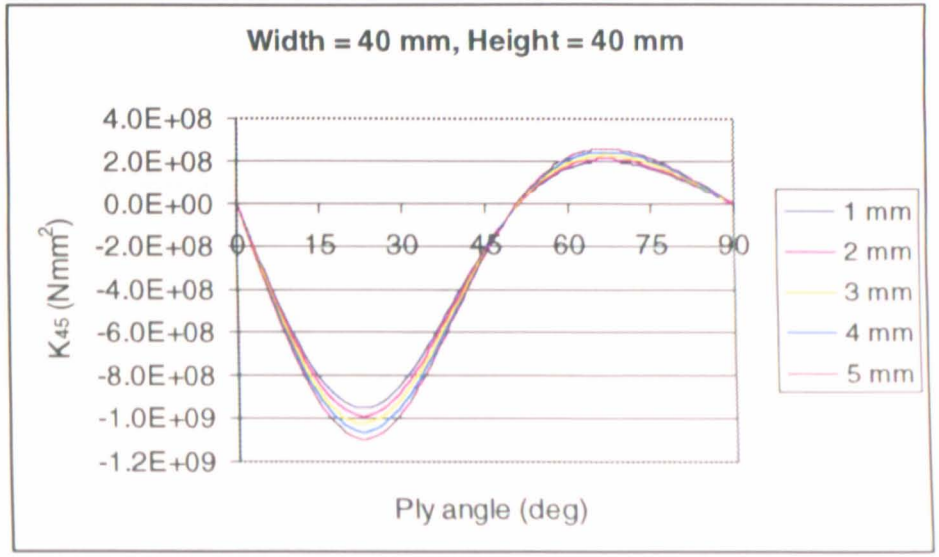
Width = 40 mm, Height = 40 mm
4.0E+08
2.0E+08
0.0E+00
-2.0E+08
-4.0E+08
-6.0E+08
-8.0E+08
-1.0E+09
-1.2E+09
K45 (Nmm2)
0
15
30
45
60
75
90
Ply angle (deg)
1 mm
2 mm
3 mm
4 mm
5 mm

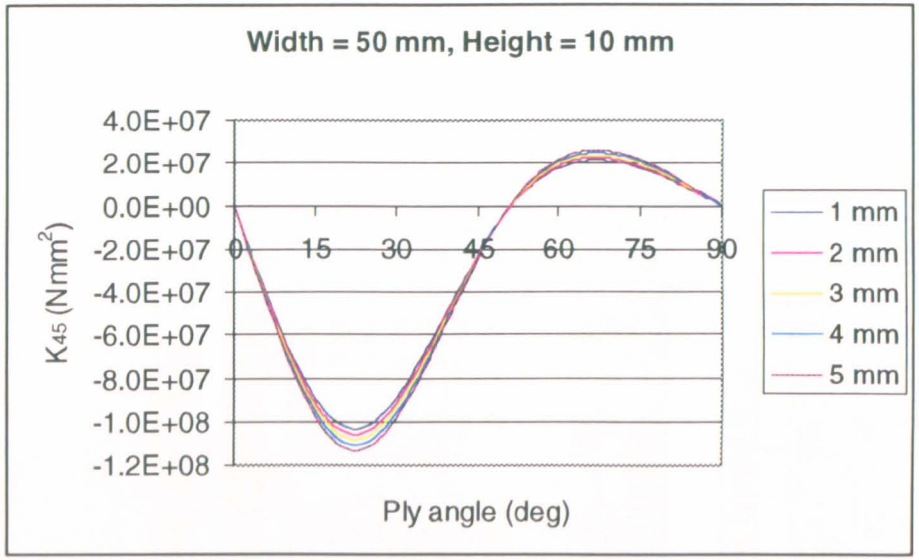
Width = 50 mm, Height = 10 mm
4.0E+07
2.0E+07
0.0E+00
-2.0E+07
-4.0E+07
-6.0E+07
-8.0E+07
-1.0E+08
-1.2E+08
0
15
30
45
60
75
90
K45 (Nmm2)
Ply angle (deg)
1 mm
2 mm
3 mm
4 mm
5 mm

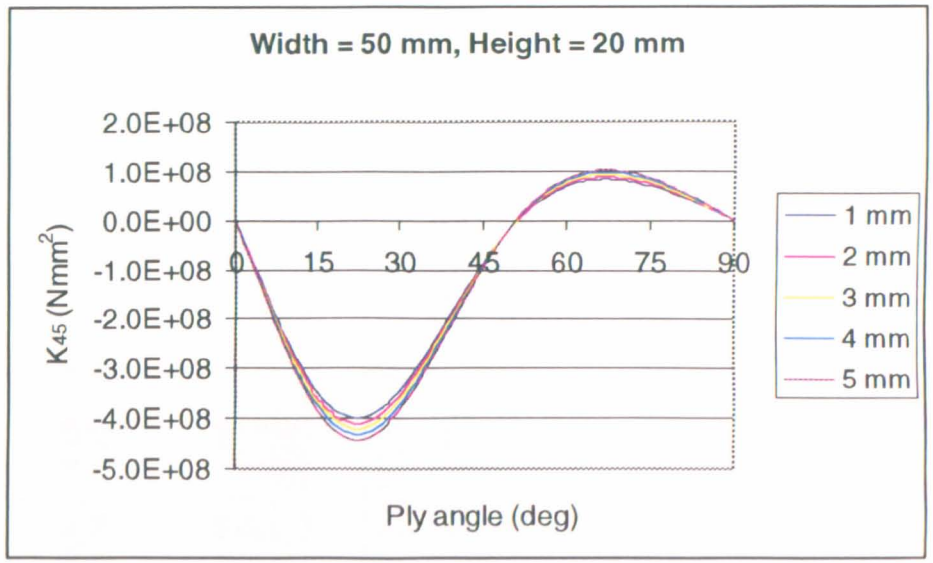
Width = 50 mm, Height = 20 mm
2.0E+08
1.0E+08
0.0E+00
-1.0E+08
-2.0E+08
-3.0E+08
-4.0E+08
-5.0E+08
0
15
30
45
60
75
90
K45 (Nmm2)
Ply angle (deg)
1 mm
2 mm
3 mm
4 mm
5 mm

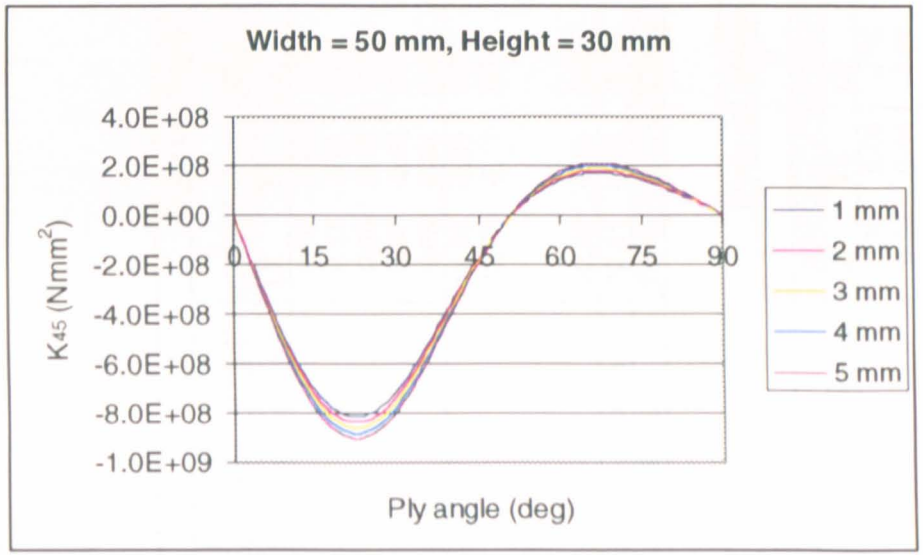
Width = 50 mm, Height = 30 mm
4.0E+08
2.0E+08
0.0E+00
-2.0E+08
-4.0E+08
-6.0E+08
-8.0E+08
-1.0E+09
0
15
30
45
60
75
90
K45 (Nmm2)
Ply angle (deg)
1 mm
2 mm
3 mm
4 mm
5 mm

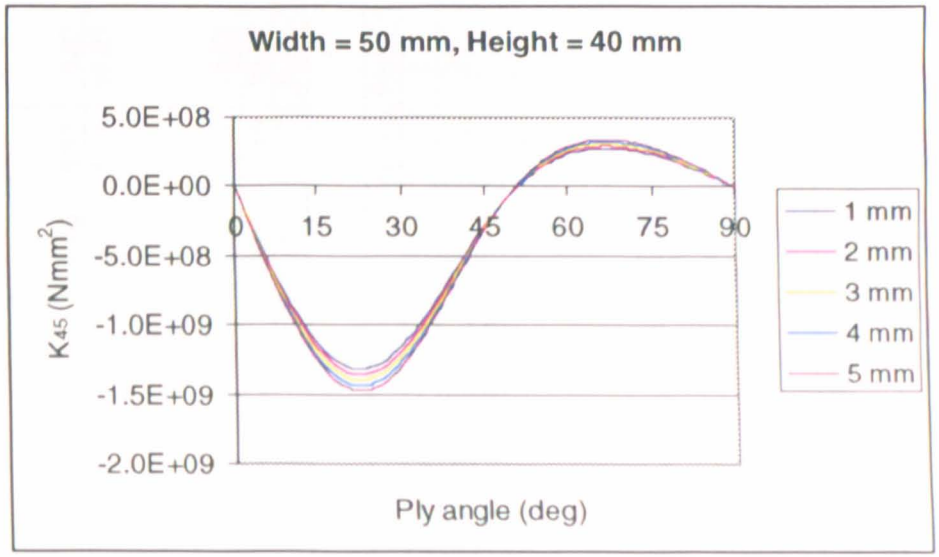
Width = 50 mm, Height = 40 mm
5.0E+08
0.0E+00
-5.0E+08
-1.0E+09
-1.5E+09
-2.0E+09
0
15
30
45
60
75
90
K45 (Nmm2)
Ply angle (deg)
1 mm
2 mm
3 mm
4 mm
5 mm

APPENDIX 6.1 FARROW'S EXPERIMENTAL RESULTS

Station A

Blade up, Station A, loaded @ 0.5kg									
Moment	1		2		3		4		SC
dist from LE mm	-352		-184		300		478		31.38
Displacement mm	LE	TE	LE	TE	LE	TE	LE	TE	
0 kg	0.00	0.00	0.00	0.00	0.00	0.00	0.00	0.00	
	0.11	0.01	-0.02	-0.08	-0.11	0.31	-0.31	0.32	
	0.00	0.00	0.00	0.00	0.00	0.00	0.00	0.00	
	0.07	-0.16	0.13	-0.23	0.00	-0.05	0.11	0.02	
Ave	**0.05**	**-0.04**	**0.03**	**-0.08**	**-0.03**	**0.07**	**-0.05**	**0.09**	
x kg	12.93	-2.01	9.79	1.54	1.02	11.80	-2.21	15.40	
	12.78	-2.17	9.74	1.26	1.12	11.33	-2.04	15.06	
Ave	**12.86**	**-2.09**	**9.77**	**1.40**	**1.07**	**11.57**	**-2.13**	**15.23**	
Disp from zero	**12.81**	**-2.05**	**9.74**	**1.48**	**1.10**	**11.50**	**-2.08**	**15.15**	
Disp LE-TE	**14.86**		**8.26**		**-10.40**		**-17.22**		**0.00**

Blade up, Station A, loaded @ 1kg									
Moment	1		2		3		4		SC
dist from LE mm	-352		-184		300		478		32.95
Displacement mm	LE	TE	LE	TE	LE	TE	LE	TE	
0 kg	0.30	0.09	0.15	0.22	0.11	0.51	0.15	0.34	
	0.42	0.04	0.30	0.09	0.15	0.22	0.11	0.51	
Ave	**0.36**	**0.07**	**0.23**	**0.16**	**0.13**	**0.37**	**0.13**	**0.43**	
x kg	13.34	-1.31	10.27	2.08	1.62	11.81	-1.47	15.46	
Ave	**13.34**	**-1.31**	**10.27**	**2.08**	**1.62**	**11.81**	**-1.47**	**15.46**	
Disp from zero	**12.98**	**-1.38**	**10.05**	**1.93**	**1.49**	**11.45**	**-1.60**	**15.04**	
Disp LE-TE	**14.36**		**8.12**		**-9.96**		**-16.64**		**0.00**

Blade up, Station A, loaded @ 1.5kg									
Moment	1		2		3		4		SC
dist from LE mm	-352		-184		300		478		29.97
Displacement mm	LE	TE	LE	TE	LE	TE	LE	TE	
0 kg	0.88	-0.66	0.75	-0.65	0.90	-0.52	0.57	-0.20	
	0.75	-0.65	0.87	-0.65	0.54	-0.20	0.09	0.26	
	0.85	-0.63	0.85	-0.63	0.57	-0.20	0.15	0.34	
			0.90	-0.52					
Ave	**0.83**	**-0.65**	**0.84**	**-0.61**	**0.67**	**-0.31**	**0.27**	**0.13**	
x kg	20.36	-2.59	15.90	2.36	2.92	16.97	-2.24	22.83	
	20.29	-2.65	15.87	2.31	2.81	17.08	-2.28	23.01	
	20.45	-2.51							
Ave	**20.37**	**-2.58**	**15.89**	**2.34**	**2.87**	**17.03**	**-2.26**	**22.92**	
Disp from zero	**19.54**	**-1.94**	**15.04**	**2.95**	**2.20**	**17.33**	**-2.53**	**22.79**	
Disp LE-TE	**21.48**		**12.10**		**-15.14**		**-25.32**		**0.00**

Station B

Blade up, Station B, loaded @ 1.5kg									
Moment	1		2		3		4		SC
dist from LE mm	-352		-184		300		478		29.61
Displacement mm	LE	TE	LE	TE	LE	TE	LE	TE	
0 kg	0.00	0.00	0.53	-0.66	0.54	-0.68	0.25	-0.25	
	0.53	-0.66	0.54	-0.68	0.25	-0.25	-0.05	-0.10	
Ave	0.27	-0.33	0.54	-0.67	0.40	-0.47	0.10	-0.18	
x kg	10.86	-5.46	7.73	-1.78	-1.53	8.73	-4.98	12.65	
Ave	10.86	-5.46	7.73	-1.78	-1.53	8.73	-4.98	12.65	
Disp from zero	10.60	-5.13	7.20	-1.11	-1.93	9.20	-5.08	12.83	
Disp LE-TE	15.73		8.31		-11.12		-17.91		0.00

Blade up, Station B, loaded @ 2.0kg									
Moment	1		2		3		4		SC
dist from LE mm	-352		-184		300		478		32.11
Displacement mm	LE	TE	LE	TE	LE	TE	LE	TE	
0 kg	0.00	0.00	0.00	0.00	0.00	0.00	0.00	0.00	
	0.59	-0.86	0.05	-0.01	-0.69	0.63	-0.48	0.62	
	0.00	0.00	0.00	0.00	0.00	0.00	0.00	0.00	
	0.09	-0.28	0.30	-0.50	0.03	-0.08	0.03	-0.05	
ave	0.17	-0.29	0.09	-0.13	-0.17	0.14	-0.11	0.14	
x kg	14.20	-7.78	9.38	-2.11	-3.10	12.46	-7.23	17.83	
	13.70	-7.28	9.58	-2.50	-2.51	11.71	-6.78	17.03	
ave	13.95	-7.53	9.48	-2.31	-2.81	12.09	-7.01	17.43	
Disp from zero	13.78	-7.25	9.39	-2.18	-2.64	11.95	-6.89	17.29	
Disp LE-TE	21.03		11.57		-14.59		-24.18		0.00

Blade up, Station B, loaded @ 2.5kg									
Moment	1		2		3		4		SC
dist from LE mm	-352		-184		300		478		28.25
Displacement mm	LE	TE	LE	TE	LE	TE	LE	TE	
0 kg	0.00	0.00	0.38	-0.59	0.18	-0.54	-0.63	0.58	
	0.30	-0.51	0.35	-0.51	-0.54	0.64	-0.65	0.45	
	0.38	-0.59	0.18	-0.54	-0.63	0.58	-1.16	1.33	
					-0.63	0.58	-1.29	1.20	
ave	0.23	-0.37	0.30	-0.55	-0.41	0.32	-0.93	0.89	
x kg	18.24	-8.50	12.72	-2.46	-3.28	15.75	-9.76	22.93	
	18.28	-8.59	12.71	-2.57	-3.43	15.85	-9.79	23.08	
					-3.39	15.92			
ave	18.26	-8.55	12.72	-2.52	-3.37	15.84	-9.78	23.01	
Disp from zero	18.03	-8.18	12.41	-1.97	-2.96	15.53	-8.84	22.12	
Disp LE-TE	26.21		14.38		-18.49		-30.96		0.00

Station C

Blade up, Station C, loaded @ 2.5kg									
Moment	1		2		3		4		SC
dist from LE mm	-352		-184		300		478		28.73
Displacement mm	LE	TE	LE	TE	LE	TE	LE	TE	
0 kg	0.00	0.00	1.58	-1.82	1.53	-1.92	0.80	-1.00	
	1.58	-1.82	1.53	-1.92	0.80	-1.00	0.33	-0.64	
ave	**0.79**	**-0.91**	**1.56**	**-1.87**	**1.17**	**-1.46**	**0.57**	**-0.82**	
x kg	9.39	-8.74	6.23	-5.14	-3.13	5.69	-6.74	10.06	
ave	**9.39**	**-8.74**	**6.23**	**-5.14**	**-3.13**	**5.69**	**-6.74**	**10.06**	
Disp from zero	**8.60**	**-7.83**	**4.68**	**-3.27**	**-4.30**	**7.15**	**-7.31**	**10.88**	
Disp LE-TE	**16.43**		**7.95**		**-11.45**		**-18.19**		**0.00**

Blade up, Station C, loaded @ 3.0 kg									
Moment	1		2		3		4		SC
dist from LE mm	-352		-184		300		478		27.20
Displacement mm	LE	TE	LE	TE	LE	TE	LE	TE	
0 kg	0.00	0.00	0.00	0.00	0.00	0.00	0.00	0.00	
	0.04	-0.46	0.00	0.24	-0.81	0.87	-0.45	0.54	
	0.00	0.00	0.00	0.00	0.00	0.00	0.00	0.00	
	0.45	-0.59	0.84	-0.82	-0.17	-0.06	-1.36	1.45	
ave	**0.12**	**-0.26**	**0.21**	**-0.15**	**-0.25**	**0.20**	**-0.45**	**0.50**	
x kg	8.39	-7.70	5.01	-3.52	-4.72	7.74	-7.78	11.69	
	8.60	-8.03	5.59	-4.42	-3.94	6.81	-8.64	12.53	
ave	**8.50**	**-7.87**	**5.30**	**-3.97**	**-4.33**	**7.28**	**-8.21**	**12.11**	
Disp from zero	**8.37**	**-7.60**	**5.09**	**-3.83**	**-4.09**	**7.07**	**-7.76**	**11.61**	
Disp LE-TE	**15.98**		**8.92**		**-11.16**		**-19.37**		**0.00**

Blade up, Station C, loaded @ 3.5 kg									
Moment	1		2		3		4		SC
dist from LE mm	-352		-184		300		478		34.84
Displacement mm	LE	TE	LE	TE	LE	TE	LE	TE	
0 kg	0.00	0.00	0.00	0.00	0.00	0.00	0.00	0.00	
	0.83	-1.77	0.01	0.49	-0.27	0.38	-0.83	0.81	
	0.00	0.00	0.00	0.00	0.00	0.00	0.00	0.00	
	0.69	-0.87	0.76	-0.98	0.05	0.17	-0.20	0.22	
ave	**0.38**	**-0.66**	**0.19**	**-0.12**	**-0.06**	**0.14**	**-0.26**	**0.26**	
x kg	10.72	-10.19	5.90	-4.14	-4.88	8.20	-9.50	14.04	
	10.44	-9.59	6.66	-5.23	-4.75	8.23	-8.87	13.35	
ave	**10.58**	**-9.89**	**6.28**	**-4.69**	**-4.82**	**8.22**	**-9.19**	**13.70**	
Disp from zero	**10.20**	**-9.23**	**6.09**	**-4.56**	**-4.76**	**8.08**	**-8.93**	**13.44**	
Disp LE-TE	**19.43**		**10.65**		**-12.84**		**-22.37**		**0.00**

APPENDIX 6.2

C++ OPTIMISATION CODE

```
////////////////////////////////////////////////
// SIMULTANEOUS LINEAR EQUATION METHOD IN C++ //
////////////////////////////////////////////////
// for problems with less than 100 variables  //
////////////////////////////////////////////////

#include <iostream.h>
#include <math.h>
#include <stdlib.h>
#include <string.h>
#include <fstream.h>
#include <iomanip.h>
#include "matfunc.cpp"

int i, j, k, ii, jj, kk;
int flag, flagA, flagB, flagC, flagSLE, best, count;
int variables; // number of design variables (equal to vectsize)
int vectsize;  // number of values in the design vector
int resultsize;
double X[100][101], res[100][101];
double Xlower[100], Xupper[100];
double range[100];
double Y[100], Z[100];
double rZ[100], target[100], weighting[100];
double obj, objnew, objbest;
double delta;

ifstream infile;
ofstream outfile;
ofstream outfile2("history.txt", ios::app);
void main()
{
      ////////////////////////////////////////
      // Remove old unwanted files that     //
      // may be hanging around and          //
      // initialise variables as necessary //
      ////////////////////////////////////////
      system("rm Xobj.txt");
      system("rm count.txt");
      count = 0;

      ////////////////////////////////////////
      // solution is initially unconverged //
      ////////////////////////////////////////
      flag = 0;

      ////////////////////////////////////
      // Read in size of design vector //
      ////////////////////////////////////
      infile.open("variables.txt");
      infile >> variables;
      infile.close();
      vectsize = variables;

      ////////////////////////////////////
```

```
// Read in size of results vector //
////////////////////////////////////
infile.open("resultsize.txt");
infile >> resultsize;
infile.close();

//////////////////////////////////////////////////
// Read in allowable range of design variables //
//////////////////////////////////////////////////
infile.open("range.txt");
for (i=0;i<variables;i++)
{
  infile >> Xlower[i];
  infile >> Xupper[i];
  range[i]=Xupper[i]-Xlower[i];
}
infile.close();

////////////////////////////
// Read in target values //
////////////////////////////
infile.open("target.txt");
for (i=0;i<resultsize;i++)
{
  infile >> target[i];
}
infile.close();

//////////////////////////
// Read in weightings //
//////////////////////////
infile.open("weighting.txt");
for (i=0;i<resultsize;i++)
{
  infile >> weighting[i];
}
infile.close();

//////////////////////////////
// Find an initial solution //
//////////////////////////////
system("FEA.out");

//////////////////////////
// Evaluate objective //
//////////////////////////
system("evalobj.out");
infile.open("Obj.txt");
infile >> objnew;
infile.close();

////////////////////////////
// read in initial design //
// vector and results     //
////////////////////////////
infile.open("X.txt");
for (j=0;j<vectsize;j++)
{
  infile   >> X[j][0];
}
infile.close();
```

```
infile.open("results.txt");
for (j=0;j<resultsize;j++)
{
  infile   >> res[j][0];
}
infile.close();

////////////////////////////////////
// Initial solution found so write //
// out all design data to Xcurrent //
////////////////////////////////////
outfile.open("Xcurrent.txt");
for (j=0;j<vectsize;j++)
{
  outfile << X[j][0] << " ";
}
for (j=0;j<resultsize;j++)
{
  outfile << res[j][0] << " ";
}
outfile << objnew << endl;
outfile.close();

////////////////////////////////////////
// As long as solution is unconverged //
// keep looking for a better solution //
////////////////////////////////////////

while (flag == 0)
{
  ////////////////////////////////////
  // read in results for current best //
  // solution from Xcurrent.txt       //
  ////////////////////////////////////
  infile.open("Xcurrent.txt");
  j=0;
  for (j=0;j<vectsize;j++)
  {
    infile >> X[j][0];
  }
  j=0;
  for (j=0;j<resultsize;j++)
  {
    infile >> res[j][0];
  }
  infile >> objnew;
  infile.close();

  ////////////////////////////////
  // read out results for current //
  // best solution to Xobj.txt    //
  ////////////////////////////////
  outfile.open("Xobj.txt");
  j=0;
  for (j=0;j<vectsize;j++)
  {
    outfile << X[j][0] << " ";
  }
  j=0;
  for (j=0;j<resultsize;j++)
  {
```

```
  outfile << res[j][0] << " ";
}
outfile << endl;
outfile.close();

//////////////////////////////////////////
// Start a count for number of iterations //
//////////////////////////////////////////
count=count+1;
outfile.open("count.txt");
{
  outfile << count;
}
outfile.close();

////////////////////////////////////////////////
// ANALYSE PERTURBED DESIGNS IN EACH DIMENSION //
////////////////////////////////////////////////
for(i=0;i<variables;i++)
{
  ///////////////////////////////////
  // start from unpeturbed design //
  ///////////////////////////////////
  for (j=0;j<vectsize;j++)
  {
    X[j][i+1]= X[j][0];
  }

  ////////////////////////////
  // PERTURB DESIGN VECTOR //
  ////////////////////////////
  if (X[i][i+1] < Xlower[i])
  {
    X[i][i+1] = Xlower[i];
  }
  X[i][i+1] = X[i][i+1]+(0.5*range[i]/count);
  if (X[i][i+1] > Xupper[i])
  {
    X[i][i+1] = X[i][i+1]-(range[i]/count);
  }

  ////////////////////////////////////////////////
  // write outperturbed design vector to X.txt //
  ////////////////////////////////////////////////
  outfile.open("X.txt");
  for (k=0;k<vectsize;k++)
  {
    outfile << X[k][i+1] << endl;
  }
  outfile.close();

  ////////////////////////////////////////
  // Find a solution for perturbed design //
  ////////////////////////////////////////
  system("FEA.out");

  ////////////////////////////////////////
  // read in results for perturbed design //
  ////////////////////////////////////////
  j=0;
  infile.open("results.txt");
```

```
for (j=0;j<resultsize;j++)
{
  infile   >> res[j][i+1];
}
infile.close();

//////////////////////////////////////////
// If results.txt is empty the analysis //
// has failed so retry the analysis     //
// perturbing a different amount        //
//////////////////////////////////////////
if (res[0][i+1] == 0)
{
   ////////////////////////////////////////////
   // Reset offending value to original value //
   ////////////////////////////////////////////
   X[i][i+1]= X[i][0];

   ////////////////////////////////////////////////
   // Perturb original value by different amount //
   ////////////////////////////////////////////////
     if (X[i][i+1] < Xlower[i])
   {
      X[i][i+1] = Xlower[i];
   }
   X[i][i+1] = X[i][i+1]+(0.25*range[i]/count);
   if (X[i][i+1] > Xupper[i])
   {
      X[i][i+1] = X[i][i+1]-(0.5*range[i]/count);
   }

   ////////////////////////////////////
   // write out alternative perturbed //
   // design vector to X.txt          //
   ////////////////////////////////////
   outfile.open("X.txt");
   for (k=0;k<vectsize;k++)
   {
      outfile << X[k][i+1] << endl;
   }
   outfile.close();

   ///////////////////////////////////
   // Find the alternative solution //
   ///////////////////////////////////
   system("FEA.out");

   ///////////////////////////////////
   // read in alternative results //
   ///////////////////////////////////
   j=0;
   infile.open("results.txt");
   for (j=0;j<resultsize;j++)
   {
     infile   >> res[j][i+1];
   }
   infile.close();

////////////
// End IF //
////////////
```

```
   }

 ////////////////////////////////////
 // We have now analysed and read  //
 // in the results for all perturbed //
 // designs, so end FOR loop       //
 ////////////////////////////////////
 }

 ////////////////////////////////////////
 // write out all data about this time //
 // step to the file Xobj.txt          //
 ////////////////////////////////////////
 i=0;
 j=0;
 k=0;
 outfile.open("Xobj.txt");
 for (i=0;i<variables+1;i++)
 {
   for (j=0;j<vectsize;j++)
   {
     outfile  << X[j][i] << " ";
   }
   for (k=0;k<resultsize;k++)
   {
     outfile  << res[k][i] << " ";
   }
   outfile  << endl;
 }
 outfile.close();

 ////////////////////////////////////////////////
 // write out all data about this time step //
 // to the files history.txt                   //
 ////////////////////////////////////////////////
 i=0;
 j=0;
 k=0;
 outfile.open("history.txt", ios::app);
 outfile << "Determining finite differences..." << endl;
 for (i=0;i<variables+1;i++)
 {
   for (j=0;j<vectsize;j++)
   {
     outfile << X[j][i] << " ";
   }
   for (k=0;k<resultsize;k++)
   {
     outfile << res[k][i] << " ";
   }
   outfile << endl;
 }
 outfile.close();

 ////////////////////////////////////////////////
 // Call Simultaneous linear equation solver //
 ////////////////////////////////////////////////
 flagSLE = 0;
 while (flagSLE == 0)
 {
   ////////////////////////////////////
```

```
// Read in data and FEA results //
// from previous design point   //
//////////////////////////////////
infile.open("Xcurrent.txt");
for (i=0;i<vectsize;i++)
{
  infile >> Y[i];
}
infile.close();

//////////////////////////////////////////////////////////
// SIMULTANEOUS LINEAR EQUATION SOLVER                  //
//////////////////////////////////////////////////////////
// Arrange results into Simultaneous linear equations   //
// Put simultaneous linear equations in to matrix form  //
// Solve equation Ax = b to get theoretical solution    //
//////////////////////////////////////////////////////////
// Analyse this solution and compare with target using  //
// same procedure as for finding the initial solution   //
//////////////////////////////////////////////////////////
// write design vector to X.txt and perform FE analysis //
//////////////////////////////////////////////////////////
system("SLE5.out");

//////////////////////////////////
// Read in data and FEA results //
// from new best design point   //
//////////////////////////////////
infile.open("best.txt");
for (i=0;i<vectsize;i++)
{
  infile >> Z[i];
}
for (j=0;j<resultsize;j++)
{
  infile >> rZ[j];
}
infile >> objbest;
infile.close();

//////////////////////////////////
// Read out data and FEA results //
// to history.txt                //
//////////////////////////////////
outfile.open("history.txt", ios::app);
outfile << "Iteration of SLE solver gives..." << endl;
for (i=0;i<vectsize;i++)
{
  outfile << Z[i] << " ";
}
for (j=0;j<resultsize;j++)
{
  outfile << rZ[j] << " ";
}
outfile << objbest << endl;
outfile.close();

//////////////////////////////////////////
// Convergence criterion for this linear step //
// Unconverged IF still improving             //
//////////////////////////////////////////
```

```
  // Move limits already imposed in SLE routine //
  ////////////////////////////////////////////////
  flagSLE = 1;
  if (objbest<objnew)
  {
    flagSLE = 0;
    objnew = objbest;
  }

  ////////////////////////////////////////////////////
  // Read data and FEA results from new best design //
  // point (currently stored as variables Z and rZ) //
  // to the file Xcurrent.txt                       //
  ////////////////////////////////////////////////////
  outfile.open("Xcurrent.txt");
  for (i=0;i<vectsize;i++)
  {
    outfile << Z[i] << " ";
  }
  for (j=0;j<resultsize;j++)
  {
    outfile << rZ[j] << " ";
  }
  outfile << objbest;
  outfile.close();

//////////////////
// End SLE loop //
//////////////////
}

////////////////////////////////////////////////////
// Apply first convergence criterion for overall //
// ie. if weighted target values have all been   //
// matched to within 1%                          //
////////////////////////////////////////////////////
flagA = 1;
for (i=0;i<resultsize;i++)
{
  if (weighting[i]*(1-target[i]/rZ[i])<-0.01)
  {
    flagA = 0;
  }
  if (weighting[i]*(1-target[i]/rZ[i])> 0.01)
  {
    flagA = 0;
  }
}
if (flagA == 1)
{
  flag = 1;
}

////////////////////////////////////////////////////
// Apply second convergence criterion to overall  //
// problem ie. if optimisation has proceeded thru //
// 5 iterations & no change in design variables   //
////////////////////////////////////////////////////
flagB = 1;
for (i=0;i<vectsize;i++)
{
```

```
        {
          if (Z[i]-X[i][0]>0.01*range[i])
          {
            flagB = 0;
          }
          if (Z[i]-X[i][0]>0.01*range[i])
          {
            flagB = 0;
          }
        }
      }
      if (count>5)
      {
        if (flagB == 1)
        {
          flag = 1;
        }
      }

      ////////////////////////////////////////
      // if solution is fully converged then //
      // write to screen and end program     //
      ////////////////////////////////////////
      if (flag == 1)
      {
        cout << "Solution converged" << endl;
      }

    ////////////////////////////
    // End overall while loop //
    ////////////////////////////
    }
    outfile.open("history.txt", ios::app);
    outfile << "Optimisation complete" << endl;
    outfile.close();
    cout << "Program finished" << endl;
}
```

APPENDIX 6.3

C++ SIMULTANEOUS LINEAR EQUATION SOLVER

```
////////////////////////////////////////////////
// SIMULTANEOUS LINEAR EQUATION SOLVER IN C++ //
////////////////////////////////////////////////
// For problems with less than 100 variables  //
////////////////////////////////////////////////

// Finds linear relationship between target variables and
// design variables and then solves the resulting simultaneous
// linear equations to match the target values

#include <iostream.h>
#include <math.h>
#include <stdlib.h>
#include <string.h>
#include <fstream.h>
#include <iomanip.h>
#include "matfunc.cpp"

int i, j, k, ii, jj, kk;
int flag, best, pivot, count;

int variables;  // no. of design variables (should equal vectsize)
int vectsize;   // no. of values in the design vector
int resultsize; // no. of targets

double X[100][101];
double XX[100][1];
double dX[100];
double Xbest[100];
double Xnew[100];
double Xupper[101];
double Xlower[101];

double res[200][101];
double resbest[200][1];
double resres[200][1];
double target[200];
double obj, objnew;

double active[101];

double wting[200];
double wttar[200];
double wtres[200][101];

double Aold[200][100];
double An[200][100];
double Anew[200][100];

double bold[100];
double bn[100];
double bnew[100];

ifstream infile;
ofstream outfile;
```

```
void main()
{
   ////////////////////////////////
   // Read in number of variables //
   ////////////////////////////////
   infile.open("variables.txt");
   infile >> variables;
   infile.close();
   vectsize = variables;

   ////////////////////////////////
   // Read in number of variables //
   ////////////////////////////////
   infile.open("resultsize.txt");
   infile >> resultsize;
   infile.close();

   ////////////////////////////////////////
   // Initialise all variables as active //
   ////////////////////////////////////////
   outfile.open("active.txt");
   for (i=0;i<variables;i++)
   {
      outfile << "1" << endl;
   }
   outfile.close();

   ////////////////////////////////////////////
   // Copy Xcurrent to Xnew and to best.txt //
   ////////////////////////////////////////////
   system("cp Xcurrent.txt Xnew.txt");
   system("cp Xcurrent.txt best.txt");

   ////////////////////////////
   // Read in target values //
   ////////////////////////////
   infile.open("target.txt");
   for (i=0;i<resultsize;i++)
   {
      infile >> target[i];
   }
   infile.close();

   ////////////////////////
   // Read in count value //
   ////////////////////////
   infile.open("count.txt");
   infile >> count;
   infile.close();

   ////////////////////////////
   // Weighted target values //
   ////////////////////////////
   infile.open("weighting.txt");
   for (i=0;i<resultsize;i++)
   {
      infile >> wting[i];
      wttar[i] = target[i]*wting[i];
   }
   infile.close();
```

```
////////////////////////////////////////////////
// Read in all data about the initial design //
// point and the perturbed solutions         //
////////////////////////////////////////////////
infile.open("Xobj.txt");
for (i=0;i<variables+1;i++)
{
   for (j=0;j<vectsize;j++)
   {
      infile >> X[j][i];
   }
   for (k=0;k<resultsize;k++)
   {
      infile >> res[k][i];
   }
}
infile.close();

////////////////////////////////////////////////////////
// Read in upper and lower limits of design variables //
////////////////////////////////////////////////////////
infile.open("range.txt");
for (i=0;i<variables;i++)
{
   infile >> Xlower[i];
   infile >> Xupper[i];
}
infile.close();

flag = 1;
while (flag == 1)
{
   ////////////////////////////
   // Read in active variables //
   ////////////////////////////
   infile.open("active.txt");
   for (i=0;i<variables;i++)
   {
      infile >> active[i];
   }
   infile.close();

   ////////////////////////////////////////////////
   // Read in data about the current design     //
   // point and the corresponding FEA solution //
   ////////////////////////////////////////////////
   infile.open("Xnew.txt");
   for (j=0;j<vectsize;j++)
   {
      infile >> XX[j][0];
   }
   for (k=0;k<resultsize;k++)
   {
      infile >> resres[k][0];
   }
   infile >> obj;
   infile.close();

   ////////////////////////////////////////////////////////
   // SIMULTANEOUS LINEAR EQUATION SOLVER                //
```

```
        //                                                          //
        // res(new)[res#] = res(old)[res#] + A[res#][0]*dX[0]       //
        //                                 + A[res#][1]*dX[1]       //
        //                                 + A[res#][2]*dX[2]       //
        ////////////////////////////////////////////////////////////

        ////////////////////////////////////////
        // Calculate gradient of each term in //
        // simultaneous linear equations      //
        ////////////////////////////////////////
        for(i=0;i<resultsize;i++)
        {
           for(j=0;j<variables;j++)
           {
              Aold[i][j]=((res[i][j+1]-res[i][0])/(X[j][j+1]-
X[j][0]))*active[j]*wting[i]/target[i];
           }
        }

        ////////////////////////////////////////////////////////////
        // Put simultaneous linear equations in to matrix form    //
        //                                                        //
        // [A][dx]  = [res(new) - res(old)]                       //
        //          = [target   - res(old)]                       //
        //          = [b]                                         //
        ////////////////////////////////////////////////////////////
        for(i=0;i<resultsize;i++)
        {
           bold[i] = wting[i]*(1 - (resres[i][0]/target[i]));
        }

        ////////////////////////////////////
        // Solve matrix equation Ax = b   //
        // to get theoretical solution    //
        ////////////////////////////////////

        ////////////////////////////////////////////////
        // initialise all variables in Anew and Bnew  //
        ////////////////////////////////////////////////
        for (i=0;i<variables;i++)
        {
           for (j=0;j<variables;j++)
           {
              Anew[i][j] = 0;
           }
        }
        for (k=0;k<resultsize;k++)
        {
           bnew[k] = 0;
        }

        ////////////////////////
        // Calculate AT*A = A1 //
        ////////////////////////
        cout << "Calculate AT*A = A1" << endl;
        for(i=0;i<variables;i++)
        {
           for(j=0;j<variables;j++)
           {
              for(k=0;k<resultsize;k++)
              {
```

```
            Anew[i][j]=Anew[i][j]+Aold[k][j]*Aold[k][i];
         }
      }
   }

   ////////////////////////
   // Calculate AT*b = b1 //
   ////////////////////////
   cout << "Calculate AT*b = b1" << endl;
   for(i=0;i<variables;i++)
   {
      for(k=0;k<resultsize;k++)
      {
         bnew[i] = bnew[i]+Aold[k][i]*bold[k];
      }
   }

   ////////////////////////////////////////////
   // Copy Anew to Aold and copy bnew to bold //
   ////////////////////////////////////////////

   i=0;
   j=0;
   for(i=0;i<variables;i++)
   {
      for(j=0;j<variables;j++)
      {
         Aold[i][j]=Anew[i][j];
      }
      bold[i]=bnew[i];
   }

   ////////////////////////////////////////////////
   // NOW TO SOLVE THE RESULTING MATRIX EQUATION  //
   //                                            //
   // [A1][dX]=[b1]                              //
   //                                            //
   // Note: [A1] is size (variables)x(variables) //
   ////////////////////////////////////////////////

   cout << "SOLVE THE MATRIX EQUATION" << endl;

   ////////////////////////////////////////////////////
   // Normalise the matrix equations (ie. so that all //
   // terms on the leading diagonal of A1 are unity). //
   // Remember to check for zeroes on the leading     //
   // diagonal                                        //
   ////////////////////////////////////////////////////

   for(i=0;i<variables;i++)
   {
      if (Aold[i][i] != 0)
      {
         for(j=0;j<variables;j++)
         {
            Anew[i][j] = Aold[i][j]/Aold[i][i];
         }
         bnew[i] = bold[i]/Aold[i][i];
      }
   }
```

```
//////////////////////////
// Copy Anew to Aold and //
// copy bnew to bold     //
//////////////////////////

i=0;
j=0;
for(i=0;i<variables;i++)
{
   for(j=0;j<variables;j++)
   {
      Aold[i][j]=Anew[i][j];
   }
   bold[i]=bnew[i];
}

//////////////////////////////////////////
// Proceed to solve the matrix equations //
// by Gauss Jordan Elimination (GJE)     //
//////////////////////////////////////////

//////////////////////////////////////////////////////////
// Longhand version of GJE for 3x3 matrix               //
//                                                      //
// An[0][0] = Ao[0][0]-Ao[pivot][0]*Ao[0][pivot];       //
// An[0][1] = Ao[0][1]-Ao[pivot][1]*Ao[0][pivot];       //
// An[0][2] = Ao[0][2]-Ao[pivot][2]*Ao[0][pivot];       //
// bn[0]    = bo[0]-bo[0]*Ao[0][pivot];                 //
//                                                      //
// An[1][0] = Ao[1][0]-Ao[pivot][0]*Ao[1][pivot];       //
// An[1][1] = Ao[1][1]-Ao[pivot][1]*Ao[1][pivot];       //
// An[1][2] = Ao[1][2]-Ao[pivot][2]*Ao[1][pivot];       //
// bn[1]    = bo[1]-bo[0]*Ao[1][pivot];                 //
//                                                      //
// An[2][0] = Ao[2][1]-Ao[pivot][0]*Ao[2][pivot];       //
// An[2][1] = Ao[2][1]-Ao[pivot][1]*Ao[2][pivot];       //
// An[2][2] = Ao[2][2]-Ao[pivot][2]*Ao[2][pivot];       //
// bn[2]    = bo[2]-bo[0]*Ao[2][pivot];                 //
//                                                      //
// An[pivot][0] = Ao[pivot][0];                         //
// An[pivot][1] = Ao[pivot][1];                         //
// An[pivot][2] = Ao[pivot][2];                         //
// bn[pivot]    = bo[pivot];                            //
//                                                      //
//////////////////////////////////////////////////////////

//////////////////////////////////////////////////////
// Generalised version for (variables)x(variables) //
//////////////////////////////////////////////////////

i=0;
j=0;
k=0;
pivot = 0;
for(pivot=0;pivot<variables;pivot++)
{
   if(Aold[pivot][pivot] != 0)
   {
      cout << "Pivot = " << pivot << endl;
      for(i=0;i<variables;i++)
      {
```

```
                for(j=0;j<variables;j++)
                {
                   An[i][j] = Aold[i][j]-
Aold[pivot][j]*Aold[i][pivot]/Aold[pivot][pivot];
                }
                bn[i] = bold[i]-
bold[pivot]*Aold[i][pivot]/Aold[pivot][pivot];
             }

             for(k=0;k<variables;k++)
             {
                An[pivot][k] = Aold[pivot][k];
             }
             bn[pivot] = bold[pivot];

             /////////////////
             // Renormalise //
             /////////////////
             i=0;
             j=0;
             for(i=0;i<variables;i++)
             {
                if (An[i][i] != 0)
                {
                   for(j=0;j<variables;j++)
                   {
                      Anew[i][j]=An[i][j]/An[i][i];
                   }
                   bnew[i] = bn[i]/An[i][i];
                }
             }

             ////////////////////////
             // Copy Anew to Aold //
             ////////////////////////
             i=0;
             j=0;
             for(i=0;i<variables;i++)
             {
                for(j=0;j<variables;j++)
                {
                   Aold[i][j]=Anew[i][j];
                }
                bold[i]=bnew[i];
             }
          }
       }

       ////////////////////////////////////////////////////////////
       // Gauss Jordan has been completed, so the vector b gives //
       // the values of delta x to solve the linear problem      //
       ////////////////////////////////////////////////////////////
       cout << "Gauss Jordan Elimination completed" << endl;
       cout << "Linear solution is given by the vector dX" << endl;
       cout << endl;

       for(i=0;i<variables;i++)
       {
          cout << "dX[" << i << "] = " << bold[i] << endl;
       }
       cout << endl;
```

```
        ////////////////////////////////////////////////////
        // ...so calculate new values of design vector Xnew //
        ////////////////////////////////////////////////////
        cout << "So the new design vector X as..." << endl;
        for (i=0;i<variables;i++)
        {
           Xnew[i] = XX[i][0]+bold[i];
           cout << "X[" << i << "] = " << Xnew[i] << endl;
        }
        cout << endl;

        ////////////////////////////////////////////////////
        // Apply move limit so that the solution doesn't move //
        // beyond the validity of the linear approximation    //
        ////////////////////////////////////////////////////
        for(i=0;i<variables;i++)
        {
           if(Xnew[i]-X[i][0]>(Xupper[i]-Xlower[i])*0.5/count)
           {
              Xnew[i]=X[i][0]+(Xupper[i]-Xlower[i])*0.5/count;
              cout << "Move limit " << i << " exceeded" << endl;
           }
           if(Xnew[i]-X[i][0]<(Xlower[i]-Xupper[i])*0.5/count)
           {
              Xnew[i]=X[i][0]-(Xlower[i]-Xupper[i])*0.5/count;
              cout << "Move limit " << i << " exceeded" << endl;
           }
        }

        ////////////////////////////////////////////
        // Check that these values of Xnew lie in //
        // the feasible design space              //
        ////////////////////////////////////////////
        flag = 0;
        for (i=0;i<variables;i++)
        {
           if (Xnew[i]<Xlower[i])
           {
              Xnew[i] = Xlower[i];
              cout << "Xnew[" << i << "] is unfeasible, so result moved to
feasible region." << endl;
              flag = 1;
              active[i] = 0;
           }
           if (Xnew[i]>Xupper[i])
           {
              Xnew[i] = Xupper[i];
              cout << "Xnew[" << i << "] is unfeasible, so result moved to
feasible region." << endl;
              flag = 1;
              active[i] = 0;
           }
        }

        ////////////////////////////////////////////////
        // Write feasible design values to file Xnew.txt //
        ////////////////////////////////////////////////
        system("rm Xnew.txt");
        cout << "The feasible solution is..." << endl;
        outfile.open("Xnew.txt");
```

```
for (i=0;i<variables;i++)
{
   cout << "X[" << i << "] = " << Xnew[i] << endl;
   outfile << Xnew[i] << endl;
}
cout << endl;
outfile.close();

////////////////////////////////////////////
// out active variables to file active.txt //
////////////////////////////////////////////
outfile.open("active.txt");
for (i=0;i<variables;i++)
{
   outfile << active[i] << endl;
}
outfile.close();

////////////////////////////////////////////
// Evaluate results for new design point //
////////////////////////////////////////////
system("cp Xnew.txt X.txt");
system("FEA.out");
infile.open("results.txt");
for (j=0;j<resultsize;j++)
{
   resres[j][0] = 0;
   infile >> resres[j][0];
}
infile.close();

////////////////////////////////////////////////////
// If results file is empty, analysis has failed //
////////////////////////////////////////////////////
if (resres[1][0]==0)
{
   ////////////////////////////////////////
   // Create a new (similar design point) //
   ////////////////////////////////////////
   system("rm Xnew.txt");
   outfile.open("Xnew.txt");
   for (i=0;i<variables;i++)
   {
      if (Xnew[i]*1.01>Xupper[i])
      {
         outfile << Xnew[i]*0.99 << endl;
      }
      if (Xnew[i]*1.01<Xupper[i])
      {
         outfile << Xnew[i]*1.01 << endl;
      }
   }
   cout << endl;
   outfile.close();
   ////////////////////////////////////////////
   // Reevaluate results for new design point //
   ////////////////////////////////////////////
   system("cp Xnew.txt X.txt");
   system("FEA.out");
   infile.open("results.txt");
   for (j=0;j<resultsize;j++)
```

```
    {
       resres[j][0] = 0;
       infile >> resres[j][0];
    }
    infile.close();
}

//////////////////////////
// Evaluate objective //
//////////////////////////
system("evalobj.out");
infile.open("Obj.txt");
infile >> objnew;
infile.close();
cout << "Objective evaluated" << endl;

////////////////////////////////////////
// Append results to data in Xnew.txt //
////////////////////////////////////////
outfile.open("Xnew.txt",ios::app);
for (j=0;j<resultsize;j++)
{
   outfile << resres[j][0] << endl;
}
outfile << objnew << endl;
outfile.close();
cout << "Results data appended" << endl;

//////////////////////////////////////////////////////
// If no improvement then revert to old best design //
//////////////////////////////////////////////////////
if (objnew>obj)
{
   flag=0;
   system("cp best.txt Xnew.txt");
}
cout << "Checked for improvement" << endl;

/////////////////////////////////////////
// Copy new best design to Xcurrent.txt //
/////////////////////////////////////////
system("cp Xnew.txt Xcurrent.txt");
system("cp Xnew.txt best.txt");
cout << "Files copied" << endl;

/////////////////////////////////////////
// Read in data for current best design //
/////////////////////////////////////////
infile.open("best.txt");
for (i=0;i<variables;i++)
{
   infile >> Xbest[i];
}
for (j=0;j<resultsize;j++)
{
   infile >> resbest[j][0];
}
infile >> obj;
infile.close();
cout << "Best design data read in" << endl;
```

```
      ////////////////////////////////////////////
      // Write data for iteration to history.txt //
      ////////////////////////////////////////////
      outfile.open("history.txt", ios::app);
      outfile << "Iteration within SLE routine..." << endl;
      for (i=0;i<variables;i++)
      {
         outfile << Xbest[i] << " ";
      }
      for (j=0;j<resultsize;j++)
      {
         outfile << resbest[j][0] << " ";
      }
      outfile << obj;
      outfile << endl;
      outfile.close();

   ////////////////////////////////////////////////////////////
   // Completed one iteration of the linear approximation //
   // This keeps looping until no further improvement in  //
   // objective function is found or all constraints have //
   // become active                                       //
   ////////////////////////////////////////////////////////////
   }

   ////////////////////////////////////
   // Reset all variables as active //
   ////////////////////////////////////
   outfile.open("active.txt");
   for (i=0;i<variables;i++)
   {
      outfile << "1" << endl;
   }
   outfile.close();

   ////////////////////////////
   // SLE routine completed //
   ////////////////////////////
   cout << "SLE5.out completed" << endl;
}
```

APPENDIX 6.4 History file from optimisation runs

RUN 1

Determining finite differences...
9 99 60 0.75 0.5 0.75 2.13676e+07 5.74998e+08 1.12291e+10 5.83582e+08 6444.28 20.781 873712
5 99 60 0.75 0.5 0.75 2.10022e+07 5.73965e+08 1.08813e+10 5.76187e+08 24496.7 28.0681 569974
9 91.75 60 0.75 0.5 0.75 2.27505e+07 5.84432e+08 1.83945e+10 5.83711e+08 12392.8 21.856 886649
9 99 50 0.75 0.5 0.75 1.8926e+07 5.02884e+08 7.34286e+09 4.73226e+08 8.53353e+06 17.8047 823114
9 99 60 0.4375 0.5 0.75 1.61909e+07 4.32986e+08 8.65166e+09 5.87101e+08 -94361.6 20.7728 873529
9 99 60 0.75 0.3125 0.75 2.14385e+07 5.76916e+08 1.12653e+10 4.33256e+08 -2.64607e+07 20.7727 873526
9 99 60 0.75 0.5 0.3125 2.0906e+07 5.65819e+08 1.11499e+10 5.80546e+08 18394.5 20.2966 854704

Iteration within SLE routine...
7.28074 95.4397 50 0.555335 0.484352 0.3125 1.58572e+07 4.18466e+08 9.0358e+09 4.6054e+08 5.31771e+06 19.8438 667062 0.0450001
This iteration of linear solver gives...
7.28074 95.4397 50 0.555335 0.484352 0.3125 1.58572e+07 4.18466e+08 9.0358e+09 4.6054e+08 5.31771e+06 19.8438 667062 0.0450001
Iteration within SLE routine...
7.28074 95.4397 50 0.555335 0.484352 0.3125 1.58572e+07 4.18466e+08 9.0358e+09 4.6054e+08 5.31771e+06 19.8438 667062 0.0450001
This iteration of linear solver gives...
7.28074 95.4397 50 0.555335 0.484352 0.3125 1.58572e+07 4.18466e+08 9.0358e+09 4.6054e+08 5.31771e+06 19.8438 667062 0.0450001

Determining finite differences...
7.28074 95.4397 50 0.555335 0.484352 0.3125 1.58572e+07 4.18466e+08 9.0358e+09 4.6054e+08 5.31771e+06 19.8438 667062
3.28074 95.4397 50 0.555335 0.484352 0.3125 1.55777e+07 4.17956e+08 8.79999e+09 4.51703e+08 5.12495e+06 28.4457 416783
7.28074 88.1897 50 0.555335 0.484352 0.3125 1.85489e+07 4.35878e+08 2.15487e+10 4.60897e+08 5.13626e+06 22.436 692245
7.28074 95.4397 60 0.555335 0.484352 0.3125 1.80517e+07 4.82929e+08 1.1874e+10 5.67996e+08 -34043.9 23.06 718679
7.28074 95.4397 50 0.242835 0.484352 0.3125 1.10322e+07 2.85114e+08 7.307e+09 4.6361e+08 5.53532e+06 19.8303 667820
7.28074 95.4397 50 0.555335 0.296852 0.3125 1.53869e+07 4.05035e+08 8.88659e+09 3.40766e+08 5.52191e+06 19.8299 667810

7.28074 95.4397 50 0.555335 0.484352 0.75 1.65191e+07 4.32227e+08 9.05964e+09 4.65333e+08 8.57999e+06 20.2126 687277

Iteration within SLE routine...
7.28074 95.4397 50 0.555335 0.484352 0.3125 1.58572e+07 4.18466e+08 9.0358e+09 4.6054e+08 5.31771e+06 19.8438 667062 0.0450001
This iteration of linear solver gives...
7.28074 95.4397 50 0.555335 0.484352 0.3125 1.58572e+07 4.18466e+08 9.0358e+09 4.6054e+08 5.31771e+06 19.8438 667062 0.0450001
Iteration within SLE routine...
7.28074 95.4397 50 0.555335 0.484352 0.3125 1.58572e+07 4.18466e+08 9.0358e+09 4.6054e+08 5.31771e+06 19.8438 667062 0.0450001
This iteration of linear solver gives...
7.28074 95.4397 50 0.555335 0.484352 0.3125 1.58572e+07 4.18466e+08 9.0358e+09 4.6054e+08 5.31771e+06 19.8438 667062 0.0450001

Determining finite differences...
7.28074 95.4397 50 0.555335 0.484352 0.3125 1.58572e+07 4.18466e+08 9.0358e+09 4.6054e+08 5.31771e+06 19.8438 667062
9.28074 95.4397 50 0.555335 0.484352 0.3125 1.60506e+07 4.1903e+08 9.15818e+09 4.63303e+08 5.42867e+06 17.4906 838354
7.28074 99.0647 50 0.555335 0.484352 0.3125 1.54452e+07 4.15604e+08 6.26909e+09 4.60514e+08 5.35652e+06 19.395 663208
7.28074 95.4397 55 0.555335 0.484352 0.3125 1.70196e+07 4.54837e+08 1.02931e+10 5.16318e+08 5.41876e+06 21.4178 692628
7.28074 95.4397 50 0.711585 0.484352 0.3125 1.80908e+07 4.79755e+08 9.84056e+09 4.59343e+08 5.24883e+06 19.8298 667805
7.28074 95.4397 50 0.555335 0.390602 0.3125 1.57269e+07 4.14498e+08 8.99884e+09 4.01234e+08 5.41009e+06 19.8298 667809
7.28074 95.4397 50 0.555335 0.484352 0.53125 1.62026e+07 4.25973e+08 9.04831e+09 4.63345e+08 7.32524e+06 20.031 677173

Iteration within SLE routine...
6.97644 94.7905 48.3712 0.494358 0.49302 0.440587 1.48227e+07 3.85008e+08 9.07961e+09 4.47535e+08 5.8947e+06 20.0706 636799 0.00871052
This iteration of linear solver gives...
6.97644 94.7905 48.3712 0.494358 0.49302 0.440587 1.48227e+07 3.85008e+08 9.07961e+09 4.47535e+08 5.8947e+06 20.0706 636799 0.00871052
Iteration within SLE routine...
7.00318 95.0569 47.8511 0.502633 0.5 0.503827 1.49691e+07 3.87649e+08 8.73846e+09 4.48385e+08 6.55341e+06 19.8469 638880 0.000312926
Iteration within SLE routine...
7.00079 94.9918 47.9831 0.49812 0.5 0.492605 1.48608e+07 3.84815e+08 8.78152e+09 4.4969e+08 6.41911e+06 19.8287 637282 9.12908e-05
This iteration of linear solver gives...
7.00079 94.9918 47.9831 0.49812 0.5 0.492605 1.48608e+07 3.84815e+08 8.78152e+09 4.4969e+08 6.41911e+06 19.8287 637282 9.12908e-05

Iteration within SLE routine...
7.00079 94.9918 47.9831 0.49812 0.5 0.492605 1.48608e+07 3.84815e+08 8.78152e+09 4.4969e+08 6.41911e+06 19.8287 637282 9.12908e-05
This iteration of linear solver gives...
7.00079 94.9918 47.9831 0.49812 0.5 0.492605 1.48608e+07 3.84815e+08 8.78152e+09 4.4969e+08 6.41911e+06 19.8287 637282 9.12908e-05
Optimisation complete

RUN 2

Determining finite differences...
2 85 40 0.125 0.125 0.125 1.04687e+07 1.56682e+08 1.80715e+10 1.62011e+08 2.49924e+06 34.6288 369214
6 85 40 0.125 0.125 0.125 1.07067e+07 1.57045e+08 1.90401e+10 1.68116e+08 2.67274e+06 24.4913 555649
2 92.25 40 0.125 0.125 0.125 6.32907e+06 1.40787e+08 9.13944e+09 1.61244e+08 2.44717e+06 28.3595 330486
2 85 50 0.125 0.125 0.125 1.13865e+07 1.88738e+08 1.78226e+10 2.15453e+08 2.41003e+06 36.9212 422471
2 85 40 0.4375 0.125 0.125 1.48489e+07 2.7814e+08 2.46235e+10 1.61432e+08 2.43122e+06 34.6162 369346
2 85 40 0.125 0.3125 0.125 1.1462e+07 1.84903e+08 1.99686e+10 2.5095e+08 2.47242e+06 34.6189 369322
2 85 40 0.125 0.125 0.5625 1.1153e+07 1.73666e+08 1.92662e+10 1.66591e+08 6.34277e+06 34.0124 388833

Iteration within SLE routine...
5.41445 92.25 50 0.4375 0.279083 0.5625 1.43775e+07 3.62587e+08 1.23681e+10 3.29496e+08 7.42531e+06 24.5108 547499 0.338101
This iteration of linear solver gives...
5.41445 92.25 50 0.4375 0.279083 0.5625 1.43775e+07 3.62587e+08 1.23681e+10 3.29496e+08 7.42531e+06 24.5108 547499 0.338101
Iteration within SLE routine...
6 92.25 50 0.428092 0.3125 0.459499 1.42915e+07 3.6e+08 1.24244e+10 3.51566e+08 6.7923e+06 23.0915 584943 0.259656
This iteration of linear solver gives...
6 92.25 50 0.428092 0.3125 0.459499 1.42915e+07 3.6e+08 1.24244e+10 3.51566e+08 6.7923e+06 23.0915 584943 0.259656
Iteration within SLE routine...
6 92.25 50 0.428092 0.3125 0.459499 1.42915e+07 3.6e+08 1.24244e+10 3.51566e+08 6.7923e+06 23.0915 584943 0.259656
This iteration of linear solver gives...

6 92.25 50 0.428092 0.3125 0.459499 1.42915e+07 3.6e+08 1.24244e+10 3.51566e+08 6.7923e+06 23.0915 584943 0.259656

Determining finite differences...
6 92.25 50 0.428092 0.3125 0.459499 1.42915e+07 3.6e+08 1.24244e+10 3.51566e+08 6.7923e+06 23.0915 584943
8 92.25 50 0.428092 0.3125 0.459499 1.4472e+07 3.60463e+08 1.26073e+10 3.54754e+08 6.95794e+06 19.7705 737734
6 95.875 50 0.428092 0.3125 0.459499 1.34297e+07 3.54021e+08 7.67148e+09 3.51483e+08 6.91656e+06 22.103 576881
6 92.25 55 0.428092 0.3125 0.459499 1.52314e+07 3.9007e+08 1.31388e+10 3.92529e+08 7.08107e+06 24.7929 610245
6 92.25 50 0.584342 0.3125 0.459499 1.68443e+07 4.30546e+08 1.34288e+10 3.50729e+08 6.73488e+06 23.0914 584941
6 92.25 50 0.428092 0.40625 0.459499 1.46769e+07 3.7083e+08 1.25691e+10 4.12043e+08 6.74681e+06 23.0916 584944
6 92.25 50 0.428092 0.3125 0.678249 1.46127e+07 3.66545e+08 1.24344e+10 3.53711e+08 8.1375e+06 23.2493 595049

Iteration within SLE routine...
6.96519 95.3452 47.8822 0.486667 0.40625 0.411845 1.44195e+07 3.74221e+08 8.30465e+09 3.92005e+08 6.00701e+06 19.7855 631545 0.0266456
This iteration of linear solver gives...
6.96519 95.3452 47.8822 0.486667 0.40625 0.411845 1.44195e+07 3.74221e+08 8.30465e+09 3.92005e+08 6.00701e+06 19.7855 631545 0.0266456
Iteration within SLE routine...
6.99952 95.0755 48.0115 0.483552 0.40625 0.490973 1.44701e+07 3.75329e+08 8.47001e+09 3.92343e+08 6.52655e+06 19.8858 638668 0.0194672
This iteration of linear solver gives...
6.99952 95.0755 48.0115 0.483552 0.40625 0.490973 1.44701e+07 3.75329e+08 8.47001e+09 3.92343e+08 6.52655e+06 19.8858 638668 0.0194672
Iteration within SLE routine...
7.00466 94.9417 47.974 0.486621 0.40625 0.487492 1.45633e+07 3.76188e+08 8.74724e+09 3.93576e+08 6.50651e+06 19.8282 637440 0.0169218
This iteration of linear solver gives...
7.00466 94.9417 47.974 0.486621 0.40625 0.487492 1.45633e+07 3.76188e+08 8.74724e+09 3.93576e+08 6.50651e+06 19.8282 637440 0.0169218
Iteration within SLE routine...
7.01021 95.0294 48.2935 0.485305 0.40625 0.481888 1.45605e+07 3.77749e+08 8.71619e+09 3.95079e+08 6.31732e+06 19.9758 640490 0.016344
This iteration of linear solver gives...
7.01021 95.0294 48.2935 0.485305 0.40625 0.481888 1.45605e+07 3.77749e+08 8.71619e+09 3.95079e+08 6.31732e+06 19.9758 640490 0.016344
Iteration within SLE routine...
7.01021 95.0294 48.2935 0.485305 0.40625 0.481888 1.45605e+07 3.77749e+08 8.71619e+09 3.95079e+08 6.31732e+06 19.9758 640490 0.016344
This iteration of linear solver gives...

7.01021 95.0294 48.2935 0.485305 0.40625 0.481888 1.45605e+07 3.77749e+08 8.71619e+09 3.95079e+08 6.31732e+06 19.9758 640490 0.016344

Determining finite differences...
7.01021 95.0294 48.2935 0.485305 0.40625 0.481888 1.45605e+07 3.77749e+08 8.71619e+09 3.95079e+08 6.31732e+06 19.9758 640490
8.34354 95.0294 48.2935 0.485305 0.40625 0.481888 1.46877e+07 3.78108e+08 8.80138e+09 3.97172e+08 6.4106e+06 18.1836 749815
7.01021 97.4461 48.2935 0.485305 0.40625 0.481888 1.42331e+07 3.75482e+08 6.5752e+09 3.95048e+08 6.38538e+06 19.6099 637427
7.01021 95.0294 51.6268 0.485305 0.40625 0.481888 1.53155e+07 4.0298e+08 9.39267e+09 4.3018e+08 6.89523e+06 21.0928 658835
7.01021 95.0294 48.2935 0.589472 0.40625 0.481888 1.61593e+07 4.21516e+08 9.25468e+09 3.94366e+08 6.26998e+06 19.9758 640487
7.01021 95.0294 48.2935 0.485305 0.46875 0.481888 1.46876e+07 3.8129e+08 8.75755e+09 4.32694e+08 6.24981e+06 19.9758 640489
7.01021 95.0294 48.2935 0.485305 0.40625 0.627721 1.47668e+07 3.8188e+08 8.72112e+09 3.96455e+08 7.21799e+06 20.0799 646803

Iteration within SLE routine...
6.99281 94.9838 47.8704 0.497154 0.46875 0.534203 1.49347e+07 3.86133e+08 8.7816e+09 4.30524e+08 6.81557e+06 19.9019 639636 0.00493363
This iteration of linear solver gives...
6.99281 94.9838 47.8704 0.497154 0.46875 0.534203 1.49347e+07 3.86133e+08 8.7816e+09 4.30524e+08 6.81557e+06 19.9019 639636 0.00493363
Iteration within SLE routine...
7.00482 95.0171 48.0536 0.495183 0.46875 0.475237 1.47744e+07 3.83576e+08 8.76096e+09 4.29897e+08 6.30086e+06 19.9128 638849 0.00265079
This iteration of linear solver gives...
7.00482 95.0171 48.0536 0.495183 0.46875 0.475237 1.47744e+07 3.83576e+08 8.76096e+09 4.29897e+08 6.30086e+06 19.9128 638849 0.00265079
Iteration within SLE routine...
6.99815 94.9851 47.892 0.498471 0.46875 0.5112 1.4923e+07 3.86011e+08 8.78851e+09 4.30537e+08 6.64191e+06 19.8809 639095 0.00263979
This iteration of linear solver gives...
6.99815 94.9851 47.892 0.498471 0.46875 0.5112 1.4923e+07 3.86011e+08 8.78851e+09 4.30537e+08 6.64191e+06 19.8809 639095 0.00263979
Iteration within SLE routine...
7.00333 95.0133 48.0499 0.495154 0.46875 0.481049 1.47826e+07 3.83728e+08 8.76464e+09 4.29925e+08 6.34354e+06 19.9191 638981 0.00235569
This iteration of linear solver gives...
7.00333 95.0133 48.0499 0.495154 0.46875 0.481049 1.47826e+07 3.83728e+08 8.76464e+09 4.29925e+08 6.34354e+06 19.9191 638981 0.00235569
Iteration within SLE routine...
7.00333 95.0133 48.0499 0.495154 0.46875 0.481049 1.47826e+07 3.83728e+08 8.76464e+09 4.29925e+08 6.34354e+06 19.9191 638981 0.00235569
This iteration of linear solver gives...

7.00333 95.0133 48.0499 0.495154 0.46875 0.481049 1.47826e+07 3.83728e+08 8.76464e+09 4.29925e+08 6.34354e+06 19.9191 638981 0.00235569

Determining finite differences...
7.00333 95.0133 48.0499 0.495154 0.46875 0.481049 1.47826e+07 3.83728e+08 8.76464e+09 4.29925e+08 6.34354e+06 19.9191 638981
8.00333 95.0133 48.0499 0.495154 0.46875 0.481049 1.48744e+07 3.83954e+08 8.82584e+09 4.31543e+08 6.42306e+06 18.5082 720970
7.00333 96.8258 48.0499 0.495154 0.46875 0.481049 1.45188e+07 3.81883e+08 7.05515e+09 4.29901e+08 6.40237e+06 19.6247 636513
7.00333 95.0133 50.5499 0.495154 0.46875 0.481049 1.53809e+07 4.03326e+08 9.27832e+09 4.59941e+08 6.4879e+06 20.7744 653182
7.00333 95.0133 48.0499 0.573279 0.46875 0.481049 1.59296e+07 4.15085e+08 9.15093e+09 4.29278e+08 6.29254e+06 19.919 638980
7.00333 95.0133 48.0499 0.495154 0.421875 0.481049 1.47716e+07 3.82154e+08 8.71435e+09 4.03915e+08 5.90197e+06 19.9191 638980
7.00333 95.0133 48.0499 0.495154 0.46875 0.590424 1.49421e+07 3.86945e+08 8.76856e+09 4.31008e+08 7.07043e+06 19.9984 643795

Iteration within SLE routine...
7.00333 95.0133 48.0499 0.495154 0.46875 0.481049 1.47826e+07 3.83728e+08 8.76464e+09 4.29925e+08 6.34354e+06 19.9191 638981 0.00235569
This iteration of linear solver gives...
7.00333 95.0133 48.0499 0.495154 0.46875 0.481049 1.47826e+07 3.83728e+08 8.76464e+09 4.29925e+08 6.34354e+06 19.9191 638981 0.00235569

Determining finite differences...
7.00333 95.0133 48.0499 0.495154 0.46875 0.481049 1.47826e+07 3.83728e+08 8.76464e+09 4.29925e+08 6.34354e+06 19.9191 638981
7.80333 95.0133 48.0499 0.495154 0.46875 0.481049 1.48538e+07 3.83924e+08 8.81323e+09 4.31281e+08 6.41674e+06 18.8126 700831
7.00333 96.4633 48.0499 0.495154 0.46875 0.481049 1.45622e+07 3.82181e+08 7.34749e+09 4.29904e+08 638145 19.6738 636919
7.00333 95.0133 50.0499 0.495154 0.46875 0.481049 1.52461e+07 3.99382e+08 9.14835e+09 4.52895e+08 6.97033e+06 20.5647 649910
7.00333 95.0133 48.0499 0.557654 0.46875 0.481049 1.57024e+07 4.08877e+08 9.07446e+09 4.29401e+08 6.33479e+06 19.919 638980
7.00333 95.0133 48.0499 0.495154 0.43125 0.481049 1.47351e+07 3.82099e+08 8.75775e+09 4.07561e+08 6.40489e+06 19.9191 638981
7.00333 95.0133 48.0499 0.495154 0.46875 0.568549 1.49107e+07 3.86324e+08 8.76779e+09 4.30807e+08 6.93982e+06 19.9826 642832

Iteration within SLE routine...
7.002 94.991 47.9249 0.500527 0.5 0.498741 1.49022e+07 3.85932e+08 8.78869e+09 4.4909e+08 6.52179e+06 19.8244 637612 0.000136563
Iteration within SLE routine...
7.00349 95.0097 48.0432 0.500549 0.5 0.494288 1.48966e+07 3.86694e+08 8.80259e+09 4.4838e+08 6.39481e+06 19.9197 639939 9.75513e-05
This iteration of linear solver gives...

7.00349 95.0097 48.0432 0.500549 0.5 0.494288 1.48966e+07 3.86694e+08 8.80259e+09 4.4838e+08 6.39481e+06 19.9197 639939 9.75513e-05
Iteration within SLE routine...
7.00349 95.0097 48.0432 0.500549 0.5 0.494288 1.48966e+07 3.86694e+08 8.80259e+09 4.4838e+08 6.39481e+06 19.9197 639939 9.75513e-05
This iteration of linear solver gives...
7.00349 95.0097 48.0432 0.500549 0.5 0.494288 1.48966e+07 3.86694e+08 8.80259e+09 4.4838e+08 6.39481e+06 19.9197 639939 9.75513e-05
Optimisation complete

RUN 3

Determining finite differences...
9 99 58 0.125 0.125 0.125 0.125 7.30208e+06 1.88417e+08 4.36759e+09 2.64417e+08 2.97855e+06 19.5159 837158
5 99 58 0.125 0.125 0.125 0.125 6.92251e+06 1.87294e+08 4.02927e+09 2.59493e+08 2.85843e+06 26.581 533430
9 91.75 58 0.125 0.125 0.125 0.125 8.68491e+06 1.97013e+08 1.1066e+10 2.64546e+08 3.18496e+06 20.6564 850095
9 99 48 0.125 0.125 0.125 0.125 6.39199e+06 1.59869e+08 3.18595e+09 2.14364e+08 2.65612e+06 16.709 783795
9 99 58 0.4375 0.125 0.125 0.125 1.32682e+07 3.55223e+08 7.11208e+09 2.63478e+08 2.97282e+06 19.529 836509
9 99 58 0.125 0.4375 0.125 0.125 7.30208e+06 1.88417e+08 4.36759e+09 2.64417e+08 2.97855e+06 19.5159 837158
9 99 58 0.125 0.125 0.3125 0.125 8.67997e+06 2.28026e+08 4.93311e+09 4.18317e+08 2.939e+06 19.5294 836507
9 99 58 0.125 0.125 0.125 0.5625 7.98471e+06 2.03738e+08 4.46265e+09 2.70716e+08 7.81283e+06 19.9802 856225

Iteration within SLE routine...
7.10019 96.1803 48 0.421001 0.125 0.3125 0.483667 1.30068e+07 3.37332e+08 7.07091e+09 3.36541e+08 6.56751e+06 19.5288 644436 0.135126
This iteration of linear solver gives...
7.10019 96.1803 48 0.421001 0.125 0.3125 0.483667 1.30068e+07 3.37332e+08 7.07091e+09 3.36541e+08 6.56751e+06 19.5288 644436 0.135126
Iteration within SLE routine...
7.00756 95.1112 48.1354 0.4375 0.125 0.3125 0.473204 1.33878e+07 3.45811e+08 8.14502e+09 3.36347e+08 6.36352e+06 19.8956 639002 0.090793
This iteration of linear solver gives...
7.00756 95.1112 48.1354 0.4375 0.125 0.3125 0.473204 1.33878e+07 3.45811e+08 8.14502e+09 3.36347e+08 6.36352e+06 19.8956 639002 0.090793
Iteration within SLE routine...

7.01234 95.0691 48.0582 0.4375 0.125 0.3125 0.484224 1.34048e+07 3.45786e+08 8.20365e+09 3.35835e+08 6.51148e+06 19.8865 639658 0.0900884
This iteration of linear solver gives...
7.01234 95.0691 48.0582 0.4375 0.125 0.3125 0.484224 1.34048e+07 3.45786e+08 8.20365e+09 3.35835e+08 6.51148e+06 19.8865 639658 0.0900884
Iteration within SLE routine...
7.01234 95.0691 48.0582 0.4375 0.125 0.3125 0.484224 1.34048e+07 3.45786e+08 8.20365e+09 3.35835e+08 6.51148e+06 19.8865 639658 0.0900884
This iteration of linear solver gives...
7.01234 95.0691 48.0582 0.4375 0.125 0.3125 0.484224 1.34048e+07 3.45786e+08 8.20365e+09 3.35835e+08 6.51148e+06 19.8865 639658 0.0900884

Determining finite differences...
7.01234 95.0691 48.0582 0.4375 0.125 0.3125 0.484224 1.34048e+07 3.45786e+08 8.20365e+09 3.35835e+08 6.51148e+06 19.8865 639658
9.01234 95.0691 48.0582 0.4375 0.125 0.3125 0.484224 1.36074e+07 3.46421e+08 8.33532e+09 3.38729e+08 6.67032e+06 17.3882 810611
7.01234 98.6941 48.0582 0.4375 0.125 0.3125 0.484224 1.29728e+07 3.42898e+08 5.30316e+09 3.35798e+08 6.60668e+06 19.398 635617
7.01234 95.0691 53.0582 0.4375 0.125 0.3125 0.484224 1.43834e+07 3.78594e+08 9.14279e+09 3.79003e+08 6.89989e+06 21.5431 665864
7.01234 95.0691 48.0582 0.59375 0.125 0.3125 0.484224 1.58735e+07 4.13483e+08 9.02128e+09 3.35042e+08 6.45857e+06 19.8864 639655
7.01234 95.0691 48.0582 0.4375 0.28125 0.3125 0.484224 1.34048e+07 3.45786e+08 8.20365e+09 3.35835e+08 6.51148e+06 19.8865 639658
7.01234 95.0691 48.0582 0.4375 0.125 0.40625 0.484224 1.3769e+07 3.55991e+08 8.31157e+09 3.93103e+08 6.47051e+06 19.8865 639658
7.01234 95.0691 48.0582 0.4375 0.125 0.3125 0.702974 1.37127e+07 3.51846e+08 8.21115e+09 3.37795e+08 7.71463e+06 20.0441 649280

Iteration within SLE routine...
7.00324 94.8887 47.9625 0.485605 0.125 0.40625 0.494072 1.45935e+07 3.77289e+08 8.80971e+09 3.93128e+08 6.71141e+06 19.8451 637710 0.0184188
This iteration of linear solver gives...
7.00324 94.8887 47.9625 0.485605 0.125 0.40625 0.494072 1.45935e+07 3.77289e+08 8.80971e+09 3.93128e+08 6.71141e+06 19.8451 637710 0.0184188
Iteration within SLE routine...
7.00324 94.8887 47.9625 0.485605 0.125 0.40625 0.494072 1.45935e+07 3.77289e+08 8.80971e+09 3.93128e+08 6.71141e+06 19.8451 637710 0.0184188
This iteration of linear solver gives...
7.00324 94.8887 47.9625 0.485605 0.125 0.40625 0.494072 1.45935e+07 3.77289e+08 8.80971e+09 3.93128e+08 6.71141e+06 19.8451 637710 0.0184188

Determining finite differences...
7.00324 94.8887 47.9625 0.485605 0.125 0.40625 0.494072 1.45935e+07 3.77289e+08 8.80971e+09 3.93128e+08 6.71141e+06 19.8451 637710
8.33657 94.8887 47.9625 0.485605 0.125 0.40625 0.494072 1.47207e+07 3.7765e+08 8.89489e+09 3.95288e+08 6.81179e+06 18.0649 746997

7.00324 97.3054 47.9625 0.485605 0.125 0.40625 0.494072 1.42557e+07 3.74949e+08 6.60923e+09 3.93097e+08 6.79124e+06 19.466 634551
7.00324 94.8887 51.2958 0.485605 0.125 0.40625 0.494072 1.52894e+07 4.01312e+08 9.4702e+09 4.26927e+08 6.98092e+06 21.0311 657311
7.00324 94.8887 47.9625 0.589772 0.125 0.40625 0.494072 1.61451e+07 4.19027e+08 9.32747e+09 3.92909e+08 6.50844e+06 19.8451 637708
7.00324 94.8887 47.9625 0.485605 0.229167 0.40625 0.494072 1.45935e+07 3.77289e+08 8.80971e+09 3.93128e+08 6.71141e+06 19.8451 637710
7.00324 94.8887 47.9625 0.485605 0.125 0.46875 0.494072 1.46951e+07 3.79592e+08 8.8457e+09 4.3104e+08 6.49632e+06 19.8451 637711
7.00324 94.8887 47.9625 0.485605 0.125 0.40625 0.639905 1.48045e+07 3.81483e+08 8.81491e+09 3.94534e+08 7.62892e+06 19.9517 644166

Iteration within SLE routine...
7.00267 95.066 48.188 0.496101 0.125 0.46875 0.501364 1.48407e+07 3.85546e+08 8.73919e+09 4.31682e+08 6.4241e+06 19.9644 640275 0.00169564
This iteration of linear solver gives...
7.00267 95.066 48.188 0.496101 0.125 0.46875 0.501364 1.48407e+07 3.85546e+08 8.73919e+09 4.31682e+08 6.4241e+06 19.9644 640275 0.00169564
Iteration within SLE routine...
7.00267 95.066 48.188 0.496101 0.125 0.46875 0.501364 1.48407e+07 3.85546e+08 8.73919e+09 4.31682e+08 6.4241e+06 19.9644 640275 0.00169564
This iteration of linear solver gives...
7.00267 95.066 48.188 0.496101 0.125 0.46875 0.501364 1.48407e+07 3.85546e+08 8.73919e+09 4.31682e+08 6.4241e+06 19.9644 640275 0.00169564

Determining finite differences...
7.00267 95.066 48.188 0.496101 0.125 0.46875 0.501364 1.48407e+07 3.85546e+08 8.73919e+09 4.31682e+08 6.4241e+06 19.9644 640275
8.00267 95.066 48.188 0.496101 0.125 0.46875 0.501364 1.49325e+07 3.85769e+08 8.80048e+09 4.33307e+08 6.49348e+06 18.5509 722259
7.00267 96.8785 48.188 0.496101 0.125 0.46875 0.501364 1.458e+07 3.83724e+08 7.04837e+09 4.31658e+08 6.48628e+06 19.674 637835
7.00267 95.066 50.688 0.496101 0.125 0.46875 0.501364 1.54092e+07 4.04879e+08 9.24534e+09 4.60878e+08 6.89581e+06 20.7901 653685
7.00267 95.066 48.188 0.574226 0.125 0.46875 0.501364 1.59901e+07 4.16979e+08 9.12794e+09 4.31026e+08 6.40448e+06 19.9643 640272
7.00267 95.066 48.188 0.496101 0.203125 0.46875 0.501364 1.48407e+07 3.85546e+08 8.73919e+09 4.31682e+08 6.4241e+06 19.9644 640275
7.00267 95.066 48.188 0.496101 0.125 0.421875 0.501364 1.47724e+07 3.83333e+08 8.72564e+09 4.03576e+08 6.48294e+06 19.9644 640275
7.00267 95.066 48.188 0.496101 0.125 0.46875 0.610739 1.49972e+07 3.88678e+08 8.74298e+09 4.32711e+08 7.13155e+06 20.0429 645044

Iteration within SLE routine...
7.00267 95.066 48.188 0.496101 0.125 0.46875 0.501364 1.48407e+07 3.85546e+08 8.73919e+09 4.31682e+08 6.4241e+06 19.9644 640275 0.00169564
This iteration of linear solver gives...
7.00267 95.066 48.188 0.496101 0.125 0.46875 0.501364 1.48407e+07 3.85546e+08 8.73919e+09 4.31682e+08 6.4241e+06 19.9644 640275 0.00169564

Determining finite differences...
7.00267 95.066 48.188 0.496101 0.125 0.46875 0.501364 1.48407e+07 3.85546e+08 8.73919e+09 4.31682e+08 6.4241e+06 19.9644 640275
7.80267 95.066 48.188 0.496101 0.125 0.46875 0.501364 1.49118e+07 3.85737e+08 8.78787e+09 4.33034e+08 6.50212e+06 18.8555 702149
7.00267 96.516 48.188 0.496101 0.125 0.46875 0.501364 1.46226e+07 3.84016e+08 7.33502e+09 4.31662e+08 6.46936e+06 19.7221 638234
7.00267 95.066 50.188 0.496101 0.125 0.46875 0.501364 1.53606e+07 4.02802e+08 9.16004e+09 4.57099e+08 6.80715e+06 20.6035 650806
7.00267 95.066 48.188 0.558601 0.125 0.46875 0.501364 1.57623e+07 4.10754e+08 9.05097e+09 4.31152e+08 6.40569e+06 19.9644 640272
7.00267 95.066 48.188 0.496101 0.1875 0.46875 0.501364 1.48407e+07 3.85546e+08 8.73919e+09 4.31682e+08 6.4241e+06 19.9644 640275
7.00267 95.066 48.188 0.496101 0.125 0.43125 0.501364 1.47932e+07 3.83912e+08 8.73225e+09 4.09207e+08 6.45993e+06 19.9644 640274
7.00267 95.066 48.188 0.496101 0.125 0.46875 0.588864 1.49664e+07 3.88071e+08 8.74223e+09 4.32518e+08 7.02784e+06 20.0273 644091

Iteration within SLE routine...
6.99604 94.9641 47.8517 0.5008 0.125 0.5 0.520918 1.49835e+07 3.87569e+08 8.82657e+09 4.48585e+08 6.69702e+06 19.8871 639271 0.00145638
Iteration within SLE routine...
7.00269 95.0084 47.9759 0.498596 0.125 0.5 0.481938 1.48497e+07 3.84656e+08 8.77163e+09 4.49489e+08 6.33658e+06 19.8149 636936 0.000418117
This iteration of linear solver gives...
7.00269 95.0084 47.9759 0.498596 0.125 0.5 0.481938 1.48497e+07 3.84656e+08 8.77163e+09 4.49489e+08 6.33658e+06 19.8149 636936 0.000418117
Iteration within SLE routine...
7.00269 95.0084 47.9759 0.498596 0.125 0.5 0.481938 1.48497e+07 3.84656e+08 8.77163e+09 4.49489e+08 6.33658e+06 19.8149 636936 0.000418117
This iteration of linear solver gives...
7.00269 95.0084 47.9759 0.498596 0.125 0.5 0.481938 1.48497e+07 3.84656e+08 8.77163e+09 4.49489e+08 6.33658e+06 19.8149 636936 0.000418117

Determining finite differences...
7.00269 95.0084 47.9759 0.498596 0.125 0.5 0.481938 1.48497e+07 3.84656e+08 8.77163e+09 4.49489e+08 6.33658e+06 19.8149 636936
7.66936 95.0084 47.9759 0.498596 0.125 0.5 0.481938 1.49148e+07 3.84836e+08 8.81605e+09 4.50763e+08 6.37473e+06 18.8027 693213
7.00269 96.2167 47.9759 0.498596 0.125 0.5 0.481938 1.46637e+07 3.83361e+08 7.58094e+09 4.49472e+08 6.37074e+06 19.6074 635196
7.00269 95.0084 49.6426 0.498596 0.125 0.5 0.481938 1.52858e+07 4.01141e+08 9.16537e+09 4.69648e+08 6.65774e+06 20.4957 648444
7.00269 95.0084 47.9759 0.550679 0.125 0.5 0.481938 1.55864e+07 4.04723e+08 9.01849e+09 4.49083e+08 6.32622e+06 19.8149 636936
7.00269 95.0084 47.9759 0.498596 0.177083 0.5 0.481938 1.48497e+07 3.84656e+08 8.77163e+09 4.49489e+08 6.33658e+06 19.8149 636936
7.00269 95.0084 47.9759 0.498596 0.125 0.46875 0.481938 1.48357e+07 3.84257e+08 8.76489e+09 4.30977e+08 6.38321e+06 19.8149 636937

7.00269 95.0084 47.9759 0.498596 0.125 0.5 0.554855 1.49575e+07 3.86845e+08 8.77431e+09 4.50246e+08 6.8529e+06 19.8686 640161

Iteration within SLE routine...
7.00545 95.0288 48.1739 0.498539 0.125 0.495877 0.49221 1.48835e+07 3.8665e+08 8.79825e+09 4.47471e+08 6.33566e+06 19.9586 640022 0.000375743
This iteration of linear solver gives...
7.00545 95.0288 48.1739 0.498539 0.125 0.495877 0.49221 1.48835e+07 3.8665e+08 8.79825e+09 4.47471e+08 6.33566e+06 19.9586 640022 0.000375743
Iteration within SLE routine...
7.00545 95.0288 48.1739 0.498539 0.125 0.495877 0.49221 1.48835e+07 3.8665e+08 8.79825e+09 4.47471e+08 6.33566e+06 19.9586 640022 0.000375743
This iteration of linear solver gives...
7.00545 95.0288 48.1739 0.498539 0.125 0.495877 0.49221 1.48835e+07 3.8665e+08 8.79825e+09 4.47471e+08 6.33566e+06 19.9586 640022 0.000375743

Determining finite differences...
7.00545 95.0288 48.1739 0.498539 0.125 0.495877 0.49221 1.48835e+07 3.8665e+08 8.79825e+09 4.47471e+08 6.33566e+06 19.9586 640022
7.57688 95.0288 48.1739 0.498539 0.125 0.495877 0.49221 1.49364e+07 3.86796e+08 8.83481e+09 4.48483e+08 6.41463e+06 19.1093 685979
7.00545 96.0645 48.1739 0.498539 0.125 0.495877 0.49221 1.47094e+07 3.85415e+08 7.68821e+09 4.47454e+08 6.39988e+06 19.7658 638394
7.00545 95.0288 49.6025 0.498539 0.125 0.495877 0.49221 1.53479e+07 4.02209e+08 9.16048e+09 4.68176e+08 6.72286e+06 20.539 650131
7.00545 95.0288 48.1739 0.543182 0.125 0.495877 0.49221 1.55279e+07 4.04274e+08 9.01728e+09 4.4709e+08 6.32194e+06 19.9494 640472
7.00545 95.0288 48.1739 0.498539 0.169643 0.495877 0.49221 1.48835e+07 3.8665e+08 8.79825e+09 4.47471e+08 6.33566e+06 19.9586 640022
7.00545 95.0288 48.1739 0.498539 0.125 0.469091 0.49221 1.48687e+07 3.86231e+08 8.79157e+09 4.3161e+08 6.37427e+06 19.9569 640101
7.00545 95.0288 48.1739 0.498539 0.125 0.495877 0.55471 1.49743e+07 3.88493e+08 8.80046e+09 4.48096e+08 6.77793e+06 20.0037 642750

Iteration within SLE routine...
7.00545 95.0288 48.1739 0.498539 0.125 0.495877 0.49221 1.48835e+07 3.8665e+08 8.79825e+09 4.47471e+08 6.33566e+06 19.9586 640022 0.000375743
This iteration of linear solver gives...
7.00545 95.0288 48.1739 0.498539 0.125 0.495877 0.49221 1.48835e+07 3.8665e+08 8.79825e+09 4.47471e+08 6.33566e+06 19.9586 640022 0.000375743
Optimisation complete

RUN 4

Determining finite differences...
5 90 45 0.25 0.25 0.25 1.07458e+07 2.43844e+08 1.45536e+10 2.67843e+08 6.79459e+06 24.9022 484074
9 90 45 0.25 0.25 0.25 1.11138e+07 2.44794e+08 1.50626e+10 2.73479e+08 5.70261e+06 17.9642 792437
5 97.25 45 0.25 0.25 0.25 8.79891e+06 2.30333e+08 4.76896e+09 2.67628e+08 5.10473e+06 22.2498 465860
5 90 55 0.25 0.25 0.25 1.21637e+07 2.87808e+08 1.47935e+10 3.42182e+08 4.93555e+06 28.2334 537146
5 90 45 0.5625 0.25 0.25 1.54985e+07 3.73509e+08 1.68317e+10 2.66521e+08 5.23006e+06 24.8917 484308
5 90 45 0.25 0.4375 0.25 1.1597e+07 2.66927e+08 1.50197e+10 3.7254e+08 5.32318e+06 24.7154 488619
5 90 45 0.25 0.25 0.6875 1.14203e+07 2.60327e+08 1.46632e+10 2.72338e+08 9.71889e+06 25.008 503694

Iteration within SLE routine...
7.60929 96.8701 53.1188 0.5625 0.4375 0.125 1.61916e+07 4.35182e+08 8.64513e+09 4.61647e+08 2.56199e+06 19.929 701476 0.39728
Iteration within SLE routine...
7.60929 96.8701 53.1188 0.5625 0.4375 0.125 1.61916e+07 4.35182e+08 8.64513e+09 4.61647e+08 2.56199e+06 19.929 701476 0.39728
This iteration of linear solver gives...
7.60929 96.8701 53.1188 0.5625 0.4375 0.125 1.61916e+07 4.35182e+08 8.64513e+09 4.61647e+08 2.56199e+06 19.929 701476 0.39728
Iteration within SLE routine...
6.86967 96.1563 48.1875 0.455001 0.4375 0.528381 1.4035e+07 3.66697e+08 7.40031e+09 4.13388e+08 6.6905e+06 19.9978 629563 0.0394434
This iteration of linear solver gives...
6.86967 96.1563 48.1875 0.455001 0.4375 0.528381 1.4035e+07 3.66697e+08 7.40031e+09 4.13388e+08 6.6905e+06 19.9978 629563 0.0394434
Iteration within SLE routine...
6.86967 96.1563 48.1875 0.455001 0.4375 0.528381 1.4035e+07 3.66697e+08 7.40031e+09 4.13388e+08 6.6905e+06 19.9978 629563 0.0394434
This iteration of linear solver gives...
6.86967 96.1563 48.1875 0.455001 0.4375 0.528381 1.4035e+07 3.66697e+08 7.40031e+09 4.13388e+08 6.6905e+06 19.9978 629563 0.0394434

Determining finite differences...
6.86967 96.1563 48.1875 0.455001 0.4375 0.528381 1.4035e+07 3.66697e+08 7.40031e+09 4.13388e+08 6.6905e+06 19.9978 629563
8.86967 96.1563 48.1875 0.455001 0.4375 0.528381 1.42282e+07 3.67249e+08 7.51611e+09 4.16531e+08 6.83508e+06 17.4338 798878
6.86967 92.5313 48.1875 0.455001 0.4375 0.528381 1.48467e+07 3.72293e+08 1.21301e+10 4.1347e+08 6.53618e+06 20.8808 637156

6.86967 96.1563 53.1875 0.455001 0.4375 0.528381 1.50956e+07 4.01903e+08 8.48718e+09 4.6786e+08 7.18842e+06 21.7016 656111
6.86967 96.1563 48.1875 0.611251 0.4375 0.528381 1.63724e+07 4.30939e+08 8.16785e+09 4.12254e+08 6.66213e+06 19.9977 629561
6.86967 96.1563 48.1875 0.455001 0.34375 0.528381 1.37244e+07 3.58119e+08 7.30572e+09 3.56372e+08 6.74886e+06 19.9979 629563
6.86967 96.1563 48.1875 0.455001 0.4375 0.747131 1.43396e+07 3.72592e+08 7.40857e+09 4.15218e+08 7.88595e+06 20.1558 639100

Iteration within SLE routine...
6.99636 95.2153 47.7613 0.492954 0.5 0.507463 1.48296e+07 3.8427e+08 8.52637e+09 4.47945e+08 6.91371e+06 19.8154 638730 0.006123
Iteration within SLE routine...
6.99636 95.2153 47.7613 0.492954 0.5 0.507463 1.48296e+07 3.8427e+08 8.52637e+09 4.47945e+08 6.91371e+06 19.8154 638730 0.006123
This iteration of linear solver gives...
6.99636 95.2153 47.7613 0.492954 0.5 0.507463 1.48296e+07 3.8427e+08 8.52637e+09 4.47945e+08 6.91371e+06 19.8154 638730 0.006123
Iteration within SLE routine...
6.99636 95.2153 47.7613 0.492954 0.5 0.507463 1.48296e+07 3.8427e+08 8.52637e+09 4.47945e+08 6.91371e+06 19.8154 638730 0.006123
This iteration of linear solver gives...
6.99636 95.2153 47.7613 0.492954 0.5 0.507463 1.48296e+07 3.8427e+08 8.52637e+09 4.47945e+08 6.91371e+06 19.8154 638730 0.006123

Determining finite differences...
6.99636 95.2153 47.7613 0.492954 0.5 0.507463 1.48296e+07 3.8427e+08 8.52637e+09 4.47945e+08 6.91371e+06 19.8154 638730
8.32969 95.2153 47.7613 0.492954 0.5 0.507463 1.49507e+07 3.84589e+08 8.60477e+09 4.50123e+08 6.98877e+06 18.0816 744906
6.99636 97.632 47.7613 0.492954 0.5 0.507463 1.45131e+07 3.82084e+08 6.42704e+09 4.47916e+08 6.95925e+06 19.4593 635769
6.99636 95.2153 51.0946 0.492954 0.5 0.507463 1.54624e+07 4.07203e+08 9.18515e+09 4.85783e+08 6.92511e+06 20.9256 655715
6.99636 95.2153 47.7613 0.597121 0.5 0.507463 1.62911e+07 4.24058e+08 9.01201e+09 4.4715e+08 6.84554e+06 19.8154 638729
6.99636 95.2153 47.7613 0.492954 0.4375 0.507463 1.47774e+07 3.82499e+08 8.51567e+09 4.10957e+08 6.98667e+06 19.8154 638731
6.99636 95.2153 47.7613 0.492954 0.5 0.653296 1.5052e+07 3.88652e+08 8.53229e+09 4.49401e+08 7.85925e+06 19.9233 645475

Iteration within SLE routine...
7.0134 95.0159 48.1313 0.498921 0.496831 0.436918 1.48039e+07 3.84881e+08 8.80219e+09 4.4698e+08 5.96042e+06 19.894 638150 0.00596881
This iteration of linear solver gives...
7.0134 95.0159 48.1313 0.498921 0.496831 0.436918 1.48039e+07 3.84881e+08 8.80219e+09 4.4698e+08 5.96042e+06 19.894 638150 0.00596881
Iteration within SLE routine...

6.99427 94.982 47.8857 0.501225 0.5 0.515112 1.49822e+07 3.87603e+08 8.81155e+09 4.48936e+08 6.6357e+06 19.8893 638950 0.000819782
Iteration within SLE routine...
7.00274 95.0078 47.9855 0.498938 0.5 0.486719 1.48623e+07 3.84943e+08 8.7754e+09 4.49648e+08 6.36128e+06 19.821 637092 0.000272677
This iteration of linear solver gives...
7.00274 95.0078 47.9855 0.498938 0.5 0.486719 1.48623e+07 3.84943e+08 8.7754e+09 4.49648e+08 6.36128e+06 19.821 637092 0.000272677
Iteration within SLE routine...
7.00521 95.0334 48.2125 0.498815 0.495251 0.499974 1.49044e+07 3.87229e+08 8.80162e+09 4.47626e+08 6.38336e+06 19.973 640563 0.000161746
This iteration of linear solver gives...
7.00521 95.0334 48.2125 0.498815 0.495251 0.499974 1.49044e+07 3.87229e+08 8.80162e+09 4.47626e+08 6.38336e+06 19.973 640563 0.000161746
Iteration within SLE routine...
7.00521 95.0334 48.2125 0.498815 0.495251 0.499974 1.49044e+07 3.87229e+08 8.80162e+09 4.47626e+08 6.38336e+06 19.973 640563 0.000161746
This iteration of linear solver gives...
7.00521 95.0334 48.2125 0.498815 0.495251 0.499974 1.49044e+07 3.87229e+08 8.80162e+09 4.47626e+08 6.38336e+06 19.973 640563 0.000161746

Determining finite differences...
7.00521 95.0334 48.2125 0.498815 0.495251 0.499974 1.49044e+07 3.87229e+08 8.80162e+09 4.47626e+08 6.38336e+06 19.973 640563
8.00521 95.0334 48.2125 0.498815 0.495251 0.499974 1.49968e+07 3.87461e+08 8.86346e+09 4.49253e+08 6.45473e+06 18.5596 722532
7.00521 96.8459 48.2125 0.498815 0.495251 0.499974 1.46414e+07 3.85388e+08 7.09797e+09 4.47602e+08 6.44929e+06 19.6803 638102
7.00521 95.0334 50.7125 0.498815 0.495251 0.499974 1.54769e+07 4.06654e+08 9.31006e+09 4.78031e+08 6.83565e+06 20.7988 653991
7.00521 95.0334 48.2125 0.57694 0.495251 0.499974 1.60252e+07 4.17894e+08 9.18263e+09 4.46948e+08 6.32909e+06 19.973 640562
7.00521 95.0334 48.2125 0.498815 0.448376 0.499974 1.48742e+07 3.86085e+08 8.79836e+09 4.19706e+08 6.4367e+06 19.973 640563
7.00521 95.0334 48.2125 0.498815 0.495251 0.609349 1.50612e+07 3.90369e+08 8.80542e+09 4.48666e+08 7.04464e+06 20.0514 645325

Iteration within SLE routine...
7.00521 95.0334 48.2125 0.498815 0.495251 0.499974 1.49044e+07 3.87229e+08 8.80162e+09 4.47626e+08 6.38336e+06 19.973 640563 0.000161746
This iteration of linear solver gives...
7.00521 95.0334 48.2125 0.498815 0.495251 0.499974 1.49044e+07 3.87229e+08 8.80162e+09 4.47626e+08 6.38336e+06 19.973 640563 0.000161746

Determining finite differences...
7.00521 95.0334 48.2125 0.498815 0.495251 0.499974 1.49044e+07 3.87229e+08 8.80162e+09 4.47626e+08 6.38336e+06 19.973 640563

7.80521 95.0334 48.2125 0.498815 0.495251 0.499974 1.4976e+07 3.87429e+08 8.85065e+09 4.49005e+08 6.43948e+06 18.8654 702346
7.00521 96.4834 48.2125 0.498815 0.495251 0.499974 1.46846e+07 3.85684e+08 7.3888e+09 4.47605e+08 -2.33265e+06 19.729 638506
7.00521 95.0334 50.2125 0.498815 0.495251 0.499974 1.54249e+07 4.04401e+08 9.22201e+09 4.74111e+08 6.74505e+06 20.61 651078
7.00521 95.0334 48.2125 0.561315 0.495251 0.499974 1.58041e+07 4.11848e+08 9.10744e+09 4.47089e+08 6.36167e+06 19.973 640561
7.00521 95.0334 48.2125 0.498815 0.457751 0.499974 1.48879e+07 3.86471e+08 8.80295e+09 4.25307e+08 6.41828e+06 19.973 640563
7.00521 95.0334 48.2125 0.498815 0.495251 0.587474 1.50303e+07 3.89762e+08 8.80467e+09 4.48472e+08 6.97136e+06 20.0358 644372

Iteration within SLE routine...
7.00369 95.0086 47.9684 0.503248 0.5 0.496333 1.49374e+07 3.8691e+08 8.79369e+09 4.49534e+08 6.47163e+06 19.8231 637647 2.97234e-05
Iteration within SLE routine...
7.00262 95.0162 48.0387 0.500988 0.5 0.498669 1.4907e+07 3.86966e+08 8.79636e+09 4.48362e+08 6.4375e+06 19.9294 639653 1.86812e-05
This iteration of linear solver gives...
7.00262 95.0162 48.0387 0.500988 0.5 0.498669 1.4907e+07 3.86966e+08 8.79636e+09 4.48362e+08 6.4375e+06 19.9294 639653 1.86812e-05
Iteration within SLE routine...
7.00262 95.0162 48.0387 0.500988 0.5 0.498669 1.4907e+07 3.86966e+08 8.79636e+09 4.48362e+08 6.4375e+06 19.9294 639653 1.86812e-05
This iteration of linear solver gives...
7.00262 95.0162 48.0387 0.500988 0.5 0.498669 1.4907e+07 3.86966e+08 8.79636e+09 4.48362e+08 6.4375e+06 19.9294 639653 1.86812e-05
Optimisation complete